Final Report

Project Title IL-33: Regulation by methotrexate in psoriasis

By   Asst. Prof. Jitlada Meephansan, MD., PhD.

December 2016

Contract No. TRG5780230

Final Report

Project Title IL-33: Regulation by methotrexate in psoriasis

Researcher

Asst. Prof. Jitlada Meephansan, MD., PhD.

Institute

Division of Dermatology, Chulabhorn International College

of Medicine, Thammasat University

Abstract

Project Code : TRG5780230

Project Title : IL-33: Regulation by methotrexate in psoriasis

Investigator : Asst. Prof. Jitlada Meephansan, MD., PhD., Division of Dermatology, Chulabhorn International College of Medicine, Thammasat University

E-mail Address : kae_mdcu@yahoo.com

Project Period : 2 years

Abstract:

Interleukin (IL)-33 is a newly cytokine of interleukin-1 family. It is a dual function protein that works as a nuclear factor and extracellular cytokine. IL-33 is constitutively expressed in endothelial cells and epithelial cells of tissues exposed to environment and can be secreted in response to tissue damage to immediately activate innate immunity and T helper (Th)-2 cell response. In addition, IL-33 actions as a nuclear factor that blocks inflammatory signals. Interestingly, it is strongly expressed in the nucleus of keratinocytes of psoriasis patients. Psoriasis, a common chronic inflammatory skin disease that affects 2-3% of Thai population, is considered as a Th1- and Th17-mediated inflammation. The responsibility of IL-33 in psoriasis has not been clearly identified. The ultraviolet radiation, especially UVB, is a phototherapy that has wide-ranging immunosuppressive potentials via different mechanisms. UVB has been used to treat psoriasis with satisfactory response.

In this study, we would like to compare IL-33 expression before and after treatment with narrowband UVB (n=4) and methotrexate (n=4). Four patients diagnosed with moderate to severe psoriasis were treated by NBUVB phototherapy, and four patients were treated by methotrexate. They were received with systematic treatment until the PASI75 was achieved or up to 12 weeks of treatment. The tissue samples from lesional psoriatic skin are taken before and after treatment. The mRNA expression of IL-33 in keratinocytes was measured using quantitative droplet digital PCR.

All of patients achieved a 75% reduction in the PASI score. For group narrowband UVB (n=4), IL-33 mRNA levels of 3 patients (75%) were downregulated after treatment with NBUVB. The median mRNA level of IL-33 was reduced from baseline 13.65 copies/μl (IQR, 7-24.25) to 2.15 copies/μl (IQR, 1.05-2.95). For group methotrexate (n=4), IL-33 mRNA levels of 3 patients (75%) were downregulated after treatment with NBUVB. The median mRNA level of IL-33 was reduced from baseline 3.5 copies/μl (IQR, 0.65-18) to 0.32 copies/μl (IQR, 0-0.82). The results obtained from data analysis revealed a reduction in IL-33 expression by Wilcoxon signed-rank test (p = 0.144). For both treatments, 6 of 8 patients (75%) achieved significant downregulated mRNA level of IL-33 (p = 0.049*). The median mRNA level of IL-33 was reduced after treatment compared to before treatment (9.4 copies/μl, 01.1-22.25 vs. 0.82 copies/μl, 0.2-2.15).

In conclusion, the IL-33 production seems particularly associates with inflammatory skin of psoriasis, and this cytokine may be regulated by anti-inflammatory treatment including NBUVB phototherapy and metrotrexate.

บทคัดย่อ

บทคัดย่อ:

อินเตอร์ลิวคิน 33 (IL-33) เป็นสมาชิกตัวล่าสุดของกลุ่มอินเตอร์ลิวคิน 1 บทบาทหน้าที่ของอินเตอร์ลิวคิน 33 นั้นประกอบด้วย nuclear function และบทบาทของ cytokine ในสภาวะปกติ IL-33 จะถูกแสดงออกใน epithelial และ endothelial cells ซึ่งเป็นเซลล์ที่สัมผัสกับสิ่งแวดล้อมภายนอกร่างกาย เซลล์เหล่านี้สามารถหลั่ง IL-33 ได้เมื่อเซลล์ดังกล่าวถูกทำลายหรือได้รับบาดเจ็บ เมื่อถูกหลั่งออกมานอกเซลล์ IL-33 ได้มีบทบาทในการกระตุ้นภูมิคุ้มกันชนิด innate และ กระตุ้นการทำงานของ Th-2 cells

โรคสะเก็ดเงินเป็นโรคผิวหนังเรื้อรังซึ่ง T cell ชนิด Th-1 และ Th-17 มีบทบาทสำคัญต่อกลไกการเกิดโรค อย่างไรก็ตาม กลไกการเกิดโรคสะเก็ดเงินในปัจจุบันยังไม่ทราบเป็นที่แน่ชัด การรักษาพื้นฐานของโรคสะเก็ดเงินคือการกดการทำงานของภูมิคุ้มกัน ในประเทศไทยนั้น การรักษานิยมใช้แสงอัลตราไวโอเลตบี รวมถึงยาเมโธเทรกเซท ซึ่งเป็นยากดภูมิคุ้มกันในเพื่อการรักษาโรคสะเก็ดเงินให้ได้ผลดี

งานวิจัยนี้นักวิจัยทำการศึกษาในคนไข้โรคสะเก็ดเงินระดับปานกลางถึงรุนแรง เพื่อเปรียบเทียบระดับ IL-33 ก่อนและหลังการรักษาด้วยแสงอัลตราไวโอเลตบี (n =4) หรือยาเมโธเทรกเซท (n=4) ผู้ป่วยทั้งหมด 8 รายได้รับการรักษา และติดตามอาการต่อเนื่อง และประเมินผลการรักษาเมื่อประเมินผลความรุนแรงของโรคสะเก็ดเงิน (PASI score) ได้คะแนนดีขึ้น 75% เทียบกับก่อนรักษา หรือได้รับการรักษาติดต่อกันนานเป็นระยะเวลา 12 สัปดาห์ การศึกษาระดับ IL-33 ทำการวัดและวิเคราะห์สารพันธุกรรม (IL-33 mRNA) จากชิ้นเนื้อบริเวณผื่นโรคสะเก็ดเงินก่อนและหลังการรักษา โดยการทำ quanlitative droplet digital PCR

ผลการศึกษาพบว่าผู้ป่วยทั้งหมดในการวิจัย (n=8) ได้รับคะแนน PASI ดีขึ้น 75% กลุ่มผู้ป่วยโรคสะเก็ดเงินที่ได้รับการรักษาโดยการฉายแสงอัลตราไวโอเลต (n=4) 3 ราย (75%)

มีระดับ IL-33 mRNA ลดลงเมื่อเทียบกับก่อนรักษา วิเคราะห์ทางสถิติพบว่าค่า median ลดลงจากก่อนรักษา 13.65 copies/μl (IQR 7-24.25) เป็น 2.15 copies/μl (IQR 1.05-2.95) สำหรับกลุ่มผู้ป่วยโรคสะเก็ดเงินที่ได้รับการรักษาด้วยยาเมโธเทรกเซท (n=4) 3 ราย (75%) มีระดับ IL-33 mRNA ลดลงเมื่อเทียบกับก่อนรักษา วิเคราะห์ทางสถิติพบว่าค่า median ลดลงจากก่อนรักษา 3.5 copies/μl (IQR 0.65-18) เป็น 0.32 copies/μl (IQR 0-0.82) ผลการศึกษาระดับ IL-33 mRNA ถูกวิเคราะห์โดย Wilcoxon signed-rank test (p=0.144) เมื่อวิเคราะห์ผลรวมจากผู้ป่วยพบว่าผู้ป่วย 6 ราย (75%) มีระดับ มีระดับ IL-33 mRNA ลดลงอย่างมีนัยสำคัญเมื่อเทียบกับก่อนรักษา (p=0.049*) วิเคราะห์ทางสถิติพบว่าค่า median ลดลงจากก่อนรักษา 9.4 copies/μl (IQR 1.1-22.25) เป็น 0.82 copies/μl (IQR 0.2-2.15)

การแสดงออกที่เพิ่มขึ้นของ IL-33 ในโรคสะเก็ดเงินน่าจะบ่งชี้ได้ว่า IL-33 มีบทบาทเกี่ยวกับการอักเสบของโรค และ cytokine ดังกล่าวสามารถควบคุมได้โดยการฉายแสงอัลตราไวโอเลตบี รวมถึงการใช้ยาเมโธเทรกเซท

คำหลัก: อินเตอร์ลิวคิน 33, แสงอัลตราไวโอเลตบี, เมตโทรเทรกเซต, โรคสะเก็ดเงิน

Executive Summary

IL-33 was first described as an inflammatory cytokine that mediate Th2-associated diseas. It is a newly discovered member of the IL-1 cytokine family that is expressed by mainly in the nucleus of cells with barrier function, such as endothelial cells and epithelial cell. Many recent studies have proposed that IL-33 is a novel 'alarmin' that, by meaning, activates multiple cells, including T helper cells, mast cells, NK and NKT cells, eosinophils, basophils, and dendritic cells and has varied contribution to pathophysiology of several inflammation and diseases.

Firstly, IL-33 was considered that it might be secreted from the nucleus of the necrosis-mediated or apoptosis cells. Then, there was a study showed that IL-33 could be transferred from nucleus to cytoplasm using the nuclear pore complex and it exists in membrane-bound cytoplasmic vesicles. This described function of IL-33 as a mechanically cytokine secreted by living cells. Nevertheless, the exact role of IL-33 remains unclear. IL-33 seems to be a cytokine with dual function, acting both as an intracellular nuclear factor with transcriptional regulatory abilities and as a traditional cytokine via activation of the ST2L receptor complex.

Interestingly, its expression is increased following varies pro-inflammatory stimulation, such as TNF-α, IFN-γ, and IL-17, which have participated in complicated immunopathogenetic of psoriasis. TNF-α could stimulate the secretion of IL-33 from immortalized keratinocytes. This was supported by other study that TNF-α and IL-17 was able to upregulate almost all IL-1 family members, including IL-33, in ex vivo healthy skin organ culture.

Psoriasis is a Th1- and Th17-mediated inflammatory skin disease, which is characterized by marked infiltration of T cells, dendritic cells, macrophages and neutrophils in psoriatic skin. Several mediators can trigger dendritic cells through keratinocyte stress or directly activate via pattern recognition receptors. Cell stress can both induce and release intracellular endogenous factors or 'damage-associated molecular pattern (DAMPs)' to extracellular environment and generate inflammation. IL-33 is one of DAMPs. From our reviews literatures, skin tissues contain a high level of IL-33 mRNA expression compared to other tissues and cell types.

Intriguingly, it has been found to be strongly expressed and noticeably higher in the nuclei of keratinocytes in psoriatic skin lesions compared with healthy skin, lichen planus which is Th1-associated disease, and atopic dermatitis which is Th2-associated inflammation. Therefore, it has been proposed to represent a novel marker of psoriasis, comparative to other inflammatory skin disorders. Moreover, recent studies revealed that epidermal IL-33 expression associates with Koebner reactions, and it may be released to induce mast cells in psoriasis biology.

UVB phototherapy has been commonly used to treat moderate to severe psoriasis with satisfactory response. Interestingly, previous studies have been demonstrated that UVB irradiation of epidermal keratinocytes resulted in a significant upregulate in IL-33 expression in vivo. Several IL-1 family members, including IL-33, are involved in UVB-induced pro-inflammatory pathway. Thus, this is the interested feature of NBUVB that we aim to investigate whether NBUVB phototherapy has an effect on the expression of IL-33 in affected psoriatic skin.

In this study, we have demonstrated for the first time that IL-33 mRNA are expressed in psoriatic lesional skin in vivo before and after treatment with NBUVB phototherapy. These expressed IL-33 mRNA levels were decreased after NBUVB therapy in psoriasis patients, which suggests that IL-33 expression associates with NBUVB radiation as well as improvement of the disease. Base on the result, we considered the discussion in two aspects.

Firstly, this outcome, the decreased IL-33 mRNA levels after treatment, raises the possibility of its involvement in pro-inflammatory role as a cytokine in psoriasis. Several recent studies can support our results in extracellular role of IL-33 as an inflammatory cytokine.

Secondly, as we have known that psoriasis is a complicated immune-mediated inflammatory disorder. Pro-inflammatory, Th1 and Th17 cytokines and chemokines such as TNF-α and IFN-γ are key cytokines in development of disease, and also are found to be involved in production of IL-33 in keratinocytes. According to the immunosuppressive effects of NBUVB phototherapy in treating psoriasis, we may assume that the suppression of these pro-inflammatory cytokines effect levels of IL-33 mRNA. NBUVB therapy might not directly decrease the IL-33 expression in psoriatic skin. Further studies with this aspect are needed.

In summary, we cannot conclude the exact function of newly cytokine, but this present study could presents evidence for a novel alarmin, IL-33, in plaque-type psoriasis through NBUVB radiation and improvement of disease. IL-33 mRNA levels are decreased after NBUVB therapy. Our findings can imply that the production of IL-33 generally associates with inflammatory skin of psoriasis, and this cytokine could be regulated by anti-inflammatory treatment. In this end, our present study may partly explain a doubful role of IL-33 cytokine in psoriasis and might be opened aspect for more investigation in the future. A limitation of this study is that the number of psoriasis patients was very small due to the limited period of time. Secondly, we did not detect a serum protein level, as well as immunohistochemical staining of IL-33, which may provide a better understanding of IL-33 expression. Further studies with larger number of subjects and IL-33 protien level as well as immunohitochemistry should be performed to validate those possible roles of this cytokine in psoriasis.

In addition, we also observed the effect of methotrexate (MTX) to IL-33 expression in keratinocyte in psoriasis patients. After methotrexate treatment, IL-33 mRNA expression were decreased in psoriatic lesional skin biopsy compared to baseline. It may imply that downregulated IL-33 expression associates with improvement of the disease due to methotrexate therapy. Therefore, we considered reporting this outcome, which is shown in the result chapter (group M), and discussing the association between IL-33 expression and psoriatic treatment modalities.

Methotrexate is considered as an effective and successful therapy and remains widely used immunosuppressive agent for treating moderate to severe psoriasis. A therapeutic mechanism of MTX in psoriasis is both anti-inflammatory and anti-proliferative properties. This drug can reduce keratinocyte proliferation by acting as folate antagonist. The diminution in pyrimidine, purines, and methylation of DNA is a result of its action. In addition, MTX acts on the adenosine metabolism and causes the release of adenosine from damaged cells by the inhibition of 5-aminoimidazole-4-carbonxamidoribonucleotide (AICAR) transformylase. Adenosine, an endogenous purine nucleoside, is an immunosuppressive mediator that inhibits PMNs adhesion molecules, macrophage-induced TNF-α, and lymphocytes proliferation.

Other immunosuppressive effects of MTX include the inhibition of proinflammatory cytokines, suppression of T and B lymphocytes, and downregulation of chemotaxis of

monocytes and neutrophils. Moreover, this drug stimulates keratinocyte apoptosis and reduces DNA synthesis. Due to the complicated pathogenesis of psoriasis, the dysregulated immunity may be a target for antipsoriatic effect of drug.

In our study, we found the IL-33 mRNA expression on lesional plaque of psoriasis patients. These mRNA levels of IL-33 were decreased after treatment with methotrexate, which proposes that IL-33 cytokine associates with methotrexate together with the disease improvement. This may be due to downregulation of inflammatory cytokines like TNF-α and IFN-γ by MTX, which are involved in IL-33 production. Another possible mechanism is that methotrexate has anti-mitotic action on psoriatic skin and apoptotic effect in keratinocytes, which are found to be potential source of IL-33 cytokine. Owning to the reduced IL-22 serum levels, MTX inhibits epidermal hyperproliferation in psoriasis, which may indirectly affect to IL-33 cytokine production from keratinocytes. In conclusion, this shows evidence for IL-33 in psoriasis through its therapies, NBUVB and methotrexate, and improvement of disease. These can support that the expression of IL-33 in psoriasis could be regulated through anti-inflammatory and immunomodulatory properties of treatments. Further study will help understand the mechanisms of release, induction, regulation and effect of this cytokine.

1. Introduction

1.1 Background and Rationale

Psoriasis is a common chronic inflammatory cutaneous condition that affected 2-3% of Thai population. This chronic disease has significant unsatisfied factors that affect patients' quality of life. The costs can lead to impaired quality of life, lost productivity, increasing overall cost related with the psoriasis management. The disease is manifested by abnormal changes in epidermal proliferation and differentiation and various immunologic, biochemical and vascular abnormalities. By the way, its cause remains unknown. Recently, the discovery of interleukin (IL)-33 as a T helper (Th) 2-mediated inflammation was proposed. Interestingly, IL-33 is strongly stained at the nucleus of keratinocytes of psoriasis, which is considered as Th-1/Th-17 mediated immune response when compared with atopic dermatitis, which is considered as Th-2/Th-1 mediated immune response. Role of IL-33 in psoriasis is still unknown. We use therapeutic models to demonstrate the IL-33 expression in keratinocytes after clinical improvement. Our results will help scientists and dermatologists for better understanding the function, the expression, the regulation of IL-33 in psoriasis as well as to develop the new therapeutic drug for psoriasis in the future.

1.2 Research question

IL-33 is the most newly cytokine of IL-1 family. It is a dual function protein that works as a nuclear factor and secreted cytokine. IL-33 is constitutively produced from epithelial cells and endothelial cells of tissues exposed to environment and can be secreted in response to alarming damage to immediately stimulate innate immune immunity and Th2-cell immunity. IL-33 also actions as an intracellular nuclear factor that inhibits inflammatory signals. Interestingly, IL-33 is strongly expressed in the nucleus of keratinocytes of psoriasis, which is a common chronic inflammatory cutaneous disease that affects 2-3% of Thai population. Psoriasis is considered as a Th1- and Th17-mediated inflammation. The role of IL-33 in psoriasis has not been clearly identified.

The ultraviolet radiation, especially UVB, is a phototherapy that has wide-ranging immunosuppressive potentials via different mechanisms. UVB has been used to treat psoriasis with satisfactory response. In this study, we would like to compare IL-33 expression before and after treatment with narrowband UVB. The tissue samples from lesional and perilesional plaques of four cases of psoriasis are taken. The mRNA

expression of IL-33 in keratinocytes is measured by a droplet digital polymerase chain reaction (ddPCR). The expression of IL-33 in the nucleus of keratinocytes in psoriasis after treatment with narrowband UVB will probably suggest the regulation and role of IL-33 in psoriasis. Additionally, this study will demonstrate another mechanism of narrowband UVB in inhibiting inflammation in psoriasis.

1.3 Specific objective

The primary objective is to investigate effect of narrowband UVB on IL-33 expression in keratinocytes of psoriasis.

1.4 Hypothesis

Increasing of IL-33 mRNA expression might be observed in keratinocyte after narrowband UVB phototherapy in psoriasis patients.

1.5 Keywords

Interleukin-33

Narrowband UVB

Psoriasis

1.6 Operation definition

Moderate to severe plaque-type psoriasis (PASI score >10)

1.7 Ethical consideration

All patients were informed about the nature, objectives, methods and expected benefits of this study. Additionally, the possible adverse events and inconvenience during the study were clearly intimated to all patients. All patients have the right to withdraw from the study and this was deprived of the bias of the physicians to continue the standard treatment. Confidentiality of the subject's data was primarily concerned. Approval of this study was obtained from Thammasat University, Ethical review committee.

1.8 Limitation

The limitations are number of cases, patient compliance, and adverse effect of NBUVB.

1.9 Expected benefits and application

Psoriasis is a chronic inflammatory skin diseases determined by polygenic inheritance, environmental factors then drives abnormal immune responses. It causes worldwide concern because of high prevalence, incurable and lifelong process that effect both physical and mental of people. The immunopathogenesis of psoriasis is very complicated. Nowadays treatment of psoriasis aims to relieve symptoms more than cure for the disease. Mechanism of the most of modalities in psoriasis treatment is broad and patients still suffer from treatments' complication. Development of translational research will help us to better understand the very complex pathogenesis of psoriasis. In the future, develop new biologic drugs that highly effective and specific for psoriasis should be concerned.

1.10 Obstacles and strategies to solve the problems

The minority of patients lost or delayed to follow up. The problem was solved by the improvement of doctor-patient relationships.

For the specimen collection, all samples were labeled the patient's code, hospital number, and date of collection in order to prevent the switching or lost of subject's specimen. The samples were kept orderly in laboratory room before the data analysis process.

Table 1.1 Administration and time schedule

	2015						2016					
	1	2	3	4	5	6	7	8	9	10	11	12
Preparation	■											
Data collection		■	■	■	■	■	■					
Data analysis							■	■	■			
Manuscript preparation									■	■	■	
Publication											■	■

2. Review of literature

Chronic inflammatory cutaneous diseases, such as lichen planus, atopic dermatitis, and psoriasis, are the most prevalent skin diseases that cause a major public health problem worldwide. They have dramatic physical, mental, social and financial ramifications for those they afflict. They are related with genetic background, defect in barrier function or hyper responses to danger stimuli and abnormal immunologic responses. Various cytokines are associated in the pathogenesis of these skin diseases.

Psoriasis is a common, chronic, inflammatory immune-mediated skin disease affecting approximately 2-3% of the world's population (1). The etiology of psoriasis seems to be multi-factorial according to polygenic inheritance, environmental factors, and abnormal immune responses. Although the disease is seldom life threatening, it certainly has a significant undesirable impact on patients' quality of life, demonstrable by physical, emotional, psychosocial wellbeing and economic burden (2, 3). Both long-term treatment costs and social costs have a negative influence on health care systems and on society in overall. There are several clinical cutaneous manifestations of psoriasis but most commonly the disease is characterized by classically well-demarcated, symmetrical, erythematous, and raised round-oval plaques with silvery dry scales that may be painful and/or often pruritic.

Epidermal keratinocytes are the main population in the epidermis, the most spacious organ, which covers the whole body. Epidermal keratinocytes respond to environmental stimuli, such as ultraviolet light, mechanical stress (4, 5) or chemical injury, which induce inflammation and infiltration of various inflammatory cells into the skin. Keratinocytes show a key role in innate immune responses in the skin via expression of Toll-like receptors, secretion of pro-inflammatory cytokines (TNF-α, IL-8, IL-1, and IL-33), chemokines, growth factors, and anti-microbial peptides in response to tissue injury or

invading microbes. Disruption of keratinocyte homeostasis can induce systemic immunological alterations. In psoriasis, keratinocytes produce high amount of cathelicidin (LL-37), an anti-microbial peptide, which bind to self-DNA, and RNA subsequently stimulates plasmacytoid dendritic cells. This mechanism breaks tolerance to self-DNA and drive autoimmune response in psoriasis (6, 7).

IL-33 is the most recently discovered cytokine as a member of IL-1 family. In human diseases, serum IL-33 is elevated in patients with allergic rhinitis (8), systemic lupus erythematosus (9), rheumatoid arthritis (10, 11), ulcerative colitis (12), human immunodeficiency virus (HIV) infection, systemic sclerosis (13), bullous pemphigoid (14), psoriatic arthritis and psoriasis vulgaris (15). Tissue IL-33 expression is upregulated in the bronchial mucosa of patients with asthma (16), the synovial tissue of patients with osteoarthritis, psoriatic arthritis, and rheumatoid arthritis (17), and in several inflammatory cutaneous diseases including atopic dermatitis, psoriasis, lichen planus, allergic contact dermatitis, chronic spontaneous urticaria, and vitiligo (18).

This cytokine was first cloned from canine vasospastic arteries induced by subarachnoid hemorrhage. IL-33 has been recognized as a ligand for the IL-1 receptor family member, ST2L. Pro-IL-33 is a 30-kDa protein that is combined of an N-terminal domain and an 18–20 kDa C-terminal cytokine domain. The 18-kDa C-terminal moiety of IL-33 is sufficient for binding to its receptor, ST2L. Binding of IL-33 cytokine to ST2L and enrollment of the IL-1RAcP induces the activation of intracellular signaling pathways typical of receptors containing a TIR domain, which include the recruitment of MyD88 protein and the activation of nuclear factor ᴋB (NF-ᴋB), ERK, p38 and JNK pathways. IL-33 activates different cells of the innate immunity (19-21), such as mast cells, eosinophils, basophils (22), NKT cells (23), dendritic cells (24) and neutrophils (25), and Th2 lymphocytes (20). Recombinant IL-33 was found to drive production of pro-inflammatory and Th2-associated cytokines in mast cells and Th2 lymphocytes (26-29). According to these findings, IL-33 is considered to the pathogenesis of Th2-type inflammation.

Despite the increasing number of studies that described the roles of mature, recombinant IL-33, substantially less is known about exact sources of IL-33. Vascular endothelial cells are the major IL-33 expressing cells in vivo (30, 31). Elevated levels of IL-33 were also found in nucleus of fibroblastic reticular cells (FRCs) of lymphoid tissues and types of epithelium, including epithelial cells of stomach and keratinocytes of skin (31).

Several publications have revealed that IL-33 expression can be increased in vitro in mesenchymal, epithelial, and myeloid cells cultured with Toll-like receptor ligands (32-35) and pro-inflammatory stimuli (10, 16, 36, 37). Tumor necrosis factor (TNF)-α is the mediator used most frequently to stimulate IL-33 production by epithelial cells. IL-1 and TNF-α can induce the production of IL-33 in synovial fibroblasts in vitro (36). In addition, the expression of ST2L on neutrophil is decreased in patients who respond to therapy with the TNF-α inhibitor (38) suggesting that both production of and cellular responses to IL-33 are modulated by pro-inflammatory cytokines. These findings suggest that pro-inflammatory cytokines induce the IL-33 production, but few reports have investigated the production of this cytokine in epidermal keratinocytes.

IL-33 was proposed as dual function protein like IL-1α, another cytokine member of IL-1 family. In the nucleus, IL-33 acts as a nuclear factor that inhibits inflammatory signals and pro-inflammatory cytokines production in keratinocytes via transcriptional suppression (39, 40). In contrast, IL-33 acts as a secreted cytokine that induces IL-8 production from keratinocytes (40) and activates immune responses.

Psoriasis is a cutaneous disease resulting from the dysregulated interaction between skin keratinocytes and infiltrating immune cells. Psoriasis is considered a mixed Th1 and Th17 cell-mediated autoimmune disease, in which the likely induction of IFN-γ and IL-17 cytokines is considered to be pathogenic (41). Recently, the expression of IL-33 was reported in psoriasis skin lesion in keratinocytes, fibroblasts and endothelial cells (19, 40), but not in serum of psoriasis patient. Induction and secretion of IL-33 from keratinocytes in psoriasis was reported after stimulation by pro-inflammatory cytokines such as TNF-α (42, 43), IFN-γ, and IL-17 (40). In contrast to rheumatoid arthritis, IL-33 could not be detectable in serum and synovial fluid of psoriasis arthritis patients (17). By the way, the function of IL-33 in psoriasis remains unknown.

The UV radiation contained in sunlight, especially UVB, has wide-ranging immunosuppressive potentials via different mechanisms. These properties of UVB include suppression of antigen presenting cells, stimulation of inhibitory cytokines synthesis e.g. IL-10, and induction of keratinocyte apoptosis. Due to these mechanisms, UVB has been used to treat psoriasis with satisfactory response. From recent study, Byrne et al. (44) and Meephansan et al. (45) demonstrated that UVB radiation could induce IL-33 expression in keratinocytes and dermal fibroblasts. More recently, Balato et al. (43) have been reported that IL-1 family members, including IL-33, are involved in UVB-induced pro-inflammatory pathway. Thus, this is the interested feature of NBUVB that we aim to

investigate whether NBUVB phototherapy has an effect on the IL-33 expression in affected psoriatic skin.

Recent development in translational research produced various clinically effective "biologics", such as cytokine-targeted antibodies, decoy-receptors, or "molecular target drugs", such as small molecular size inhibitors for signal transduction. Therapeutic antibodies and inhibitors targeted for some of the inflammatory cytokines have been proved effective in treating chronic inflammatory skin diseases, such as psoriasis (46), which imply that studies on the production mechanisms of inflammatory cytokines related to skin diseases would be of importance in future therapeutic development in dermatology.

Interleukin-33 and psoriasis

Many current publications have showed that IL-33 expression is increased in lesional skin of psoriasis compared with normal skin (42, 47, 48). Hueber et al. (19) demonstrated that IL-33 and ST2 expression are upregulated in human lesional psoriatic plaques compared with perilesional and normal healthy skin. Moreover, IL-33 is strongly expressed in the nuclei of keratinocyte in psoriasis which is considered as a Th1 and Th17 mediated disease, compared with atopic dermatitis which is Th2 related disease, and lichen planus which relate to Th1 cells (40). According to the discovered structure of IL-33, It shows the property to act both as an extracellular cytokine, stimulating ST2L receptor, and as an intracellular factor, controlling gene transcription. However, the clearly role of IL-33 in psoriasis remain not well know.

Relatively studies have shown the association between IL-33 and psoriasis. IL-33 was found in both nucleus and cytoplasm of disease keratinocytes and it was also detectable in the cells junctions, being suggestion that psoriatic keratinocytes can secrete IL-33 (42, 43). Suttle et al. (49) also reported the decrease in IL-33 immunostaining biopsies in the Koebner-positive psoriasis patients, which can reflex the release of IL-33 after skin injury by tape-stripping. Interestingly, proinflammatory cytokine, TNF-α, dose- and time-dependently activated IL-33 mRNA expression in normal skin culture ex vivo. Likewise, TNF-α potentially stimulated gene expression of IL-33 in normal human epidermal sheets and psoriatic skin (50). Moreover, the levels of IL-33 were significantly reduced after TNF-α inhibitors therapy (50, 51). Hueber et al. (19) demonstrated that ST2-deficient mice develop reduced keratinocyte proliferation in a topical phorbol esters-induced development of inflammation. They also showed that IL-33 functions as an

alarmin and it can trigger mast cell and neutrophil activation leading to psoriatic lesion of the skin. Balato et al. (42) also evaluated the role of IL-33 through mast cell activation in promoting inflammatory cascade.

Furthermore, Mitsui et al. (15) recently investigated that serum IL-33 levels are significantly elevated in patients with psoriasis, particularly correlated with serum TNF-α levels, and these elevation were decreased after anti-TNF-α treatment. Therefore, they suggested that IL-33 is a general indicator for inflammation in psoriasis. However, Tamagawa-Mineoka et al. (52), Balato et al. (42) and Talabot-Ayer et al. (17) revealed the contrary result that serum IL-33 expression was not detectable in psoriasis patients. By the way, the pathophysiology of IL-33 remains complicated and all these evidences support that this cytokine has several doubtful roles that remain to be solve.

3. Research methodology

3.1 Study sample

3.1.1 Target population

Patients presenting to Out Patients Department (OPD) of Dermatology, Thammasat University Hospital and Thailand Tobacco Monopoly Hospital, who had been diagnosed with moderate to severe plaque-type psoriasis achieving the inclusion criteria were included in the study.

3.1.2 Sample size

A total of 11 patients are recruited for this study.

$$N \text{ (Pair)} = \frac{[Z\alpha - Z\beta]^2 \sigma^2}{d^2}$$

$\alpha = 0.05$ $Z\alpha = 1.645$

$\beta = 0.2$ Power = 0.8

d = mean difference = 220

σ = SD of the within pair difference = 281.8

N (Pair) = 10.1 subjects

Drop out rate 10% = 11 subjects

3.1.3 Inclusion criteria

- Patient aged $\geq$ 18 years old

- Moderate to severe plaque-type psoriasis (Psoriasis Area and Severity Index; PASI >10) patient

3.1.4 Exclusion criteria

- Patients' refusal to participate the study

- Patient taking other treatment for psoriasis; topical therapies within 2 weeks, and systemic therapies within 4 weeks prior the study period

- Patient with contraindication of narrowband UVB (e.g. xeroderma pigmentosum, other inherited disorder associated with UV-induced carcinogenesis, photodermatosis, history of skin cancer)

- Patient with known history of photosensitivity

- Patient suffering from psoriatic arthritis

- Patient with IL-33 associated diseases (e.g. rheumatoid arthritis, atopic dermatitis, systemic lupus erythematosus, ulcerative colitis, asthma, HIV infection)

- Patient with cancer condition, autoimmune disease and immunocompromised conditions

- Pregnant and lactating women

- Unreliable and poor compliance patient

3.1.5 Discontinuation criteria

- Patients' refusal to participate the study

- Patient suffering serious adverse effect of phototherapy

- Unreliable and poor compliance patient

3.2 Research design

This experimental before - after study will be conducted at the Department of Dermatology, Thammasat University Hospital and Thailand Tobacco Monopoly Hospital

UVB   IL-33 expression

Increasing of IL-33 mRNA expression ?

Psoriasis skin
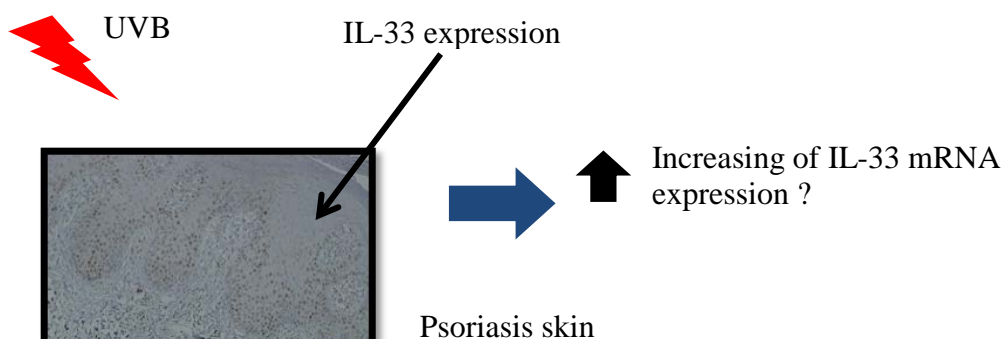
between Jul y 2015 and April 2016.

Figure 3.1 Research design

3.3 Materials and methods

3.3.1 Informed consent process

- Patients are fully informed of the nature, objective, expected benefit, and complication of this study.

- The formal consent form was taken from participants.

3.3.2 History taking

The collected data include

- Patients' personal history: age, gender, body mass index, skin type, occupation, smoking habits, drinking habits, underlying disease, current medication, and family history.

- Patients' disease history: age of disease onset, duration of disease, site of lesions, pruritus intensity measured by Visual Analogue Scale, history of prior treatment and response, and history of arthritis.

- Patients' information for exclusion criteria such as history of photosensitivity, pregnancy, and lactation.

3.3.3 Physical examination

- Weight and height measurement

- Disease evaluation will be established regarding the erythema, scale, thickness, site, and size of the psoriatic plaque. The Psoriasis Area Severity Index (PASI; <10=mild, ≥ 10=moderate to

3.3.4 Tissue collection

- The skin biopsy (fully developed lesion, peri-lesional skin) will be collected at baseline and following 12 weeks of treatment or when the PASI score is improved more than 75%.
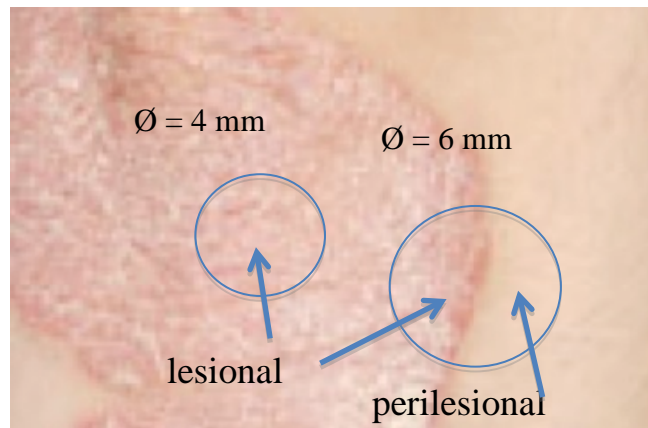
Figure 3.2 Tissue collection

3.3.5 Intervention and follow up

- Before each phototherapy session, the participants' skin type will be evaluated. The starting UVB doses are 0.20 to 0.30, J/cm^2 according to the skin types then increase by 10% to 20% with each treatment. The patients have 3 sessions each week. Dose increments continue until lesion clearance, which is defined as 75% reduction in PASI score or achieved 12 weeks of treatment.

- Follow up will be done every 2 weeks for the first month, then every 4 weeks until clearance. At clearance of disease, the phototherapy will be tape off and the topical treatment is used for maintenance.

- Patients will be ask about pinkness, tenderness, burning sensation, pruritic symptom, and any abnormal lesion of the skin from the previous session.

3.4 Outcome measurement

Skin biopsies are used to detect mRNA level of IL-33 by Droplet Digital^{TM} PCR Technology and they are used to detect protein level of IL-33 by immunohistochemical staining.

3.4.1 Skin biopsies preparation

- Skin biopsies (4 mm-sized of lesional, 6 mm-sized of peri-lesional skin) are collected in cryotubes.

- The tissues are immediately cryopreserved at -80° Celsius, where they were kept until molecular analysis.

3.4.2 Materials for outcome measurement

- RNeasy® Mini Kit

- ImProm-II^{TM} Reverse Transcription System

- ddPCR^{TM} Supermix for Probes Assay

3.4.3 RNA extraction, cDNA synthesis, and droplet digital PCR

The lesional skin biopsies before and after NB-UVB therapy were cryopreserved at -80° Celsius until RNA extraction. An RNAeasy mini kit (Qiagen, Inc., Hilden, Germany) was used for total RNA extraction from lesional psoriatic skin biopsies. Complementary DNA was generated from 5.7-29.61 ng/μl RNA using an ImProm-II^{TM} Reverse Transcription System (Promega Madison, USA) according to the manufacturer's instructions. The PCR primers and probes for human IL-33 (Hs00369221_m1) and the housekeeping gene, glyceraldehyde-3-phosphate dehydrogenase (GAPDH), were obtained from Applied Biosystems (Norwalk, CT). Sample preparation for droplet generation was performed using the Droplets Digital PCR reaction supermix for probes (Bio-Rad, Hercules, CA). In a 20 μl PCR reaction, 2 μl of cDNA was added to 10 μl of 2x supermix (Qx200 ddPCR EvaGreen Supermix, Bio-Rad) with the addition of IL-33 gene-specific primers and GAPDH primers, respectively. The reaction mixture was converted into droplets using an Automated Droplet Generator (Bio-Rad) and end-point PCR was performed. All the primers were diluted to optimize signal-to-noise and thresholds were set using non-template control wells.

3.4.4 Droplet Digital Polymerase Chain Reaction (ddPCR) Technology

3.4.4.1 Sample preparation

- Bio-Rad ddPCR supermixes for Probes are specific for the droplet chemistry.

- Prepare the PCR reaction by combining 2x PCR supermix, 20x primers and probe, and cDNA sample. Mix by vortexing in short pulses; centrifuge briefly.

- Insert the DG8 cartridge into the holder with the notch in the cartridge at the upper left of the holder.

- Transfer 20 μl of each prepared sample to the sample wells (middle row) of the DG8 cartridge.

- Dispense the droplet generation oil in the reagent trough.

3.4.4.2 Droplet generation

- Correct placement of the gasket over the cartridge holder. The gasket must be securely hooked on both ends of the holder.

- Place loaded cartridge into QX200 droplet generator.

- Generate 20,000 nanoliter sized droplets per sample 2 minutes for 8 samples.

3.4.4.3 Preparation for PCR

- Pipet 40 μl of the contents of the top wells (the droplets).

- Dispense droplets into a single column of a 96-well PCR plate.

- Seal the PCR plate with foil immediately after transferring droplets to avoid evaporation.

- Use pierceable foil plate seals that are compatible with the PX1^{TM} PCR plate sealer. Set the plate sealer temperature to 180° Celsius and time to 5 seconds.

- When heat sealing is complete, the PX1 door opens automatically. Remove the plate from the block for PCR in thermal cycler. Begin thermal cycling (PCR) within 30 minutes of sealing the plate.

- The resultant droplets were then subjected to amplification as follows: one cycle at 95°C for 10 minutes, 40 cycles at 94°C for 30 seconds, and 60°C for 1 minute, and a final cycle at 98°C for 10 minutes with a ramp speed of 2.5^{o}C/s in a C1000 Touch Thermal Cycler (Bio-Rad).

3.4.4.4 Droplets reading

- Following PCR amplification of the nucleic acid target in the droplets, the plate containing the droplets is loaded in QX200 droplet reader.

- Entire 96-well plate read in approximately 2.5 hours.

3.4.4.5 ddPCR data analysis by software

The data analysis was performed using QuantaSoft Software (Bio-Rad). The data can be viewed as a 1-D plot with each droplet from a sample plotted on the graph of fluorescence intensity vs. droplet number. All the samples were normalized to the GAPDH control with graphs representing data normalized to the indicated comparison condition.

3.5 Data analysis

Data were analyzed using SPSS version 23 for statistic. The results were given in form of proportion or percentage for qualitative data, median, mean and standard deviation for quantitative data. The equivalent nonparametric statistics, Wilcoxon signed rank test, was used to compare levels of IL-33 expression before and after NBUVB treatment. Statistical significance was considered when p-value <0.05.

	Qualitative data	Quantitative data
Data summarization	Proportion	Mean
	Percentage	Standard deviation
		Median
		Interquartile
Test of difference		Wilcoxon signed rank

The qualitative data were presented in table. While, the quantitative data were presented in histogram charts or box-and-whisker plot.

4. Results

A total 13 patients with widespread plaque-type psoriasis were enrolled. They were divided into two groups according to their treatment.

Group NBUVB (group N) (n=7) received a NBUVB phototherapy, 4 patients completed the study (the treatment, follow-up, and laboratory process): 1 patient lost follow-up, and 2 biopsy tissues were unextractable.

Group Methotrexate or MTX (group M) (n=6) received a methotrexate treatment, 4 patients completed the study (the treatment, follow-up, and laboratory process): 2 biopsy tissues were unextractable.

4.1 Group NBUVB (group N)

4.1.1 Baseline characteristics

Four patients, all males (100%), who had been diagnosed with plaque type psoriasis with PASI score >10 were included in this study. None of the subject in this study showed evidence of contraindications as the result of administration of narrowband UVB therapy.

The mean ± SD age of subjects was 53.75 ± 14.24 years and the median age was 56.5 years. The mean ± SD and median number of body mass index (BMI) was 27.15 ± 2.47 and 27.25, respectively. Two patients (50%) had Fitzpatrick skin type III and other halves (50%) had Fitzpatrick skin type IV. The alcohol-drinking history was found in two patients (50%).

The mean ± SD age of disease onset was 44 ± 19.66 years and the median was 45 years. Each patient in this study had lesions on scalp and nails which do not always occur within the population of psoriasis sufferers. The mean ± SD and median numbers of disease duration were 9.75 ± 8.10 years, and 9 years with a range from 2 to 19 years. Family history of psoriasis with first-degree relative was found in two patients (50%). The underlying diseases of all subjects are shown in Table 9.1.

Table 4.1 Baseline characteristics for each psoriasis patient (group N)

Case	Sex	Age	Skin type	BMI	Smoking	Alcohol drinking	Age of onset (y)	Duration of disease (y)	FH of psoriasis	Duration of NBUVB (w)	Underlying disease
1	M	68	IV	24.4	No	No	66	2	No	8	T2DM
2	M	56	III	25.8	No	Yes	52	4	No	9	HT
3	M	34	III	29.7	No	No	20	14	Yes	9	None
4	M	57	IV	28.7	No	Yes	38	19	Yes	11	Type 2 DM, HT, DLP

y, years; *w*, weeks; *BMI*, body mass index; *DM*, diabetes mellitus; *HT*, hypertension; *DLP*, dyslipidemia

Table 4.2 PASI scores and IL-33 mRNA levels for each psoriasis patient (group N)

Case	PASI score		mRNA IL-33 (copies/μl)	
	Baseline	After NBUVB	Baseline	After NBUVB
1	16.0	1.1	14.5	1.7
2	14.3	1.7	34.0	0.4
3	14.5	1.5	1.2	3.3
4	23.3	2.7	12.8	2.6

Table 4.3 Analyzed baseline characteristics (group N)

	Group N (n=4)	
	Mean ± SD Max)	Median (Min,
	Frequency (%)	
Age (years)	53.75 ± 14.24	56.5 (34, 68)
Sex		
Female	0 (0%)	
Male	4 (100%)	
Skin type		
III	2 (50%)	
IV	2 (50%)	
BMI	27.15 ± 2.47	27.25 (24.4, 29.7)
Smoking	0 (0%)	
Alcohol	2 (50%)	
Age of onset	44 ± 19.66	45 (20, 66)
Duration (years)	9.75 ± 8.1	9 (2, 19)
Lesion on scalp	4 (100%)	
Lesion on nails	4 (100%)	
Family history of psoriasis	2 (50%)	
Duration of treatment (weeks)	9.25 ± 1.26	9 (8, 11)
Underlying disease		
None	1 (25%)	
Hypertension	2 (50%)	
Type II diabetes mellitus	2 (50%)	
Dyslipidemia	2 (50%)	

Values presented as frequency (%), Mean ± SD, and Median (Min, Max).

BMI, body mass index

4.1.2 Clinical response and PASI score

After treatment with NBUVB, all patients (100%) achieved improvement with 75% reduction in PASI score.
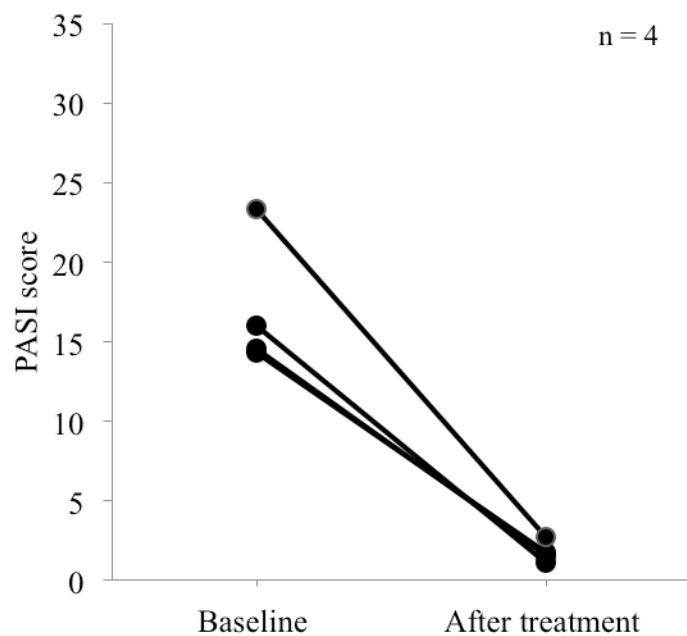
Figure 4.1 Serial changes in PASI scores before and after NBUVB treatment

The median PASI score at baseline was 15.25 with an interquartile range between 14.4 and 19.55.

The median PASI score after NBUVB treatment was 1.6 with an interquartile range between 1.3 and 2.2.

The results obtained from data analysis revealed that a Wilcoxon signed-rank test showed a reduction in PASI score (p = 0.068).

4.1.3 Baseline and after treatment analysis of IL-33 mRNA levels

After treatment with NBUVB, 3 of 4 pateints (75%) achieved downregulated mRNA level of IL-33.
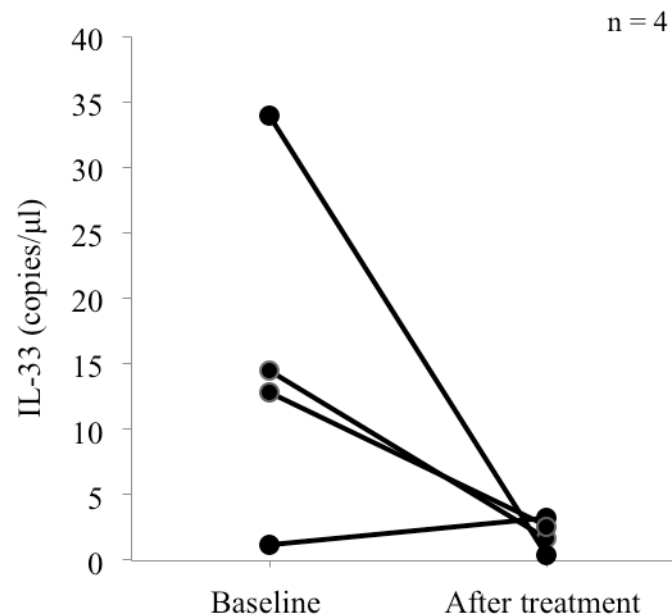
Figure 4.2 Serial changes in IL-33 mRNA levels before and after NBUVB treatment

The median IL-33 mRNA level at baseline was 13.65 copies/μl with an interquartile range between 7 and 24.25.

The median IL-33 mRNA level after NBUVB treatment was 2.15 copies/μl with an interquartile range between 1.05 and 2.95.

The results obtained from data analysis revealed that a Wilcoxon signed-rank test showed a reduction in mRNA level of IL-33 (p = 0.144).
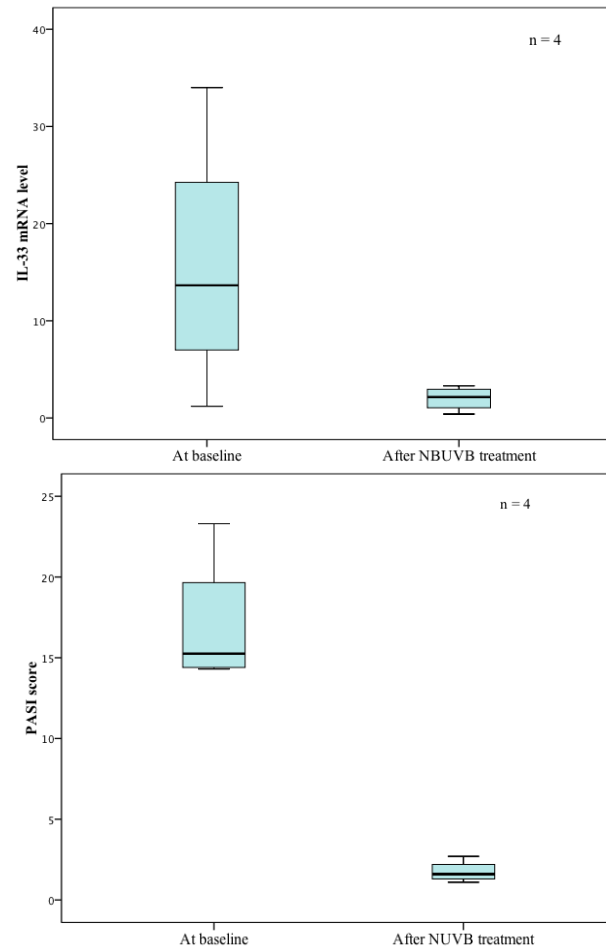
Figure 4.3 Comparison of PASI score (upper) and IL-33 mRNA levels (lower) at baseline and after NUVB treatment in psoriasis patients. Horizontal bars represent the median.

Table 4.4 Baseline and after treatment analysis (group N).

Median (IQR) and *p*-value of Wilcoxon signed ranks test (n=4)

	At baseline	After NUVB treatment	p-value
PASI score	15.25 (14.40, 19.65)	1.6 (1.3,2.2)	0.068
IL-33 expression (copies/μl)	13.65 (7,24.25)	2.15 (1.05,2.95)	0.144

Values presented as median (IQR). *p*-value corresponds Wilcoxon signed ranks test.

4.2 Group Methotrexate (group M)

4.2.1 Baseline characteristics

Four patients, Three males (75%) and one female (25%), who had been diagnosed with plaque type psoriasis with PASI score >10 were included in this study. None of the subject in this study showed evidence of contraindication.

The mean ± SD age of subjects was 48 ± 20.85 years and the median age was 51 years. The mean ± SD and median number of body mass index (BMI) was 30.05 ± 9.09 and 27.45. Two patients (50%) had Fitzpatrick skin type III and other halves (50%) had Fitzpatrick skin type IV. Smoking history was found in one patient (25%) and alcohol-drinking history was found in two patients of group M (50%).

The mean ± SD age of disease onset was 35.5 ± 21.61 years and the median was 27.5 years. Each patient in this study had lesions on scalp and nails. The mean ± SD and median numbers of disease duration were 8.77 ± 9.75 years, and 6.5 years with a range from 0.08 to 22 years. Family history of psoriasis with first-degree relative was found in two patients (50%). The underlying diseases of all subjects are shown in Table 9.5.

Table 4.5 Baseline characteristics for each psoriasis patient (group M)

Case	Sex	Age	Skin type	BMI	Smoking	Alcohol drinking	Age of onset (y)	Duration of disease (y)	FH of psoriasis	Duration of MTX (w)	Underlying disease
1	M	54	IV	22.4	Yes	Yes	32	22	Yes	10	Type 2 DM
2	F	20	III	43.1	No	No	20	0.083	Yes	10	None
3	M	70	III	26.3	No	No	3	3	No	8	BPH
4	M	48	IV	28.6	Yes	No	10	10	No	9	None

y, years; *w*, weeks; *BMI*, body mass index; *DM*, diabetes mellitus; *BPH,* benign prostatic hypertrophy

Table 4.6 PASI scores and IL-33 mRNA levels for each psoriasis patient (group M)

Case	PASI score		mRNA IL-33 (copies/μl)	
	Baseline	After MTX	Baseline	After MTX
1	26.3	6	1	0
2	10.2	2.2	6	0
3	15.3	3.6	0.3	0.64
4	10.6	2.4	30	1

Table 4.7 Analyzed baseline characteristics (group M)

	Group M (n=4)	
	Mean ± SD Max)	Median (Min,
	Frequency (%)	
Age (years)	48 ± 20.85	51 (20, 70)
Sex		
Female	1 (25%)	
Male	3 (75%)	
Skin type		
III	2 (50%)	
IV	2 (50%)	
BMI	30.05 ± 9.09	27.45 (22.2, 43.1)
Smoking	2 (50%)	
Alcohol	1 (25%)	
Age of onset	35.5 ± 21.61	27.5 (20, 67)
Duration (years)	8.77 ± 9.75	6.5 (0.08, 22)
Lesion on scalp	4 (100%)	
Lesion on nails	4 (100%)	
Family history of psoriasis	2 (50%)	
Duration of treatment (weeks)	9.25 ± 0.96	9.5 (8, 10)
Underlying disease		
None	2 (50%)	
Benign prostate gland hyperplasia	1 (25%)	
Type II Diabetes mellitus	1 (25%)	

Values presented as frequency (%), Mean ± SD, and Median (Min, Max).

BMI, body mass index

4.2.2 Clinical response and PASI score

After treatment with MTX, all patients (100%) achieved improvement with 75% reduction in PASI score.
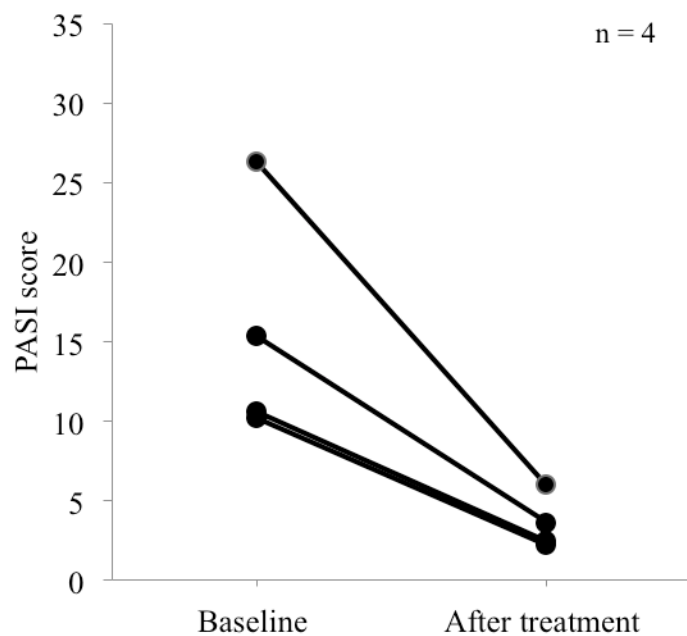
Figure 4.4 Serial changes in PASI scores before and after MTX treatment

The median PASI score at baseline was 12.95 with an interquartile range between 10.4 and 20.8.

The median PASI score after MTX treatment was 3 with an interquartile range between 2.3 and 4.8.

The results obtained from data analysis revealed that a Wilcoxon signed-rank test showed a reduction in PASI score (p = 0.068).

4.2.3 Baseline and after treatment analysis of IL-33 mRNA levels

After treatment with MTX, 3 of 4 pateints (75%) achieved downregulated mRNA level of IL-33.
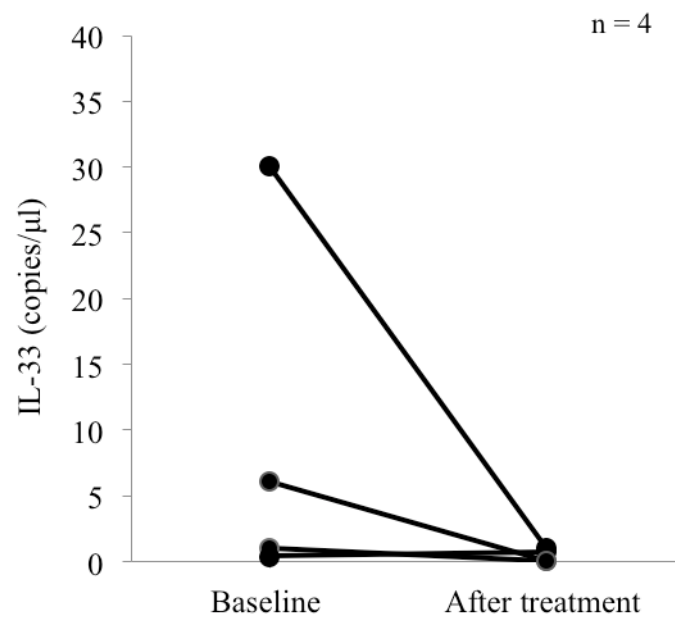
Figure 4.5 Serial changes in IL-33 mRNA levels before and after MTX treatment

The median IL-33 mRNA level at baseline was 3.5 copies/μl with an interquartile range between 0.65 and 18.

The median IL-33 mRNA level after MTX treatment was 0.32 copies/μl with an interquartile range between 0 and 0.82.

The results obtained from data analysis revealed that a Wilcoxon signed-rank test showed a reduction in mRNA level of IL-33 (p = 0.144).
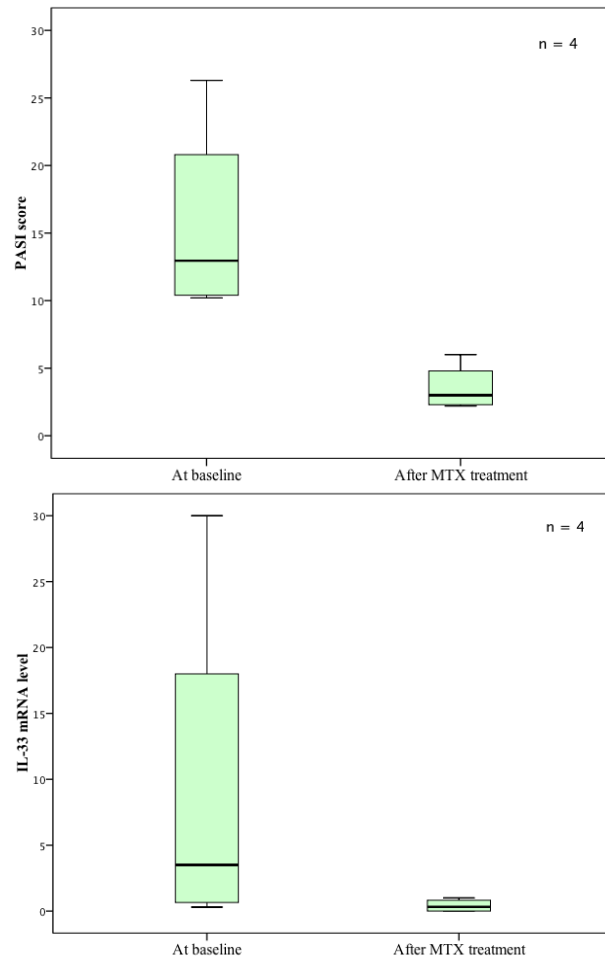
Figure 4.6 Comparison of PASI score (upper) and IL-33 mRNA levels (lower) at baseline and after MTX treatment in psoriasis patients. Horizontal bars represent the median.

Table 4.8 Baseline and after treatment analysis (group M).

Median (IQR) and *p*-value of Wilcoxon signed ranks test (n=4)			
	At baseline	After MTX treatment	*p*-value
PASI score	12.95 (10.4, 20.8)	3 (2.3, 4.8)	0.068
IL-33 expression (copies/μl)	3.5 (0.65, 18)	0.32 (0, 0.82)	0.144

Values presented as median (IQR). *p*-value corresponds Wilcoxon signed ranks test.

4.3 Group NBUVB and Methotrexate (group N+M)

4.3.1 Baseline characteristics

Eight patients, seven males (87.5%) and one female (12.5%), who had been diagnosed with plaque type psoriasis with PASI score >10 were included in this study. None of the subject in this study showed evidence of treatment contraindication.

The mean ± SD age of subjects was 50.88 ± 16.81 years and the median age was 55 years. The mean ± SD and median number of body mass index (BMI) was 28.6 ± 6.36 and 27.45. Four patients (50%) had Fitzpatrick skin type III and other halves (50%) had Fitzpatrick skin type IV. Smoking history was found in two patients (25%) and alcohol-drinking history was found in three patients (37.5%).

The mean ± SD age of onset was 39.75 ± 19.66 years and the median was 35 years. Each patient in this study had lesions on scalp and nails. The mean ± SD and median numbers of disease duration were 9.26 ± 8.31 years, and 7 years with a range from 0.08 to 22 years. Family history of psoriasis with first-degree relative was found in four patients (50%). The underlying diseases of all subjects are shown in Table 4.9.

Table 4.9 Baseline characteristics for each psoriasis patient (group N+M)

Case	Sex	Age	Skin type	BMI	Smoking	Alcohol drinking	Age of onset (y)	Duration of disease (y)	FH of psoriasis	Duration of treatment (w)	Underlying disease
1	M	68	IV	24.4	No	No	66	2	No	8	Type 2 DM
2	M	56	III	25.8	No	Yes	52	4	No	9	HT
3	M	34	III	29.7	No	No	20	14	Yes	9	None
4	M	57	IV	28.7	No	Yes	38	19	Yes	11	Type 2 DM, HT, DLP
5	M	54	IV	22.4	Yes	Yes	32	22	Yes	10	Type 2 DM
6	F	20	III	43.1	No	No	20	0.083	Yes	10	None
7	M	70	III	26.3	No	No	3	3	No	8	BPH
8	M	48	IV	28.6	Yes	No	10	10	No	9	None

y, years; *w*, weeks; *BMI*, body mass index; *DM*, diabetes mellitus; *HT*, hypertension; *DLP*, dyslipidemia; *BPH,* benign prostatic- gland hypertrophy

Table 4.10 Analyzed Baseline characteristics (group N+M)

	Group N+M (n=8)	
	Mean ± SD Max) Frequency (%)	Median (Min,
Age (years)	50.88 ± 16.81	55 (20, 70)
Sex		
Female	1 (12.5%)	
Male	7 (87.5%)	
Skin type		
III	4 (50%)	
IV	4 (50%)	
BMI	28.6 ± 6.36	27.45 (22.2, 43.1)
Smoking	2 (25%)	
Alcohol	3 (37.5%)	
Age of onset	39.75 ± 19.66	35 (20, 67)
Duration (years)	9.26 ± 8.31	7 (0.08, 22)
Lesion on scalp	8 (100%)	
Lesion on nails	8 (100%)	
Family history of psoriasis	4 (50%)	
Duration of treatment (weeks)	9.25 ± 1.04	9 (8, 11)
Underlying disease		
None		
Hypertension	3 (37.5%)	
Type II diabetes mellitus	1 (12.5%)	
Dyslipidemia	2 (25%)	
Benign prostate gland	1 (12.5%)	
hyperplasia	1 (12.5)	

Values presented as frequency (%), Mean ± SD, and Median (Min, Max).

BMI, body mass index

4.3.2 Clinical response and PASI score

The median PASI score at baseline was 14.9 with an interquartile range between 12.45 and 19.65. A skewed right distribution is shown in the histogram. (Figure 4.7)
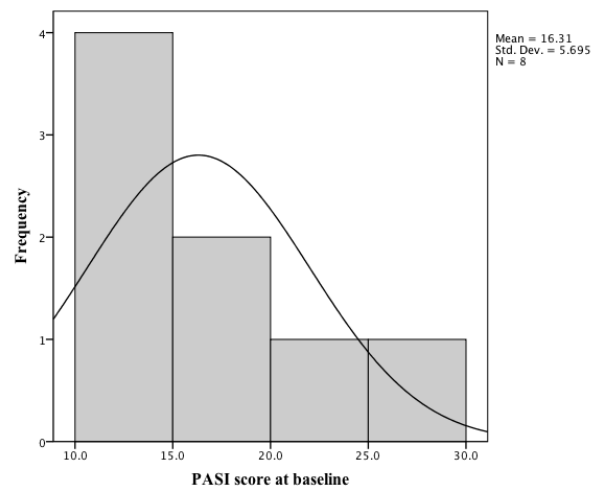

Figure 4.7 Histogram shows PASI score at baseline (group N+M)

The median PASI score after NBUVB and methotrexate treatments was 2.3 with an interquartile range between 1.6 and 3.15. A skewed right distribution is shown in the histogram. (Figure 4.8)
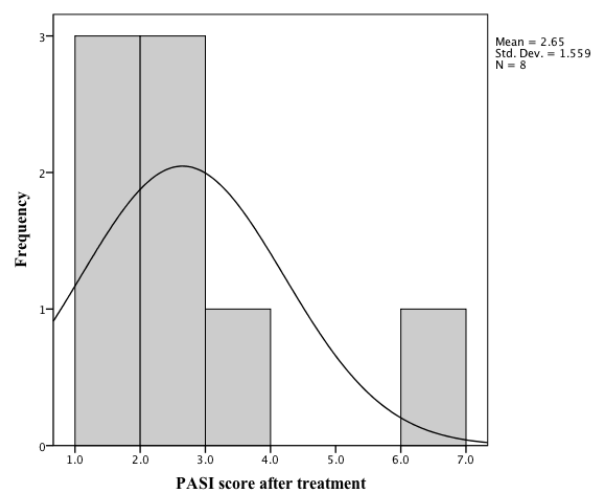
Figure 4.8 Histogram shows PASI score after treatment (group N+M)

After NUVB and methotrexate treatments, all patients (100%) achieved improvement with 75% reduction in PASI score.

The results obtained from data analysis revealed that a Wilcoxon signed-rank test showed a significant reduction in PASI score (p = 0.012*).
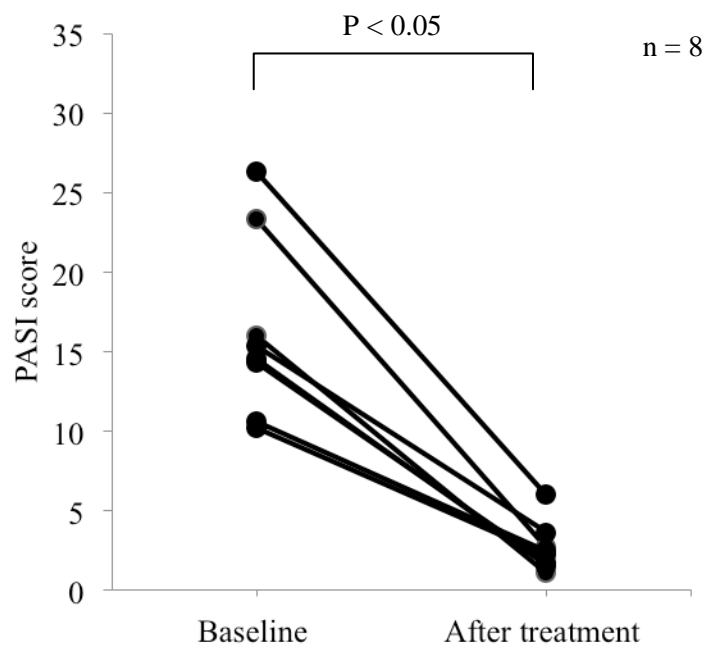
Figure 4.9 Serial changes in PASI scores before and after treatment

4.3.3 Baseline and after treatment analysis of IL-33 mRNA levels

The median IL-33 mRNA level at baseline was 9.4 copies/μl with an interquartile range between 1.1 and 22.25. A skewed right distribution is shown in the histogram. (Figure 4.10)
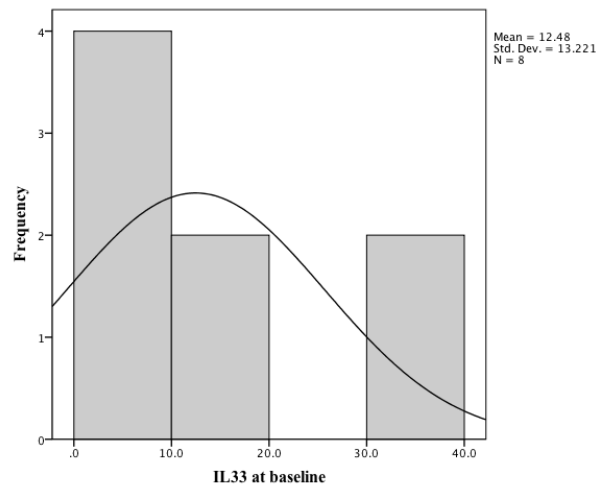
Figure 4.10 Histogram shows IL-33 mRNA levels at baseline (group N+M)

The median IL-33 mRNA level after NBUVB and methotrexate treatments was 0.82 copies/μl with an interquartile range between 0.2 and 2.15. A skewed right distribution is shown in the histogram. (Figure 4.11)
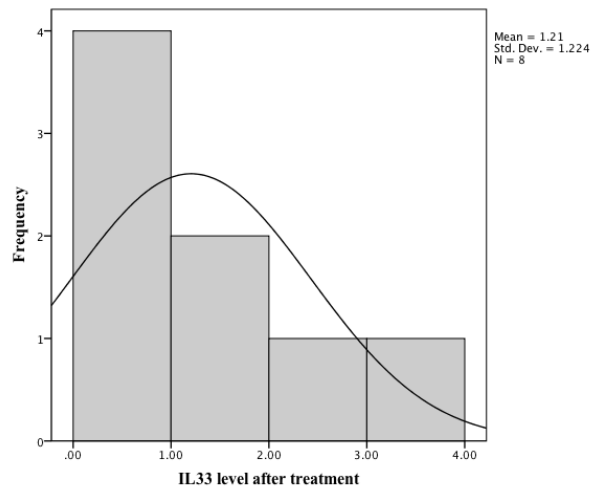
Figure 4.11 Histogram shows IL-33 mRNA after treatment (group N+M)

After NUVB and methotrexate treatments, 6 of 8 patients (75%) achieved downregulated mRNA level of IL-33. The median mRNA level of IL-33 was reduced after treatment compared to before treatment (9.4 copies/μl, 01.1-22.25 vs. 0.82 copies/μl, 0.2-2.15).

The results obtained from data analysis revealed that a Wilcoxon signed-rank test showed a reduction in mRNA level of IL-33 (p = 0.049*).
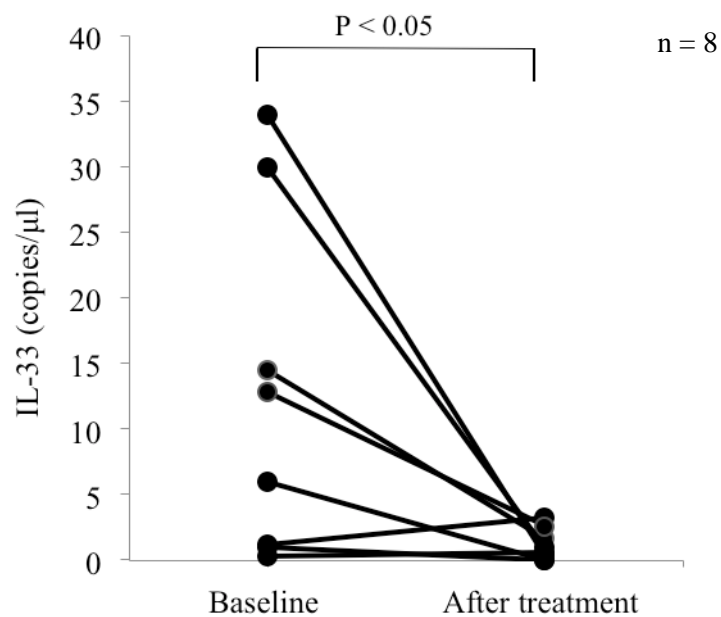
Figure 4.12 Serial changes in IL-33 mRNA levels before and after treatment
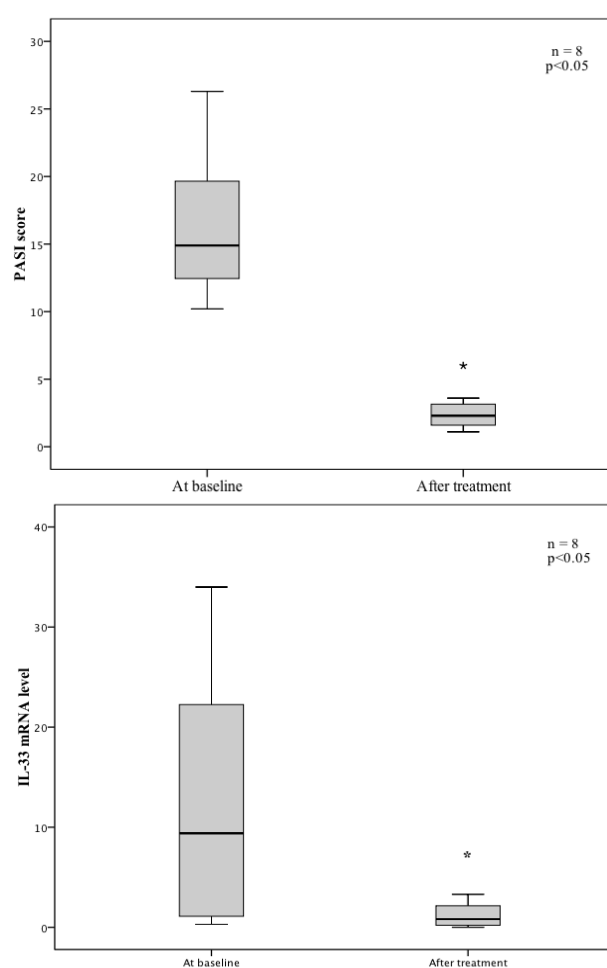
Figure 4.13 Comparison of PASI scores (upper) and IL-33 mRNA levels (lower) at baseline and after NBUVB and methotrexate treatment in psoriasis patients. Horizontal bars represent the median.

Table 4.11 Baseline and after treatment analysis (group N+M).

Median (IQR) and p-value of Wilcoxon signed ranks test (n=8)			
	At baseline	After treatment	p-value
PASI score	14.9 (12.45, 19.65)	2.3 (1.6, 3.15)	0.012*

IL-33 expression (copies/μl)	9.4 (1.1, 22.25)	00.82 (0.2, 2.15)	0.049*

Values presented as median (IQR). *p*-value corresponds Wilcoxon signed ranks test.

5. Discussion

5.1 Discussion

IL-33 was first described as an inflammatory cytokine that mediate Th2-associated disease (29). It is a newly discovered member of the IL-1 cytokine family that is expressed by mainly in the nucleus of cells with barrier function, such as endothelial cells and epithelial cell (31, 131). Many recent studies have proposed that IL-33 is a novel 'alarmin' that, by meaning, activates multiple cells, including T helper cells, mast cells, NK and NKT cells, eosinophils, basophils, and dendritic cells and has varied contribution to pathophysiology of several inflammation and diseases.

Firstly, IL-33 was considered that it might be secreted from the nucleus of the necrosis-mediated or apoptosis cells. Then, Kakkar et al. (132) studies showed that IL-33 could be transferred from nucleus to cytoplasm using the nuclear pore complex and it exists in membrane-bound cytoplasmic vesicles. This described function of IL-33 as a mechanically cytokine secreted by living cells. Nevertheless, the exact role of IL-33 remains unclear. IL-33 seems to be a cytokine with dual function, acting both as an intracellular nuclear factor with transcriptional regulatory abilities and as a traditional cytokine via activation of the ST2L receptor complex.

Interestingly, its expression is increased following varies pro-inflammatory stimulation, such as TNF-α, IFN-γ, and IL-17, which have participated in complicated immunopathogenetic of psoriasis. Balato et al. (42) have studied that TNF-α could stimulate the secretion of IL-33 from immortalized keratinocytes. This was supported by other study (43) that TNF-α and IL-17 was able to upregulate almost all IL-1 family members, including IL-33, in ex vivo healthy skin organ culture. Moreover, Meephansan et al. (40) showed similarly evidence that IL-33 expression may be regulated by IFN-γ in a dose- and time-dependent manner.

Psoriasis is a Th1- and Th17-mediated inflammatory skin disease, which is characterized by marked infiltration of T cells, dendritic cells, macrophages and neutrophils in psoriatic skin. Several mediators can trigger dendritic cells through keratinocyte stress or directly activate via pattern recognition receptors. Cell stress can both induce and release intracellular endogenous factors or 'damage-associated

molecular pattern (DAMPs)' to extracellular environment and generate inflammation. IL-33 is one of DAMPs. From our reviews literatures, skin tissues contain a high level of IL-33 mRNA expression compared to other tissues and cell types (29).

Intriguingly, it has been found to be strongly expressed and noticeably higher in the nuclei of keratinocytes in psoriatic skin lesions compared with healthy skin, lichen planus which is Th1-associated disease, and atopic dermatitis which is Th2-associated inflammation (19, 40). Therefore, it has been proposed to represent a novel marker of psoriasis, comparative to other inflammatory skin disorders. Moreover, recent studies revealed that epidermal IL-33 expression associates with Koebner reactions, and it may be released to induce mast cells in psoriasis biology.

UVB phototherapy has been commonly used to treat moderate to severe psoriasis with satisfactory response. Interestingly, Byrne et al. (44) and Meephansan et al. (45) have been demonstrated that UVB irradiation of epidermal keratinocytes resulted in a significant upregulate in IL-33 expression in vivo. Balato et al. (43) recently reported that IL-1 family members, including IL-33, are involved in UVB-induced pro-inflammatory pathway. Thus, this is the interested feature of NBUVB that we aim to investigate whether NBUVB phototherapy has an effect on the expression of IL-33 in affected psoriatic skin.

In this study, we have demonstrated for the first time that IL-33 mRNA are expressed in psoriatic lesional skin in vivo before and after treatment with NBUVB phototherapy. These expressed IL-33 mRNA levels were decreased after NBUVB therapy in psoriasis patients, which suggests that IL-33 expression associates with NBUVB radiation as well as improvement of the disease. Base on the result, we considered the discussion in two aspects.

Firstly, this outcome, the decreased IL-33 mRNA levels after treatment, raises the possibility of its involvement in pro-inflammatory role as a cytokine in psoriasis. Balato et al. (42) have revealed that IL-33 was visible in psoriatic keratinocyte nucleus, cytoplasm, and in the junctions between keratinocytes. It showed same results in primary keratinocytes and ex vivo skin organ culture, confirming that it was secreted by immortalized psoriatic keratinocytes. Suttle et al. (49) also reported the decrease in IL-33 immunostaining biopsies in the Koebner-positive psoriasis patients, which can reflex the release of IL-33 after skin injury by tape-stripping. Our results agree with

those previous studies showing that IL-33 mRNA were reduced, although not significant, after treatment with TNF-α inhibitors in plaque psoriasis patients (51). Furthermore, most recently studies by Mitsui et al. (15) indicate that IL-33 is a general indicator for inflammation in psoriasis. They have investigated that serum IL-33 levels are significantly elevated in patients with psoriasis, particularly correlated with serum TNF-α levels, and these serum IL-33 were reduced after anti-TNF-α treatment. These can support our results in extracellular role of IL-33 as an inflammatory cytokine.

Secondly, as we have known that psoriasis is a complicated immune-mediated inflammatory disorder. Pro-inflammatory, Th1 and Th17 cytokines and chemokines such as TNF-α and IFN-γ are key cytokines in development of disease (53, 54), and also are found to be involved in production of IL-33 in keratinocytes (40, 42, 50). According to the immunosuppressive effects of NBUVB phototherapy in treating psoriasis, we may assume that the suppression of these pro-inflammatory cytokines effect levels of IL-33 mRNA. NBUVB therapy might not directly decrease the IL-33 expression in psoriatic skin. Further studies with this aspect are needed.

Interestingly, the study outcome shows a contrast with our hypothesis, which proposed whether the increasing of IL-33 expression might be observed in keratinocyte after NUVB phototherapy in psoriasis patients. It also differences with prior studies by Byrne et al. (44) and Meephansan et al. (45), which are reported the elevation of IL-33 expression after UVB exposure in the human skin sample ex vivo or cultured normal human epidermal keratinocytes (NHEKs), respectively. In current study, we selectively investigated an effect of NUVB exposure in keratinocytes of plaque psoriasis patients. Thus, it is an in vivo study. The discrepancy between those previous studies might be due to the different experimental models.

In the other hand, UVB radiation probably increases the production of IL-33 in psoriatic keratinocytes. But, its therapeutic effects cause a depletion of varies cell populations that are involved in psoriasis immunopathogenesis, including epidermal and dermal T cells, dendritic cells, and macrophages. Reduced levels of inflammatory cytokines such as TNF-α, IFN-γ, as well as IL-17 could be the consequence of an anti-inflammatory effect of phototherapy on varieties of cells. As this concern, a similar inhibitory cascade could also occur in a production of IL-33.

In summary, we cannot conclude the exact function of newly cytokine, but this present study could presents evidence for a novel alarmin, IL-33, in plaque-type psoriasis through NBUVB radiation and improvement of disease. IL-33 mRNA levels are decreased after NBUVB therapy. Our findings can imply that the production of IL-33 generally associates with inflammatory skin of psoriasis, and this cytokine could be regulated by anti-inflammatory treatment. In this end, our present study may partly explain a doubtful role of IL-33 cytokine in psoriasis and might be opened aspect for more investigation in the future. A limitation of this study is that the number of psoriasis patients was very small due to the limited period of time. Secondly, we did not detect a serum protein level, as well as immunohistochemical staining of IL-33, which may provide a better understanding of IL-33 expression. Further studies with larger number of subjects and IL-33 protien level as well as immunohitochemistry should be performed to validate those possible roles of this cytokine in psoriasis.

5.2 Effect of methotrexate to IL-33 expression in psoriasis

According to one of study limitations, the sample size of NBUVB-treated group is not large. We also observed the effect of methotrexate (MTX) to IL-33 expression in keratinocyte in psoriasis patients. After methotrexate treatment, IL-33 mRNA expression were decreased in psoriatic lesional skin biopsy compared to baseline. It may imply that downregulated IL-33 expression associates with improvement of the disease due to methotrexate therapy. Therefore, we considered reporting this outcome, which is shown in the previous chapter (group M), and discussing the association between IL-33 expression and psoriatic treatment modalities.

Methotrexate is considered as an effective and successful therapy and remains widely used immunosuppressive agent for treating moderate to severe psoriasis. A therapeutic mechanism of MTX in psoriasis is both anti-inflammatory and anti-proliferative properties. This drug can reduce keratinocyte proliferation by acting as folate antagonist. The diminution in pyrimidine, purines, and methylation of DNA is a result of its action (57). In addition, MTX acts on the adenosine metabolism and causes the release of adenosine from damaged cells by the inhibition of 5-aminoimidazole-4-carbonxamidoribonucleotide (AICAR) transformylase. Adenosine, an endogenous purine

nucleoside, is an immunosuppressive mediator that inhibits PMNs adhesion molecules, macrophage-induced TNF-α, and lymphocytes proliferation (58).

Other immunosuppressive effects of MTX include the inhibition of proinflammatory cytokines, suppression of T and B lymphocytes, and downregulation of chemotaxis of monocytes and neutrophils. Moreover, this drug stimulates keratinocyte apoptosis and reduces DNA synthesis (59, 60). Due to the complicated pathogenesis of psoriasis, the dysregulated immunity may be a target for antipsoriatic effect of drug. From recent study, Meephansan et al. (61) reveled that MTX reduces serum levels of interleukin-22, an important cytokine that stimulates keratinocyte proliferation and skin inflammation in psoriasis.

In our study, we found the IL-33 mRNA expression on lesional plaque of psoriasis patients. These mRNA levels of IL-33 were decreased after treatment with methotrexate, which proposes that IL-33 cytokine associates with methotrexate together with the disease improvement. This may be due to downregulation of inflammatory cytokines like TNF-α and IFN-γ by MTX (62), which are involved in IL-33 production. Another possible mechanism is that methotrexate has anti-mitotic action on psoriatic skin and apoptotic effect in keratinocytes, which are found to be potential source of IL-33 cytokine. Owning to the reduced IL-22 serum levels, MTX inhibits epidermal hyperproliferation in psoriasis, which may indirectly affect to IL-33 cytokine production from keratinocytes. In conclusion, this shows evidence for IL-33 in psoriasis through its therapies, NBUVB and methotrexate, and improvement of disease. These can support that the expression of IL-33 in psoriasis could be regulated through anti-inflammatory and immunomodulatory properties of treatments. Further study will help understand the mechanisms of release, induction, regulation and effect of this newly cytokine.

6. Conclusions

IL-33 is a newly cytokine of IL-1 family. It is a dual function protein that works as a cytokine and nuclear factor. IL-33 is strongly expressed in the nucleus of keratinocytes of psoriasis, which is considered as a Th-1 and Th-17 mediated inflammation. The role of IL-33 in psoriasis has not been clearly elucidated. The narrowband ultraviolet B (NBUVB) radiation is a phototherapy that has wide-ranging immunosuppressive potentials via different mechanisms. UVB has been used to treat psoriasis with satisfactory response. A therapeutic mechanism of MTX in psoriasis is both anti-inflammatory and anti-proliferative properties.

In this thesis, we studied IL-33 expression before and after treatment with narrowband UVB or methotrexate. Eight patients with moderate to severe psoriasis were given treatment until the PASI75 was achieved or up to 12 weeks of treatment. The tissue samples were collected from lesional skin. The expression of IL-33 mRNA in keratinocytes is shown a droplet digital polymerase chain reaction (ddPCR). All of patient achieved a 75% PASI score reduction. IL-33 mRNA levels of 6 patients (75%) were downregulated after treatment with NBUVB or methotrexate.

In conclusion, we expected that the expression of IL-33 in the nucleus of keratinocytes in psoriasis after treatment would probably suggest the regulation and function of IL-33 in psoriasis. The biology of IL-33 is complex. Its production seems particularly associates with inflammatory skin of psoriasis, and this cytokine may be regulated by anti-inflammatory treatment including NBUVB phototherapy.

7. Recommendations

-   Further studies with a larger number of subjects in order to obtain the stronger power of studies and to clarify the possible mechanisms of IL-33 in psoriasis

-   Further studies with immunohistochemical studies to achieve further evidence of IL-33 expression in psoriatic keratinocytes.

-   Further studies with the IL-33 protein expression to provide the potential function of IL-33 cytokine, according to its complexity and unclearly biologic mechanisms.

8. Reference

1.   Perera GK, Di Meglio P, Nestle FO. Psoriasis. Annu Rev Pathol. 2012;7:385-422.

2.   Langley RG, Krueger GG, Griffiths CE. Psoriasis: epidemiology, clinical features, and quality of life. Ann Rheum Dis. 2005;64 Suppl 2:ii18-23; discussion ii4-5.

3.   Radtke MA, Augustin M. Economic considerations in psoriasis management. Clin Dermatol. 2008;26(5):424-31.

4.   Yano S, Komine M, Fujimoto M, Okochi H, Tamaki K. Activation of Akt by mechanical stretching in human epidermal keratinocytes. Experimental Dermatology. 2006;15(5):356-61.

5.   Yano S, Komine M, Fujimoto M, Okochi H, Tamaki K. Mechanical stretching in vitro regulates signal transduction pathways and cellular proliferation in human epidermal keratinocytes. J Invest Dermatol. 2004;122(3):783-90.

6.   Ganguly D, Chamilos G, Lande R, Gregorio J, Meller S, Facchinetti V, et al. Self-RNA-antimicrobial peptide complexes activate human dendritic cells through TLR7 and TLR8. J Exp Med. 2009;206(9):1983-94.

7.   Lande R, Gregorio J, Facchinetti V, Chatterjee B, Wang YH, Homey B, et al. Plasmacytoid dendritic cells sense self-DNA coupled with antimicrobial peptide. Nature. 2007;449(7162):564-9.

8.   Sakashita M, Yoshimoto T, Hirota T, Harada M, Okubo K, Osawa Y, et al. Association of serum interleukin-33 level and the interleukin-33 genetic variant with Japanese cedar pollinosis. Clin Exp Allergy. 2008;38(12):1875-81.

9.   Mok MY, Huang FP, Ip WK, Lo Y, Wong FY, Chan EY, et al. Serum levels of IL-33 and soluble ST2 and their association with disease activity in systemic lupus erythematosus. Rheumatology (Oxford). 2010;49(3):520-7.

10.   Matsuyama Y, Okazaki H, Tamemoto H, Kimura H, Kamata Y, Nagatani K, et al. Increased levels of interleukin 33 in sera and synovial fluid from patients with active rheumatoid arthritis. J Rheumatol. 2010;37(1):18-25.

11.   Mu R, Huang HQ, Li YH, Li C, Ye H, Li ZG. Elevated serum interleukin 33 is associated with autoantibody production in patients with rheumatoid arthritis. J Rheumatol. 2010;37(10):2006-13.

12.   Pastorelli L, Garg RR, Hoang SB, Spina L, Mattioli B, Scarpa M, et al. Epithelial-derived IL-33 and its receptor ST2 are dysregulated in ulcerative colitis and in experimental Th1/Th2 driven enteritis. Proc Natl Acad Sci U S A. 2010;107(17):8017-22.

13.   Yanaba K, Yoshizaki A, Asano Y, Kadono T, Sato S. Serum IL-33 levels are raised in patients with systemic sclerosis: association with extent of skin sclerosis and severity of pulmonary fibrosis. Clin Rheumatol. 2011;30(6):825-30.

14.   Wakatabi K, Komine M, Meephansan J, Matsuyama Y, Tsuda H, Tominaga S, et al. The levels of soluble ST2 in sera and bullous fluid from patients with bullous pemphigoid. Eur J Dermatol. 2012;22(3):333-6.

15.   Mitsui A, Tada Y, Takahashi T, Shibata S, Kamata M, Miyagaki T, et al. Serum IL-33 levels are increased in patients with psoriasis. Clin Exp Dermatol. 2016;41(2):183-9.

16.   Prefontaine D, Lajoie-Kadoch S, Foley S, Audusseau S, Olivenstein R, Halayko AJ, et al. Increased expression of IL-33 in severe asthma: evidence of expression by airway smooth muscle cells. J Immunol. 2009;183(8):5094-103.

17.   Talabot-Ayer D, McKee T, Gindre P, Bas S, Baeten DL, Gabay C, et al. Distinct serum and synovial fluid interleukin (IL)-33 levels in rheumatoid arthritis, psoriatic arthritis and osteoarthritis. Joint Bone Spine. 2012;79(1):32-7.

18.   Balato A, Raimondo A, Balato N, Ayala F, Lembo S. Interleukin-33: increasing role in dermatological conditions. Arch Dermatol Res. 2016.

19.   Hueber AJ, Alves-Filho JC, Asquith DL, Michels C, Millar NL, Reilly JH, et al. IL-33 induces skin inflammation with mast cell and neutrophil activation. Eur J Immunol. 2011;41(8):2229-37.

20.   Komai-Koma M, Xu D, Li Y, McKenzie AN, McInnes IB, Liew FY. IL-33 is a chemoattractant for human Th2 cells. Eur J Immunol. 2007;37(10):2779-86.

21.   Pushparaj PN, Tay HK, H'Ng S C, Pitman N, Xu D, McKenzie A, et al. The cytokine interleukin-33 mediates anaphylactic shock. Proc Natl Acad Sci U S A. 2009;106(24):9773-8.

22.   Suzukawa M, Iikura M, Koketsu R, Nagase H, Tamura C, Komiya A, et al. An IL-1 Cytokine Member, IL-33, Induces Human Basophil Activation via Its ST2 Receptor. The Journal of Immunology. 2008;181(9):5981-9.

23.   Bourgeois E, Van LP, Samson M, Diem S, Barra A, Roga S, et al. The pro-Th2 cytokine IL-33 directly interacts with invariant NKT and NK cells to induce IFN-gamma production. Eur J Immunol. 2009;39(4):1046-55.

24.   Rank MA, Kobayashi T, Kozaki H, Bartemes KR, Squillace DL, Kita H. IL-33-activated dendritic cells induce an atypical TH2-type response. J Allergy Clin Immunol. 2009;123(5):1047-54.

25.   Alves-Filho JC, Sonego F, Souto FO, Freitas A, Verri WA, Jr., Auxiliadora-Martins M, et al. Interleukin-33 attenuates sepsis by enhancing neutrophil influx to the site of infection. Nat Med. 2010;16(6):708-12.

26.   Ali S, Huber M, Kollewe C, Bischoff SC, Falk W, Martin MU. IL-1 receptor accessory protein is essential for IL-33-induced activation of T lymphocytes and mast cells. Proc Natl Acad Sci U S A. 2007;104(47):18660-5.

27.   Iikura M, Suto H, Kajiwara N, Oboki K, Ohno T, Okayama Y, et al. IL-33 can promote survival, adhesion and cytokine production in human mast cells. Lab Invest. 2007;87(10):971-8.

28.   Moulin D, Donze O, Talabot-Ayer D, Mezin F, Palmer G, Gabay C. Interleukin (IL)-33 induces the release of pro-inflammatory mediators by mast cells. Cytokine. 2007;40(3):216-25.

29.   Schmitz J, Owyang A, Oldham E, Song Y, Murphy E, McClanahan TK, et al. IL-33, an interleukin-1-like cytokine that signals via the IL-1 receptor-related protein ST2 and induces T helper type 2-associated cytokines. Immunity. 2005;23(5):479-90.

30.   Kuchler AM, Pollheimer J, Balogh J, Sponheim J, Manley L, Sorensen DR, et al. Nuclear interleukin-33 is generally expressed in resting endothelium but rapidly lost upon angiogenic or proinflammatory activation. Am J Pathol. 2008;173(4):1229-42.

31.   Moussion C, Ortega N, Girard JP. The IL-1-like cytokine IL-33 is constitutively expressed in the nucleus of endothelial cells and epithelial cells in vivo: a novel 'alarmin'? PLoS One. 2008;3(10):e3331.

32.   Hudson CA, Christophi GP, Gruber RC, Wilmore JR, Lawrence DA, Massa PT. Induction of IL-33 expression and activity in central nervous system glia. Journal of Leukocyte Biology. 2008;84(3):631-43.

33.   Nile CJ, Barksby E, Jitprasertwong P, Preshaw PM, Taylor JJ. Expression and regulation of interleukin-33 in human monocytes. Immunology. 2010;130(2):172-80.

34.   Reh DD, Wang Y, Ramanathan M, Jr., Lane AP. Treatment-recalcitrant chronic rhinosinusitis with polyps is associated with altered epithelial cell expression of interleukin-33. Am J Rhinol Allergy. 2010;24(2):105-9.

35.   Shimosato T, Fujimoto M, Tohno M, Sato T, Tateo M, Otani H, et al. CpG oligodeoxynucleotides induce strong up-regulation of interleukin 33 via Toll-like receptor 9. Biochem Biophys Res Commun. 2010;394(1):81-6.

36.   Palmer G, Talabot-Ayer D, Lamacchia C, Toy D, Seemayer CA, Viatte S, et al. Inhibition of interleukin-33 signaling attenuates the severity of experimental arthritis. Arthritis Rheum. 2009;60(3):738-49.

37.   Wood IS, Wang B, Trayhurn P. IL-33, a recently identified interleukin-1 gene family member, is expressed in human adipocytes. Biochem Biophys Res Commun. 2009;384(1):105-9.

38.   Verri WA, Jr., Souto FO, Vieira SM, Almeida SC, Fukada SY, Xu D, et al. IL-33 induces neutrophil migration in rheumatoid arthritis and is a target of anti-TNF therapy. Ann Rheum Dis. 2010;69(9):1697-703.

39.   Ali S, Mohs A, Thomas M, Klare J, Ross R, Schmitz ML, et al. The dual function cytokine IL-33 interacts with the transcription factor NF-kappaB to dampen NF-kappaB-stimulated gene transcription. J Immunol. 2011;187(4):1609-16.

40.   Meephansan J, Tsuda H, Komine M, Tominaga S, Ohtsuki M. Regulation of IL-33 expression by IFN-gamma and tumor necrosis factor-alpha in normal human epidermal keratinocytes. J Invest Dermatol. 2012;132(11):2593-600.

41.   Kastelan M, Massari LP, Pasic A, Gruber F. New trends in the immunopathogenesis of psoriasis. Acta Dermatovenerol Croat. 2004;12(1):26-9.

42.   Balato A, Lembo S, Mattii M, Schiattarella M, Marino R, De Paulis A, et al. IL-33 is secreted by psoriatic keratinocytes and induces pro-inflammatory cytokines via keratinocyte and mast cell activation. Exp Dermatol. 2012;21(11):892-4.

43.   Balato A, Schiattarella M, Lembo S, Mattii M, Prevete N, Balato N, et al. Interleukin-1 family members are enhanced in psoriasis and suppressed by vitamin D and retinoic acid. Arch Dermatol Res. 2013;305(3):255-62.

44.   Byrne SN, Beaugie C, O'Sullivan C, Leighton S, Halliday GM. The immune-modulating cytokine and endogenous Alarmin interleukin-33 is upregulated in skin exposed to inflammatory UVB radiation. Am J Pathol. 2011;179(1):211-22.

45.   Meephansan J, Komine M, Tsuda H, Tominaga S, Ohtsuki M. Ultraviolet B irradiation induces the expression of IL-33 mRNA and protein in normal human epidermal keratinocytes. J Dermatol Sci. 2012;65(1):72-4.

46.   Asahina A, Nakagawa H, Etoh T, Ohtsuki M, Adalimumab MSG. Adalimumab in Japanese patients with moderate to severe chronic plaque psoriasis: efficacy and safety results from a Phase II/III randomized controlled study. J Dermatol. 2010;37(4):299-310.

47.   Meephansan J, Komine M, Tsuda H, Karakawa M, Tominaga S, Ohtsuki M. Expression of IL-33 in the epidermis: The mechanism of induction by IL-17. J Dermatol Sci. 2013;71(2):107-14.

48.   Theoharides TC, Zhang B, Kempuraj D, Tagen M, Vasiadi M, Angelidou A, et al. IL-33 augments substance P-induced VEGF secretion from human mast cells and is increased in psoriatic skin. Proc Natl Acad Sci U S A. 2010;107(9):4448-53.

49.   Suttle MM, Enoksson M, Zoltowska A, Chatterjee M, Nilsson G, Harvima IT. Experimentally induced psoriatic lesions associate with rapid but transient decrease in interleukin-33 immunostaining in epidermis. Acta Derm Venereol. 2015;95(5):536-41.

50.   Balato A, Di Caprio R, Canta L, Mattii M, Lembo S, Raimondo A, et al. IL-33 is regulated by TNF-alpha in normal and psoriatic skin. Arch Dermatol Res. 2014;306(3):299-304.

51.   Vageli DP, Exarchou A, Zafiriou E, Doukas PG, Doukas S, Roussaki-Schulze A. Effect of TNF-alpha inhibitors on transcriptional levels of pro-inflammatory interleukin-33 and Toll-like receptors-2 and -9 in psoriatic plaques. Exp Ther Med. 2015;10(4):1573-7.

52.   Tamagawa-Mineoka R, Okuzawa Y, Masuda K, Katoh N. Increased serum levels of interleukin 33 in patients with atopic dermatitis. J Am Acad Dermatol. 2014;70(5):882-8.

53.   Kim J, Krueger JG. The immunopathogenesis of psoriasis. Dermatol Clin. 2015;33(1):13-23.

54.   Zhang J. Yin and yang interplay of IFN-gamma in inflammation and autoimmune disease. J Clin Invest. 2007;117(4):871-3.

55.   Miller AM. Role of IL-33 in inflammation and disease. J Inflamm (Lond). 2011;8(1):22.

56.   Kakkar R, Hei H, Dobner S, Lee RT. Interleukin 33 as a mechanically responsive cytokine secreted by living cells. J Biol Chem. 2012;287(9):6941-8.

57.   Shen S, O'Brien T, Yap LM, Prince HM, McCormack CJ. The use of methotrexate in dermatology: a review. Australas J Dermatol. 2012;53(1):1-18.

58.   Cronstein B. How does methotrexate suppress inflammation? Clin Exp Rheumatol. 2010;28(5 Suppl 61):S21-3.

59.   Saporito FC, Menter MA. Methotrexate and psoriasis in the era of new biologic agents. J Am Acad Dermatol. 2004;50(2):301-9.

60.   Ranganathan P, McLeod HL. Methotrexate pharmacogenetics: the first step toward individualized therapy in rheumatoid arthritis. Arthritis Rheum. 2006;54(5):1366-77.

61.   Meephansan J, Ruchusatsawat K, Sindhupak W, Thorner PS, Wongpiyabovorn J. Effect of methotrexate on serum levels of IL-22 in patients with psoriasis. Eur J Dermatol. 2011;21(4):501-4.

62.   Thirupathi A, Elango T, Subramanian S, Gnanaraj P. Methotrexate regulates Th-1 response by suppressing caspase-1 and cytokines in psoriasis patients. Clin Chim Acta. 2016;453:164-9.

9. Appendices

<center>

APPENDIX A

PASI SCORE ASSESSMENT

</center>

Table A1 Formula for PASI score calculation

Score	0	1	2	3	4	5	6
Erythema	None	Slight	Moderate	Severe	Very severe		
Induration							
Scaling							
Area (%)	0	1-9	10-29	30-49	50-69	70-89	90-100

Head (H)	0.1
Upper limbs (UL)	0.2
Trunk (T)	0.3
Lower limbs (LL)	0.4

PASI score = Total (H) + Total (UL) + Total (T) + Total (LL)

Total (H)   = 0.1 x [E(H)   + I(H)   +S(H)]   x Area

Total (UL)   = 0.2 x [E(UL)   + I(UL)   +S(UL)]   x Area

Total (T)   = 0.3 x [E(T)   + I(T)   +S(T)]   x Area

Total (LL)   = 0.4 x [E(LL)   + I(LL)   +S(LL)]   x Area

APPENDIX B

PATIENT RECORD FORM

แบบฟอร์มบันทึกข้อมูลสำหรับผู้ร่วมการวิจัย

วันที่................................... ลำดับที่...................................

ชื่อ-สกุล...

โทร...................................

HN............................ โรงพยาบาล ☐ ธรรมศาสตร์เฉลิมพระเกียรติ ☐ ยาสูบ

<u>ข้อมูลทั่วไป</u>

1. เพศ ☐ ชาย ☐ หญิง อายุ.................ปี เชื้อชาติ
....สัญชาติ..................................
อาชีพ...ภูมิลำเนา..................................

2. น้ำหนัก.............กิโลกรัม ส่วนสูง...................เซนติเมตร เส้นรอบเอว.................
เซนติเมตร

3. ดื่มสุรา ☐ ไม่ดื่ม ☐ ดื่ม ปริมาณต่อวัน.....................ระยะเวลา
....

4. สูบบุหรี่ ☐ ไม่สูบ ☐ สูบ ปริมาณต่อวัน.....................ระยะเวลา
....

5. โรคประจำตัว
....
ยาที่ใช้อยู่ในขณะนี้ หรือใช้เป็นประจำ
....
ประวัติแพ้ยา...

<u>ข้อมูลเกี่ยวกับโรคสะเก็ดเงิน</u>

1. วินิจฉัยโรคสะเก็ดเงินมานาน..............เดือน...............ปี อายุที่เริ่มเป็นโรค
....

2. การรักษาที่ได้รับมาก่อนหน้านี้และการตอบสนองต่อการรักษา
ยาทา โปรดระบุ ....
ยารับประทาน เคย ..... ไม่เคย .....

a. ยาเมโทรเทรคเซต (Methotrexate)　　　เคย .....　　　ไม่เคย .....

b. ยาไซโคลสปอริน (Cyclosporin A)　　　เคย .....　　　ไม่เคย .....

c. ยาอะซิเทรตติน (Acitretin)　　　　เคย .....　　　ไม่เคย .....

การฉายแสงอัลตร้าไวโอเลต　　　　　　เคย .....　　　ไม่เคย .....

ยาฉีด　　　　　　　　　　　　　　เคย .....　　　ไม่เคย .....

อื่นๆ　โปรดระบุ

....

3. ประวัติบุคคลในครอบครัวมีโรคสะเก็ดเงิน............ไม่มี...........มี ระบุ.........................

4. มีโรคข้อสะเก็ดเงินร่วมด้วย　　　　　............ไม่มี...........มี ระบุ.........................

5. บริเวณที่เป็นสะเก็ดเงิน

a. หนังศีรษะ　　มี ...... ไม่มี .....

b. ผิวหนัง　　　มี ...... ไม่มี .....

c. เล็บ　　　　มี ...... ไม่มี .....

ข้อมูลเกี่ยวกับสิ่งส่งตรวจ

1. CODE...

2. Anti-HIV...

3. Others..

ข้อมูลสำหรับการวิเคราะห์

	Baseline	1st month	2nd month	3rd month
PASI Score				
IL-33 mRNA level				

การรักษา

ครั้งที่	NUVB (mJ/cm^2) or MTX	หมายเหตุ
1		
2		
3		
4		
5		
6		
7		
8		
9		
10		
11		
12		
13		
14		
15		
16		
17		
18		
19		
20		
21		

22		
23		
24		

APPENDIX C

PATIENT PICTURES

Baseline   1st month

2nd month

Figure C1 Pictures of case 1

Baseline   1st month

2nd month

Figure C2 Pictures of case 2

Baseline

1st month

2nd month

Figure C3 Pictures of case 3

Baseline

1st month

2nd month

3rd month

Figure C4 Pictures of case 4

APPENDIX D

IL-33 CONCENTRATION
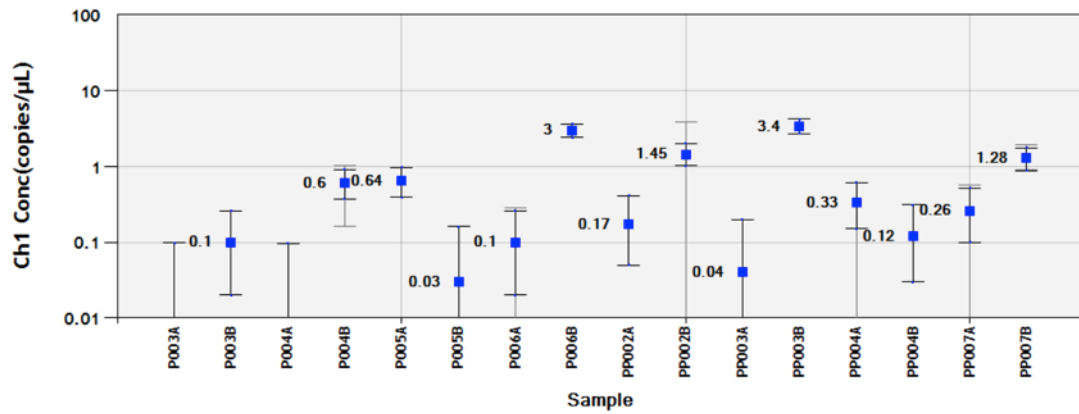
Figure D1 IL-33 concentration

- Use merge well function for merge duplicated well

- Calculate sample concentration

- P, group methotrexate; PP, group NBUVB

- B, baseline; A, after treatment

10. Output

10.1 International Journal Proceeding

Subpayasarn U, Ponnikorn S, Meephansan J. **Moderate to severe plaque type psoriasis and its treatment: Methotrexate.** The 13th Asia Pacific Federation of Pharmacologist (APFP) Meeting.

10.2 International Conference Publication

Pittayapruek P, Meephansan J, Prapapan O, Komine M, Ohtsuki M. **Role of Matrix Metalloproteinases in Photoaging and Photocarcinogenesis**. International Journal of Molecular Sciences. 2016;17(6):868.

10.3 International Conference

Meephansan J. **Effect of narrowband UVB on IL-33 expression on keratinocytes in psoriasis.** The 31st Annual Meeting of the Japanese Society for Psoriasis Research, Utsunomiya city, Japan

APFP 2016

The 13th Asia Pacific Federation of Pharmacologist (APFP) Meeting
"New Paradigms in Pharmacology for Global Health"
1st – 3rd February 2016
The Berkeley Hotel Pratunam, Bangkok, Thailand

LETTER OF ACCEPTANCE

5th April, 2016

Authors: Urairack Subpayasarn, Saranyoo Ponnikorn , Jitlada Meephansan

Manuscript title: Moderate to severe plaque type psoriasis and its treatment: Methotrexate

Dear Authors,

Thank you for submitting your paper to the 13th Asia Pacific Federation of Pharmacologist (APFP) Meeting which held in 1st-3rd February, 2016 at the Berkeley Hotel, Bangkok, Thailand. I am pleased to inform you that the reviewers feel your paper has substantial merit for publication. **Therefore, on behalf of the Conference Academic Committees, I am pleased to inform you that your research manuscript has been accepted for publication in the Proceedings of the 13th Asia Pacific Federation of Pharmacologist (APFP) Meeting** and the hard copy of the proceeding will be issue soon.

Regards,

W. Tassaneeyakul

Professor WichittraTassaneeyakul, Ph.D.
Chair of the Conference Academic Committees, APFP2016 Meeting

Head of Department of Pharmacology
Faculty of Medicine, KhonKaen University
KhonKaen 40002
Tel: 6681 659 4623

APFP 2016

The 13th Asia Pacific Federation of
Pharmacologist (APFP) Meeting
"New Paradigms in Pharmacology for Global Health"

1st – 3rd February 2016
The Berkeley Hotel Pratunum,
Bangkok, Thailand

Organized by The Pharmacological and Therapeutic Society of Thailand

Conference Host

The Pharmacological and Therapeutic Society of Thailand

The Asia Pacific Federation of Pharmacologists

Co-hosted by

Chulabhorn Ubternational College of Medicine, Thammasat University, Bangkok, Thailand

Chulalongkorn University, Bangkok, Thailand

Naresuan University, Phitsanulok, Thailand

Thailand Center of Excellence for Life Sciences

Thailand Convention & Exhibition Bureau

Organising Committee

Conference Chair

Professor Kesara Na-Bangchang

Advisory Committee

Professor Dr. Boonchua Dhorranintra
Professor Amnuay Thithapandha
Major General Associate Professor Borpit Klangkalya
Major General Sunan Rojanavipat
Associate Professor Jintana Sattayasai
Associate Professor Chaicharn Sangdee
Associate Professor Pornpen Pramyothin
Udom Chantharaksri
Professor Samuel HH Chan
Professor John Miners
Professor Alastair Stewart
Professor Masayoshi Mishina
Professor Nafeeza Mohd Ismail
Professor Wen-Chang Chang
Professor Guan-Hua Du
Professor Zhi-Bin Lin
Professor Masamitsu Iino
Professor Jong-Keun Kim
Dr. Herbert Ho
Associate Professor Wong Wai-Shiu Fred
Associate Professor Peter Molenaar

Academic

Professor Wichittra Tassaneeyakul
Professor Veerapol Kukongviriyapan
Associate Professor Mayuree Tantisira
Associate Professor Srichan Pornjirasilp
Associate Professor Supornchai Kongpatanakul
Associate Professor Supeecha Wittayalertpanya
Associate Professor Pithi Chanvorachote
Associate Professor Dr. Werawath Mahatthanatrakul
Associate Professor Chonlaphat Sukasem
Assistant Professor Wacharee Limpanasithikul
Assistant Professor Pornpun Vivithanaporn
Assistant Professor Sakonwun Praputbut
Witoo Luangbudnark

Fundraising

Associate Professor Dr. Supornchai Kongpatanakul
Associate Professor Mayuree Tantisira
Associate Professor Supatra Srichairat
Associate Professor Srichan Pornjirasilp
Associate Professor Supeecha Wittayalertpanya
Associate Professor Dr.Adisak Wongkajornsilp
Associate Professor Chonlaphat Sukasem

Registration

Associate Professor Chandhanee Itthipanichpong
Assistant Professor Orapin Wongsawatkul
Assistant Professor Suree Jianmongkol
Associate Professor Dr. Uraiwan Panich
Assistant Professor Puongtip Kunanusorn
Assistant Professor Wandee Udomuksorn
Assistant Professor Panot Tangucharit
Dr. Wannarasmi Ketchart
Dr. Kitipong Soontrapa
Jiraporn Kuesap

Finance

Associate Professor Supeecha Wittayalertpanya
Associate Professor Payong Wanikiat
Assistant Professor Pasarapa Towiwat
Associate Professor Chonlaphat Sukasem
Supannikar Tawinwung
Piyanuch Wonganan
Warabhorn Meesart

Conference Rooms and Food

Associate Professor Sumana Chompootaweep
Dr. Wannarasmi Ketchart
Jiraporn Kuesap
Kanyarat Boonprasert

Secretariat

Associate Professor Rattima Jeenapongsa
Assistant Professor Wanna Chaijaroenkul
Assistant Professor Pornpun Vivithanaporn
Assistant Professor Ornrat Lohitnavy

Conference Document

Associate Professor Supatra Srichairat
Associate Professor Dr.Adisak Wongkajornsilp
Associate Professor Laddawal Phivthongngam
Associate Professor Chonlaphat Sukasem
Dr. Pajaree Chariyavilaskul
Siwanon Jirawatnotai
Kanyarat Boonprasert
Piyanuch Wonganan
Yamaratee Jaisin
Oranun Kerdpin

Reception and Social Activity

Major General Associate Professor Nisamanee Satyapan
Associate Professor Dr.Naowarat Suthamnatpong
Assistant Professor Pornpun Vivithanaporn
Colonel Assistant Professor Jeeranut Tankanitlert
Colonel Dr. Sarawut Jindarat
Major Janeyuth Chaisakul
Yamaratee Jaisin
Tullayakorn Plengsuriyakarn
Supannikar Tawinwung
Dr. Pajaree Chariyavilaskul
Sirada Srihirun

Public Relations and Information Technology

Associate Professor Rattima Jeenapongsa
Assistant Professor Ornrat Lohitnavy
Assistant Professor Pornpun Vivithanaporn
Associate Professor Chonlaphat Sukasem
Tullayakorn Plengsuriyakarn

Reviewers

Professor Kesara Na-Bangchang	Chulabhorn International College of Medicine, Thammasat University
Associate Professor Dr.Nathawut Sibmooh	Department of Pharmacology Faculty of Science, Mahidol University
Associate Professor Dr.Uraiwan Panich	Department of Pharmacology Faculty of Medicine Siriraj Hospital, Mahidol University
Associate Professor Bunkerd Kongyingyoes	Department of Pharmacology Faculty of Medicine, Khon Kaen University
Associate Professor Chonlaphat Sukasem	Department of Pathology, Faculty of Medicine, Ramathibodi Hospital; Mahidol University
Associate Professor Darawan Pinthong	Department of Pharmacology Faculty of Science, Mahidol University
Associate Professor Jarupa Viyoch	Faculty of Pharmaceutical Sciences Naresuan University
Associate Professor Nantaka Khorana	Faculty of Pharmaceutical Sciences Naresuan University
Associate Professor Waree Tiyaboonchai	Faculty of Pharmaceutical Sciences Naresuan University
Assistant Professor Laddawan Senggunprai	Department of Pharmacology Faculty of Medicine, Khon Kaen University
Assistant Professor Ornrat Lohitnavy	Faculty of Pharmaceutical Sciences Naresuan University
Assistant Professor Pornpun Vivithanaporn	Department of Pharmacology Faculty of Science ,Mahidol University

Assistant Professor Sakonwun Praputbut

Faculty of Pharmaceutical Sciences
Naresuan University

Assistant Professor Thanasak Teaktong

Faculty of Pharmaceutical Sciences
Naresuan University

Assistant Professor Wacharee Limpanasithikul

Department of Pharmacology
Faculty of Medicine, Chulalongkorn University

Dr.Pajaree Chariyavilaskul

Department of Pharmacology
Faculty of Medicine, Chulalongkorn University

Dr.Wannarasmi Ketchart

Department of Pharmacology
Faculty of Medicine, Chulalongkorn University

Atchariya Yosboonruang

School of Pharmaceutical Sciences
University of Phayao

Piyanuch Wonganan

Department of Pharmacology
Faculty of Medicine, Chulalongkorn University

Sirada Srihirun

Department of Pharmacology
Faculty of Dentistry, Mahidol University

Siwanon Jirawatnotai

Department of Pharmacology
Faculty of Medicine Siriraj Hospital,
Mahidol University

Witoo Luangbudnark

Faculty of Pharmaceutical Sciences
Naresuan University

Scientific Program

Day 1: Mon 1st February 2016

7.30-8.30	Registration		
8.30-9.00	**Mayfair Grand Ballroom (A+B+C Merged Room)**		
	Opening Ceremony - *Prof. Piyasakol Sakolsatayadorn, Minister of Public Health Thailand* - *Prof. Kesara Na-Bangchang, The President of Pharmacological and Therapeutics Society of Thailand* - *Prof. Samuel HH Chan, The President of Asia Pacific Federation of Pharmacologists*		
9.00-9.45	**Plenary session 1**		
	"Move Pharmacogenomics Discovery to Medical Practice" *Prof. Yuan-Tsong Chen, Academia Sinica, Taiwan & Duke Medical Center, USA*		
9.45-10.00	**Coffee Break**		
10.00-12.00	**Mayfair Ballroom A**	**Mayfair Ballroom B**	**Mayfair Ballroom C**
	<u>Session 1A:</u> **Role of Pharmacogenomics in Drug Efficacy and Safety**	<u>Session 1B:</u> **Neuropharmacology**	<u>Session 1C:</u> **Novel Molecular Targets for Cancer Therapy and Diagnosis**
	Chair: Prof. Amnuay Thithapandha, Mahidol University, Thailand *Co-chair*: Prof. Wichittra Tassaneeyakul, Faculty of Medicine, Khon Kaen University, Thailand	*Chair:* Prof. Jong-Keun Kim, Chonnam National University Medical School, Republic of Korea *Co-chair*: Prof. Masayoshi Mishina, Ritsumeikan University, Japan	*Chair:* Prof. Wen-Chang Chang, Taipei Medical University, Taiwan *Co-Chair:* Prof. Apiwat Mutirangura, Chulalongkorn University, Thailand
	Speakers: 1. **"Pharmacogenomics for the Clinical Implementation in Korea"** *Prof. Jae-Gook Shin, Inje University, Busan, Republic of Korea* 2. **"Pharmacogenomics Guided Treatment in Clinical Practice: Experience in Thailand"** *Assoc. Prof. Chonlaphat Sukasem, Mahidol University, Thailand* 3. **"Pharmacogenomics of Antiepileptics: In Search of Genetic Biomarkers for Drug Responsiveness"** *Prof. Zahurin Mohamed, University of Malaya, Malaysia*	*Speakers:* 1. **"From Synapse Pharmacology to Mental Health"** *Prof. Masayoshi Mishina, Ritsumeikan University, Japan* 2. **"Excitatory Projection from Entorhinal Cortex to Hippocampus Instructs the Anti-epileptic Effect of Low-frequency Stimulation in Temporal Lobe Epilepsy"** *Prof. Zhong Chen, Zhejiang University, China* 3. **"Effect of Ethanol and Acetaldehyde on Human Psychomotor Function, Physiological Response and Alcohol Dependence"** *Prof. Jong-Keun Kim, Chonnam National University Medical School, Republic of Korea*	*Speakers:* 1. **"Inhibition of Lung Tumorigenesis by Targeting Transcription Factor Sp1"** *Prof. Wen-Chang Chang, Taipei Medical University, Taiwan* 2. **"The Role of Epigenetic Regulation on Repetitive Sequences in Cancer Development"** *Prof. Apiwat Mutirangura, Chulalongkorn University, Thailand* 3. **"Anti-tumor Effect of Ganoderma lucidum Polysaccharide Peptide Mediated by Immunological Mechanism"** *Prof. Zhi-Bin Lin, Peking University Health Science Center, China*

10.00-12.00 (cont.)	Mayfair Ballroom A	Mayfair Ballroom B	Mayfair Ballroom C
	Session 1A: Role of Pharmacogenomics in Drug Efficacy and Safety	**Session 1B:** Neuropharmacology	**Session 1C:** Novel Molecular Targets for Cancer Therapy and Diagnosis
			4. **"Caveolin as a Target for Cancer Therapy"** *Assoc. Prof. Pithi Chanvorachote, Chulalongkorn University, Thailand*
12.00-13.00	**Mayfair Grand Ballroom (A+B+C Merged Room)**		
	Luncheon Symposium supported by TCELS Thailand		
	"Development of herbal medicine from bench to shelf" **Speaker:** *Dr. Tzung Hsien Lai, Institute of Pharmaceutics, Development Center for Biotechnology, Taiwan* **Modulator:** *Dr. Nares Damrongchai, TCELS, Thailand*		
13.00-13.45	**Plenary Session 2**		
	"Roles of Melatonin in Controlling Alzheimer's Disease" *Prof. Piyarat Govitrapong, Mahidol University, Thailand*		
13.45-15.30	• **Poster Presentation (Session 1)** • **Coffee Break/ Booth**		
15.30-17.00	Mayfair Ballroom A	Mayfair Ballroom B	Mayfair Ballroom C
	Session 2A: Metabolomics and Advanced Medicine *Chair:* Prof. Amnuay Thithapandha, Mahidol University, Thailand *Co-chair:* Asst. Prof. Nipan Israsena Na Ayuthaya, Chulalongkorn University, Thailand	**Session 2B:** Novel Pharmacotherapy for HIV *Chair:* Prof. Kiat Ruxrungtham, Chulalongkorn University, Thailand *Co-Chair:* Dr. Timothy R. Cressey, Programmed for HIV prevention and treatment, Thailand	**Session 2C:** Cholangiocarcinoma and Its Clinical Implications *Chair:* Prof. Veerapol Kukongviriyapan, Khon Kaen University, Thailand *Co-Chair:* Prof. Bin Tean Teh, National Cancer Centre, Singapore
	Speakers: 1. **"Metabolomics in the Study of Cancer Mechanisms and Diagnosis"** *Dr. Frank Gonzalez, National Cancer Institute, National Institute of Health, USA* 2. **"Personalized Medicine for Neurodegenerative Diseases"** *Asst. Prof. Nipan Israsena Na Ayuthaya, Chulalongkorn University, Thailand* 3. **"Impact of Sigma-1 Receptor in Amyotrophic Lateral Sclerosis Therapy"** *Prof.Kohji Fukunaga, Tohoku University, Japan*	*Speakers:* 1. **"Novel Anti-HIV Medicine"** *Prof. Kiat Ruxrungtham, Chulalongkorn University, Thailand* 2. **"Antiretroviral Therapy for HIV Infection in Adults and Adolescents: Recommendations for a Public Health Approach"** *Prof. Somnuek Sungkanuparph, Ramathibodi Hospital, Mahidol University, Thailand* 3. **"Application of Pharmacokinetics for Optimizing Antiretroviral Therapy and Drug-Drug Interactions"** *Dr. Timothy R. Cressey, Harvard School of Public Health/ Programmed for HIV Prevention and Treatment, Thailand*	*Speakers:* 1. **"Liver Fluke and Cholangiocarcinoma in Thailand"** *Assoc. Prof. Chawalit Pairojkul, Khon Kaen University, Thailand* 2. **"Genetic Landscape of Cholangiocarcinoma and Its Clinical Implication"** *Prof. Bin Tean Teh, National Cancer Centre, Singapore* 3. **"Targeting of Aberrant Antioxidant Gene Expression as a Therapeutic Strategy Against Cholangiocarcinoma"** *Prof. Veerapol Kukongviriyapan, Khon Kaen University, Thailand*
18.30-20.30	**Welcome reception** (drink and light snack, free for all participants)		

Day 2: Tue 2nd February 2016

7.45-8.30	**Mayfair Grand Ballroom (A+B+C Merged Room)**		
	Early Bird Lecture supported by Elsevier Publishing		
	"How to Write Scientific Paper for Successful Submission to High Impact Factor Journals " *Prof. Rob Verpoorte, Editor in chief, Journal of Ethnopharmacology*		
8.30-9.15	**Plenary session 3**		
	"Discovery of New Drug Targets for Inflammatory Diseases: Endogenous Modulators of Pro-resolving Signaling" *Prof. Young-Joon Surh, Seoul National University, Republic of Korea*		
9.15-10.15	**Coffee Break/ Booth**		
10.15-12.00	**Mayfair Ballroom A**	**Mayfair Ballroom B**	**Mayfair Ballroom C**
	Session 3A: Signaling and Transporters	**Session 3B: Advance in Xenobiotic Metabolism**	**Session 3C: Models in Drug Discovery & Development**
	Chair: Prof. Shuh Narumiya, Kyoto University, Japan *Co-chair:* Prof. Naohiko Anzai, Chiba University, Japan	*Chair:* Prof. John Miners, Flinder University, Australia *Co-Chair:* Prof. Wichittra Tassaneeyakul, Khon Kaen University, Thailand	*Chair:* Prof. Kazuhisa Sekimizu, University of Tokyo, Japan *Co-Chair:* Dr. Joel Tarning, Mahidol University, Thailand
	Speakers: 1. **"Prostaglandin Receptor and Signaling as Potential Drug Targets"** *Prof. Shuh Narumiya, Kyoto University, Japan* 2. **"Manipulating Calcium Signals to Cope with Neurodegenerative Diseases"** *Prof. Masamitsu Iino, University of Tokyo, Japan* 3. **"Renal Tubular Urate Transporters as Targets for New Drug Discovery and Development"** *Prof. Naohiko Anzai, Chiba University, Japan*	*Speakers:* 1. **"Inhibition of Human UDP-glucuronosyl-Transferase Enzymes: Implications for Drug-drug and Drug-endobiotic Interactions"** *Prof. John Miners, Flinders University, Australia* 2. **"Metabolic Activation of Xenobiotics by Polymorphic Drug-metabolizing Enzymes"** *Prof. Hiroshi Yamazaki, Showa Pharmaceutical University, Japan* 3. **"*In Vitro* Approaches for Drug Metabolism Studies – Focus On Cytochromes P450"** *Assoc. Prof. Ong Chin Eng, Monash University, Malaysia*	*Speakers:* 1. **"Silkworm Model for Drug Discovery and Drug Development"** *Prof. Kazuhisa Sekimizu, University of Tokyo, Japan* 2. **"Population Pharmacokinetic-Pharmacodynamic Modeling in Tropical Medicine Research"** *Assoc. Prof. Joel Tarning, Mahidol University, Thailand* 3. **"Nanotechnology Application in Pharmacology"** *Asst. Prof. Amornpun Sereemaspun, Chulalongkorn University, Thailand*
12.00-13.00	**Mayfair Ballroom A**	**Mayfair Ballroom B**	**Mayfair Ballroom C**
	Luncheon Symposium supported by Thai-Otsuka Co., Ltd.	**Luncheon Symposium supported by Takeda Thailand**	**Luncheon Symposium supported by Sanofi Pasteur Thailand**
	"Consideration for Interchangeability of Psychiatric Drugs" **Speaker:** *Asst. Prof. Dr. Julraht Konsil, Khon Kaen University, Thailand* **Modulator:** *Dr. Nipatt Karnjanathanalers, Chulalongkorn University, Thailand*	**"Pharmacological actions Based Upon Its Pathophysiology"** **Speaker:** *Assoc. Prof. Dr. Naeti Suksomboon, Mahidol University, Thailand* **Modulator:** *Assoc. Prof. Dr. Srichan Phornchirasilp, Mahidol University, Thailand*	**"New perspectives in dengue prevention: Results from phase III dengue vaccine efficacy studies in Asia and Latin America"** **Speaker:** *Prof. Usa Thisyakorn, Chulalongkorn University, Thailand* **Modulator:** *Assoc Prof. Dr. Supatra Srichairat, Eastern Asia University, Thailand*

13.00-13.45	**Mayfair Grand Ballroom (A+B+C Merged Room)**		
	Plenary session 4		
	"Drug Discovery from Traditional Chinese Medicine: The Effect of Salvianolic acid A on Metabolic Syndrome" *Prof. Guanhua Du, Institute of Materia Medica, Chinese Academy of Medical Sciences & Peking Union Medical College, China*		
13.45-15.30	**Mayfair Ballroom A**	**Mayfair Ballroom B**	**Mayfair Ballroom C**
	Session 4A: Drug Discovery & Development in Infectious Diseases *Chair:* Prof. Stephen A. Ward, Liverpool School of Tropical Medicine, UK *Co-chair:* Prof. Kesara Na-Bangchang, Thummasat University, Thailand	**Session 4B: Antioxidants and Oxidative Stress Disorders** *Chair:* Prof. Samuel Chan, Chung Gung Memorial Hospital, Taiwan *Co-Chair:* Assoc. Prof. Supornchai Kongpatanakul, Mahidol University, Thailand	**Session 4C: CVS and Endocrine Pharmacology** *Chair:* Prof. Nipon Chattipakorn, Chiang Mai University, Thailand *Co-Chair:* Prof. Yasufumi Sato, Tohoku University, Japan
	Speakers: 1. **"The Importance of Academia in the Discovery and Development of Antiparasitic Drugs"** *Prof. Stephen A. Ward, Liverpool School of Tropical Medicine, UK* 2. **"Medicinal Chemistry of Tetraoxane-based Antimalarials; Towards a Drug Candidate that Circumvents K13-dependent Artemisinin Resistance"** *Prof. Paul Michael O'Neill, University of Liverpool, UK* 3. **"Preventive Chemotherapy for Neglected Tropical Diseases: Opportunities and Challenges"** *Dr. Vicente Belizario, University of the Philippines, Philippines*	*Speakers:* 1. **"The Role of Oxidative Stress in Developmental Programming of Hypertension"** *Prof. Julie YH Chan, Chang Gung Memorial Hospital, Taiwan* 2. **"Vitamin E Isoform γ-Tocotrienol Protects Against Obstructive Airway Diseases"** *Assoc. Prof. Wong Wai-Shiu Fred, National University of Singapore, Singapore* 3. **"Paeonol Protects Against Tunicamycin Induced Endothelial Dysfunction in Mice by Inhibition of Oxidative Stress"** *Prof. Mohd Rais Mustafa, University of Malaysia, Malaysia*	*Speakers:* 1. **"A Novel Link between Inhibition of Angiogenesis and Tolerance to Vascular Stress"** *Prof. Yasufumi Sato, Tohoku University, Japan* 2. **"Adipokines as Novel Therapeutic Targets for Vascular Disease"** *Prof. Chao-Yu Miao, Second Military Medical University, China* 3. **"Angel and Demon Effects of Antidiabetic Drugs on the Heart in Metabolic Syndrome"** *Prof. Nipon Chattipakorn, Chiang Mai University, Thailand*
15.30-17.00	• **Poster Presentation (Sesssion 2)** • **Coffee Break /Booth**		
17.00-21.30	**Welcome dinner (Siam Niramit) – Additional price**		

Day 3: Wed 3rd February 2016

8.30-10.00	Mayfair Ballroom A	Mayfair Ballroom B	Mayfair Ballroom C
	Session 5A: Drug toxicity: Prediction and Mechanism	**Session 5B: Controlling Exacerbation of Chronic Respiratory Disease: Current and Innovative Approaches**	**Session 5C: Standards & Regulation in Drug Discovery & Development: Good Clinical Practice & Ethics**
	Chair: Prof. Tsuyoshi Yokoi, Nagoya University, Japan *Co-Chair:* Prof. Veerapol Kukogviriyapan, Khon Kaen University, Thailand	*Chair:* Prof. Alastair Stewart, University of Melbourne, Australia *Co-Chair:* Assoc. Prof. Judith CW Mak, Hong Kong SAR, China	*Chair:* Prof. Juntra Karbwang, Nagasaki University, Japan *Co-chair:* Assoc. Prof. Supeecha Wittayalertpanya, Chulalongkorn University, Thailand
	Speakers: 1. **"Approaches to Predict Drug-induced Liver Injury"** *Prof. Tsuyoshi Yokoi, Nagoya University, Japan* 2. **"Role of Xenobiotic-responsive Nuclear Receptors in Hepatotoxicity"** *Prof. Kouichi Yoshinari, University of Shizuoka, Japan* 3. **"Predict Cardiac Toxicity by Using Stem Cells Derived Cardiomyocytes"** *Dr. Jufeng Wang, National Institutes for Food and Drug Control, China*	*Speakers:* 1. **"Controlling Exacerbation of Chronic Respiratory Disease: Mechanisms and Targets"** *Prof. Alastair Stewart, University of Melbourne, Australia* 2. **"Airway Smooth Muscle Contractility: Novel Drug Targets"** *Asst. Prof. Thai Tran, National University of Singapore, Singapore* 3. **"Mesenchymal Stem Cell Treatment in Chronic Obstructive Airway Disease"** *Assoc. Prof. Judith CW Mak, University of Hong Kong, Hong Kong SAR, China*	*Speakers:* 1. **"GCP & Ethics in Clinical Research: Academia's Perspective"** *Prof. Chitr Sitthi-Amorn, Chulalongkorn University, Thailand* 2. **"GCP & Ethics in Clinical Research: EC's Perspective"** *Assoc. Prof. Thipaporn Tharavanij, Thammasat University, Thailand* 3. **"GCP & Ethics in Clinical Research: Sponsor's Perspective"** *Dr. Pravich Tanyasittisuntorn Medical Research Network of the Consortium of the Thai Medical Schools, Thailand*
10.00-10.45	**Coffee Break/ Booth**		
10.45-12:00	Mayfair Ballroom A	Mayfair Ballroom B	Mayfair Ballroom C
	Oral Presentation **(O-01-O-04)**	**Oral Presentation** **(O-05-O-08)**	**Oral Presentation** **(O-09-O-013)**
	Chair: Assoc. Prof. Mayuree Tantisira, Burapha University, Thailand	*Chair:* Assoc. Prof. Adisak Wongkajornsilp, Faculty of Medicine Siriraj Hospital, Mahidol University, Thailand	*Chair:* Assoc. Prof. Nathawut Sibmooh, Mahidol University, Thailand
	O-01 Development BDNF Incorporated PLGA Nanoparticles and Evaluation Its Ability to Cross Blood-Brain Barrier using an *in vitro* Model *Dr. Siti Norsyafika Kamarudin, Universiti Teknologi MARA, Malaysia* **O-02 Cytotoxic Effect of Novel 1-substituted 5-(phenyl)aminouracil Derivatives as Potential Anti-dengue Virus Agents on Vero 76 Cells** *Dr. Noor Fahitah Abu Hanipah, Universiti Teknologi MARA, Malaysia*	**O-05 Possible Role of Perivascular Adipose Tissue in Resistant Mesenteric Artery of Spontaneously Hypertensive Rat** *Dr. Chin-Chen Wu, National Defence Medical Centre, Taiwan* **O-06 CUMS–induced Depression Alter Saxagliptin Pharmacokinetics in GK Rats** *Dr. Xu Feng, Shanghai Jiaotong University, China*	**O-09 Characterization of Bladder Selectivity Based on *in vivo* Drug-Receptor Binding of Antimuscarinic Agents for Treatment of Overactive Bladder** *Dr. Shizuo Yamada, University of Shizuoka, Japan* **O-10 Hepatoprotective Activity and Metabolic Profile of the Anthocyanin rich Extract of *Hibiscus sabdariffa* Calyces** *Dr. Sayed H. Seif el-Din, Theodor Bilharz Research Institute, Egypt*

10.45-12:00 (Cont)	Mayfair Ballroom A	Mayfair Ballroom B	Mayfair Ballroom C
	Oral Presentation (O-01-O-04)	Oral Presentation (O-05-O-08)	Oral Presentation (O-09-O-013)
	O-03 Nitrosative Stress-induced Defunct Baroreflex underpins High Mortality in a Rat Model of Hepatic Encephalopathy *Dr. Ching-Yi Tsai, Chang Gung Memorial Hospital, Taiwan* **O-04 Differential Alteration of Sympathetic Norepinephrine Transporter in Mesenteric Arteries and Veins in DOCA-salt hypertensive rats** *Dr. Sutheera Sangsiri, Michigan State University, USA*	**O-07 AAV-mediated *MECP2* Gene Delivery in Mouse Models of Rett Syndrome** *Dr. Thishnapha Vudhironarit, University of Glasgow, , UK* **O-08 Pharmacokinetics Guided Exploration of Potential Antimalarial Therapy** *Dr. Muhammad Wahajuddin, CSIR Central Drug Research Institute, India*	**O-11 Magnesium Status, Oxidative Stress and Inflammation: Links and Possible Therapeutic Targets in Glaucomatous Neuropathy?** *Dr. Igor Iezhitsa, Universiti Teknologi MARA, Malaysia* **O-12 Dexamethasone Treatment of Cultured Human Trabecular Meshwork Cells: Effect on Secretion of Fibronectin and Alpha Smooth Muscle Actin** *Dr. Nurul Ainsya Bakry, Universiti Teknologi MARA, Malaysia* **O-13 Co-culture of Immortalized Keratinocytes and Immune Cells to Investigate Sulfur Mustard Toxicity and Potential Treatments** *Dr.Balszuweit Frank, Bundeswehr Institute of Pharmacology and Toxicology, Germany*
12.00-13.00	Mayfair Ballroom A	Mayfair Ballroom B	Mayfair Ballroom C
	Luncheon Symposium supported by Pfizer Thailand	Luncheon Symposium supported by SCIEX	Luncheon Symposium supported by GPO, Thailand
	"Variability on Design of Bioequivalence: Questions on Drugs with Complicated Pharmacokinetic Properties" **Speaker:** *Asst. Prof. Dr. Julraht Konsil, Khon Kaen University, Thailand* **Modulator:** *Dr. Porranee Puranajoti, International Bio Service Co., Ltd., Thailand*	**"Liquid-chromatography Mass-spectrometry Applications for Small Molecule, Peptide and Protein-based drugs"** **Speaker:** *Vincent Lau, Technical Marketing Manager SCIEX (ASEAN)* **Modulator:** *Dr. Piboon Pornmanee, Application Specialist, SCIEX*	**"Brahmi, A Medicinal Plant for Memory Improvement: From Lab to Market"** **Speaker:** *Assoc. Prof. Dr. Kornkanok Ingkaninan, Naresuan University, Thailand* **Modulator:** *Asst. Prof. Dr. Nanteetip Limpeanchob, Naresuan University, Thailand*

13.00-15.00	Mayfair Ballroom A	Mayfair Ballroom B	Mayfair Ballroom C
	Session 6A: Ethnopharmacology & Alternative Medicines I	**Session 6B**: Ethnopharmacology & Alternative Medicines II	**Session 6C**: Systems Approach to Polypharmacology and Drug Discovery
	Chair: Prof. Rob Verpoorte, Leiden University, The Netherland *Co-Chair*: Assoc. Prof. Mayuree Tantisira, Burapha University, Thailand	*Chair:* Prof. Yongxiang Zhang, Beijing Institute of Pharmacology and Toxicology, China *Co-chair:* Prof. Cecilia C. Maramba-Lazarte, University of the Philippines, Philippines	*Chair:* Assoc. Prof. Somponnat Sampattavanich, Faculty of Medicine, Siriraj Hospital, Mahidol University, Thailand *Co-Chair:* Dr. Siwanon Jirawatnotai, Faculty of Medicine, Siriraj Hospital, Mahidol University, Thailand
	Speakers: 1. **"Synergy: Easier to Say Than to Prove"** *Prof. Rob Verpoorte, Leiden University, Netherland* 2. **"Pharmacokinetics and Disposition of Bioactive Herbal Compounds after Intravenous Dosing of Antiseptic XueBiJing Injection in Human Subjects and Rats"** *Prof. Chuan Li, China Academy of Chinese Medicine, China* 3. **"Wound Healing Activity of Standardized Extract of *Centella asiatica* ECa 233 and its Application"** *Assoc. Prof. Mayuree Tantisira, Burapha University, Thailand* 4. *"Reactive Oxygen Species Mediated Anticancer Effects of Natural Products in Lung Cancer Cells"* *Assoc. Prof. Xiuping Chen, University of Macau, China*	*Speakers:* 1. **"New Drug Discovery from Traditional Medicine: Experience from Chinese Traditional Medicine"** *Prof. Yongxiang Zhang, Beijing Institute of Pharmacology and Toxicology, China* 2. **"Tocotrienol Delays Cataractogenesis in STZ-induced Diabetic Rats"** *Prof. Nafeeza Mohd Ismail,Universiti Teknologi, Malaysia* 3. **"Integrated Research in the Development of Herbal Medicines: the Philippines"** *Prof. Cecilia C. Maramba-Lazarte, University of the Philippines, Philippines*	*Speakers:* 1. **"Tracking Cellular Effects of Signal Transduction and Metabolic Inhibitors in Living Cells"** *Prof. John Albeck, University of California, Davis, USA* 2. **"Image-based Phenotypic Profiling: Using Cellular Effects to Predict Drug Target and Toxicity"** *Asst. Prof. Lit-Hsin Loo, Bioinformatics Institute, A*STAR, Singapore* 3. **"Scientific Basis of Differences between β-blockers and Relevance for Therapeutics"** *Assoc. Prof. Peter Molenaar, Queensland University of Technology, Australia* 4. **"Macrophage Disruption of Sympathetic Neurovascular Transmission in Salt-sensitive Hypertension"** *Prof. James J. Galligan, Michigan State University, USA*
15.00-15.30	**Coffee Break**		
15.30-16:30	**Mayfair Grand Ballroom (A+B+C Merged Room)**		
	Poster Presentation Awards **Announcement of 14th APFP** - *The President of Pharmacological Society in Taiwan* **Closing remark** - *Prof. Kesara Na-Bangchang, The President of Pharmacological and Therapeutics Society of Thailand* - *Prof. Samuel HH Chan, The President of Asia Pacific Federation of Pharmacologists*		
16.30-18:00	**Annual Meeting of Members of The Pharmacological and Therapeutic Society of Thailand**		

Table of Content

RESEARCH ARTICLE

Preliminary investigation of oxidized regenerated cellulose/polycaprolactone composite as a synthetic dura substitute in a rabbit model

Ticomporn Luangwattanawilai[1], Visut Rawiwet[2], Sadudee Patamatham[3], Sorayouth Chumnanvej[3], Jintamai Suwanprateeb[4], Kasem Rattanapinyopituk[5], Somkiat Huaijantug[6], Chaowaphan Yinharnmingmongkol[6], Warinkarn Hemstapat[1]

[1]*Department of Pharmacology, Faculty of Science, Mahidol University, Bangkok, 10400 Thailand*
[2]*Central Animals Facility, Faculty of Science, Mahidol University, Bangkok, 10400 Thailand*
[3]*Department of Surgery, Faculty of Medicine, Ramathibodi Hospital, Mahidol University, Bangkok, 10400 Thailand*
[4]*Biomaterials Laboratory, Biomedical Engineering Research Unit, National Metal and Materials Technology Center (MTEC), Pathumthani 12120, Thailand.*
[5]*Department of Veterinary Pathology, Faculty of Veterinary Science, Chulalongkorn University, Bangkok, 10330 Thailand*
[6]*Department of Clinical Sciences and Public Health, Faculty of Veterinary Science, Mahidol University, Nakhonpathom 73170, Thailand*

Address correspondence and reprint request to: Warinkarn Hemstapat, Department of Pharmacology, Faculty of Science, Mahidol University, Bangkok Thailand.
E-mail address: warinkarn.hem@mahidol.ac.th

Abstract

Although a number of ideal dural substitutes have been developed, their manufacturing processes are rather complicated and costly. In addition, many of them have been associated with complications such as cerebrospinal fluid leakage, meningitis, and a chronic inflammatory reaction. In this study, two novel synthetic dural substitutes (P10 and P20) based on the mixture of oxidized regenerated cellulose (ORC) and polycaprolactone (PCL) were implanted and evaluated at 1 month post-implantation and compared with pericranium (autologous dura graft) in a rabbit model. The results showed that no signs of systemic and CSF infections as well as no evidence of infection and inflammatory response in the implantation sites were found in any groups. Histologically, both synthetic dural substitutes could enhance dural regeneration without causing any complications or tissue reactions. Interestingly, a new dura formation was found to be comparable between P10 and autologous group. These preliminary findings suggested that these new dural substitutes were well tolerated and exhibited excellent biocompatibility as well as enhancing the dural regeneration in this rabbit model. However, long-term study is required to confirm their effectiveness.

Keywords: Synthetic dural substitute, oxidized regenerated cellulose (ORC), polycaprolactone (PCL), rabbit model

Introduction

Over the past decades, a number of dural substitutes have been proposed and their efficacies have been evaluated. However, dural substitutes currently employed in clinical practice are expensive and some may not be readily available in some countries. In addition, many of them cause serious life-threatening complications, including cerebrospinal fluid (CSF) leakage, meningitis, and a chronic inflammatory reaction. Due to the lack of suitable dural substitutes, a novel dural substitute that could demonstrate the superior properties is needed. Dural substitutes that are the most commonly used in clinical practice are those that made of collagen matrix, which either obtained from bovine[1,2] or equine origin[3,4]. Despite their effectiveness, they are very expensive and may carry a risk of zoonotic transmission[1,3,4].

Recently, we have reported a new synthetic dural substitute, which was developed based on the combination of oxidized regenerated cellulose (ORC) and polycaprolactone (PCL)[5]. It showed that the physical and mechanical properties of the composites were closed to those of natural human dura mater. In addition, *in vitro* viability and proliferation tests (unpublished data) also revealed that mouse fibroblast could survive and proliferate on these composites, suggesting their non-toxic properties. Thus, this study was aimed to further assess their performances by mean of *in vivo* evaluation in a rabbit model.

Materials and Methods

Synthetic dural substitutes

Synthetic dural substitutes were prepared as described previously[5]. Two formulations were selected based on our previous finding, which are composed of ORC and 10 or 20 part of PCL in 100 part of N-methyl-2-pyrrolidone, respectively (P10 and P20). They were then sterilized by gamma irradiation at 25 kGy prior to implantation into the animals.

Animals

Fifteen male New Zealand white rabbits (2.5-3 kg) were obtained from National Laboratory Animal Center, Mahidol University, Thailand. Ethical approval of this study was obtained and approved by the Faculty of Science, Mahidol University Animal Care and Use Committee. Animals were housed in a temperature controlled room (20 ± 2ºC) with a 12/12 hour light/dark cycle and maintained at humidity $60 \pm 10\%$. Standard laboratory food and water were supplied *ad libitum*. The animals were randomly divided into three groups: autologous control group (implanted with pericranium), P10 group (implanted with a synthetic dural substitute P10) and P20 group (implanted with a synthetic dural substitute P20).

Dural implantation

The rabbits were pre-medicated by using the mixture of dextomitor (5µg/kg), midazolam (0.5 mg/kg) and ketamine (7 mg/kg) administered by a single intramuscular injection to provide sedation and analgesia in order to allow endotracheal intubation. The level of anesthesia was then maintained with 3-5% isoflurane inhalational anaesthesia. In brief, the

5 cm rostral-to-caudal linear incision was made at the right parietal region and a 1×1.5 cm^2 craniectomy at the right parietal region was created using a high-speed electrical drill. A dural defect (4 mm in diameter) was created under microscopic observation. This dural defect was repaired by suturing the edge of the native dura with either an autologous dural graft or ORC/PCL composites (P10 and P20) by using 5-0 non-absorbable silk. Finally, the scalp was then closed by using 2-0 non-absorbable nylon.

Examination of blood and cerebrospinal fluid (CSF)

At one month post-implantation, animals were anesthetized via ear vein injection using a mixture of ketamine (10 mg/kg) and xylazine (1.0 mg/kg), in which the level of anesthesia was maintained with 3% isoflurane. Whole blood and CSF samples were drawn from the saphenous vein and cisterna magna, respectively for evaluating the systemic infection and meningoencephalitis.

Tissue preparation and histological analysis

Following blood and CSF collecting, animals were euthanized and the whole brain along with tissues including dural substitutes with overlying bone and underlying brain was removed and preserved in 10% buffered formalin for 3-5 days. The tissue was then decalcified in 10% EDTA for 2 weeks and embedded in paraffin block. Serial sections (4 µm) were cut and stained with hematoxylin/eosin (H&E). Histological slides were assessed in semi-quantitative fashion for reactions of the host tissue, tissue infiltration into the defects and overall dural healing (n=5/group) (Table 1).

Statistical Analysis

Statistical analysis was performed using GraphPad Prism (version 6). All data were expressed as the mean and standard error of the mean (mean ± SEM). Statistical significance was determined using one-way analysis of variance (ANOVA), followed by Tukey's multiple comparisons test. The *p* value was set at $p < 0.05$ for the significant different between groups.
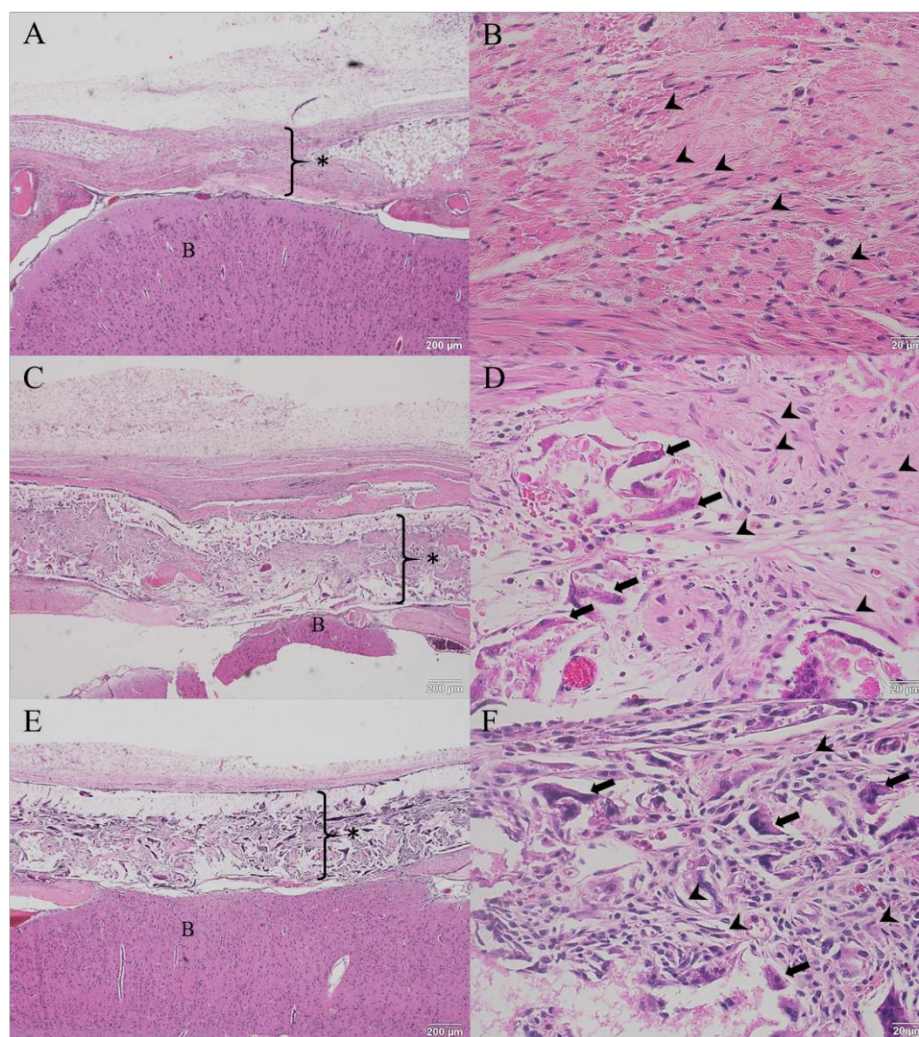
Results and Discussion

Two synthetic dural substitutes were successfully implanted into the animals. All animals recovered well post-implantation as observed by a gradual increase in their body weights. They remained healthy with no neurological impairment and post-operative complications such as CSF leakage. These data suggested that the composites exhibited a water-tight seal which is an essential property for an ideal dural substitute. In addition, no polymorphonuclear leukocytes (PMN) infiltration was observed in the implantation sites, indicating no infection and inflammatory responses. This data was consistent with the results obtained from blood and CSF tests, in which the completed blood count values were found to be in the normal range and no white blood cells were detected in the CSF samples of all the animals (data not shown).

Histologically, no significant difference in a degree of fibrosis and the attachment degree between autologous dural graft and two synthetic dural substitutes with adjacent tissues was observed. Both samples could enhance the dural regeneration, but P10 was found to have greater ability and was comparable to that of autologous group (Figure 2). Interestingly, a significant increase in the mean scores for bone remodeling markers, including vascularization and infiltration of osteoclast was observed in the implantation sites of both synthetic dural substitutes compared to that of autologous group (Figure 2).

Table 1. Semi-quantitative scoring criteria of histological studies

1. Adhesion to adjacent tissue		**4. Vascularization**	
4	Extensive adhesion	4	Abundant vascularization
3	Moderate adhesion	3	Moderate vascularization
2	Mild adhesion	2	Mild vascularization
1	Few adhesion	1	Few vascularization
0	None	0	None
2. Dura formation and Dura rearrangement		**5. Foreign body response (Macrophage or Foamy cells)**	
4	Dura formation > 75% with thin dura structure	4	Abundant infiltration of macrophages and giant cells
3	Dura formation 50-75% of bone excision area with thin dura structure or Dura formation > 75% with thick dura structure	3	Moderate infiltration of macrophages and giant cells
2	Dura formation 25-50% of bone excision area	2	Occasional infiltration of macrophage
1	Dura formation <25% of bone excision area	1	Few infiltration of macrophage
0	No dura formation	0	None
3. Degree of fibrosis		**6. Bone remodeling**	
4	Severe fibrosis	4	Abundant osteoclasts
3	Moderate fibrosis	3	Moderate number of osteoclasts
2	Mild fibrosis	2	Small number of osteoclasts
1	Few fibrosis	1	Few osteoclasts
0	None	0	None

Figure 1. H&E staining of tissue around the dural graft 1 month after implantation with either an autologous dural graft (A, B) or ORC/PCL composites (P10: C, D & P20: E, F) in rabbits. The remaining of synthetic dural substitutes (P10: C, D & P20: E, F) were observed. Fibrosis pattern in the synthetic dural substitutes were similar to autologous grafts after implantation. No hemorrhage and meningo-encephalitis were observed in all rabbits. Arrowhead indicated fibroblasts in fibrous tissue after implantation with dural substitutes and the arrow indicated the osteoclasts. Both P10 & P20 could enhance the dural regeneration, but P10 was found to have greater ability and was comparable to that of autologous group. Asterisk (*) = dural substitutes, B = brain, Bar = 200 μm (A, C, E) & 20 μm (B, D, F).
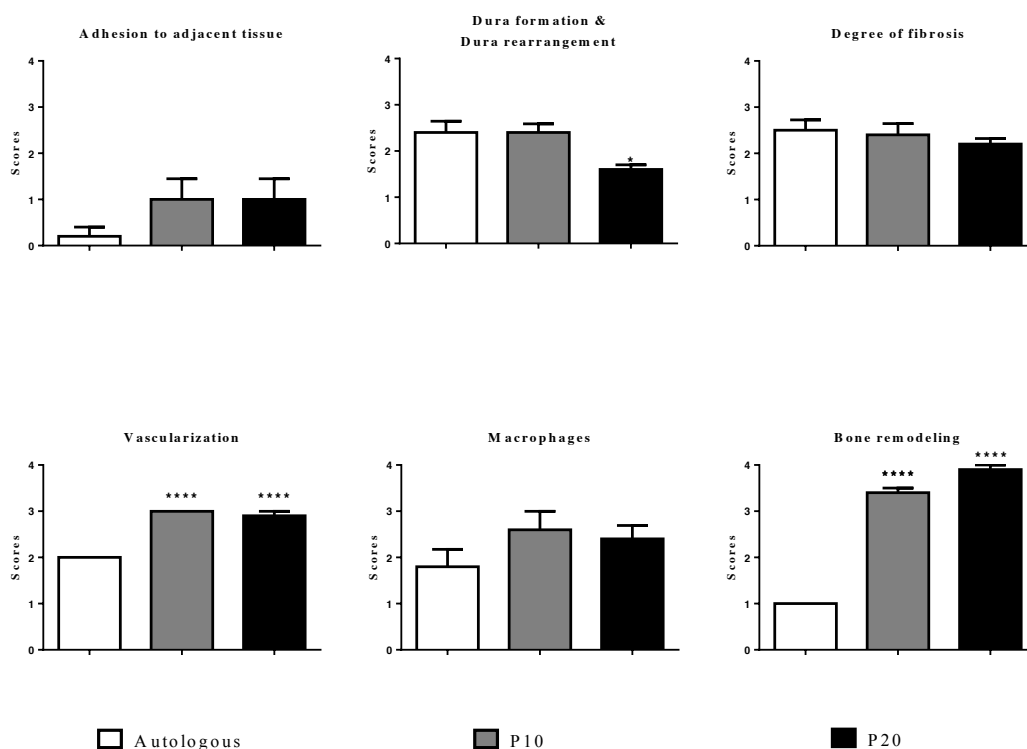
Figure 2. Histological scoring of the implantation sites for autologous, P10 and P20 groups after 1 month post-implantation. Histological examination was graded in semi-quantitative fashion. Data were expressed as mean ± SEM of five animals in each group. Statistically significant differences were determined using one-way analysis of variance (ANOVA), followed by Tukey's multiple comparisons test, *$p<0.05$, ****$p<0.0001$ versus autologous group.

Besides, our current finding also demonstrated that both formulations of new synthetic dural substitutes could enhance the bone remodeling process. However, further studies are required to investigate this finding.

Conclusion

The present finding demonstrated that the new synthetic dural substitutes based on the mixture of ORC and PCL are well tolerated and exhibited excellent biocompatibility as well as enhancing the dural regeneration in the rabbit model. These composites could potentially be employed as alternative dural substitutes that are biocompatible and safe to use. However, long-term *in vivo* investigation is required to confirm their effectiveness.

Acknowledgements

References

1. Costa BS, Cavalcanti-Mendes Gde A, Abreu MS, Sousa AA. Clinical experience with a novel bovine collagen dura mater substitute. Arq Neuropsiquiatr. 2011;69(2A):217-20.
2. Van Calenbergh F, Quintens E, Sciot R, Van Loon J, Goffin J, Plets C. The use of Vicryl Collagen as a dura substitute: a clinical review of 78 surgical cases. Acta neurochirurgica. 1997;139(2):120-3.
3. Parlato C, di Nuzzo G, Luongo M, Parlato RS, Accardo M, Cuccurullo L, et al. Use of a collagen biomatrix (TissuDura) for dura repair: a long-term neuroradiological and neuropathological evaluation. Acta neurochirurgica. 2011;153(1):142-7.
4. Knopp U, Christmann F, Reusche E, Sepehrnia A. A new collagen biomatrix of equine origin versus a cadaveric dura graft for the repair of dural defects--a comparative animal experimental study. Acta neurochirurgica. 2005;147(8):877-87.
5. Theeranattapong T, Luangwattanawilai T, Suwanprateeb J, Suvannapruk W, Chumnanvej S, Hemstapat W. Physical and Mechanical Characterizations of Oxidized Regenerated Cellulose/Polycaprolactone Composite for Use as a Synthetic Dura Mater. Key Engineering Materials. 2015; 659: 19-23.

RESEARCH ARTICLE

Chondrogenic induction ability of adipose-derived mesenchymal stem cells (ASCs) from infrapatellar fat pad and subcutaneous adipose tissues: a preliminary study in a rat model of osteochondral defect

Orada Sriwatananukulkit[1], Ticomporn Luangwattanawilai[1], Narongrit Srikaew[2], Tulyapruek Tawonsawatruk[3], Kasem Rattanapinyopituk[4], Warinkarn Hemstapat[1]

[1]Department of Pharmacology, Faculty of Science, Mahidol University, Bangkok, 10400 Thailand
[2]Research Centre, Faculty of Medicine, Ramathibodi Hospital, Bangkok, 10400 Thailand
[3]Department of Orthopedics, Faculty of Medicine, Ramathibodi Hospital, Bangkok, 10400 Thailand
[4]Department of Veterinary Pathology, Faculty of Veterinary Science, Chulalongkorn University, Bangkok, 10330 Thailand

Address correspondence and reprint request to: Warinkarn Hemstapat, Department of Pharmacology, Faculty of Science, Mahidol University, Bangkok Thailand.
E-mail address: warinkarn.hem@mahidol.ac.th

Abstract

Mesenchymal stem cell (MSC)-based therapy has been received a lot of attention as a promising strategy for the treatment of a full-thickness articular cartilage defect, in which bone marrow derived mesenchymal stem cells (BM-MSCs) has been one of the most commonly used sources of MSCs. However, the focus has recently been shifted to adipose tissue-derived mesenchymal stem cells (ASCs). The chondrogenic potential of ASCs extracted from both infrapatellar fat pad (IF-ASCs) and subcutaneous adipose tissues (SC-ASCs) harvested from the knee of OA patients has recently been investigated and compared *in vitro*. In this study, we investigated the chrondrogenic differentiation characteristics of scaffold free cartilage constructs derived from IF-ASCs and SC-ASCs after implantation into an osteochondral defect of the rat knee for 4 weeks. The results showed that scaffold free cartilage constructs derived from both sources were stained positive for safranin-O and toluidine blue as well as immunostaining for collagen type II, confirming their chondrogenic differentiation ability. In addition, the results from histological grading score revealed that after implantation for 4 weeks, the chondrogenic differentiation characteristics of these cartilage constructs still remained and no significant difference between them were observed. These preliminary finding suggested that the chondrogenic potential of these scaffold free cartilage constructs derived from IF-ASCs and SC-ASCs can be preserved 4 weeks post-implantation. However, further study for longer duration is required to confirm this result.

Keywords: Rat model of osteochondral defect, adipose-derived mesenchymal stem cell, infrapatellar fat pad, subcutaneous adipose tissues, chondrogenic differentiation

Introduction

It is well accepted that cartilage injury when left untreated; it can increase a patient's chance of later developing osteoarthritis (OA). Recently, cell-based therapy has increasingly received a lot of attention as one of the alternative strategies to repair full-thickness cartilage defects. For instance, bone marrow-derived mesenchymal stem cells (BM-MSCs) are the most commonly used cells for repairing bone and cartilage defects[1]. In addition, adipose tissue-derived mesenchymal stem cells (ASCs) have been reported to serve as superior alternative to BM-MSCs for the cartilage tissue engineering due to their abundance, ease of harvesting and less invasive than performing bone marrow extraction[2]. More recently, an *in vitro* study comparing the sources of ASCs obtained from infrapatellar fat pad (IF-ASCs) and subcutaneous adipose tissues (SC-ASCs) have been reported, in which both of them were demonstrated to exhibit chondrogenic differentiation potentials[3]. However, whether their differentiation potentials can be retained after implantation in an *in vivo*, this was the subject to be investigated in the present study.

Materials and Methods

Preparation of 3D cartilage constructs

Human ASCs were harvested from two different sources, including infrapatellar fat pad (IF) and subcutaneous adipose tissue (SC). IF was collected from patients who underwent total knee arthroplasty, while SC was obtained by liposuction from patients who received cosmetic surgery. After harvesting, ASCs from both sources were isolated. To prepare 3D cartilage constructs, adipose tissues were digested by collagenase type I to obtain ASCs. These cells were then cultured in completed medium containing DMEM-low glucose medium supplemented with 10% fetal bovine serum, 1% penicillin/streptomycin, 1% L-glutamine and 0.1% fungizome until 3ʳᵈ passages. Prior to implantation, the characteristic of ASCs was confirmed, in which immunophenotypes including CD73, CD90, CD105, CD 34, CD45 and HLA-DR were evaluated by using flow cytometry. In addition, ASCs' karyotype as well as differentiation abilities to chondrogenic-, adipogenic- and osteogenic-ASCs were also determined. To obtain the cartilage construct, approximately 1.0×10^6 IF-ASCs and SC-ASCs were used and cultured in chondrogenic media for 21 days as previously described[4]. The cartilage construct were then divided into 2 parts. The first part was used to confirm the chondrogenic differentiation characteristic, while another part was used for implantation in the osteochondral defect of the rat.

Animal study: 3D cartilage constructs implantation in osteochondral defect rat model

Six weeks old male Wistar rats (160- 180 g) were obtained from National Laboratory Animal Center, Mahidol University, Thailand. Ethical approval of this study was obtained and approved by the Faculty of Science, Mahidol University Animal Care and Use Committee. Animals were housed in pair in a temperature-controlled room (20 ± 2ºC), maintained at humidity 60 ± 10%, and a 12 h/12 h dark-light cycle. Standard laboratory rat food and water were supplied *ad libitum*. Wistar rats were divided into two groups: 1. Osteochondral defect

group implanted with IF-ASCs (n=2), 2. Osteochondral defect group implanted with SC-ASCs (n=3). The osteochondral defect was created as previously described with some modifications[5]. Briefly, a medial parapatellar incision was made on the right knee joint of the animal. The patellar was dislocated laterally to expose a better access to the articular surface of the femoral condyle. Two full-thickness osteochondral defects with a diameter of 1.2 mm and 3 mm depth were created by using Kirschner wires (K-wires) to drill on both medial and lateral femoral condyles until reaching the bone marrow region. IF-ASCs were then implanted into medial femoral condyle whereas SC-ASCs were implanted into lateral femoral condyle. After 4 weeks post-implantation, the animals were euthanized and both knee joints were collected for further histological analysis.

Histological and immunohistochemical analyses

Cartilage constructs and femoral condyles were preserved in 10% buffered formalin for 2 days. Femoral condyles, but not cartilage constructs were then decalcified with 10% EDTA for 2 weeks followed by paraffin embedding and sectioning. Sections were then stained with Hematoxylin and Eosin (H&E) to detect general morphology as well as safranin-O/fast green and toluidine blue to detect proteoglycan contents of matrix. In addition, immunohistochemical staining for collagen type-II (Merck Millipore, Germany) was also assessed by using standard immunochemistry techniques as previously described[6,7]. To assess the tissue regeneration, histological slides were evaluated in semi-quantitative fashion according to the following criteria established in Table 1. Criteria for evaluation were based on previously described with some modifications[8].

Table 1. Semi-quantitative criteria for evaluating the regenerated tissue in the repaired osteochondral defect.

Filing of defect in percentage	Grading	Matrix staining : Toluidine blue	Grading
100	0	Normal	0
75	1	Reduced	1
50	2	Significantly reduced	2
25	3	Faint	3
0	4	None	4
Reconstitution of osteochondral junction	**Grading**	**Matrix staining : Immunohistochemistry**	**Grading**
Yes	0	High	0
Almost	1	Moderate	1
Not close	2	None	2
Matrix staining : Safranin-O staining	**Grading**	**Cell morphology**	**Grading**
Normal	0	Normal	0
Reduced	1	Mostly hyaline and	1
Significantly reduced	2	fibrocartilage	
Faint	3	Mostly fibrocartilage	2
None	4	Some fibrocartilage but most non-chondrocytic cells	3
		Non-chondrocytic cells only	4

Statistical analysis

All data were expressed as the mean and standard deviation (mean ± SD). Semi-quantitative histology scores were compared using non-parametric Mann Whitney tests and GraphPad Prism software (version 6.0). The p value was set at $p < 0.05$ for the significant different between two groups.

Results and Discussion

*Preparation of 3D cartilage constructs*

Both IF-ASCs and SC-ASCs expressed the positive marker including CD73, CD90, CD105, but not CD 34, CD45 and HLA-DR. In addition, ASCs' karyotypes were found to be normal and their ability to differentiate into chondrogenic, adipogenic and osteogenic lineage were also observed (unpublished work; data not shown).

*Histology and immunohistochemistry of cartilage construct*

After 21 days of culture in chondrogenic media, both IF-ASCs and SC-ASCs cartilage constructs displayed round with white opaque color in which more solid texture was noted for IF-ACSs. Histologically, staining of these cartilage constructs with H&E revealed cells with rounded appearance and they were surrounded by an abundant extracellular matrix. In addition, the results also revealed that both cartilage constructs stained positively for safranin-O and toluidine blue (data not shown) as well as immunostained with collagen type II (Figure 1). This result suggested that the cartilage constructs obtained from both sources can produce proteoglycans matrix and collagen type II, which are the main components in the articular cartilage, confirming their chondrogenic differentiation ability. Similar results of both cartilage constructs were also observed after implantation in the rat femoral condyles for 4 weeks as indicated by a positive staining for safranin-O and toluidine blue (data not shown) as well as immunostained with collagen type II (Figure 2). Additionally, cartilage lacunae were also observed in the implanted constructs (Figure 2), suggesting the presence of mature chondrocytes.

Moreover, the present data also showed that the mean histological scores for IF-ASCs and SC-ASCs were 12.2 ± 3.2 and 10.3 ± 1.5, respectively, in which no significant difference between these constructs were observed (Figure 3). Therefore, this present study suggested that the cartilage constructs derived from both IF-ASCs and SC-ASCs can retain their chondrogenic differentiation characteristics after 4 weeks implantation such that they exhibited similar chrondrogenic ability regardless of their source of origin.
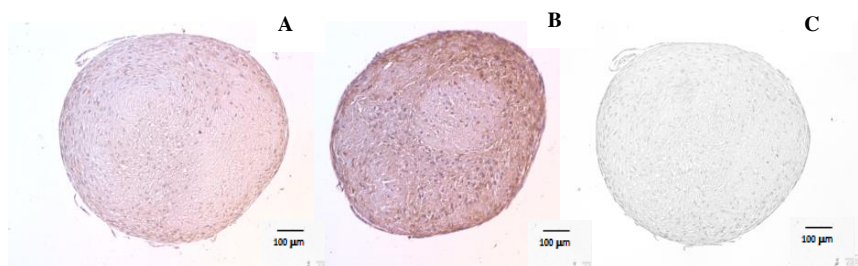
Figure 1. Immunohistochemical staining of collagen type II. Representative 3D cartilage constructs derived from IF-ASCs (A), SC-ASCs (B) and IgG staining as controls (C).
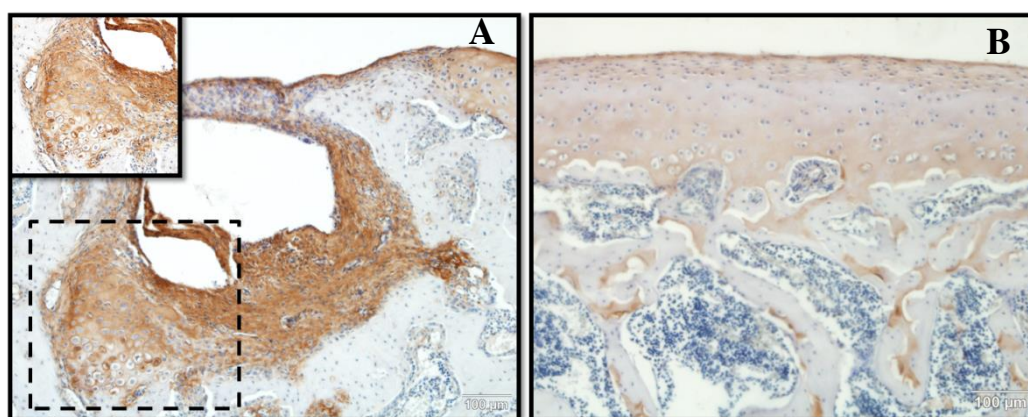
Figure 2. Immunohistochemical staining for collagen type II of implanted cartilage constructs derived from SC-ASCs (A) in osteochondral defects at 4 weeks post-implantation and normal cartilage (B). Black dotted line indicated the area of cartilage lacunae where the mature chondrocytes were observed.
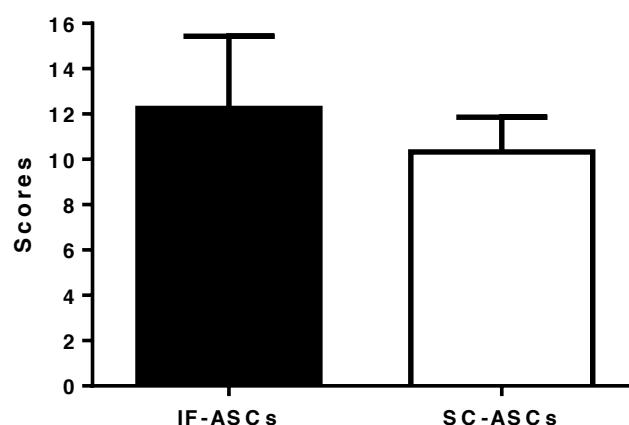
Figure 3. Histological grading scores of the regenerated tissue in the repaired osteochondral defect. Results from IF-ASCs (n = 2) and SC-ASCs (n = 3) groups are shown. All data were expressed as the mean and standard deviation (mean ± SD). Semi-quantitative histology score were compared using non-parametric Mann Whitney tests. The p value was set at $p < 0.05$ for the significant different between two groups.

Conclusion

This study demonstrated that the cartilage construct derived from both IF-ASCs and SC-ASCs can retain their chondrogenic differentiation characteristics after implantation into an osteochondral defect of the rat for 4 weeks. Although, this study is a proof of concept experiment showing cartilage constructs derived from adipose tissue either from infra-patellar fat pad or from subcutaneous source can maintain their chondrogenic phenotype *in vivo,* the further investigation in an appropriate cartilage injury model should be done to determine their potential for cartilage regeneration.

Acknowledgements

References

1. Kristjansson B, Honsawek S. Current perspectives in mesenchymal stem cell therapies for osteoarthritis. Stem cells Int. 2014; 1-13.
2. Peng L, Jia Z, Yin X, Zhang X, Liu Y, Chen P, et al. Comparative analysis of mesenchymal stem cells from bone marrow, cartilage, and adipose tissue. Stem Cells Dev. 2008; 17(4): 761-73.
3. Lopa S, Colombini A, Stanco D, de Girolamo L, Sansone V, Moretti M. Donor-matched mesenchymal stem cells from knee infrapatellar and subcutaneous adipose tissue of osteoarthritic donors display differential chondrogenic and osteogenic commitment 2014. Eur Cells Mater. 2014; 27: 298-311.
4. Ye K, Felimban R, Traianedes K, Moulton SE, Wallace GG, Chung J, et al. Chondrogenesis of infrapatellar fat pad derived adipose stem cells in 3D printed chitosan scaffold. PloS one. 2014; 9(6): 1-9.
5. Dausse Y, Grossin L, Miralles G, Pelletier S, Mainard D, Hubert P, et al. Cartilage repair using new polysaccharidic biomaterials: macroscopic, histological and biochemical approaches in a rat model of cartilage defect. Osteoarthritis and cartilage. 2003; 11(1): 16-28.
6. Otsuka Y, Mizuta H, Takagi K, Iyama K, Yoshitake Y, Nishikawa K, et al. Requirement of fibroblast growth factor signaling for regeneration of epiphyseal morphology in rabbit full-thickness defects of articular cartilage. Dev Growth Differ. 1997; 39(2): 143-56.
7. Anraku Y, Mizuta H, Sei A, Kudo S, Nakamura E, Senba K, et al. The chondrogenic repair response of undifferentiated mesenchymal cells in rat full-thickness articular cartilage defects. Osteoarthritis and cartilage. 2008;16(8):961-4.
8. Pineda S, Pollack A, Stevenson S, Goldberg V, Caplan A. A semiquantitative scale for histologic grading of articular cartilage repair. Acta Anat (Basel). 1992; 143(4): 335-40.

RESEARCH ARTICLE

Comparative study on hot flushes model in both sexes of rats: a preliminary study

Panida Chamawan[1], Krittiya Thisayakorn[2], Srichan Phornchirasilp[1]

[1]*Pharmacology and Biomolecular Sciences Program, Department of Pharmacology, Faculaty of Pharmacy, Mahidol University, Bangkok, Thailand*
[2]*Pharmaceutical and Natural Product Department (PNPD), Thailand Institute of Scientific and Technological Research (TISTR), Pathum Thani, Thailand*

Address correspondence and reprint request to: Department of Pharmacology, Faculty of Pharmacy, Mahidol University, Bangkok, Thailand.
E-mail address: panida.cha@mahidol.ac.th

Abstract

Hot flush is a symptom that relates with sex hormone deficiency. It is the reflection of a disorder of hypothalamic thermoregulatory mechanisms. This symptom can be found in both postmenopausal women and andropause men and may disturb their quality of life. The hallmarks of hot flushes include cutaneous vasodilatation and increase in peripheral blood flow. The objective of this study was to evaluate the effects of vasodilator substances on hot flushes simulation in both female and male Wistar rats. Calcitonin gene-related peptide (CGRP) (10 μg/kg) as the potent vasodilator was intravenously (i.v.) injected in both sexes of rats. Leuprorelin acetate (1 mg/kg), the potent GnRH-analogue, was also subcutaneously (s.c.) injected in both sexes of rats. Tail skin temperature (TST) and core body temperature were measured. CGRP significantly elevated female's tail skin temperature when compared with saline-treated female rats. While, leuprorelin acetate significantly elevated male's tail skin temperature when compared with saline-treated male rats. The results obtained from this study may be used to develop an animal model for screening the substances that are proposed to relieve hot flushes in human.

Keywords: Hot flush, Calcitonin gene-related peptide (CGRP), GnRH-analogue, Leuprorelin acetate, tail skin temperature, core body temperature

Introduction

Hot flushes are the symptoms that mostly been found in postmenopausal women and andropause men. These symptoms generally begin with a sudden outpouring of sweat, and then increasing in heart rate and peripheral blood flow resulting in skin temperature elevation.[1] Vasomotor symptoms in postmenopausal women result from a disorder of hypothalamic thermoregulatory mechanisms that link to the lack of sex hormone. The thermoneutral zone is narrow down in postmenopausal women caused by losing of thermoregulation of autonomic thermoeffectors such as vessels, muscle, and skin.[1] Hot flushes relate with an imbalance of heat dissipated activation and heat loss mechanisms. Tail skin temperature (TST) is often used to

represent cutaneous vasodilatation in rat model. Rat's tail is a primary exchange organ because it has an extensive vascularization, a lack of fur, and a high surface area to volume ratio.[2] Using vasodilator substances can induce vasodilatation in order to mimic hot flushes in animal models. Calcitonin gene-related peptide (CGRP) is a 37-amino-acid, potent vasodilator neuropeptide and has been found abundant in urine[3] and plasma[4] in postmenopausal women. Leuprorelin acetate is a gonadotropin releasing hormone receptor agonist (GnRH-analogues) that suppresses luteinizing hormone (LH) and follicle stimulating hormone (FSH) from anterior pituitary gland, and subsequently suppresses sex hormone production. It can cause skin temperature increasing in patients whom treated with chronic leuprorelin administration such as prostate cancer, endometriosis, central precocious puberty, and polycystic ovary syndrome. The activation of these thermoeffectors can be used to mimic hot flushes in animal model. Therefore, the aim of this study was to evaluate the effects of vasodilator substances on hot flushes simulation in both sexes of rats.

Materials and Methods

Handling and testing in animal were in accordance with the "Guidelines for the care and use of laboratory animals" approved by the Thailand Institute of Scientific and Technological Research (TISTR) Animal Care and Use Committee, Pathum Thani, Thailand

Animals

Male Wistar rats weighting 300-350 g and female Wistar rats weighting 200-250 g were purchased from National Laboratory Animal Center, Mahidol University, Salaya, Nakornpathom. The rats were maintained on 12 h light/ dark schedule at a temperature of 23±1 °C, with free access to food and water. All measurements of tail skin and core body temperatures were performed between 08.00-12.00 h, and the room temperature was maintained at 23±1 °C throughout the recording period.

Drug and reagents

Rat αCGRP was purchased from Sigma Aldrich (USA) and dissolved in saline on the day of use. Leuprorelin acetate 3.75 mg was purchased from Takeda (Japan) and dissolved in solvent that accompanied with a prefilled syringe.

Measurement of αCGRP-induced increasing of tail skin temperature

10 µg/ml rat αCGRP was intravenously injected at dose of 10 µg/kg of body weight in both male and female rats. A digital thermometer probe (TL8009, Keyan Technology Co. Ltd., China) was taped to the dorsal surface of the tail about 3 cm from its tip. The mean tail skin temperature was measured at 10-min intervals throughout the 120-min experiment. The core body temperature was anally measured by mercury thermometer (CRW-23A, Jianggsu Yuyue Medical Instruments Co. Ltd., China) at 30-min intervals throughout the experiment. These data were expressed as △ tail skin temperature; whereas the average tail skin temperature in each corresponding period after rat CGRP administration – the basal tail skin temperature in each rat.

*Measurement of leuprorelin-induced increasing of tail skin temperature*

3.75 mg/ml leuprorelin acetate was subcutaneously injected at dose of 1 mg/kg of body weight daily in both male and female rats. A digital thermometer probe (TL8009, Keyan Technology Co. Ltd., China) was taped to the dorsal surface of the tail about 3 cm from its tip. The mean tail skin temperature was measured everyday at 09.00 AM or in the morning throughout the 14-day experiment. The core body temperature was measured by mercury thermometer (CRW-23A, Jianggsu Yuyue Medical Instruments Co. Ltd., China). These data were expressed as Δ tail skin temperature as described above.

Statistical analysis

All data represent the mean ± S.E.M. Statistical analysis was performed using one-way analysis of variance (ANOVA) followed by Dunnett's test. A value of $P<0.05$ was considered for statistical significance.
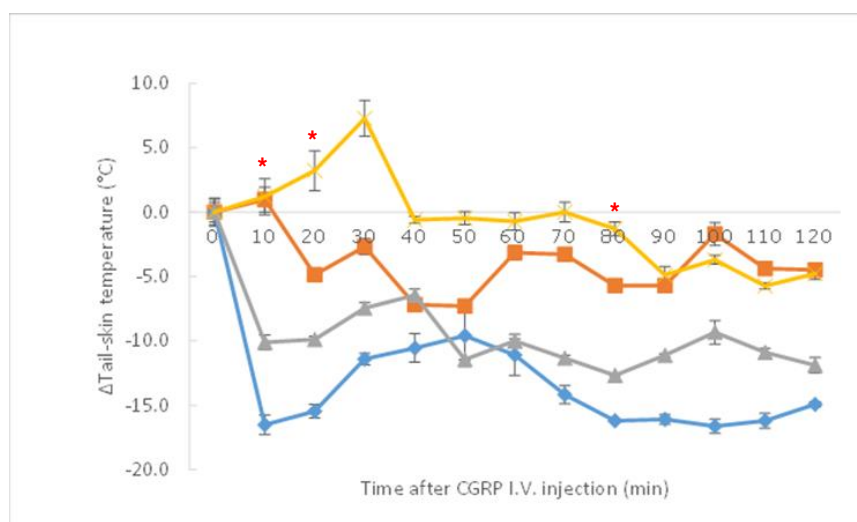
Figure 1. Effects of αCGRP on tail skin temperature change in both sexes of rats. Each value is expressed as the mean ± S.E.M. (n=3). Significance with Dunnett's test following a one-way ANOVA [*p < 0.05*] vs. saline-treated rats. [■- control male rats, ▲- CGRP male rats, ◆-control female rats, ✕- CGRP female rats, * significant when p< 0.05]
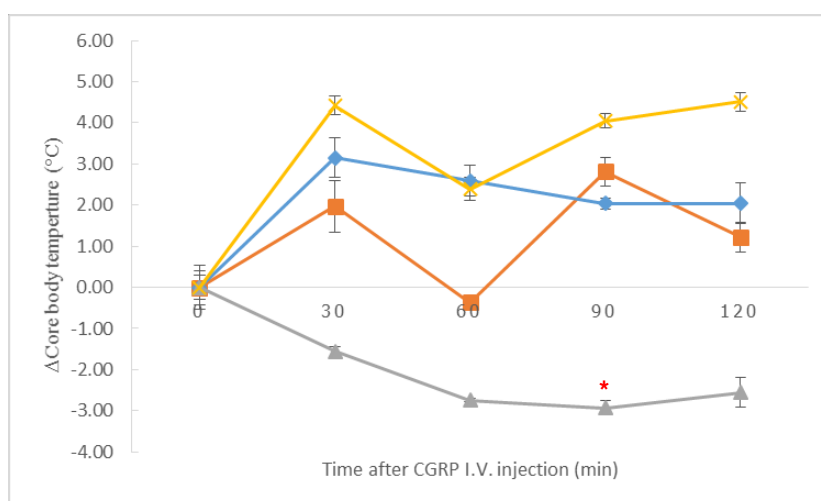
Figure 2. Effects of CGRP on core body temperature change in both sexes of rats. Each value is expressed as the mean ± S.E.M. (n=3). Significance with Dunnett's test following a one-way ANOVA [p < 0.05] vs. saline-treated rats. [■- control male rats, ▲- CGRP male rats, ◆-control female rats, ×-CGRP female rats, * significant when p< 0.05]
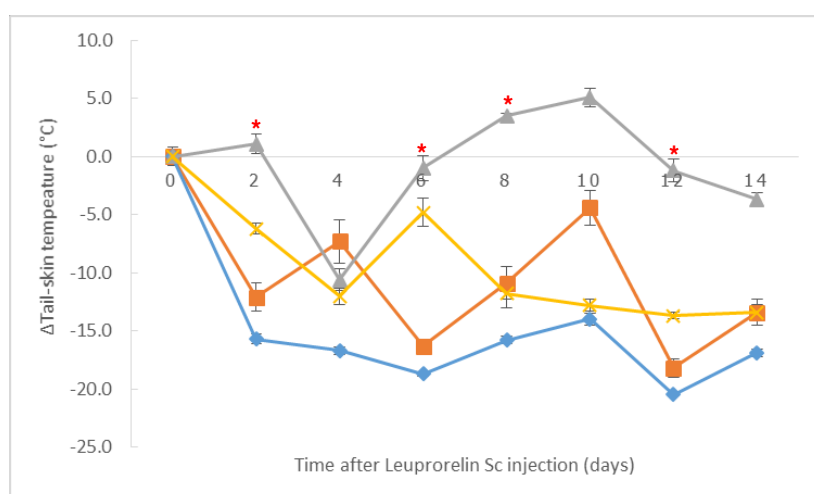
Figure 3. Effects of leuprorelin on tail skin temperature change in both sexes of rats. Each value is expressed as the mean ± S.E.M. (n=3). Significance with Dunnett's test following a one-way ANOVA [p < 0.05] vs. saline-treated rats. [■- control male rats, ▲- leuprorelin male rats, ◆-control female rats, ×-leuprorelin female rats, * significant when p< 0.05]
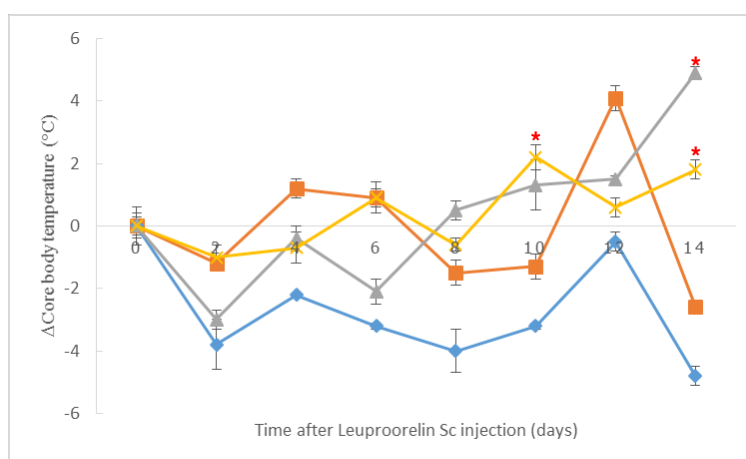
Figure 4. Effects of leuprorelin on core body temperature change in both sexes of rats. Each value is expressed as the mean ± S.E.M. (n=3). Significance with Dunnett's test following a one-way ANOVA [$p < 0.05$] vs. saline-treated rats. [■- control male rats, ▲- leuprorelin male rats, ◆-control female rats, ✕-leuprorelin female rats, * significant when $p < 0.05$]

Results

Effects of αCGRP on tail skin and core body temperatures

20 minutes after injection, αCGRP at 10 µg/kg significantly ($p < 0.05$) elevated the maximal tail skin temperature in female, but not in male rats when compared with saline-treated group (Fig. 1). While, the △ core body temperature in every group was not statistically significant as shown in Fig. 2.

Effects of leuprorelin acetate on tail skin and core body temperatures

Maximal tail skin temperature in male rats was significantly ($p < 0.05$) elevated after 8 days of leuprorelin acetate injection, but not in female rats when compared with saline-treated group (Fig. 3). Leuprorelin acetate increased △ core body temperature in leuprorelin-treated male and female groups only at the end of the trial that exhibited in Fig. 4.

Discussion

In the previous study,[5,6] CGRP has been shown to synergize the responses of ovariectomized animal model for increasing peripheral blood flow and elevating tail skin temperature. In this study, we demonstrated that αCGRP significantly elevated tail skin temperature in intact female, but not in male rats. These results suggest that the expression of αCGRP and its receptor in intact female rats may sensitive to rat αCGRP more than in male rats.[7] This substance is probably useful to be applied in perimenopause female rats setting as a non-invasive hot flush model that can be used in the screening for hot flush-relieving drugs.

Leuprorelin acetate (known as leuprolide acetate), a potent gonadotropin releasing hormone receptor (GnRHR) agonist, was continuously administered. It acted as an inhibitor of gonadotropin secretion leading to sex hormone deficiency. This manipulation resulted in tail

skin temperature elevation. In male rats, tail skin temperature decreased after 4 days of leuprorelin acetate injection. Possibly, it is a result of "flare phenomenon"[8], which is the effect of the increasing level of testosterone during the first 4 days of administration, and then the tail skin temperature was decreased to reach castrate levels in 8 days when leuprorelin acetate was still continuously administered.

The changes in core body temperature in every αCGRP-treated group were not statistically significant, while leuprorelin acetate increased Δ core body temperature in both leuprorelin-treated male and female groups at the end of the trial (day 10-14 of the experiment). Although, leuprorelin acetate increased sex hormone initially, continuous administration produces an inhibition of the hypophyseal-gonadal axis and a suppression of circulating LH, FSH, and sex hormone levels within 2-4 weeks.[9] Since leuprorelin inhibited sex hormone production, it caused losing of central thermoregulation.[10, 11]

Conclusion

We demonstrated that αCGRP and leuprorelin acetate may possibly be used to elevate tail skin temperature in female and male rats, respectively. However, further studies are still needed to confirm the results of this study in order to develop an animal model for screening of hot flush-relieving substances in human.

Acknowledgements

References

1. Freedman RR, Physiology of hot flashes. Am J Hum Biol. 2001; 13:453-64.
2. Gordon CJ, Thermal biology of the laboratory rat. Physiol Behav. 1990; 47:963-91.
3. Wyon Y, Frisk J, Lundeberg T, Theodorsson E, Hammar M. Postmenopausal women with vasomotor symptoms have increased urinary excretion of calcitonin gene-related peptide. Maturitas. 1998; 30:289-94.
4. Wyon YA, Spetz AC, Theodorsson GE, Hammar ML. Concentrations of calcitonin gene-related peptide and neuropeptide Y in plasma increase during flushes in postmenopausal women. Menopause. 2000; 7:25-30.
5. Kawasaki H, Takasaki K, Saito A, Goto K. Calcotonin gene related peptide acts as novel vasodilator neurotransmitter in mesenteric resistance vessels of the rats. Nature. 1988; 335:164-7.
6. Noguchi M, Yazurihara M, Ikarashi Y. Effects of the vasoactive neuropeptides calcitonin gene-related peptide, substance P and vasoactive intestinal polypeptide on the skin temperature in ovariectomized rats. Neuropeptides. 2002a; 175:327-32.
7. Stucky NL, Gregory E, Winter MK, He YY, Hamilton ES, MaCarson KE, and Berman NEJ. Sex Differences in Behavior and Expression of CGRP-Related Genes in a Rodent Model of Chronic Migraine. Headache. 2011; 51(5):674-92.
8. Wilson AC, Meethal SV, Bowen RL, Atwood CS. Leuprolide acetate: a drug of diverse clinical applications. Expet Opin Investig Drugs. 2007; 16(11):1-13.

9. Schally AV, Comura-Schally AM, Nagy A. Hypothalamic hormones and cancer. Front Neuroendocrinol. 2001; 22:248-91.

10. Katsrup E. Drug facts and Comparisons. St. Louis: Wolters Kluwer; 2003.

11. Lacy C, Armstrong L, Goldman M, Lance L, editors. Drug Information Handbook. Cleveland: Lexi-Comp, Inc.; 2003.

RESEARCH ARTICLE

Cefazolin impregnated oxidized regenerated cellulose/polycaprolactone composite for using as antibacterial synthetic dural substitute

Arunnee Sanpakitwattana[1], Jintamai Suwanprateeb[2], Waraporn Suvannapruk[2], Sorayouth Chumnanvej[3], Warinkarn Hemstapat[1]

[1]*Department of Pharmacology, Faculty of Science, Mahidol University, Bangkok 10400 Thailand*
[2]*Biomaterials Laboratory, Biomedical Engineering Research Unit, National Metal and Materials Technology Center (MTEC), Pathumthani 12120, Thailand*
[3]*Neurosurgical Unit, Surgery Department, Faculty of Medicine Ramathibodi Hospital, Bangkok 10400 Thailand*

Address correspondence and reprint request to: Warinkarn Hemstapat, Department of Pharmacology, Faculty of Science, Mahidol University, Bangkok Thailand.
E-mail address: warinkarn.hem@mahidol.ac.th

Abstract

A local and sustained antibiotics delivery to the surgical site has been foreseen as a way to help preventing post-neurosurgical infection as well as lowering the systemic adverse effects resulted from higher dose intravenous injection. Recently, a novel synthetic dural substitute which was developed by the combination of oxidized regenerated cellulose (ORC) and polycaprolactone (PCL) has offered several advantages including low cost, simple production as well as similar mechanical properties to natural human dura mater. It was hypothesized that this synthetic dural substitute could be modified to act as antibiotic carrier for localized release application. In this study, cefazolin impregnated ORC/PCL composite was prepared by incorporating cefazolin at the concentration of 25, 50 and 100 mg mL^{-1} in N-methyl-2-pyrrolidone which was used as solvent for PCL in the solution impregnation process. It was found that the incorporation of cefazolin resulted in the samples having greater density, but lower thickness compared to the ORC/PCL composite alone. Tensile modulus was observed to increase with increasing cefazolin concentration. Inversely, tensile strength and strain at break were slightly lower than those of ORC/PCL composite. All the samples displayed biphasic releasing profile including burst release of high amount of cefazolin initially and followed by a continuous and small release afterward for at least ten days which was the maximum periods in this study. Cefazolin released concentration was found to still be above the minimum inhibition concentration against *S. aureus*.

Keywords: synthetic dural substitute, antibiotic carrier, cefazolin, drug release

Introduction

Post-neurosurgical infection could lead to severe consequences including meningitis, brain abscess, and intracranial infection[1]. With this concern, a dural substitute that can provide local and sustained release of antibiotic to surgical site would be beneficial to prevent post-

neurosurgical infection[2]. Moreover, this local release could minimize the administration of higher dose intravenous antibiotics injection which lowering systemic adverse effects for patient[3]. Cefazolin is an antibiotic which is considered as the first line drug of choice because of its most effectiveness against *Staphylococcus aureus* (*S. aureus*) and Coagulase-negative staphylococci (CoNS) which are the major causes of the post-neurosurgical infection[4]. Recently, a novel dural substitute based on the combination of oxidized regenerated cellulose (ORC) and polycaprolactone (PCL) was successfully developed which displayed similar properties to those of natural human dura mater[5]. This study was aimed to fabricate and to characterize the physical and mechanical properties of cefazolin impregnated ORC/PCL for possibly using as an antibacterial dural substitute, which provide both tissue regeneration and initial localized antibiotic prophylaxis. Cefazolin releasing profile from the developed samples was also investigated.

Materials and Methods

Raw Materials

All the raw materials including polycaprolactone ($M_w \sim 80,000$, Sigma-Aldrich), oxidized regenerated cellulose (Surgicel®, Ethicon Inc.) and N-methyl-2-pyrrolidone (Pharmasolve™, Ashland Inc.) were purchased and used in the as-received form. The antibiotic used was cefazolin sodium (Fazolin®, Siam Bheasach Co., Ltd.) and was supplied in the powder form.

Sample preparation

Formulation P20 of ORC/PCL composite (20 g in 100 ml of N-methyl-2-pyrrolidone) was selected to be employed in this study based on the previous result, in which this formulation was easy to prepare and its mechanical properties were found to be in the range of natural human dura mater[5]. ORC/PCL composites were fabricated by solution infiltration process by coating prepared PCL solutions using a blade onto both sides of oxidized regenerated cellulose knitted sheet and followed by recoating the PCL solution on one side of the infiltrated sheet. Various concentrations of cefazolin (25, 50 and 100 mg mL^{-1}) were dissolved in N-methyl-2-pyrrolidone making PCL solutions used to prepare cefazolin impregnated composite (designated P20_25, P20_50 and P20_100, respectively) instead of a typical drug-free PCL solution (P20). After processing, the samples were washed in water and dried in the oven at 40°C to remove the solvent.

Characterizations

Bulk density of the samples was determined by dividing the weight of the sample by its volume which was measured by a precision balance (Sartorious) and a vernier caliper (Mitutoyo), respectively. The volume each sample was calculated by multiplying the width, the length and the thickness. Tensile testing was carried out by a universal testing machine (Instron 55R4502) equipped with a 10 kN load cell. All tests were carried out at 23 °C and 50

% RH and a constant crosshead speed of 50 mm min^{-1}. Tensile properties such as tensile modulus, tensile strength and tensile strain at break were then determined.

Cefazolin release determination

Preliminary investigation of the cefazolin released profile was carried out by cutting the samples into square sheets (1×1 cm^2). Each sample was placed in a plastic bottle containing 5 ml of deionized (DI) water and stored in an incubator at 37°C. At every 24 hrs, the solution was collected and filtered with syringe filter. The sample was removed, slightly blotted with paper, and placed in new bottle containing fresh DI water. The absorbance of the solution was then measured by UV-VIS spectrophotometer (Spectrum measurement) at a wavelength of 270 nm and compared with a standard curve to quantify the amount of cefazolin. The test was carried out in triplicate for up to ten days and the results were reported as mean values ± standard deviation (SD).

Statistical Analysis

All data were expressed as the mean and standard deviation (mean ± SD). Statistical analysis was performed using GraphPad Prism (version 6). Statistical significance was determined using one-way analysis of variance (ANOVA), followed by Tukey's multiple comparisons test. The *p* value was set at $p < 0.05$ for the significant difference between groups.

Results and Discussion

Table 1 showed the comparison of bulk density and thickness of fabricated samples. It was found that bulk density of all cefazolin impregnated ORC/PCL composites was greater than that of ORC/PCL composite, but the thickness was lower. However, density and thickness of the cefazolin impregnated composite were relatively unchanged with the increase in concentration of cefazolin used. The differences between ORC/PCL composite and cefazolin impregnated ORC/PCL composites were thought to be resulted from the amount of incorporated cefazolin itself in couple with the effect of cefazolin on the increase in viscosity of the PCL solution due to the restriction of polymer chain movement[6]. Figures 1-3 showed tensile properties of cefazolin impregnated ORC/PCL composites compared to ORC/PCL composite. Tensile modulus was observed to increase with increasing cefazolin concentration in the sample. Tensile strength and strain at break of all cefazolin impregnated composites were lower than those of ORC/PCL composite, but were in the similar ranges regardless of the concentration of cefazolin. These results indicated that the incorporation of cefazolin in the ORC/PCL composites caused the composites to be stiffer and less ductile. However, tensile properties of all cefazolin impregnated composites were still within the range of human dura mater[7-9] (11.2-171.5 MPa, 1.3-27.1 MPa and 16.0-49.7% for tensile modulus, strength and strain at break, respectively).

Table 1. Bulk density and thickness of the fabricated samples.

Samples	Bulk Density (g cm^{-3})	Thickness (mm)
P20	0.519 ± 0.09	0.88 ± 0.04
P20_25	0.663 ± 0.04	0.69 ± 0.02
P20_50	0.632 ± 0.01	0.67 ± 0.02
P20_100	0.626 ± 0.05	0.65 ± 0.01
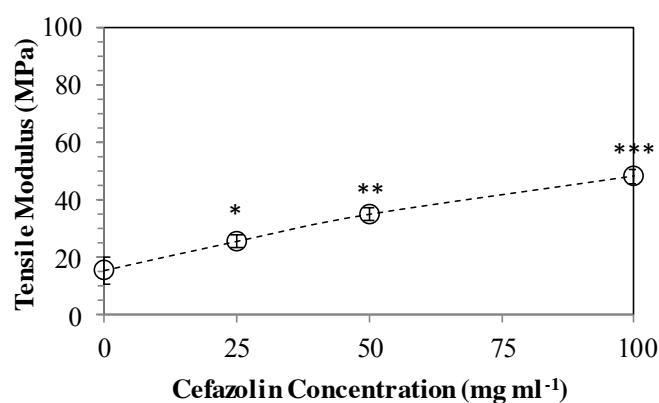
Figure 1. Influence of cefazolin concentration incorporated in the ORC/PCL composite on tensile modulus. Samples that do not share the same symbols are significantly different (p<0.05).
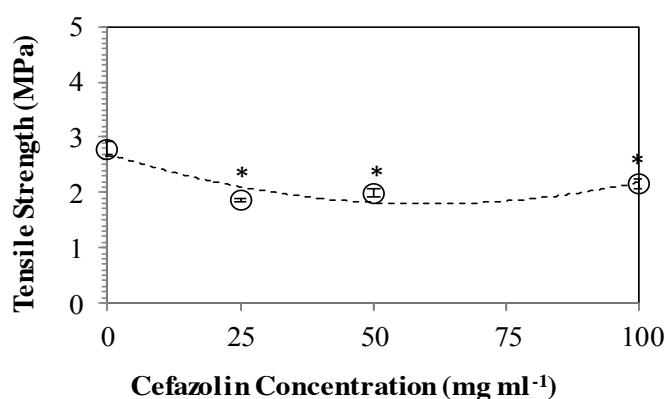
Figure 2. Influence of cefazolin concentration incorporated in the ORC/PCL composite on tensile strength, *p<0.05 versus P20 group.
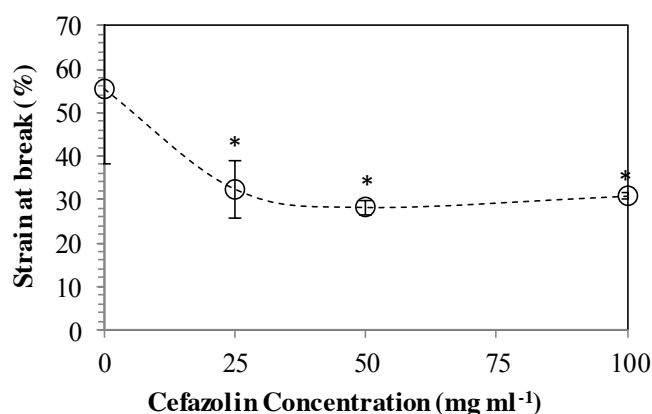
Figure 3. Influence of cefazolin concentration incorporated in the ORC/PCL composite on tensile strain at break, *p<0.05 versus P20 group.

Figure 4 showed the releasing characteristic of the cefazolin impregnated ORC/PCL composites. It could be seen that all the samples displayed similar releasing profile including burst release of high amount of cefazolin initially and followed by a significantly small, but slow release afterward. The amount of cefazolin burst release increased with increasing the cefazolin concentration in the processing step. The lowest concentration of cefazolin in media during a slow release after day 1 was found to be about 1.0 µg mL-1 per day which was still above the minimum inhibition concentration) 0.9 µg mL-1 against S. aureus10. The cefazolin released profiles tended to follow the power law model, for example, Korsmeyer-Peppas model11. The release pattern could be related to the fast release of the cefazolin absorbed on the sample surfaces and from dissolved ORC component during the initial period and followed by a slow release of the drug from the PCL matrix.
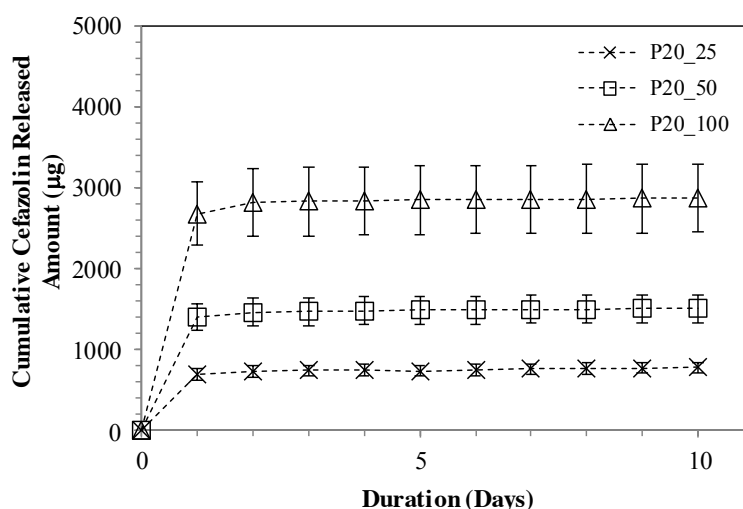
Figure 4. Cumulative antibiotic releasing profile of three cefazolin impregnated ORC/PCL composites.

Conclusion

Cefazolin impregnated ORC/PCL composites were successfully fabricated which still had the physical and mechanical properties in the range of natural dura mater. Cefazolin could be loaded and continuously released from the composites in DI water for at least ten days displaying biphasic releasing profile. These results indicated the potential use of cefazolin impregnated ORC/PCL composites as antibacterial synthetic dural substitute. However, the study for longer duration and in other media, for example, artificial cerebrospinal fluid will be further investigated for evaluating their effectiveness.

Acknowledgements

References

1. Bassetti M, Righi E, Astilean A, Corcione S, Petrolo A, Farina EC, et al. Antimicrobial prophylaxis in minor and major surgery. Minerva Anestesiol. 2015; 81(1):76-91.
2. Wang G, Liu SJ, Ueng SW, Chan EC. The release of cefazolin and gentamicin from biodegradable PLA/PGA beads. Int J Pharm. 2004; 273 (1-2):203-12.
3. Wang H, Dong H, Kang CG, Lin C, Ye X, Zhao YL. Preliminary exploration of the development of a collagenous artificial dura mater for sustained antibiotic release. Chin Med J (Engl). 2013; 126 (17):3329-33.
4. Liu W, Ni M, Zhang Y, Groen RJ. Antibiotic prophylaxis in craniotomy: a review. Neurosurgical rev. 2014; 37 (3):407-14.
5. Theeranattapong T, Luangwattanawilai T, Suwanprateeb J, Suvannapruk W, Chumnanvej S, Hemstapat W. Physical and Mechanical Characterizations of Oxidized Regenerated Cellulose/Polycaprolactone Composite for Use as a Synthetic Dura Mater. Key Engineering Materials. 2015; 659: 19-23.
6. Büyükyaylaci S, Joshi YM, Peck GE, Banker GS. Polymeric Pseudolatex Dispersions as a New Topical Drug Delivery System. In: Anderson JM, Kim SW, editors. Recent Advances in Drug Delivery Systems. New York: Plenum Press; 1984. p. 291-307
7. van Noort R, Black MM, Martin TRP, Meanley S. A study of the uniaxial mechanical properties of human dura mater preserved in glycerol. Biomaterials. 1981; 2: 41-5.
8. van Noort R, Martin TRP, Black MM, Barker AT, Montero CG. The mechanical properties of human dura mater and the effects of storage media. Clin Phys Physiol Meas. 1981; 2: 197–203.
9. Zarzur E. Mechanical properties of the human lumbar dura mater. Arq Neuropsiquiatr. 1996; 54: 455-60.
10. Ahmed SYE, Sanousi SME. Susceptibility of hospital *Staphylococcus aureus* isolates against cephalosporins using manual E-test. Journal of Natural and Medical Sciences. 2014; 15 (2): 36-43.
11. Dash S., Murthy PN, Nath L, Chowdhury P. Kinetic modeling on drug release from controlled drug delivery systems. Acta Poloniae Pharmaceutica-Drug Research. 2010; 67(3): 217-23.

RESEARCH ARTICLE

Molecular analysis of *Pfmrp1*, *Pfnhe1*, *Pfmc-2tm* and *Pfgch1* in *Plasmodium falciparum* isolates from Mae sot, Tak province

Pimwan Thongdee[1,2], Jiraporn Kuesap[2], Kesara Na-Bangchang[1,3]*

[1]Graduate Program in Bioclinical Sciences, Chulabhorn International College of Medicine, Thammasat University, Pathumthani 12121, Thailand
[2]Graduate Program in Biomedical Sciences, Faculty of Allied Health Sciences, Thammasat University, Pathumthani 12121, Thailand
[3]Center of Excellence in Pharmacology and Molecular Biology of Malaria and Cholangiocarcinoma, Thammasat University, Pathumthani 12121, Thailand
*Corresponding author

Address correspondence and reprint request to: Kesara Na-Bangchang 99 Moo 18 Klongnung, Klongluang, Pathumthani12121, Thailand. Tel.: +66 2 5644440 79x1803; fax: +66 2 5644398.
E-mail address: kesaratmu@yahoo.com (K. Na-Bangchang).

Abstract

The sensitivity of ten *Plasmodium falciparum* isolates collected from Mae Sot district, Tak province in 2012, to chloroquine, quinine and artemisinin was investigated in association with polymorphisms of the parasite resistant genes, *i.e., Plasmodium falciparum* multidrug resistance protein 1 (*pfmrp1*: SNP at amino acid positions 191 and 437), *Plasmodium falciparum* sodium hydrogen exchanger 1 (*pfnhe1*: at the microsatellite in ms4760 locus), *Plasmodium falciparum* maurer's cleft two transmembrane proteins (*pfmc-2tm*: new SNPs), and *Plasmodium falciparum* GTP cyclohydrolase 1 (*pfgch1*: new SNPs). Results revealed non-synonymous mutations at the position 437 of *pfmrp1* of which the amino acids were DNNND repeat. For *pfnhe1*, the amino acids were NHNDNHNNDDD repeat. For *pfmc-2tm*, non-synonymous mutations at the positions 189, 190, 192, 194, 196 and 197 were found. All isolates carried wild type *pfgch1*. These genetic markers should be further validated for monitoring of antimalarial drug resistance.

Keywords: Antimalarial drug resistance, *Plasmodium falciparum* multidrug resistance protein 1, *Plasmodium falciparum* sodium hydrogen exchanger 1, *Plasmodium falciparum* maurer's cleft two transmembrane proteins, *Plasmodium falciparum* GTP cyclohydrolase 1

Introduction

Malaria is one of the major public health problems in tropical countries. Globally, an estimated 3.3 billion people in 97 countries and territories are at risk of being infected with malaria, and 1.2 billion are at high risk[1]. Resistance to antimalarial drugs has been documented for *Plasmodium falciparum*, *Plasmodium malariae*, and *Plasmodium vivax*. Resistance of *P. falciparum* to antimalarial drugs has been observed for almost all of the available drugs

including chloroquine, mefloquine, quinine, sulfadoxine-pyrimethamine (Fansidar™), and more recently, artemisinin derivatives. The geographical distributions and rates of spread have varied considerably[2]. In Thailand, resistance to chloroquine was first reported in 1961[3]. Resistance to sulfadoxine–pyrimethamine and mefloquine were reported in 1083 and 1989, respectively[4].

Plasmodium falciparum multidrug resistance associated protein (*Pfmrp*) belongs to the C subfamily of ABC transporters play role in the transport of glutathione, glucuronate, as well as glucuronide and sulfate conjugated compounds[5]. *Pfmrp* localizes to the parasite plasma membrane and membrane-bound vesicles in asexual stages[6]. The gene knock-out parasite lines were shown to increase intracellular glutathione accumulation and increased susceptibility to several antimalarial drugs,including chloroquine, quinine and artemisinins[6].

Resistance to quinolone antimalarials involves multiple transporters, in particular mutations in the *Plasmodium falciparum* chloroquine resistance transporter (*pfcrt*) and *Plasmodium falciparum* multidrug resistance 1 (*pfmdr1*) genes. A quantitative trait loci (QTL) analysis confirmed these remarks and recommended an additional role of a newly discovered locus on chromosome 13 interacting with other loci, further highlighting the complex network of gene interactions involved in the acquisition of a quinoline resistance phenotype. Among 100 predicted genes, this locus harbors a homolog of the Na^+/H^+ exchanger (*pfnhe1*), with a polymorphic coding microsatellite (ms4760) associated with quinine susceptibility[7]. Recently, new genetic markers of resistance of *P. falciparum* to artemisinin-based combination treatment (ACT), *Plasmodium falciparum* GTP cyclohydrolase I (*pfgch1*) and *Plasmodium falciparum* maurer's cleft two transmembrane proteins (*pfmc-2tm*) have been discovered[8].

The objective of this study was to investigate the distribution and diversity of the genetic polymorphisms of *Plasmodium falciparum* multidrug resistance protein 1 (*pfmrp1*), *Plasmodium falciparum* sodium hydrogen exchanger 1 (*pfnhe1*), *Plasmodium falciparum* GTP cyclohydrolase 1 (*pfgch1*), and *Plasmodium falciparum* maurer's cleft two transmembrane (*pfmc-2tm*) in *Plasmodium falciparum* isolates in Thailand. Ten *P. falciparum*-infected blood samples were collected from Mae Sot district, Tak province in 2012 for investigation of the distribution and diversity of the genetic polymorphisms of these genes by Nested-PCR and Sequencing.

Materials and Methods

Analysis of genetic polymorphisms of pfmrp1, pfnhe1, pfmc-2tm, and pfgch1 genes of Plasmodium falciparum isolates

The analysis of genetic polymorphisms of *pfmrp1*, *pfnhe1*, *pfgch1*, and *pfmc-2tm* genes were performed in 10 *P. falciparum* isolates collected from the area of multidrug resistance along the Thai-Myanmar border Mae Sot district, Tak province of Thailand[9].

Amplification of pfmrp1 single-nucleotide polymorphisms (SNPs): PCR amplification followed by sequencing was used to detect SNPs in *pfmrp* at amino acid positions 191 and 437. The primers *pfmrp*-501F and *pfmrp*-1409R (Table 1) were used for amplification and sequencing. The PCR cycling conditions were as follows: denaturation at 94°C for 2 min, followed by 40 cycles of 94°C for 30 sec, 52°C for 30 sec, 72°C for 1 min, and then 72°C for 15 min. All PCR products were verified on 1% agarose gels. The amplified fragments were performed to recover or concentrate DNA fragments (50bp-10kb) from an agarose gel or any other enzymatic reaction by using a Gel/PCR DNA Fragments Extraction Kit (Gene aid, New Taipei, Taiwan). The purified DNA was sent to 1st BASE DNA Sequencing Company (Selangor Darul Ehsan, Malaysia) for sequence analysis.

Amplification of pfnhe-1 microsatellites: A sequence containing the ms4760 microsatellite locus was amplified using *pfnhe*-3802F and *pfnhe*-4322R primers (Table 1). Gene amplification and sequencing followed the previously described procedures for *pfmrp1*.

Amplification of pfmc-2tm: The *pfmc-2tm* gene was amplified and sequenced using *pfmc-2tm* oligos and *pfmc-2tm* internal oligos primers (Table 1). Gene amplification and sequencing followed the previously described procedures for *pfmrp1*.

Amplification of pfgch1: The *pfgch1* gene was amplified and sequenced by using *pfgch1*-oligos and *pfgch1*-internal oligos primers (Table 1). Gene amplification and sequencing followed the previously described procedures for *pfmrp1*.

Data analysis

The amino acid sequences were aligned using the Gap4 program (version 4.10) available from http://www.mrclmb.cam.ac.uk/pubseq/_manual/gap4_windows_2.html. For investigation of the relatedness of the sequences, a Clustal C program was used to create synonymous SNPs in *pfmrp1*, *pfnhe1*, *pfmc-2tm*, and *pfgch1* (ANGIS, http://www.angis.org.au). Unique DNA sequences described in this paper have been deposited in the GenBank.

Results

Analysis of genetic polymorphisms of pfmrp1, pfnhe1, pfmc-and pfgch1 genes of Plasmodium falciparum isolates

Genetic diversity of pfmrp1 gene of P. falciparum malaria: Result of amino acid sequence analysis of the *pfmrp1 gene* of each isolate was compared to the Accession No. NC_004325 sequence from the GenBank. The gene consists of 7,109 bp that are translated into 2,369 amino acids. Non-synonymous mutations at position 437 were detected, *i.e.*, from serine (S) to alanine (A) (S437A) in 9 out of 10 samples (90%).

Genetic diversity of pfnhe1 gene of P.falciparum malaria: Result of amino acid sequence analysis of the *pfnhe1* gene of each isolate was compared to the Accession No.

GQ845118 sequence (318 bp), GQ845119 (312 bp), and GQ465284 (403 bp) from the GenBank. The amino acid repeats detected were DNNND and NHNDNHNNDDD (Table 2).

Table 1 Primers used for amplification of the *pfmrp1*, *pfnhe1*[10], *pfmc-2tm*, and *pfgch1* genes

Gene	PCR (position)	Primer	Sequence (5'-3')
pfmrp1	191,437	*pfmrp*-501F *pfmrp*-1409R	TTTCAAAGTATTCAGTGGGT GGCATAATAATTGATGTAAA
pfnhe1	ms4760 microsatellite locus	*pfnhe*-3802F *pfnhe*-4322R	TTATTAAATGAATATAAAGA TTTTTTATCATTACTAAAGA
pfmc-2tm	965, 1210	*pfmc-2tm* oligos* *pfmc-2tm* internal oligos*	AAACACCATCTTTTACCTTTTGAA AGCATCGTGCTCTTTAACTCC
pfgch1	469, 618	*pfgch1*-oligos* *pfgch1*-internal oligos*	ATTTGGATTGTTTCAACGACCT CATGTCAGGAAAATAACGAGCA

*new designed primer

Table 2 Frequency of the mutations of *pfnhe1* ms4760 haplotypes in 10 *P. falciparum* isolates

Mutations of *pfnhe1* gene		
No.DNNND repeat	No. NHNDNHNNDDD repeat	No. genotype profile
2	1	ms-6 = 1(10%)
3	1	ms-7 = 9(90%)

Genetic diversity of pfmc-2tm: Result of the amino acid sequence analysis of the *pfmc-2tm* gene of each isolate was compared to the Accession No. NC_000910 from the GenBank. The gene consists of 1,018 bp that are translated into 339 amino acids. The polymorphisms of the gene in the 9 isolates are shown in Table 3. Analysis of gene mutation in 1 isolate revealed neither mutation nor wild-type genotype.

Table 3 Frequency of the mutations of *pfmc-2tm* gene in 10 *P. falciparum* isolates

Mutations of *pfmc-2tm* gene					
189	190	192	194	196	197
F=8(88.9%)	I=6(66.7%)	L=7(77.8%)	F=8(88.9%)	I=7(77.8%)	H=1(11.1%)
Y=1(11.1%)	S=3(33.3%)	S=2(22.2%)	N=1(11.1%)	N=2(22.2%)	Y=8(88.9%)

Genetic diversity of pfgch1: Result of the amino acid sequence analysis of *pfgch1* was compared with the Accession No. NC_004,316 from the GenBank. The gene consists of 1,520 bp that are translated into 506 amino acids. All carried wild-type genotype of *pfgch1*.

Discussion

ACTs remain the most effective treatment for uncomplicated *P. falciparum* malaria. Artemisinin derivatives are very effective in rapidly reducing the parasite biomass, and when combined with an effective partner medicine, they are likely to clear all parasites successfully[4]. Recently, artemisinin resistance was found in Cambodia and areas along the Thai-Cambodian border[11]. There has been no confirmed report of artemisinin on the Thai-Myanmar border. The present study reports on the genetic polymorphisms of *pfmrp1*, *pfnhe1*, *pfmc-2tm*, and *pfgch1* genes of *P. falciparum* isolates collected from Mae Sot district, Tak province, the area of multidrug resistance *P. falciparum*. The polymorphism of *pfmrp1* gene at position 437 was found at high frequency (90%). For *pfnhe* 1, three repeats of DNNND of the gene were detected at high frequency (90%). The polymorphism of *pfmc-2tm* gene at position 197 was detected at high frequency (89%).

Pfmrp1 has been shown to associate with increased susceptibility of *P. falciparum* to several antimalarial drugs, including chloroquine, quinine, and artemisinins. The current results show that all isolates carried *Pfmrp1* gene consisting of the amino acid histidine (H191) as that was reported previously in Thailand[12]. Furthermore, there was a change in amino acids at the position 437 (S437A) from serine (S) to alanine (A) in 9 samples (90%) as that was reported from Cambodian isolates[12]. Based on results of a previous study in Thailand isolates, the F1390I allele significantly modulated the *in vitro* drug response phenotypes. Carriers of the F1390 allele were less susceptible to artemisinin, mefloquine and lumefantrine, with average IC_{50}'s of 8.96 (60.92), 121.71 (612.17) and 15.56 (61.71) nM, respectively. The IC_{50}'s of the isolates carrying 1390I allele were 3.30 (60.86), 37.25 (69.31) and 6.08 (61.87) nM, respectively[13]. Mutations of *pfnhe1* was associated with quinine resistance in *P. falciparum* isolates in Viet Nam[14]. The results showed genotype profile of ms-6 at frequency of 1% similarly to that found in Vietnam[14] and ms-7 at frequency of 9% similarly to that found in Thailand[12]. For ACT resistance, were found non-synonymous mutations of the *pfgch1* was found at amino acid positions 189, 190, 192, 194, 196 and 197. Confirmation of these observations is required in a larger number of *P. falciparum* isolates.

References

1. World Health Organization. World malaria report 2014. Geneva : WHO; 2014.
2. World Health Organization. Guidelines for the treatment of malaria. Geneva: WHO; 2010.
3. Harinasuta T, Suntharasamai P, Viravan C. Chloroquine-resistant falciparum malaria in Thailand. Lancet. 1965; 2(7414): 657-660.
4. World Health Organization. Global report on antimalarial efficacy and drug resistance: 2000-2010. Geneva : WHO; 2010.
5. Ambudkar SV, Kimchi-Sarfaty C, Sauna ZE, Gottesman MM. P-glycoprotein: from genomics to mechanism. Oncogene. 2003; 22(47): 7468-7485.
6. Raj DK, Mu J, Jiang H, Kabat J, Singh S, Sullivan M, Fay MP, McCutchan TF, Su XZ. Disruption of a *Plasmodium falciparum* multidrug resistance-associated protein (*pfmrp*) alters its fitness and transport of antimalarial drugs and glutathione. J Biol Chem. 2009; 284(12): 7687-7696.
7. Pelleau S, Bertaux L, Briolant S, Ferdig MT, Sinou V, Pradines B, et al. Differential association of *Plasmodium falciparum* Na+/H+ exchanger polymorphism and quinine responses in field- and culture-adapted isolates of *Plasmodium falciparum*. Antimicrob Agents Chemother. 2011; 55(12): 5834-5841.
8. Mok S, Imwong M, Mackinnon MJ, Sim J, Ramadoss R, Yi P, et al. Artemisinin resistance in *Plasmodium falciparum* is associated with an altered temporal pattern of transcription. BMC Genomics. 2011; 12: 391.
9. Thongdee P, Chaijaroenkul W, Kuesap J, Na-Bangchang K. Nested-PCR and New ELISA-Based NovaLisa Test Kit for Malaria Diagnosis in an Endemic Area of Thailand. Korean J Parasitol. 2014; 52(4): 377-381.
10. Pradines B, Briolant S, Henry M, Oeuvray C, Baret E, Amalvict R, et al. Absence of association between pyronaridine in vitro responses and polymorphisms in genes involved in quinoline resistance in *Plasmodium falciparum*. Malar J. 2010; 9: 339.
11. Noedl H, Se Y, Sriwichai S, Schaecher K, Teja-Isavadharm P, Smith B, et al. Artemisinin resistance in Cambodia: a clinical trial designed to address an emerging problem in Southeast Asia. Clin Infect Dis. 2010; 51(11): e82-89.
12. Briolant S, Henry M, Oeuvray C, Amalvict R, Baret E, Didillon E, et al. Absence of association between piperaquine in vitro responses and polymorphisms in the *pfcrt*, *pfmdr1*, *pfmrp*, and *pfnhe* genes in *Plasmodium falciparum*. Antimicrob Agents Chemother. 2010; 54(9): 3537-3544.
13. Veiga MI, Ferreira PE, Jornhagen L, Malmberg M, Kone A, Schmidt BA, et al. Novel polymorphisms in *Plasmodium falciparum* ABC transporter genes are associated with major ACT antimalarial drug resistance. PLoS One. 2011; 6(5): e20212.

14 Sinou V, Quang le H, Pelleau S, Huong VN, Huong NT, Tai le M, et al. Polymorphism of *Plasmodium falciparum* Na$^{(+)}$/H$^{(+)}$ exchanger is indicative of a low in vitro quinine susceptibility in isolates from Viet Nam. Malar J. 2011; 10: 164.

RESEARCH ARTICLE

Effects of a standardized extract of *Centella asiatica* ECa233 on human keratinocyte migration

Sawana Singkhorn[1], Mayuree H Tantisira[2] and Wanida Sukketsiri[1*]

[1]*Department of Pharmacology, Faculty of Science, Prince of Songkla University, Hat Yai, Songkhla, Thailand, 90112*
[2]*Faculty of Pharmaceutical Sciences, Burapha University, Mueang District, Chonburi, Thailand, 20131*

Address correspondence and reprint request to: Department of Pharmacology, Faculty of Science, Prince of Songkla University, Hat Yai, Songkhla, 90112, Thailand. Tel.: +66 74 288171; Fax: +66 74 446678
E-mail address: wanida.su@psu.ac.th

Abstract

Re-epithelialisation is a pivotal event in the healing of skin wounds. The purpose of this study was to investigate the migration effects of standardized extract of *Centella asiatica* ECa233 in human skin keratinocyte cells. Cytotoxicity was determined using the MTT assay. The result showed that exposure to ECa233 at concentration 0, 0.001, 0.01, 0.1, 1, 10 and 100 µg/mL after 24, 48 and 72 h were not affected keratinocyte cells viability when compared to the control. Moreover, wound-healing assay showed that ECa233 (0.1, 1, and 10 µg/mL) significantly increased the migration of keratinocyte cells after 48 h. This result indicated that standardized extract of *Centella asiatica* ECa233 may promote wound repair by facilitating keratinocyte cell migration.

Keywords: *Centella asiatica*, ECa233, wound healing, migration

Introduction

Cutaneous wound healing, a complex biological process, is involving in 3 phases of inflammation, cell proliferation, and tissue remodeling. Several cell types have been involved in the process of wound repair, such as keratinocytes, and fibroblasts[1]. The process of re-epithelialisation has drawn considerable attention because of its critical for intact epidermal function. Delays or defects in re-epithelialisation frequently cause a chronic wound and/or non-healing wound.

Centella asiatica Linn. has long been used in complementary traditional medicine in order to improve mental clarity, wound healing, and treat skin conditions such as leprosy and psoriasis[2]. In addition, *C. asiatica* contains several bioactive compounds, including asiatic acid, madecassic acid, asiaticoside, and madecassoside[3]. Wound healing effects of standardized extract of *C. asiatica* ECa233 have been demonstrated in animal model of second degree burn wound. It has been demonstrated that ECa233 increases cutaneous blood flow[4] and possess

anti-inflammatory and antioxidant effect[4,5]. The anti-inflammatory effect of ECa233 has been shown to effectively decreased myeloperoxidase activity and also reduces tissue damage by decreased reactive oxygen species production[6]. As mentioned above, ECa233 has drawn considerable attention owing to its pharmacological effects related to wound repair such as wound healing, anti-inflammatory effect and anti-oxidative effect. Therefore, the aim of this study was to elucidate the effect of standardized extract of *C. asiatica* ECa233 on keratinocyte cell migration.

Materials and Methods

Cells culture and reagents

The human keratinocyte cell line (HaCaT) was obtained from the Cell Line Service, Heidelberg, Germany. The cells were cultured in Dulbecco's Modified Eagle's Medium (DMEM) supplemented with 10 % fetal bovine serum, 2 mM L-glutamine and 1% antibiotics (100 U/ml penicillin and 100 µg/ml streptomycin) in a humidified atmosphere containing 5 % CO_2 at 37°C. Standardized extract of *Centella asiatica* ECa233 was provided by Associate Professor Dr. Mayuree Tantisira, Faculty of Pharmaceutical Sciences, Burapha University, Thailand.

Cell viability assay

Cell viability was determined by 3 - (4 ,5 - dimethylthiazol-2 - yl)-2 ,5 - diphenyl tetrazoliumbromide (MTT) assay. Cells were cultured at a density of 1×10^4 cells/well in a 96 well plate and treated with standardized extract of *Centella asiatica* ECa233 at 0, 0.001, 0.01, 0.1, 1, 10 and 100 µg/mL for 24, 48 and 72 h. After treatment, MTT solution (5.0 mg/mL) was added into the well and incubated for 2 h at 37 °C. After removal of the MTT solution, the formazan crystals were solubilized with DMSO. The intensity of the formazan product was measured at 570 nm using a microplate reader (Bio-tex, USA).

Cell migration assay

Cell migration was determined using a scratch wound-healing assay. Cells (1.5×10^5 cells/well) were grown to a 100% confluent monolayer in a 24-well plate, and a wound spaces was made by using sterile micropipette tip. Then, the wells were washed with phosphate-buffered saline and incubated with standardized extract of *Centella asiatica* ECa233 at 0, 0.1, 1, and 10 µg/mL for 0, 24, 48 and 72 h. The wound spaces were examined using a phase-contrast microscope fluorescence microscope (Olympus IX71, Japan). The wound closure area was calculated by using ImageJ program. The data were expressed as % wound closure area calculated based on the following formula:

$$\% \text{ Wound closure area} = \frac{\text{Wound closure area}}{\text{Wound closure area (time 0)}} \times 100$$

Results

1. *Effects of standardized extract of Centella asiatica ECa233 on keratinocyte cell viability*

Cells viability was determined using MTT assay. It was shown that standardized extract of *Centella asiatica* ECa233 did not significantly decrease keratinocyte cell viability at concentration 0.001, 0.01, 0.1, 1, 10 and 100 µg/mL after 24, 48 and 72 hours of treatment when compare to the control (Figure 1).
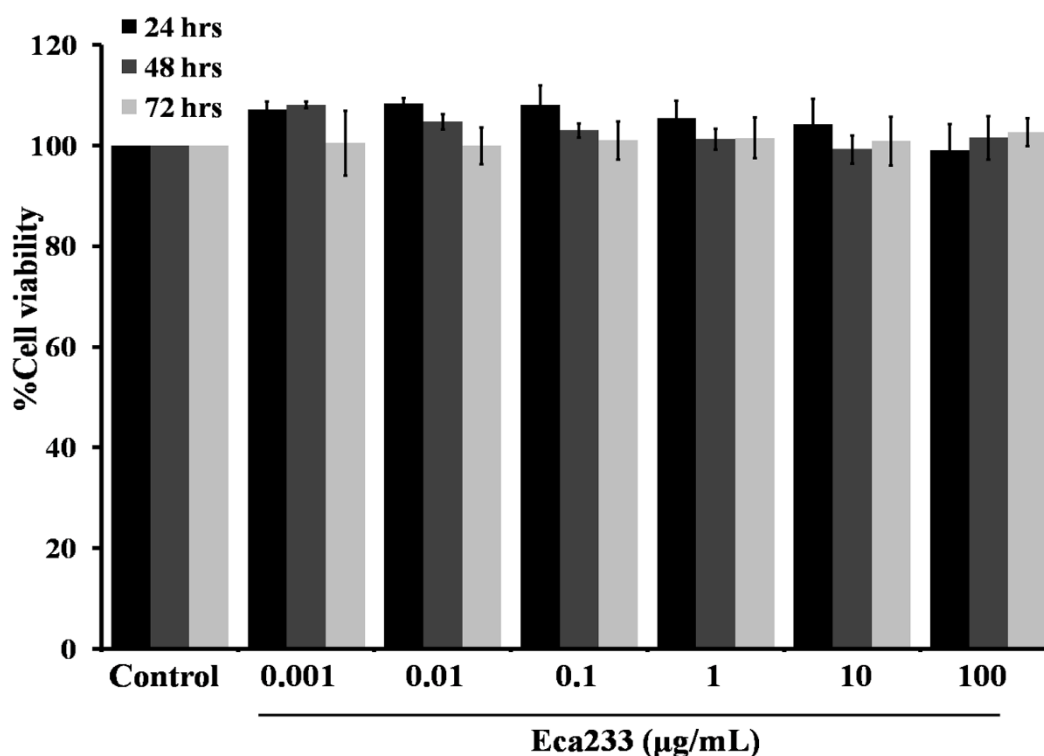
Figure 1. Cytotoxicity effects of standardized extract of *Centella asiatica* ECa233 in keratinocyte cells. Cells were treated with various concentrations (0.001-100 µg/mL) of Eca233 for 24, 48 and 72 hour. Cell viability was determined by the MTT assay. Data shown are mean values ± SEM of four independent experiments.

2. *Effects of standardized extract of Centella asiatica ECa233 on keratinocyte cell migration*

The migration behavior of the human keratinocytes was determined by a scratch wound-healing assay. After the cells were treated with ECa233 for 24, and 48 h at various concentrations (0.1-10 µg/mL), ECa233 significantly enhanced the migration of the cells across the wound space in a dose-and time-dependent manner when compare to the control (Figure 2).
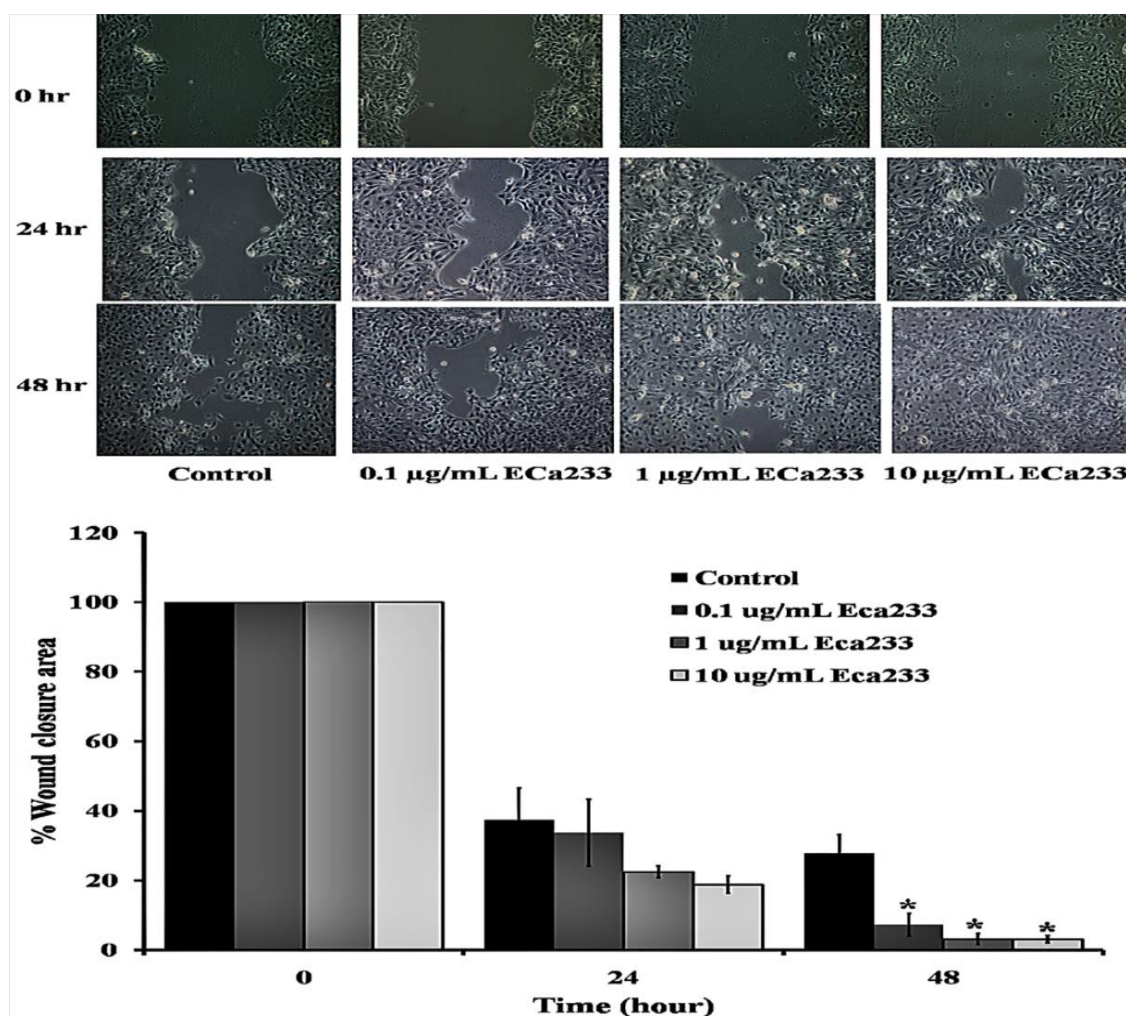
Figure 2. Effects of standardized extract of *Centella asiatica* ECa233 on keratinocyte cell migration. Cells were treated with various concentrations (0.1-10 µg/mL) of Eca233 for 24, and 48 hour. Cell migration was determined by a scratch wound-healing assay. Data shown are mean values ± SEM of four independent experiments. *$P<0.05$ compared to the time 0.

Discussion and conclusion

Keratinocyte proliferation and migration is the key processes for normal wound epithelialisation and restoring barrier function in cutaneous wound[7]. In this study, we demonstrated that standardized extract of *Centella asiatica* ECa233 induces keratinocyte migration. Treatment of the cells with standardized extract of *Centella asiatica* ECa233 (0.1, 1, and 10 µg/mL) did not cause significant cytotoxicity and proliferative effects. Thus, the concentrations of ECa233 at 0.1-10 µg/mL were used in the subsequent migratory experiments. In the present study, keratinocyte cells were treated with standardized extract of *Centella asiatica* ECa233 for 24, 48 and 72 h with various doses (0.1, 1, and 10 µg/mL). Standardized extract of *Centella asiatica* ECa233 was found to increase keratinocyte cell migration in dose- and time-dependent manner. These findings were consistent with those observed in rat[4,5] who reported that ECa233 increased wound repair in incision and burn wound in both normal and diabetic rats. Thus, our finding supported the wound healing effects of ECa233, of which the

mechanism was to increase keratinocyte cell migration. However, the underlying mechanisms of ECa 233 on keratinocyte migration will thus important to explore in further study.

In conclusion, this study demonstrated that treatment with standardized extract of *Centella asiatica* ECa233 enhanced the motility of the cells across the wound space keratinocyte cells. Interestingly, our study might provide support for the potential use of ECa233 as a therapeutic agent on wound-healing.

Acknowledgements

References

1. Gurtner GC, Werner S, Barrandon Y, Longaker MT. Wound repair and regeneration. Nature. 2008; 453: 314–21.
2. Cheng CL, Koo MWL. Effects of *Centella asiatica* on ethanol induced gastric mucosal lesions in rats. Life Sciences. 2000; 67: 2647–53.
3. Brinkhaus B, Lindner M, Schuppan D, Hahn EG. Chemical, pharmacological and clinical profile of the East Asian medical plant *Centella asiatica*. Phytomedcine. 2000; 7: 427–48.
4. Wannarat K, Tantisira MH, Tantisira B. Wound Healing Effects of a Standardized Extract of *Centella asiatica* ECa 233 on Burn Wound in Rats. Thai J Pharmacol. 2009; 31: 120-3.
5. Hamid AA, Shah MdZ, Muse R, Mohamed S. Characterisation of antioxidative activities of various extracts of *Centella asiatica* (L) Urban. Food Chemistry. 2002; 77: 465–9.
6. Ruengprasertkit C, Hongprasong N, Tantisira B, Tantisira MH. Preliminary study of effects of a standardized extract of *Centella asiatica* ECa233 on minor aphthous ulcers. CU Dent J. 2010; 33: 131-42.
7. Meyer M, Müller A-K, Yang J, Moik D, Ponzio G, Ornitz DM, et al. FGF receptors 1 and 2 are key regulators of keratinocyte migration *in vitro* and in wounded skin. J Cell Sci. 2012; 125: 5690–701.

RESEARCH ARTICLE

Astaxanthin and wound healing

Atiya Rungjang MD[1], Saranyoo Ponnikorn PhD[2], Werayut Yingmema DVM[3], Jitlada Meephansan MD PhD[1]

[1]*Division of Dermatology, Chulabhorn International College of Medicine, Thammasat University, Pathum Thani, 12120, Thailand*
[2]*Chulabhorn International College of Medicine, Thammasat University, Pathum Thani, 12120, Thailand*
[3]*Laboratory Animal Centers, Thammasat University, Pathum Thani, 12120, Thailand*

Abstract

Wound healing is a complex reaction of the organism to injury. The successful wound healing requires the execution of three major overlapping phases: inflammation, proliferation, and remodeling. Reactive oxygen species (ROS) are involved in all phases of wound healing. It is shown that large amount of ROS, which is called oxidative stress, is harmful to these processes. The correct balance between oxidative and antioxidative forces is needed for favorable wound healing. Astaxanthin, a member of the xanthophyll group, is a red-orange carotenoid. It is recognized as a most powerful antioxidant. In this study, we investigated the effect of topical astaxanthin on cutaneous wound healing. Full-thickness dermal wound was done in 36 healthy female mice, then divided into two groups. Mice were treated with topical astaxanthin 78.9 uM (5% extraction) or vehicle twice daily for 15 days. Wound areas were determined on daily serial photographs. We found that astaxanthin significantly accelerated wound closure in treatment mice compared to control group. Astaxanthin treatment improves wound healing since contraction takes place earlier in astaxanthin-treated in comparison to vehicle-treated mice by wound area assessment method. These results suggest that astaxanthin may have an effect on improving cutaneous wound healing.

Keywords: wound healing, astaxanthin, reactive oxygen species

Introduction

Wound healing is a complex reaction of the organism to physical injuries that result in an opening or break of the skin. Various cell types including leucocytes, keratinocytes, fibroblasts, and macrophages as well as cytokines are involved in this dynamic process that results in the closure of the wound and restoration of a barrier function.[1-3] Repair of injured tissues occurs as a sequence of events briefly divided into three overlapping phases "inflammation, proliferation and remodeling". In the coagulation and inflammatory phase: cutaneous injury affecting primarily the epithelial and endothelial compartments, results in coagulation cascade forming blood clot and the release of proinflammatory mediators. Blood clot within the vessel lumen provides hemostasis; the clot within the injury site acts as a

provisional matrix for cell migration, further formation of new extracellular matrix (ECM), a reservoir for cytokines and growth factors. Inflammatory white cells functions are debridement of necrotic material and bacteria and production of certain critical cytokines. 24–48 hours after injury, monocytes replace neutrophils and change to tissue macrophages that phagocytose and kill bacteria, scavenge tissue debris and release several growth factors stimulating migration and proliferation of fibroblasts, endothelial cells and keratinocytes and production and modulation of extracellular matrix, during which "reepithelialization and angiogenesis" of proliferation/migration phases take place. The remodeling phase begins 5–7 days after injury to breakdown of excess macromolecules. Cells within the wound are returned to a stable phenotype and extracellular matrix material is altered.[4-6]

All phases in skin wound healing are involved with reactive oxygen species (ROS). ROS may promote wound angiogenesis by inducing VEGF expression in wound-related cells such as keratinocytes and macrophages.[7] However, excess quantities of such compounds are dangerous due to their very high reactivity because they may react with various cellular components such as proteins, lipids, carbohydrates, and DNA. This situation may cause oxidative damage that are also involved in many natural and pathological processes, including aging cancer, diabetes mellitus, atherosclerosis, neurological degeneration, angiogenesis, and metastasis.[8] Overexposure to ROS is deleterious to wound healing process due to the harmful effects on cells and tissues.[9, 10] To inhibit wound site injury by oxidative stress, antioxidants have been applied to balance oxidative stress on the wound sites.[11] Kumin et al. reported that the over expression of peroxiredoxin, which is an antioxidant enzyme that quenchs free radicals resulted in the enhancement of wound closure in aged mice.[12]

Astaxanthin, a biological antioxidant, is a pigment in xanthophylls family, the oxygenated derivatives of carotenoids whose synthesis in plants derives from lycopene. Common sources of natural astaxanthin are the green algae *Haematococcus pluvialis* and the red yeast *Phaffia rhodozyma*. It was reported to exhibit strong free radical scavenging activity and to protect cells against lipid peroxidation and the oxidative damage.[13] Lee et al. demonstrated that astaxanthin inhibited the expression of a number of pro-inflammatory mediators (such as nitric oxide).[14] Also, health benefits such as cardiovascular disease prevention, immune system boosting, bioactivity against helicobacter pylori, and cataract prevention were reported.[15-17]

The objective of the present study was to evaluate the effect of topical astaxanthin extract on full-thickness cutaneous wound healing in mice model. We assess the change of wound area during the process of wound repair.

Materials and Methods

Drugs

The astaxanthin solution, composed of 78.9 µM (5.0%w/w) of astaxanthin extracted from *Haematococcus pluvialis*, was supplied by China Jiangsu International Economic and Technical Cooperation. The vehicle was Chremophore RH 40 Glycerin.

Animals

Young female Balb/c mice (8-week-old) were procured from the National Laboratory Animal Center. A total of 36 studied mice were assigned to treatment group (N=18) and control group (N=18). During the experiments, the animals were housed under Strict hygienic conventional standard, maintained under controlled environmental conditions (12-hour light/dark cycle, temperature approximately 23°C), and provided with standard laboratory food and water ad libitum. Study protocol was approved by Thammasat University's Animal Ethical Committee and conducted according to Ethical Principals and Guidelines for the Use of Animals for Scientific Purpose

Full-thickness wounds were created on the back of mice under sterile conditions. Mice were anesthetized with inhaled isoflurane before the procedure. After shaving and cleaning with 70% ethanol, the dorsal skin was picked up and punched through two layers of skin with a sterile disposable biopsy punch (4 mm in diameter) to generate two wounds on the dorsal skin. Each wound site was digitally photographed until complete wound closure was observed as shown in Figure 1.

The wounds were treated topically twice daily with 5% astaxanthin in treatment group and vehicle in control group (0.025 mL/wound). A digital image of each wound with a scale was daily recorded. For the wound contraction study, a template containing a 10 mm diameter circular window was used to standardize the size of each wound and wound areas were determined on photographs using Adobe Illustrator CS3. Changes in wound areas overtime were expressed as the percentage of the decrease in wound areas. The mice were humanely euthanized with 5-8% Isoflurane at experimental end-point.

Statistical analysis was done using SPSS statistic program. The data were expressed as mean ± standard error of the mean (X ± SEM). General linear model; ANOVA was conducted for comparisons. A p value of < 0.05 was considered as significance.
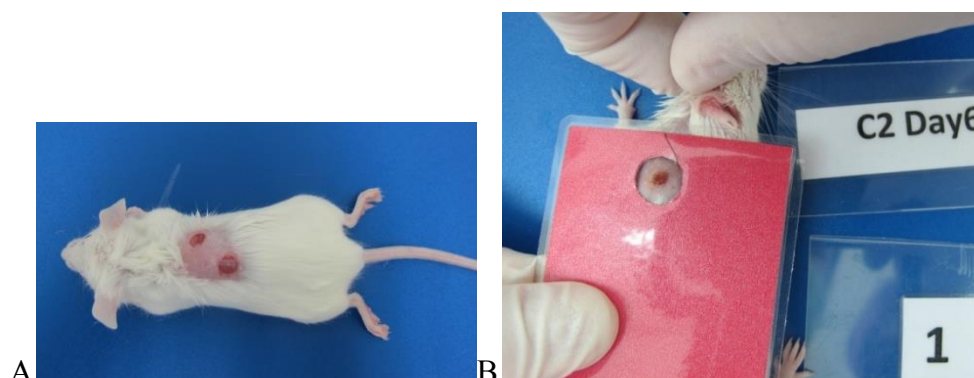
Figure 1. Wound measurement and analysis. **A**. On day 0, two circular excisional wounds (4 mm in diameter) were created in the dorsal skin of female Balb/c mice. **B**. Each wound site was digitally photographed at the indicated time intervals, and wound areas were determined on photographs using Adobe Illustrator software. Changes in wound areas over time were expressed as the percentage of the area reduction.

Results

The effect of astaxanthin on wound healing was studied in two groups of animal models (see "Materials and Methods"). Wound areas were analyzed throughout the healing process. Astaxanthin 5% extract applied topically on the wounds showed significant acceleration of wound closure which was clearly visible at the 3rd day of the experiment (Figure 2a). On day 9 after wounding, the astaxanthin-treated wounds had already lost their eschars and appeared fully epithelialized, whereas the wounds of control mice demonstrated only partial epithelialization and still carried scab. A complete wound closure of control group was observed by day 12 after the injury. The results of the wound model are presented in Figure 2b. The mean of original wound area of astaxanthin-treated group was larger than control group (14.12 mm^2 vs. 12.72 mm^2). On the 1st day post-injury, wound area of astaxanthin-treated group was maximally decreased to 8.69 mm^2 (38.46% reduction of the original wound area), whereas the control group showed slower rate at 14.39% to 10.89 mm^2. On day 6 after wounding, the closure of the wound in astaxanthin-treated group was more pronounced (90% closed with the remaining wound area of 1.86 mm^2) than control group (72.96% closed with the remaining wound area of 3.44 mm^2). Statistical analysis indicated that wound closure in astaxanthin-treated mice was significantly accelerated as compared with control mice at p value <0.05. A significant difference between 2 groups has been observed since the second day after operation and continued until the sixth day.

(a.)

(b.)
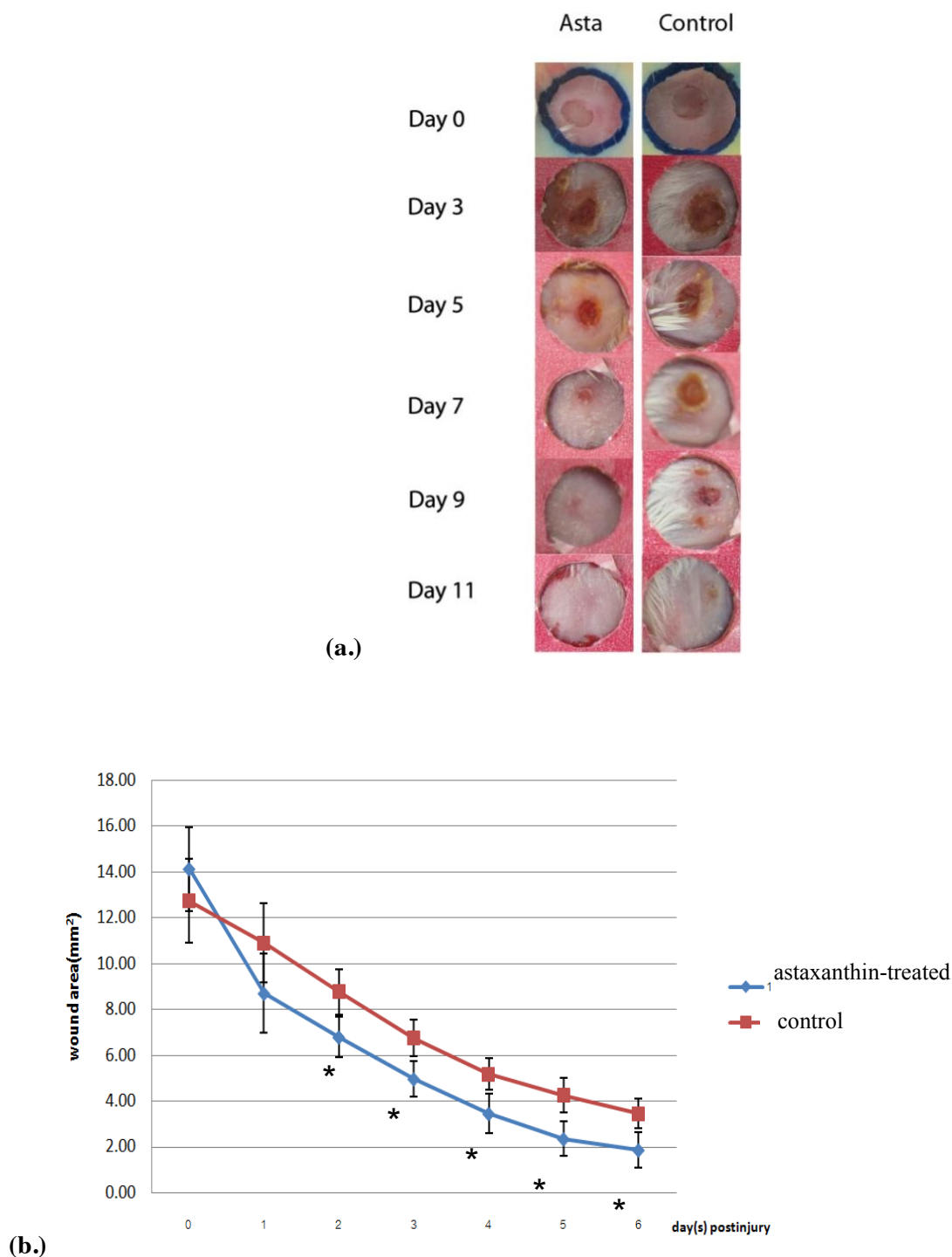
Figure 2. Acceleration of wound healing in Astaxanthin treated mice.

(a.) Representative photographs from astaxathin-treated and control mice showing the macroscopic wound closure on different days post-injury. The size of wounds was determined from photographs. **(b**.) At the time points indicated, the wound area was determined using image analysis and expressed as Mean ± SEM of astaxanthin-treated-group (1) in comparison with the control group (2), N=18 each. * : significant decrease as compared to the control group at the same time point.

Discussion

Wound healing process is regulated by various factors, including cells, growth factors, cytokines, and hormones. During inflammation, reepithelization, and tissue remodeling, ROS are involved in all of these phases.[18] The proper amounts of ROS play an important role in the wound healing[19, 20] as they provide defense against invading bacteria and assist in cellular signaling. When the generation of free radicals exceeds the capacity of the defenses, these highly active molecules may cause reversible or irreversible cell injury by harmful structural changes, which is called oxidative stress. In addition to these, several studies have demonstrated that overexpression of H_2O_2 impairs wound closure, whereas low doses fairly facilitated closure.[10, 12]This suggested that the favorable wound healing requires a delicate balance between oxidative and anti-oxidative forces. Numerous studies have reviewed antioxidant effect of astaxanthin.[21-23] Our study results support that astaxanthin, a powerful quencher of reactive oxygen and nitrogen species shorten the period of wound healing by clinical assessment. Significant accelerated healing effects of astaxanthin were observed in the phase of inflammation and proliferation including formation of granulation tissue and epithelization. This effect could be mediated by scavengin ROS in the wound resulted in suppression of inflammation. The main source of ROS during inflammation is NADPH-oxidase in plasma membrane of neutrophils and macrophages which are major cells in these phases. Astaxanthin may also suppress expression of adhesion molecules during these processes leading to inhibition of these inflammatory cells infiltration.[18] In addition, Mizuta and colleagues have demonstrated that during the healing process of vocal fold, the expression of procollagen type 1 increased significantly in the astaxanthin-treated group.[20] Collagen is essential as a scaffold for wound healing. Therefore, astaxanthin may promote healing through inducing expression of procollagen type 1. As its strong antioxidant activity contributes to favorable wound healing, future studies may support the implication of astaxanthin as a novel redox-based strategy to treat wounds.

Conclusion

In the present study, astaxanthin accelerates healing of full-thickness dermal wounds. Considering the results obtained, we believe that the astaxanthin extracted from *Haematococcus pluvialis*, might become a useful alternative medicine for the cutaneous wound healing.

Acknowledgements

References

1. Barrientos S, Stojadinovic O, Golinko MS, Brem H, Tomic-Canic M. Growth factors and cytokines in wound healing. Wound Rep Reg. 2008;16:585-601.

2. Galeano M, Torre V, Deodato B, Campo GM, Colonna M, Sturiale A, et al. Raxofelast, a hydrophilic vitamin E-like antioxidant, stimulates wound healing in genetically diabetic mice. SURGERY 2001;129:467-77.

3. Esposito D, Rathinasabapathy T, Schmidt B, Shakarjian MP, Komarnytsky S, Raskin I. Acceleration of cutaneous wound healing by brassinosteroids. Wound Repair Regen. 2013;21:688-96.

4. Singer Aj, Clark RaF. Cutaneous wound healing. The New England Journal of Medicine. 1999:738-46.

5. Talekar YP, Das B, Paul T, Talekar DY, Apte KG, Parab PB. Evaluation of wound healing potential of aqueous and ethanolic extracts of tridax procumbens linn. In wiar rats. Asian Journal of Pharmaceutical and Clinical Research. 2012;5:141-5.

6. Powers CJ, McLeskey SW, Wellstein A. Fibroblast growth factors, their receptors and signaling. Endocrine-Related Cancer. 2000(7):165-97.

7. Ojha N, Roy S, He G, Biswas S, Velayutham M, Khanna S, et al. Assessment of wound-site redox environment and the significance of Rac2 in cutaneous healing. Free Radic Biol Med. 2008;44:682–91.

8. Yoon S-O, Park S-J, Yoon SY, Yun C-H, Chung A-S. Sustained production of H2O2 activates pro-matrix metalloproteinase-2 through receptor tyrosine kinases/phosphatidylinositol 3-kinase/NF-kB pathway. The Journal Of Biological Chemistry. 2002;277:30271-82.

9. Edwin S, Jarald EE, Deb L, Jain A, Kinger H, Dutt KR, et al. Wound healing and antioxidant activity of Achyranthes aspera. Pharmaceutical Biology. 2008;46:824-8.

10. Sen CK, Roy S. Redox signals in wound healing. Biochim Biophys Acta 2008;1780:1348–61.

11. Kim H-L, Lee J-H, Kwon BJ, Lee MH, Han D-W, Hyon S-H, et al. Promotion of full-thickness wound healing using epigallocatechin-3-O-Gallate/Poly (Lactic-Co-Glycolic Acid)membrane as temporary wound dressing. Artificial Organs. 2014;38:411-7.

12. Ku¨min A, Huber C, Ru¨licke T, Wolf E, Werner S. Peroxiredoxin 6 is a potent cytoprotective enzyme in the epidermis. The American Journal of Pathology. 2006;169:1194-205.

13. Hussein G, Nakamura M, Qi Zhao BTI, Hirozo Goto CUS, Watanabe H. Antihypertensive and neuroprotective effects of astaxanthin in experimental animals. Biol Pharm Bull. 2005;28:47-52.

14. Gross GJ, Lockwood SF. Acute and chronic administration of disodium disuccinate astaxanthin (CardaxTM) produces marked cardioprotection in dog hearts. Molecular and Cellular Biochemistry. 2005;272:221-7.

15. Higuera-Ciapara I, Félix-Valenzuela L, Goycoolea FM. Astaxanthin: a review of its chemistry and applications. Critical Reviews in Food Science and Nutrition. 2006;46:185-96.

16. Nishigaki I, Rajendran P, Venugopal R, Ekambaram G, Sakthisekaran D, Nishigaki Y. Cytoprotective role of astaxanthin against glycated protein/iron chelate-induced toxicity in human umbilical vein endothelial cells. Phytother Res. 2010;24:54-9.

17. Lee S-J, Bai S-K, Lee K-S, Namkoong S, Na H-J, Ha K-S, et al. Astaxanthin Inhibits nitric oxide production and inflammatorygene expression by suppressing IκB kinase-dependentNF-κB activation. Mol Cells. 2003;16:97-105.

18. Demianenko IA, Vasilieva TV, Domnina LV, Dugina VB, Egorov MV, Ivanova OY, et al. Novel mitochondria-targeted antioxidants, "Skulachev-Ion derivatives, accelerate dermal wound healing in animals. Biochemistry (Moscow). 2010;75:274-80.

19. Bedard K, Krause k-H. The NOX family of ROS-generating NADPH oxidases: physiology and pathophysiology. Physiol Rev. 2007;87:245-313.
20. Mizuta M, Hirano S, Hiwatashi N, Tateya I, Kanemaru S-i, Nakamura T, et al. Effect of astaxanthin on vocal fold wound healing. The Laryngos cope. 2014;124:E1-E7.
21. Yuan J-P, Peng J, Yin K, Wang J-H. Potential health-promoting effects of astaxanthin: A high-value carotenoid mostly from microalgae. Mol Nutr Food Res. 2011;55:150-65.
22. Wolf AM, Asoh S, Hiranuma H, Ohsawa I, Iio K, Satou A, et al. Astaxanthin protects mitochondrial redox state and functional integrity against oxidative stress. Journal of Nutritional Biochemistry. 2010;21:381-9.
23. Hussein G, Sankawa U, Goto H, Matsumoto K, Watanabe H. Astaxanthin, a Carotenoid with potential in human health and nutrition. J Nat Prod. 2006;69:443-9.

RESEARCH ARTICLE

Antimicrobial activities of stingless bee propolis from mangosteen orchard

Boonyadist Vongsak[1]*, Kulwara Poolpol[2], Sumet Kongkiatpaiboon[3], Sasipawan Machana[1]

[1]*Faculty of Pharmaceutical Sciences, Burapha University Chonburi, 20131, Thailand*
[2]*Faculty of Allied Health Sciences Burapha University Chonburi, 20131, Thailand*
[3]*Drug Discovery and Development Center, Thammasat University, Pathum Thani, 12120, Thailand*

Address correspondence and reprint request to: Boonyadist Vongsak, Faculty of Pharmaceutical Sciences, Burapha University Chonburi 20131, Thailand.
E-mail address: boonyadist@buu.ac.th.

Abstract

Propolis has been relied on numerous therapeutic purposes such as treatment of cold, ulcer and inflammation. The biological activities and chemical constituents of each type of propolis mainly depend on geographical regions and on the bee species. In the study, the propolis from three stingless bee species, *Tetragonula pagdeni* Schwarz, *Lepidotrigona ventralis* Smith, and *Lepidotrigona terminata* Smith, which are commercially cultivated in artificial hives in fruit gardens was collected in the same orchard and compared antimicrobial activity. The active compound from the species that demonstrated the strongest activity were identified. Gram-positive bacteria: *Staphylococcus aureus*, gram-negative bacteria: *Escherichia coli*, *Enterobacter* sp., *Proteus mirabilis*, anaerobic bacteria: *Propionibacterium acnes* and pathogenic yeast: *Candida albicans* were tested. All extracts revealed antimicrobial activity of *S. aureus* and *P. acnes*. The extract of *T. pagdeni* propolis exhibited the highest antimicrobial activity with 8 mm and 9 mm of inhibition zone of *S. aureus* and *P. acnes*, respectively at concentration 100 µg/disc. While, the propolis extracts of *L. ventralis* and *L. terminata* at concentration 10 mg/disc demonstrated comparable size of inhibition zone of *S. aureus* and *P. acnes*. The minimal inhibition concentrations of *T. pagdeni* extract were 31.25 µg/ml against *S. aureus* and 15.625 µg/ml against *P. acnes*. Thus, the extract of *T. pagdeni* propolis was selected for further identification of the active compound. Alpha-mangostin was identified as the possible active compound by chromatographic method. In conclusion, *T. pagdeni* propolis extract could be suggested as good source for utilizing as antimicrobial agent and for further development as pharmaceutical products.

Keywords: Antimicrobial, stingless bees, Propolis, mangosteen

Introduction

Propolis is one of natural products that exhibits extensive pharmacological activity such as antiviral, antibacterial, antifungal, antioxidant, anti-inflammatory, antitumor activities and is also listed in the Chinese Pharmacopoeias and London Pharmacopoeias.[1,2] Nevertheless, the

1st-3rd Feb 2016, Bangkok, Thailand

biological activities and chemical divergence of propolis depend on bee species and the flora at site of bee collection. For example, propolis from North America and Europe regions' main compounds contain mostly cinnamic acids and their esters, flavones, flavanones, while that from Brazil mainly consist of diterpenic acids, prenylated *p*-coumaric acids.[3,4] In addition, different races of honeybees collected at the similar area established varying potency. Stingless bees: *Trigona incisa*, *Timia apicalis*, *Trigona fusco-balteata* and *Trigona fuscibasis*, from Indonesia revealed different degree of cytotoxicity. *Apis mellifera caucasica* showed a greater antibacterial activity than *Apis mellifera carnica* and *Apis mellifera anatolica*.[5,6]

In Thailand and India, stingless bee propolis is widely applied for the treatment of maladies such as acne, toothache and inflammation.[7,8] Antimicrobial, antiproliferative and antioxidant activities of some species of stingless bee propolis were investigated.[9] However, the study of propolis from Thai stingless bees, (*Tetragonula pagdeni* Schwarz, *Lepidotrigona ventralis* Smith, and *Lepidotrigona terminata* Smith), which are commercially cultivated in artificial hives in fruit gardens and used in several preparations in Thailand, is limited. Thus, the objective of the present work was to compare antimicrobial effect of propolis from three stingless bee species in the same area of Thai mangosteen orchard. In addition, the active compound from the species producing the strongest antimicrobial activity was identified.

Materials and Methods

Propolis sample and preparation

Propolis of *Tetragonula pagdeni* Schwarz, *Lepidotrigona ventralis* Smith, and *Lepidotrigona terminata* Smith were collected from the mangosteen garden in December from Makham district, Chanthaburi province, Thailand in 2014, and kept in the dark at 0 °C until use. The stingless bees were identified by Dr.Chama Inson, Department of Entomology, Faculty of Agriculture, Kasetsart University. The voucher specimens (*Tetragonula pagdeni* No.1214003, *Lepidotrigona ventralis* No.1214001 and *Lepidotrigona terminata* No.1214002) were deposited at Faculty of Pharmaceutical Sciences, Burapha University, Thailand.

Propolis from different bee species (20 g) was separately cleaned and cut into small pieces and was then sonicated with 80% ethyl alcohol (400 ml) at 40 °C for 30 min. The suspension was centrifuged at 3,000 g for 5 min at 20 °C. The supernatant was kept while the pellet was re-extracted using the same procedure. The supernatants were pooled together and evaporated in a rotary evaporator. Each extract was dewaxed by sonication with 100 ml of hexane at 40°C for 20 min and centrifuged at 2,000 g for 5 min at 20°C. The supernatant was discarded while the crude residue was kept and stored in the dark at 0 °C.

Microorganisms

The pathogenic microorganisms used in this study were: gram-positive bacteria including *Staphylococcus aureus*, *Propionibacterium acnes* and gram-negative bacteria including *Escherichia coli*, *Enterobacter aerogenes* ATCC13048, and *Proteus mirabilis*. Important pathogenic yeast, *Candida albicans* was also used in this study. The bacteria and

yeast were obtained from Faculty of Allied Health Sciences, Burapha University, Thailand. Moreover, they were tested with many antibiotics and showed no resistant strains. All strains were confirmed by cultural and biochemical characteristics and stored at 4ºC for further use. Anaerobic jar was used for the growth of *P. acnes* in all experiment of the study.

Antimicrobial activities test

Antimicrobial activity of each extract was determined using a modified Kirby-Bauer disc diffusion method. Briefly, the microorganisms were cultured in nutrient broth (Criterion, Hardy Diagnostics) at 35-37 ºC for 18-24 h, and then collected by centrifugation and washed with PBS. The cell suspensions were adjusted with McFarland standard no. 0.5 density to obtain a final concentration of approximately 10^8 CFU/ml by using densitometer (DEN-1 McFarland Densitometer). After that they were spread onto Muller Hinton Agar (Criterion, Hardy Diagnostics). The extracts were tested using 6 mm sterilized filter paper discs (GE Healthcare Life Sciences). Discs were impregnated with 10 µl of the extract in different concentrations. Incubation was done at 35 ºC for 18 – 24 h. Inhibition zone of each extract was observed and indicated for its antimicrobial activity of the extracts. The diluent of the extracts (1% DMSO) was used as a negative control. Ampicillin (10 µg/disc), gentamycin (10 µg/disc), penicillin G (10 Units/disc), chloramphenicol (30 µg/disc), kanamycin (30 µg/disc), and tetracycline (30 µg/disc) (Oxoid) were served as positive controls for antimicrobial activity.

Broth microdilution test

The minimum inhibitory concentration (MIC) of the extracts was determined using conventional broth microdilution method according to the CLSI guideline. The extracts were prepared in Mueller-Hinton broth in different concentrations, and then added into each well of sterile 96-well microtiter plate (50 µl/well). The adjusted bacterial suspension in Mueller-Hinton broth was added to each well (50 µl/well). Finally, final concentrations of the extract of 1 mg/ml to 0.98 µg/ml and final inoculum concentration of 1×10^5 CFU/ml were obtained. The plate was incubated for 18-24 hours at 35-37°C. A control well containing the growth medium, the bacteria, and the extract were also set-up. The minimum inhibitory concentration (MIC) of the extracts was defined as the lowest concentration of the extract that inhibits the visible bacterial growth.

Separation of active compound by thin-layer chromatography

The propolis extract from *Tetragonula pagdeni* that exhibited the strongest activity was selected to separate the bioactive compounds. The crude residue was subjected to column chromatography (3 × 20 cm, Silica gel (0.063 – 0.200 mm) with 20% ethyl acetate in hexane as a mobile phase monitored by thin-layer chromatography. The fraction was applied to pTLC with dichloromethane (triple run) as a mobile phase. The pure compound was dissolved in 99.98% $CDCl_3$ (ca. 5 mg in 0.7 ml) and transferred into 5 mm NMR sample tube (Promochem, Wesel, Germany). Spectra were recorded by the Bruker Topspin software on a Bruker AVANCE 400 spectrometer (Bruker, Rheinstetten, Germany). The NMR data was compared with the previous study and reported as alpha-mangostin.

Table 1. Antimicrobial activity of *T. pagdeni* propolis extract against microorganisms

Microorganisms	Concentration of the *T. pagdeni* propolis extract (per disc)			
	Size of inhibition zone (mean ± SD)			
	100 µg	50 µg	10 µg	1% DMSO
S. aureus	8.0 ± 0.0 mm	6.7 ± 0.3 mm	-	-
Propionibacterium acnes	9.0 ± 0.0 mm	-	-	-
E. coli	-	-	-	-
Enterobacter aerogenes	-	-	-	-
Proteus mirabilis	-	-	-	-
Candida albicans	-	-	-	-

Table 2. Antimicrobial activity of *L. ventralis* propolis extract against microorganisms

Microorganisms	Concentration of the *L. ventralis* propolis extract (per disc)				
	Size of inhibition zone (mean ± SD)				
	20 mg	10 mg	1 mg	100 µg	1% DMSO
S. aureus	7.5 ± 0.7 mm	7.0 ± 0.0 mm	-	-	-
Propionibacterium acnes	11.0 ± 0.0 mm	9.0 ± 0.0 mm	-	-	-
E. coli	-	-	-	-	-
Enterobacter aerogenes	-	-	-	-	-
Proteus mirabilis	-	-	-	-	-
Candida albicans	-	-	-	-	-

Table 3. Antimicrobial activity of *L. terminata* propolis extract against microorganisms

Microorganisms	Concentration of the *L. terminata* propolis extract (per disc)				
	Size of inhibition zone (mean ± SD)				
	20 mg	10 mg	1 mg	100 µg	1% DMSO
S. aureus	10.5 ± 0.7 mm	8.0 ± 0.0 mm	-	-	-
Propionibacterium acnes	12.0 ± 0.0 mm	8.0 ± 0.0 mm	-	-	-
E. coli	-	-	-	-	-
Enterobacter aerogenes	-	-	-	-	-
Proteus mirabilis	-	-	-	-	-
Candida albicans	-	-	-	-	-

Results

The antimicrobial effect of the extracts

Determination of antimicrobial activity of each extract against *S. aureus, P. acnes, E. coli, Enterobacter aerogenes, P. mirabilis,* and *C. albicans* by disc diffusion method was measured by measuring the zone of inhibition. One hundred microgram, 50 and 10 µg per disc of *T. pagdeni* propolis extract were used for determination of their antimicrobial activities against those microorganisms. *T. pagdeni* propolis at the concentration of 100 µg showed inhibitory effect against *S. aureus* and *P. acnes,* as indicated by the inhibition zone of 8 and 9 mm, respectively. Moreover, the extract at the concentration of 50 µg can inhibit S. aureus (Table 1).

L. ventralis propolis extract at the concentrations of 20 mg, 10 mg, 1 mg and 100 µg were tested. The extract at the concentration of 20 and 10 mg showed antibacterial activity against *S. aureus* and *P. acnes* (Table 2). Antibacterial activity against *S. aureus* expressed as inhibition zone of 11 and 8 mm was produced by *L. terminata* propolis at the concentration of 20 and 10 mg, respectively. *P. acnes* was also inhibited by *L. terminata* propolis at the same concentrations of 20 and 10 mg producing inhibition zone of 12 and 8 mm, respectively (Table 3).

T. pagdeni propolis was selected for investigation of minimal inhibition concentration (MIC) because the species exhibited the strongest activity and extracts of (*L. ventralis* and *L. terminata*) could not be dissolved in the culture media. *T. pagdeni* propolis extract using 2-fold serial dilution method ranging from 1 mg/ml to 0.98 µg/ml was tested for MIC value against the *S. aureus* and *P. acnes.* The extract showed MIC of 31.25 µg/ml against *S. aureus* whereas it has greater activity against *P. acnes* by showing MIC of 15.625 µg/ml. The extracts provided antimicrobial activities in a dose-dependent manner. Moreover, alpha-mangostin, an active compound identified in *T. pagdeni* propolis extract, had antibacterial effect against *S. aureus* (inhibition zone of 10 mm) and *P. acnes* (inhibition zone of 9 mm).

Discussion

Propolis is utilized for medicinal and nutraceutical purposes. Most of studies describe the antimicrobial activity of propolis extract collected by European honey bee, *Apis mellifera.* Stingless bee propolis is a kind of propolis collected by stingless bee species, a large group of eusocial insect, that play a part in plant pollination in tropical regions. However, pharmacological activity of its propolis needs elucidation.[8,9]

Propolis from some stingless bee species has been suggested to provide strong antibacterial activity against Gram-positive bacteria, particularly, *Staphylococcus* strains, but weaker activity against Gram-negative bacteria. Our study indicated that Thai stingless bee propolis from mangosteen orchard has antibacterial activity for gram-positive bacteria, *S. aureus* and *P. acnes,* although the extracts at concentration of 20 mg/disc were not effective against some gram-negative bacteria and fungi. In addition, *T. pagdeni* propolis extract

demonstrated the strongest activity and alpha-mangostin could be one of active compounds responsible for its antibacterial activity.

Conclusion

This study has suggested that different stingless bee propolis cultivated in mangosteen orchard may be further developed as antimicrobial agents. Moreover, the propolis extract of *T. pagdeni* provided the strongest antibacterial activities among the extracts studied and alpha-mangostin could possibly be applied as a marker compound for standardization of the extracts.

Acknowledgements

References

1. Sforcin JM, Bankova V. Propolis: Is there a potential for the development of new drugs? J Ethnopharmacol. 2011;133(2):253-60.
2. Zhang H, Wang G, Beta T, Dong J. Inhibitory properties of aqueous ethanol extracts of propolis on alpha-glucosidase. Evid Based Complement Alternat Med. 2015;2015:7.
3. Bankova V. Chemical diversity of propolis and the problem of standardization. J Ethnopharmacol. 2005;100(1–2):114-7.
4. Sforcin JM. Propolis and the immune system: a review. J Ethnopharmacol. 2007;113(1):1-14.
5. Silici S, Kutluca S. Chemical composition and antibacterial activity of propolis collected by three different races of honeybees in the same region. J Ethnopharmacol. 2005;99(1):69-73.
6. Kustiawan PM, Puthong S, Arung ET, Chanchao C. *In vitro* cytotoxicity of Indonesian stingless bee products against human cancer cell lines. Asian Pac J Trop Biomed. 2014;4(7):549-56.
7. Choudhari MK, Punekar SA, Ranade RV, Paknikar KM. Antimicrobial activity of stingless bee (*Trigona sp*.) propolis used in the folk medicine of Western Maharashtra, India. J Ethnopharmacol. 2012;141(1):363-7.
8. Umthong S, Phuwapraisirisan P, Puthong S, Chanchao C. *In vitro* antiproliferative activity of partially purified *Trigona laeviceps* propolis from Thailand on human cancer cell lines. BMC Complement Altern Med. 2011;11:37
9. da Cunha MG, Franchin M, de Carvalho Galvao LC, de Ruiz AL, de Carvalho JE, Ikegaki M, et al. Antimicrobial and antiproliferative activities of stingless bee *Melipona scutellaris* geopropolis. BMC Complement Altern Med. 2013;13:23.

RESEARCH ARTICLE

Inhaled nebulized sodium nitrite has no effect on oxidative stress in healthy volunteers; a preliminary study

Jirada Kaewchuchuen[1], Tipparat Parakaw[1], Sirada Srihirun[2], Supeenun Unchern[1], Nathawut Sibmooh[1]

[1]*Department of Pharmacology, Faculty of Science, Mahidol University, Bangkok 10400, Thailand*
[2]*Department of Pharmacology, Faculty of Dentistry, Mahidol University, Bangkok 10400, Thailand*

Address correspondence and reprint request to: Nathawut Sibmooh, Department of pharmacology, Faculty of Science, Mahidol University.
E-mail address: Nathawut.sib@mahidol.ac.th

Abstract

Nitrite, a bioactive derivative of nitric oxide (NO), has been shown to reduce pulmonary artery pressure (PAP), and is under clinical trial for treatment of pulmonary hypertension in thalassemia. However, the effect of nitrite on oxidative stress has not been reported in humans. Here, we aimed to examine the effect of inhaled nebulized sodium nitrite (37.5 mg single dose) on oxidative stress in 7 healthy subjects. Nitrite in whole blood was measured by chemiluminescence. Thiobarbituric reactive substances (TBARs), markers of lipid peroxidation, and reduced glutathione (GSH) were determined. The nitrite levels increased from the baseline (0.14 μM) to the maximum concentration (1.92 μM) immediately after nebulization, and decreased with the half-life of 30 minutes. TBARs in plasma and erythrocytes were unchanged, while the reduced glutathione (GSH) in erythrocytes were also unchanged. We conclude that nitrite has no effect on oxidative stress. Further study with larger number of subjects is required to ensure the safety of inhaled nitrite.

Keywords: Oxidative stress, thiobarbituric reactive substances, reduced glutathione

Introduction

Pulmonary hypertension is a life-threatening complication in thalassemia. It is characterized by restriction of blood flow through the pulmonary arterial circulation. Nowadays, the evidence-based treatment for pulmonary hypertension in thalassemia is lacking. Although NO is pulmonary vasodilator effective in pulmonary hypertension, it is unstable gas and inconvenient for use in this chronic clinical setting. In contrast, nitrite is a stable product of NO, and converted to NO under hypoxic acidotic condition. Nitrite inhalation can reduce pulmonary artery pressure in hypoxia-induced pulmonary hypertension in lambs[1]. Thus, there is a potential for development of inhaled nitrite as a drug. Inhaled sodium nitrite is currently under clinical trial for pulmonary hypertension in thalassemia[2].

Nitrite plays an important role in biological functions at the physiological concentration. Nitrite at high concentrations causes toxicities including hypotension, methemoglobinemia, and increased oxidative stress[3]. An in vitro study with sodium nitrite at high doses reveals an increase in oxidative stress in human erythrocytes. High-dose sodium nitrite (0.1-10.0 mM) induces oxidative stress in erythrocytes as demonstrated by membrane damage, protein oxidation, lipid peroxidation, and altered metabolic pathways[3]. Sodium nitrite enhances expression of markers of renal oxidative stress in guinea pigs[4].

In this study, we aim to investigate the effect of inhaled nitrite at pharmacologic dose on oxidative stress in healthy volunteers by determination of TBARs and erythrocytic GSH following nitrite inhalation.

Materials and Methods

Subjects

Three male and four female healthy subjects, average age of 23.27±0.63 years, enrolled in this study. The study was approved by the Committee on Human Rights Related to Research Involving Human Subjects from Faculty of Medicine Ramathibodi Hospital, Mahidol University, Bangkok, Thailand (ID 03-56-27).

Sodium nitrite nebulization

Sodium nitrite solution was prepared by Faculty of Pharmacy, Chulalongkorn University. Sodium nitrite at 37.5 mg single dose was delivered to subjects by 15-minutes nebulization using Beurer IH 25/1 nebulizer (Beurer GmbH Company, Ulm, Germany). As assessed by right heart catherization, the mean pulmonary arterial pressure was reduced during 40-mg sodium nitrite nebulization (unpublished data).

Blood sample collection

Venous blood was collected using ethylenediaminetetraacetic acid (EDTA) (1.8 mg/mL) as anticoagulant before inhalation, immediately 10 and 60 minutes after inhalation for oxidative stress markers. The blood was collected at before inhalation, immediately, 30 and 60 minutes after inhalation for measurement of whole blood nitrite levels. Whole blood samples were centrifuged at 14,000 g, room temperature, for 2 minutes to separate plasma and erythrocytes.

Determination of nitrite in whole blood

Since nitrite has a short half-life (about 30 minutes), the nitrite-preserving solution containing 0.8 M ferricyanide, 10 mM N-Ethylmaleimide (NEM), and 1%NP-40[5] was added to the whole blood samples. The preserved samples were kept frozen at -80ºC within 1 week until measurement. The samples were deproteinated with ice-cold methanol (1:1 v/v), mixed for 1 minute, and centrifuged at 14,000 g for 4 minutes at 4ºC. Supernatant was injected into column that contains tri-iodide solution. Nitrite levels were measured by the Chemiluminescence-NO analyzer (CLD88, ECO Medics, Duernten, Switzerland).

Determination of TBARs in plasma and erythrocytes

Lipid peroxidation was determined by spectrofluorometry using thiobarbituric acid assay[6]. Briefly, plasma was 2.5-fold diluted with deionized-distilled water. Protein in erythrocyte was precipitated in 10% trichloroacetic acid. Diluted plasma or supernatant of erythrocyte extract were mixed with 100 mM butylated hydroxytoluene , 10% trichloroacetic acid, ethylene diaminetetraacetic acid. Then, 1% thiobarbituric acid was added into samples and incubated at 90˚C for 1 hour. TBARs were extracted by 1 mL butanol. TBARs were determined at 531 nm excitation and 553 nm emission. Tetraethoxypropane was used as a standard.

Measurement of GSH in erythrocytes

GSH was determined by spectrofluorometry using ophthalaldehyde[7]. Briefly, erythrocytes were 24-fold diluted with 0.1 M sodium phosphate-EDTA buffer. Samples were deproteinated by meta-phosphoric acid. Supernatant was mixed with 100 µl of ophthalaldehyde and incubated at dark, room temperature for 15 minutes. GSH was determined at 340 nm excitation and 420 nm emission.

Statistical analysis

Data were expressed as means ± SEM (n=7). Comparison test was done by one-way analysis of variance (ANOVA) with Tukey's multiple comparison test. P-value < 0.05 was considered statistically significant.
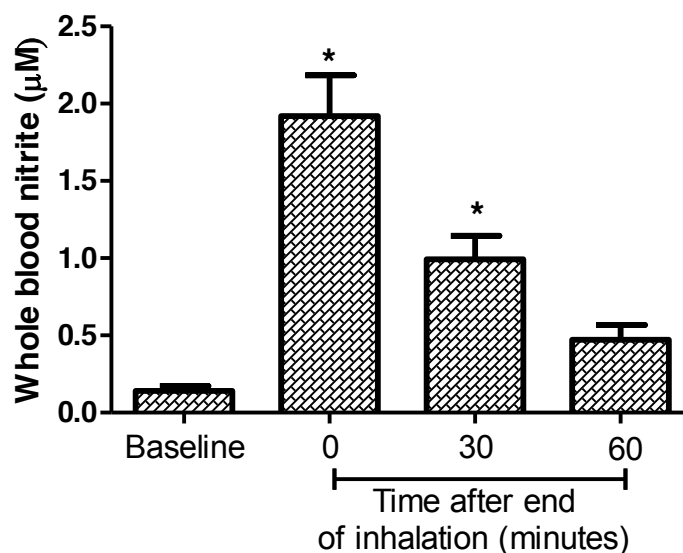
Figure 1 Whole blood nitrite levels at time before, immediately after, 30- and 60-minutes after 37.5 mg sodium nitrite inhalation (n=7) . *Whole blood nitrite levels significantly decreased between baseline and immediately after nitrite inhalation and between baseline and 30 minutes after inhalation.

Results

Nitrite in blood

Immediately after 15-minute nebulization of sodium nitrite (37.5 mg), the nitrite levels in whole blood significantly increased from 0.14 to 1.92 μM ($P < 0.05$). The whole blood nitrite levels at 30 minutes after nitrite inhalation also increased than before inhalation ($P < 0.05$). Afterward, nitrite decreased with half-life of 30 minutes (Figure 1).

Lipid peroxidation in plasma and erythrocytes

TBARs were measured as markers of lipid peroxidation. Inhalation of sodium nitrite (37.5 mg) had no effect on lipid peroxidation in plasma and erythrocyte (Figure 2a and 2b)
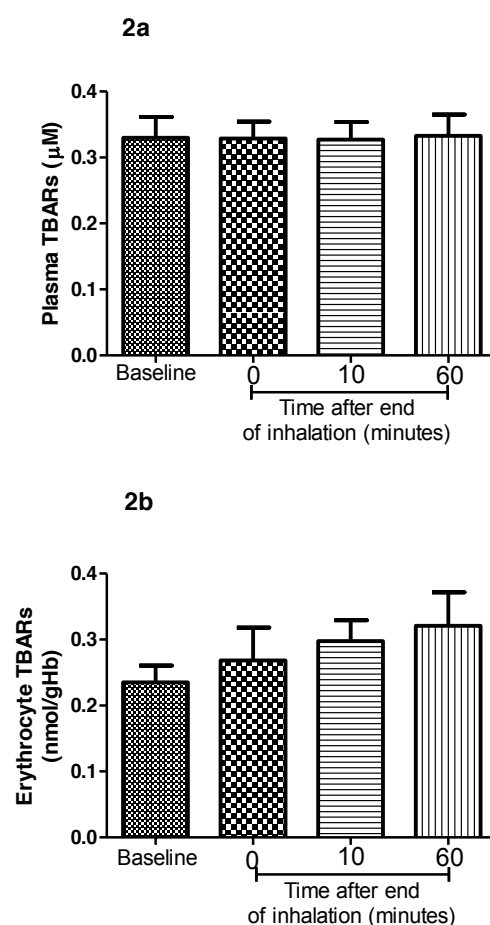
Figure 2 TBARs levels in plasma (a) and erythrocytes (b) at time before, immediately after 10 and 60-minutes after 37.5-mg sodium nitrite inhalation (n=7).

GSH in erythrocytes

GSH was measured as antioxidant marker. Sodium nitrite inhalation (37.5 mg) had no effect on GSH level in erythrocytes (Figure 3).
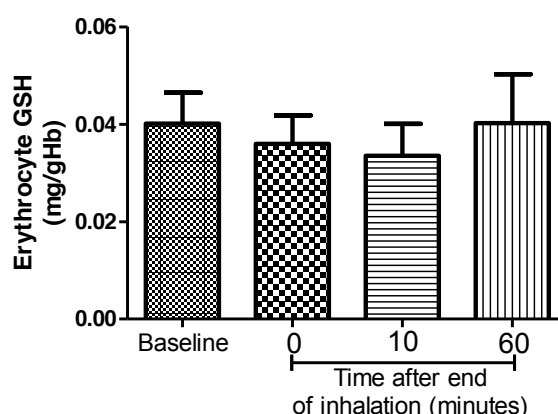
Figure 3 Reduced glutathione (GSH) in erythrocytes at time before, immediately after 10 and 60-minutes after 37.5-mg sodium nitrite inhalation (n=7).

Discussion and Conclusion

Nitrite was reduced to NO that has multiple biological effects including vascular relaxation[8] and platelet inhibition[9]. Nitrite is extensively undergoing clinical investigations for treatment of cardiovascular disorders such as hypertension[10], pulmonary hypertension[1], and cerebral vasospasm after subarachnoid hemorrhage[11].

One of the concerns is nitrite-induced oxidative stress. Nitrite is converted to NO by reductase activity of heme-containing proteins. Then, NO may increase oxidative and nitrosative stress by reacting with superoxide anion (O_2^-) to form toxic peroxynitrite ($OONO^-$) leading to the subsequent decrease in activity of antioxidant enzymes[3]. An in vitro study showed that sodium nitrite at 0.1-0.5 mM incubated for 30 minutes induced oxidative damage to human erythrocytes[3]. However, the maximum blood nitrite concentration in our study was 1.92 μM which was lower than that of in vitro report. Thus, it is unlikely that nitrite at pharmacologic dose would increase oxidative stress in vivo.

In our study, 37.5-mg dose of nitrite was chosen because nitrite at 40 mg could reduce mean pulmonary arterial pressure in thalassemia patient with pulmonary hypertension (unpublished data). So we demonstrate that sodium nitrite at 37.5-mg single dose is safe without any change in hemodynamics and has no effect on oxidative stress.

In summary, we provide data to ensure the safety of inhaled sodium nitrite and encourage its advancement into clinical trial. The long-term effect of nitrite on oxidative requires further investigation.

Acknowledgements

References

1. Hunter CJ, Dejam A, Blood AB, Shields H, Kim-Shapiro DB, Machado RF, et al. Inhaled nebulized nitrite is a hypoxia-sensitive NO-dependent selective pulmonary vasodilator. Nat Med. 2004;10(10):1122-7.
2. Effect of inhaled nebulized nitrite on pulmonary arterial pressure in thalassemia patients with pulmonary arterial hypertension [internet].2015 [cited 2015 Dec 14]. Available from: http:// clinicaltrials.in.th
3. Ansari FA, Ali SN, Mahmood R. Sodium nitrite-induced oxidative stress causes membrane damage, protein oxidation, lipid peroxidation and alters major metabolic pathways in human erythrocytes. Toxicology in Vitro. 2015 ;29(7):1878-86.
4. Baek JH, Zhang X, Williams MC, Hicks W, Buehler PW, D'Agnillo F. Sodium nitrite potentiates renal oxidative stress and injury in hemoglobin exposed guinea pigs. Toxicology. 2015;333:89-99.
5. Piknova B, Schechter AN. Measurement of Nitrite in Blood Samples Using the Ferricyanide-Based Hemoglobin Oxidation Assay. Methods in molecular biology (Clifton, NJ). 2011;704:39-56.
6. Dawn-Linsley M, Ekinci FJ, Ortiz D, Rogers E, Shea TB. Monitoring thiobarbituric acid-reactive substances (TBARs) as an assay for oxidative damage in neuronal cultures and central nervous system. Journal of Neuroscience Methods. 2005;141(2):219-22.
7. Hissin PJ, Hilf R. A fluorometric method for determination of oxidized and reduced glutathione in tissues. Analytical Biochemistry. 1976;74(1):214-26.
8. Cosby K, Partovi KS, Crawford JH, Patel RP, Reiter CD, Martyr S, et al. Nitrite reduction to nitric oxide by deoxyhemoglobin vasodilates the human circulation. Nat Med. 2003;9(12):1498-505.
9. Srihirun S, Sriwantana T, Unchern S, Kittikool D, Noulsri E, Pattanapanyasat K, et al. Platelet Inhibition by Nitrite Is Dependent on Erythrocytes and Deoxygenation. PLoS ONE. 2012;7(1):e30380.
10. Calvert JW, Lefer DJ. Clinical translation of nitrite therapy for cardiovascular diseases. Nitric Oxide. 2010;22(2):91-7.
11. Pluta RM, Dejam A, Grimes G, Gladwin MT, Oldfield EH. Nitrite infusions to prevent delayed cerebral vasospasm in a primate model of subarachnoid hemorrhage. JAMA. 2005;293(12):1477-84.

RESEARCH ARTICLE

The effect of Ayurved Siriraj Ha-Rak recipe on pain and edema in rat models

Wassamun Suksawad[1], Pinpilai Jutasompakorn[1], Uraiwan Panich[1], Pravit Akarasereenont[1, 2], Pinpat Tripatara[1]

[1]*Department of Pharmacology, Faculty of Medicine Siriraj Hospital, Mahidol University, Bangkok 10700, Thailand*
[2]*Center of Applied Thai Traditional Medicine, Faculty of Medicine Siriraj Hospital, Mahidol University, Bangkok 10700, Thailand*

Address correspondence: Pinpat Tripatara, Department of Pharmacology, Faculty of Medicine Siriraj Hospital, Mahidol University, Bangkok 10700, Thailand.
E-mail address: pinpat.tri@mahidol.ac.th

Abstract

Ha-Rak recipe has been used widely in Thailand for relief of fever. Ha-Rak recipe has been included in the list of herbal medicinal products since 2011 by National Drug Committee of Thailand. Its extract was found to reduce fever, decrease tissue damage, and reduce pain and edema in animal studies. However, there is no evidence to support the use of this herbal medicine in a form of mixed crude herbs as in the list of herbal medicinal products. This study aimed to investigate the effect of Ayurved Siriraj Ha-Rak recipe (AVS022) powder of the crude herbs on pain and edema in rats.

Three animal models were used in this study to investigate the effects of AVS022 in different modalities of inflammation, hotplate test for the thermal pain, formalin test for the chemical pain, and carrageenan induced paw edema for the swelling. In the hot plate test, the positive control 10 mg/kg indomethacin, significantly reduced the reaction time to hot plate test at nearly all time points starting at 75 min after administration. When compared with vehicle control, oral administration of AVS022 at dose of 300, 1000, or 3000 mg/kg does not increase reaction time to the thermal stimulus or decrease the licking response to the pain caused by formalin in early phase (0-5 min). However, all doses of AVS022 significantly reduced the licking response to the pain caused by formalin in late phase (20-30 min). Interestingly, the effect of AVS022 on the pain induced by formalin has the same trend with the effects observed in indomethacin treated group. In carrageenan induced paw edema model, indomethacin and all doses of AVS022 exhibited the strong and moderate anti-edematous effect, respectively.

In conclusion, AVS022 possess peripheral analgesic activity in rats. Furthermore, it possessed anti-edematous effect which may involve the inhibitory effect on inflammatory or pain mediators. Therefore, the AVS022 may be a potential herbal recipe for analgesic and anti-edematous activities.

Keywords: Ayurved Siriraj Ha-Rak**,** pain, edema

Introduction

Inflammation is the common health problems. The description of acute inflammatory response in term of cardinal signs are redness, heat, swelling, pain, and loss of function.[1] The common drugs used to treat inflammation, non-steroidal anti-inflammatory drugs (NSAIDs) have many side effects such as gastrointestinal irritation and ulcer, especially from classical NSAIDs, and increased cardiovascular risk, from selective cyclooxygenase-2 (COX-2) inhibitors.[2-3]

The use of herbal medicine as the alternative treatment is increasing in Thailand. However, most of the herbal plants used as medicine are still lacking scientific evidence to support their efficacy. The Ha-Rak recipe is a traditional medicine that has been indicated for treatment of fever in the 2011 Thailand Herbal Medicine Essential Drug List for both children and adults.[4] Besides oral administration, it can be topically used to treat many inflammatory skin conditions such as urticarial and dermatitis.[5-6] Moreover, the extraction of Ha-Rak recipe possessed both antipyretic and anti-nociceptive properties.[7] The recipe composed of five herbal dried roots, Ching Chi *(Capparis micracantha DC)*, Thao yaai mom *(Clerodendrum petasites S.Moore)*, Khonthaa (*Harrisonia perforata Merr.*), Ma duea chumphon (*Ficus racemosa Linn.*) and Ya Nang *(Tiliacora triandra Diels.)*, in equal weight. Its individual component also has various effects including antipyretics[8] and anti-inflammation.[8-10] These previous reports suggested that Ha-Rak recipe may have the pharmacological efficacies similar to NSAIDs, which have been known to possess analgesic, antipyretics, and anti-inflammation effects. However, these studies in the literature used combination of hydroethanolic extracts instead of crude drugs of the root as stated in Thailand Herbal Medicine Essential Drug List. Therefore, this study investigated the effects of Ayurved Siriraj Ha-Rak recipe (AVS022), as crude drug, on pain and edema, in order to provide scientific evidence supporting therapeutic use of Thai herbal medicines in the future.

Materials and Methods

Chemicals and Instruments

λ-Carrageenan (C3889, Sigma-Alrich Co., USA.), 37% Formaldehyde solution (F1635, Sigma-Alrich Co., USA), Indomethacin (Sigma-Alrich Co., USA), Thiopental Sodium for injection BP (Jagsonpal Pharmaceuticals LTD, India), Plethysmometer (Kent scientific corporation, USA.), Hot plate (series 8, IITC Life Science, USA.) were used in this experiment.

Plant Materials and Preparation of AVS022

AVS022 powder was prepared by Manufacturing Unit of Herbal Medicines and Products, Center of Applied Thai Traditional Medicine (CATTM), Faculty of Medicine, Siriraj Hospital, Mahidol University, Thailand under standard Good Manufacturing Practice. The plant materials were authenticated by experienced Thai traditional practitioners. Then, they were underwent crushing to small powder and screening for quality control. Using the dose translation formula based on body surface area,[11] the dosage of AVS022 used in the study was

calculated, from the 3000-4500 mg/day[1] dose range in clinical use stated in Thailand Herbal Medicine Essential Drug List 2011, to be 300, 1000, and 3000 mg/kg/day.

Animal

Male Wistar rats (200-250 g) obtained from the National Laboratory Animal Center, Mahidol University, Salaya, Nakhon Pathom, Thailand, were used in this study. They were acclimatized in the environmentally controlled condition, $25\ 2\pm^0C$ and 12 h light/ dark cycle, for at least 1 week before the experiment. Food and water were given *ad libitum* unless otherwise specified. The experimental protocol was approved by Siriraj Animal Care and Use Committee (SiACUC), Faculty of Medicine Siriraj Hospital, Mahidol University, Bangkok, Thailand. The rats were divided into 5 groups and received treatment by gastric feeding as followed;

1. Vehicle control (distilled water 40 ml/kg)[12]
2. 300 mg/kg AVS022
3. 1000 mg/kg AVS022
4. 3000 mg/kg AVS022
5. 10 mg/kg positive control indomethacin

Hotplate test

The rats were placed on a hot plate maintained the temperature at 54 °C ± 0.5 °C for the measurement of the latency time of nociceptive responses such as licking of a hind paw at 60, 75, 90, 105, 120, 135, 150, 180 and 210 minutes after treatment. Cut-off time for preventing of the tissue damage was 30 seconds.[13-15] Baseline of latency time response was measured at 60 min before treatment.

Formalin test

At 60 minutes after oral treatment, 100 µl of 2.5% formalin in 0.9% normal saline was injected subcutaneously to a right hind paw. Time spent licking the injected paw was recorded and expressed as total licking time in the early phase (0-5 minutes) and the late phase (20-30 minutes) of the formalin injection.[16-18]

Carrageenan-induced hind paw edema

The initial right hind paw volume of the rats was measured just before the treatment as baseline. At 1 h after oral treatment, 100 µl of 1% (w/v) carrageenan in 0.9% normal saline was subcutaneously injected into the subplantar region of the right hind paw.[19] The volume of right hind paw was measured and recorded using a Plethysmometer (Kent scientific corporation, USA) at 1, 2, 3, 4 and 5 h after carrageenan injection. The data were expressed as percentage of swelling compared with the baseline hind paw volume of each rat measured just before the oral treatment. The percentage of edema inhibition were calculated as[20]

$$\%EIx = \frac{EVx\ of\ control\ group - EVx\ of\ treatment\ group}{EVx\ of\ control\ group} \times 100,$$

where, %EIx is the percentage of edema inhibition at time x of the treatment, and EVx is the edema volume (ml) at time x which calculated as the increase of paw volume (ml) at time x from its baseline volume.

Statistical Analysis

The behavioral observation data from hotplate test and formalin test were expressed as mean ± SD. The data from the measurement of paw edema was expressed as mean ± SEM. Statistical comparison was analyzed by using Two-way analysis of variance (ANOVA) and Bonferroni post hoc test. The *p* value of less than 0.05 were considered significant.

Results

Effects of AVS022 on the hotplate test in rats

When compared with vehicle control, AVS022 at dose of 300, 1000 or 3000 mg/kg did not significantly alter the reaction time at 60, 75, 90, 105, 120, 135, 150, 180 and 210 min after administration, whereas, the positive control 10 mg/kg indomethacin, significantly increase latency of nociceptive response to hot plate test at nearly all time points starting at 75 min after administration (Table 1). Hence, the results indicated that AVS022 did not increase the latency of nociceptive response for the thermal stimulation by hot plate in rats.

Effects of AVS022 on the formalin test in rats

When compared with vehicle control, treatment of 10 mg/kg indomethacin or AVS022 at dose 300, 1000, or 3000 mg/kg for 60 min did not significantly reduced the licking time (sec) spent in the early phase (0-5 min) (Figure 1a). However, in the late phase (20-30 min), AVS022 at dose 300, 1000, or 3000 mg/kg significantly decreased the licking time by 45.33%, 29% and 39.19% , respectively when compared with vehicle control (Figure 1b). This effect was also seen with 10 mg/kg indomethacin which intensively inhibited the licking time by 65.56% when compared with vehicle control. The results indicated AVS022 at dose of 300, 1000, or 3000 mg/kg decreased the licking time in late phase (20-30 min) of chemical pain stimulated by formalin in rats.

Effects of AVS022 on carrageenan-induced hind paw edema in rats

When compared with vehicle control, the standard indomethacin at 10 mg/kg strongly decreased the hind paw edema at 2, 3, 4 and 5 h after carrageenan injection (Table 2). Although the effect of AVS022 was not strong as the effect of indomethacin, AVS022 at dose of 300, 1000, or 3000 mg/kg also significantly decreased the hind paw edema at 2, 3, 4 and 5 h after carrageenan injection (Table 2). Therefore, the results indicated that AVS022 also possessed the anti-edematous effect against carrageenan.

Table 1. Analgesic effect of AVS022 on nociceptive response to the thermal stimulus

Treatment	Latency of nociceptive response (s) at different time interval									
	baseline	0 min	15 min	30 min	45 min	60 min	75 min	90 min	120 min	150 min
Control distilled water	9.50 ± 2.43	8.64 ± 2.73	7.89 ± 2.24	8.40 ± 3.97	7.84 ± 3.57	7.98 ± 3.13	6.45 ± 1.19	7.08 ± 2.56	6.69 ± 2.47	6.66 ± 2.26
300 mg/kg AVS022	9.35 ± 2.32	7.81 ± 2.33	9.24 ± 3.94	8.46 ± 1.51	10.79 ± 4.22	9.51 ± 4.41	10.19 ± 3.32	8.78 ± 0.90	6.81 ± 1.86	8.87 ± 3.76
1,000 mg/kg AVS022	9.53 ± 3.20	7.56 ± 1.32	8.84 ± 0.86	9.69 ± 2.93	8.94 ± 2.89	9.51 ± 2.75	9.12 ± 2.30	8.14 ± 2.03	9.26 ± 3.33	7.92 ± 2.44
3,000 mg/kg AVS022	9.32 ± 1.79	10.09 ± 2.33	9.94 ± 2.51	9.20 ± 2.76	10.03 ± 2.87	9.42 ± 3.71	8.84 ± 1.04	8.27 ± 1.73	10.33 ± 2.27	10.08 ± 4.73
10 mg/kg indomethacin	9.94 ± 2.85	9.75 ± 2.51	$11.41 \pm 2.06^{*}$	$11.84 \pm 2.83^{*}$	$12.56 \pm 4.18^{***}$	$12.99 \pm 5.37^{***}$	$12.72 \pm 3.89^{***}$	$11.38 \pm 3.30^{**}$	$11.08 \pm 3.87^{**}$	$12.37 \pm 5.02^{***}$

Latency time of nociceptive response at baseline and at different time after oral administration of 300, 1000, or 3000 mg/kg AVS022, 10 mg/kg indomethacin, or vehicle control. Data are means ± SD (N= 8-15). *p <0.05, **p <0.01, ***p <0.001 *versus* control.

Table 2. Anti-edematous effect of AVS022 on carrageenan-induced paw edema

Treatment	Time after carrageenan injection									
	1 h		2 h		3 h		4 h		5 h	
	EV (ml)	%EI	EV (ml)	%EI	EV (ml)	%EI	EV (ml)	%EI	EV (ml)	%EI
Control (distilled water)	0.067±0.008	-	0.123±0.010	-	0.167±0.020	-	0.178±0.020	-	0.172±0.020	-
300 mg/kg AVS022	0.032±0.005	52.44	0.046±0.008***	62.28	0.082±0.010***	51.07	0.087±0.010***	51.39	0.100±0.010***	41.68
1,000 mg/kg AVS022	0.041±0.007	38.91	0.067±0.009**	45.46	0.086±0.010***	48.30	0.084±0.010***	52.73	0.095±0.010***	44.36
3,000 mg/kg AVS022	0.040±0.006	40.69	0.059±0.008**	52.30	0.091±0.010***	45.24	0.106±0.010***	40.55	0.105±0.010**	38.65
10 mg/kg indomethacin	0.025±0.005	61.23	0.027±0.006***	76.60	0.037±0.008***	77.38	0.039±0.006***	75.79	0.050±0.009***	69.25

Paw edema volume was measured at 1, 2, 3, 4, and 5 h after carrageenan injection in rats treated with oral administration of 300, 1000, or 3000 mg/kg AVS022, 10 mg/kg indomethacin, or vehicle control at 60 min prior to hind paw carrageenan injection. Data are means ± SEM (N= 8-20). **p<0.01 or ***p<0.001 *versus* control. EV, Edema volume; EI, Edema inhibition.
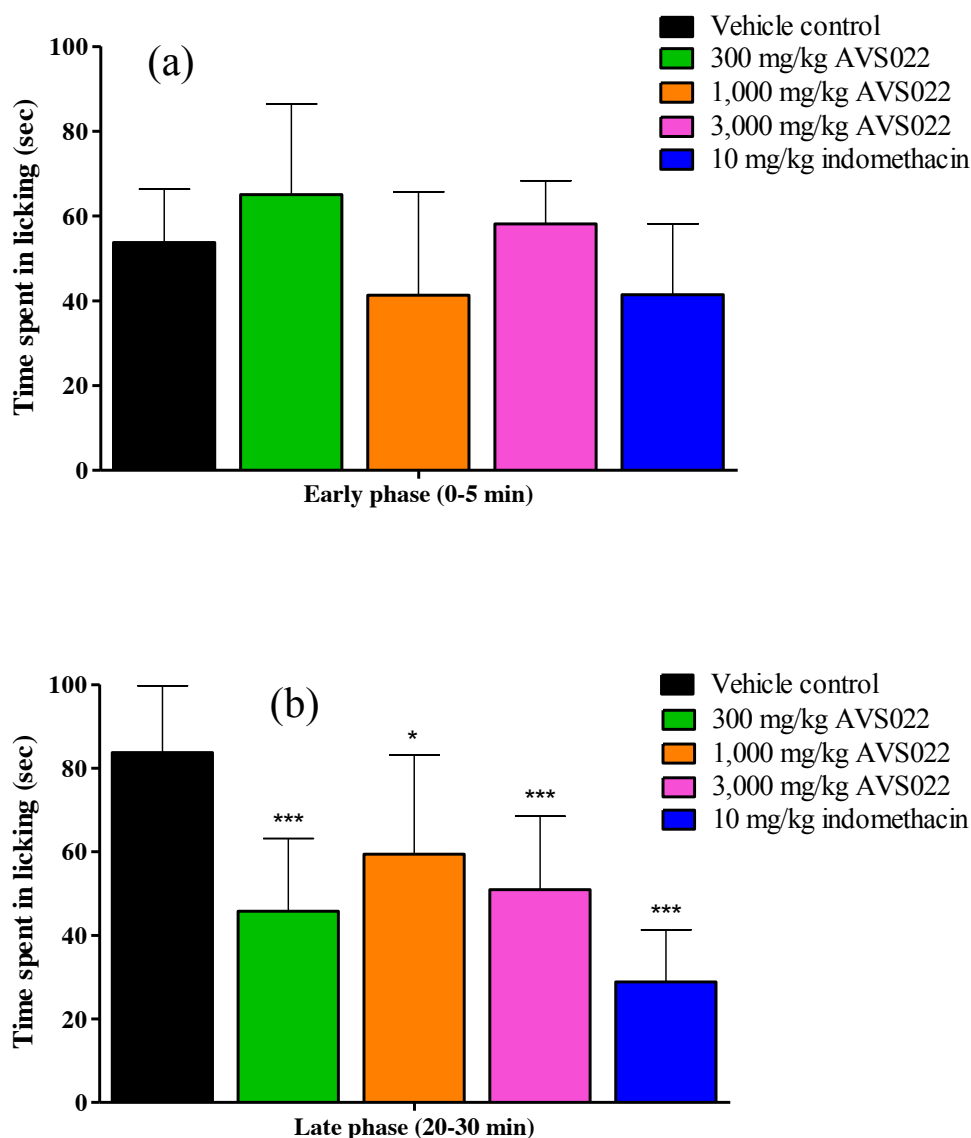
Figure 1. Analgesic effect of AVS022 on nociceptive response to the chemical stimulus Response to chemical stimulus was recorded as licking time spent in (a) early phase or (b) late phase after treatment with oral administration of 300, 1000, or 3000 mg/kg AVS022, 10 mg/kg indomethacin, or vehicle control at 60 min prior to subcutaneous formalin injection. Data are means ± SD (N= 7-8). *p <0.05, **p <0.01, ***p <0.001 *versus* control.

Discussion

Ayurved Siriraj Ha-Rak recipe (AVS022) is a traditional medicine that has been indicated for treatment of fever in the 2011 Thailand Herbal Medicine Essential Drug List for both children and adults[4]. It consists of the equal weight of five Thai herbal roots which are

Ching Chi *(Capparis micracantha DC)*, Thao yaai mom *(Clerodendrum petasites S.Moore)*, Khonthaa (*Harrisonia perforata Merr*.), Ma duea chumphon (*Ficus racemosa Linn*.) and Ya Nang *(Tiliacora triandra Diels.)*.

The previous study of the extract of Ha-Rak recipe indicated that it possessed antipyretic and antinociceptive properties in animal models.[7, 21] Herein, the AVS022 in dried powder from crushed roots, instead of the extract, is used by oral administration to demonstrate the analgesic and anti-edematous effects in rats.

The hotplate test measures the response of noxious stimulus. It reflects activity in thermally sensitive afferent fiber and activity of Aδ and C fiber[22-23] and is suitable for identifying centrally, but not peripherally acting analgesic drug. From the result, all doses of AVS022 do not reduce nociceptive response in hotplate test, so it does not has the effect on supraspinal activity or central pathway mechanism, which is different from the previous study of its extract.[7]

The formalin test is an applicable and reliable model of nociception. There are 2 types of response, early phase and late phase (second phase). Early phase (0-5 min) is mediated by the central effect via a direct stimulation of the nociceptors by chemical irritant. Late phase (10-30 min) response is most likely secondary to development of an inflammatory response mediated by the peripheral effect via the release of chemical mediators such as histamine, serotonin, prostaglandin and bradykinin.[16, 24] Both phases are sensitive to centrally acting drugs such as opiods,[24] but only late phase that is also sensitive to non-steroidal anti-inflammatory drugs (NSAIDs) and corticosteroids.[24] All doses of AVS022 showed analgesic activity only on late phase of formalin test, suggesting the inhibition of peripheral nociception associated with inflammatory response, but not the central effect. However, 300 mg/kg of AVS022 decreased licking time better than 1,000 and 3,000 mg/kg, indicating the bi-phasic dose response[25] which is the result from the effects on different pathways and with the different potency of each component in the recipe.

The carrageenan induced paw edema is commonly used as an experimental animal model for acute inflammation. Edema formation due to carrageenan injection in the rat paw is the biphasic events with initial phase and second phase.[26] The initial phase occurs within first to second hours after carrageenan injection which releases cytoplasmic enzymes and serotonin from mast cell to increase prostaglandin, histamine and bradykinin in the inflammatory area.[26-27] The second phase occurs 3-5 hours after carrageenan injection. Macrophage stimulated by dermal tissue injuries, releases much interleukin-1 (IL-1) to induce accumulation of polymorphonuclear cells (PMNs) in the inflamed area, then leading to the induction of paw swelling. Other mediators such as prostaglandin, bradykinin, protease and lysosomal enzyme were also found in the second phase.[27-28] All doses of AVS022 inhibited paw edema formation at 2-5 hours, suggesting that its mechanism of action possibly involves both phases of edema formation.

Conclusion

The Ayurved Siriraj Ha-Rak recipe (AVS022) possesses peripheral analgesic activity, as well as anti-edematous effect. Both of which are probably mediated via inhibitory effect on the release of pain and/or inflammatory mediators. Therefore, the AVS022 may be a potential herbal recipe for analgesic and anti-edematous activities.

Acknowledgements

References

1. Nathan C. Point of control in inflammation. [review article] Nature. 2002;420(6917):846-52.
2. Bäck M, Yin L, Ingelsson E. Cyclooxygenase-2 inhibitors and cardiovascular risk in a nation-wide cohort study after the withdrawal of rofecoxib. Eur Heart J. 2012;33(15):1928-33.
3. Lanza FL. A review of gastric ulcer and gastroduodenal injury in normal volunteers receiving aspirin and other non-steroidal anti-inflammatory drugs. Scand J Gastroenterol. 1989;24(suppl 163):24-31.
4. Thai National Drug Committee. National list of herbal medicinal products A.D. 2011. Bangkok: Ministry of Public Health. 2011:1-54.
5. ธมลวรรณ ทับพึ่ง, ธนภรณ์ ตั้งจิตปิยะนนท์, ศุณิตา มากชูชิต, อรุณพร อิฐรัตน์. การศึกษาฤทธิ์ต้านการก่อภูมิแพ้ของตำรับยาเบญจโลกวิเชียร (ห้าราก). วารสารการแพทย์แผนไทยและแพทย์ทางเลือก 2552;7:123
6. วรัมพา สุวรรณรัตน์, มะลิ อาจริยะกุล, อรุณพร อิฐรัตน์, สมบูรณ์ เกียรตินันทน์. การศึกษาทางคลินิกระยะที่ 1 เรื่องความปลอดภัยของสารสกัดตำรับยาเบญจโลกวิเชียร และสารสกัดสมุนไพรเดี่ยวที่ (ห้าราก) เป็นส่วนประกอบของตำรับ. ธรรมศาสตร์เวชสาร 2555;4:767-76
7. Jongchanapong A, Singharachai C, Palanuvej C, Ruangrungsi N, Towiwat P. Antipyretic and antinociceptive effects of BEN-CHA-LO-KA-WI-CHIAN REMEDY. J Health Res. 2010;24(1):15-22
8. Panthong A, Kanjanapothi D, Taesotikul T, Wongcome T, Reutrakul V. Anti-inflammatory and antipyretic properties of *Clerodendrum petasites S. Moore*. J Ethnopharmacol. 2003;85(1):151-6.
9. Mandal SC, Maity TK, Das J, Saba BP, Pal M. Anti-inflammatory evaluation of *Ficus racemosa Linn*. leaf extract. J Ethnopharmacol. 2000;72(1-2):87-92.
10. Tangsucharit P, Kukongviriyapan V, Kukongviriyapan U, Airarat W. Screening for analgesic and anti-inflammatory activities of extracts from local vegetables in Northeast Thailand. Srinagarind Med J. 2006;21(4):305-10.
11. Reagan-Shaw S, Nihal M, Ahmad N. Dose translation from animal to human studies revisited. FASEB J. 2008;22(3):659-61.

12. Diehl KH, Hull R, Morton D, et al. A good practice guide to the administration of substances and removal of blood, including routes and volumes. J Appl Toxicol. 2001;21(1):15-23.
13. Woolf G, MacDonald AL. The evaluation of the analgesic action of pethidine hydrochloride (Dermorol). J Pharmacol Exp Ther. 1944; 80:300-7
14. Parker AG, Peraza GG, Sena J, Silva ES, Vaz MRC, Furlong EB, et al. Antinociceptive effects of the aqueous extract of *Brugmansia suaveolens* flowers in mice. Biol Res Nurs. 2007;8(3):234-9.
15. Muccillo-Baisch AL, Parker AG, Cardoso GP, Cezar-Vaz MR, Soares MC. Evaluation of the analgesic effect of aqueous extract of *Brugmansia suaveolens* flower in mice: possible mechanism involved. Biol Res Nurs. 2010;11(4):345-50.
16. Hunskaar S, Berge OG, Hole K. Dissociation between antinociceptive and anti-inflammatory effects of acetylsalicylic acid and indomethacin in the formalin test. Pain. 1986;25(1):125-32
17. Hunskaar S, Hole K. The formalin test in mice: dissociation between inflammatory and non-inflammatory pain. Pain. 1987;30(1):103-14
18. Jaijoy K, Soonthornchareonnon N, Panthong A, Sireeratawong S. Anti-inflammatory and analgesic activities of the water extract from the fruit of *Phyllanthus emblica* Linn. Int J of App Res in Nat Products. 2010;3(2):28-35.
19. Winter CA, Risley EA, Nuss GW. Carrageenan-induced edema in hind paw of the rat as an assay for anti-inflammatory drug. Proc Soc Exp Biol Med. 1962; 111:544-7.
20. Mbiantcha M, Kamanyi A, Teponno RB, Tapondjou AL, Watcho P, Nguelefack TB. Analgesic and anti-Inflammatory properties of extracts from the bulbils of *Dioscorea bulbifera* L. var sativa (Dioscoreaceae) in mice and rats. Evid Based Complement Alternat Med. 2011;2011:1-9.
21. Konsue A, Sattayasai J, Puapairoj P, Picheansoont C. Antipyretic effects of Bencha-Loga-Wichien herbal drug in rats. Thai J Pharmacol. 2008;29(1):79-82.
22. Ibironke GF, Ajiboye KI. Studies on the anti-inflammatory and analgesic properties of *Chenopodium ambrosioides* leaf extract in rat. Int J Pharmacol. 2007;3:111-5
23. Sabina E, Chandel S, Rasool MK. Evaluation of analgesic, antipyretic and ulcerogenic effect of Withaferin A. Int J Integr Biol. 2009;6(2):52-56
24. Shibata M, Ohkubo T, Takahashi H, Inoki R. Modified formalin test: characteristic biphasic pain response. Pain. 1989;38(3):347-52
25. Di Veroli GY, Fornari C, Goldlust I, Mills G, Koh SB, Bramhall JL et al. An automated fitting procedure and software for dose response curves with multiphasic features. Sci Rep. 2015;5(14701):1-11
26. Vinegar R, Schreiber W, Hugo R. Biphasic development of carrageenin edema in rats. J Pharmacol Exp Ther. 1969;166(1):96-103
27. Vinegar R, Truax JF, Selph JL, Johnton PR, Venable AL, McKenzie KK. Pathway to carrageenan-induced inflammation in the hind limb of the rat. Fed Proc. 1987;46(1):118-26
28. Crunkhorn P, Meacock SC. Mediator of the inflammation induced in the rat paw by carrageenan. Br J Pharmacol. 1971;42(3):392-402

RESEARCH ARTICLE

Preliminary study of hypoglycemic effect of palmyra palm fruit fiber water extract on fasting blood glucose level in streptozotocin-induced diabetic rats

Karnsasin Seanoon[1], Supaporn Kansenalak[1], Uraporn Vongvatcharanon[2], Sukanya Dej-adisai[3] and Wandee Udomuksorn[1]*

[1]*Department of Pharmacology, Faculty of Science, Prince of Songkla University, Hatyai, Songkhla 90110, Thailand*
[2]*Department of Anatomy, Faculty of Science, Prince of Songkla University, Hatyai, Songkhla 90110, Thailand*
[3]*Department of Pharmacognosy and Pharmaceutical Botany, Faculty of Pharmaceutical Sciences, Prince of Songkla University, Hatyai, Songkhla 90110, Thailand*

Address correspondence and reprint request to: Wandee Udomuksorn, Department of Pharmacology, Faculty of Science, Prince of Songkla University, Hatyai, Songkhla 90110, Thailand.
E-mail address: wandee.u@psu.ac.th

Abstract

Borassus flabellifer Linn. or palmyra palm belonging to Arecaceae family has been reported using male flower, fruit pulp and inflorescence part for hypoglycemic activity in Thailand and India traditional medicine. There is no scientific proved evidence in animal diabetic model. This study aimed to evaluate the effect of palmyra palm fruit fiber water extract (PFWE) on fasting blood glucose (FBG) level in streptozotocin (STZ)-induced diabetic rats. Male Wistar rats were devided into 7 groups (n=5) which were group 1 normal control, group 2 normal rats orally treated with PFWE 1,000 mg/kg, group 3 diabetic control, group 4 diabetic orally treated with glibenclamide 1 mg/kg, group 5, 6 and 7 diabetic orally treated with PFWE 500, 1,000 and 2,000 mg/kg, respectively. The animals were induced by STZ 50 mg/kg, i.p. and fasting blood level >200 mg/dl was the criteria to be diabetic rat. The result showed that PFWE 500, 1,000 and 2,000 mg/kg, p.o. significantly decreased FBG ($p<0.05$) after PFWE treatment for 3 days (136.80±31.54, 122.00±23.87 and 116.40±22.94 mg/dl) compared with diabetic control (381.00±33.38 mg/dl) while glibenclamide group (325.00±58.73 mg/dl) did not have effect. We can summarized that PFWE has potential to be hypoglycemic drug, the mechanism of action and the major composition of PFWE isolation should be explored further.

Keywords: Palmyra palm fruit fiber, diabetes mellitus, fasting blood sugar level

Introduction

Diabetes mellitus, which has become a major health problem around the world, is categorized as a metabolic disease characterized by increased blood glucose level resulting from defects in insulin secretion, failure of insulin to act on its targets tissue, or both. India, China and the United States are the largest number of people with diabetes and the incidence is increasing day by day.[1] Currently available therapies for diabetes include exercise, insulin

and various oral hypoglycaemic drugs. Although oral drugs have beneficial effects on promoting insulin secretion from β-cell, increasing insulin sensitivity of target organs, inhibiting α-glucosidase and increasing GI hormone to provide lowering blood sugar in diabetes, while they have many side effects and drug resistance would occur after long-term using.[2,3]

Borassus flabellifer Linn. belonging to Arecaceae family, is widely distributed and cultivated in tropical Asian countries such as Thailand, India, Myanmar, Sri Lanka, etc.[4] This plant is traditionally used for treating hyperglycemia including diabetes mellitus in Phra Nakhon Si Ayutthaya Province (Thailand). The fruit contains a yellow–orange pulp and brown fiber covering 1-3 nuts. The pulp contains pectin, sugar, carotenoids and numerous steroidal saponins (flabelliferins).[5] One of these flabelliferins, termed flabelliferin-II (tetraglycoside) was suspected to reduce weight gain in ICR mice[6] and fruit pulp can significantly inhibit the expected increase in blood glucose after a glucose challenge, while enhancing the level of faecal glucose, thus suggesting an inhibition of intestinal glucose uptake.[7] For toxicity study, there is no toxicity of fruit pulp in liver, kidney, hematological parameters and histology of major organs.[8] There is no scientific evidence about the effect of *B. flabellifer* fruit fiber on blood glucose level. Therefore, this study was objected to investigate the effect of *B. flabellifer* fruit fiber on blood glucose level in streptozotocin-induced diabetic rats.

Materials and Methods

Animals

Male Wistar rats, weighting 230-250 g were obtained from the Southern Laboratory Animal Facility, Faculty of Science, Prince of Songkla University, Hatyai, Songkhla, Thailand. The animals were housed in the Southern Laboratory Animal Facility with fresh water and standard food available ad libitum. They were maintained at 12 h light and dark cycles and with room temperature maintained at 22–25ºC in the animal house. The animal protocol was approved by the Animal Ethics Committee, Prince of Songkla University, Thailand (No.34/2555)

Preparation of plant extracts

Fruits of *B. flabellifer* were collected from Sathingpra, Songkhla Province (Thailand). Fruit fiber were chopped and blended into small pieces. They were extracted repeatedly with petroleum ether, ethyl acetate, ethanol and water, respectively for 3 days (x 3 times of each). All filtrates were pooled and the solvent was evaporated by rotary evaporator or hot water bath. The water extracts of *B. flabellifer* gave a percentage yield of 30%. The extracted yields were stored at 4ºC until using.

Induction of diabetes mellitus in rats

Diabetes was induced with a streptozotocin (STZ) which was dissolved in cool and fresh 0.1 M citrate buffer (pH 4.5) at dose of 50 mg/kg, i.p. Diabetes was considered at 4 days after STZ injection by cutting tail tip and determining the fasting blood glucose (FBG) level

using a glucometer (Accu-Chek Performa, Roche Diagnostics, Germany). Only animals with FBG levels above 200 mg/dl were considered to be diabetic rat.

Experimental design

Total of 35 rats were sorted into 7 groups (n=5). Group 1 normal control (non-diabetic) and received distilled water, Group 2 normal rats and received water extracts of *B. flabellifer* (PFWE) 1,000 mg/kg, p.o., Group 3 diabetic control and received distilled water, Group 4 diabetic rats (DM) and received standard drug glibenclamide 1 mg/kg, p.o. Group 5, 6 and 7 diabetic rats and received PFWE 500, 1,000 and 2,000 mg/kg, p.o., respectively. All treatments of water extracts were continued once daily at 12.00 noon for 3 days. Blood glucose levels were estimated at day 0 and day 3 of treatment by cutting tail tip and using a glucometer (Accu-Chek Performa, Roche Diagnostics, Germany).

Statistical analysis

All quantitative data were presented as mean ± standard error of the mean (SEM). Difference between means were analyzed by One-way analysis of variance (ANOVA) followed by Tukey's post-hoc test for the comparison between groups. The differences between groups were considered significant at *p<0.05*.

Results

In the preliminary experiments, the effect of palmyra palm fruit fiber water extract (PFWE) 500, 1,000 and 2,000 mg/kg were studied on the fasting blood glucose in normal and diabetic rats. The results showed that oral administration of PFWE 500, 1,000 and 2,000 mg/kg, p.o. significantly decreased FBG (*p<0.05*) after PFWE treatment for 3 days (136.80±31.54, 122.00±23.87 and 116.40±22.94 mg/dl) when compared with diabetic control (381.00±33.38 mg/dl) while glibenclamide group had FBG level 325.00±58.73 mg/dl, which slightly decreased blood glucose level however the effect was not significant when compared with diabetic control group. In addition, normal rats orally received PFWE 1,000 mg/kg showed no effect on blood glucose level after PFWE treatment for 3 days (106.60±5.46 mg/dl) when compared with normal control group (117.60±7.17 mg/dl) (figure 1).

Discussion

The chemical induced diabetes mellitus in experimental rats is executed using STZ that selectively destroys pancreatic β-cells is convenient and simple to use.[9] STZ causes a degeneration of β-cells of the islets of langerhans and induces hyperglycemia. The hypoglycemic activity of palmyra palm fruit fiber water extract (PFWE) has not been reported previously and its molecular mechanism has not yet been described. In this study, we found the preliminary antihyperglycemic potency of PFWE. The results show that administration of PFWE 500, 1,000 and 2,000 mg/kg in diabetic rats caused a significant (*p<0.05*) reduction in blood glucose level at 3 days after oral administration. This may be due to the stimulation of pancreatic β-cells for a short duration of insulin release against high blood glucose level by this

extract, as same as the activity produced by synthetic oral drugs, glibenclamide, which is responsible for the increase in sensitization and stimulation of β-cells against blood glucose. But in this study, group treated with glibenclamide 1 mg/kg slightly decreased blood glucose level however the effect was not significant because glibenclamide provided a delay onset of its hypoglycemic action and prolonged decrease in blood glucose without any appreciable effect on the initial glucose treatment.[10]
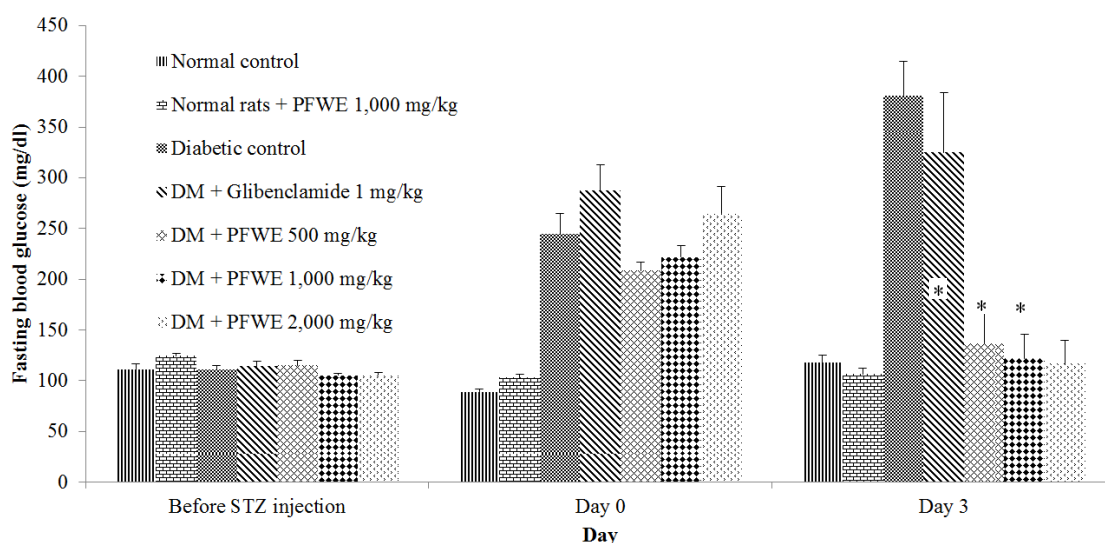
Figure 1. Effect of palmyra palm fruit fiber water extract (PFWE) on fasting blood glucose (FBG) level after 3 days oral administration in normal and diabetic rats. [Control group ( ), diabetic group ( ), normal rats+PFWE 1,000 mg/kg ( ), glibenclamide 1 mg/kg ( ), DM+PFWE 500 mg/kg ( ), DM+PFWE 1,000 mg/kg ( ) and DM+PFWE 2,000 mg/kg ( )] Data is expressed as the mean ± SEM (n=5). * indicates significant difference at $p<0.05$ compared with diabetic control group at the same time.

Conclusion

The present finding indicates that the palmyra palm fruit fiber water extract is able to decrease fasting blood glucose in streptozotocin-induced diabetic rats. From this study suggests that the palmyra palm fruit fiber may have potential pharmacological properties beyond antidiabetic effects. Further studies, doing long duration experimental model of hypoglycemic activity, an isolation of principle compounds and other *in vivo* study to elucidate the mechanism should be done.

Acknowledgements

of Songkla University. I would like to express my great thank to Department of Pharmacognosy and Pharmaceutical Botany, Faculty of Pharmaceutical Sciences for supply of the palmyra palm fruit fiber water extract and Department of Pharmacology and Department of Anatomy, Faculty of Sciences, Prince of Songkla University for instruments and experimental facilities.

References

1   American Diabetes Association (ADA). Position statement: Standards of medical care in diabetes-2015. Diabetic care 2015;38:S1-S94.
2   Michael J, Fowler MD. Diabetes treatment, part 2: oral agents for glycemic management. Clin Diabetes 2007;25:131-4.
3   Bolen S, Feldman L, Vassy J, Wilson L, Yeh HC, Marinopoulos S, et al. Systematic review: comparative effectiveness and safety of oral medications for type 2 diabetes mellitus. Ann Intern Med 2007;147:386-99.
4   Yoshikawa M, Xu F, Morikawa T, Pongpiriyadacha Y, Nakamura S, Asao Y et al. Medicinal Flowers XII (1) New Spirostane-Type Steroid Saponins with antidiabetogenic activity from Borassus flabellifer. Chem Pharm Bull 2007;55:308-16.
5   Thabrew MI, Jansz ER. Nutritive importance of palmyrah products. Recent research development. Environ Biol 2004;1:43-60.
6   Ariyasena DD, Jayasekera S, Jansz ER, Abeysekera AM. Effect of palmyrah (Borassus flabellifer L.) fruit pulp on weight gain by mice. Vidyodaya J Sci 2002;9:99-105.
7   Uluwaduge DI, Thabrew MI, Jansz ER. The effect of flabelliferins of the palmyrah fruit pulp on intestinal glucose uptake in ICR mice. J Natn Sci Foundation 2005;4:37-41.
8   Uluwaduge DI, Thabrew MI, Jansz ER. Preliminary report on the absence of toxicity of the fruit pulp palmyrah (Borassus flabellifer) in ICR mice. J Natn. Sci Foundation 2005;1:37-41.
9   Elsner M, Guldbakke B, Tiedge M, Munday R, Lenzen S. Relative importance of transport and alkylation for pancreatic b-cell toxicity of streptozotocin. Diabetol. 2000;43:1528-33.
10 Ikenoue T, Okazaki K, Fujitani S, Tsuchiya Y, Akiyoshi M, Maki T, Kondo N. Effect of a new hypoglycemic agent, A-4166 [(-)-N-(trans-4-isopropylcyclohexanecarbonyl)-D-phenylalanine], on postprandial blood glucose excursion: comparison with voglibose and glibenclamide. Biol Pharm Bull. 1997;20:354-9.

RESEARCH ARTICLE

Moderate to severe plaque type psoriasis and its treatment: Methotrexate

Urairack Subpayasarn[1], Saranyoo Ponnikorn[2], Jitlada Meephansan[1]

[1]*Division of Dermatology, Chulabhorn international college of medicine, Thammasat University, PathumThani, 12120, Thailand.*
[2]*Chulabhorn international college of medicine, Thammasat University, PathumThani, 12120, Thailand.*

Address correspondence and reprint request to: Jitlada Meephansan, Chulabhorn international college of medicine, Thammasat University, PathumThani, Thailand.
E-mail address: kae_mdcu@yahoo.com

Abstract

Psoriasis is a common, chronic skin disease affecting approximately 2-3% of the world's population. The disease is usually manifested as well-demarcated, erythematous, and raised oval plaques with silvery scales. Although there is no current cure for psoriasis, several treatments can minimize symptoms and help control disease. Systemic therapy is considered the best treatment for moderate to severe psoriasis, which includes conventional systemic, phototherapy, photochemotherapy (PUVA), and, more recently, biological agents. Methotrexate is a highly effective therapy for treating moderate to severe plaque-type psoriasis. This study was to assess the efficacy of methotrexate in treating chronic plaque-type psoriasis.

Methods: This study was conducted at the Department of Dermatology, Thammasat University Hospital between March and December 2015. Six patients age between 20 and 70, diagnosed with moderate to severe plaque-type psoriasis with PASI score >10 participated in the study. Once a week, subjects were given a dose of 7.5-20 mg oral or subcutaneous methotrexate. Demographic profiles (age of onset, gender), body mass index, smoking habits, duration of disease, site of lesions, pruritus intensity measured by Visual Analogue Scale (VAS), severity of disease measured by Psoriasis Area and Severity Index (PASI) score were recorded before and at the end of treatment. End point clearance was 75% reduction in PASI.

Results: Six patients, four males (66.67%) and two females (33.33%). The mean ± SD age was 46.17 ± 21.30 years. Both PASI scores and VAS for pruritus had improved ($p < 0.05$). The mean PASI score showed clearance and comparable improvement from a mean 20.70 ± 10.79 to 4.72 ± 3.08. The mean VAS score of pruritus showed comparable improvement from a mean 5.83 ± 2.31 to 0.67 ± 0.82. The mean number of weeks required for achieving clearance (PASI 75) was 12.33 ± 4.63 weeks.

Conclusion: Methotrexate is the mainstay in the standard treatment of moderate to severe plaque-type psoriasis especially in developing countries due to its cost-effectiveness. Efficacy of methotrexate provided satisfactory disease improvement and improved quality of life.

Keywords: plaque psoriasis, psoriasis vulgaris, methotrexate

Introduction

Psoriasis is a common, chronic, inflammatory immune mediated skin disease affecting approximately 2 - 3% of the world's population. The etiology of psoriasis seems to be multi-factorial including polygenic inheritance, environmental factors, and abnormal immune responses. Although the disease is rarely life-threatening, it certainly has a significant undesirable impact on patients' quality of life, demonstrable by physical, emotional, psychosocial wellbeing and economic burden.[1, 2] Both long-term treatment costs and social costs have a negative impact on health care systems and on society in overall.[3]

There are several clinical cutaneous manifestations of psoriasis but most commonly the disease is characterized by classically well-demarcated, symmetrical, erythematous, and raised round-oval plaques with silvery dry scales that may be painful and/or often pruritic. Plaque psoriasis is the most common variety that affects around 80% to 90% of patients.[3-7] The lesions are predominantly distributed on the scalp, elbows, knees, and lumbosacral area and in the site of injury or trauma. The Psoriasis Area and Severity Index (PASI) score is a measure of psoriasis severity that evaluates affected body surface area, erythema, induration, and scale of psoriatic lesions. Typically, the PASI score is calculated before, during, and after treatment to determine disease response to the therapy. A 75% reduction in the PASI (PASI 75) is largely used to assess the effectiveness of any individual therapy in clinical trial.[4]

The immunopathogenesis of psoriasis is actually complicated. However, several recent studies have shown that immune system plays an important role; both innate and adaptive immunity. The dysregulated interactions between immune components and cutaneous cell types initiate the inflammation cascades. Dendritic cells and T cells are considered as key cell types, and type I interferon, interferon-gamma, TNF-alpha and interleukin-17 are recognized as key cytokines, which are the important signatures in psoriatic skin lesions.[3, 6, 8, 9]

Though there is no current cure for psoriasis, various therapies can potentially minimize the symptoms and help control the disease including topical modalities as the first line treatment and systemic therapies for the extensive disease. Systemic therapy is considered as the proper management for moderate to severe psoriasis, which include conventional systemic, ultraviolet (UV) light therapy, photochemotherapy (PUVA), and, more recently, biological agents. [10]

Recently, biological agents have been used more widely in treating psoriasis. Therefore, patients have additional options with better efficacy and safety profiles. However, conventional systemic therapies still play a significant role in treatment of extensive psoriasis in developing countries because they are effective and affordable. Of all the systemic therapies, *methotrexate* is the most commonly used conventional therapy which is highly effective in treating moderate to severe plaque-type psoriasis.[11] Methotrexate is known to competitively inhibits dihydrofolatereductase enzyme, thus has an antiproliferative effect due to inhibiting DNA synthesis on psoriatic lesions.[10-12]

In 2002, Kumar *et al.*[13] reviewed the data that has shown more than 75% improvement occurred in 88% methotrexate-treated psoriasis patients in 8.5 ± 5.1 weeks. Naldi et al.,[14] proposed that methotrexate might reduce the severity of psoriasis by at least 50% in at least 75% of patients. Moreover, in a retrospective study over 26 years by Haaustein *et al.*,[15] the effect of methotrexate treatment was good in 76%, moderate in 18% and poor in 6% of psoriasis patients.

In Thailand, there are limitations of psoriasis treatment. The limited availability of phototherapy devices and the high cost of biological modalities make them inaccessible to many people. Therefore, this study aims to evaluate the efficacy of methotrexate in the treatment of chronic plaque-type psoriasis. So that it can be offered as a cost-effective treatment for psoriasis patients. This clinical trial has never been done in our country.

Materials and Methods

This study was conducted at the Department of Dermatology, Thammasat University Hospital between March and December 2015. The study was approved by the Ethics Committee of Thammasat University, and the formal consent was obtained from patients after they are fully informed of the nature of this study.

Initially the study included all patients age 18 years and above who had been diagnosed with moderate to severe plaque-type psoriasis. The severity of psoriasis was classified according to the Psoriasis Area and Severity Index (PASI ;<10=mild, 10-15=moderated, >15=severe). This study excluded patients taking other treatments for the disease, suffering from psoriatic arthritis, other autoimmune disease, immunosuppression, cancer, active infection (e.g. septicemia, tuberculosis, HIV infection), severe hepatic, renal, hematological or other systemic disorders, and alcoholism. Patients with known history of methotrexate intolerance and pregnant and lactating women were also excluded.

The diagnosis was made on a clinical manifestation; a history was taken concerning age, age of onset, family history, occupation, duration of disease, presence and severity of itching, and history of previous treatment. Physical examination was established regarding the erythema, scale, thickness, site, and size of the psoriatic plaque. The PASI score evaluation was conducted with each subject before starting the study and repeated every four weeks until clearance occurred. Female subjects of reproductive age were counseled to take contraceptive precautions during methotrexate therapy and one month after stopping the medication. Male subjects were advised to take the precautions while on methotrexate and three months after stopping treatment.

Before starting the study, subjects were asked to discontinue any systemic therapy or phototherapy for at least four weeks, and any topical therapy for at least two weeks. Liver function tests (LFT), complete blood cell counts (CBC), renal function tests, and HIV-antibody were conducted prior to initiation of the treatment. CBC and LFT were repeated every two weeks for the first four weeks and then once every four weeks during the therapy.

Finally six patients from Out Patients Department of Dermatology (OPD), Thammasat University Hospital, who had been diagnosed with moderate to severe plaque type psoriasis fulfilling the inclusion criteria, were included in the study after the informed consent had been obtained.

Once a week, a dose of between 7.5 and 20 mg of methotrexate was administered either orally or subcutaneously to each subject. The starting dose was given depending on the subjects' weight and severity of disease. The dosage was adjusted according to the clinical response. A folic acid supplement was given daily to minimize gastrointestinal side effects or early bone-marrow suppression. As the beginning of the study, baseline data comprising the PASI scores were obtained for each subject. Subsequently further data were obtained during monthly follow up. The end point clearance was 75% reduction in PASI score.

The collected data included demographic profile (age of onset, gender), body mass index, skin type, smoking habits, duration of disease, site of lesions, pruritus intensity measured by Visual Analogue Scale (VAS), the impact of psoriasis on patient's quality of life measured by Dermatology Life Score Index (DLQI) questionnaire, severity of disease measured by PASI score before and at the end of treatment. Data were analyzed by SPSS version 23 for statistic. The results were given in form of percentage for qualitative data, mean and standard deviation for quantitative data. Otherwise, equivalent nonparametric statistics (Wilcoxon signed rank test) was used.

Results

Six patients, four males (66.67%) and two females (33.33%) age between 20 and 70 (Mean ± SD 46.17 ± 21.30) who had been diagnosed with plaque type psoriasis with PASI score >10 were included in the study. Each patient in this study had lesions on scalp and nails which do not always occur within the population of psoriasis sufferers.

The baseline laboratory parameters were normal in each of the six subjects. None of the subject in this study showed evidence of contraindications as the result of administration of methotrexate. Importantly, during the study and in subsequent follow-ups with subjects no adverse effects arising from the treatment regimen were observed. This included both mild symptoms and/or serious events which would have led to cessation of treatment.

Table 1 illustrates the demographic data of the subjects. The mean number of body mass index (BMI) was 26.93 ± 8.94. The mean age of onset was 35.0 ± 18.95 years. The mean number of disease duration was 10.18 ± 10.93 years.

The results obtained from data analysis revealed that both PASI scores and VAS for pruritus had improvement with statistical significance ($p < 0.05$). The mean PASI score showed clearance and comparable improvement from a mean 20.70 ± 10.79 to 4.72 ± 3.08. The mean VAS score of pruritus showed comparable improvement from a mean 5.83 ± 2.31 to 0.67 ± 0.82. The mean DLQI score showed comparable improvement from mean 11.67 ± 7.39 to 2.67

± 1.97. [Table1]. While A Wilcoxon signed-rank test showed a statistically significant reduction in PASI score ($p = 0.013$), in VAS for pruritus ($p = 0.013$) and in DLQI score ($p = 0.015$) [Figure2].

Table 1. Demographic profiles on study patients.

	Methotrexate (n=6)
Age (years)	
Range	20 - 70
Mean ± SD	46.17 ± 21.30
Gender	
Female (%)	2 (33.33)
Male (%)	4 (66.67)
Mean BMI ± SD	26.93 ± 8.94
Mean age of onset (years) ± SD	35.0 ± 18.95
Mean duration of psoriasis (years) ± SD	10.18 ± 10.93
Lesion on nails (%)	6 (100)
Lesion on scalp (%)	6 (100)
Family history of psoriasis (%)	3 (50)
PASI score at baseline	
Range	10.2 - 38
Mean ± SD	20.70 ± 10.79
PASI score at the end of MTX treatment	
Range	2.2 - 10.4
Mean ± SD	4.72 ± 3.08
Mean clearance time for psoriasis (weeks)	12.33 ± 4.63
Mean cumulative dose of MTX (mg) ± SD	150.83 ± 90.41
VAS for pruritus at baseline	
Range	2 - 8
Mean ± SD	5.83 ± 2.31
VAS for pruritus at the end of MTX treatment	0 - 2
Range	0.67 ± 0.82
Mean ± SD	
DLQI at baseline	2 – 20
Range	11.67 ± 7.39
Mean ± SD	
DLQI at the end of MTX treatment	1 – 6
Range	2.67 ± 1.97
Mean ± SD	

BMI, body mass index*; MTX*, methotrexate*; PASI*, Psoriasis Area and Severity Index; *DLQI*, dermatology life quality index.
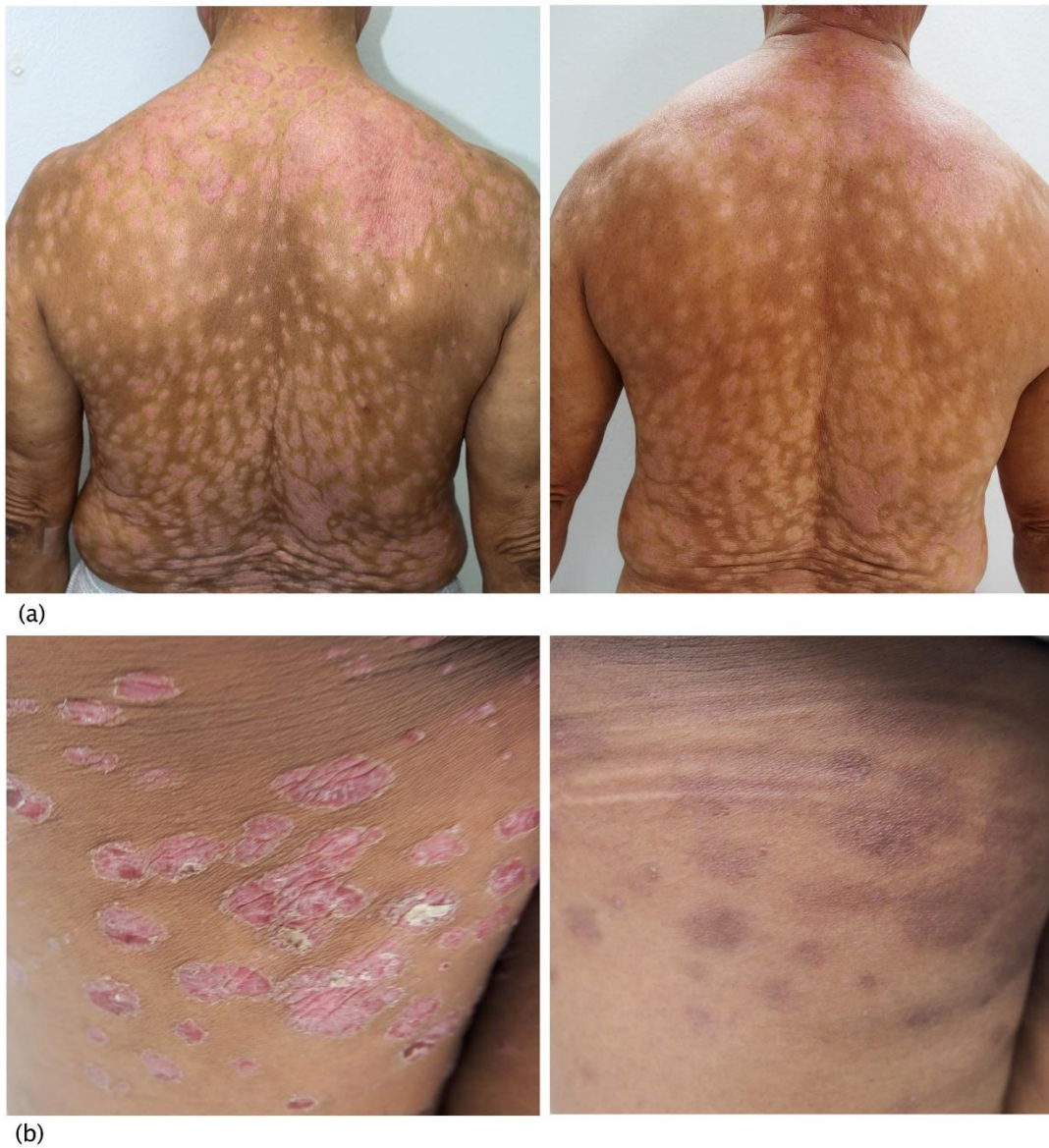
Figure 1. Pictures of two subjects with moderate to severe plaque type psoriasis at baseline and at the 75% improvement of PASI score (PASI 75) after initiation of methotrexate therapy. The endpoint results were achieved after 8 weeks (a) and 10 (b) weeks of treatment.
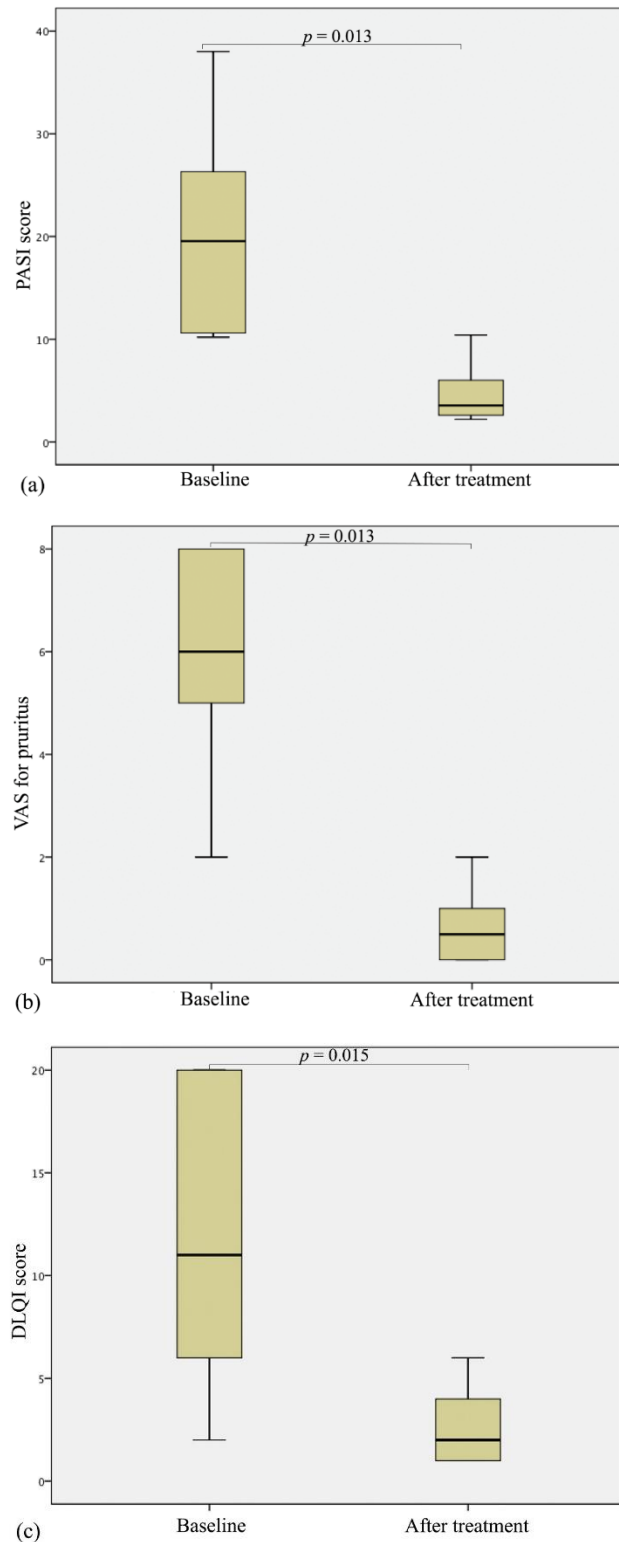
Figure 2. Comparison of PASI score (a), VAS score for pruritus (b) and DLQI score (c) at baseline and after treatment (PASI 75) with methotrexate in psoriasis patients. Horizontal bars represent the mean.

Discussion

Psoriasis is a genetic, multi-system chronic disorder that may have extensive impact on patients' quality of life, psycho-social morbidity, and social-economic status. From our experience, most patients with psoriasis require high efficacy, cost effective, rapid control and ease of administration of therapies.

In a review done by Naldi *et al*.,[14] management of moderate to severe psoriasis is often initiated with either narrowband or broadband UVB phototherapy followed by photochemotherapy or PUVA. However, to be effective phototherapy treatment has to be taken at least two to three times a week depending on patient preference. According to Lebwohl *et al*.,[16] the principle of combining, rotational, and sequential treatments is preferred in order to improve effectiveness and reduce the risk of side effects.

Guidelines issued by Britain's National Institute for Health and Clinical Excellence[7] and Hsu *et al*.,[17] advocate use of methotrexate as the first choice systemic agent for patients with extensive psoriasis. The authors cited immediately before also note that cyclosporin and acitretin can effectively control psoriasis in many cases, but use is limited by toxicity and sometimes sub-optimal efficacy for plaque psoriasis. The results of our study are consistent with the administration of methotrexate as an effective agent calculated by PASI score before, during, and after treatment of plaque psoriasis.

An earlier study of Opmeer BC *et al*.,[18] indicated improvement in methotrexate-treated PASI score from 13.4 ± 3.6 to 5.0 ± 4.5 during treatment of 16 weeks duration. In another study by Hroch *et al*.,[19] PASI decreased from 24.0 ± 8.0 at baseline to 8.0 ± 6.1 in treatment regime of a 110 days duration with 47% of PASI 75. In a more recent study undertaken by Haider *et al*.,[20] the mean baseline PASI score was 14.8 ± 4.2 and at the end of eight weeks treatment it was 4.9 ± 4.3. In our study, the mean PASI score showed improvement (PASI 75) and comparable improvement from a mean of 20.70 ± 10.79 to 4.72 ± 3.08 during treatment ranged from 8 to 20 weeks.

In a retrospective study, Kumar *et al*.[13] reviewed data on 244 psoriasis patients. PASI 75 was achieved in 88% of patients in 8.5 ± 5.1 weeks. Sandhu *et al*.[21] reported PASI 75 was achieved in 5.3 weeks with methotrexate-treated patients. In present study, the mean clearance time for psoriasis (PASI 75) was 12.33 ± 4.63 weeks. In comparison, the clearance time in our study was longer than the two studies mentioned earlier. This may result from the very limit sample size of only six subjects. Further, result from our study showed the mean VAS for pruritus improved from 5.83 ± 2.31 to 0.67 ± 0.82; this may prove to be an interesting finding about the role of methotrexate in relieving itching symptoms in psoriasis patients.

Once a week, a dose of between 7.5 and 15 mg of methotrexate was administered either orally or subcutaneously to each subject for the first week depending on psoriasis severity and patient's body weight. Guidelines published by Menter *et al*.[10] and Naldi *et al*.[14] recommended a starting dose of 2.5 to 5 mg due to the risk of adverse effects. However, Montaudie *et.al*.[22]

concluded in their systematic review that the initial dose of methotrexate should be between 5 to 15 mg per week due to dose-dependent response. According to this review, 60% of patients achieved a PASI 75 within 16 weeks if the starting dose of methotrexate is 15 mg per week. From the latest RCT-based report published in 2015[23], the author also suggests a starting dose of 15 mg per week methotrexate with laboratory control after one week in healthy patients.

Advances in psoriasis treatment continue to this day. Certain type of drugs can interrupt the specific mechanisms of inflammatory and immune responses that occur during psoriasis process. A combination therapy of methotrexate and new biological agents appears to be more advantageous due to the additional or synergistic actions in advanced therapy for psoriasis.[11, 12, 24] Continued clinical use of methotrexate presents an intriguing challenge when dealing in the context of the new agents, more so, since methotrexate remains an inexpensive medication, but one with known potential for hepatotoxicity and bone marrow suppression.

In summary, available clinical data show that methotrexate is effective in the treatment of moderate to severe plaque type psoriasis. Currently, there is no universal standard of managing patients with extensive psoriasis. The risks and benefits of systemic therapy have to be weighed cautiously for each patient to achieve optimal psoriasis treatment and minimize toxicity.

Conclusion

The efficacy of methotrexate leads to marked improvement in psoriasis and thus improved quality of life. Treatment with methotrexate for moderate to severe plaque-type psoriasis brings satisfactory disease control especially in developing countries due to cost-effectiveness. Further studies are needed to assess the role of methotrexate in reducing itching symptoms in psoriasis patients.

Conflict of interest: The author declares that they have no conflict of interest.
Limitation: This study is not a randomised trial, and the sample size is very small.

References

1. Langley RG, Krueger GG, Griffiths CE. Psoriasis: epidemiology, clinical features, and quality of life. Ann Rheum Dis. 2005;64 Suppl 2:ii18-23; discussion ii4-5.
2. Radtke MA, Augustin M. Economic considerations in psoriasis management. Clin Dermatol. 2008;26(5):424-31.
3. Nestle FO, Kaplan DH, Barker J. Psoriasis. New England Journal of Medicine. 2009;361(5):496-509.
4. Menter A, Gottlieb A, Feldman SR, Van Voorhees AS, Leonardi CL, Gordon KB, et al. Guidelines of care for the management of psoriasis and psoriatic arthritis: Section 1. Overview of psoriasis and guidelines of care for the treatment of psoriasis with biologics. J Am Acad Dermatol. 2008;58(5):826-50.
5. Cohen SN, Baron SE, Archer CB, British Association of D, Royal College of General P. Guidance on the diagnosis and clinical management of psoriasis. Clin Exp Dermatol. 2012;37 Suppl 1:13-8.

6. Boehncke W-H, Schön MP. Psoriasis. The Lancet. 2015;386(9997):983-94.
7. National Clinical Guideline C. National Institute for Health and Clinical Excellence: Guidance. Psoriasis: Assessment and Management of Psoriasis. London: Royal College of Physicians (UK) Copyright (c) National Clinical Guideline Centre - October 2012.; 2012.
8. Kim J, Krueger JG. The immunopathogenesis of psoriasis. Dermatol Clin. 2015;33(1):13-23.
9. Sabat R, Philipp S, Hoflich C, Kreutzer S, Wallace E, Asadullah K, et al. Immunopathogenesis of psoriasis. Exp Dermatol. 2007;16(10):779-98.
10. Menter A, Korman NJ, Elmets CA, Feldman SR, Gelfand JM, Gordon KB, et al. Guidelines of care for the management of psoriasis and psoriatic arthritis: section 4. Guidelines of care for the management and treatment of psoriasis with traditional systemic agents. J Am Acad Dermatol. 2009;61(3):451-85.
11. Dogra S, Mahajan R. Systemic methotrexate therapy for psoriasis: past, present and future. Clin Exp Dermatol. 2013;38(6):573-88.
12. Saporito FC, Menter MA. Methotrexate and psoriasis in the era of new biologic agents. Journal of the American Academy of Dermatology. 2004;50(2):301-9.
13. Kumar B, Saraswat A, Kaur I. Short-term methotrexate therapy in psoriasis: a study of 197 patients. Int J Dermatol. 2002;41(7):444-8.
14. Naldi L, Griffiths CE. Traditional therapies in the management of moderate to severe chronic plaque psoriasis: an assessment of the benefits and risks. Br J Dermatol. 2005;152(4):597-615.
15. Haustein UF, Rytter M. Methotrexate in psoriasis: 26 years' experience with low-dose long-term treatment. Journal of the European Academy of Dermatology and Venereology. 2000;14(5):382-8.
16. Lebwohl M, Menter A, Koo J, Feldman SR. Combination therapy to treat moderate to severe psoriasis. Journal of the American Academy of Dermatology. 2004;50(3):416-30.
17. Hsu S, Papp K, Lebwohl MG, et al. COnsensus guidelines for the management of plaque psoriasis. Archives of Dermatology. 2012;148(1):95-102.
18. Opmeer BC, Heydendael VR, de Borgie CM, et al. Costs of treatment in patients with moderate to severe plaque psoriasis: Economic analysis in a randomized controlled comparison of methotrexate and cyclosporine. Archives of Dermatology. 2004;140(6):685-90.
19. Hroch M, Chladek J, Simkova M, Vaneckova J, Grim J, Martinkova J. A pilot study of pharmacokinetically guided dosing of oral methotrexate in the initial phase of psoriasis treatment. J Eur Acad Dermatol Venereol. 2008;22(1):19-24.
20. Haider S, Wahid Z, Najam Us S, Riaz F. Efficacy of Methotrexate in patients with plaque type psoriasis. Pak J Med Sci. 2014;30(5):1050-3.
21. Sandhu K, Kaur I, Kumar B, Saraswat A. Efficacy and safety of cyclosporine versus methotrexate in severe psoriasis: a study from north India. J Dermatol. 2003;30(6):458-63.
22. Montaudie H, Sbidian E, Paul C, Maza A, Gallini A, Aractingi S, et al. Methotrexate in psoriasis: a systematic review of treatment modalities, incidence, risk factors and monitoring of liver toxicity. J Eur Acad Dermatol Venereol. 2011;25 Suppl 2:12-8.
23. Menting SP, Dekker PM, Limpens J, Hooft L, Spuls PI. Methotrexate Dosing Regimen for Plaque-type Psoriasis: A Systematic Review of the Use of Test-dose, Start-dose, Dosing Scheme, Dose Adjustments, Maximum Dose and Folic Acid Supplementation. Acta Derm Venereol. 2015.
24. Warren RB, Griffiths CE. Systemic therapies for psoriasis: methotrexate, retinoids, and cyclosporine. Clin Dermatol. 2008;26(5):438-47.

RESEARCH ARTICLE

Effects of chronic kidney disease on intestinal drug transporters in a mouse model

Varumporn Sukkummee[1], Supeecha Wittayalertpanya[2], Piyanuch Wonganan[2], Pajaree Chariyavilaskul[2], Asada Leelahavanichkul[3]

[1]*Inter-department of pharmacology, Graduate School, Chulalongkorn University, Bangkok 10330, Thailand*
[2]*Department of Pharmacology, Faculty of Medicine, Chulalongkorn University, Bangkok 10330, Thailand*
[3]*Department of Microbiology, Faculty of Medicine, Chulalongkorn University, Bangkok 10330, Thailand*

Address correspondence: Varumporn Sukkummee, Inter-department of Pharmacology, Graduate School, ChulalongkornUniversity, Bangkok, Thailand.
E-mail address: varum_sk@hotmail.com

Abstract

Chronic kidney disease (CKD) is associated with an increased bioavailability of drugs by a poorly understood mechanism. The present study aim to investigate the repercussion of CKD on major intestinal transporters involved in drug extrusion including P-glycoprotein (P-gp) and Multidrug resistance-associated protein 2 (Mrp2). Two groups of mice were studied: CKD and control. CKD was induced by a chronic ischemic reperfusion (I/R) in a mouse model. The left renal artery was ligated for 50 minutes then right nephrectomy was performed 7 days afterwards. Twenty eight days later, mice were sacrificed. Serum was harvested to measure serum creatinine and urea levels using QuantichromTM assay kit. P-gp and Mrp2 mRNA levels were measured using the real-time polymerase chain reaction. Serum creatinine and urea levels were significantly higher in the CKD group than control group ($p<0.05$). When compared the effect of CKD on intestinal transporters to control group, P-gp mRNA levels was reduced by 73% ($p<0.05$) in mice with CKD. However, Mrp2 mRNA level remained unchanged. In conclusion, CKD is associated with a decrease in intestinal transporters involving to drug extrusion. This reduction could explain the increased bioavailability of drugs in CKD.

Keywords: chronic kidney disease (CKD), mouse, drug transporters, intestine

Introduction

Chronic kidney disease (CKD) is a presence of structural or functional abnormalities of kidneys or GFR less than 60 ml/min/1.73m^2 for at least three months.[1] The incidence of CKD in Thailand has increased steadily over the past decade.[2] Patients with CKD has been shown to significantly reduce the renal clearance and alter bioavailability of drugs predominantly metabolized by the intestine. Dose adjustment of kidney-excreted drugs is mostly necessary

adjusted according to the glomerular filtration rate.[3] Despite dosage adjustment, CKD patients still suffer from a great number of drug adverse effects.[4] Patients with CKD usually require numerous medicines to control uremic-associated complications. The CKD itself is an important risk factor for systemic accumulation of drugs and may cause adverse effects or ineffective therapy. Oral bioavailability, i.e., the quantity of drug reaching the blood circulation, depends on different factors, such as intestinal drug transport and liver metabolisms.[5] The most important intestinal efflux transporters are P-gp and MRP2. However, very few studies have described the repercussions of CKD on intestinal drug transporters. In addition, a CKD mouse model induced by ischemic reperfusion (I/R) of one kidney followed by nephrectomy of the other side of the kidney has not been established. The present study, therefore evaluated the changes in mRNA expression of major intestinal drug transporters in an experimental CKD using chronic ischemic reperfusion model.

Materials and Methods

Animal Model

Male ICR mice with age of 6 to 8 weeks and weight of 25 to 40 g were obtained from the National Laboratory Animal Center, Mahidol University, Salaya, Nakorn Pathom, Thailand. All animals were housed as 5 animals/cage in the 12:12 light-dark cycle at 25±2 ºC at the Faculty of Medicine, Chulalongkorn University's animal laboratory facilities. Animals were allowed an acclimatization period of at least 7 days before the experiments. The experimental protocol was approved by the Ethics Committee for animal study of the Faculty of medicine, Chulalongkorn University.

Studies were performed in two groups of mice: CKD and control group. The mRNA expression levels of intestinal drug transporters were measured in 6 mice per group. CKD was induced by chronic ischemic reperfusion (I/R) model. The left renal artery was ligated for 50 minutes then right nephrectomy was performed 7 days afterwards. The surgical procedures were done under isoflurane anesthesia. All mice were weighed daily. Twenty eight days after right nephrectomy operation, CKD mice were sacrificed. Blood and intestinal tissue samples were harvested. Kidney function was assessed by serum creatinine and serum urea. Serum creatinine and serum urea was determined by QuantichromTM assay kit (Hayward, CA, USA).

RNA Isolation and Real time RT-PCR Analysis

At the time of sacrifice, whole tissue in part of jejunal was rinsed with ice-cold normal saline before snap frozen in liquid nitrogen. Samples were kept at -80°C until RNA isolation. Total RNA was extracted from frozen tissue using TRIzol reagent (Invitrogen, Burlington, ON, Canada) according to the manufacturer's instructions. After that, one microgram of total RNA was used to prepare cDNA using ImProm-II Reverse Transcription System (Promega). The mRNA encoding for P-gp (mdr1a) and Mrp2 was measured by TaqMan gene expression assays from Applied Biosystems (Carlsbad, CA). The expression levels of interested genes in CKD group were normalized to GAPDH and expressed in relative to those in control group using the $2^{-\Delta\Delta CT}$ method.

Data analysis

The results are expressed as mean ± S.E.M. Differences between groups were assessed using an unpaired Student's *t* test or an analysis of variance test. The threshold of significance was $p < 0.05$.

Results

Biochemical Parameters and Body Weight in CKD and Control Mice.

Table 1 presents the biochemical parameters and body weight of both CKD and control groups. Compared with control group, CKD mice had higher levels of serum creatinine (0.478±0.031 versus 0.295±0.035 mg/dL, *p*<0.05) and serum urea (45.573±7.660 versus 25.782±1.025 mg/dL, *p*<0.05). Body weight in CKD mice was significantly reduced with respect to the control group (32.804±1.126 versus 37.369±0.210 g, *p*<0.05).
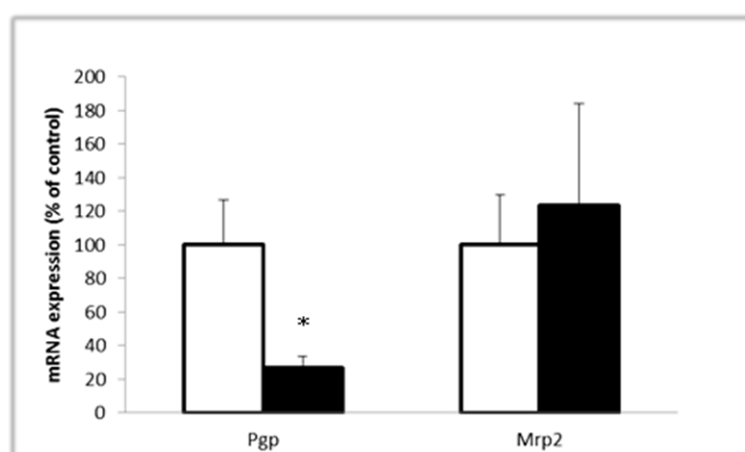
mRNA Expression of Intestinal Drug Transporters in CKD Mice.

Figure 1 shows the results of the analysis of mRNA coding for intestinal transporters. There was a significant increase in mRNA for the excretion transporters P-gp (73%, *p*<0.05) when compared with control, however mRNA expression for the import transporter Mrp2 remained unchanged.

Table 1. Characteristics of CKD mouse and control

	Control (n=6)	CKD (n=6)	*p*-value
Body weight (g)	37.369±0.61	32.804±1.126	*p*<0.05
Serum creatinine (mg/dL)	0.295±0.035	0.478±0.031	*p*<0.05
Serum urea (mg/dL)	25.782±1.025	45.573±7.660	*p*<0.05

Values are means ± S.E.M.; n= 6/group. CKD, chronic kidney disease.

Figure 1. mRNA encoding intestinal drug transporters in CKD (black bars) and control (white bars) mice were measured by quantitative real-time PCR. mRNA levels of interested genes in CKD mice normalized to GAPDH were expressed in relative to those in control mice using the $2^{-\Delta\Delta CT}$ method with GAPDH as a reference gene. The mean relative quantity of control rats was arbitrarily defined as 100%. Data are the mean±S.E.M. of six animal in each group. *p*<0.05 compared with control mice.

Discussion

Compared to a previous reported of CKD model by Naud J. [6], our model takes a shorter time for CKD induction, and shows a higher animal survival rate, suggesting that ischemic reperfusion of one kidney followed by nephrectomy of the other can be a new technique to develop CKD *in vivo*.

The purpose of this study was to evaluate the effect of CKD on the mRNA expression of two intestinal excretion transporters (Pgp and Mrp2). We have developed CKD mice using a chronic ischemic reperfusion (I/R) model to be used for assessing the effect of CKD on gene expression of two major intestinal drug efflux transporters. Our results demonstrated that the mRNA expression of P-gp was significantly reduced in CKD mouse model. Uremic serum in CKD may lead to the modifications in drug transporters, suggesting that uremic toxins such as indoxyl sulfate, para-aminohippuric acid, involved in modulation of drug transporters.[7] However, we found that Mrp2 mRNA expression was not statistical significance similar to previously published by Naud J.[6] P-gp was a major excretion intestinal drug transporter. These findings could explain the increased bioavailability of drugs in CKD patients. CKD alters intestinal drug transport producing a clinically significant impact on drug disposition and increasing the risk for adverse drug reactions.

Conclusion

In conclusion, CKD induced a decrease in mRNA expression of P-gp, the most important intestinal drug efflux transporter, whereas the mRNA expression of Mrp2 remained unchanged. Our results suggested that reduction in P-gp may play an important role in accumulation of drugs and increased in drug absorption in patients with CKD.

Acknowledgements

References

1   National kidney foundation. Kidney disease outcome quality initiative (K/DOQI) guideline.Am J Kidney Dis.2002 39(2) : S17-S31.
2   Ingsathit A, Thakkinstian A, Chaiprasert A, Sangthawan P, Gojaseni P, Kiattisunthorn K, et al. Prevalence andrisk factors of chronic kidney disease in the Thai adult population: Thai SEEK study. Nephrol DialTransplant.2010 Jan 22;25(5):1567-1575
3   Veau C, Leroy C, Banide H, Auchere D, Tardivel S, Farinotti R, Lacour B, Effect of chronic renal failure on the expression and function of rat intestinal P-glycoprotein in drug excretion. Nephrology dialysis transplant.2001;16 :1607-1614.
4   Matzke GR and Frye RF. Drug administration in patients with renal insufficiency: minimising renal and extrarenal toxicity. Drug Saf.1997;16:205–231.

5   Nolin TD, Frye RF, and Matzke GR. Hepatic drug metabolism and transport in patients with kidney disease. Am J Kidney Dis.2003;42:906–925.

6   Naud J, Michaud J, Boisvert C, Desbiens K, Leblond F, Mitchell A, et al. Down-Regulation of Intestinal Drug Transporters in ChronicRenal Failure in Rats. Pharmacology and experimental therapeutics. 2007;320(3):978-85.

7.   Enomoto A and Niwa T. Roles of organic anion transporters in the progression of chronic renal failure. Ther Apher Dial. 2007;11:S27–S31.

RESEARCH ARTICLE

Antimicrobial and antibiofilm formation activities of chrysazin on Bacillus species

Marion Micheler[1], Chanida Palanuvej[2], Santad Chanprapaph[3*]

[1]*Inter-department of Pharmacology, Graduate School, Chulalongkorn University, Bangkok, 10330, Thailand;*
[2]*College of Public Health Sciences, Chulalongkorn University, Bangkok, 10330, Thailand;*
[3]*Department of Pharmacology and Physiology, Faculty of Pharmaceutical Sciences, Chulalongkorn University, Bangkok, 10330, Thailand*

Address correspondence and reprint request to Santad Chanprapaph, Department of Pharmacology and Physiology, Faculty of Pharmaceutical Sciences, Chulalongkorn University, Bangkok, 10330, Thailand
E-mail address: schanprapaph@yahoo.com.

Abstract

Bacillus species are the pathogens associated with food poisoning, localized infections and systemic infections. The existences of such pathogens in various environments arise from the formation of biofilms. The ability of microorganisms to form biofilms increases the potential of antibiotic resistance of the bacteria at last. The aim of this study was to evaluate the antimicrobial and antibiofilm activities of chrysazin, the major bioactive compound found in *Xyris indica* Linn., on *B. cereus* and *B. subtilis* using *in vitro* studies. We examined antibacterial activities using broth microdilution method. MIC values of chrysazin against *B. cereus* and *B. subtilis* were 7.81 and 15.63 µg/ml, respectively. Furthermore, MBC values of chrysazin against both microorganisms were greater than 500 µg/ml. The results showed MBC/MIC ratios of chrysazin against both microorganisms were greater than 4. Therefore, chrysazin was considered to have bacteriostatic effect against both microorganisms. The antibiofilm potentials of chrysazin were analyzed at various concentrations (1/2-32 MIC) and chrysazin at highest concentration (32 MIC) showed the maximum inhibition on biofilm formation with the percentage of inhibition for *B. cereus* and *B. subtilis* 77.56% and 73.86%, respectively. In conclusion, chrysazin had antimicrobial activities against both microorganisms. In addition, *B. cereus* was more susceptible to chrysazin than *B. subtilis*. Furthermore, chrysazin also has antibiofilm activities against both microorganisms and inhibitory effects on biofilm formation of chrysazin were concentration dependent manner with statistically significant ($p < 0.05$ for each chrysazin concentration comparing to control). This information may lead to further step for development of antimicrobial drugs in mammals.

Keywords: Chrysazin, *Bacillus cereus*, *Bacillus subtilis*, Antimicrobial, Biofilm

Introduction

Bacillus cereus cause serious and potentially fatal non-gastrointestinal-tract infections and severe ocular infections.[1] *Bacillus subtilis* produces toxin known as subtilisin that causes hypersensitivity reactions and the oral, dermal and pulmonary acute toxicity. Moreover, it causes disease in severely immunocompromised patients.[2] Biofilms of Bacillus species are recognized as a serious problem and important contaminants in food industry settings.[3] The resistance increasing to antibacterial agents, bioresources have tremendous potential in providing bioactive compounds for the development of new lead candidates.[4] In this study, we investigated chrysazin that is the major bioactive compound found in *Xyris indica* Linn. for its antimicrobial activity and inhibitory effect of the biofilm formation on *B. cereus* and *B. subtilis*.

Materials and Methods

Inoculum preparation

Inoculums were prepared by streaking *B. cereus* (ATCC 11778) and *B. subtilis* (ATCC 6633) on Mueller Hinton Agar (MHA). They were incubated at 37 °C for 24 hours and transferred to a tube containing 10 mL of normal saline solution. The turbidity was adjusted to an optical density of 0.08-0.10 at 625 nm, using UV/Visible spectrophotometer (1×10^8 CFU/ml) and diluted 1:100 with Mueller Hinton Broth (MHB).[5]

Preparing chrysazin stock solution

Chrysazin stock solution was prepared at 1,000 μg/ml in 10% Dimethyl sulfoxide by dissolving 0.1 g of chrysazin powder in 10 ml of Dimethyl sulfoxide (99.9% purity, Labscan, Thailand), then 1 ml of the solution was added in the flask containing normal saline solution 9 ml.

Determination of the minimal inhibitory concentration (MIC) and minimal bactericidal concentration (MBC)

MICs were determined using a broth microdilution method recommended by the M07-A9 document.[5] The serially diluted 2-folded from chrysazin stock solution 100 μL were added into a sterile 96 well plate (final concentration ranging from 0.24-500 μg/ml). Then, 100 μL of bacterial suspension were added (final concentration are 5×10^5 CFU/ml). All plates were incubated at 37°C for 24 hours and MIC was defined as the lowest concentration that inhibited visible growth of the organism. Then, spotted suspension in the wells of MIC and higher concentrations on MHA and incubated. The lowest concentration that prevents any growth of bacteria was recorded as the MBC.

Inhibition of biofilm formation assay

Bacterial suspensions were diluted with 1.5% glucose of MHB (1:100). The 96-well plates were filled with 100 μl of each strain and 100 μl of chrysazin (the concentration at 1/2MIC, MIC, 2MIC, 4MIC, 8MIC, 16MIC and 32MIC). All plates were incubated at 37°C for 24 hours. Then, medium were removed and washed three times with 300 μl of sterile deionized water (DI). Bacteria were fixed with 250 μl of methanol. Biofilm cells were stained with 250

µl of 1% crystal violet for 15 min. The adherent cells were extracted with 33% (v/v) glacial acetic acid. Absorbance of each well was measured at 570 nm using a UV/Visible spectrophotometer.[6]

$$\% \text{ inhibition} = \frac{(\text{OD negative control} - \text{OD sample}) \times 100}{(\text{OD negative control})}$$

Statistical Analysis

Statistical significance between groups was evaluated using one-way ANOVA.

Results

Table 1. *In vitro* antibacterial activity of chrysazin against *B. cereus* and *B. subtilis*

Substances	Bacteria	MIC (µg/ml)	MBC (µg/ml)	MBC/MIC
Chrysazin	*B. cereus* (ATCC 11778)	7.81	>500	>64
Gentamicin (Positive Control)	*B. cereus* (ATCC 11778)	0.12	0.12	1
Chrysazin	*B. subtilis* (ATCC 6633)	15.63	>500	>32
Gentamicin (Positive Control)	*B. subtilis* (ATCC 6633)	0.12	0.12	1
Gentamicin (Quality Control)	*S. aureus* (ATCC 29213)	0.06	0.06	1
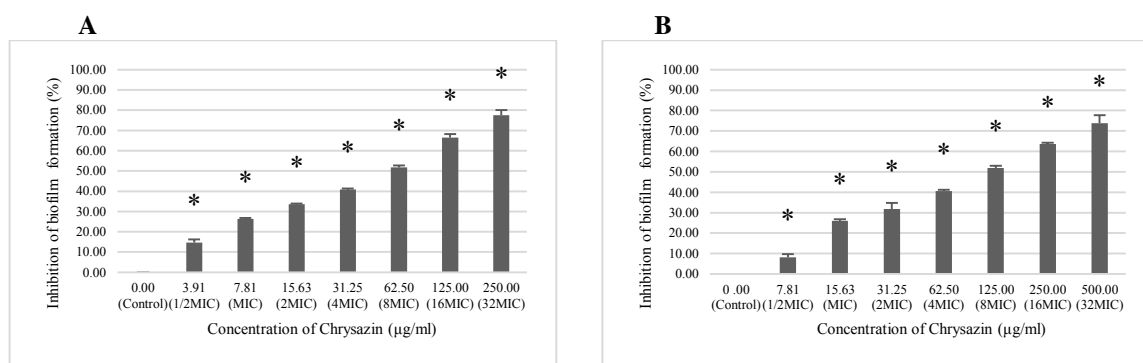
Figure 1. The inhibitory effect on the biofilm formation of chrysazin against *B. cereus* (A) and *B. subtilis* (B), Error bars represent the mean ± SEM, *$p < 0.05$.

MIC values of chrysazin against *B. cereus* and *B. subtilis* were 7.81 and 15.63 µg/ml, respectively. Furthermore, MBC values of chrysazin against both microorganisms were greater than 500 µg/ml. The results showed MBC/MIC ratios of chrysazin against both microorganisms were greater than 4. The antibiofilm potentials of chrysazin were analyzed at various concentrations (1/2-32 MIC) and chrysazin at highest concentration (32 MIC) showed the maximum inhibition on biofilm formation with the percentage of inhibition for *B. cereus* and *B. subtilis* 77.56% and 73.86%, respectively.

Discussion and Conclusion

The findings of this study indicated that chrysazin had antimicrobial activities against both microorganisms and *B. cereus* was more susceptible to chrysazin than *B. subtilis*. To determine the action of chrysazin on the bacterial strains by using MBC/MIC ratios. If the ratio MBC/MIC is equal to 1 or 2, Chrysazin will be considered to have bactericidal effect. If the ratio is greater than or equal to 4, Chrysazin will be considered to have bacteriostatic effect.[7] Therefore, chrysazin possessed not only bacteriostatic effect but also antibiofilm activities against both *B. cereus* and *B. subtilis* whereas inhibitory effects on biofilm formation of chrysazin were concentration dependent manner with statistically significant ($p < 0.05$). We, therefore, suggested that chrysazin has a potential to develop as a new candidate for antimicrobial drug and antibiofilm agent. However, it should be investigated the antimicrobial and antibiofilm formation activities on other bacterial strains in the future.

References

1. Bottone, E.J. *Bacillus cereus*, a Volatile Human Pathogen. Clin Microbiol Rev. 2010: 382–398.
2. Bilbiie, V. and Pozsgi, N. Bacteriologie Medicala. Medicala Bucuresti Ed. 1985; 11.
3. O'Toole, G., Kaplan, H.B., and Kolter, R. Biofilm formation as microbial development. Annual Review of Microbiology. 2000: 49–79.
4. Bilge, S. and Ilkay, O. Discovery of drug candidates from some Turkish plants and conservation of biodiversity. Pure Applied Chemistry. 2005: 53–64.
5. Clinical and Laboratory Standards Institute (CLSI). Methods for Dilution Antimicrobial Susceptibility Tests for Bacteria that Grow Aerobically; Approved Standard-Ninth Edition. CLSI Documents M07-A9, Clinical and Laboratory Standards Institute; 2012.
6. Sandasi, M., Leonard, C.M., and Viljoen, A.M. The *in vitro* antibiofilm activity of selected culinary herbs and medicinal plants against Listeria monocytogenes. Lett. Appl. Microbiol. 2010: 30-35.
7. Berche, P., Gaillard, J.L., and Simonet, M. In Nosocomial Infections Caused by Bacteria and Their Prevention in Bacteriology. Edited by Flammarion Medicine Sciences. 1988: 64-71.

RESEARCH ARTICLE

Measurement of antiretroviral drug levels prior to HIV-1 resistance testing to predict detection of HIV-1 resistance mutations for patients with virologic failure

Jiraporn Khamkon[1], Tanawan Samleerat[2], Pimpinun Panyathi[1], Nicole Ngo-Giang-Huong[1], Wasna Sirirungsi[2], Tim R Cressey[1,3,4], Kesara Na-Bangchang[5*]

[1]*PHPT/ IRD UMI 174 Faculty of Associated Medical Sciences, Chiang Mai University, Chiang Mai 50200 Thailand;*
[2]*Department of Medical Technology, Faculty of Associated Medical Sciences, Chiang Mai University, Chiang Mai 50200 Thailand;*
[3]*Harvard T.H Chan School of Public Health, Boston, USA;*
[4]*Department of Molecular & Clinical Pharmacology, University of Liverpool, UK; 5Chulabhorn International College of Medicine, Thammasat University, Pathum Thani, 12120, Thailand*

Address correspondence and reprint request to: Prof. Kesara Na-Bangchang, Ph.D. Chulabhorn International College of Medicine at Thammasat University 95 Phahonyothin Rd Klonglung, Pathum Thani Thailand 12120. E-mail address: kesaratmu@yahoo.com

Abstract

In Thailand more than 275,000 HIV infected patients are receiving antiretroviral drugs under the National AIDS Program. HIV genotypic resistance testing is performed for patients with confirmed virologic failure (HIV-1 RNA >2,000 copies/mL) to select the optimal drug regimen. It is critical that the resistance testing is performed when patients are on treatment to ensure detection of any resistance mutations selected under drug pressure. Treatment discontinuation prior to resistance testing can result in the outgrowth of wild-type virus and thus a decrease or loss of sensitivity to detect the resistant viruses. The Clinical Microbiology Service Unit (CMSU) at the Faculty of Associated Medical Sciences, Chiang Mai University provides HIV-1 drug resistance service within the National Health Security Office (NHSO) program. Approximately 20% of samples tested had no resistance mutations detected. Our objective was to assess if measuring antiretroviral plasma drug levels prior to HIV-1 resistance testing can predict the detection of resistance mutations. We performed a retrospective analysis of plasma samples tested at CMSU for resistance in 2013. Drug resistance genotyping was performed using the ViroSeq HIV-1 Genotyping System V2.8. Samples of patient receiving non-nucleoside reverse-transcriptase inhibitors (NNRTIs) or protease inhibitors (PI) plus 2 nucleoside reverse-transcriptase inhibitors (NRTIs) with resistance results available were selected for drug measurement. NNRTI and PI plasma drug concentrations were determined using validated reversed-phase high performance liquid chromatography assays. The sensitivity and specificity of drug concentration measurements to predict the detection of resistance were determined. Of 138 patients with one sample tested: 102 patients were receiving a NNRTI-based regimen and 36 were receiving a PI-based regimen. Overall, 48 of 138 (35%) had no detectable drug concentration. Among these samples, 36 (75%) had no drug resistance mutation detected. In the 90 samples with a detectable drug concentration 19 samples

had no drug resistance detected. Sensitivity and specificity of detectable drug concentrations to predict the detection of resistance was 86% and 65%, respectively. The sensitivity and specificity were 84% and 50% for patients receiving NNRTI and 100% and 76% for those receiving PI. In conclusion, this preliminary assessment suggests that the detection of plasma PI drug concentrations may help to predict the detection of PI-associated resistance mutations by consensus sequencing in that sample, while for patients receiving NNRTI-based regimen drug concentrations may be less useful to predict the detection of NNRTI-associated resistance mutations. Further analyses are needed to confirm the utility of drug measurement to predict the detection of NNRTI and PI resistance mutations prior to genotype testing.

Keywords: Antiretroviral, Drug measurements, HIV genotypic resistance testing

Introduction

In 2013, the estimated number of people living in Thailand with HIV was 440,000 cases, approximately 1.1% of adults (aged 15-49), and 286,214 patients were receiving HIV treatment under the National AIDS Program.[1-2] Combination antiretroviral therapy (cART) can suppress viral replication and enable the body's immune cells to return to normal levels.

Antiretroviral treatment is provided through several programs in Thailand, including the National AIDS Program (NAP) under the National Health Security Office (NHSO), and the Social Welfare Program under the Social Security Office (SSO). Antiretroviral treatment guidelines have recently changed in Thailand and it is now recommended that adults or adolescents initiate ART at any level of CD4+ T-cell count.[2]

A major challenge of HIV treatment is that the HIV genome frequently mutates about one mutation per round of replication, due to the lack of proofreading activity of the HIV reverse transcriptase enzyme.[3] Viruses resistant to antiretroviral drugs can emerge when the drug pressure is not sufficient to block viral replication. Poor patient drug adherence and/or suboptimal drug exposure increases the risk of selecting drug resistance mutations. HIV-1 drug resistance is the most common cause of therapeutic failure and subsequent HIV disease progression.

Clinical assessment and laboratory follow-up are important to detect early treatment failure. Treatment failure can be defined as virological failure, immunologic failure, and/or clinical progression.[4] The Thai National Guidelines recommends using virological failure criteria defined as plasma HIV-1 RNA viral load greater than 200 copies/mL after six months of antiretroviral treatment.[2] The National program provides free HIV-1 RNA quantification tests two times in the first year, then once a year thereafter if plasma viral load is lower than 50 copies/mL.[2] Continuing a non-suppressive regimen, especially with NNRTI-based regimens, increase the risk of selecting drug resistance.[5-7] Therefore virologic failure should be identified

early to prevent the accumulation of drug resistant associated mutations and preserve future antiretroviral treatment options.

The Clinical Microbiology Service Unit (CMSU) at the Division of Clinical Microbiology, Department of Medical Technology, Faculty of Associated Medical Sciences, Chiang Mai University has been providing a service for HIV-1 drug resistance genotyping under both the NHSO and SSO programs since 2009. HIV-1 drug resistance genotype (ViroSeq, Abbott Molecular) is determined and reported to clinicians for clinical management. Approximately, 3,000 plasma samples from almost 100 hospitals in Thailand (10 provinces) have been tested at the CMSU. A HIV genotypic resistance test is approximately 200 USD/test. In 2013-2014, plasma samples from 1,106 HIV-infected patients receiving cART within the NHSO program were sent to the CMSU for a HIV-1 drug resistance genotype test and among these samples 246 (22%) had no HIV drug resistance detected.

HIV-1 drug resistance genotype testing generally requires a HIV-1 RNA level >1000 copies/mL to ensure successful amplification. [2] Discontinuation of ART prior to the test will result in a decrease or loss of sensitivity to detect the resistant viruses due to replication of wild-type virus. It is possible that detecting the presence of plasma drug concentrations prior to performing an HIV-1 resistance testing may help ensure that the genotyping is performed when drug pressure is present to maximize the sensitivity of detecting the presence of drug resistant viruses.

Our objective was to assess if measuring antiretroviral plasma drug levels prior to HIV-1 resistance testing can predict the detection of resistance mutations by consensus sequencing.

Materials and Methods

Study Population

We performed a retrospective analysis of plasma drug concentrations in samples sent to the CMSU for HIV-1 drug resistance testing in 2013. Eligible samples were from HIV-infected adults with virological failure. Subjects were included in this analysis if receiving antiretroviral treatment consisting of 2 NRTIs and either a PI or a NNRTI. Five drugs, nevirapine, efavirenz, lopinavir, indinavirand ritonavir were measured.

Blood specimen

All plasma samples were stored at -20°C or -70°C until analysis and identified by a numeric code.

Ethical Consideration and Approval

The Human Research Protection Committee at the Faculty of Associated Medical Sciences, Chiang Mai University approved the study on April 30, 2015 (reference number: AMSEC-58EM-003).

Determination of Drug resistance mutations

Drug resistance genotyping of the HIV pol gene was performed using the ViroSeq HIV-1 Genotyping System V2.8 (Abbott Diagnostics, U.S.A.). The HIV sequences were compared to the CRF01-AE reference sequence using the Stanford HIVseq program Version 7.0 (http://hivdb.stanford.edu/pages/algs/HIVseq.html).

Definition of level of drug resistance

For this analysis, drug resistance interpretations were classified into 2 groups: (1) "Presence of drug resistance" -, low-level, intermediate or high-level resistance to specific drug detected, and (2) "Absence of drug resistance" - if virus remains potential low-level resistance or susceptible to the specific ARV drug.

Determination of plasma drug level

To quantify nevirapine concentrations in human plasma a validated reversed-phase high performance liquid chromatography (HPLC) assay with ultraviolet detection was performed.[8] Efavirenz, lopinavir, indinavir and ritonavir plasma concentrations were determined using a validated HPLC assay with ultraviolet detection.[9]

Quantification of plasma drug concentrations

The calibration curve range was linear over the range 50-15,000 ng/mL for nevirapine, 50-20,000 ng/mL for ritonavir, 100-20,000 ng/mL for efavirenz and lopinavir. The lower limit of quantification (LLOQ) was 38 ng/mL for indinavir, 50 ng /mL for nevirapine and ritonavir, 100 ng /mL for efavirenz and lopinavir. Samples were classified as "Drug detected" if the drug concentration was above the LLOQ whereas "No drug detected" was stated if drug concentration were below the LLOQ.
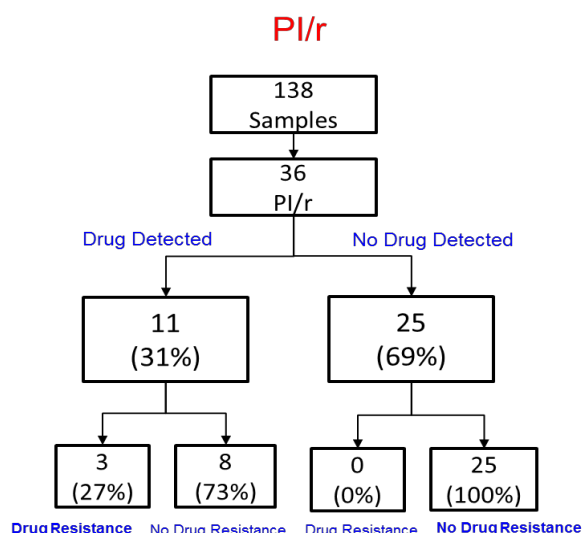
Results

Plasma samples sent to the CMSU from January to December 2013 were selected for analysis. The median plasma HIV RNA viral load was 4.19 $\log_{10}$ copies/mL (range: 3.31- 6.35 $\log_{10}$ copies/mL). Overall, 102 patients were treated with an NNRTI-based regimen (efavirenz n=35 and nevirapine n=67) while 36 were under PI based regimen of which 100% were ritonavir boosted (indinavir n=5 and lopinavir n=31).

Forty-eight samples (35%) had drug concentrations below the LLOQ. In this group, no drug resistance was detected in 35 (73%) samples and 13 (27%) had drug resistance detected (see Figure 1). Drug concentrations were above the LLOQ in 90 samples (65%). Among these samples, 71 had drug resistance detected and 19 had no drug resistance detected. The negative predictive value (NPV) of the presence of drug concentrations above the LLOQ to predict the detection of drug resistance was 74%; the positive predictive value (PPV) was79%. Sensitivity and Specificity were 85% and 65% respectively.
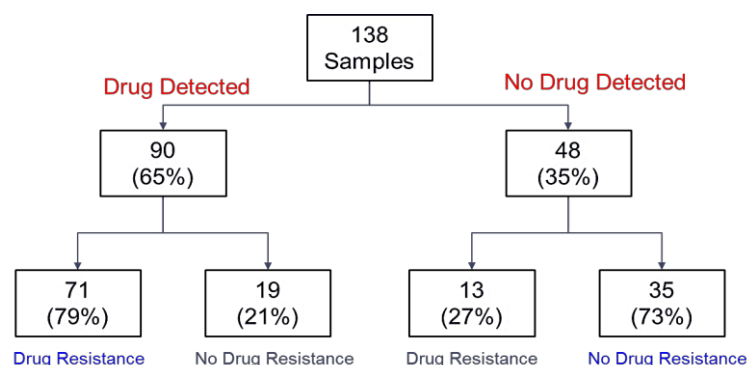
Figure 1 Summary of drug level measurements result and HIV drug resistance result

A separate analysis was performed based on the drug class. The NPV, PPV, sensitivity and specificity for subjects receiving NNRTI-based treatment were 43%, 87%, 84% and 50%. The NPV, PPV, sensitivity and specificity for subjects receiving PI-based treatment were 100%, 27%, 100% and 76% respectively (see figure 2).

Figure 2 Summary of PI/r drug level measurements result and HIV drug resistance result

Discussion

In this pilot study, we assessed if the presence of plasma drug concentration could predict the detection of HIV drug resistance mutations by consensus sequencing. We tested 138 plasma samples from ART-experienced patients followed within the National AIDS Program (NAP). Our results showed that 35% of plasma samples had drug below the limit of detection and among these samples 73% had no drug resistance detected. The negative predictive value (NPV) was 74%. For subjects receiving PI-based regimens the negative predictive value was 100%, suggesting that drug level detection may be more useful to predict the detection of drug resistance than for patients receiving NNRTIs.

Antiretroviral drug concentration measurements have been useful in several scenarios in routine clinical practice.[10] A prospective cohort study in Cameroon compared adherence of fixed-dose combinations of nevirapine/stavudine/lamivudine using nevirapine plasma level monitoring and self-report by patients and found that self-reported adherence was significantly higher than adherence measures by nevirapine level monitoring. The authors concluded that nevirapine plasma concentration monitoring provides an accurate measurement of adherence compared to self-report.[11] Furthermore, therapeutic drug monitoring (TDM) may serve to confirm non-adherence in cases of virologic failure without resistance.[12]

A limitation of the study is that the sample size is relatively small and further samples, particularly for the HIV protease inhibitors, are needed in order to make firm conclusions. Of note, the NRTIs plasma concentrations within the antiretroviral regimen were not quantified; however, plasma half-life of the NRTIs commonly used is Thailand (i.e. ZDV, 3TC) are relatively short and undetectable concentrations may not correspond to poor drug adherence. Also the level measured only reflects recent drug adherence and does provide information on the long-term drug adherence. Accurate information about timing of food intake, dose intake, genetic factors, pathological condition and the time of blood collection were not available in the NAP database. However, based on the plasma elimination half-life of the antiretroviral drugs measured (NNRTIs and ritonavir-boosted protease inhibitors) it would be expected that the drug would be detectable within the normal dosing period for an adherence patient.

If the clinical decision is made to perform a HIV drug resistance test it is only useful if drug pressure is present to maximize the sensitivity of detecting the presence of drug resistant viruses. If no drug is present the wild-type viruses will likely be detected and it would be a waste of time (and money) to perform the test. The idea to detect the presence of drug in the plasma before performing the resistance test may help ensure that the optimal sample is used for testing and prevent testing samples that will not be interpretable. For example, if no drug is detected the physician can provide adherence counseling and then request a new samples when the patient is thought to be more adherent.

Conclusion

In conclusion, this preliminary assessment suggests that the detection of plasma PI drug concentrations may help to predict the detection of PI-associated drugs resistance by consensus sequencing in that sample, while for patients receiving NNRTI-based treatment drug concentrations may be less useful to predict the detection of NNRTI-associated drug resistance. Further analyses are needed to confirm the utility of drug measurement to predict the detection of NNRTI and PI resistance mutations prior to genotype testing.

Acknowledgements

References

1. UNAIDS. HIV and AIDS estimates 2014. Available from: http://www.unaids.org/en/regionscountries/countries/thailand.
2. CDCThailand. Thailand National Guideline for HIV/AIDS treatment and prevention 2014: Bureau of AIDS and stis Thailand; 2014. 498 p.
3. Gianotti N, Moretti F, Tambussi G, Capiluppi B, Ferrari M, Lazzarin A. The rationale for a study on HIV-1 reverse transcriptase mutations and outcome of antiretroviral therapy with two nucleoside analogs. Journal of biological regulators and homeostatic agents. 1999;13(3):158-62.
4. Mack N, Evens EM, Tolley EE, Brelsford K, Mackenzie C, Milford C, et al. The importance of choice in the rollout of ARV-based prevention to user groups in Kenya and South Africa: a qualitative study. Journal of the International AIDS Society. 2014;17(3 Suppl 2):19157.
5. Ferrer E, Navarro A, Curto J, Medina P, Rozas N, Barrera G, et al. Long-term fat redistribution in ARV-naive HIV+ patients initiating a non-thymidine containing regimen in clinical practice. Journal of the International AIDS Society. 2014;17(4 Suppl 3):19553.
6. CDCThailand. Thai national guidelines for antiretroviral therapy in HIV-1 infected adults and adolescents2010.
7. de Maat MM, Huitema AD, Mulder JW, Meenhorst PL, van Gorp EC, Mairuhu AT, et al. Subtherapeutic antiretroviral plasma concentrations in routine clinical outpatient HIV care. Ther Drug Monit. 2003;25(3):367-73.
8. Hollanders RM, van Ewijk-Beneken Kolmer EW, Burger DM, Wuis EW, Koopmans PP, Hekster YA. Determination of nevirapine, an HIV-1 non-nucleoside reverse transcriptase inhibitor, in human plasma by reversed-phase high-performance liquid chromatography. J Chromatogr B Biomed Sci Appl. 2000;744(1):65-71.
9. Günthard HF, Aberg JA, Eron JJ, et al. Antiretroviral treatment of adult hiv infection: 2014 recommendations of the international antiviral society–usa panel. JAMA. 2014;312(4):410-25.
10. Perrone V, Cattaneo D, Radice S, Sangiorgi D, Federici AB, Gismondo MR, et al. Impact of therapeutic drug monitoring of antiretroviral drugs in routine clinical management of patients infected with human immunodeficiency virus and related health care costs: a real-life study in a large cohort of patients. ClinicoEconomics and outcomes research : CEOR. 2014;6:341-8.
11. Kouanfack C, Laurent C, Peytavin G, Ciaffi L, Ngolle M, Nkene YM, et al. Adherence to Antiretroviral Therapy Assessed by Drug Level Monitoring and Self-Report in Cameroon. JAIDS Journal of Acquired Immune Deficiency Syndromes. 2008;48(2):216-9.
12. Charania MR, Marshall KJ, Lyles CM, Crepaz N, Kay LS, Koenig LJ, et al. Identification of evidence-based interventions for promoting HIV medication adherence: findings from a systematic review of U.S.-based studies, 1996-2011. AIDS and behavior. 2014;18(4):646-60.

RESEARCH ARTICLE

Quantification of lopinavir and ritonavir in dried blood spots using liquid chromatography-triple quadrupole mass spectrometry

Yardpiroon Tawon[1,2], Kesara Na-Bangchang[2], Gonzague Jourdain[1], Marc Lallemant[1,3], Tim R Cressey[1,3,4]

[1]*Program for HIV Prevention and Treatment (PHPT/IRD 174), Faculty of Associated Medical Sciences, Chiang Mai University 50200, Thailand;*
[2]*Center of Excellence in Pharmacology and Molecular Biology of Malaria and Cholangiocarcinoma, Graduate Program in Bioclinical Sciences, Chulabhorn International College of Medicine, Thammasat University, Pathumthani, Thailand;*
[3]*Harvard T.H Chan School of Public Health, Boston, MA 02115, USA;4Department of Molecular & Clinical Pharmacology, University of Liverpool, UK.*

Abstract

Lopinavir/ritonavir is widely used as part of combination antiretroviral treatment in HIV-infected adults and children in Thailand. Lopinavir is a HIV protease inhibitor and is administered with low dose ritonavir to enhance its bioavailability. Antiretroviral drug measurement can be useful for the clinical management of patients with drug toxicities, drug-drug interactions, as well as optimization of dosing for pregnant women and young children. Drug measurements are performed using plasma samples and they require storage and shipping under frozen conditions. Dried blood spots (DBS) is an alternative sample matrix for drug measurement as they can be stored at room temperature and shipped in the normal post. We developed and validated a liquid chromatography-triple quadrupole mass spectrometry (LC-MS/MS) assay to measure lopinavir and ritonavir from DBS. Sample preparation involved a liquid-liquid extraction. Chromatographic separation was performed on a Gemini Polar Reversed Phase C18 column (150 x 2.0 mm ID, 5µm) using a stepwise gradient. The calibration curve was linear over the range 0.05 to 20 µg/mL. The lower limit of quantification was 0.05 µg/mL. The assay average accuracy was 102-112% for lopinavir and 90-112% for ritonavir. The assay precision (inter- and intra assay) expressed as coefficient of variation (%CV) was <6% for lopinavir and <9.0% for ritonavir. The recoveries for lopinavir and ritonavir were 82.1% and 102.6%, respectively. Both drugs were stable in DBS stored at room temperature for at least 3 months. No effect from the sample hematocrit (30-60%) was observed. Concentrations of lopinavir and ritonavir in paired plasma and DBS samples collected from 50 HIV-infected patients (median age 19 years) during 0.1-12.3 hours after the last doses were measured using the developed method. Plasma and DBS concentrations for lopinavir and ritonavir were highly correlated (Pearson correlation r = 0.913 and r = 0.952, respectively). The Bland-Almond plot indicated no proportional bias between the DBS and plasma assays (p>0.05). However, lopinavir and ritonavir concentrations were 31.6% and 16.4% lower in DBS than in plasma, respectively. In conclusion, the LC-MS/MS assay validated for the quantification of lopinavir and ritonavir in DBS is robust, accurate and precise. Lopinavir and ritonavir concentrations in DBS are lower than plasma. Current target drug concentrations are

based on plasma concentration thresholds therefore drug concentrations determined from DBS need to be adjusted to estimate the plasma concentrations before interpretation. Further analysis of paired DBS-plasma samples is needed to establish an equation to predict plasma concentrations from DBS concentrations.

Keywords: lopinavir, ritonavir, dried blood spots, LC-MS/MS

Introduction

Lopinavir (LPV) and ritonavir (RTV) are HIV protease inhibitors. Lopinavir and ritonavir are substrates for cytochrome CYP3A4 and because ritonavir is a potent inhibitor of CYP3A coadminstration significantly increases the bioavailability of lopinavir. Lopinavir is coformulated with low dose ritonavir in a single tablet formulation (LPV/RTV 200/50 mg tablets) and is administered twice daily.

In Thailand, the recommended first-line antiretroviral treatment regimens are composed of a dual nucleoside reverse transcriptase inhibitor (NRTI) backbone plus non-nucleoside reverse transcriptase inhibitor (NNRTI), e.g. TDF+3TC plus EFV. This first line regimen is also recommendation for HIV-infected pregnant women. For patients who cannot take a NNRTI lopinavir/ritonavir is recommended to replace the NNRTI. Lopinavir/ritonavir is also recommended as part of antiretroviral drug regimens for children. LPV/rtv is part of the preferred 1st line regimen for HIV-infected infants less than 3 years of age[1].

Therapeutic drug monitoring (TDM) of antiretroviral drugs is not routinely recommended but can be considered in special clinical circumstances, such as for patients with renal or hepatic impairment, pregnant women, children and in cases of suspected drug-drug interactions to maximize efficacy and/or minimize drug toxicity[2]. Standard drug measurement methods require plasma samples but this can limit its widespread use as the samples must be processed (i.e. centrifuge) and then stored and shipped under frozen conditions. Dried blood spots (DBS) is a possible alternative sample for drug measurement as they can be shipped under ambient conditions through the standard mail (the dry matrix is considered none pathogenic). DBS sample collection can also be less invasive and uses smaller blood volumes. Consequently, drug measurement using DBS is increasingly being used in drug discovery, drug development, and therapeutic drug monitoring.

The US FDA does not currently accept standalone DBS data as a replacement for liquid matrices for registration studies. If a bioanalytical method for analyte is already developed for a liquid matrix, one can usually modify and apply it to DBS. DBS methods must be developed and validated to meet the same validation acceptance criteria. The comparison of drug concentrations in DBS and plasma is also required as the current efficacy and toxic concentrations thresholds for antiretroviral drugs are based on plasma drug concentrations; thus
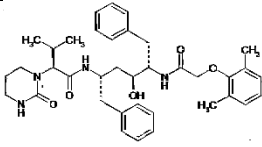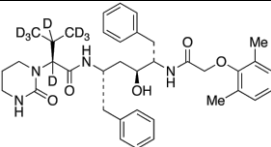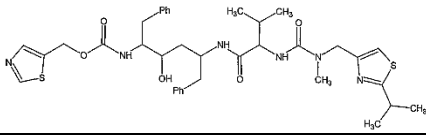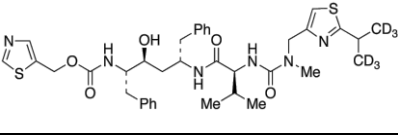
if DBS are to be used as an alternative sample matrix it is important to determine the agreement between DBS and plasma concentrations to facilitate interpretation[3].

Our objectives were to validate a method to determine LPV and RTV concentrations in dried blood spot using liquid chromatography-triple quadrupole mass spectrometry (LC-MS/MS) and to compare LPV and RTV concentrations in paired plasma and dried blood spots samples from HIV-infected patients in Thailand.

Materials and Methods

Chemicals and Reagents

Lopinavir, lopinavir-d8, ritonavir and ritonavir-d6 were obtained from Toronto Research Chemicals Inc, Canada. Acetronitrile (HPLC grade), Ethyl Acetate and Methanol (HPLC grade) were obtained from JT. Baker. Acetic acid (glacial) 100% and Ammonium Acetate were obtained from Merck. The chemical structure of each compound is shown in Figure 1.

Lopinavir: $C_{37}H_{48}N_4O_5$	Lopinavir-d8: $C_{37}H_{40}D_8N_4O_5$ (Internal Standard for LPV)
Ritonavir: $C_{37}H_{48}N_6O_5S_2$	Ritonavir-d6: $C_{37}H_{42}D_6N_6O_5S_2$ (Internal Standard for RTV)

Figure 1. Structure of the lopinavir, ritonavir and internal standards

Equipment

The quantification of lopinavir and ritonavir in plasma and DBS were analyzed using liquid chromatography-triple quadrupole mass spectrometry (LC-MS/MS). An Agilent HPLC 1100 series coupled with an Agilent Triple Quad MS 6430 system was used with Mass Hunter Software for data acquisition.

Chromatographic and Mass Spectrometric Conditions for DBS Assay

The chromatographic and MS conditions were based on a published method to quantify LPV and RTV in human plasma[4]. Chromatographic separations were performed on a Gemini Polar Reversed Phase C18 column (150 mm x 2.0 mm ID, particle size 5µm) connected with Security Guard Cartridges AQ C18: 4.0 mm x 2.0 mm ID, cat no. AJ0-7596. A stepwise gradient was used at a flow rate of 0.25 mL/min. At time zero the flow consist of 15% mobile

phase A (100% Methanol) and 85% mobile phase B (10 mM ammonium acetate buffer: 10 mM acetic acid: methanol (43:22:35 %v/v). The percentage of mobile phase A was increased to 85% from time 0 to 0.1 minutes. The 85% mobile phase A and 15% mobile phase B was maintained from 0.1 to 10 minutes. At 10.1 minutes the percentage of mobile phase A was decreased from 85% to 15% and continues to recondition the system with 15% of mobile phase A and 85% of mobile phase B until 15 minutes. Total run time is 15 minutes. The triple quadrupole mass spectrometer was operated in positive mode. The source temperature was set at 350°C. The nebulizer was set at 50 psi (air). The drying gas (N_2) was flow at 10 L/min of gas flow. The multiple reaction monitoring (MRM) mode was used for the quantification analysis. MRM transitions for each analyte are given in Table 1.

Table 1. MS QQQ Mass Spectrometer Parameters

Analyte Compound	Precursor Ion	Product Ion	Dwell	Frag (V)	CE (V)
LPV	629.80	447.2	50	128	8
LPV-d8	637.86	191.2	50	128	18
Internal Standard	**Precursor Ion**	**Product Ion**	**Dwell**	**Frag (V)**	**CE (V)**
RTV	721.90	296.1	50	128	16
RTV-d6	727.99	302.2	50	168	14

Preparation of Standard calibration samples, Internal standards and Quality Controls

Stock solutions of all analytes (LVP, LPV-d8, RTV and RTV-d6) were prepared by dissolving in methanol to make a final concentration of 1.0 mg/mL. The stock solution of LPV and RTV were diluted with human blank plasma to an intermediate working solution at a concentration of 100,000 ng/mL. This working solution was further diluted with whole blood (K2-EDTA) to prepare the calibration samples at nine levels in the range 50 to 20,000 ng/mL. Internal Quality Control Samples were prepared similarly by diluting the intermediate working solution in plasma into whole blood (K2-EDTA) to yield three levels: QC low at 150 ng/mL, QC medium at 1,500 ng/mL and QC High at 16,000 ng/mL. Each calibrator and internal quality control samples were spotted (50 µL) on separate Whatman Protein Saver 903 Cards. The cards were dried at room temperature overnight and then stored with a desiccant at -20ºC. A working solution of both internal standards was prepared by mixing spiked stock solutions of LPV-d8 and RTV-d5 into DI water to obtain a final concentration of 500 ng/mL.

Sample Preparation

The extraction procedure was modified based on a previously published assay to measure NRTIs in DBS[5]. The entire DBS was cut out using a 1/2-Inch hole punch and place it into an appropriately labelled 1.5 mL micro tube. 150 µL of the Internal Standard-mixture in water was added into the micro-tube and then left to equilibrate at room temperature for 10 minutes. After that, methanol was added and the tubes were sonicated for 15 minutes. Ethyl acetate was then added to each tubes and vortex for 1 minute, followed by centrifugation at 12,000 rpm (16,060xg) for 5 minutes. The supernatant was transferred to a new tube and evaporated under nitrogen gas. Once the sample was dry it was reconstitution in mobile phase

B (10 mM ammonium acetate buffer: 10 mM acetic acid: methanol (43:22:35 %v/v). 10 µL of sample matrix was injected in to the HPLC-MS-QQQ by automatic injector.

Method Validation

The DBS method were validated following the Bioanalytical Method Validation based on the US FDA[6] and European Medicines Agency (EMA) guidelines[7].

Matrix effect, Percentage recovery and Process Efficiency

Three sets of samples were prepared at three levels low, medium and high. Each set was prepared in five replicates. Set 1: "No matrix"- analytes and IS were spiked in mobile phase. Set 2: "Post-extraction"- analytes and IS were spiked in extracted blank whole blood spotted DBS samples. Set 3: "Pre-extraction" - analytes and IS were spiked in whole blood and spot on DBS samples and then analyzed. Each replicate was from a different source of blank DBS. The matrix effect was determined by calculating the ratio of the signal of the Post-extraction spike/No matrix. The percentage recovery was determined by calculating the ratio of the signal of the Pre-extraction spike/Post-extraction spike. The process efficiency was determined by calculating the ratio of the signal of the Pre-extraction spike/No matrix.

Selectivity/Concomitant Medications

Blank plasma sample (matrix sample processed without analyte and internal standard) from six individual sources and plasma samples from persons receiving both antiretroviral and non-antiretroviral drugs were analyzed to assess is the presence of interfering compounds.

Inter- and Intra Assay Accuracy and precision

The accuracy and precision of the assay was determined by analysis of spiked DBS samples with known amounts of antiretroviral drugs at 4 levels of the calibration curve: Lower Limit of Quantification (LLOQ, 50 ng/mL), Low QC (150 ng/mL), Medium QC (1,500 ng/mL) and High QC (16,000 ng/mL). Six replicate DBS samples of LLOQ, Low QC, Medium QC and High QC in 3 separate analytical runs were analyzed.

Carry-over

To determine the possibility of any sample carry-over between sample runs, three injections of extracted blank DBS samples (DBS from blank whole blood) were run after a run containing the highest calibration curve standard for each analyte.

Stability

The stability of LPV and RTV under various conditions was determined. The following tests were performed: the stability of analytes in whole blood at 2-8°C before spotting, the stability after five freeze/thaw cycles at -20°C and the stability of the extracted diluent in the autosampler at 4°C for one week.

The short-term and long-term stability in DBS were also determined: for one week (at room temperature, at 2-8 °C and at -20 °C) and for three months (at room temperature and at -20°C).

Hematocrit effect

Hematocrit is currently identified as the single most important parameter influencing the spread of blood on DBS cards, which could impact the validity of the results generated by DBS methods, affecting the spot formation, spot size, drying time, homogeneity, and ultimately, the robustness and reproducibility of the methods. DBS samples were prepared at low level (QC Low) and high level (QC High) from whole blood with 30% hematocrit and 60% hematocrit then analyzed and compared with the control DBS sets prepared from whole blood with 45% hematocrit.

DBS spotting, pipette versus calibrated capillary

Even though the exactly volume of blood is used for DBS spotting but the spotting technique can be affect the validity of the results. The validation of DBS spotting effect was performed by spotting the DBS with the blood at Low QC and High QC on Whatman 903 filter paper using a calibrated capillary (50μL) was compared with a control set prepared by using a micropipette (50μL).

Comparison of the DBS concentrations versus plasma concentrations in HIV-infected patients

To assess whether lopinavir and ritonavir concentrations in plasma and DBS are similar, 50 paired plasma and DBS samples from HIV infected patients receiving LPV/RTV based regimen within the PHPT observational cohort study were tested. All samples were identified by a patient identification code (PID). The study protocol was approved by the Institute for Development of Human Research Protection (IHRP) committee at the Thai Ministry of Public health on 05 March 2013. The number of sample size was based on the Clinical and Laboratory Standards Institute (CLSI) Guidelines for 'Measurement Procedure Comparison and Bias Estimation Using Patient Samples'[8] stated that a minimum of 40 patient specimens are required for method comparison and bias estimation. The LC-MS/MS assay to quantify lopinavir and ritonavir in plasma was served as the 'standard' method and the DBS LC-MS/MS assay was the 'candidate' method. The LC-MS/MS assay to quantify lopinavir and ritonavir in plasma was previously internally validated at the Program for HIV Prevention and Treatment laboratory, Faculty of Associated Medical Sciences, Chiang Mai University. Lopinavir and ritonavir were extracted from plasma using protein precipitation and the standard calibration curve was linear over the range 50 to 20,000 ng/mL for lopinavir and ritonavir.

The comparison of lopinavir and ritonavir concentrations in plasma and dried blood spots was performed using linear regression analysis and Bland-Altman plots. A statistical analysis was performed using SPSS Statistic Software (version 22).

Results

Lopinavir and ritonavir DBS Assay Development

A typical chromatogram showing the MRM chromatographic peak of all analytes are shown in Figure. 2. The retention times of RTV and LPV were 7.8 and 8.5 minutes, respectively. The stable-isotope-labeled internal standards (RTV-d6 and LPV-d8) had the same retention time as the analytes.

Method Validation

Matrix Effect, Percentage Recovery and Process efficiency

The % matrix effect for RTV and LPV were 93.5% and 120.7%, respectively. The % matrix effect for internal standards were 93.3% for RTV-d6-IS and 107.5% for LPV-d8-IS. There was an enhancement matrix effect for LPV and minor suppression for RTV. All analytes (LPV and RTV) were quantified using the area ratio of analytes and internal standard. The peak area of the isotopic internal standards has an enhancement for LPV-d8-IS and minor suppression for RTV-d6-IS, similar to their corresponding analytes. The matrix effect was considered acceptable: % matrix effect of area ratio for LPV/LPV-d8-IS and RTV/LPV-d6-IS peak area were 102.1% and 95.7%, respectively. The % recovery and % process effect were also acceptable for all analytes (Table 2).

Calibration Curves and Lower Limit of Quantification (LLOQ)

The calibration curves over the range 50-20,000 ng/mL for LPV and RTV were plotted and fitted using 1/x2 weighted linear regression of the peak area ratios (drug peak area/I.S. peak area) versus concentrations. All the calibration curves showed good linear correlation. The coefficient of determination (R^2) for the calibration curve for lopinavir and ritonavir were > 0.990 and > 0.994, respectively.

The lower limit of quantification (LLOQ) was 50 ng/mL for all analytes. The peak area response at LLOQ of and RTV were at least 5 times the response compared to blank response.

Inter- and Intra Assay Accuracy and precision

A summary of the assay precision and accuracy results are shown in Table 3. The assay average accuracy was 102-112% for lopinavir and 90-112% for ritonavir. The assay precision (inter- and intra assay) expressed as coefficient of variation (%CV) was <5% for lopinavir and <8.0% for ritonavir (Table 3).
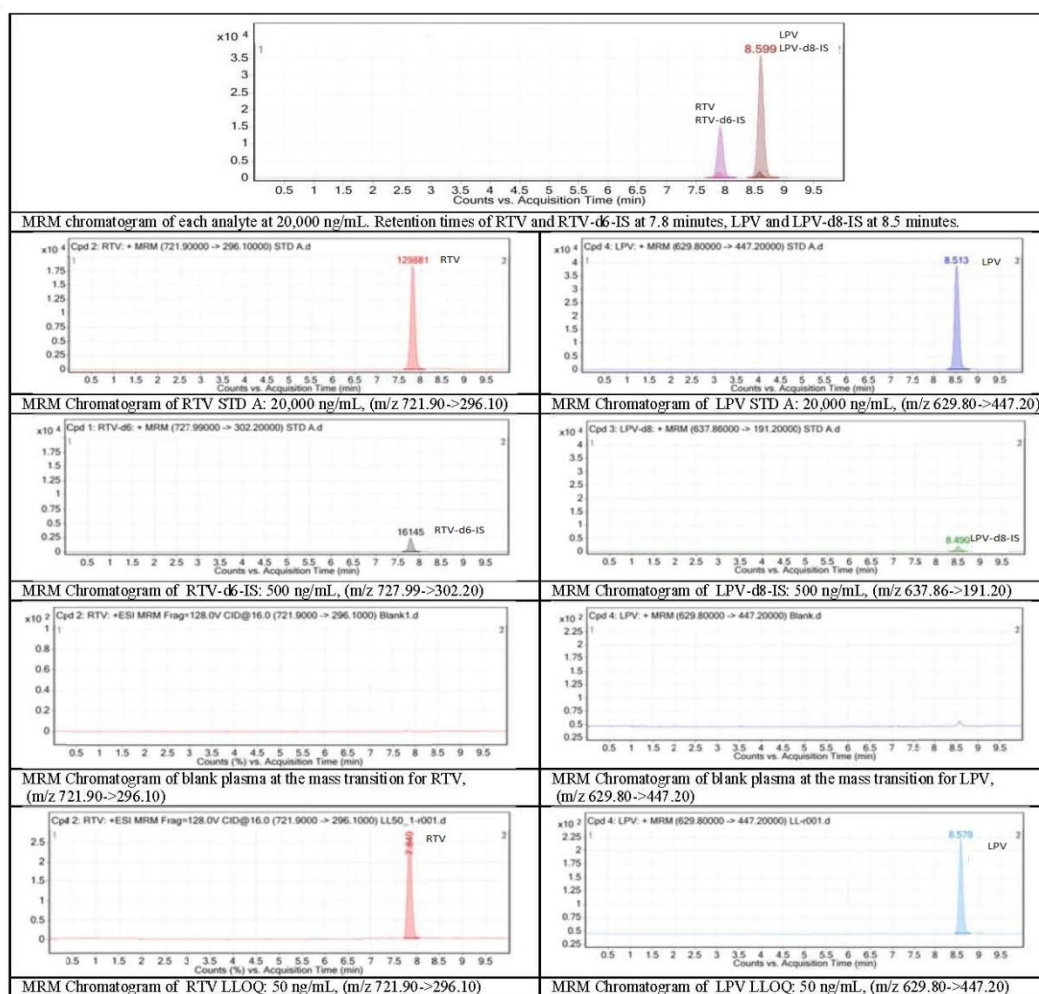
Figure 2. MRM chromatogram for lopinavir and ritonavir. RTV and RTV-d6-IS peaks were at 7.8 minutes, LPV and LPV-d8-IS peaks at 8.5 minutes.

Table 2. Matrix Effect (ME), Recovery (RE), and Process Efficiency (PE) for LPV and RTV in DBS

Analyte	Validation parameters		Analyte	IS	Area Ratio (Analyte/IS)
LPV	Matrix Effect (ME)	Range	96.7 - 139.3	96.2 - 117.9	92.0 - 118.2
		Mean	120.7	107.5	102.1
	Recovery (RE)	Range	74.7 - 92.7	86.6 - 101.6	82.5 - 107.6
		Mean	82.1	92.9	100.4
	Process efficiency (PE)	Range	89.7 - 109.9	97.7 - 102.1	91.0 - 96.0
		Mean	97.9	99.3	97.6
RTV	Matrix Effect (ME)	Range	85.4 - 96.0	86.4 - 105.7	90.9 - 113.4
		Mean	93.5	93.3	95.7
	Recovery (RE)	Range	97.7 - 108.7	93.1 - 107.0	98.6 - 105.2
		Mean	102.6	100.9	101.8
	Process efficiency (PE)	Range	92.9 - 100.4	90.0 - 98.5	95.6 - 111.8
		Mean	95.7	93.7	102.7

TABLE 3. Inter- and Intra Assay Accuracy and precision

Analyte	Level	Conc. (ng/mL)	Intra Assay (n = 6)			Inter Assay (n=18)		
			% Accuracy	% Variation	SD	% Accuracy	% Variation	SD
LPV	LLOQ	50	101.93 - 104.04	3.11 - 5.57	1.63-2.84	102.90	4.38	2.25
	Low	150	103.03 - 109.46	0.81 - 4.82	1.33-7.45	106.67	4.09	6.54
	Med	1500	108.40 - 109.33	1.54 - 4.04	25.04 - 66.01	108.92	2.57	42.07
	High	16000	109.60 - 111.50	1.88 - 4.94	334.30 - 886.95	110.75	3.17	562.49
RTV	LLOQ	50	90.18 - 105.59	2.65 - 5.61	1.20 – 2.81	98.43	8.04	3.96
	Low	150	103.92 - 110.90	2.65 - 5.25	2.87 – 8.18	107.07	4.23	6.80
	Med	1500	109.00 - 110.75	1.37 - 4.68	22.81 – 76.48	110.13	2.94	48.55
	High	16000	106.74 - 111.54	1.72 - 6.38	307.25 – 1101.95	108.72	4.31	750.41

Stability

Both LPV and RTV have been shown to be stable in whole blood at 4°C for 24 hours before spotting and in DBS after freeze thaw for 5 cycles, at 2-8 °C for 1 week and at -20ºC and at room temperature for 3 months. The stability data are shown in Table 4.

Table 4. Stability Data for LPV and RTV in DBS under various conditions and storage

Stability Condition/ Variation parameters	LPV				RTV			
	Low		High		Low		High	
	% mean diff	% CV	% mean diff	% CV	% mean diff	% CV	% mean diff	% CV
In whole blood at 4°C for 24 hours	105.79	3.05	95.11	7.48	107.48	3.54	92.85	7.35
Freeze Thaw 5 cycles	105.44	7.35	97.41	1.75	103.78	8.36	93.01	1.76
In injection matrix at 2-8°C for 1 week	107.67	0.75	100.14	0.43	110.24	1.31	98.57	0.37
In DBS at room temperature for 1 week	109.96	2.05	108.74	4.29	110.52	3.61	103.65	5.55
In DBS at 2-8°C for 1 week	112.46	0.66	105.96	5.28	111.22	1.14	102.82	8.40
In DBS at room temperature for 3 months	92.19	4.55	97.57	5.52	92.99	7.07	92.73	5.62
In DBS at -20°C for 3 months	95.46	7.68	98.44	0.72	93.67	8.05	98.26	0.21

The effect from Hematocrit variation and DBS spotting, pipette versus calibrated capillary

There is no effect from hematocrit to the measurement of LPV and RTV in DBS at the Hematocrit value in between 30-60%. DBS spotting by using calibrated capillary is not different from using micropipette. Overall results were acceptable. The data are shown in Table 5.

Table 5. The effect of Hematocrit and DBS preparation technique for LPV and RTV in DBS

Variation parameters	LPV				RTV			
	Low		High		Low		High	
	% mean diff	% CV	% mean diff	% CV	% mean diff	% CV	% mean diff	% CV
Hct (30%)	98.09	5.60	98.05	2.26	102.40	4.56	99.57	2.72
Hct (60%)	98.44	4.41	100.23	3.74	104.30	4.82	99.83	4.69
Prepare DBS by using 50 uL calibrated capillary tube	92.09	2.26	101.93	0.79	102.15	7.28	105.44	0.43

Comparison of DBS and plasma concentrations in HIV-infected patients[13,14,15]

Concentrations of lopinavir and ritonavir in paired plasma and DBS samples from 50 HIV-infected patients (median age 19 years old) between 0.1 to 12.3 hours post-dose were determined.

The relationship between drug concentrations in DBS and plasma samples for lopinavir are shown in Figure 3a and for ritonavir in Figure 3c. Plasma and DBS concentrations for lopinavir and ritonavir were highly correlated (Pearson correlation r = 0.913 and r =0.952, respectively), although the DBS concentrations for both lopinavir and ritonavir were lower than in plasma. The Bland-Almond plot for lopinavir and ritonavir are shown in Figure 3b and Figure 3d, respectively. The mean percent difference between DBS and plasma [(DBS conc.-Plasma conc.)/mean%] was 31.6% lower (95% confidence interval (CI): -59.2% to -4.0%; p=0.378) for lopinavir and 16.4% lower (95% CI: -43.1% to +10.3%; p=0.080) for ritonavir.

Discussion

We reported the validation of a new method for the quantification of lopinavir and ritonavir in DBS. A new validated method was simple and rapid. The total run time of the assay is 15 minutes. The assay suppression and matrix background were removed by using two steps of extraction (precipitation extraction and following with the liquid-liquid extraction). The assay average accuracy (inter- and intra assay) was 102-112% for lopinavir and 90-112% for ritonavir. The assay precision (inter- and intra assay) expressed as coefficient of variation (%CV) was <6.0% for lopinavir and <9.0% for ritonavir. The recoveries for lopinavir and ritonavir were 82.1% and 102.6%, respectively. Both drugs were stable in DBS stored at room temperature for at 3 months. Several LC-MS/MS assays for the quantification of lopinavir and ritonavir in DBS have been reported[9-12] but the impact of different hematocrit values was not performed as part of the assay validation. A patient's hematocrit is an important factor for DBS samples as it can affect the spread of blood on the card and thus the volume of blood per punched spot, especially when only a 'partial punch' hole is used for testing. We observed no effect of sample hematocrit (30-60%) in the assay developed. In addition, limited data are available assessing the degree of agreement between lopinavir and ritonavir concentrations quantified in plasma and in DBS samples. Koal *et al*[9] reported a good correlation (R=0.984) between antiretroviral drugs concentrations in paired plasma and DBS from 70 patients (containing either atazanavir, saquinavir, LPV, RTV or efavirenz). Roland *et al*.[10] reported a

strong correlation between plasma and DBS concentrations in 19 HIV-infected children for both LPV (R=0.921) and RTV (R=0.877). Despite the strong correlation reported it is also important to determine the agreement between the two methods to quantify the drug concentrations.
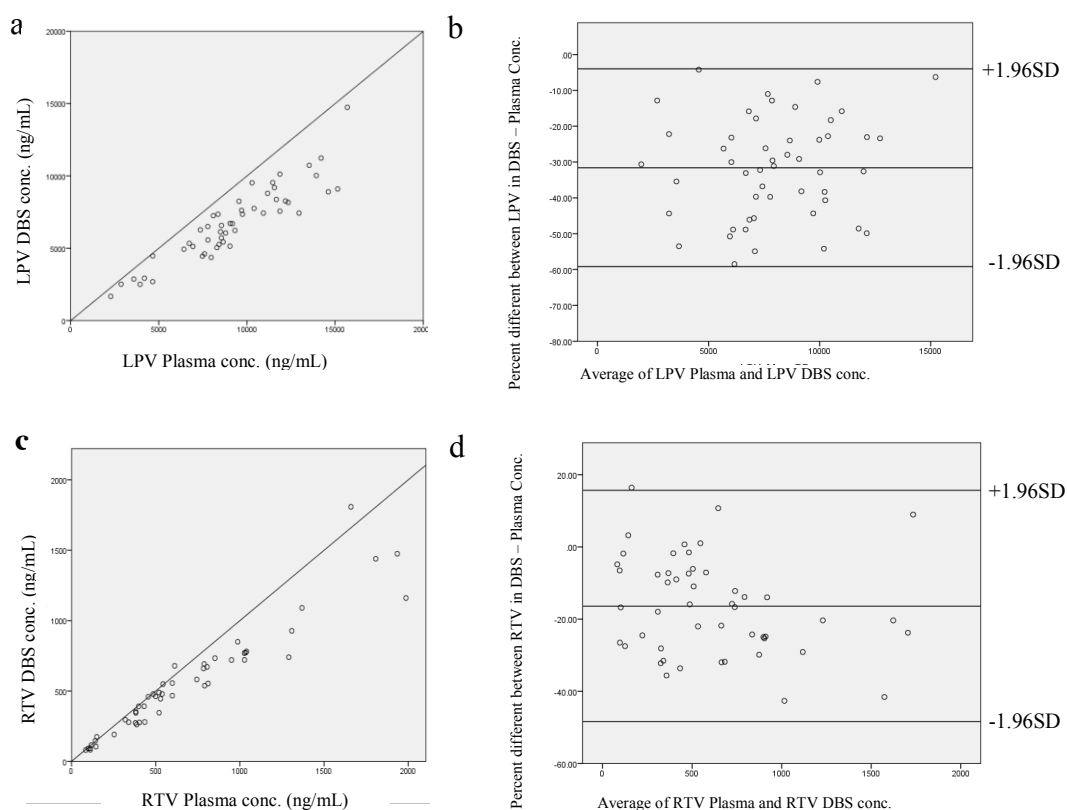
Figure 3 (a) Comparison of LPV concentrations measured in DBS versus plasma (b) Bland-Altmand plot of percent difference between LPV concentrations in DBS (DBS assay) versus with plasma (plasma assay) (c) Comparison of RTV concentrations in DBS versus plasma (d) Bland-Altmand plot of percent difference between RTV concentrations in DBS (DBS assay) versus plasma (plasma assay).

We also found a strong correlation between LPV and RTV concentrations between DBS and plasma concentrations. The Bland-Almond plots showed there was no proportional bias (p>0.05) between the DBS and plasma methods. However, lopinavir were 31.6% lower and ritonavir 16.4% lower in DBS than in plasma. The different drug concentrations in DBS and plasma could be due to the diffusion of the drug between blood cells and fraction of drug bound to plasma protein (fbpp). This observed difference between the sample matrixes could lead to a different interpretation of the result. To confirm that correlation between drug DBS and plasma concentrations and to establish an equation to predict plasma concentrations from DBS concentrations a larger number of paired samples from patients (e.g. 100 to 200) should be assessed. Finally, a limitation of our study was that DBS samples were prepared from a venous blood sample. Often DBS are prepared from a finger prick and it will be important to

determine if the drug concentrations in a DBS prepared from a venous or finger prick (i.e. capillary) are similar.

Conclusion

The validated LC-MS/MS assay for the quantification of lopinavir and ritonavir in Dried Blood Spots (DBS) was robust, accurate and precise. DBS sample collection is ideal for neonates and small children as it is less invasive and only requires a small blood volume. In addition, DBS samples are considered non-infectious so can be shipped by standard post mail without temperature control. DBS samples are also preferable in remote areas with no equipment for plasma collection and facilities for sample storage and shipment under frozen condition.

In paired DBS-plasma samples from HIV-infected patients both lopinavir and ritonavir concentrations were lower in DBS than in plasma samples. Current efficacy and toxic antiretroviral concentration thresholds for clinical management are based on plasma drug concentrations. Thus, DBS results need to be adjusted to estimate the corresponding plasma concentration before interpretation. Additional paired DBS-plasma samples need to be tested to establish an equation to predict plasma concentrations from DBS concentrations. The DBS assay developed can be useful for the clinical management by providing qualitative results or semi-quantitative results to monitor drug adherence and drug toxicity of the patients.

Acknowledgements

References

1. Thai Bureau of AIDS TB and STIs D, Ministry of Public Health. Thailand National Guidelines on HIV/AIDS Treatment and Prevention 2014. DDC, Ministry of Public Health, 2014.
2. AIDSinfo. Guidelines for the Use of Antiretroviral Agents in Pediatric HIV Infection: AIDSinfo; 2015 [updated March 5, 2015; cited 2015 Sept 8, 2015]. Panel's Recommendations Regarding the Role of Therapeutic Drug Monitoring in Management of Pediatric HIV Infection]. Available from: https://aidsinfo.nih.gov/guidelines/html/2/pediatric-arv-guidelines/108/role-of-therapeutic-drug-monitoring-in-management-of-pediatric-hiv-infection.
3. Li W. Handbook of LC-MS Bioanalysis, Best Practices, Experimental Protocols, and Regulations: John Wiley & Sons, Inc.; 2014.
4. Ter Heine R, Alderden-Los CG, Rosing H, Hillebrand MJ, van Gorp EC, Huitema AD, et al. Fast and simultaneous determination of darunavir and eleven other antiretroviral drugs

for therapeutic drug monitoring: method development and validation for the determination of all currently approved HIV protease inhibitors and non-nucleoside reverse transcriptase inhibitors in human plasma by liquid chromatography coupled with electrospray ionization tandem mass spectrometry. Rapid Commun Mass Spectrom. 2007;21(15):2505-14.

5. Anton Joubery SC JN, Peter Smith, Belinda Holtzhauzen, Lubbe Wiesner. The development and validation of an LC-MS/MS method for the determination of Abacavir, Efavirenz, Lamivudine, Nevirapine, Stavudine and Zidovudine in Dried Blood Spots (DBS). 17th World Congress on Basic and Clinical Pharmacology; 13-18 July; South Africa2014.

6. U.S.FDA. Antiretroviral drugs used in the treatment of HIV infection 2015 [updated Oct 08; cited 2015 Nov, 11]. Available from:
http://www.fda.gov/ForPatients/Illness/HIVAIDS/Treatment/ucm118915.htm.

7. EMA. Guideline on bioanalytical method validation: European Medicines Agency (EMA), Committee for Medicinal Products for Human Use (CHMP); 2011 [updated 21 July 2011]. Available from:
http://www.ema.europa.eu/docs/en_GB/document_library/Scientific_guideline/2011/08/WC500109686.pdf.

8. Clinical and Laboratory Standards Institute. Method comparison and bias estimation using patient samples. second edition (interim version) ed. CLSI, USA2005.

9. Koal T, Burhenne H, Romling R, Svoboda M, Resch K, Kaever V. Quantification of antiretroviral drugs in dried blood spot samples by means of liquid chromatography/tandem mass spectrometry. Rapid Commun Mass Spectrom. 2005;19(21):2995-3001.

10. Ter Heine R, Rosing H, van Gorp EC, Mulder JW, van der Steeg WA, Beijnen JH, et al. Quantification of protease inhibitors and non-nucleoside reverse transcriptase inhibitors in dried blood spots by liquid chromatography-triple quadrupole mass spectrometry. J Chromatogr B Analyt Technol Biomed Life Sci. 2008;867(2):205-12.

11. Meesters RJ, van Kampen JJ, Reedijk ML, Scheuer RD, Dekker LJ, Burger DM, et al. Ultrafast and high-throughput mass spectrometric assay for therapeutic drug monitoring of antiretroviral drugs in pediatric HIV-1 infection applying dried blood spots. Anal Bioanal Chem. 2010;398(1):319-28.

12. Watanabe K, Varesio E, Hopfgartner G. Parallel ultra-high pressure liquid chromatography-mass spectrometry for the quantification of HIV protease inhibitors using dried spot sample collection format. J Chromatogr B Analyt Technol Biomed Life Sci. 2014; 965:244-53.

13. Westgard JO. Use and interpretation of common statistical tests in method comparison studies. Clin Chem. 2008;54(3):612.

14. Hanneman SK. Design, analysis, and interpretation of method-comparison studies. AACN Adv Crit Care. 2008;19(2):223-34.

15. Giavarina D. Understanding Bland Altman analysis. Biochem Med (Zagreb). 2015;25(2):141-51.

RESEARCH ARTICLE

Effects of dihydroartemisinin on the inhibition of cell proliferation and migration in tamoxifen resistant breast cancer cells.

Nisakorn Pornsomchai[1*], Wacharee Limpanasithikul[2], Wannarasmi Ketchart[2]

[1]*Master of Science Program in Pharmacology, Graduate school, Chulalongkorn University, Bangkok 10330, Thailand;*
[2]*Department of Pharmocology, Faculty of Medicine, Chulalongkorn University, Bangkok 10330, Thailand*

Address correspondence and reprint request to: Department of Pharmacology, Faculty of Medicine, Chulalongkorn University, Bangkok, Thailand.
E-mail address: kignisakorn@gmail.com

Abstract

Acquired resistance to tamoxifen (TAM) is a major clinical problem in patients with ER-positive breast cancer, since the treatment is very limited. The effects of DHA on the inhibition of proliferation and migration of ER-positive breast cancer cells (MCF-7) and TAM resistant breast cancer cells (MCF-7/LCC-2) were investigated. DHA significantly decreased cell proliferation in the concentration-dependent manner with the IC50 value of 26.89 µM and 36.93 µM at 48 hours after DHA treatment in MCF-7 and MCF-7/LCC-2 cells respectively which were determined by MTT test. DHA also decreased cell migration in tamoxifen resistant cells at 10–40 µM range determined by scratch assay. The preliminary result obtained from this study indicated that DHA were able to inhibit cell proliferation and migration in ER-positive breast cancer cells and tamoxifen resistant cells.

Keywords: dihydroartemisinin, tamoxifen, drug resistance, breast cancer cells, cell proliferation, cell migration

Introduction

Breast Cancer is the most common cancer in woman all over the world. It is also the leading cause of death for women in Thailand (1). In addition, 70% of breast cancer patients are classified as estrogen receptor (ER) positive (2). US national institutes of Health (NIH) suggests that ER positive breast cancer patients should receive continuous anti-estrogen therapy for 5 years after the surgery as an adjuvant therapy (3). Tamoxifen, a selective estrogen receptor modulators (SERMs), is commonly used to treat this particular type of breast cancer. It competes to bind to estrogen receptor instead of estrogen and prevent cancer cells growth (4). Although this drug seems to be very promising, 40% of patients developed tamoxifen resistance after 1-3 years, resulted in increasing chances of cancer cell survival and invasion to other organs or metastasis (5). The treatment for tamoxifen resistance is very limited due to few choices of drug available and these drugs also develop resistance later on. Thus, it is crucial

to find another medication to treat those patients who are tamoxifen resistant to improve survival rate. The recent study found that dihydroartemisinin (DHA), one of the sesquiterpene lactones isolated from *Artemisia annua*, active metabolite of artemisinin, has the anti-malarial and anti-cancer property by reducing cell growth, tumor progression and metastasis of ER negative breast cancer cells (6), pancreatic cancer (7) and fibrosarcoma (8). Sesquiterpene lactones are known to interfere with the activity of *NF-kB* by alkylating its p65 unit (6). The previous study shown that *NF-kB* also involved in tamoxifen resistant mechanism in breast cancer cells (9). DHA can inhibit proliferation of pancreatic cancer cells by reduced expression of *C-MYC* and *Cyclin-D* gene that involved in cell proliferation and both are ER target genes (7). Recent reports demonstrated that *NF-kB*, *C-MYC* and *Cyclin-D* associate with drug resistant mechanism in breast cancer cells and DHA has been shown to inhibit *NF-kB*, *C-MYC* and *Cyclin-D* genes in other cancer cells. However, the effect of DHA on tamoxifen resistant breast cancer cells has not been elucidated. Thus, this research serves to study the effect of DHA on tamoxifen resistant breast cancer cells, in order to develop new therapy for the advance stage or metastatic ER positive breast cancer patients.

Materials and Methods

Cell culture and reagent

The human breast adenocarcinoma cell line MCF-7 (ATCC, USA) and tamoxifen resistant breast cancer cell line MCF-7/LCC-2 (Dr. Robert Clarke, Georgetown University Medical center, Washington DC, USA) were maintained in MEM media and supplemented with 5% FBS, 1% penicillin and streptomycin, 1% Amphotericin B in a 5% CO_2 atmosphere at 37° C. Dihydroartemisinin (DHA) and 4-hydroxytamoxifen (4- OHT) were purchased from Sigma-Aldrich.

Cell viability assay

Antiproliferation effect were determined by the 3-(4,5-dimethylthiazol-2-yl)-2,5 diphenyltetrazolium bromide (MTT) assay. Cells were seeded in 96-well plates at a density of 5000 cells per well. After 24 hours, cells were treated to varying concentrations of DHA (6.25, 12.5, 25, 50, 100 µM). MTT (5 mg/ml) was added to each well after DHA treatment for 48 hours and then MTT was aspirated and 100 µL of dimethyl sulfoxide (DMSO) was added to the cells and dissolved the blue formazan crystals. The absorbance was obtained from microplate reader at a wavelength of 570 nm. Percentage of cell viability by was calculated using the following formula:

$$\% \text{ cell viability} = \left(\frac{\text{ODsample} - \text{ODblank}}{\text{ODcontrol} - \text{ODblank}}\right) \times 100$$

Scratch assay

To determine the effect of DHA on cell migration, cells were seeded in 6-well plates at a density of 500,000 cells per well. After 24 hours, three straight scratches were made with a P200 µl pipette tip to create a wound. The cell debris was removed by washing with serum free

medium. After that, MCF-7/LCC-2 cells were treated with DHA in various concentration of 10, 20, 40 µM and 0.2% DMSO was used as a control for 48 hours. Digital images of cells was captured by a phase contrast microscope at 0, 24 and 48 hours after scratching. Scratch area was measured using ImageJ software (National Institutes of Health, Bethesda, MD, USA). Percentage of wound closure was calculated using the following formula:

$$\% \text{ wound closure} = \left(\frac{\text{migrated cell surface area}}{\text{total surface area}}\right) \times 100$$

Statistical Analysis

The results are expressed as mean ± S.E.M. Differences between groups were assessed by using an ANOVA test. The threshold of significance is $p < 0.05$

Results

DHA inhibited cell proliferation in ER-positive and tamoxifen resistant cells.

The inhibition of cell proliferation was investigated by MTT assay. The viability was assessed at 48 hours after the treatment with DHA in 5 concentrations (6.25, 12.5, 25, 50, 100 µM). DHA treatment exhibited statistically significant in the inhibition of cell proliferation in dose dependent manner (figure1). The IC50 values of DHA in MCF-7, MCF-7/LCC-2 at 48 hours were 29.06 µM and 36.93 µM respectively.
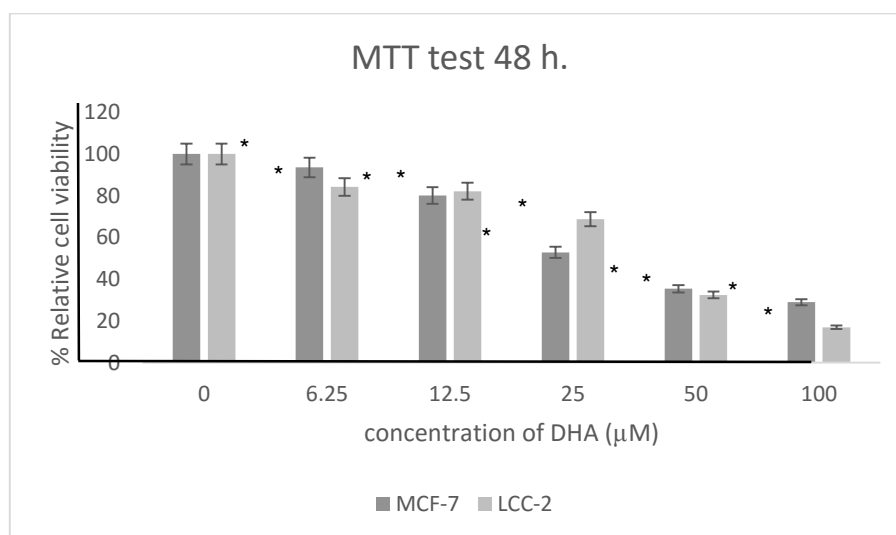
Figure 1. Effect of DHA on cell viability in wild type (MCF-7) and tamoxifen resistant breast cells (MCF-7/LCC-2). The percentage of cell viability of MCF-7, MCF-7/LCC-2 cells after the treatment with DHA at concentration 6.25-100 µM for 48 hours. Each value represented the mean ± S.E.M. (n=3). *p<0.05. Data are the representative of three independent experiments.
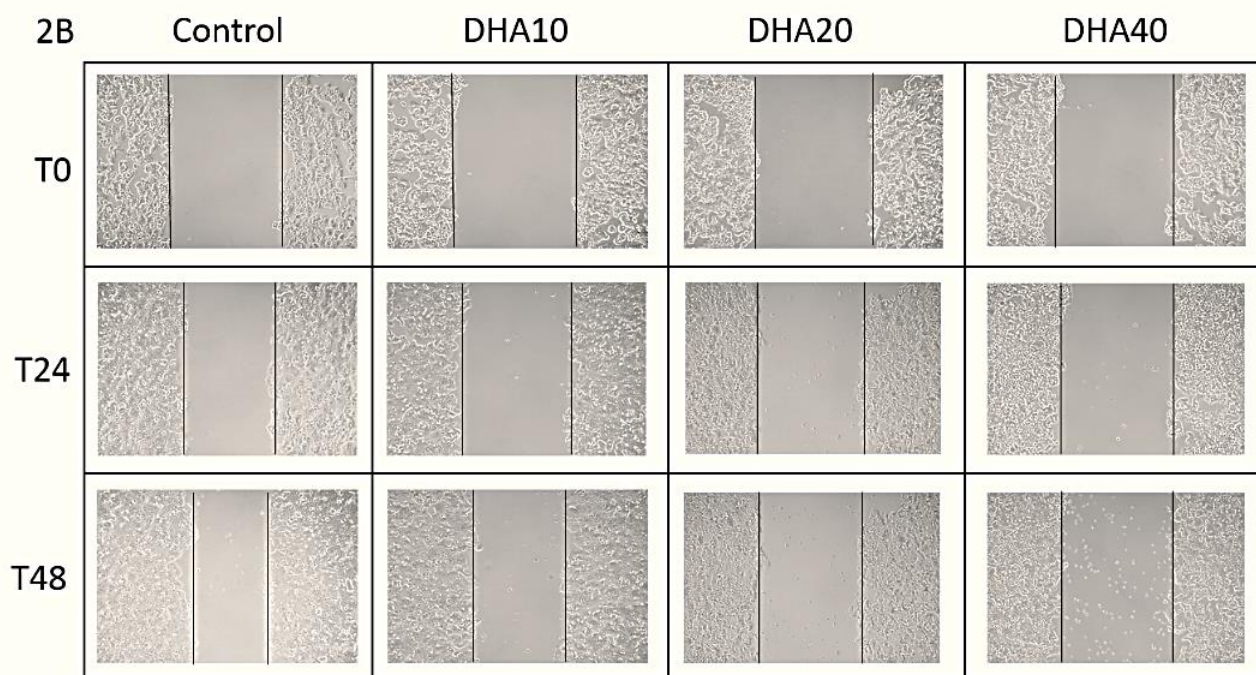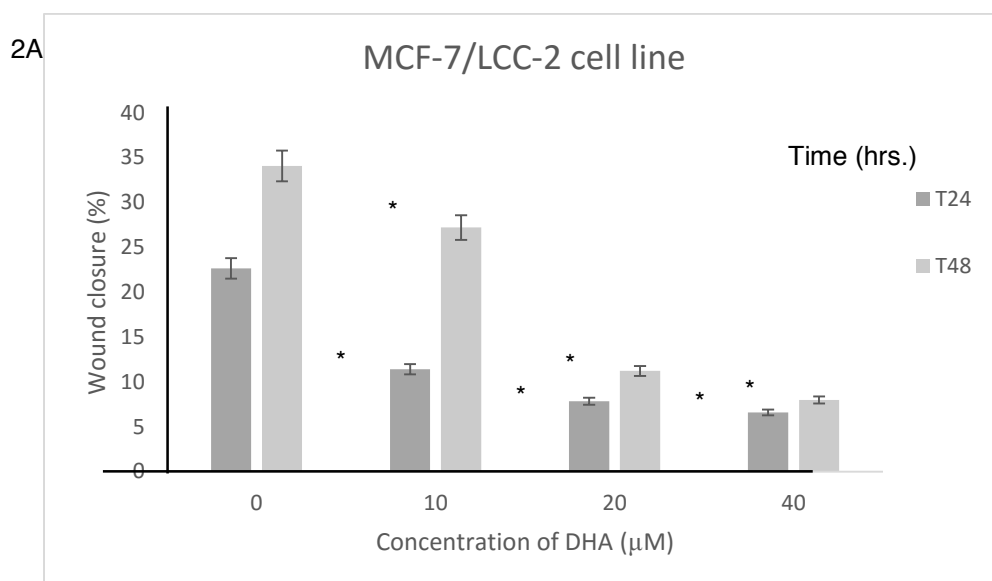
DHA inhibited cell migration in tamoxifen resistant cells

Since DHA has been shown to inhibit cell migration in fibrosarcoma HT1080 cells (10) and human umbilical vein endothelial (HUVE) cells (11), scratch assay was carried out to observe the effect of DHA on cell migration as shown in figure 2. The result of the study after treatment with DHA for 24 and 48 hours shown that the percentage of wound closure was significantly decreased when compare with the control group. At 24 hours after treatment with DHA in concentration 0 (used 0.2% DMSO as control group), 10, 20 and 40 µM, the percentage of wound closure were 22.45, 11.4, 7.84, 6.59 respectively. The result of the same concentration at 48 hours after treatment with DHA shown that the wound closure percent were 34.07, 27.2, 11.27, 7.98 respectively. The recent study shown that the higher concentration of DHA was related to the less percent wound closure when the time changing from 24 to 48 hours.

Discussion

Breast cancer is one of the most common types of cancer in female worldwide. Thus, the development of novel drug to improve patient quality of life is urgently required. DHA is currently used as anti-malarial drug. The anticancer properties of DHA have been studied since its identification. DHA have been demonstrated to induced cell cycle arrest or apoptosis in various tumor cell types such as pancreatic cancer (7). However, the effect of DHA in ER positive breast cancer has not been studied. Our recent study observed that DHA had anti-proliferation effect on ER-positive breast cancer cells (MCF-7) and tamoxifen resistant breast cells (MCF-7/LCC-2) by reducing the percentage of cell viability after the treatment with DHA in various concentrations for 48 hours. DHA can inhibit cell proliferation of MCF-7 cell lines in time and dose dependent manner. Due to the characteristic of MCF-7 cells which are non-invasive, we tested ability of DHA in the inhibition of migration only in more invasive MCF-7/LCC-2 cells. As the drug concentration gradually increased, the migration distance of MCF-7/LCC-2 cells was shortened, indicating the gradual decrease in the migration ability of MCF-7/LCC-2 cells. Thus, DHA can inhibit cell migration in MCF-7/LCC-2.However, this method was used for screening the effect of DHA in migration process and the result of this study may result from proliferation process of the cells. Invasion assay and the expression of genes involved in cell invasion should be performed to confirm this effect.

Figure 2. Effect of DHA on cell migration in tamoxifen resistant breast cancer cells (MCF-7/LCC-2). (2A) Graph showed the percentage of wound closure. (2B) digital image of MCF-7/LCC-2 cells after treated with DHA at 0-40 µM for 24 and 48 hours by scratch assay. Each value represented the mean ± S.E.M. (n=3). *p<0.05. Data are the representative of three independent experiments.

Conclusion

The results of the present study demonstrated that DHA is able to inhibit cell proliferation in dose dependent manner with IC50 in micromolar range and has inhibitory effect on cell migration. Thus, this study was a preliminary data to support the effects of DHA as anticancer agents for ER positive and tamoxifen resistant breast cancer cells. However, further experiments to investigate in molecular mechanisms are needed to explain the effect of DHA in order to use for the treatment of advance stage ER positive and tamoxifen resistant breast cancer patients.

Acknowledgements

References

1. Chaiwerawattana A. Breast cancer. Cancer in Thailand 2010;4:48.
2. Anderson W.F, Chatterjee N, Ershler W.B, Brawley O.W. Estrogen receptor breast cancer phenotypes in the Surveillance. Epidemiology and End Results database Breast Cancer Research 2002;76:27–36.
3. Yang JJ, Park SK, Cho LY, Han W, Park B, Kim H, et al. Cost-effectiveness analysis of 5 years of postoperative adjuvant tamoxifen therapy for Korean women with breast cancer retrospective cohort study of the Korean Breast Cancer Society Database. Clinical Therapeutics 2010;32:1122–1138.
4. Brauch H, Jordan VC. Targeting of tamoxifen to enhance antitumour action for the treatment and prevention of breast cancer: the ''personalised'' approach. European Journal of Cancer 2009;45:2274–83.
5. Ring A, Dowsett M. Mechanisms of tamoxifen resistance. Endocrine-Related Cancer 2004;11:643–658.
6. Shuqun Z, Yinan M, Jiantao J, Zhijun D, Xiaoyan G, Xiaoran Y, Wentao X and Weili M. Inhibition of urokinase-type plasminogen activator expression by dihydroartemisinin in breast cancer cells. Oncology letter 2014;7:1375-1308.
7. Chen H, Sun B, Pan S, Jiang H, Sun X. Dihydroartemisinin inhibits growth of pancreatic cancer cells In vitro and In vivo. Anti-Cancer Drugs 2009;20:131–140.
8. Moore C, Lai H, Li R, Ren L, McDougall A, Singh N, Chou K. Oral administration of dihydroartemisinin and ferrous sulfate retarded implanted fibrosarcoma growth in the rat. Cancer Letter 1995;98:83–87.
9. Sas L, Lardon F, Vermeulen P, Hauspy J, Van P, Pauwels P, Dirix L, van Laere S. The interaction between ER and NFκB in resistance to endocrine therapy. Breast Cancer Res. 2012;14:212.

10. Yong H, Hyo Y, Hyung K, Eun H, Gye L, Hye J. Suppression of PMA-induced tumor cell invasion by dihydroartemisinin via inhibition of PKCa/Raf/MAPKs and NF-kB/AP-1-dependent mechanisms. Biochemical pharmacology 2010;79:1714–1726.
11. Huan-Huan C, Hui-Jun Z, Xin F. Inhibition of human cancer cell line growth and human umbilical vein endothelial cell angiogenesis by artemisinin derivatives in vitro. Pharmacological Research 2003;48:231–236.

RESEARCH ARTICLE

Inhaled nebulized nitrite decreases platelet activity in healthy volunteers

Tipparat Parakaw[1,2], Kran Suknuntha[1], Pornpun Vivithanaporn[1], Supeenun Unchern[1], Nathawut Sibmooh[1], Sirada Srihirun[2]*

1Department of Pharmacology, Faculty of Science, Mahidol University, Bangkok, Thailand, 10400
2Department of Pharmacology, Faculty of Dentistry, Mahidol University, Bangkok, Thailand, 10400

Address correspondence and reprint request to: Sirada Srihirun Department of Pharmacology, Faculty of Dentistry, Mahidol University
E-mail address: Sirada.srh@mahidol.ac.th.

Abstract

Nitrite, a nitric oxide (NO) metabolite, inhibits platelet activation through its conversion to NO. In this study, we investigated the effect of inhaled nebulized nitrite on human platelets *ex vivo*. Seven healthy volunteers were administered 37.5-mg sodium nitrite by inhaled nebulization. Levels of platelet activation before and immediately after inhalation were measured by aggregometry and flow cytometry using P-selectin, and activated glycoprotein aGPIIb/IIIa expression in response to adenosine 5' diphosphate (ADP) and U46619, a thromboxane A_2 (TXA_2) agonist. After nebulization, the nitrite level in whole blood increased from 0.15 ± 0.03 to 1.7 ± 0.23 μM. Nitrite decreased platelet aggregation and P-selectin expression induced by ADP. However, nitrite had no effect on ADP-induced aGPIIb/IIIa expression and U46619 induced P-selectin and aGPIIb/IIIa expression. In conclusion, inhaled nitrite decreases platelet activation, and may have potential to use in patients with platelet hyperactivation.

Keywords: Platelet, nitrite, nitric oxide, inhalation.

Introduction

Nitric oxide (NO) is an endogenous vasodilator and platelet inhibitor[1,2]. In circulation, NO is constitutively synthesized by endothelial nitric oxide synthase (eNOS). In platelets, NO increases cGMP, which further causes deactivation of glycoprotein IIb/IIIa (GPIIb/IIIa) receptors and P-selectin expression on platelet surface leading to platelet inhibition[3]. NO is also generated from nitrite anion (NO_2^-) by reductase activity of heme-containing proteins such as deoxyhemoglobin[4]. Because NO is unstable, nitrite which is a more stable metabolite of NO, has been investigated for an alternative treatment. Our previous *in vitro* study demonstrated the antiplatelet activity of nitrite in the presence of erythrocytes under hypoxic condition[5].

Nitrite inhalation has been entered phase II trial for treatment of pulmonary hypertension[6]. In phase I clinical trial, nitrite reached peak concentration time (T_{max}) immediately after inhalation and had half-life ($t_{1/2}$) of 35 minutes[7]. The maximum tolerated

dose was 90 mg. The major adverse effect was transient asymptomatic orthostasis and no serious adverse effect was reported.

In this study, we aimed to determine the effect of inhaled sodium nitrite *ex vivo* at dose of 37.5 mg (almost half of maximum tolerated dose) on platelet activity in healthy subjects. The levels of platelet activation before and after nitrite inhalation were measured by aggregometry and flow cytometry.

Materials and Methods

Sodium nitrite ($NaNO_2$) nebulizer was prepared by Faculty of Pharmaceutical Science, Chulalongkorn University. Sodium nitrite was administrated to volunteers by Beurer Inhalator Nebuliser IH25/1 model (Exeter, NH, USA). Adenosine 5' diphosphate (ADP) was purchased from Sigma (St Louis, MO, USA). U46619 were purchased from Calbiochem (Billerica, MA, USA). Sodium nitrite, ADP and U46619 were dissolved in PBS pH 7.4.

Monoclonal antibodies: Fluorescein isothiocyanate (FITC)-labeled anti-human PAC-1, Phycoerythrin (PE)-labeled anti-human CD62P and Phycoerythrin cyanine5 (PEcy5)-labeled anti-human CD42b were purchased from BD bioscience (San Jose, CA, USA).

Subjects

This study was approved by Ramathibodi Hospital Ethics Committee (ID 03-56-27). Seven healthy volunteers with 31.7±1.6 years of age who signed informed consent enrolled in the study. Subjects who had history of smoking, heart disease, hemoglobinopathy, platelet function disorders, asthma, or COPD were excluded from this study.

Blood sample collection

The venous blood was collected using 3.8% sodium citrate as an anti-coagulant. Whole blood was 2-fold diluted with phosphate buffer saline (PBS) for platelet aggregation measured by an aggregometer (Chronolog, Havertown, PA, USA). Whole blood was 10-fold diluted with PBS for measurement of platelet surface markers by FC500 flow cytometer (Cytomics FC 500, Beckman coulter, Brea, CA, USA). For measurement of nitrite in blood, the whole blood was mixed immediately with the nitrite-stabilizing solution containing 0.8 M potassium hexacyanoferrate (III), 10 mM N-ethylmaleimide (NEM), and 5% nonidet P-40 (NP40) dissolved in nitrite-free deionized water. The preserved samples were stored at -80 °C and the measurement was done within 2 weeks.

The effect of inhaled nitrite on platelet aggregation

Citrated (3.8%) whole blood was collected before 37.5-mg nitrite inhalation (baseline measurement) and immediately after inhalation. Platelet aggregation induced by 20 μM ADP was measured for 6 minutes by impedance aggregometry.

The effect of inhaled nitrite on expression of platelet surface markers

Diluted whole blood was incubated with PEcy5-labeled CD42b, FITC-labeled PAC-1 and PE-labeled CD62P and platelet agonists either ADP (20 μM) or U46619 (20 μM) for 10 minutes at room temperature. Then, samples were fixed with 1% paraformaldehyde and kept at 4 °C. The platelet population was identified by light scatter and anti-CD42b antibody. Percentage of platelets positively expressed P-selectin and aGPIIb/IIIa were calculated from 10,000 events positive for CD42b.

Measurement of nitrite in blood

The nitrite levels in whole blood were measured by tri-iodide based chemiluminescence assay. Whole blood samples were mixed with methanol and centrifuged at 14,000 g for 5 minutes. Supernatant was injected into a purge vessel containing tri-iodide solution and the nitrite levels were measured by a chemiluminescence NO analyzer (Eco medics CLD88, Duernten, Switzerland).

Statistical analysis

Data processing and statistical analysis were analyzed by GraphPad Prism® version 4 (GraphPad software Inc., San Diego, CA, USA). Data represents mean ± SEM. Wilcoxon matched-pairs signed rank test was used to compare with acceptable *P*-value < 0.05.

Results

Whole blood nitrite

Whole blood samples from healthy volunteers were collected before and immediately after nitrite inhalation. The levels of nitrite were determined by chemiluminescence NO analyzer. After inhalation of 37.5-mg nitrite, whole blood nitrite levels increased from 0.15 ± 0.03 to 1.70 ± 0.23 μM. (figure 1).
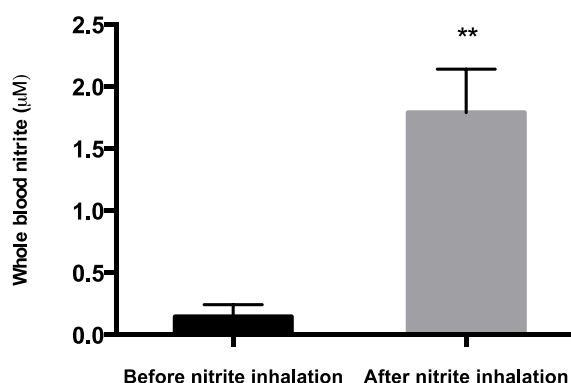
Figure 1: Nitrite levels in whole blood before and immediately after inhalation. Whole blood was collected in nitrite-stabilizing solution before and after inhalation. Tri-iodide based chemiluminescence was used to measure the level of nitrite in whole blood. Data are mean ± SEM (n=7). *P*-value < 0.05 (Mann-Whitney test)

The effect of inhaled nitrite on platelet aggregation

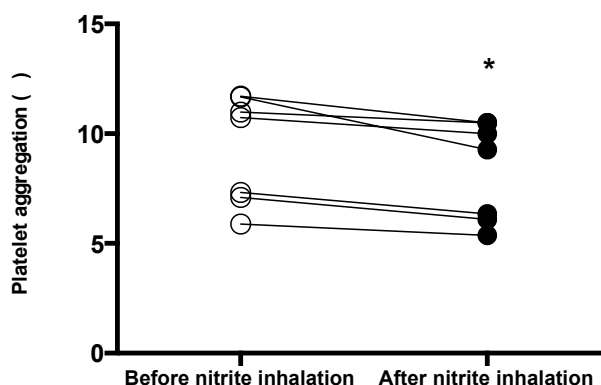The levels of platelet aggregation before and after inhalation were measured *ex vivo* by impedance aggregometry. After nitrite inhalation, platelet aggregation induced by ADP decreased significantly ($P = 0.02$ by Wilcoxon matched-pairs signed rank test). Platelet aggregation decreased from 10.73 (7.10 to 11.67) to 9.27 (6.10 to 10.49) ohm; median (interquartile range) (figure 2).

The effect of inhaled nitrite on P-selectin and aGPIIb/IIIa expression

P-selectin and aGPIIb/IIIa expression before and after inhalation was induced by 20 μM ADP and U46619, and determined by flow cytometry. After inhalation, P-selectin expression induced by ADP significantly decreased ($P = 0.02$ by Wilcoxon matched-pairs signed rank test). The percentage of ADP-induced P-selectin expression before and after nitrite inhalation was 30.65 (17.68-39.40) and 24.63 (17.17-37.80), respectively; median (interquartile range) (figure 3A). However, inhalation of nitrite had no effect on ADP-induced aGPIIb/IIIa expression and U46619-induced P-selectin and aGPIIb/IIIa expression (figure 3B-D).

Figure 2: The effect of inhaled nitrite on platelet aggregation induced by ADP. Whole blood samples were collected before (baseline) and after nitrite inhalation. Platelet aggregation in whole blood was induced by 20 μM ADP and measured by impedance aggregometry. *$P < 0.05$ tested by Wilcoxon matched-pairs signed rank test (n = 7).

Discussion

Our results demonstrated the inhibitory effect of inhaled nitrite on platelet activity *ex vivo*. The aggregometry showed that inhaled nitrite reduced platelet aggregation induced by ADP. In addition, the expression of P-selectin induced by ADP decreased after nitrite inhalation. However, the expressions of aGPIIb/IIIa induced by ADP, P-selectin and aGPIIb/IIIa induced by U46619 were not changed.

Inhalation of 37.5-mg nitrite increased whole blood nitrite to the maximum concentration of 1.7 μM, which was lower than the level reported elsewhere (estimated plasma nitrite of 4.5 uM at the same dose)[7]. This may result from the efficiency of nebulizer. However, the plasma nitrite of 0.4-0.6 μM was shown to decrease platelet activation[8].
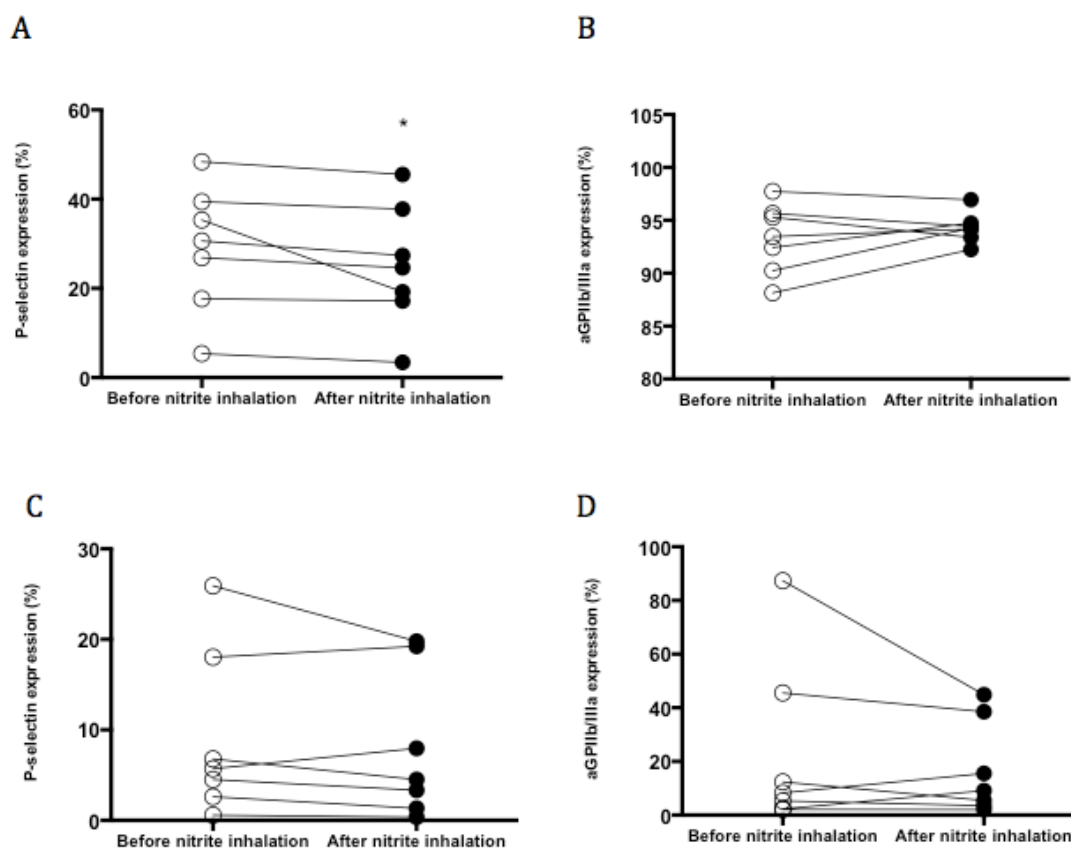
Figure 3: The effect of inhaled nitrite on P-selectin and aGPIIb/IIIa expression. Platelets in 10-fold diluted whole blood samples were stimulated by 20 μM ADP or U46619. ADP-induced P-selectin expression (A), ADP-induced aGPIIb/IIIa expression (B), U46619-induced P-selectin expression, (C) and U46619-induced aGPIIb/IIIa expression (D) were measured by flow cytometry. *$P < 0.05$ tested by Wilcoxon matched-pairs signed rank test (n = 7).

Our *ex vivo* study demonstrated that nitrite inhalation decreased ADP-induced platelet aggregation and P-selectin expression, which is consistent with the previous *in vitro* anti-platelet effect of nitrite reported by our group[5,9]. On the contrary, inhaled nitrite could not inhibit ADP-induced aGPIIb/IIIa expression. Our results showed that ADP induced almost 100% of aGPIIb/IIIa expression. It is possible that the nitrite level in this study may not be enough to inhibit the effect of ADP on aGPIIb/IIIa expression. An *ex vivo* study showed that 65 μg/ml aspirin has less inhibitory effect on the expression of aGPIIb/IIIa than the inhibitory effect on the expression of P-selectin (36.5% versus 81%)[10]. Therefore, aGPIIb/IIIa expression may be more difficult to inhibit than P-selectin. However, inhaled nitrite had no effect on

U46619-induced P-selectin and aGPIIb/IIIa expression with unknown reason. Therefore, these results should be further confirmed in larger number of subjects.

The anti-platelet effect of nitrite may arise from nitrite reduction to NO. Heme-containing proteins such as deoxyhemoglobin may be responsible for nitrite reduction to NO[11]. cGMP, a marker of NO, in platelets increased after incubation with nitrite *in vitro*[12]. Therefore, the anti-platelet mechanism of inhaled nitrite *ex vivo* needs further investigation.

Conclusion

Inhaled nitrite decreases platelet aggregation and P-selectin expression induced by ADP *ex vivo*. The results support the idea that inhaled nitrite may have potential benefit for treat patients with platelet hyperaggregation. However, the effect of inhaled nitrite on platelets needs further studies in a larger group of population.

Acknowledgements

References

1. Samama CM, Diaby M, Fellahi JL, Mdhafar A, Eyraud D, Arock M, et al. Inhibition of platelet aggregation by inhaled nitric oxide in patients with acute respiratory distress syndrome. Anesthesiology. 1995;83(1):56-65.
2. George TN, Johnson KJ, Bates JN, Segar JL. The effect of inhaled nitric oxide therapy on bleeding time and platelet aggregation in neonates. The Journal of pediatrics. 1998;132(4):731-4.
3. Irwin C, Roberts W, Naseem KM. Nitric oxide inhibits platelet adhesion to collagen through cGMP-dependent and independent mechanisms: the potential role for S-nitrosylation. Platelets. 2009;20(7):478-86.
4. Kim-Shapiro DB, Gladwin MT. Mechanisms of nitrite bioactivation. Nitric oxide : biology and chemistry / official journal of the Nitric Oxide Society. 2014;38:58-68.
5. Srihirun S, Sriwantana T, Unchern S, Kittikool D, Noulsri E, Pattanapanyasat K, et al. Platelet inhibition by nitrite is dependent on erythrocytes and deoxygenation. PloS one. 2012;7(1):e30380.
6. A service of the U.S. National Institute of Health [internet}. 2015 [cited 2015 July 26]. Available from: http://clinicaltrails.gov
7. Rix PJ, Vick A, Attkins NJ, Barker GE, Bott AW, Alcorn H, Jr., et al. Pharmacokinetics, pharmacodynamics, safety, and tolerability of nebulized sodium nitrite (AIR001) following repeat-dose inhalation in healthy subjects. Clinical pharmacokinetics. 2015;54(3):261-72.

8. Webb AJ, Patel N, Loukogeorgakis S, Okorie M, Aboud Z, Misra S, et al. Acute blood pressure lowering, vasoprotective and anti-platelet properties of dietary nitrate via bioconversion to nitrite. Hypertension. 2008;51(3):784-90

9. Akrawinthawong K, Park JW, Piknova B, Sibmooh N, Fucharoen S, Schechter AN. A Flow Cytometric Analysis of the Inhibition of Platelet Reactivity Due to Nitrite Reduction by Deoxygenated Erythrocytes. PloS one. 2014;9(3)

10. Le Guyader A, Pacheco G, Seaver N, Davis-Gorman G, Copeland J, McDonagh PF. Inhibition of platelet GPIIb-IIIa and P-selectin expression by aspirin is impaired by stress hyperglycemia. Journal of diabetes and its complications. 2009;23(1):65-70.

11. Kim-Shapiro DB, Gladwin MT. Mechanisms of nitrite bioactivation. Nitric oxide : biology and chemistry / official journal of the Nitric Oxide Society. 2014;38:58-68.

12. Borgognone A, Loka T, Chimen M, Rainger E, Feelisch M, Watson S, et al. Nitrite is a cGMP generator in isolated platelets. BMC Pharmacology and Toxicology. 2015;16(Suppl 1):A65.

RESEARCH ARTICLE

Low-density lipoprotein oxidation in subjects with chronic cadmium exposure

Pornthip Tomuang[1], Thanaporn Sriwantana[2], Witaya Swaddiwudhipong[3], Sirada Srihirun[4], Pornpun Vivithanaporn[2], Supeenun Unchern[2], Nathawut Sibmooh[2,*]

[1]*Toxicology Program, Faculty of Science, Mahidol University, Bangkok 10400, Thailand*
[2]*Department of Pharmacology, Faculty of Science, Mahidol University, Bangkok 10400, Thailand*
[3]*Department of Community and Social Medicine, Mea Sot Hospital, Tak Province 63100, Thailand*
[4]*Department of Pharmacology, Faculty of Dentistry, Mahidol University, Bangkok 10400, Thailand*

Correspondence: Nathawut Sibmooh, Department of Pharmacology Faculty of Science, Mahidol University, Rama 6 Road, Bangkok 10400, Thailand.
E-mail: Nathawut.sib@mahidol.ac.th

Abstract

Cadmium exposure has been reported to be associated with cardiovascular disorders. In this study, we aimed to investigate the low-density lipoprotein (LDL) oxidation in subjects with high-level cadmium exposure. LDL was separated from plasma of cadmium-exposed subjects who lived in Mae Sot District, Tak Province, Thailand. The concentrations of protein, cholesterol, and lipid peroxidation markers (thiobarbituric acid reactive substances, TBARs; conjugated diene, CD; and lipid hydroperoxide, LOOH) were measured in LDL. Cadmium-exposed subjects had higher levels of total cholesterol, LDL cholesterol and triglycerides than non-exposed subjects. The levels of cholesterol, CD, LOOH, and TBARs were elevated in LDL of cadmium-exposed subjects. The ratio of CD/cholesterol and TBARs/cholesterol also increased in cadmium group when compared with non-exposed group. The levels of protein and LOOH/cholesterol ratio were not different between cadmium and control groups. We conclude that subjects with chronic cadmium exposure have pro-atherosclerotic lipid profile, and increased LDL oxidation.

Keywords: Cadmium, Cardiovascular disease, Lipid peroxidation, LDL oxidation

Introduction

Cadmium is an environmental pollutant found in the northwestern part of Thailand. Cadmium ore is found as refining zinc by-product from zinc mine [1, 2]. Cadmium has long half-life, approximately 30 years, in human. Chronic low-level cadmium exposure is reported in general population [3], which may be due to cigarette smoking and ingestion of contaminated food. The low-level exposure as demonstrated by urinary or plasma cadmium levels is related with hypertension and abnormal lipid profile[4]. In this study, we investigated LDL oxidation by measurement of TBARs, CD and LOOH in subjects with chronic cadmium exposure. Cadmium exposure causes an increase in plasma lipid peroxidation (TBARs)[5]. In population

with low-level cadmium exposure (geometric mean of blood cadmium of 1.16 µg/L), blood cadmium correlates with triglyceride and triglyceride/HDL-cholesterol ratio[6]. However, the LDL oxidation in subjects with high-level chronic cadmium exposure has never been reported. Because oxidized LDL plays important role in the development of atherosclerosis, increased oxidized LDL may be a marker of atherosclerosis in cadmium-exposed subjects.

Materials and Methods

Subjects and clinical parameters

This study has been approved by the Ramathibodi Hospital Ethics Committee (ID 05-54-20). Cadmium in whole blood and urine was measured by atomic absorption spectrophotometry (AAnalysis 600, PerkinElmer, Waltham, MA, USA). Baseline clinical parameters were determined at laboratory of Ramathibodi Hospital. The subjects participated in the study were classified into control non-exposed and cadmium-exposed groups. The control group (healthy volunteers) consisted of 10 females with 40-55 years of age (mean ± SEM = 48.0 ± 2.2 years). The cadmium-exposed group consisted of 10 females with 40-55 years of age (mean ± SEM = 50.6 ± 2.7 years). Inclusion criteria for healthy volunteers were urinary cadmium levels < 1 µg/g creatinine. Inclusion criteria for cadmium exposures were urinary cadmium levels ≥ 1 µg/g creatinine. Both healthy and cadmium-exposed volunteers agreed to participate in the study and signed an informed consent form. The cadmium-exposed and healthy volunteers who had history of hypertension, heart failure, ischemic heart diseases, COPD, diabetes mellitus, thyroid disease, chronic liver disease, cigarette smoking, chronic alcohol consumption, addictive substance and pregnancy were excluded from the study.

Blood collection and plasma preparation

Blood was collected by using EDTA (1.5 mg/mL) as anticoagulant after 12 h of fasting. Plasma was separated by centrifugation (Kubota 5900 centrifuge with swinging bucket rotor) at 3,500 rpm for 15 minutes at 4ºC, and then stored at -80ºC.

Lipoprotein Separation

Plasma lipoproteins were separated by sequential density gradient using ultracentrifugation (OptimaTM L-100xp with Ti 90 rotor, Beckman Coulter, Fullerton, California, USA) at 548,000g, 4 ºC. The plasma was adjusted to desired density by Mork's salt solution and Stock's solution. LDL was obtained at density between 1.019–1.063 g/mL[7]. The separated lipoprotein was dialyzed against 10 mM phosphate buffer saline (PBS), pH 7.4 to remove EDTA and salts from the density solutions. Plasma lipoprotein was packed in dialysis membrane and dialyzed in PBS with continuous stirring at 4ºC overnight. The dialyzed plasma lipoprotein was collected and stored at -80ºC.

Lipoprotein composition

The composition of LDL was determined by following methods: protein by modified Lowry's method[8] and total cholesterol by cholesterol enzymatic kit (Cholesterol LiquiColor, Stanbio, Boerne, TX, USA).

Lipid Peroxidation

Conjugated diene (CD) is a marker of initial-phase lipid peroxidation. CD was measured in 100 μg protein/mL of LDL. The optical density (OD) at 234 nm was measured immediately using spectrophotometry (GBCCintra 10e UV-Vis spectrometers)[9]. The amount of CD was calculated using molar extinction coefficient ($\varepsilon 234 = 29{,}500$ M^{-1}. cm^{-1})[10].

Lipid hydroperoxide (LOOH) is a marker of propagation-phase lipid peroxidation. LOOH levels reacted with ferricthiocyanate reagent for 30 min in 100 μg protein/mL of lipoprotein suspension, and were measured at $OD_{500\ nm}$ using spectrophotometry (GBCCintra 10e UV-Vis spectrometers)[11]. H_2O_2 was used as standard.

TBARs are markers of final-phase lipid peroxidation. TBARs were measured by spectrofluorometric method (LS 55, Fluorescence spectrometer, PerkinElmer, Boston, Massachusetts, USA)[12].

Statistical Analysis

Statistical analysis was performed by Graphpad Prism, version 5.0 (GraphPad Software Inc., San Diego, CA, USA) using Student t-test or Mann Whitney U-test, depending on the normality of distribution. Significance for all analyses were assumed at *$P<0.05$*.

Results

Background characteristics of subjects

Cadmium-exposed subjects had higher levels of total cholesterol, LDL-cholesterol, triglyceride, serum creatinine, blood cadmium and urinary cadmium than control non-exposed subjects (unpaired t-test *$P < 0.05$*) (table 1). On the other hand, BMI and HDL-cholesterol were lower in cadmium-exposed than non-exposed subjects. There was no difference in age, blood pressure, hematocrit, hemoglobin, red blood cell count, white blood cell count, platelet count, and urinary β2-microglobulin between cadmium and control groups.

Cholesterol and protein content in LDL

The cholesterol content in LDL of cadmium-exposed subjects was significantly higher than LDL of control group (*$P < 0.05$*) (Fig. 1a). No difference in protein content between cadmium group and control group was observed (Fig. 1b).

Lipid peroxidation

Lipid peroxidation makers including CD, LOOH and TBARs showed the increased levels in LDL of cadmium-exposed subjects compared with control non-exposed subjects (*$P < 0.05$*) (Fig. 2a-2c). The CD/cholesterol ratio and TBARs/cholesterol ratio increased in cadmium-exposed subjects compared with those of control group (*$P < 0.05$*) (Fig. 2d, 2f). No difference in LOOH/cholesterol ratio was noted (Fig. 2e).

Table 1. Background characteristics of subjects

Parameters	Non-exposed	Cadmium-exposed	*P*-value
N	10	10	
Gender (F)	10	10	
Age (years)	48.00 ± 2.23	50.60 ± 2.66	0.4635
BMI (kg/m^2)	29.33 ± 1.65	23.85 ± 1.16	0.0144*
Systolic blood pressure (mmHg)	130.10 ± 4.46	119.6 ± 4.20	0.1038
Diatolic blood pressure (mmHg)	75.90 ± 2.95	76.60 ± 2.27	0.8531
Mean blood pressure (mmHg)	112.00 ± 3.53	105.30 ± 3.34	0.1813
Hematocrit (%)	37.47 ± 1.26	39.22 ± 0.78	0.2533
Hemoglobin (g/dL)	12.24 ± 0.42	12.94 ± 0.30	0.1936
Red blood cells (10^6/µL)	4.754 ± 0.16	4.44 ± 0.12	0.1374
White blood cells (10^3/µL)	6.73 ± 0.32	7.28 ± 0.38	0.0815
Platelets (10^3/µL)	238.80 ± 26.94	270.60 ± 18.69	0.345
Total cholesterol (mg/dL)	170.50 ± 11.64	220.90 ± 9.71	0.0038*
LDL cholesterol (mg/dL)	95.10 ± 9.44	152.00 ± 8.14	0.0002*
HDL cholesterol (mg/dL)	62.60 ± 5.097	44.10 ± 2.81	0.0052*
Triglyceride (mg/dL)	100.40 ± 11.13	200.80 ± 17.46	0.0001*
Creatinine (mg%)	0.66 ± 0.034	1.03 ± 0.09	0.0008*
BUN (mg%)	11.00 ± 0.68	11.27 ± 0.66	0.7785
Blood cadmium (µg/L)	0.38 ± 0.22	5.46 ± 4.45	0.0001*
Urinary cadmium (µg/g creatinine)	0.76 ± 0.71	5.82 ± 3.80	0.0001*
Urinary β$_2$-microglobulin (µg/g creatinine)	45.91 ± 73.53	95.88 ± 111.60	0.6128

Data are means ± SEM. except blood cadmium, urinary cadmium and urinary β$_2$-microglobulin which are geometric mean ± geometric SD. BMI, body mass index; BUN, Blood urea nitrogen. *$P < 0.05$ (Student's t test)
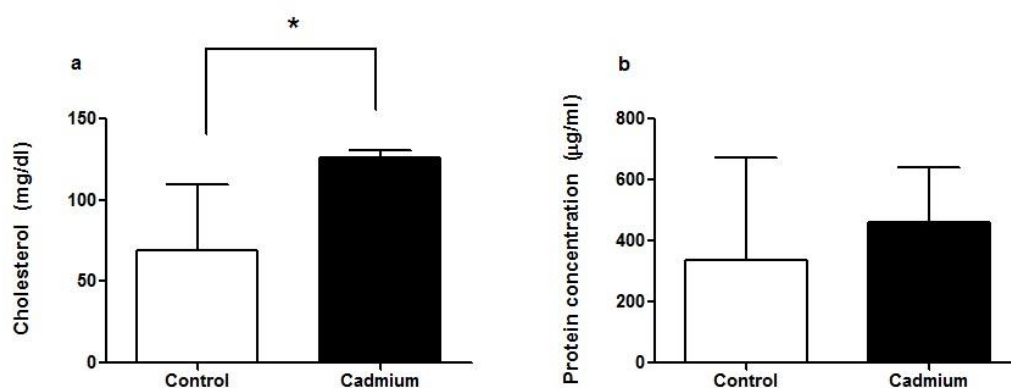
Figure 1. Biochemical composition of LDL obtained from control non-exposed (N = 10) and cadmium-exposed subjects (N = 10). a Total cholesterol (mg/dL). b Protein content (µg/mL). Data are means ± SEM. *$P < 0.05$ (Mann Whitney test).
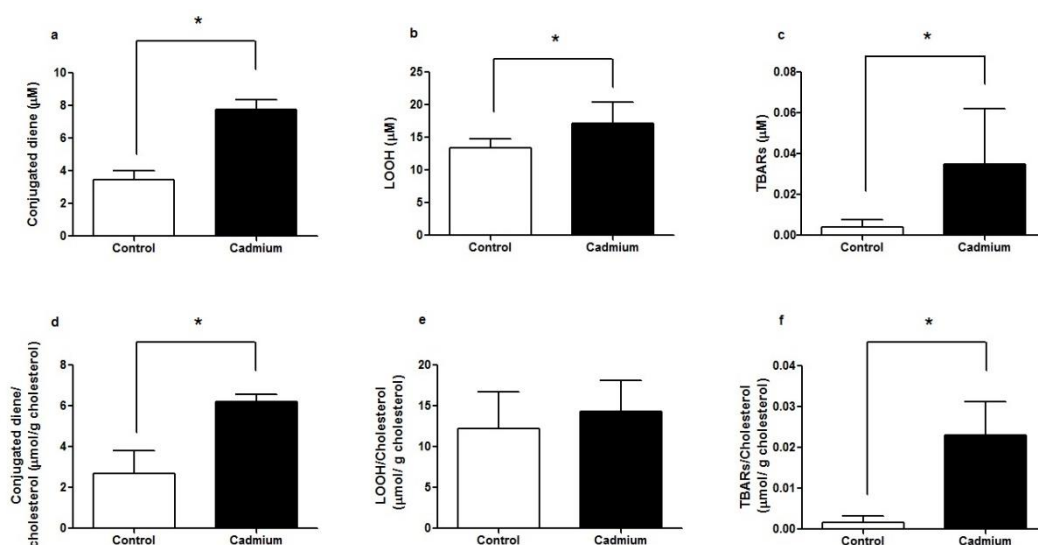
Figure 2. Lipid peroxidation markers in LDL of control non-exposed (N = 10) and cadmium-exposed subjects (N = 10). a Conjugated diene (CD, μM). b Lipid hydroperoxide (LOOH, μM). c Thiobarbituric acid reactive substances (TBARs, μM). d–f Ratio of CD, LOOH, and TBARs to cholesterol (μmol/g cholesterol). Data are means ± SEM. *P<0.05 (Mann Whitney test).

Discussion

Our study demonstrates proatherosclerotic change in lipid profile of cadmium-exposed subjects; namely, increased LDL cholesterol, decreased HDL cholesterol, and increased triglyceride. The cholesterol content and lipid peroxidation markers increased in LDL of subjects with chronic cadmium exposure, indicating an increased LDL oxidation. In population with low-level cadmium exposure, blood cadmium correlates with triglyceride and triglyceride/HDL-cholesterol ratio[6]. We provide further information that subjects with chronic cadmium exposed have elevated LDL oxidation. The abnormal lipid profile together with increased oxidized LDL may be associated with the risk of atherosclerosis and vascular disorders such as coronary artery disease in cadmium-exposed subjects.

In animal study, cadmium affects lipid metabolism causing alterations in the serum lipid components towards proatherosclerosis profile. TBARs, CD, and LOOH were increased in the liver of cadmium-treated rats[13]. These are consistent with our human data showing that cadmium-exposed subjects have proatherosclerotic lipid profile and increased oxidized LDL, which are risks of atherosclerosis.

Conclusion

Here, we show that subjects with chronic cadmium exposure have proatherosclerotic plasma lipid profile and elevated oxidized LDL.

Acknowledgements

References

1. Jarup L. Cadmium overload and toxicity. Nephrol Dial Transplant. 2002;17 Suppl 2:35-9.
2. Satarug S, Baker JR, Urbenjapol S, Haswell-Elkins M, Reilly PE, Williams DJ, et al. A global perspective on cadmium pollution and toxicity in non-occupationally exposed population. Toxicol Lett. 2003;137(1-2):65-83.
3. Jarup L, Berglund M, Elinder CG, Nordberg G, Vahter M. Health effects of cadmium exposure--a review of the literature and a risk estimate. Scand J Work Environ Health. 1998;24 Suppl 1:1-51.
4. Messner B, Bernhard D. Cadmium and cardiovascular diseases: cell biology, pathophysiology, and epidemiological relevance. Biometals. 2010;23(5):811-22.
5. Erdogan Z, Erdogan S, Celik S, Unlu A. Effects of ascorbic acid on cadmium-induced oxidative stress and performance of broilers. Biol Trace Elem Res. 2005;104(1):19-32.
6. Kim K. Blood cadmium concentration and lipid profile in Korean adults. Environ Res. 2012;112:225-9.
7. Havel RJ, Eder HA, Bragdon JH. The distribution and chemical composition of ultracentrifugally separated lipoproteins in human serum. J Clin Invest. 1955;34(9):1345-53.
8. Markwell MA, Haas SM, Bieber LL, Tolbert NE. A modification of the Lowry procedure to simplify protein determination in membrane and lipoprotein samples. Anal Biochem. 1978;87(1):206-10.
9. Esterbauer H, Striegl G, Puhl H, Rotheneder M. Continuous monitoring of in vitro oxidation of human low density lipoprotein. Free Radic Res Commun. 1989;6(1):67-75.
10. Kleinveld HA, Hak-Lemmers HL, Stalenhoef AF, Demacker PN. Improved measurement of low-density-lipoprotein susceptibility to copper-induced oxidation: application of a short procedure for isolating low-density lipoprotein. Clin Chem. 1992;38(10):2066-72.
11. Mihaljevic B, Katusin-Razem B, Razem D. The reevaluation of the ferric thiocyanate assay for lipid hydroperoxides with special considerations of the mechanistic aspects of the response. Free Radic Biol Med. 1996;21(1):53-63.
12. Kovachich GB, Mishra OP. Lipid peroxidation in rat brain cortical slices as measured by the thiobarbituric acid test. J Neurochem. 1980;35(6):1449-52.
13. Prabu SM, Shagirtha K, Renugadevi J. Amelioration of cadmium-induced oxidative stress, impairment in lipids and plasma lipoproteins by the combined treatment with quercetin and alpha-tocopherol in rats. J Food Sci. 2010;75(7):T132-40.

RESEARCH ARTICLE

Increased nitric oxide levels in human breast cancer tissue

Nannapat Phiewphong[1], Ronnarat Suvikapakornkul[2], Piyadon Sathavorasmith[3], Pornpun Vivithanaporn[4], Nathawut Sibmooh[4,*]

[1]*Toxicology graduate program in multidisciplinary, Faculty of Science, Mahidol University, Bangkok, Thailand, 10400*
[2]*Department of Surgery, Faculty of Medicine Ramathibodi Hospital, Mahidol University, Bangkok, Thailand, 10400*
[3]*Thalassemia research center, Institute of molecular biosciences, Mahidol University, Nakhon Phathom, Thailand, 73170*
[4]*Department of Pharmacology, Faculty of Science, Mahidol University, Bangkok, Thailand, 10400*

Address correspondence and reprint request to: Nathawut Sibmooh, Department of Pharmacology, Faculty of Science, Mahidol University.
E-mail address: Nathawut.sib@mahidol.ac.th

Abstract

Several *in vivo* and *in vitro* studies show increased nitric oxide (NO) level in breast cancer together with elevated level of nitric oxide synthase (NOS) activity. In this study, we aimed to investigate the level of nitrite, a bioactive metabolite of NO, using chemiluminescence method, and determine the expression levels of endothelial NOS (eNOS) and inducible NOS (iNOS) using real-time PCR in control and breast cancer tissues obtained from 15 patients. We found that the nitrite levels increased in breast cancer tissues compared with control tissues. The expression of eNOS mRNA was higher in breast cancer tissues while iNOS expression was not different between two groups. In conclusion, breast cancer tissues have increased NO levels associated with increased eNOS expression. NO could be used as a biomarker of breast cancer and inhibition of NO synthesis may be a therapeutic strategy.

Keywords: Breast cancer, nitric oxide, nitrite, nitric oxide synthase.

Introduction

Breast cancer is the common cancer with high incidence rate in women worldwide in both developed and developing countries[1]. NO has been documented as a key signaling molecule that promotes breast carcinogenesis[2]. In breast cancer, NO may be synthesized by eNOS in endothelial cells or iNOS in inflammatory cells. The increased expression of NOS has been found in human breast cancer tissues[3] and in breast cancer cell lines[4]. Increased eNOS and iNOS activities have been reported in breast cancer tissues from patients[5]. Interestingly, high NOS activity is associated with high tumor grade[5]. All these findings suggest that increased NO and NOS expression may involve in carcinogenesis of breast cancer. However, NO concentration in breast cancer tissues derived from patients has never been reported. In this

study, we measured nitrite (a bioactive NO derivative) and NOS expression in breast cancer tissues.

Materials and Methods

Breast tissues

This study has been approved by the Ramathibodi Hospital Ethics Committee. Fifteen human breast tissues were obtained from the Department of Surgery, Faculty of Medicine Ramathibodi Hospital, Mahidol University, Bangkok, Thailand. Breast cancer and adjacent control tissues were dissected by gross visualization from the same breast.

Tri-iodide based chemiluminescence

Breast tissues were homogenized in the homogenized solution containing nitrite stabilizer (1 mM potassium cyanide, 12 mM potassium ferricyanide, 10 mM N-ethylmaleimide, and 12 μM diethylene triamine pentaacetic acid). Nitrite in 200 μl of homogenated samples was measured by tri-iodide chemiluminescence assay using analyzer CLD 88 (ECO medics, Durnten, Switzerland)[6,7]. Each data point is represented as average of duplicate measurement.

Real-time PCR

Total RNA was extracted from homogenated sample using total RNA purification kit (Jena Bioscience, Jena, Germany). 1 μg of total RNA was reversed transcribed using superscript III transcriptase (Invitrogen, Waltham, MA, USA). Gene expression of eNOS and iNOS was quantified by measuring the fluorescence intensity using iTaq[TM] Universal SYBR Green Supermix (Bio-Rad) on an Applied Biosystems real time PCR 7500 system.

Results

Elevated nitrite levels in breast cancer tissues from patients.

The nitrite level was determined by the tri-iodide based chemiluminescence, and reported as nmol per gram of tissue. The median of nitrite level was higher in breast cancer than those in control breast tissues (21.26 vs. 13.59 nmol/g tissue, N = 15) (*P = 0.0020, Wilcoxon test) (Figure 1).

The mRNA expression levels of genes associated with NO synthesis in breast cancer tissues.

To determine whether the increased NO levels were produced by the upregulation of eNOS and/or iNOS, mRNA expression of NOS genes were analyzed in control breast and breast cancer tissues (N = 15 each) by real-time PCR. The eNOS and iNOS mRNA expression was shown as relative fold change (RFC) of NOS mRNA normalized to GAPDH mRNA. The eNOS mRNA expression in breast tissues was significantly higher in breast cancer tissues compared with control breast tissues (*P = 0.0125, Wilcoxon test) (Figure 2). The iNOS

mRNA expression was not different between control and breast cancer tissues ($P = 0.4212$, Wilcoxon test) (Figure 3).
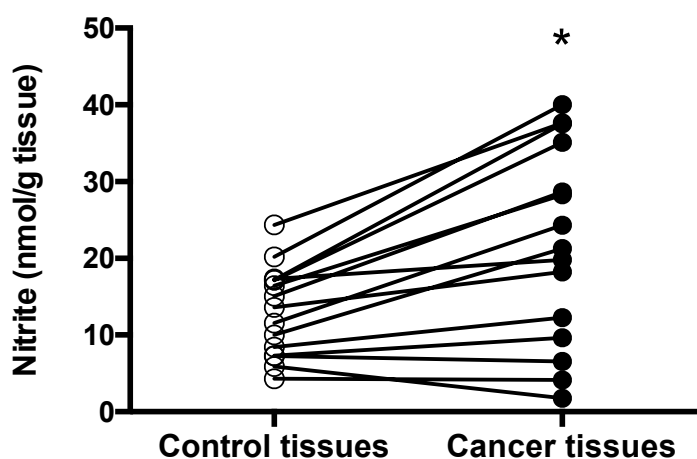
Figure 1. Nitrite levels in control and breast cancer tissues. *$P = 0.0020$ (Wilcoxon test).
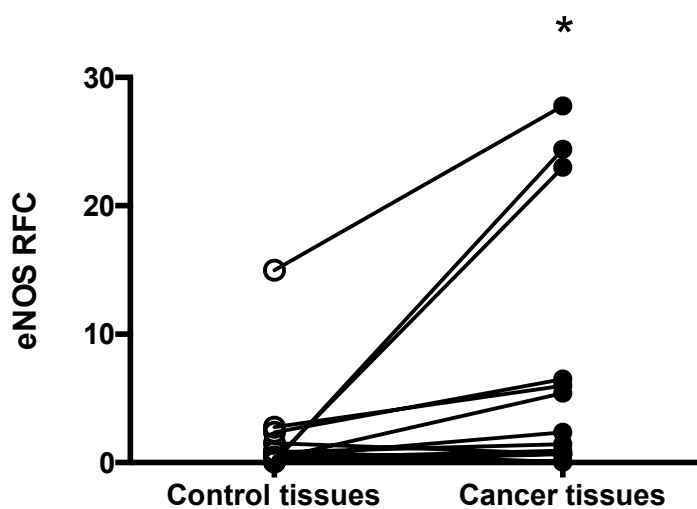
Figure 2. The eNOS mRNA levels in control and breast cancer tissues. The mRNA levels were expressed as relative fold change (RFC) compared with GAPDH. *$P = 0.0125$ (Wilcoxon test).
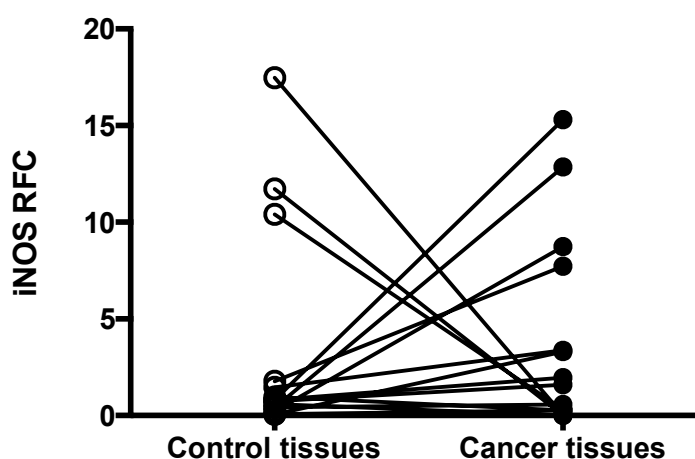
Figure 3. The iNOS mRNA levels in control and breast cancer tissues. The mRNA levels were expressed as relative fold change (RFC) compared with GAPDH. $P = 0.4212$ (Wilcoxon test).

Conclusions and discussion

Breast cancer tissues have higher NO and eNOS expression than control tissues. The high level of nitrite in breast cancer tissues suggests that NO is important for cancer cell growth. From our results, NO is likely produced by eNOS as the eNOS expression increases in breast cancer tissues. The increased eNOS expression in human breast cancer is consistent with previous reports demonstrated by immunocytochemistry[3]. The iNOS expression has a trend toward increase in cancer compared with control tissue although the difference does not reach statistical significance. Thus, more patients are required to confirm these results.

Elevated NO in breast cancer was shown by spin-trapping electron paramagnetic resonance spectroscopy[3]. However, the NO concentration in breast cancer tissues had never been reported. NOS inhibition could reduce the tumor growth in female nude mice injected with GFP-tagged human breast cancer cells[2]. Induction of iNOS expression by components of tumor microenvironment was correlated with increased nitrite[2]. Furthermore, the eNOS expression was found in stromal structures and tumor cells of invasive breast cancer and links to increased vascular density, and high tumor grade and stage[8].

Collectively, our study provides the additional evidences of elevated NO concentration and eNOS expression in human breast cancer tissues. The high NO levels in breast tissues may be used as a prognostic marker, and suggests the novel therapeutic target.

Acknowledgements

References

1. Global Burden of Disease Cancer C. The Global Burden of Cancer 2013. JAMA Oncol. 2015;1(4):505-27.
2. Heinecke JL, Ridnour LA, Cheng RYS, Switzer CH, Lizardo MM, Khanna C, et al. Tumor microenvironment-based feed-forward regulation of NOS2 in breast cancer progression. Proc Natl Acad Sci USA. 2014;111(17):6323-8.
3. Loibl S, von Minckwitz G, Weber S, Sinn H-P, Schini-Kerth VB, Lobysheva I, et al. Expression of endothelial and inducible nitric oxide synthase in benign and malignant lesions of the breast and measurement of nitric oxide using electron paramagnetic resonance spectroscopy. Cancer. 2002;95(6):1191-8.
4. Alagöl H, Erdem E, Sancak B, Turkmen G, Camlibel M, Bugdayci G. Nitric oxide biosynthesis and malondialdehyde levels in advanced breast cancer. Aust N Z J Surg. 1999;69(9):647-650.
5. Thomsen LL, Miles DW, Happerfield L, Bobrow LG, Knowles RG, Moncada S. Nitric oxide synthase activity in human breast cancer. Br J Cancer. 1995;72(1):41-4.
6. Samouilov A, Zweier JL. Development of Chemiluminescence-Based Methods for Specific Quantitation of Nitrosylated Thiols. Anal Biochem. 1998;258(2):322-30.
7. Yang BK, Vivas EX, Reiter CD, Gladwin MT. Methodologies for the sensitive and specific measurement of S-nitrosothiols, iron-nitrosyls, and nitrite in biological samples. Free Radic Res. 2003;37(1):1-10.
8. Vakkala M, Paakko P, Soini Y. eNOS expression is associated with the estrogen and progesterone receptor status in invasive breast carcinoma. Int J Oncol. 2000;17:667-671.

RESEARCH ARTICLE

Fluorescent interference from doxorubicin in flow cytometric analysis of p-glycoprotein expression

Udomsak Udomnilobol[1], Noppadol Sa-Ard-Iam[2], Suree Jianmongkol[1,*]

[1]*Department of Pharmacology and Physiology, Faculty of Pharmaceutical Sciences, Chulalongkorn University, Bangkok 10330, Thailand*
[2]*Immunology Laboratory, Faculty of Dentistry, Chulalongkorn University, Bangkok 10330, Thailand*

Address correspondence and reprint request to: Suree Jianmongkol; Department of Pharmacology and Physiology, Faculty of Pharmaceutical Sciences, Chulalongkorn University, Bangkok 10330, Thailand. Tel.: +66 2 218 8318; Fax: +66 2 218 8324.
E-mail address: Suree.j@pharm.chula.ac.th

Abstract

P-glycoprotein (P-gp) is a drug efflux transporter relevant in both pharmacodymamic and pharmacokinetic aspects. The expression of this transporter can be altered by several drugs and natural substances, which would subsequently affect its function. Doxorubicin-induced P-gp upregulation as determined by flow cytometry with the use of fluorochrome-conjugated antibody (Ab) was reported in a number of studies. As known, this technique reflects the amount of P-gp expression on the cell surface. This study demonstrated the potential misleading data arising from the doxorubicin interference on the fluorescent signal of FITC-labeled P-gp as measured by flow cytometric technique. The Caco-2 cells were treated with doxorubicin for 24 hours. Then, the cells were washed and further incubated in the presence or absence of FITC-conjugated anti-human P-gp Ab for flow cytometric analysis. Our results showed that doxorubicin significantly increased fluorescent intensity in the concentration-dependent manner. The fluorescent signal of the Ab-labeled and unlabeled groups were comparable. These data suggested that doxorubicin interfered with the fluorescent signal of FITC-conjugated P-gp on the cell surface. An increase in the fluorescent signal in the doxorubicin-treated cells resulted from doxorubicin rather than an increase of P-gp expression. Thus, researchers should be aware of the intrinsic fluorescent property of any substances used in the flow cytometric experiment with fluorescent-labeled proteins. If there is a potential for interference on the fluorometric reading, conventional western blot should be chosen to determine protein expression.

Keywords: doxorubicin, FITC, flow cytometry, interference, P-glycoprotein

Introduction

P-glycoprotein (P-gp) is an ATP-binding cassette transporter responsible for limiting cellular uptake of several therapeutic drugs. An overexpression of P-gp at cancer cell

membrane can reduce intracellular accumulation of cytotoxic agents, subsequently leading to chemotherapeutic failure. In addition, alteration of P-gp expression at intestinal cells may change absorption of its drug substrates-such as digoxin.[1] Thus an alteration of P-gp expression can influence drug safety and efficacy. The expression of this transporter can be altered by several drugs and natural substances such as rifampin, doxorubicin, and piperine.[2-4] Therefore, effects of any new compounds on P-gp expression have been subjected for investigation early in drug development process.

Methods for detection of protein expression are fundamental research tools in the life science area. Western blot analysis is a popular procedure involving the uses of gel electrophoresis, protein transfer, and immunoblotting. It is widely used to determine specific cellular proteins. Although this technique is highly sensitive and reliable, it requires several processing steps which are tedious and time-consuming.[5] Recently, flow cytometry has been applied to investigate protein expression with the use of fluorochrome-conjugated antibody (Ab).[3] This method requires only a process to fix the Ab-labeled cells for the measurement of their fluorescent intensity and, therefore, provides better speed and is more convenient. It should be noted that flow cytometry does not involve protein separation. Fluorescent signal generated from common dyes such as fluorescein isothiocyanate (FITC) used in flow cytometry can be interfered by other substances present in the experiment.[6] A number of drugs and natural compounds, particularly those with highly conjugated double bonds or fused aromatic rings can also exhibit fluorescence and cause misinterpretation of the labeled target protein.[7, 8] Hence, analytical methods involving fluorometry should be designed and performed carefully.

Doxorubicin, an anthracycline antibiotic used as an anticancer drug, has been widely used as a P-gp inducer.[3, 9-12] Doxorubicin is known to possess intrinsic fluorescent property with a broad emission spectrum.[13] Flow cytometric analysis of cell surface P-gp expression in doxorubicin-treated cells might therefore be unsuitable due to the interference from doxorubicin-mediated fluorescence. Therefore, this study aimed to examine the potential misleading data arising from the fluorescent interference in flow cytometric determination of cell surface protein. We demonstrated herein an interfering effect of doxorubicin on the fluorescent signal of FITC-labeled P-gp on the surface of Caco-2 cells as measured by flow cytometric technique.

Materials and Methods

Materials

Doxorubicin HCl was purchased from Merck Millipore (Darmstadt, Germany). FITC mouse anti-human P-gp Ab was purchased from BD Biosciences (San Jose, CA, USA). Dulbecco's Modified Eagle's Medium (DMEM) and L-glutamine were purchased from Gibco Life Technologies (Grand Island, NY, USA). Fetal bovine serum was obtained from Biochrom AG (Berlin, Germany). Penicillin G, streptomycin, non-essential amino acids, and paraformaldehyde were purchased from Sigma Aldrich (St. Louis, MO, USA).

Cell culture

The colorectal adenocarcinoma cells (Caco-2, HTB-37™) were obtained from American Type Culture Collection (ATCC, Mannassas, VA, USA). Cells were routinely subcultured at 70% confluence and maintained at 37°C in 5% CO_2-95% air atmosphere in Dulbecco's modified Eagle's medium (DMEM), supplemented with 10% heat-inactivated fetal bovine serum (FBS), 1% non-essential amino acid, 1% penicillin G/streptomycin, and 2 mM L-glutamine.

Flow cytometry

The Caco-2 cells (passage no. 60-65) were seeded onto a 24-well plate at the density of 14,000 cells/cm^2. The cells grew into monolayer and reached its confluency within 5 days after seeding. The culture media was changed every 2 days. The cells at day 20 after seeding were treated with various concentrations of doxorubicin (up to 100 μM) for 24 hours. After treatment, the cells were washed three times and trypsinized with trypsin-EDTA solution at 37°C. The cells were suspended in ice-cold phosphate buffered saline (PBS) and subsequently centrifuged at 5,000 rpm, 4°C for 4 minutes. The cell pellets were divided into Ab-labeled and unlabeled groups. The cells in the first group were resuspended in ice-cold PBS and incubated with FITC-anti-human P-gp Ab in the dark at 4°C for 30 minutes. They were subsequently washed with ice-cold PBS containing 2% FBS, and centrifuged at 5,000 rpm, 4°C for 4 minutes. The cell pellets were fixed with 1% paraformaldehyde in PBS. The cells in the unlabeled group were collected and fixed using similar processes as mentioned above, except that they were not treated with the FITC-conjugated Ab. The intensity of FITC fluorescence was measured by BD FACSCalibur flow cytometer (BD Biosciences, CA, USA) at 488 and 535 nm for excitation and emission wavelengths, respectively. The fluorescent intensity of 10,000 events was used for data analysis.

Statistical analysis

Data were expressed as mean ± standard error of the mean (SEM) from three duplicated experiments. Multiple comparisons were statistically analyzed by Kruskal-Wallis test, followed by Mann-Whitney *U* test with Bonferroni correction. Comparison between the Ab-labeled and unlabeled groups in each treatment with doxorubicin was performed by the Mann-Whitney *U* test. Statistical significance was considered at $p < 0.05$.

Results

We determined the expression of P-gp on the cell surface with FITC-labeled P-gp Ab. The cells in the solvent control group (0.5% DMSO) which were incubated with P-gp Ab showed a significant increase in fluorescent intensity, suggesting the presence of considerable amount of expressed P-gp in these cells (Figures 1 and 2).

Treatment of the cells with the non-cytotoxic concentrations of doxorubicin (3, 10, 50, and 100 μM) for 24 hours increased the fluorescent intensity in concentration-dependent manner (Figure 2). In the cells treated with 3 μM of doxorubicin, the intensity of the

fluorescence between Ab-labeled and unlabeled cells was statistically different. Upon increasing the concentration of doxorubicin, fluorescent signals of the Ab-labeled cells were apparently equal to those of the unlabeled cells (Figures 1 and 2). Our data clearly demonstrated that doxorubicin, particularly at concentrations higher than 3 μM, was able to interfere with the fluorescent signal of FITC-conjugated Ab on the cell surface.
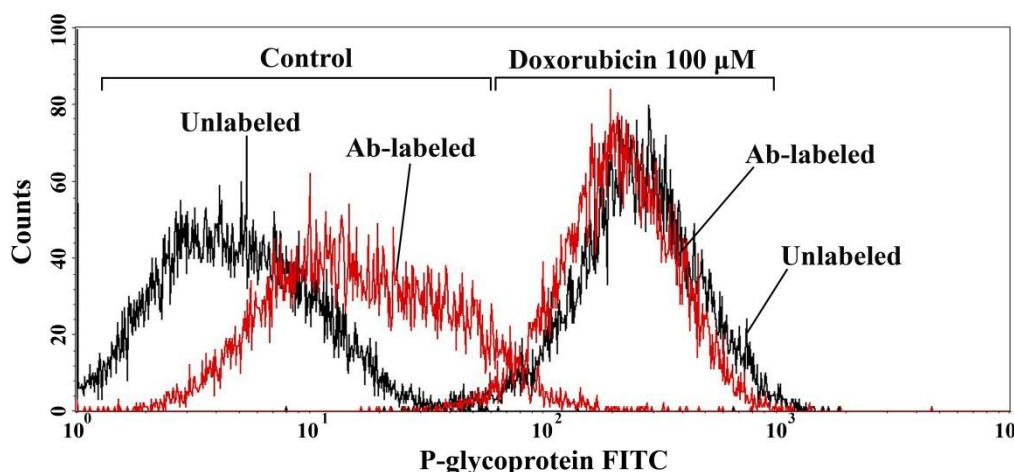
Figure 1. Representatives of flow cytometric analysis of fluorescent intensity in the Caco-2 cells after treatment with either 0.5% DMSO (control) or doxorubicin 100 μM in the FITC-conjugated anti-P-gp Ab labeled (red line) and the unlabeled groups (black line).
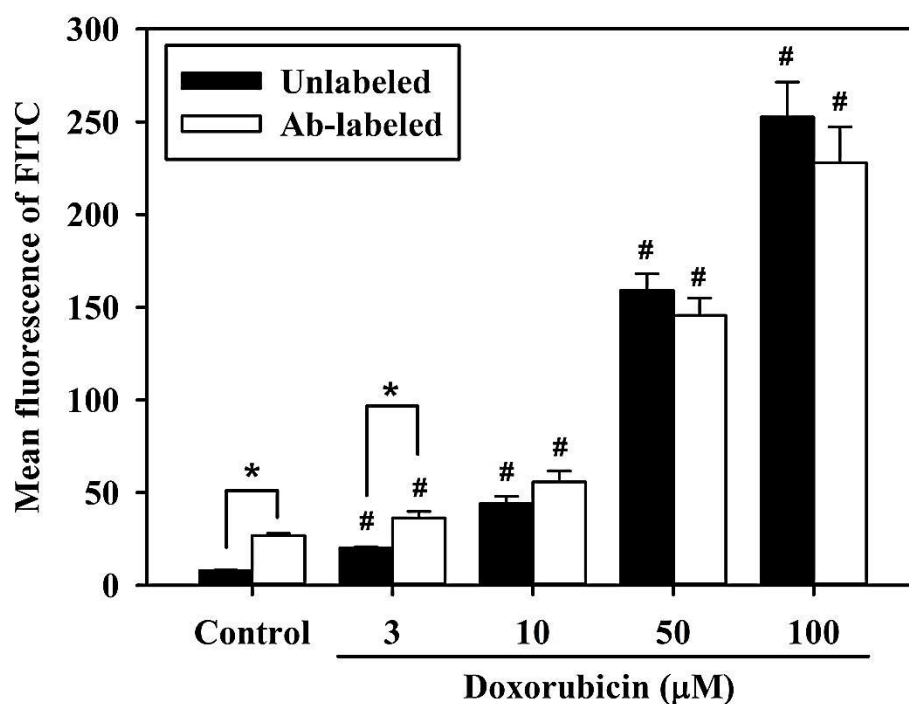
Figure 2. Effect of doxorubicin on fluorescent intensity of the FITC-Ab labeled (open bar) and the unlabeled groups (solid bar). The cells were treated with doxorubicin at various concentrations for 24 hours. Doxorubicin was washed out three times with PBS before flow cytometric analysis. Data were expressed as mean ± SEM (n=3). $^*p < 0.05$ vs the unlabeled group. $^#p < 0.05$ vs control.

Discussion

Flow cytometry using fluorochrome-conjugated Ab provides a fast and simple method to determine the expression of cell surface proteins including membrane transporters. Two common fluorochromes widely used to conjugate with P-gp Ab are FITC and phycoerythrin. The emission spectrum of FITC and phycoerythrin was commonly measured at 530/30 nm and 585/42 nm, respectively. In this study, we used a commercially available FITC-conjugated Ab to label the cell surface P-gp of the doxorubicin-treated Caco-2 cells. Our results clearly showed that the fluorescent signal from the doxorubicin-treated cells was not exclusively different from the FITC-labeled P-gp. Increased doxorubicin concentration correlated well with fluorescent signal from the doxorubicin-treated cells. It was likely that the fluorescence reflected an accumulation of doxorubicin rather than an increase in P-gp expression. Doxorubicin permeates through cell membrane and is retained in lysosomes by pH trapping.[14] Increasing its concentration or treatment period could either enhance its intracellular accumulation. Moreover, the doxorubicin-washout step with PBS prior to labeling the cells with Ab was insufficient to abolish the interfering effect of doxorubicin on fluorescence readings. Eventually, the fluorescent intensity of FITC-labeled P-gp was interfered by doxorubicin when fluorescent signal of the cells was measured by flow cytometric technique. It was reported that fluorescent signal of doxorubicin interfered with certain fluorescent dyes such as phycoerythrin and propidium iodide in flow cytometric analysis.[6, 15] Our finding was the first to demonstrate that doxorubicin could cause fluorescent interference with FITC in particular when the high concentrations of doxorubicin were applied. In addition, application of the fluorescence compensation technique to correct spectral overlap in flow cytometry could not reduce doxorubicin interference in this experiment setting.

Conclusion

Thus, researchers should be aware of the intrinsic fluorescent property of any substances used in the flow cytometric experiment with fluorescent-labeled proteins. Overlooking this issue may lead to misinterpretation and a false positive result. Potential interference on the fluorescent signal of target proteins could be avoided by selecting the fluorescent dye with the least overlapping spectrum with a tested substance. It should be noted that the degree of interference depends on the concentration and retention period of the fluorochrome within the cells. Higher concentration of fluorochrome causes greater interference on the signal of the labeled target protein. If there is a potential for interference on the fluorometric reading, conventional western blot should be chosen to determine protein expression.

Acknowledgements

References

1. Wessler JD, Grip LT, Mendell J, Giugliano RP. The P-glycoprotein transport system and cardiovascular drugs. J Am Coll Cardiol. 2013;61(25):2495-502.
2. Qiang F, Kang KW, Han HK. Repeated dosing of piperine induced gene expression of P-glycoprotein via stimulated pregnane-X-receptor activity and altered pharmacokinetics of diltiazem in rats. Biopharm Drug Dispos. 2012;33(8):446-54.
3. Budde T, Haney J, Bien S, Schwebe M, Riad A, Tschope C, et al. Acute exposure to doxorubicin results in increased cardiac P-glycoprotein expression. J Pharm Sci. 2011;100(9):3951-8.
4. Haslam IS, Jones K, Coleman T, Simmons NL. Rifampin and digoxin induction of MDR1 expression and function in human intestinal (T84) epithelial cells. Br J Pharmacol. 2008;154(1):246-55.
5. MacPhee DJ. Methodological considerations for improving Western blot analysis. J Pharmacol Toxicol Methods. 2010;61(2):171-7.
6. Krishan A, Ganapathi RN, Israel M. Effect of adriamycin and analogs on the nuclear fluorescence of propidium iodide-stained cells. Cancer Res. 1978;38(11 Pt 1):3656-62.
7. Skoog DA, Holler FJ, Crouch SR. Principles of Instrumental Analysis: Thomson Brooks/Cole; 2007.
8. Vogel AI, Mendham J. Vogel's Textbook of Quantitative Chemical Analysis: Longman; 2000.
9. Mealey KL, Barhoumi R, Rogers K, Kochevar DT. Doxorubicin induced expression of P-glycoprotein in a canine osteosarcoma cell line. Cancer Lett. 1998;126(2):187-92.
10. Silva R, Carmo H, Dinis-Oliveira R, Cordeiro-da-Silva A, Lima SC, Carvalho F, et al. In vitro study of P-glycoprotein induction as an antidotal pathway to prevent cytotoxicity in Caco-2 cells. Arch Toxicol. 2011;85(4):315-26.
11. Bao L, Hazari S, Mehra S, Kaushal D, Moroz K, Dash S. Increased expression of P-glycoprotein and doxorubicin chemoresistance of metastatic breast cancer is regulated by miR-298. Am J Pathol. 2012;180(6):2490-503.
12. Liu Z, Duan ZJ, Chang JY, Zhang ZF, Chu R, Li YL, et al. Sinomenine sensitizes multidrug-resistant colon cancer cells (Caco-2) to doxorubicin by downregulation of MDR-1 expression. PLoS One. 2014;9(6):e98560.
13. Karukstis KK, Thompson EH, Whiles JA, Rosenfeld RJ. Deciphering the fluorescence signature of daunomycin and doxorubicin. Biophys Chem. 1998;73(3):249-63.
14. Yamagishi T, Sahni S, Sharp DM, Arvind A, Jansson PJ, Richardson DR. P-glycoprotein mediates drug resistance via a novel mechanism involving lysosomal sequestration. J Biol Chem. 2013;288(44):31761-71.
15. Reddy LH, Couvreur P. Macromolecular Anticancer Therapeutics: Springer Verlag; 2010.

RESEARCH ARTICLE

A comparative study of antioxidant and antiplatelet activity of pomelo juice extracted from three cultivars

Jindaporn Janprasit[1], Paveena Yamanont[1], Rataya Luechapudiporn[2], Noppawan Phumala Morales[1]

[1] Department of Pharmacology, Faculty of Science, Mahidol University, Bangkok, 10400, Thailand
[2] Department of Pharmacology and Physiology, Faculty of Pharmaceutical Sciences, Chulalongkorn University, Bangkok, 10330, Thailand

Address correspondence and reprint request to: Noppawan Phumala Morales, Department of Pharmacology, Faculty of Science, Mahidol University, Bangkok, 10400, Thailand.
E-mail address: noppawan.phu@mahidol.ac.th

Abstract

Several studies have reported the protective effect of polyphenol-rich diet to cardiovascular diseases (CVD) thru antioxidant and antiplatelet activity. This study aimed to evaluate antioxidant activity and inhibitory effect of pomelo on human platelet aggregation. The nitrite content, total phenolic content, total flavonoid content and antioxidant activity were determined in juice extracted from three cultivars of pomelo; Thong Dee, Khao Tang Kwa and Khao Yai. All of pomelo juice contained phenolic content approximately 6 mM of gallic acid equivalence while contained nitrite content in range of 3-6 μM. The *in vitro* effect of pomelo juice on ADP-induced human platelet aggregation was investigated. Pomelo juice affected the maximum aggregation in dose-dependent manner and also altered the response curve in to biphasic shape. The juice extract from Thong Dee showed highest antioxidants and antioxidant activity and highest effect on platelet aggregation. The mechanism of action in related to active compounds in various cultivars of pomelo will be further investigated.

Keywords: pomelo juice, antioxidant, antiplatelet

Introduction

Platelets are one of blood cells that are necessary for physiologic processes of hemostasis. Conversely, they also involve in atherothrombosis, which is the major cause of cardiovascular diseases (CVD). Atherothrombosis, the leading cause of mortality in developed countries, is explained as the formation of thrombi overlaid on atherosclerotic lesion disruption[1].

Several epidemiological studies have reported the protective effect of diets in the prevention of CVD[2-5]. Thus, the food or food component, which maintain or improve health, is regarded as functional food. This fact has brought the enormous interest on the antiplatelet activity of dietary components, including polyphenols and flavonoids. Several natural

components that found in grape, onion, and tomato have been reported to exert the preventive role against CVD thru inhibition of platelet aggregation[6-7].

Interestingly, some of natural polyphenols presenting in diet affected to the platelet function, even if it is not well defined that their native compounds, metabolites, or combination of both exerted their *in vivo* antiplatelet activities[8]. The natural form of polyphenols mostly found as glycoside.

The pomelo (*Citrus maxima* Merr.*)* is the largest of all nature citrus fruits that is widely consumed in Thailand. There are many cultivars that are cultivated in Thailand, namely Thong Dee, Khao Tang Kwa and Khao Yai. Pomelo enrich with vitamin C, antioxidant and flavonoids (i.e. kaemferol, myricetin, apigenin, luteolin and hesperetin). The nutritive composition and content depend on cultivar[9]. Previous study have confirmed that pomelo juice enrich with flavonoids in glycoside form[10-11]

The aim of this study is to evaluate antioxidant activity of pomelo juice extracted from 3 different cultivars, including Thong Dee, Khao Tang Kwa and Khao Yai. Furthermore, the inhibitory effect of pomelo juice on human platelet aggregation is investigated.

Materials and Methods

Pomelo juice preparation

Three cultivars of pomelo were studied: Thong Dee (TD), Khao Yai (KY) and Khao Tang Kwa (KT). The pomelo pulps (500 g) were blended and filtered to obtain pomelo juice. The samples of pomelo juice were centrifuge 10,000 g before performing assays.

Griess assay

The griess assay was performed using sulfanilamide and N-(1-Naphthyl)ethylenediamine dihydrochloride (NED) to determine total nitrite (NO_2^-). The juice or standard (50 µl) was mixed with 1% sulfanilamide in 5% phosphoric acid (50 µl) for 5 minutes and 0.1% NED (50 µl) was then added and mixed well. Then, it was incubated at room temperature in dark for 5 minutes. The absorbance of reaction was measured at 520 nm with microplate multimode reader (Varioskan Flash, Thermo Scientific, USA).

Total phenolic content

The total phenolic content was determined using the Folin-Ciocalteau method compared to standard compound, gallic acid. The juice or standard (20 µl) was mixed with 10%v/v Folin-Ciocalteau reagent (100 µl) for 2 minute and 7.5% sodium carbonate solution (80 µl) was then added and mixed well. Then, it was incubated at room temperature for 60 minutes. The absorbance of reaction was measured at 765 nm with a microplate multimode reader.

Total flavonoid content

The flavonoids content was determined using aluminum chloride ($AlCl_3$) compared to standard compound, quercetin. The juice or standard (100 µl) was mixed with 2% $AlCl_3$ in ethanol (100 µl). Then, it was incubated at room temperature for 60 minutes. The absorbance of reaction was measured at 420 nm with a microplate multimode reader.

DPPH radical scavenging assay

The DPPH radical scavenging assay was performed to evaluate antioxidant activity compared to standard compound, trolox. The juice or standard (100 µl) was mixed with 500 µM DPPH (100 µl). Then, it was incubated at room temperature in dark for 10 minutes. The absorbance of reaction was measured at 520 nm with a microplate multimode reader.

Ferric ion reducing antioxidant power (FRAP) assay

The FRAP assay also was used to evaluate the antioxidant activity compared to standard compound, ascorbic acid. The juice or standard (20 µl) was mixed with FRAP reagent (180 µl). Then, it was incubated at room temperature for 10 minutes. The absorbance of reaction was measured at 593 nm with a microplate multimode reader.

FRAP reagent is the mixture of 300 mM acetate buffer (pH 3.6), 10 mM TPTZ, 20 mM Ferric Chloride ($FeCl_3$) and water in 10:1:1:1.2 ratio.

Statistical analysis

The value of nitrite content, total polyphenolic content, total flavonoid contents and antioxidant activities was shown in mean ± SD and used one way analysis of variance (One-way ANOVA) following Bonferroni's Multiple Comparison Test (Graphpad Prism, USA)

Platelet preparation

The blood sample was obtained from male free-drug healthy volunteer and anticoagulated with 3.8% sodium citrate (approved by the Committee on Human Rights Related to Research Involving Human Subjects, Faculty of Medicine Ramathibodi Hospital, Mahidol University, Protocol Number: ID 08-58-28). Platelet-rich plasma (PRP) was prepared by centrifugation at 200 g for 10 minutes. After that the rest was centrifuged at 2,330 g for 10 minutes to obtain platelet-poor plasma (PPP). PPP was used to dilute PRP in ratio 1:1.

Platelet aggregation study

The platelet aggregation was studied by turbidimetric method. PRP samples were stimulated using ADP as agonists. It was monitored in an aggregometer (AggRAM, Helena Biosciences, UK) at 37°C under continuous stirring at 1,000 rpm.

PRP samples (295 µl) was pre-incubated with10 µl of 50% or 100% pomelo juice (TD, KY and KT) for 5 and 30 minutes at 37°C in aggregometer. Then, it was stimulated with 5 µl of 8 µM ADP (as shown in final concentration). The extent of platelet aggregation was

estimated by measuring the maximum height above the baseline reached by the aggregation curve within 5 minutes following stimulation (Maximum aggregation).

The %inhibition was calculated by comparison maximum aggregation between control and treated as shown in below equation.

$$\%inhibition = \frac{Max.\,aggregation_{control} - Max.\,aggregation_{treated}}{Max.\,aggregation_{control}} \times 100$$

Results

Determination of nitrite content, total polyphenolic content, total flavonoid contents and antioxidant activities

Results of nitrite content, total phenolic content, total flavonoids content and antioxidant activities were shown in Table 1. The results showed that TD had higher phenolic and flavonoids content than others, but the significant difference was not observed between KT and KY. TD also had higher antioxidant activity than others.

Table 1. Nitrite content, total phenolic content, total flavonoids content and antioxidant activities of pomelo juice

Parameters	Value [a]		
	TD	KT	KY
Nitrite content (μM)	3.41 ± 0.48[**]	5.53 ± 0.27	4.37 ± 0.62
Total phenolic content (GAE[b], mM)	2.39 ± 0.02[**,##]	2.06 ± 0.08	2.00 ± 0.04
Total flavonoids content (QE[b], μM)	6.85 ± 0.54[**]	6.00 ± 0.33	6.32 ± 0.05
DPPH assay (TEAC[b], mM)	5.21 ± 0.38[*]	3.98 ± 0.21	4.84 ± 0.62
FRAP assay (VCEAC[b], mM)	4.59 ± 0.45[*]	3.37 ± 0.07	3.90 ± 0.36

[a] The value shown in mean ± SD, n=3
[b] Abbreviations: Gallic acid equivalence (GAE), Quercetin equivalence (QE), Trolox equivalent antioxidant capacity (TEAC) and vitamin C equivalent antioxidant (VCEAC)
[*] $p < 0.05$ when compared to KT
[**] $p < 0.01$ when compared to KT
[##] $p < 0.01$ when compared to KY

Antiplatelet activity of pomelo juice

PRP sample was pre-incubated with pomelo juice and then stimulated with 8 μM ADP. In control, without pomelo juice, ADP-induced platelet aggregation was about 87-94% as shown in Figure 1. The pomelo juice affected to ADP-induced platelet aggregation depending on incubation time and concentration.

Figure 1a and 1b showed that the lower concentration of pomelo juice (50%) had slightly inhibitory effect on the value of maximum aggregation. However, all of them altered the aggregation curve into biphasic shape. KY marginally decreased the value of maximum aggregation to 77.8% after 5 minutes of pre-incubation while TD and KT marginally decreased the value of maximum aggregation to 76.1% and 82.5%, respectively after 30 minutes of pre-incubation.

(a) 50% pomelo juice, 5 minutes
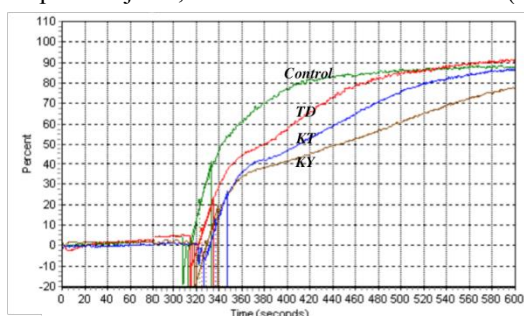
(c) 100% pomelo juice, 5 minutes
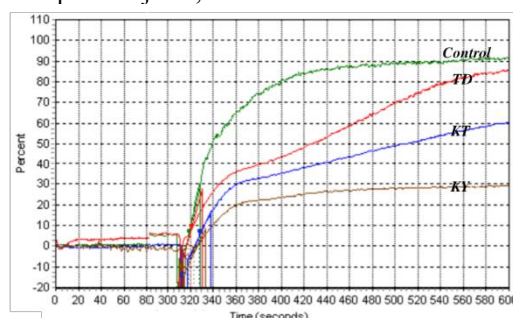
(b) 50% pomelo juice, 30 minutes
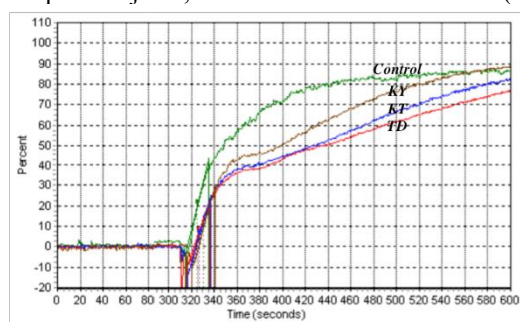
(d) 100% pomelo juice, 30 minutes
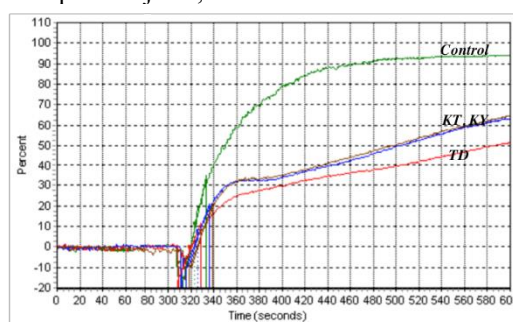
Figure 1. Platelet aggregations after incubation with pomelo juice for 5 and 30 minutes (TD; Thong Dee, KT; Khao Tang Kwa and KY; Khao Yai)

Platelet samples were pre-incubated with 100% pomelo juice for 5 minutes as shown in Figure 1c. The results shown KY greatly decreased the value of maximum aggregation (29.5%) followed by KT (60.4%) and TD (85.8%). For 30 minutes of incubation time (Figure 1d), TD decreased the value of maximum aggregation to 51.6%, while KT and KY shown similarly response curve.

The maximum aggregation and %inhibition, which was calculated comparing to control of each group, were shown in Table 2.

Table 2. The maximum aggregation of pomelo juice pre-incubated platelet and percentage inhibition of maximum aggregation of pomelo juice

Incubation time	Sample Name	Maximum aggregation (%)		% Inhibition	
		50% juice	100% juice	50% juice	100% juice
5 minutes	**TD**	91.5	85.8	-	6.7
	KT	86.8	60.4	2.0	34.3
	KY	77.8	29.5	12.2	67.9
30 minutes	**TD**	76.1	51.6	12.6	45.1
	KT	82.5	63.4	5.3	32.6
	KY	88.5	64.7	-	31.2

Discussion

Pomelo juice from TD, KT and KY contained high polyphenol content as shown in gallic acid equivalence. The phenolic content was in millimorlar level which was corresponded to levels of antioxidant activities as demonstrated by values obtained from DPPH and FRAP assay. On the other hand, the value of flavonoids content was in micromolar. The value may underestimate because of the limitation of technique of flavonoids assay that due to high content of water in pomelo juice may enhance dissociation between flavonoids and aluminum (III)[12]. Therefore, flavonoids content will be further determined by high performance liquid chromatography (HPLC) technique.

The results demonstrated that pomelo juice had inhibitory effect on platelet function. Although the low concentration and shorter pre-incubation time had not significant effect on maximum platelet aggregation, the biphasic shape of the curve may indicate that pomelo juice altered the activation and delay aggregation process. Several lines of evidences have indicated the roles of flavonoids as antiplatelet functions thru several mechanisms including inhibition of ADP receptors (P2Y1 and P2Y12)[6-7]. Activation of platelet induced the production of free radicals that involve in the platelet aggregation pathway[13-15]. Therefore, mechanism related to antioxidants should be considers. In addition, three cultivars of pomelo juice (TD, KT and KY) have nitrite content in range 3-6 μM. We also suspected the effect of nitrite which it is product of nitric oxide (NO). NO is chemical compound that potentially inhibit platelet aggregation[16-17]. The mechanism of antiplatelet activity of pomelo juice will be investigated.

Conclusion

Pomelo juice had high content of antioxidants and exhibited antiplatelet activity. The potency of antiplatelet activity depended on concentration, incubation time and cultivars. TD showed the highest potency among cultivars. The extract mechanism of antiplatelet activity will be future investigated.

Acknowledgements

References

1. Viles-Gonzalez JF, Fuster V, Badimon JJ. Atherothrombosis: A widespread disease with unpredictable and life-threatening consequences. Eur Heart J. 2004;25(14):1197-207.
2. de Lorgeril M, Renaud S, Salen P, Monjaud I, Mamelle N, Martin JL, et al. Mediterranean alpha-linolenic acid-rich diet in secondary prevention of coronary heart disease. The Lancet. 1994;343(8911):1454-9.
3. Estruch R, Ros E, Salas-Salvadó J, Covas M-I, Corella D, Arós F, et al. Primary prevention of cardiovascular disease with a mediterranean diet. New Engl J Med. 2013;368(14):1279-90.
4. Fuentes E, Castro R, Astudillo L, Carrasco G, Alarcon M, Gutierrez M, et al. Bioassay-guided isolation and HPLC determination of bioactive compound that relate to the antiplatelet activity (Adhesion, Secretion, and Aggregation) from Solanum lycopersicum. Evid Based Complement Alternat Med. 2012;2012:10.
5. Hu FB. Plant-based foods and prevention of cardiovascular disease: an overview. The American Journal of Clinical Nutrition. 2003;78(3):544S-51S.
6. Fuentes E, Palomo I. Antiplatelet effects of natural bioactive compounds by multiple targets: Food and drug interactions. J Funct Foods. 2014;6:73-81.
7. Vilahur G, Badimon L. Antiplatelet properties of natural products. Vascul Pharmacol. 2013;59(3–4):67-75.
8. Mattiello T, Trifiro E, Jotti GS, Pulcinelli FM. Effects of pomegranate juice and extract polyphenols on platelet function. J Med Food. 2009;12(2):334-9.
9. Kongkachuichai R, Charoensiri R, Sungpuag P. Carotenoid, flavonoid profiles and dietary fiber contents of fruits commonly consumed in Thailand. International Journal of Food Sciences and Nutrition. 2010;61(5):536-48.
10. Kawaii S, Tomono Y, Katase E, Ogawa K, Yano M. Quantitation of Flavonoid Constituents in Citrus Fruits. Journal of Agricultural and Food Chemistry. 1999;47(9):3565-71.
11. Zhang M, Duan C, Zang Y, Huang Z, Liu G. The flavonoid composition of flavedo and juice from the pummelo cultivar (Citrus grandis (L.) Osbeck) and the grapefruit cultivar (Citrus paradisi) from China. Food Chem. 2011;129(4):1530-6.
12. Zhang J, Wang J, Brodbelt JS. Characterization of flavonoids by aluminum complexation and collisionally activated dissociation. J Mass Spectrom. 2005;40(3):350-63.
13. Pignatelli P, Pulcinelli FM, Lenti L, Paolo Gazzaniga P, Violi F. Hydrogen Peroxide Is Involved in Collagen-Induced Platelet Activation. Blood. 1998;91(2):484-90.
14. Iuliano L, Pedersen JZ, Pratico D, Rotilio G, Violi F. Role of hydroxyl radicals in the activation of human platelets. Eur J Biochem. 1994;221(2):695-704.
15. Iuliano L, Colavita AR, Leo R, Praticò D, Violi F. Oxygen Free Radicals and Platelet Activation. Free Radical Biol Med. 1997;22(6):999-1006.
16. Wang GR, Zhu Y, Halushka PV, Lincoln TM, Mendelsohn ME. Mechanism of platelet inhibition by nitric oxide: in vivo phosphorylation of thromboxane receptor by cyclic GMP-dependent protein kinase. Proc Natl Acad Sci U S A. 1998;95(9):4888-93.
17. Riddell DR, Owen JS. Nitric oxide and platelet aggregation. Vitam Horm. 1999;57:25-48.

RESEARCH ARTICLE

Detection of mutation in dopamine receptor (DRD2) in Malay male subjects with co-occurring amphetamine-type stimulant (ATS) and opioid dependence: a preliminary study

Ruzilawati Abu Bakar[1], Deeza Syafikah Mohd Sidek[1], Nor Afina Mohd Din[1], Vicknasingam Balasingam Kasinather[2] and Imran Ahmad[3]

[1]*Department of Pharmacology, School of Medical Sciences, Universiti Sains Malaysia, Kelantan, Malaysia.*
[2]*Centre for Drug Research, University Sains Malaysia, Penang, Malaysia.*
[3]*Department of Family Medicine, School of Medical Sciences, Universiti Sains Malaysia, Kelantan, Malaysia.*

Address correspondence and reprint request to: Ruzilawati Abu Bakar, Department of Pharmacology, School of Medical Sciences, Universiti Sains Malaysia, Kelantan, Malaysia,
Email: ruzila@usm.my

Abstract

Drug addiction remains a worldwide problem, and its negative impact on society is increasing. The dopaminergic pathways of the mesolimbic and nigrostriatal systems have been shown to be involved in the reward pathway of drugs of abuse. One of the genes, dopamine receptor (DRD2) gene was reported to play a large role in the rewarding effects of drugs of abuse. Many have reported an association between the DRD2 locus and drug abuse. There has been no prior study reported for this gene in Malay Male subjects with co-occurring amphetamine-type stimulant (ATS) and opioid dependence, so far. Therefore, the aim of the present study was to investigate the frequencies of DRD2 gene polymorphism among Malay Male subjects with co-occurring amphetamine-type stimulant (ATS) and opioid dependence. The study was conducted in 20 Malay Male subjects with co-occurring amphetamine-type stimulant (ATS) and opioid dependence and 50 control subjects. DNA was extracted from leucocytes and the allele was determined by a polymerase chain reaction–restriction fragment length polymorphism (PCR-RFLP). The PCR product was digested with restriction enzymes *Taq*I. In this study, there were no mutations detected in DRD2 allele for the control subjects as all subjects were found to be wild-type. While the genotype frequencies for DRD2 gene in co-occurring amphetamine-type stimulant (ATS) and opioid dependence subjects are A1/A1= 20% (4), A1/A2= 55% (11) and A2/A2= =25% (5).Larger sample size is needed to confirm the association of this gene with addiction among Malay subjects.

Keywords: DRD2 gene; Malay Male: co-occurring amphetamine-type stimulant (ATS) and opioid dependence; PCR-RFLP

Introduction

Drug addiction remains a worldwide problem, and its negative impact on society is increasing[1, 2]. It is a chronic relapsing disorder in which compulsive drug-seeking and drug-taking behaviour persists despite serious negative consequences.

Dopamine is a neurotransmitter in the central nervous system[3.] Dopamine is largely produced in neuronal cell bodies in two areas of the brainstem: the substantia nigra and the ventral tegmental area[4]. Previous studies have shown that there were interactions between the dopaminergic system in reward and drug dependence and withdrawal[5]. The dopaminergic pathways of the mesolimbic and nigrostriatal systems have been shown to be involved in the reward pathway[6,7].

Dopamine receptor D2 gene (DRD2) appears to play a large role in the rewarding effects of drugs of abuse. Many have reported an association between the DRD2 locus and drug abuse[8]. It has been postulated that substance abuse may be related to a structural deficit in the dopaminergic reward system[9]. The most frequently examined polymorphism linked to DRD2 gene is the Taq1A restriction fragment length polymorphism (RFLP) which has been associated with a reduction in D2 receptor density[10]. The pharmacological perspective suggests that diminished responsiveness in the dopaminergic system associated with the DRD2 Taq A1 allele would have a greater contribution as a genetic risk factor in drug abuse, especially for amphetamines[11].

The aim of this study was to investigate the frequency of DRD2 gene polymorphism among Malay Male subjects with co-occurring amphetamine-type stimulant (ATS) and opioid dependence by using a polymerase chain reaction-restriction fragment length polymorphism (PCR-RFLP).

Materials and Methods

Subjects

A total of 20 Malay Male subjects with co-occurring amphetamine-type stimulant (ATS) and opioid dependence and 50 control subjects were recruited. All subjects were given informed consent form to participate in the study. The study was approved by Ethics Committee of School of Medical Sciences, Universiti Sains Malaysia.

DNA Extraction

Three ml of venous blood was drawn into a tube containing EDTA and stored at -20°C until the isolation of genomic DNA. Genomic DNA was isolated from the leucocytes using QIAamp DNA Blood Mini Kit (Qiagen, USA) and the allele was determined by a polymerase chain reaction-restriction fragment length polymorphism (PCR-RFLP). DNA purity and concentration was measured by spectrophotometer, Biophotometer Uvette (Eppendorf, Germany) at 280 nm absorbance

Molecular analysis

      Genotyping of DRD2 gene polymorphism was performed using polymerase chain reaction/restriction fragment length polymorphism (PCR/RFLP) method as describe by Dan T.A et al. (2007). The PCR reaction was carried out in a total volume of 25 µl consisting of 10x PCR buffer with KCl, 0.3 µmol/l of each primer as listed in Table 1, 0.16 µmol/l of dNTPs, 0.7 mmol/l of MgCl2 and 0.5 U Taq DNA polymerase (MBI Fermentas Inc., USA). After an initial incubation at 95˚C for 15 min, the PCR products were amplified for 35 cycles of 30 sec at 94˚C, annealing at 55˚C for 30 sec, extension at 75˚C for 1 min and final extension at 72˚C for 7 min. The 300 bp PCR product was then digested with TaqI enzyme (BioLabs Inc., New Zealand) for 2 hours at 65˚C. The digested products were visualized under UV light on 1.4% ethidium bromide agarose gel with 100 bp ladder.
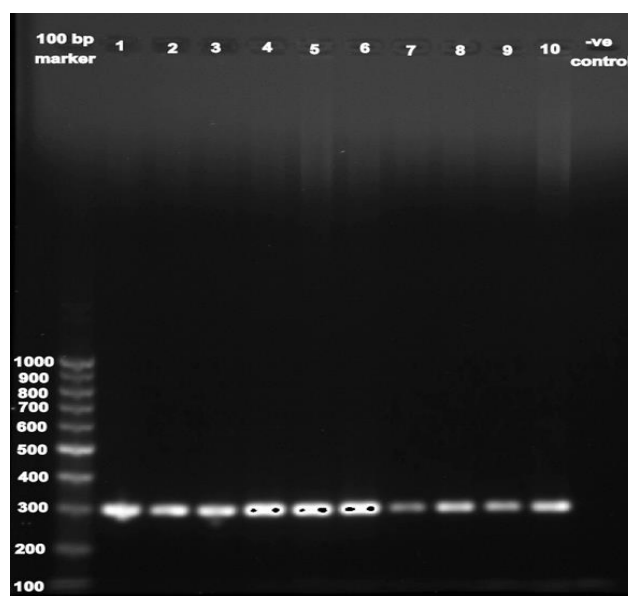
Figure 1. Agarose gel electrophoresis for PCR or DRD2 gene (300 bp fragments).
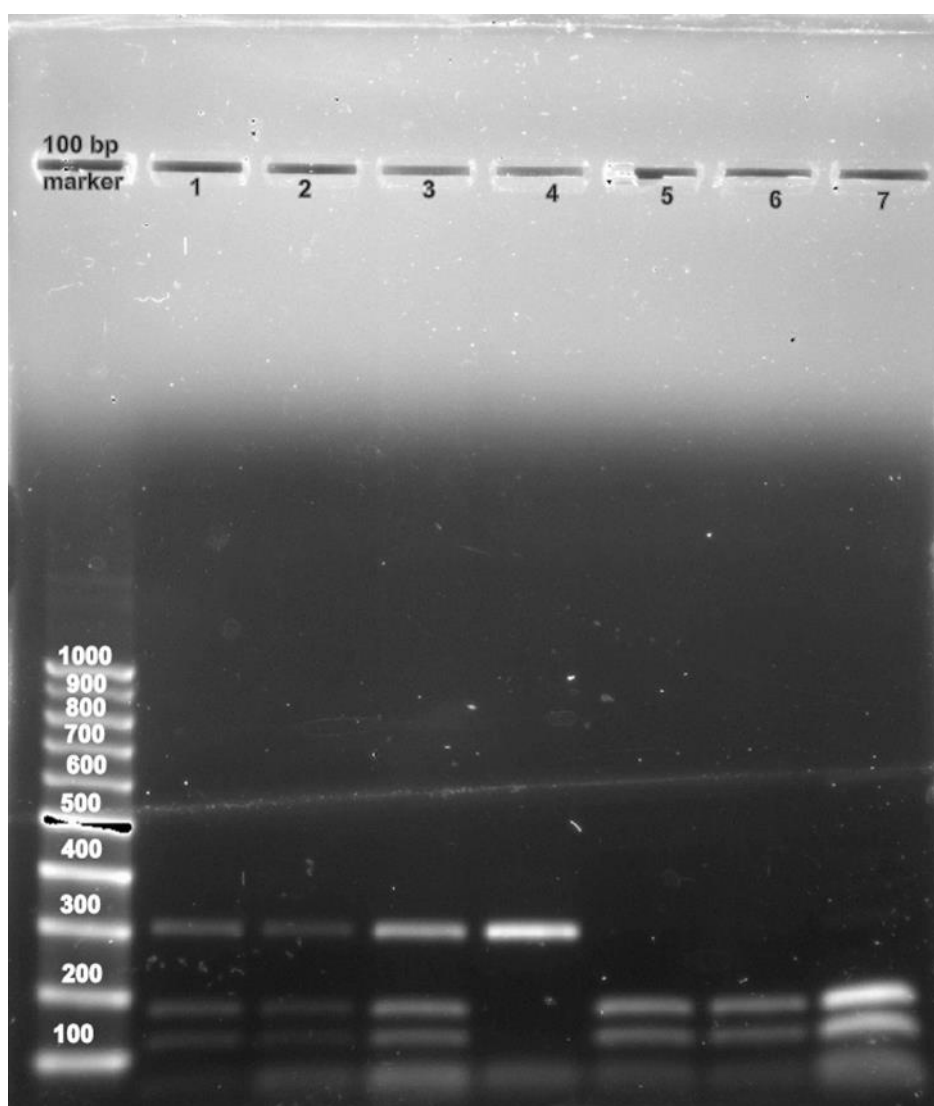
Figure 2. PCR-RFLP result after digestion with Taq A1 restriction enzyme. Lane 1, 2 and 3 show a heterozygous A1/A2 wild-mutant alleles with 125bp, 175bp and 300bp fragment. Lane 4 shows a homozygous wild-type A1/A1 with 300bp fragment. Lane 5, 6 and 7 show homozygous A2/A2 with 125bp and 175bp fragments.

Results and Discussion

In all reactions, correct lengths of expected PCR products were obtained. Figure 1 shows the PCR products for DRD2 gene with the band size of 300 bp. In the PCR-RFLP analyses, restriction enzymes used in the present study was found to have worked. Figure 2 shows PCR-RFLP result after digestion with Taq A1 restriction enzyme. The wild-type allele, A1/A1 allele, remained uncut (300 bp), whereas the mutant allele, A2/A2 allele was digested into 125 bp and 175 bp. The presence of three fragments at 125 bp, 175 bp and 300 bp were observed as A1/A2 allele which consists of both wild-mutant alleles. PCR-RFLP is one of the most reliable methods used for recognition of genetic mutations. The method is based on specific PCR product cut by restriction endonucleases which is capable of cutting the double-

stranded DNA[12]. TaqI restriction analysis of the polymorphism of the DRD2 gene is rapid and less complex compared to other methods

To our knowledge, the present study describes for the first time polymorphisms of DRD2 among Malay Male subjects with co-occurring amphetamine-type stimulant (ATS) and opioid dependent and control subjects. In this study, there were no mutations detected in DRD2 allele for the control subjects as all subjects were found to be wild-type. While the genotype frequencies for DRD2 gene in co-occurring amphetamine-type stimulant (ATS) and opioid dependence subjects are A1/A1= 20% (4), A1/A2= 55% (11) and A2/A2= =25% (5). About half of our drug addict subjects are having A1/A2 allele. Many studies were conducted to find an association between Taq1A polymorphisms and alcoholism[13], cocaine dependence [14] and smoking status [15,16]. Our result is in contrast to the results of DRD2 Taq1A polymorphism Turkish population where they found that A1/A1 genotype in cannabinoid addict samples were higher than in control group[17].

This is a preliminary study. Therefore, in order to confirm the association of this gene with co-occurring amphetamine-type stimulant (ATS) and opioid dependence among Malay Male population a larger sample size is needed. The clinical relevance of the genetic variants of DRD2 in this population and drug addiction is still under our investigation.

Conclusion

In conclusion, the PCR-RFLP method described in our study can be used to screen for and detect DRD2 Taq A1 mutations.

Acknowledgements

References

1. National Drug Information (NADI), National drug Agency, Malaysia, 2005. Annual Report, 5–21.
2. Chawarski MC, Schottenfeld RS, Mazlan M. Heroin dependence and HIV infection in Malaysia. Drug & Alcohol Depend. 2006 April; 82:S39-S42.
3. Molinoff PB and Axelrod J. Biochemistry of catecholamines. Annu Rev Biochem. 1971; 40:465–500.
4. Pitchers KK, Coppens CM, Beloate LN, Fuller J, Van S, Frohmader KS, Laviolette SR, Lehman MN, Coolen LM. Endogenous opioid-induced neuroplasticity of dopaminergic neurons in the ventral tegmental area influences natural and opiate reward. J Neurosci. 2014 Jun 25; 34(26):8825-8836
5. Kreek MJ and Vocci FJ. History and current status of opioid maintenance treatments: blending conference session. J Subst Abuse Treat. 2002; 23:93–105.

6. Di Chiara G and Imperato A. Drugs abused by humans preferentially increase synaptic dopamine concentrations in the mesolimbic system of freely moving rats. Proc Natl Acad Sci USA. 1988; 85:5274–5278.
7. Herz A. Bidirectional effects of opioids in motivational processes and the involvement of D1 dopamine receptors. NIDA Res Monogr. 1988; 90:17–26.
8. Noble EP. Addiction and its reward process through polymorphisms of the D2 dopamine receptor gene: a review. Eur Psychiatry. 2000; 15:79–89.
9. George FK. Addiction is a Reward Deficit and Stress Surfeit Disorder Front Psychiatry. 2013; 4: 72. 1-18
10. Neville MJ, Johnstone EC, Walton RT. Identification and characterization of ANKK1: a novel kinase gene closely linked to DRD2 on chromosome band 11q23.1.   Hum Mutat. 2004; **23**: 540-545.
11. Kenneth B, Thomas JH, Chen B, William D, Abdalla B, Roger LW, Eric RB, Margaret M, Marlene O-B, Nicholas D, Mark G. Neurogentics of Dopaminergic Receptor Super-sensitivity in Activation of Brain Reward Circuitry and Relapse: Proposing "Deprivation-Amplification Relapse Therapy" (DART), Postgrad Med. 2009 Nov; 121(6): 176–196.
12. Topic E. Pharmacogenetics and clinical laboratory. Biochem Medica 1999; 9: 97-106
13. Suraj SH, Ghosh PK, Saraswathy KN. DRD2 and ANKK1 gene polymorphisms and alcohol dependence: a case-control study among a Mendelian population of East Asian ancestry. Alcohol Alcohol. 2013 Jul-Aug; 48(4):409-14.
14. Lohoff FW, Bloch PJ, Hodge R, Nall AH, Ferraro TN, Kampman KM, Dackis CA, O'Brien CP, Pettinati HM, Oslin DW. Association analysis between polymorphisms in the dopamine D2 receptor (DRD2) and dopamine transporter (DAT1) genes with cocaine dependence. Neurosci Lett. 2010 Apr 5; 473(2):87-91.
15. Ohmoto M, Takahashi T, Kubota Y, Kobayashi S, Mitsumoto Y. Genetic influence of dopamine receptor, dopamine transporter, and nicotine metabolism on smoking cessation and nicotine dependence in a Japanese population. BMC Genet. 2014 Dec 20;15:151.
16. Sieminska A, Buczkowski K, Jassem E, Niedoszytko M, Tkacz E. Influences of polymorphic variants of DRD2 and SLC6A3 genes, and their combinations on smoking in Polish population. BMC Med Genet. 2009 Sep 17;10:92.
17. Nacak M1, Isir AB, Balci SO, Pehlivan S, Benlier N, Aynacioglu S.. Analysis of Dopamine D2 Receptor (DRD2) Gene Polymorphisms in Cannabinoid Addicts. J Forensic Sci. 2012 Nov;57(6):1621-4.

RESEARCH ARTICLE

Overstimulation of β-ARs induces the upregulation of paracrine factors in neonatal rat cardiac myocytes

Narawat Nuamnaichati[1], Vilasinee Hirunpanich Sato[1], Primchanien Moongkarndi[2], Supachoke Mangmool[1]

[1]*Department of Pharmacology, Faculty of Pharmacy, Mahidol University, Bangkok 10400, Thailand*
[2]*Department of Microbiology, Faculty of Pharmacy, Mahidol University, Bangkok 10400, Thailand*

Address correspondence and reprint request to: Supachoke Mangmool, Department of Pharmacology, Faculty of Pharmacy, Mahidol University.
E-mail address: supachoke.man@mahidol.ac.th

Abstract

Overstimulation of β-adrenergic receptor)β-AR(and cardiac injury can cause cardiac myocyte to increase the synthesis and secretion of several growth factors and cytokines (paracrine factors) which could activate cardiac fibroblasts in a paracrine manner and thereafter could lead to cardiac fibrosis. Cardiac fibrosis is characterized by overproduction of extracellular matrix components (e.g., collagen I, collagen III), induction of cardiac fibroblast proliferation, expression pro-contractile protein of myofibroblast (e.g., α-SMA) and stiffening of myocardium, and is often a secondary condition that develops in response to myocardial infarction, hypertension, or heart failure. Therefore, this study aimed to identify which paracrine factors upregulated by β-AR overstimulation and to investigate molecular mechanism of β-AR-mediated upregulation of these paracrine factors in cardiac myocytes. This study reported that overstimulation of β-ARs by isoproterenol (ISO) increased mRNA expression of connective tissue growth factor (CTGF), vascular endothelial growth factor (VEGF) and interleukin-8 (IL-8) in neonatal rat cardiac myocytes. The upregulation of these growth factors and cytokines significantly peaked at 3-6 hours after stimulation and decreased thereafter. Conversely, overstimulation of β-ARs did not significantly induce upregulation of transforming growth factor-beta (TGF-β), insulin-like growth factor-1 (IGF-1), brain-derived neurotrophic factor (BDNF), interleukin-1β (IL-1β), and interleukin-6 (IL-6). Furthermore, ISO did not increase the mRNA expression of CTGF, VEGF and IL-8 in pretreatment with either propranolol (a potent, non-selective β-AR antagonist) or a specific adenylate cyclase inhibitor, 2'3-dideoxyadenosine)ddA(, suggesting these effects of ISO are mediated through cAMP dependent pathway. Moreover, this study showed that paracrine factors released by cardiac myocytes following ISO stimulation were necessary for the induction of cardiac fibroblast proliferation and upregulation of collagen III and of α-SMA, supporting that overstimulation of β-ARs on cardiac myocytes can induce cardiac fibrosis.

Keywords: β-Adrenergic receptor (β-AR), cardiac fibroblast, cardiac fibrosis, cardiac myocyte, cytokine, growth factor, paracrine factor

Introduction

Cardiovascular diseases (CVDs) are the leading cause of morbidity and mortality in the world. In Thailand, the number of patient with heart diseases (e.g., heart failure, angina and myocardial infarction) and hypertension is rising rapidly over decade and has become a major public health problem.

In the heart, β-AR stimulation by catecholamine serves as the powerful regulatory mechanism to enhance myocardial performance and maintenance of cardiac homeostasis[1]. Whereas prolong and overstimulation of β-ARs promotes detrimental signaling to cause several pathological cardiac dysfunction apoptosis, myocardial hypertrophy and heart failure, high blood pressure, and cardiac remodeling such as fibrosis[2,3,4]. In physiological condition, mammalian heart consists of approximately 70% non-myocytic cells (cardiac fibroblasts are the majority of the non-myocytic cells) and 30% cardiac myocytes of the total number cardiac cells[5]. Crosstalk between cardiac fibroblasts and cardiac myocytes is important for both cardiac development and the heart's ability to respond to tissue injury during remodeling.

In the heart, norepinephrine (NE) activates both protein kinase A) PKA(and protein kinase C) PKC(pathways by α_1- and β_1-ARs, respectively and thereby induced cardiac hypertrophy[6, 7]. Furthermore, NE also upregulates VEGF in rat cardiac myocytes by a paracrine mechanism[8], supporting that stimulation of adrenergic receptor of cardiac myocytes induced the releasing of fibrogenic proteins, VEGF to affect on cardiac fibroblasts. In human cardiac cells maintained in primary culture, these cells are able to synthesize and to secrete cytokines such as IL-6 and IL-11[9]. These cytokines could be involved in an autocrine and/or a paracrine networks regulating myocardial cytoprotection, hypertrophy and fibrosis. Baudino et al. also showed consistent data that angiotensin II (Ang II), TGF-β, IL-6, IL-11, VEGF and tumor necrosis factor-alpha (TNF-α) are involved in autocrine and paracrine regulation of myocyte hypertrophy, fibroblast proliferation, and extracellular matrix (ECM) protein turnover and deposition[10]. Moreover, β-AR stimulation by ISO significantly increases gene expression of IL-6. IL-6 protein levels in serum and mouse myocardium are also significantly increased in response to ISO treatment[11]. Thus, it is possible that β-AR overstimulation on the cell surface of cardiac myocytes by ISO increases synthesis and secretion of several paracrine factors. After that, they could stimulate cardiac fibroblasts in paracrine fashion to cause fibroblast proliferation, cell differentiation into myofibroblast, and impaired ECM synthesis. These conditions eventually mediate cardiac fibrosis which develops in response to heart diseases.

Materials and Methods

Reagents

Isoproterenol, propranolol, were purchased from Sigma-Aldrich. 2′,5′-Dideoxy-adenosine (ddA) was purchased from Calbiochem. Dulbecco's Modified Eagle Medium (DMEM), fetal bovine albumin (FBS), 0.25% trypsin-EDTA solution, penicillin/streptomycin (P/S) solution were purchased from Gibco.

Isolation of neonatal rat cardiac myocytes and fibroblasts

The animal in this study were handled according to approved protocol and animal welfare regulations of the author's institutional Review Boards of Faculty of Pharmacy, Mahidol University (Protocol no. PYR002/2556). A Sprague Dawley rat (pregnant) was from National Laboratory Animal Center, Mahidol University. The experiments were performed by using cardiac myocytes and cardiac fibroblasts that were isolated from the ventricles of 1-2 day-old Spraque-Dawley rats. Cardiac myocytes were plated on gelatin-coated plates and cultured in DMEM containing 10% FBS, 5 mM taurine, 1 µg/ml insulin, 1 µg/ml transferrin, 10 ng/ml selenium and 1% (v/v) P/S solution.

mRNA expression analysis

Growth factors (e.g., BDNF, CTGF, IGF-1, TGF-β and VEGF), cytokines (e.g., IL-1β, IL-6, and IL-8), α-SMA and collagen III mRNA expressions were determined by real-time quantitative polymerase chain reaction)RT-qPCR(method. The mRNA purification was conducted using Thermo Scientific GeneJET RNA Purification Kit. Quantitative mRNA analysis was performed on Mx3005p Real Time PCR system using the KAPA SYBR FAST One step RT-qPCR kit following the manufacturer's instructions and expressed as fold over basal.

Cell proliferation assay

Cardiac fibroblast proliferation was assessed by MTT assay, which is based on the transformation of yellow tetrazolium salt of MTT by mitochondria of living cells to an insoluble formazan salt which has purple color. Cardiac fibroblasts ($2x10^4$ cells/well) were plate in 96-well plates in DMEM containing 1% FBS and 1% P/S and incubated overnight. The cells were treated with the medium obtained from ISO-stimulated cardiac myocytes for 24 hours. After that, cells were added 100 µl of MTT solution (concentration 1 mg/ml dissolve in DMEM) to each well and incubated at 37^oC. Untransformed MTT was removed by aspiration, and formazan crystals were dissolved in 100 µl DMSO. The samples were mixed thoroughly and were quantified spectroscopically at absorbance 570 nm using Microplate reader. The percentage of cell viability was calculated according to the following equation.

Cell viability (%) = (Absorbance of treated cells /Absorbance of control cells) x100

Data analysis

All results were showed as mean ± standard error of mean (S.E.M). The different between each group were determined by using analysis of variance (ANOVA). A difference was considered to be statistically significant if the *P* value is less than 0.05.

Results

Overstimulation of β-ARs increased mRNA expressions of CTGF, VEGF and IL-8

We investigated the effects of ISO-mediated β-AR stimulation on upregulation of growth factors and cytokines from neonatal rat cardiac myocytes. We found that ISO

stimulation for 3-6 hours significantly increased the mRNA expression of CTGF, VEGF and IL-8 in neonatal rat cardiac myocytes (Figure 1). Whereas, overstimulation of β-ARs with ISO did not significantly induce the mRNA expression of TGF-β, BDNF, IGF-1, IL-1β, and IL-6 (Figure 2).

β-AR-induced mRNA expression of CTGF , VEGF and IL-8 is dependent of adenylate cyclase (AC)

Our previous results showed that overstimulation of β-ARs played an important role in the synthesis of several growth factors and cytokines, especially CTGF, VEGF and IL-8 in cardiac myocytes. Thus, we next investigated the signaling pathway of β-AR-mediated upregulation of these growth factors and cytokines. After ISO stimulation for 6 hours, the mRNA expression levels of CTGF, VEGF and IL-8 markedly increased compared to that of non-treated group)vehicle : H_2O((Figure 3). ISO did not increase the mRNA expression levels of CTGF, VEGF and IL-8 in the presence of propranolol (a potent, non-selective β-AR antagonist) as pretreatment, suggesting these effects of ISO are mediated through receptor-dependent pathway.

mRNA expression of paracrine factors
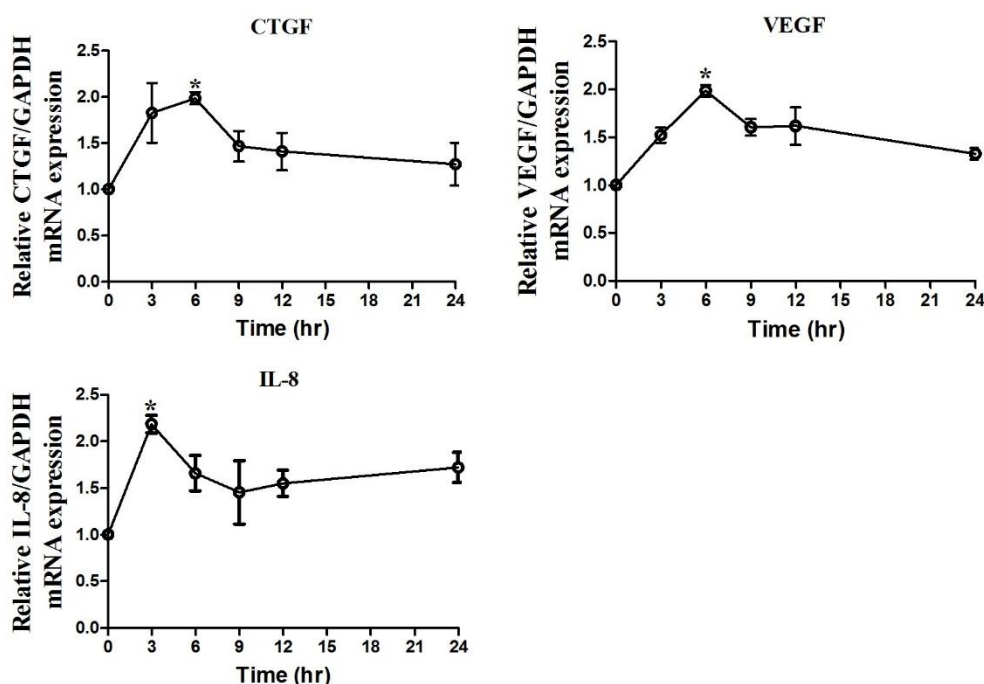
Figure 1. Overstimulation of β-ARs increases mRNA levels of CTGF, VEGF and IL-8. CTGF, VEGF and IL-8 mRNA expression levels in cardiac myocytes were assayed by RT-qPCR. Serum-starved cells were stimulated with 10 μM ISO for the indicated times at 37°C. The mRNA expression was analyzed using specific primer for growth factor and cytokine genes. GAPDH served as a loading control. The mRNA levels were quantified, expressed as fold increase over non-treated group (H_2O) and shown as the mean ± SEM (n=3). ***P*<0.05 versus non-treated group.

mRNA expression of paracrine factors
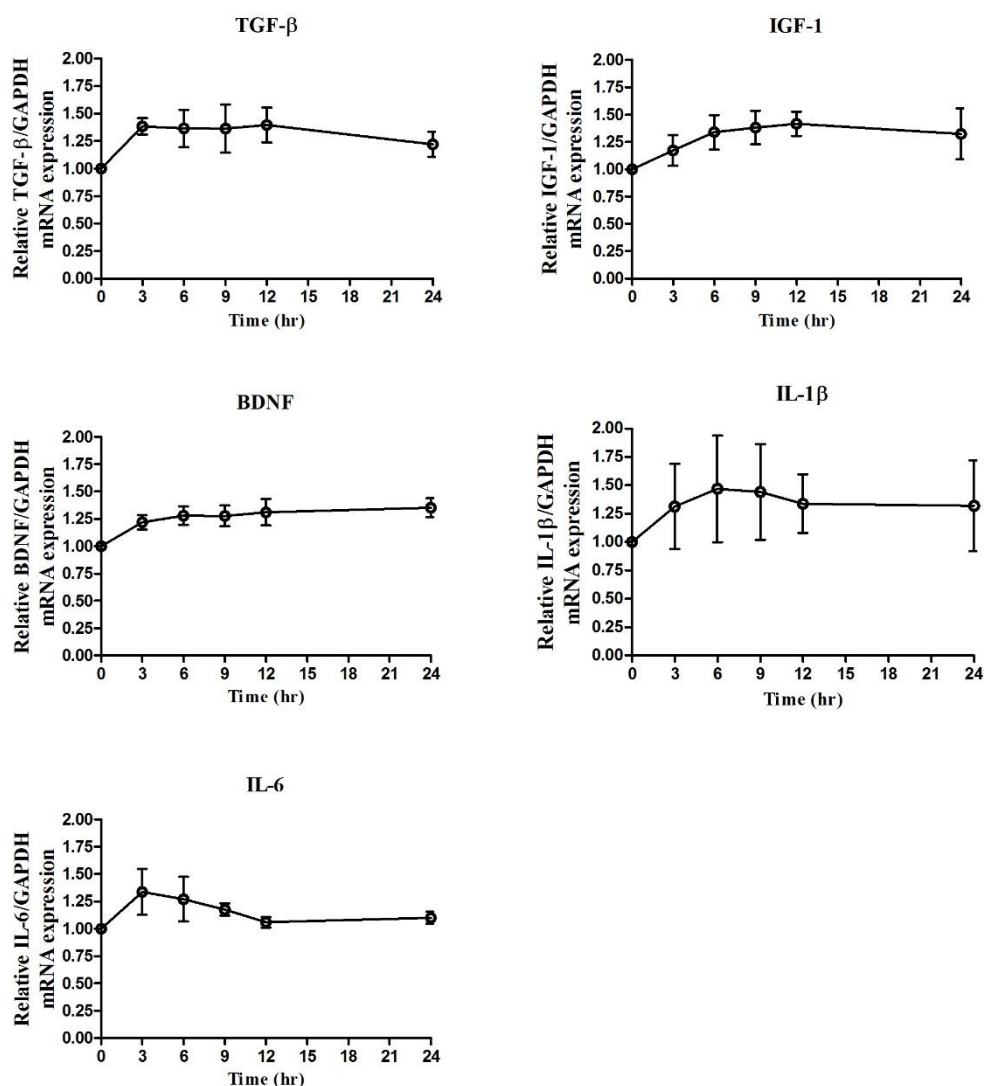
Figure 2. Effects of ISO on mRNA expression of growth factors and cytokines. Growth factors (e.g., TGF-β, IGF, BDNF), and cytokines (e.g., IL-1β, IL-6) mRNA expression levels in cardiac myocytes were assayed by RT-qPCR. Serum-starved cells were stimulated with 10 μM ISO for the indicated times at 37 °C. The mRNA expression was analyzed using specific primer for growth factor and cytokines genes. GAPDH served as a loading control. The mRNA levels were quantified, expressed as fold increase over non-treated group (H_2O) and shown as the mean ± SEM (n=3).
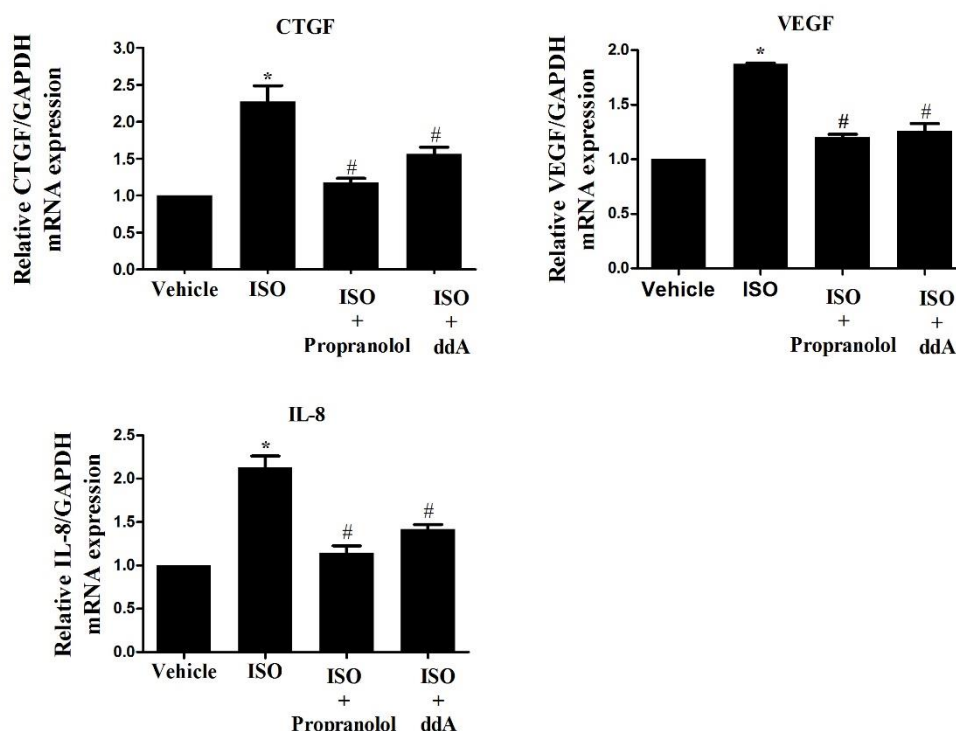
Figure 3. Overstimulation of β-ARs by ISO induced mRNA expression of CTGF, VEGF and IL-8 is dependent of cAMP. Serum-starved cardiac myocytes were pretreated with or without either 10 μM propranolol or 1 μM ddA before treatment with vehicle (DMEM) or 10 μM ISO at 37°C for 6 hours. The mRNA expression was analyzed using specific primer for growth factor and cytokine genes. GAPDH served as a loading control. The mRNA levels were quantified, expressed as fold increase over non-treated group (vehicle: H_2O) and shown as the mean ± SEM (n=3).*P<0.05 versus non-treated group; #P<0.05 versus ISO-stimulated group.

After agonist binding, β-AR can couple with α subunit of heterotrimeric G protein (Gα$_s$), which results in activation of AC, followed by elevation of cAMP levels. We next investigated whether cAMP-dependent pathway plays a role in β-AR-induced the upregulation of CTGF, VEGF and IL-8 in cardiac myocytes. We found that the effects of ISO were inhibited by pretreatment with specific adenylate cyclase inhibitor, 2'3-dideoxyadenosine (ddA) (Figure 3), confirming that β-AR-mediated upregulation of CTGF, VEGF and IL-8 is cAMP dependent.

Paracrine factors released by cardiac myocytes after β-AR overstimulation are required for the induction of cardiac fibroblast proliferation and upregulation of collagen III and of α-SMA.

Based on the results from our experiments, overstimulation of β-ARs mediates the release of growth factors and cytokines from cardiac myocytes. It is possible that these growth factors and cytokines activate cardiac fibroblasts in a paracrine manner. Then, the activated cardiac fibroblasts increase the synthesis of ECM protein, induce cell proliferation, and

enhance the cells differentiation into myofibroblasts which are identified by α-SMA. Thus, we next tested whether the paracrine factors secreted from cardiac myocytes into the medium after β-AR overstimulation can induce cardiac fibroblast proliferation, cardiac fibroblasts differentiation into myofibroblasts and ECM upregulation in a paracrine manner. As shown in figure 4, after ISO stimulation, the medium from culture of cardiac myocytes can cause the cell proliferation of cardiac fibroblasts) Figure 4(. Moreover, cardiac fibroblasts treated with medium from cardiac myocytes following ISO stimulation showed the induction of collagen III and α-SMA mRNA expression (Figure 5). These results suggest the paracrine factors released by cardiac myocytes following ISO stimulation are necessary for the induction of fibroblast proliferation and upregulation of collagen III and of α-SMA, leading to cardiac fibrosis.

Discussion and conclusion

Stimulation of β-ARs induces the release of paracrine factors such as growth factors and cytokines from cardiac myocytes. The paracrine activities of cardiac myocytes are important for regulating the function of cardiac fibroblasts. For instance, NE-mediated β-AR activation induces the upregulation of vascular endothelial growth factor (VEGF) in rat cardiac myocyte. Moreover, β-AR stimulation by ISO significantly increases gene expression of IL-6[8]. Indeed, it is known that catecholamine treatment induces the production and secretion of paracrine factors but, presently, the mechanism by which β-AR activate this effect is largely unknown. In this study, we found that overstimulation of β-AR with ISO significantly increased the gene expressions of CTGF, IL-8, and VEGF (Figure 1), whereas ISO did not increase the production of TGF-α, IGF-1, BDNF, IL-1β, and IL-6 in cardiac myocytes. β-ARs (Gs protein-coupled receptors) signal through a variety of mechanisms that impact cardiac function, including contractility, hypertrophy and remodeling. Gs protein-dependent and G protein-independent (β-arrestin-dependent) pathways each have the capacity to initiate numerous intracellular signaling cascades to mediate these effects[12]. After agonist binding, β-AR can couple with α subunit of heterotrimeric G protein ($G\alpha_s$), which results in activation of AC, followed by elevation of cAMP levels. We found that the effects of ISO were inhibited by pretreatment with specific adenylate cyclase inhibitor, ddA (Figure 3), confirming that β-AR-mediated upregulation of CTGF, VEGF, and IL-8 is cAMP dependent. Previous studies have reported that Ang-II, CTGF, TGF-β, TNF-α, VEGF, IL-6 and IL-11 are related with autocrine and paracrine regulation of myocyte hypertrophy, fibroblast proliferation, fibroblast differentiation into myofibroblast and ECM synthesis[13, 14]. Cardiac remodeling, including cardiac fibrosis is characterized by the induction of cardiac fibroblasts proliferation[15], differentiation into myofibroblasts[16], and excessive production of ECM such as collagen I and collagen III. Our study found that paracrine factors released by cardiac myocytes following ISO stimulation were necessary for the induction of cardiac fibroblast proliferation and upregulation of collagen III and of α-SMA, supporting that overstimulation of β-ARs of cardiac myocytes can induce cardiac fibrosis. We believe that understanding the mechanism of β-AR-mediated production and secretion of paracrine factors in the heart will provide a novel therapeutic strategy against cardiovascular diseases such as cardiac fibrosis.
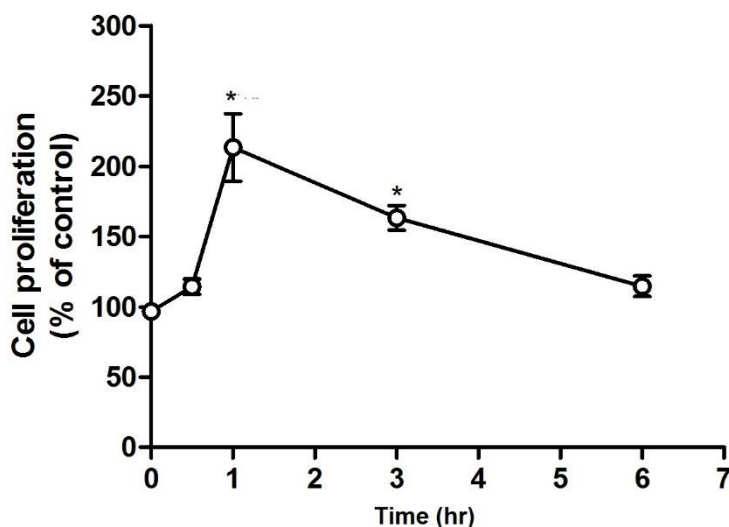
Figure 4. Effects of paracrine factors released by cardiac myocytes following ISO stimulation on induction of cardiac fibroblast proliferation. Cardiac myocytes were treated with or without 10 µM ISO at 37°C for the indicated times. After ISO stimulation, the medium in each well, from stimulated cardiac myocytes, were added into cultured dishes containing cardiac fibroblast and then incubated further at 37°C for 24 hours. Cell proliferation was quantified by MTT assay. The data were expressed as the percentage relative to the non-treated group (H₂O), and shown as the mean ± SEM (n=3). *$P<0.05$ versus non-treated group (H₂O).
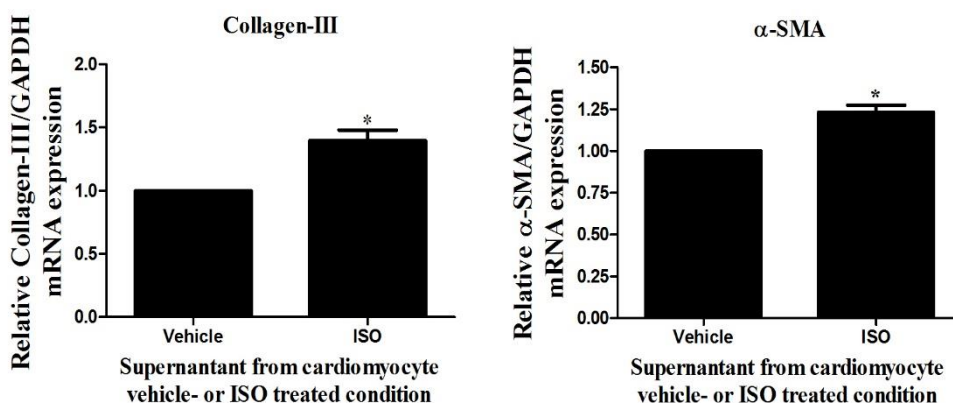
Figure 5. Effects of paracrine factors released by cardiac myocyte following ISO stimulation on collagen III and α-SMA mRNA expression. Cardiac myocytes were treated with or without 10 µM ISO at 37°C for 3 hours. After ISO stimulation, the medium in each well, from stimulated cardiac myocytes, were added into cultured dishes containing cardiac fibroblast and then incubated further for 6 hours. The mRNA expression was analyzed using specific primer for collagen III and α-SMA genes. GAPDH served as a loading control. The mRNA levels were quantified, expressed as fold increase over vehicle (non-treated group : H₂O) and shown as the mean ± SEM (n=3). *$P<0.05$ versus non-treated group.

Acknowledgements

References

1. Rockman HA, Koch WJ, Lefkowitz RJ. Seven-transmembrane-spanning receptors and heart function. Nature. 2002;415:206-12.
2. Zhu WZ, Wang SQ, Chakir K, Yang D, Zhang T, Brown JH, et al. Linkage of β1-adrenergic stimulation to apoptotic heart cell death through protein kinase A–independent activation of Ca2+/calmodulin kinase II. J Clin Invest. 2003;111:617-25.
3. Sun Y, Kiani MF, Postlethwaite AE, Weber KT. Infarct scar as living tissue. Basic Res Cardiol. 2002;97:343-7.
4. Bos R, Mougenot N, Findji L, Médiani O, Vanhoutte PM, Lechat P. Inhibition of Catecholamine-Induced Cardiac Fibrosis by an Aldosterone Antagonist. J Cardiovasc Pharmacol. 2005;45:8-13.
5. Ottaviano FG, Yee KO. Communication Signals Between Cardiac Fibroblasts and Cardiac Myocytes. J Cardiovasc Pharmacol. 2011;57:513-21.
6. Simpson P. Stimulation of hypertrophy of cultured neonatal rat heart cells through an alpha 1-adrenergic receptor and induction of beating through an alpha 1- and beta 1-adrenergic receptor interaction. Evidence for independent regulation of growth and beating. Circ Res.56:884-94.
7. Karliner JS, Kagiya T, Simpson PC. Effects of pertussis toxin on alpha 1-agonist-mediated phosphatidylinositide turnover and myocardial cell hypertrophy in neonatal rat ventricular myocytes. Experientia. 1990;46:81-4. eng.
8. Weil J, Benndorf R, Fredersdorf S, Griese DP, Eschenhagen T. Norepinephrine upregulates vascular endothelial growth factor in rat cardiac myocytes by a paracrine mechanism. Angiogenesis. 2003;6:303-9.
9. Ancey C, Corbi P, Froger J, Delwail A, Wijdenes J, Gascan H, et al. Secretion of il-6, il-11 and lif by human cardiomyocytes in primary culture. Cytokine. 2002;18:199-205.
10. Baudino TA, Carver W, Giles W, Borg TK. Cardiac fibroblasts: friend or foe? Am J Physiol Heart Circ Physiol. 2006;291:1015-26.
11. Yin F, Li P, Zheng M, Chen L, Xu Q, Chen K, et al. Interleukin-6 family of cytokines mediates isoproterenol-induced delayed STAT3 activation in mouse heart. J Biol Chem. 2003;278:21070-5.
12. Tilley DG. G protein-dependent and –independent signaling pathways and their impact on cardiac function. Circ Res. 2011;109:217-30.
13. Zhao T, Zhao W, Meng W, Liu C, Chen Y, Sun Y. Vascular endothelial growth factor-C: its unrevealed role in fibrogenesis. Am J Physiol Heart Circ Physiol. 2014;306:789-96.
14. Leask A. TGF-β, cardiac fibroblasts, and the fibrotic response. Circ Res. 2007;74:207-12.
15. Olson ER, Naugle JE, Zhang X, Bomser JA, Meszaros JG. Inhibition of cardiac fibroblast proliferation and myofibroblast differentiation by resveratrol. Am J Physiol Heart Circ Physiol. 2005;288:1131-8.
16. Naugle JE, Olson ER, Zhang X, Mase SE, Pilati CF, Maron MB, et al. Type VI collagen induces cardiac myofibroblast differentiation: implications for postinfarction remodeling. Am J Physiol Heart Circ Physiol. 2005;290:323-30.

RESEARCH ARTICLE

Anti-inflammatory activities of Thai rice bran extracts

Warintra Sawangsri[1], Primchanien Moongkarndi[2], Malyn Ungsurungsie[3], Supachoke Mangmool[1,4]

[1]*Department of Pharmacology; Faculty of Pharmacy, MahidolUniversity, Bangkok10400, Thailand*
[2]*Department of Microbiology, Faculty of Pharmacy, MahidolUniversity, Bangkok10400, Thailand*
[3]*Research and Development Division, S&J International Enterprises Public Company Limited, Bangkok10120, Thailand*
[4]*Center of Excellence for Innovation in Drug Design and Discovery, Faculty of Pharmacy, MahidolUniversity, Bangkok10400, Thailand*

Address correspondence and reprint request to: Supachoke Mangmool, Department of Pharmacology, Faculty of Pharmacy, Mahidol University, Bangkok 10400, Thailand
E-mail address: supachoke.man@mahidol.ac.th

Abstract

Rice bran extract contains several compounds that have health-supportive properties including anti-inflammation. The inflammation is the mechanism that involves with immune systems by release and synthesis of various pro-inflammatory mediators. However, the anti-inflammatory activities of Thai rice bran extracts has been scarcely studied and so is still unclear. In this study, the anti-inflammatory-activity with molecular mechanisms of Thai rice bran extracts on the inhibition of inflammation in L929 fibroblast cells was performed. Three samples of Thai rice bran extract from *Hom Dang*, *Hom Red Rose*, and *Hom Dum Sukhothai II* were investigated using LPS-stimulated L929 cells. Before studying the anti-inflammatory potentials of these extracts, we tested their cytotoxicity and found that the highest concentration to be non-toxic was 1/10 dilution (v/v).While in the test of cell inflammation, it was observed that the treatment of L929 fibroblast cells with10 µg/ml of LPS for 12 hours significantly increased the mRNA expression of TNF-α, COX-2, IL-6, and IL-10, whereas iNOS was induced remarkably when cells were treated with LPS for 6 hours comparing to the control (vehicle) group. In the study on anti-inflammatory activity, pretreatment of the above cells with the studied Thai rice bran extracts at 1/10 dilution (v/v) reduced the LPS-induced TNF-α and iNOS mRNA expressions, which were similar to the effects shown by indomethacin (10 µM) and dexamethasone (10µM). Among these three Thai rice bran extracts, *Hom Red Rose* bran extract exhibited the highest activity on inhibition of LPS-induced TNF-α and iNOS. All bran extracts, however, tended to inhibit LPS-induced COX-2 and IL-6 mRNA expression. As shown in the results, all three Thai rice bran extracts exhibited anti-inflammatory effects through the inhibition of inflammatory mediator production in LPS-induced L929 cells. In further study, the effects of Thai rice bran extracts on inflammatory mediators (e.g., PGE_2 and TNF-α) secretion will be performed by ELISA technique.

Keywords: Rice bran extract, L929, anti-inflammatory activity, TNF-α, COX-2, IL-6, inflammatory mediators

Introduction

Inflammation is defensive mechanisms, which respond to foreign substances or invading organisms. The results of these mechanisms such as immune responses and phagocytosis or neutralization are beneficial to host. However, inflammation itself can sometime cause symptoms of chronic diseases, including gout, rheumatoid arthritis[1], osteoporosis, diabetes, cancer, bowel diseases[2], atherosclerosis and coronary artery disease[3].

Activated inflammatory cells (e.g. endothelial cells, circulating white blood cells, connective tissue cells, and components of the extracellular matrix) increase the secretion of autacoids, prostanoids, and cytokines that lead to the development of the immune responses. The cyclooxygenase (COX) is an enzyme responsible for formation of prostanoids and its pathway is a well-known target of many anti-inflammatory drugs like NSAIDs. The arachidonic acid is converted into prostaglandins like prostaglandin E_2 (PGE_2) by pro-inflammatory enzymes, COX-1 andCOX-2[4]. In inflammation, prostaglandins have major effects on blood vessels by increasing vascular permeability that causes edema, erythema and pain[1]. The inflammatory cells produce several inflammatory mediators such as inflammatory cytokines (e.g. tumor necrosis factor-α (TNF-α), interleukin-6 (IL-6), interleukin-8 (IL-8), and interleukin-10 (IL-10)) and chemokines. These mediators play an important role in inflammatory processes[5]. Moreover, nitric oxide (NO) is a free radical, which also involves in the inflammatory process. The production of NO is catalyzed by nitric oxide synthase (NOS) such as inducible NOS (iNOS)[6]. NO can induce COX and increase the production of IL-1 and TNF-α[7].

In skin inflammation, skin cells such as keratinocytes, fibroblasts, and endothelial cells are stimulated by antigens and inflammatory stimuli e.g., ultraviolet (UV) radiation, TNF-α, IL-1, and lipopolysaccharide (LPS). These activated skin cells produce cytokines that involve in inflammatory reaction. The skin inflammation can cause chronic inflammatory skin diseases such as psoriasis[8]andskin cancer and aging skin[9].

The LPS is a main component of the outer membrane of gram-negative bacteria. It induces inflammatory responses through Toll-like receptor (TLR) proteins signaling pathways[10]. In fibroblast cells, LPS increases the COX-2 production[11] and cytokines production and secretion especially IL-6 then, plays an important role in the inflammatory stimulation[12]. Overproduction of these inflammatory mediators causes inflammation. Therefore, the inhibition of inflammatory mediator production and secretion is essential in inflammatory disorders treatment.

Rice is a major socio-economic crop product in many countries including Thailand. Its rice bran has been extensively studied to possess several important health-enhancing properties including anti-oxidative, anti-carcinogenic[13], anti-inflammatory, hypocholesterolemic and anti-diabetic[14] effects. The rice bran extracts have been found to compose of well-known micronutrients and phytochemicals e.g., vitamin E[15], gamma-oryzanol, anthocyanin[16], which are strong anti-oxidant agents. It so has been used as ingredient in cosmetic and food

supplement products to help increase moisture and reduce skin wrinkles. There are studies showed some Thai rice bran extracts had the essential ingredients[7] which can be developed for the use in cosmetics and health care products.

Many studies revealed that rice bran extract and its compounds had shown anti-inflammatory effects tested by both cell cultures and animal models such as phytosterylferulate could inhibit NF-κB activity in colitis induced by dextran sulphate sodium in mice targeted to use in therapy and/or prevention of gastro-intestinal inflammatory diseases[17]. In addition, some studies showed that the rice bran extract could inhibit LPS-induced inflammation by decreasing the production and the secretion of many inflammatory mediators such as COX-1, COX-2, IL-6, etc[6].

However, the molecular mechanistic-activity of Thai rice bran extracts on inhibition of LPS-induced inflammation in fibroblast cells from subcutaneous connective tissue (L929; mouse fibroblast cell line) has not been investigated. The purpose of this study is to study anti-inflammatory effects of Thai rice bran extracts in such cells by evaluating their inhibitory potentials on LPS-induced L929 cells and determining the production and secretion of inflammatory mediators from such cells.

Materials and Methods

Chemicals and reagents

Dulbecco's Modified Eagle's Medium (DMEM), Trypsin 0.25% EDTA, fetal bovine serum (FBS), penicillin-streptomycin solution, MTT solution, DMSO were purchased from Biowest Co. (NY, MO, USA), Jena Bioscience Co. (Germany), and Roche (Germany). Lipopolysaccharide (LPS) from *Salmonella enterica* serotype typhimurium and indomethacin were purchased from Sigma-Aldrich (St, Louise, MO, USA). Three Thai rice bran extracts, *Hom Dang*, *Hom Red Rose*, and *Hom Dum Sukhothai II* that were extracted by 50% hydroglycol, were generous gifts from Prof. Malyn Ungsurungsie (Research and development division, SJI, Thailand).

Cell culture

L929 cells were cultured in DMEM with 10% FBS and penicillin-streptomycin solution diluted 1:100 and incubated in a humidified atmosphere of 5% CO_2 incubator under temperature 37°C. Cell were grown in culture dishes and passaged by trypsinization every 3-5 days.

Cell toxicity testing by using MTT assay

The MTT (3-[4,5-dimethylthiazol-2-yl]-2,5-diphenyltetrazolium bromide), a water-soluble yellow tetrazolium salt, is converted to an insoluble purple formazan by active mitochondrial dehydrogenases of living cells. Cell viability was determined by the MTT assay. Briefly, L929 cells were seeded in 96-well culture plates at a 1.0×10^4 cells/well density in 200 μL of DMEM supplemented with 1% FBS for 24 hours before treated with solvent (vehicle

control; DMEM) and the solutions of Thai rice bran extracts 1/100,000 – 2 (v/v; volume per volume from extracts). This experiment was performed in two replicated wells and incubated for 36 hours. The medium was washed out and replaced with 200 μL of DMEM and added 50 μL of MTT solution (2 mg/mL). After incubated for 4 hours, the medium was removed and the formed purple formazan crystals were solubilized with 150 μL of DMSO. The absorbance of treated and control cell plates were read by using a Tecan microplate reader at wavelength 570 nm. The results were the absorption values of the solution at 570 nm, which directly represents relative cell number. The percentage of cell viability was calculated according to the following equation and shown in graph between the percentage of cell viability and solution concentrations.

Cell viability (%) = (absorbance of treated cells / absorbance of control cells) x 100

The mRNA expression of inflammatory mediator measurement

L929 cells were stimulated by 10 μg/ml of LPS to produce inflammatory mediators such as TNF-α, COX-2, IL-6, IL-8, IL-10, and iNOS. These cells were divided into four groups; cells without LPS stimulation (control group; H_2O), cells stimulated by LPS, cells pretreated with the dilution of three Thai rice bran extracts, *Hom Dang*, *Hom Red Rose*, and *Hom Dum Sukhothai II*, at concentration of 1/10 v/v for 1 hour before stimulated by LPS, and cells pretreated with either 10 μM of dexamethasone or 10 μM of indomethacin as positive control for 1 hour before stimulated by LPS. The mRNA expression of inflammatory mediators in each group was determined by RT-qPCR. The mRNA from L929 cells of each group was extracted by using RNeasy kits (Qiagen) and purified by using Thermo Scientific GeneJET RNA Purification Kit. The concentration of mRNA was detected by KAPA SYBR FAST One-step RT-qPCR kits (KAPA Biosystems, Wilmington, MA) and analyzed by Mx 3005p Real Time PCR system (Stratagene) following the manufacturer's instructions. The primer sets designed from mouse are shown in Table 1. Relative mRNA expression levels were normalized to the level of the housekeeping internal control mouse gene, glyceraldehyde-3-phosphate dehydrogenase (GAPDH).

Statistical analysis

Results were expressed as mean ± standard error of mean (S.E.M.). The difference between each group was analyzed by using one-way analysis of variance (ANOVA). The level of significance was set at *P*-value < 0.05.

Results

Cell toxicity of Thai rice bran extracts

MTT assay was performed to evaluate cell toxicity and optimal concentration of the bran extracts from *Hom Dang*, *Hom Red Rose*, and *Hom Dum Sukhothai II* before studying anti-inflammatory activities of these three Thai rice bran extracts in LPS-stimulated L929 cells. The tested extracts were diluted ten-fold and by then run for MTT assay. Results showed that

Hom Dang bran extract at concentration less than 1 v/v was not toxic to L929 cells as cell survival was more than 80% compared with the control (vehicle group). While above such the concentrations or at 1 and 2 v/v, the cell viability of L929 were significantly less than 50% and 20%, respectively, (Figure 1A) when compared with the control. For *Hom Red Rose* bran extract, the concentrations of 1/10– 1/100,000 v/v were not toxic to L929 cells, but at 1 and 2 v/v, the cell viability of L929 were significantly decreased to be only 30% and 15%, respectively, compared with the control (Figure 1B). In case of *Hom Dum Sukhothai II* bran extract at 1– 1/100,000 v/v, the cell viability of L929 were more than 70% which showed non-toxic to L929 cells, while the two-fold dilution decreased cell viability to 16% compared with the control (Figure 1C).

Table 1. Gene specific primers for RT-qPCR (mouse)

Gene specific primer		Sequences
TNF-α	Sense	5′-ATGAGCACAGAAAGCATGATC-3′
	Antisense	5′-TACAGGCTTGTCACTCGAATT-3′
COX-2	Sense	5′-TGCATGTGGCTGTGGATGTCATCAA-3′
	Antisense	5′-CACTAAGACAGACCCGTC ATCTCCA-3′
IL-6	Sense	5′-GACAAAGCCAGAGTCCTTCAGAGAG-3′
	Antisense	5′-CTAGGTTTGCCGAGTAGATCTC-3′
IL-8	Sense	5′-ATGACTTCCAAGCTGGCCGTG-3′
	Antisense	5′-TTATGAATTCTCAGCCCTCTTCAAAAACTTCTC-3′
IL-10	Sense	5′-GCTGGACAACATACTGCTAACC-3′
	Antisense	5′-ATTTCCGATAAGGCTTGGCAA-3′
iNOS	Sense	5′-GTGTTCCACCAGGAGATGTTG-3′
	Antisense	5′-CTCCTGCCCACTGAGTTCGTC-3′
GAPDH	Sense	5′-GCCTGCTTCACCACCTTC-3′
	Antisense	5′-GGCTCTCCAGAACATCATCC-3′
COX-1	Sense	5′-AGTGCGGTCCAACCTTATCC-3′
	Antisense	5′-CCGCAGGTGATACTGTC GTT-3′
IL-1β	Sense	5′-CAGGATGAGGACATGAGCACC-3′
	Antisense	5′-CTCTGCAGACTCAAACTCCAC-3′
TGF-β1	Sense	5′-GCGGACTACTATGCTAAAGAGG-3′
	Antisense	5′-GTAGAGTTCCACATGTTGCTCC-3′

The effects of Thai rice bran extracts on inflammatory mediator production.

Before measured the effects of Thai rice bran extracts on inflammatory mediator production, the inflammatory stimulation of LPS was investigated by measurement of mRNA expression using RT-qPCR. L929 cells were stimulated with 10 µg/ml LPS at 1, 3, 6, 12, and 24 hours. After treatment with LPS for 12 and 24 hours, the mRNA expression of TNF-α was significantly increased when compared with the control (0hr) (Figure 2A). For COX-2, the mRNA expression was significantly increased by LPS for 6, 12, and 24 hours compared with the control (0hr) (Figure 2B). However, the mRNA expressions of IL-6 and IL-10 were increased after treatment with LPS for 12 hours (Figure 2C and D, respectively). In addition,

treatment with LPS significantly increased the iNOS mRNA expression and reached to the maximum level after 6 hour LPS stimulation (Figure 2E).
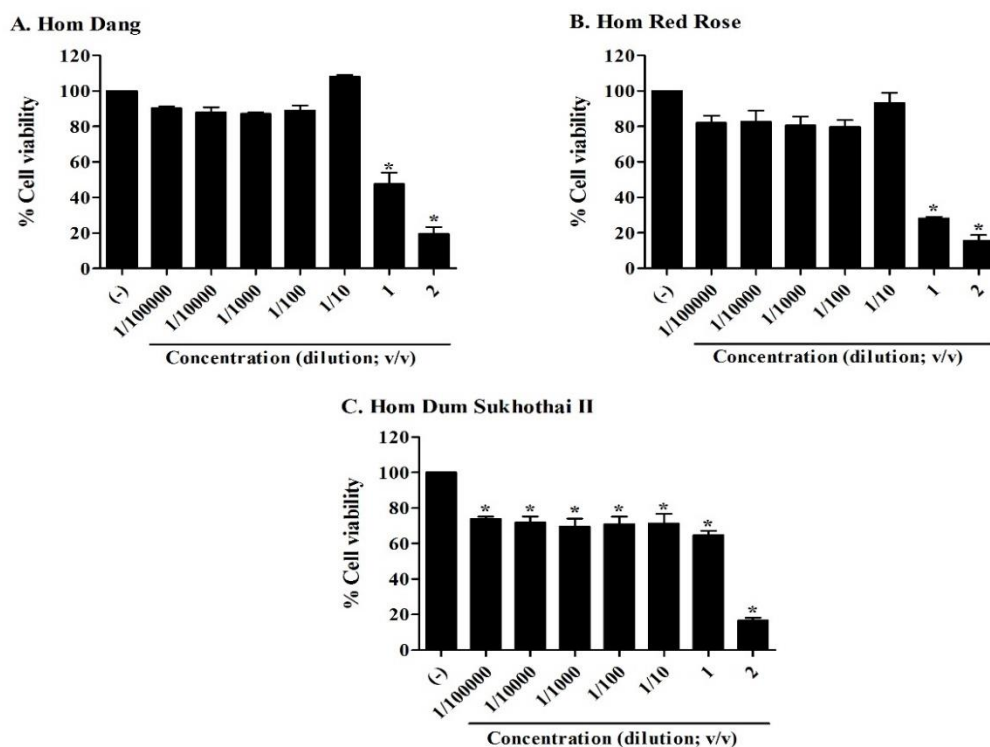
Figure 1. Cell viability of Thai rice bran extracts on L929 cells by MTT assay. L929 cells were treated with the dilution of Thai rice bran extracts, *Hom Dang* (A), *Hom Red Rose* (B), and *Hom Dum Sukhothai II* (C), respectively, at concentrations of 1/100,000 – 2 (v/v; volume per volume from extracts) for 36 hours. Cell viability were shown as mean ± SEM (n=3). *$P<0.05$ vs. the control.
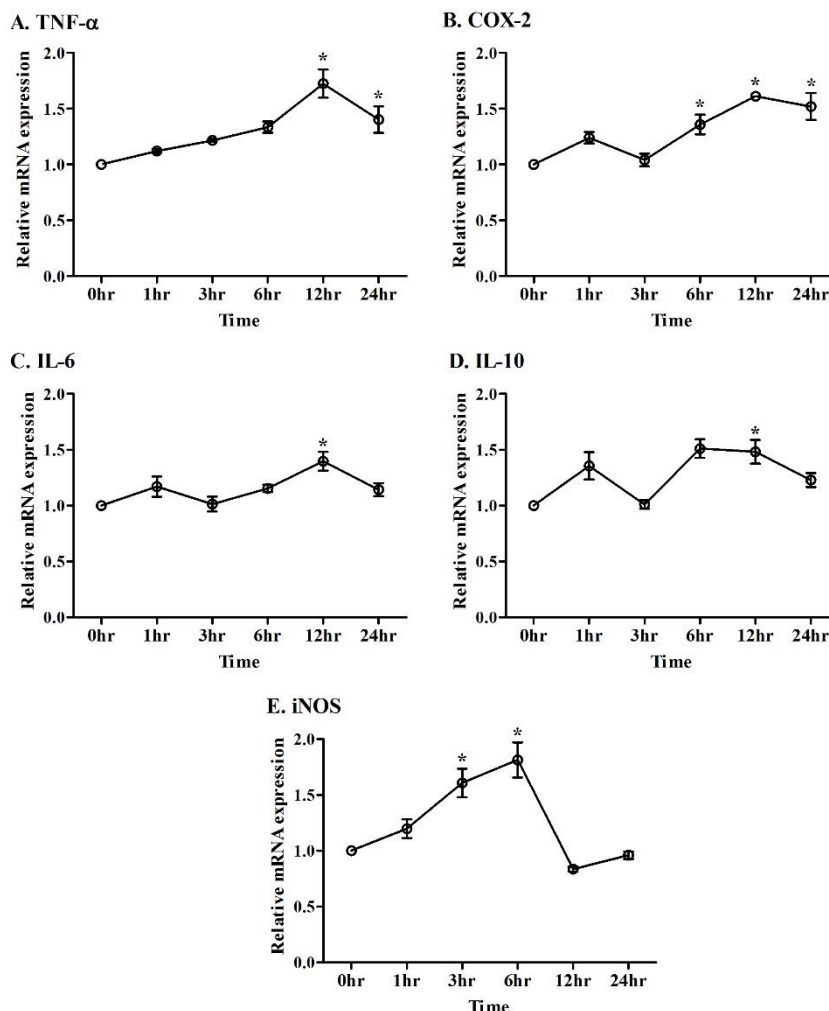
Figure 2. The changes in the mRNA expressions of TNF-α, COX-2, IL-6, IL-10, and iNOS in LPS-stimulated L929 cells at various time points by RT-qPCR(A-E). L929 cells were stimulated by 10 µg/ml of LPS at 1, 3, 6, 12, and 24 hours. Relative TNF-α (A), COX-2 (B), IL-6 (C), IL-10 (D) and iNOS (E) mRNA levels were quantified and shown as the mean ± SEM (n=3).*$P<0.05$ vs. the control (vehicle group).

However, treatment with LPS did not increase the mRNA expressions of IL-8, COX-1, IL-1β, and TGF-β1 (Figure 3A-D).
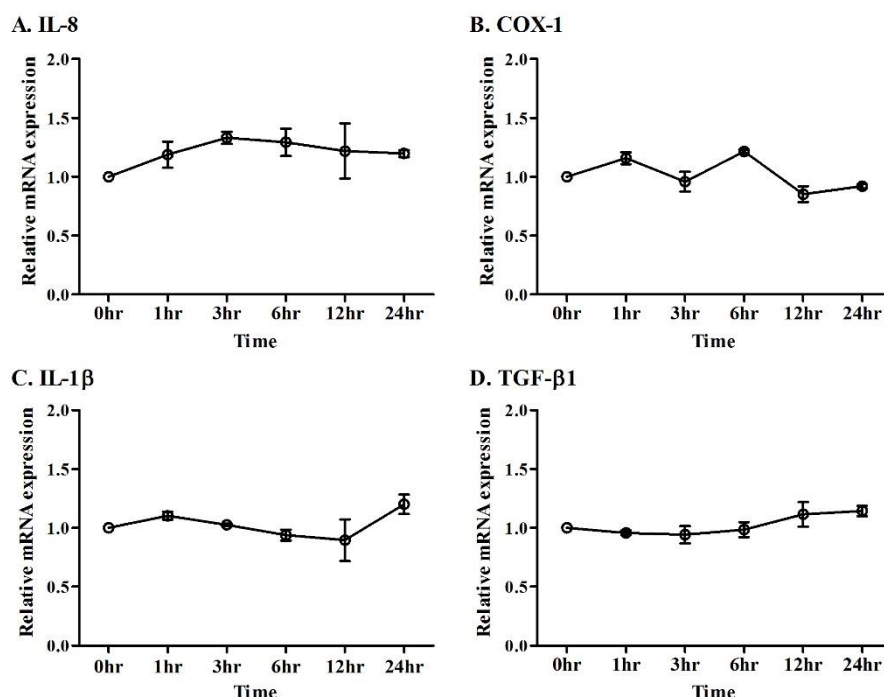
Figure 3. The changes in the mRNA expressions of IL-8, COX-1, IL-1β, and TGF-β1 in LPS-stimulated L929 cells at various time points by RT-qPCR. (A-D)L929 cells were stimulated by 10 µg/ml of LPS at 1, 3, 6, 12, and 24 hours. Relative IL-8 (A), COX-1 (B), IL-1β (C) and TGF-β1 (D) mRNA levels were quantified and shown as the mean ± SEM (n=3).*$P<0.05$ vs. non-stimulation (0 hour).

To determine the anti-inflammatory activities of Thai rice bran extracts, L929 cells were pretreated with dilutions of Thai rice bran extracts for 1 hour before stimulated by 10 µg/ml LPS for 12 hours. The levels of mRNA of inflammatory mediators in treatment with Thai rice bran extracts dilutions were evaluated and compared with the untreated cells by using RT-qPCR. The changes in the mRNA expressions of TNF-α, COX-2, IL-6, IL-10and iNOS as relative ratio to GAPDH are shown in Figure 4. The dilutions of *Hom Dang*, *Hom Red Rose*, and *Hom Dum Sukhothai II* bran extracts significantly reduced the up-regulated the mRNA expressions of TNF-α (Figure 4A) and iNOS (Figure 4B) compared with no treatment in LPS-stimulated L929 cells which showed the similar results to those of indomethacin and dexamethasone. Moreover, treatment with these three Thai rice bran extracts tended to inhibit LPS-induced COX-2 and IL-6 mRNA expression (Figure 4C and 4D, respectively). Taken together, these results indicated that Thai rice bran extracts exhibit the anti-inflammatory activity in L929 cells by inhibiting LPS-induced inflammatory mediator production.
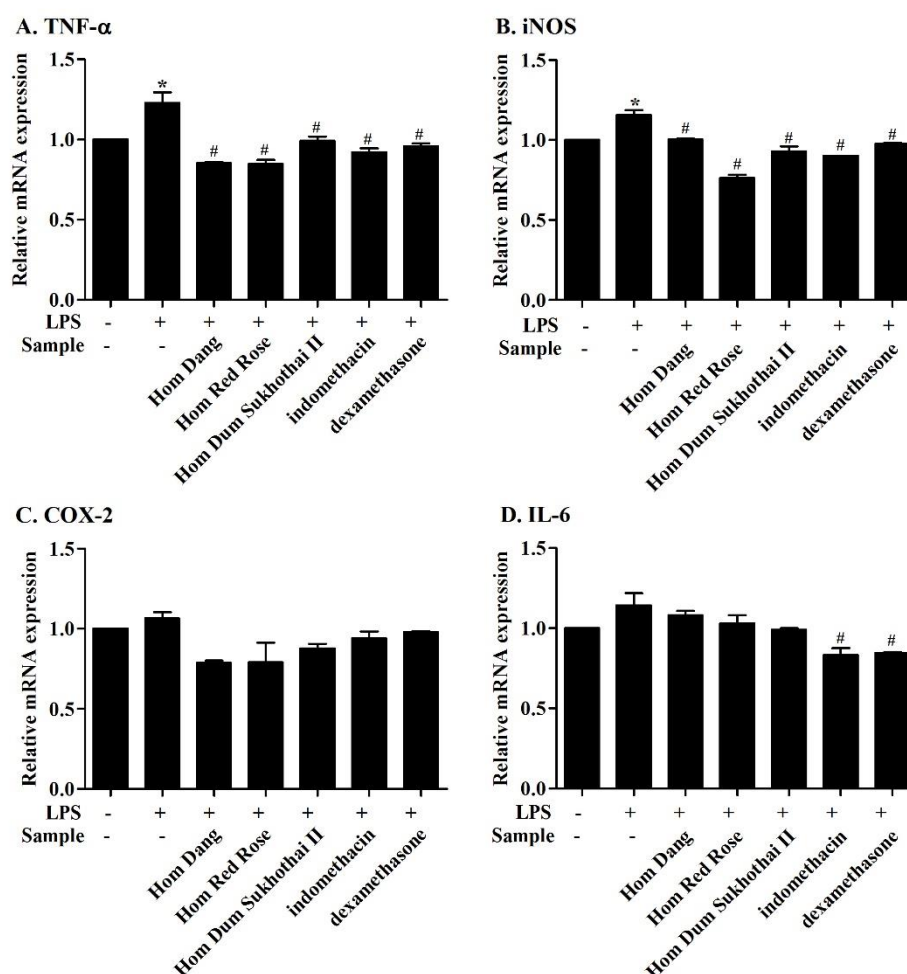
Figure 4. The changes in the mRNA expressions of TNF-α (A), iNOS (B), COX-2 (C), and IL-6 (D) in LPS-stimulated L929 cells by RT-qPCR. L929 cells were treated with the dilutions of *Hom Dang*, *Hom Red Rose*, and *Hom Dum Sukhothai II* extracts at concentration of 1/10 (v/v; volume per volume from extracts) for 1 hour before stimulated by 10 µg/ml LPS for 12 hours. Relative TNF-α (A), iNOS (B), COX-2 (C), and IL-6 (D) mRNA levels were quantified and shown as the mean ± SEM (n=3).*P<0.05 vs. control; #P<0.05 vs. LPS stimulation.

Discussion and Conclusion

The skin is an important defense to the invasion from outside the body as well as for maintenance the homeostasis inside. Innate immunity is the first line of defense in the skin. To counterattack the invasion, the innate immunity induces inflammatory mediators, including cytokines and chemokines. However, these inflammatory mediators can cause chronic inflammatory diseases and also induce prematurely aged in skin[18]. Fibroblast is one type of skin cells, which can be stimulated by antigen and inflammatory stimuli and produces inflammatory mediators[8]. Rice bran has many healthy benefits, including anti-inflammation[14]. Rice bran extract has anti-inflammatory effects in both cell line and animal experiments[19,6].

It was found that the dilutions of *Hom Dang*, *Hom Red Rose*, and *Hom Dum Sukhothai II* bran extracts at 1/10 v/v were not toxic to L929 cells and this concentration was used to

evaluate the inhibition of L929 cells-induced inflammatory mediators production and secretion. To induced intracellular inflammation, we used LPS as chemical-stimulant. The LPS can increases the production of COX-2[11] and cytokines production and secretion in fibroblast cells[12]. The time point for stimulate L929 cells by LPS was detected by using RT-qPCR. After stimulating the cells by LPS for 12 hours, the mRNA expressions of TNF-α, COX-2, IL-6, and IL-10 were significantly increased compared with the control. However, the production of IL-8, COX-1, IL-1β, and TGF-β1 were not significantly increased by LPS stimulation in L929 cells.

The effects on inflammatory mediator production, the treatment with the dilutions of *Hom Dang*, *Hom Red Rose*, and *Hom Dum Sukhothai II* bran extracts significantly exhibited the reduction of TNF-α and iNOS mRNA expressions, especially the dilution of *Hom Red Rose* bran extract. It had the greatest inhibition activities. Moreover, treatment with the dilutions of these three Thai rice bran extracts presented the reduction of the TNF-α and iNOS mRNA expressions similar to positive controls, indomethacin 10 µM and dexamethasone 10 µM.

As the study of germinated brown rice extract[6], the extract also has anti-inflammatory effects by inhibiting protein expressions of iNOS, COX-2, TNF-α, IL-1β, and IL-6 compared with LPS-induced macrophage cells. Unfortunately, we could not demonstrate that IL-1β mRNA expression was significantly increased with LPS stimulation in L929 cells, so we cannot use to detect anti-inflammatory activity. Moreover, the treatment with *Hom Dang*, *Hom Red Rose*, and *Hom Dum Sukhothai II* bran extracts did not show significantly decrease the mRNA expressions of COX-2 and IL-6 on LPS-induced L929 cells but we could see the tendency of inhibition.

In addition, these three of Thai rice are the colored rice. Previously, the components of colored rice bran extracts were investigated anti-inflammatory effects such as gamma-oryzanol and anthrocyanin. The gamma-oryzanol in colored rice bran extracts had strong inhibition activity on the NO production in LPS-IFN-γ-activated macrophage cells compared with the control gamma-oryzanol[7]. Also as Anthrocyanidins, the sugar-free counterparts of anthrocyanins, possessed anti-inflammatory activities by inhibiting COX-2 expression in LPS-stimulated macrophage cells and iNOS protein/mRNA expression in LPS-induced murine macrophage cells[20,21]. Some studies have revealed that the anthrocyanidins inhibited nuclear translocation of nuclear factor-kappa B (NF-κB) by inhibiting on degradation of IκB-α and also suppressed NF-κB through down-regulation of MAPK pathways[20,22].

Therefore, many components in colored rice bran extracts were found to be anti-inflammatory agents. As shown in our results, all three Thai rice bran extracts exhibited anti-inflammatory effects by inhibiting the production of inflammatory mediators. In further study, we will study the effects of Thai rice bran extracts on inflammatory mediator secretion such as PGE_2 and TNF-α.

Acknowledgements

References

1. FurstDE, Munster T. Nonsteroidal anti-Inflammatory drugs, disease-modifying antirheumatic drugs, nonopioid analgesics, & drugs used in gout. In: Fultin J, Ransom J, Nogueira I, Davis K, editors. Basic & clinical pharmacology. 8th ed. New York:McGraw-Hill; 2001.p. 596-623.
2. Libby P. Inflammatory mechanisms: The molecular basis of inflammation and disease. Nutri Rev. 2007;65(12):140-6.
3. Hansson GK. Inflammation, atherosclerosis, and coronary artery disease. N Engl J Med. 2005;352:1685-95.
4. Roschek B, Fink R, Li D, McMichael M, Tower C, Smith R, ed al. Pro-inflammatory enzymes, cyclooxygenase 1, cyclooxygenase 2, and 5-lipooxygenase, inhibited by stabilized rice bran extracts. J Med Food. 2009;12(3): 615–23.
5. Sperber K. Mononuclear phagocytic cells. In: Sigal LH, Ron Y, editors. Immunology and inflammation: basic mechanisms and clinical consequences. Singapore: McGrew-Hill; 1994. p. 330-2.
6. Debneth T, Park SR, Kim da H, Jo JE, Lim BO. Anti-oxidant and antiinflammatory activities of Inonotus obliquus and germinated brown rice extracts. Molecules. 2013;18:9293-304.
7. Chalermpong S. Antioxidant and anti-inflammatory activities of gamma-oryzanol rich extracts from Thai purple rice bran. J Med Plants Res. 2012;6(6):1070-7.
8. Mantovani A, DinarelloCA, Ghezzi P**. Pharmacology of cytokines**.1st ed. Oxford : Oxford University Press; c2000.
9. Bennett MF, Robinson MK, Baron ED, Cooper KD. Skin immune systems and inflammation: protector of the skin or promoter of aging?. J Investig Dermatol Symp Proc. 2008;13(1):15-9.
10. Miyake K. Innate recognition of lipopolysaccharide by Toll-like receptor 4–MD-2. Trends Microbiol. 2004;12(4): 186–192.
11. Noguchi K, Shitashige M, Yanai M, Morita I, Nishihara T, Murota S, et al. Prostagladin production via induction of cyclooxygenase-2 by human gingival fibroblasts stimulated with lipopolysaccharides. Inflammation. 1996;20:555-68.
12. Kent LW, Rachemtulla F, Michalek SM. Interleukin (IL)-1 and Porphyromonas gingivalis lipopolysaccharide stimulation of IL-6 production by fibroblasts derived from healthy or periodontally diseased human gingival tissue. J Periodontol. 1999;70:274-82.
13. Kim SP, Kang MY, Nam SH, Friedman M. Dietary rice bran component γ-oryzanol inhibits tumor growth in tumor-bearing mice. Mol Nutr Food Res. 2012;56(6):935-44.
14. Lai MH, ChenYT, Chen YY, Chang JH, Cheng HH. Effects of rice bran oil on the blood lipids profiles and insulin resistance in type 2 diabetes patients. J Clin Biochem Nutr. 2012;51(1):15-8.
15. Chotimakorn C, Benjakul S, Silalai N. Antioxidant components and properties of five long-grained rice bran extracts from commercial available cultivars in Thailand. Food Chem. 2008;111:636-41.

16. Choi SP, Kim SP, Kang MY, Nam SH,Friedman M. Protective Effects of Black Rice Bran against Chemically-Induced Inflammation of Mouse Skin. J Agric Food Chem. 2010;58:10007-15.
17. Islam MS, Murata T, Fujisawa M, Nagasaka R, Ushio H, Bari AM, et al. Anti-inflammatory effects of phytosteryl ferulates in colitis induced by dextran sulphate sodium in mice. Br J Pharmacol. 2008;154(4):812-24.
18. Geusens B, Mollet I, Anderson CD, Terras S, Roberts MS, Lmbert J. Changes in skin immunity with age and disease. In: Dayan N, Wertz PW, editors. Innate immune system of skin and oral mucosa: Properties and impact in pharmaceutics, cosmetics, and personal care products. Singapore: A John willey & Sons, Inc.; 2011. p. 217-50.
19. Park DK, Park HJ. Ethanol extract of Antrodia camphorata Grown on germinated brown rice suppresses inflammatory responses in mice with acute DSS-induced colitis. Evid Based Complement Alternat Med. 2013;2013:1-12.
20. Hou DX, Yanagita T, Uto T, Masuzaki S, Fujii M. Anthocyanidins inhibit cyclooxygenase-2 expression in LPS-evoked macrophages: structure-activity relationship and molecular mechanism involved. Biochem. Pharmacol. 2005; 70:417-425.
21. Hämäläinen M, Nieminen R, Vuorela P, Heinonen M, Moilanen E. Anti-inflammatory effects of flavonoids: genistein, kaempferol, quercetin, and daidzein inhibit STAT-1 and NF-κB activations, whereas flavone, isorhamnetin, naringenin, and pelargonidin inhibit only NF-κB activation along with their inhibitory effect on iNOS expression and NO production in activated macrophages. Mediators Inflamm. 2007:1-10.
22. Jeong JW, Lee WS, Shin SC, Kim GY, Choi BT, Choi YH. Anthocyanins downregulate lipopolysaccharide-induced inflammatory responses in BV2 microglial cells by suppressing the NF-κB and Akt/MAPKs signaling pathways. Int J Mol Sci. 2013;14(1):1502-15.

RESEARCH ARTICLE

In vitro activity of pomelo relevant to treatment of Alzheimer's disease.

Piangkamol Sonphueng[1], Pornthip Waiwut[2], Yoawared Chulikhit[1], Supawadee Doadee[1], Chantana Boonyarat[1]*

[1]*The Faculty of Pharmaceutical Sciences, Khon Kaen University, Khon Kaen 40002, Thailand*
[2]*The Faculty of Pharmaceutical Sciences, Ubon Ratchathani University, Ubon Ratchathani 34190, Thailand*

*Address correspondence and reprint request to: Chantana Boonyarat, The Faculty of Pharmaceutical Sciences, Khon Kaen University, Khon Kaen 40002, Thailand
E-mail address: chaboo@kku.ac.th

Abstract

In searching for a promising candidate for treatment of Alzheimer/dementia, the effect of the ethanol extract of pomelo cultivar "Kao Numpueng" (KN) on pathological cascade of Alzheimer's disease (AD) was investigated by *in vitro* and cell culture models. The result exhibited that the ethanol extract of KN showed antioxidant activity by both 2,2′-azino-bis-3-ethylbenzthiazoline-6-sulphonic acid (ABTS) and 1,1-diphenyl-2-picrylhydrazyl (DPPH) assay with IC_{50} values of 0.29 and 0.95 mg/mL, respectively. The result from Ellman method indicated that the KN extract could not inhibit acetylcholinesterase function. In addition, for ThioflavinT assay which studies an effect on beta amyloid aggregation indicated that the KN extract at the concentration of 0.1 mg/mL was able to inhibit beta amyloid aggregation with inhibitory percentage value of 22.92. From the neuroprotection study in cell culture revealed that the ethanol extract of KN could reduce neuronal death induced by oxidative stress and beta amyloid toxicity. The overall results indicated that the KN extract possesses multimode of action involved with AD pathology cascade including antioxidant, anti-aggregation of beta amyloid, and neuroprotection against oxidative stress and beta amyloid toxicity. Thus, the pomelo cultivar "Kao Numpueng" might be a potential candidate for further developing as drug for Alzheimer's disease

Keywords: Pomelo, Alzheimer, antioxidant, beta amyloid aggregation inhibitor, acetylcholinesterase inhibitor, neuroprotection

Introduction

Alzheimer's disease (AD) is a multifaceted neurodegenerative disorder characterized by loss of memory, progressive deficits in cognitive functions, and severe behavioral abnormalities. Currently, AD is increasing in elder people over 65 years and affects over 35 million people worldwide[1]. In line with an increase in average life expectancy, the number of affected persons is expected to triple by 2050 if the lack of an efficient treatment persists[2]. Thus, AD is considered one of essentially troublesome diseases for Public Health System.

The cause of AD is unclear, but it has been found to be related with the decrease of acetylcholine neurotransmitter, the accumulation of beta amyloid (Aβ) and neurofibrillary triangle and the occurrence of oxidative stress (OS)[3-6]. Todate, only four drugs in the market, including donepezil, galantamine, rivastigmine and memantin, have been approved for AD treatment[7]. However, these drugs that modulate such a single target could only enable a palliative treatment instead of curing or preventing AD. Due to the multi-pathogenesis of AD, the classical approach modulating at one target may be inadequate in this complex disease. Therefore, searching the candidates acting at multiple sites of pathologic cascade has become a new strategy for development of new drugs for AD. In recent years, plant-derived drug research has become more promising and also a better alternative for synthetic medicine and therapeutics in spite of many challenges. Natural plant, a rich source of biological and chemical diversity, may be a potential multi-target drug for treatment of AD. Several natural plants, vegetables and fruits were developed and researched to cure and prevent AD including ginkgo[8], Brahmi[9], Blueberry[10] .

Pomelo (*Citrus grandis* (L.) Osbeck) is the largest citrus fruit. Many cultivars are grown in Thailand including Tong Dee, Tha. Knoi, Kao Yai, Kao Paen, Kao Nampheung, Kao Tanggwa, Kao Hom, Kao Phuang and Pattavee [11] . Citrus fruits have been recognized as a good source of bioactive compounds including carotenoids, flavonoids, and linonoids. Citrus fruit extracts are also found to have active anti-inflammatory, anti-tumor, anti-fungal and blood clot inhibition properties[12]. However, the effect of citrus fruit on neurodegenerative diseases especially AD have not been reported. Therefore, the aim of our study was to evaluate the effects of the pomelo cultivar "Kao Numpueng" extract on the biological activities related AD pathological cascade, namely antioxidant, AChE activity and Aβ aggregation. In addition, the neuroprotective effects against oxidative stress and Aβ toxicity of the extracts were also investigated in a cell culture model.

Materials and Methods

Materials

Analytical grade reagents were purchased from Sigma-Aldrich (SM Chemical supplies Co., Ltd, Thailand), Merck (Merck, Thailand) and Fluka (SM Chemical supplies Co., Ltd, Thailand) and were used as supplied. All solvents were routinely distilled prior to use.

Preparation of sample

The pomelo cultivar "Kao Numpueng" (KN) were collected from Chaiyaphum provinces, Thailand. Dried and finely powdered fruit pulp of KP (250 g) was extracted with 1 L of ethanol at room temperature for 7 day. The extract was evaporated by a rotary evaporator and then kept at -20°C until analysis.

1. *In vitro antioxidant activity assays [13,14]*

The radical scavenging activity of the ethanol extract of KN was measured by both the 2,2′-azino-bis-3-ethylbenzthiazoline-6-sulphonic acid (ABTS) and 1,1-diphenyl-2-picrylhydrazyl (DPPH) method.

The ABTS was dissolved in water to obtain a 7 mM concentration of ABTS stock solution. ABTS radical cation (ABTS$^{•+}$) was generated by adding 2.45 mM potassium persulfate to the ABTS stock solution and keeping it in the dark at room temperature for 12–16 h. The ABTS$^{•+}$ solution was diluted with ethanol to give an absorbance of 0.70±0.02 at 734 nm. The 50 µL of the test compounds were allowed to react with 100 µL of ABTS$^{•+}$ solution. The absorbance was taken 15 min after initial mixing. Trolox was used as a standard.

The DPPH assay was performed as described by Pichaiyongvongdee. One hundred µL of the test compound was added to 100 µL of 0.2 mM DPPH solution. After a 30 min of reaction at room temperature, the absorbance of the solution was measured at 517 nm. The free radical scavenging activity of each fraction was determined by comparing its absorbance with that of a control. The ability to scavenge the DPPH radical was calculated using the following equation:

$$\text{DPPH scavenging activity (\%)} = (A0 - A1)/A0 \times 100$$

Where A0 is the absorbance of the control and A1 is the absorbance of the sample.

2. *In vitro AChE inhibitory activity assay [15]*

The ethanol extract of KN was investigated for their acetylcholinesterase (AChE) inhibitory activity through the modified Ellman's spectrophotometric method. The assay was performed in 96-well plate by adding 25 µL of 1 mM acetylthiocholine iodide used as substrate in the assay, 125 µL of 1 mM 5, 5'-dithiobis-(2 nitrobenzoic acid) (DTNB), 25 µL of 0.1 M phosphate buffer pH 7.4, 25 µL of the extracts in various concentrations and 50 µL of 0.2 Units/ml AChE from an electric eel (type VI-S), respectively. At least five concentrations of the test compounds were assayed. The absorbance changes at 405 nm were detected every 30 s over the period of 5 min with a microplate reader. The enzyme activity and the percent inhibition were determined.

3. *In vitro assay for AB aggregation inhibition by thioflavin T assay [16]*

Thioflavin-T (ThT) fluorescence assay was used to monitor the aggregation state of Aβ1–42. The assay was performed as described by Levine with minor modification. Briefly, twenty-five µM of Aβ1–42 in 50 mM phosphate buffer, pH 7.4, was incubated at 37 °C with various concentrations of the extract for 48 h. After incubation, the samples were mixed with 50 µM glycine/NaOH buffer (pH 9.2) containing 5 µM ThT. Fluorescence intensities were measured at an excitation wavelength of 446 nm and an emission wavelength of 490 nm. The fluorescence intensities were recorded, and the percentage of inhibition on aggregation was calculated by using the following equation: (1 - IFi/IFc) * 100% in which IFi and IFc were the

fluorescence intensities obtained for absorbance in the presence and absence of the test compound, respectively, after subtracting the background fluorescence of 5 μM ThT in the blank buffers.

4. Effect on H_2O_2-induced oxidative cell damage in neuroblastoma cells [17]

Neuroblastoma cells (SH-SY5Y) were cultured in Dulbecco's Modified Eagle Medium (DMEM)/F12 containing 50 IU/ml penicillin, 50 g/ml streptomycin, 2 mM L-glutamine, and 10% fetal bovine serum. Cultures were maintained at 37ºC in a humidified incubator in an atmosphere of 5% CO_2. For assays, the SH-SY5Y cells were seeded in a 96-well plate and incubated for 48 h. After this incubation period, the cells were treated with various concentrations of test compounds for 2 h. After removing the unabsorbed test compounds, the cells were treated with hydrogen peroxide (H_2O_2) for 2 h to induce oxidative stress. The cell viability was determined by 3-(4,5-dimethyl-2-thiazolyl)-2,5-diphenyl-2H-tetrazolium bromide (MTT) colorimetry. The optical density of each well was measured at 55o nm in a microplate reader.

5. Effect on Aβ-induced cell damage in neuroblastoma cells [17]

Lyophilized Aβ1-42 (Sigma) was reconstituted in sterile water at a concentration of 2 mM and keep at -80 °C until use. Aliquots were diluted with a culture medium to achieve a final concentration of 25 μM and then incubated at 37°C for 72 h to form aggregated amyloid.

Neuroblastoma cells (SH-SY5Y) were cultured in Dulbecco's modified Eagle's medium (DMEM) /F12 containing 50 IU/ml penicillin, 50 g/ml streptomycin, 2 mM L-glutamine, and 10% fetal bovine serum. Cell cultures were maintained at 37°C in an atmosphere of 95% humidified air and 5% CO_2. For assays, SH-SY5Y cells were sub-cultured into a 96 well plate for 24 h. Then, the cells were incubated with aggregated Aβ1-42 (25 μM) without or with various concentrations of the extract for 24 h. Cell viability was determined by staining the cells with 0.5 mg/mL of MTT. The absorption was measured by a well plate reader at 550 nm.

Statistical analysis

The results are expressed as mean $\pm$ SD (n = 4-6). Statistical significance was determined by one way analysis of variance (ANOVA). For all statistical analysis, significance levels were set at p value < 0.05.

Results and discussion

Due to the multi-pathogenesis of AD, the agents acting at multiple sites of pathologic cascade seem to be a potential drug for AD treatment. Pomelo, a rich source of biological and chemical diversity, may be a potential multi-target drug for treatment of this disease. There are a rich variety of pomelo cultivars, including Tong Dee, Tha. Knoi, Kao Yai, Kao Paen, Kao Nampheung, Kao Tanggwa, Kao Hom, Kao Phuang and Pattavee. Among them, Kao Nampheung had the highest phenolic content[11]. The polyphenolic compounds from plants are

known to possess several bioactivities including antioxidant, antithrombotic, anti-Aβ aggregation, anticancer, and antidiabetic activities[18-21]. Therefore, the pomelo cultivar "Kao Numpueng" (KN) was chosen to evaluate its neuroprotection for AD in this study. The effect of KN extract on the biological activities related AD pathological cascade, namely antioxidant, AChE activity and Aβ aggregation was investigated. In addition, the neuroprotective effects against oxidative stress and Aβ toxicity of the extracts were also determined in a cell culture model.

1. In vitro antioxidant activity assays

The reduction of the oxidative stress is a crucial aspect in designing agents for AD treatment. We examined the antioxidant activities of the ethanol extract of Pomelo cultivar. "Kao Numpueng" (KN) by using the ABTS and DPPH radical scavenging method. Its ability to scavenge radicals was shown as IC_{50}, the test compound's concentration resulting in 50% inhibition of free radical. Trolox, a water-soluble vitamin E analogue, was used as a reference standard. Our results showed that the KN extract had the ability to scavenge both ABTS and DPPH radicals with IC_{50} of 0.28 and 0.95 mg/mL, respectively, as shown in Table 1. Trolox used as a positive control exhibited ABTS and DPPH radical scavenging activity with IC_{50} of 28.29 and 26.12 µM, respectively.

Table 1. The effects of the KN extract on radical scavenging, AChE activity and Aβ aggregation.

Compounds	DPPH assay[a] (IC_{50})	ABTS assay[a] (IC_{50})	AChE assay[b] (IC_{50})	Aβ aggregation assay (% Inhibition)
Tacrine (µM)	nd	nd	0.42 ± 0.16	nd
Trolox (µM)	26.12 ± 2.32	28.29± 1.41	nd	nd
Curcumin	nd	nd	nd	38.96 ± 6.90 (at 10 µM)
pomelo extract (mg/mL)	0.95± 0.01	0.29 ± 0.07	>1.00	22.92 ± 3.54 (at 0.1 mg/mL)

nd = not determine
[a]Data are expressed as IC_{50}, the test compound's concentration that inhibits 50%of free radicals (mean ± SD).
[b]AChE from electric eel; IC_{50}, inhibitor's concentration that inhibits 50% of AChE (mean ± SD).

2. In vitro AChE inhibitory activity assay

AD has also been found to be associated with a cholinergic deficit in the post-mortem brain characterized by a significant decrease in acetylcholine amount. The main role of AChE is to rapidly hydrolyze acetylcholine at the cholinergic synapses, ending the transmission of nerve impulses[4]. Therefore, inhibition of AChE appears to be a useful therapeutic path to reduce, at least temporarily, the cognitive deficit in AD. In this experiment, the effect of KN extract on AChE activity was evaluated according to the spectrophotometric method of Ellman. It is well known that the anti-amnesic effects of tacrine are due to AChE inhibition in brain.

Tacrine was used as a positive control. The result exhibited that the ethanol extract of KN does not show ability to inhibit AChE until the concentration of 1 mg/mL (Table 1).

3. In vitro assay for Aβ aggregation inhibition by thioflavin T assay

The key hallmark of AD pathogenesis is the formation of toxic Aβ plaques in the brain of AD patients. Therefore, preventing or reducing the aggregation of Aβ has been the primary goal of a number of therapeutic strategies under development or in clinical trials. In the present study, we examined the effects of KN on the inhibition of Aβ aggregation using the Th-T fluorescence assay. Table 1 shows the percentage of inhibition on aggregation of KN extract. As shown in Table 1, The KN extract were found to inhibit the aggregation of Aβ1–42 with % Inhibition of 22.92 at the concentration of 0.1 mg/mL.

4. Effect on H_2O_2-induced oxidative cell damage in SH-SY5Y cells

The neuroprotective effect against oxidative stress of the KN extract was determined by colorimetric MTT [3-(4,5-dimethyl-2-thiazolyl)-2,5-diphenyl-2H-tetrazolium bromide] assay in the neuroblastoma cell (SH-SY5Y). H_2O_2 was used to induce oxidative damage and curcumin was included as a reference compound. SH-SY5Y cells were treated with 0 to 1 mM concentrations of H_2O_2 in order to determine the concentration of H_2O_2 which kills 50% of cells. The results showed that H_2O_2 reduced the viability of SH-SY5Y cells in a concentration dependent manner, the IC_{50} was found to be 250 µM after treatment with H_2O_2 for 2 h. At this concentration, the cell viability was about 50% of the control viability. Therefore, for subsequent protection experiment, H_2O_2 at a concentration of 250 µM was used to treat the cells for 2 h. As reported in Figure 1, treatment of the neuronal cell with our test compounds significantly increased the cell viability compared with the H_2O_2 only treated control. The KN extract showed a significant effect at the dose of 1- 100 μg/mL when compared with the H_2O_2 only treated control. The results obtained from ABTS and DPPH assays reveal that our extract possesses antioxidant activity. Thus, the neuroprotective action against oxidative stress of the KN extract might be enhanced by the antioxidant action.

5. Effect on Aβ-induced cell damage in SH-SY5Y cells

The neuroprotective effects of the KN extracts were determined against the Aβ1-42 peptide induced toxicity in SH-SY5Y neuroblastoma cells. To determine the concentration of Aβ1-42 which reduce cell viability significantly, the cells were treated with various concentration of Aβ1-42. The result showed that Aβ1-42 significantly decreased cell viability in a concentration dependent. A concentration of 25 µM was chosen to induce toxicity to SH-SY5Y cells in the subsequent experiment. In this test, curcumin at 10 µM was used as a reference compound which significantly increased cell viability with p-value less than 0.01 compared with the Aβ1-42 only treated group. Both of the KN extract and curcumin showed a similar neuroprotective effect against Aβ1-42 peptide induced neurotoxicity (Figure. 2). Treatment of SH-SY5Y cells with the KN extract at concentrations of 1 - 100 μg/ml significantly reduced the cell viability loss evoked by Aβ1-42 peptide. The result obtained from anti-aggregation assay indicated that our extract could inhibit Aβ aggregation. Thus, the

protective action against the Aβ1-42 peptide of the KN extract might be enhanced by the antioxidant and anti-Aβ aggregation action.
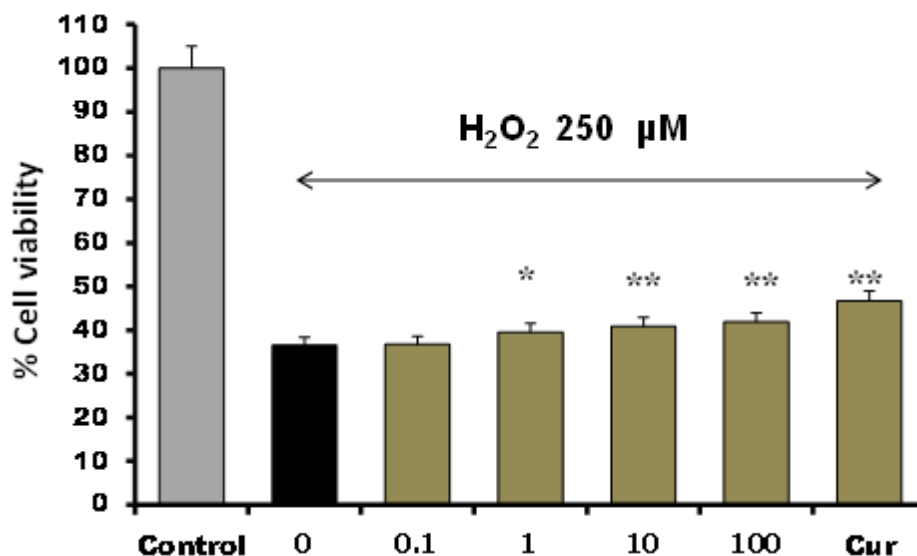
Figure 1. Effect of the KN extract (0.1-100 μg/mL) on H_2O_2-induced oxidative cell damage in neuroblastoma cells. Curcumin at 10 μM was used as a reference standard. Data are means ± SD (n = 5) *p < 0.05 and **p<0.01 compared to the H_2O_2-treated control group.
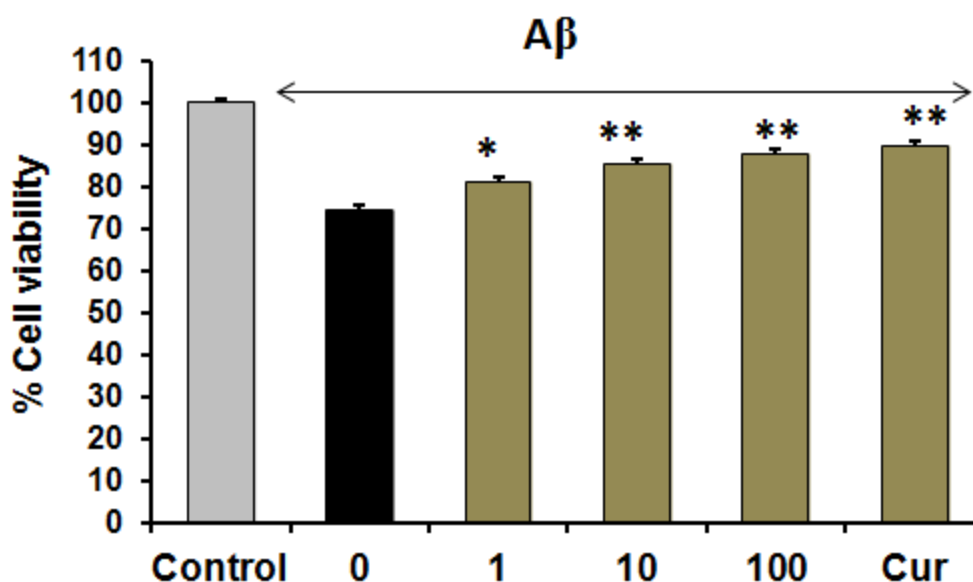
Figure 2. Effect of the extract of KN on Aβ1-42 peptide-induced neurotoxicity in SH-SY5Y cells. The cell viability of SH-SY5Y cells was determined by MTT assay, after 24 h of incubation with Aβ1-42 peptide (25 μM) in the presence or absence of various concentrations of test compounds (1-100 μg/mL). The values are reported as mean + SD (n = 5) *p < 0.05 and **p<0.01 compared to the Aβ1-42 -treated control group.

Conclusion

The results of the present study indicate that the KN extract possesses multimode of action involved with AD pathology cascade including antioxidant, anti-aggregation of Aβ, and neuroprotection against oxidative stress and Aβ toxicity. Thus, the Pomelo cultivar "Kao Numpueng" might be a potential candidate for further developing as drug for Alzheimer's disease.

Acknowledgements

References

1. Rodrı´guez-Franco MI, Ferna´ndez-Bachiller MI, Pe´rez C, et al. Novel tacrine-melatonin hybrids as dual-acting drugs for alzheimer disease, with improved acetylcholinesterase inhibitory and antioxidant properties. *Journal of Medicinal Chemistry* 2006; 49: 450-462.
2. Ferri CP, Prince M, Brayne C, Brodaty H, Fratiglioni L, Ganguli M, et al. Global prevalence of dementia: a Delphi consensus study. *The Lancet* 2005; 366: 2112-2117.
3. Floyd RA, Hensley K. Oxidative stress in brain aging. Implications for therapeutics of neurodegenerative diseases. *Neurobiology of Aging* 2002; 23: 795-807.
4. Wilkinson DG, Francis PT, Schwam E, Payne-Parrish J. Cholinesterase inhibitors used in the treatment of Alzheimer's disease: the relationship between pharmacological effects and clinical efficacy. *Drugs Aging* 2004; 21: 453-478.
5. Ohnishi S, Takano K. Amyloid fibrils from the viewpoint of protein folding. *Cellular and Molecular Life Sciences* 2004; 61 (5): 511–24.
6. Goedert M, Spillantini MG, Crowther RA. Tau proteins and neurofibrillary degeneration. *Brain Pathology* 1991; 1(4): 279–86.
7. Danuello A, Romeiro N, Giesel G, et al. Molecular Docking and Molecular Dynamic Studies of Semi-Synthetic Piperidine Alkaloids as Acetylcholinesterase Inhibitors. *J Braz. Chem Soc* 2012; 23: 163-170.
8. Wesnes KA, Ward T, McGinty A, Petrini O. The memory enhancing effects of a Ginkgo biloba/Panax ginseng combination in healthy middle-aged volunteers. *Psychopharmacology* 2000; 152: 353-361.
9. Nathan PJ, Tanner S, Lloyd J, Harrison B, Curran L, Oliver C, Stough C. Effects of a combined extract of Ginkgo biloba and Bacopa. *Human Psychopharmacology Clinical and*
10. Shih PH, Chan YC, Liao JW, Wang MF, Yen GC. Antioxidant and cognitive promotion effects of anthocyanin-rich mulberry (Morus atropurpurea L.) on senescence-accelerated mice and prevention of Alzheimer's disease. *The Journal of Nutritional Biochemistry* 2010; 21(7):598-605.
11. Makynen K, Jitsaardkul S, Tachasamran P, et at. Cultivar variations in antioxidant and antihyperlipidemic properties of pomelo pulp (Citrus grandis [L.] Osbeck) in Thailand . *Food Chemistry* 2013; 139: 735-743.
12. Theppakorn T, Chaiwong S. Bioactive Compounds in Pummelo and Grapefruit. *King Mongkut's Agricultural Journal* 2015; 29(2): 90-99.
13. Arnao MB, Cano A, Acosta M. The hydrophilic   and lipophilic contribution to total antioxidant activity. *Food Chem* 2001; 73: 239–244.

14. Pichaiyongvongdee S, Ratiporn B, Haruenkit R. Total Polyphenol Content and Antioxidant Properties in Different Tissues of Seven Pomelo (Citrus grandis (L.) Osbeck) Cultivars. *Natural Sciences* 2014; 43: 28 – 36.

15. Ellman G L, Courtney KD, Andres VJ, Featherstone RM. A new and rapid olorimetric determination of acetylcholinesterase activity. *Biochem*. *Pharmacol* 1996; 7: 88-95.

16. Levine H . Thioflavine T interaction with synthetic Alzheimer's disease β-amyloid peptides: Detection of amyloid aggregation in solution. *Protein science* 1993; 2(3): 404-410.

17. Park HR, Lee H, Park H, et al. Neuroprotective effects of Liriope platyphylla extract against hydrogen peroxide-induced cytotoxicity in human neuroblastoma SH-SY5Y cells. *BMC Complementary and Alternative Medicine* 2015; 15: 2-11.

18. Duarte J, Vizcaino FP, Utrilla P, Jimenez J, Tamargo J, and Zarzuelo A. Vasodilatory effects of flavonoids in rat aortic smooth muscle. Structure–activity relationships. *General Pharmacology: The Vascular System* 1993; 24: 857–862.

19. Pandey KB, and Rizvi SI. Plant polyphenols as dietary antioxidants inhuman health and disease. *Oxidative Medicine and Cellular Longevity* 2009; 2: 270.

20. Ren W, Qiao Z, Wang H, Zhu L, and Zhang L. Flavonoids: Promising anticancer agents. *Medicinal Research Reviews* 2003; 23: 519–534.

21. Vessal M, Hemmati M, and Vasei M. Antidiabetic effects of quercetin in streptozocin-induced diabetic rats. Comparative Biochemistry and Physiology Part C: *Toxicology & Pharmacology* 2003; 135: 357–364.

RESEARCH ARTICLE

Optimization of the extraction method for *Atractylodes lancea* (Thunb.) DC.

Siriprapa Warathumpitak[1], Tullayakorn Plengsuriyakarn[1], Juntra Karbwang[2], Kesara Na-Bangchang[1]

[1]*Center of Excellence in Pharmacology and Molecular Biology of Malaria and Cholangiocarcinoma, Graduate Program in Bioclinical Sciences, Chulabhorn International College of Medicine, Thammasat University, Pathumthani 12121, Thailand*
2*Department of Clinical Product Development, Institute of Tropical Medicine, Nagasaki University, Nagasaki, Japan*

Address correspondence and reprint request to: Professor Kesara Na-Bangchang, Center of Excellence in Pharmacology and Molecular Biology of Malaria and Cholangiocarcinoma, Graduate Program in Bioclinical Sciences, Chulabhorn International College of Medicine, Thammasat University, Pathumthani 12121, Thailand
E-mail address: kesaratmu@yahoo.com

Abstract

Cholangiocarcinoma (CCA) is the cancer of bile duct with high incidence and mortality rate in the northeastern region of Thailand. *Atractylodes lancea* (Thunb.) DC. (AL) has been used as crude extract in different preparations for treatment of various diseases in China, Japan, and Thailand. It contains several bioactive components including atractylodin, β-eudesmol, hinesol, and atractylone. The aim of the study was to optimize the extraction method/condition for AL using three different extraction procedures, *i.e*., maceration, sonication, and heat-reflux. Cytotoxicity of the extracts, β-eudesmol, atractylodin, and 5-fluorouracil (5-FU: reference control) on CCA cell line CL-6 and normal human embryonic fibroblast cell line OUMS-36T-1F was evaluated using standard MTT assay. The cytotoxic activities represented by IC_{50} (concentration that inhibits cell growth by 50%: mean $\pm$ SD) values of the crude ethanolic extracts prepared by sonication, maceration and heat-reflux were 26.15 ± 0.47, 33.02 ± 0.18, and 33.61 ± 4.70 µg/ml, respectively. The maceration, although not the most efficient method, was selected for further optimization due to its simplicity, cost-effectiveness, and applicability for large scale production. Results showed that 24 hours maceration twice, provided the most suitable condition to prepare the extract with regard to the extraction yield and cytotoxic activity (9.95% yield, IC_{50}: 33.15 ± 2.50 µg/ml). The IC_{50} of β-eudesmol, atracylodin, and 5-FU were 29.60 ± 1.00, 45.69 ± 3.40 and 107.72 ± 1.69 µg/ml, respectively. This extraction procedure and condition will be used for further development of the oral pharmaceutical formulation for preclinical studies.

Keywords: *Atractylodes lancea*, chologiocarcinoma, cytotoxicity, extraction method, maceration

Introduction

Cholangiocarcinoma (CCA) is the cancer of bile duct originating from the malignant transformation of epithelial cell that lines the biliary tract. This type of cancer is found worldwide including in the United States of America, Canada, Australia, and South-East Asia [1]. The highest incidence is reported from South-East Asia particularly the northeastern region of Thailand where consumption of improperly cooked or fermented food that contains *Opisthorchis viverrini* is common [2-3]. Treatment strategies for CCA include surgery, radiation, chemotherapy, and liver transplant [4]. Nevertheless, all of them remain unsatisfactory with high mortality rate. Clinical efficacy of the currently used standard chemotherapeutic drugs such as 5-flurouracil (5-FU) is low [5]. New alternative drugs are urgently needed to control this cancer.

The rhizomes of *Atractylodes lancea* (Thunb.) DC. (AL) has been used in traditional medicine in China, Japan, and Thailand for treatment of several diseases including digestive disorder, rheumatoid, arthritis, night blindness, fever, and common cold [6]. Previous studies have demonstrated promising cytotoxic activity of the crude ethanolic extract of AL against the CCA cell line CL-6 [7]. However, the most efficient extraction method that provides extract with highest yield and potent cytotoxic activity has never been investigated. The aim of the present study was to evaluate the efficiency of the three extraction methods for AL, *i.e.*, maceration, sonication, and heat-reflux. In addition, optimization of the extraction condition of the selected extraction method was also performed. The efficiency of the extraction method/condition was evaluated based on cytotoxic activities (MTT assay) of the extracts against the CCA cell line CL-6 in comparison with normal human embryonic fibroblast cell line OUMS-36T-1F.

Materials and Methods

1. Plant materials

The rhizome of AL (grown in Heilongjiang, China) was purchased from local supplier in Nakhonprathom province of Thailand. The plant species was confirmed by macroscopic and microscopic characterization. The rhizome was pulverized, kept in sealed plastic bag and stored in dry condition.

2. Chemical and reagents

MTT (Sigma-Aldrich, USA), dimethylsulfoxide (Ameresco, USA), 5-fluorouracil (Wako Pure Chemical Industries, Ltd., Osaka, JPN), RPMI, and DMEM medium, fetal bovine serum, and antibiotic-antimycotic solution (Gibco BRL Life Technologies, NY, USA) were obtained commercially.

3. Cell culture

The cholangiocarcinoma cell line CL-6 was established and kindly provided by Associate Professor Dr. Adisak Wongkajornsilp of the Department of Pharmacology, Faculty of Medicine (Siriraj Hospital), Mahidol University and normal human embryonic fibroblast

cell line OUMS-36T-1F was purchased from JCRB Cell Bank, Japan, were cultured in RPMI and DMEM medium, respectively, with supplementation of 10% heat-inactivated fetal bovine serum and 100-IU/mL antibiotics-antimycotics. All cells were maintained at 37°C in a 5% CO_2 atmosphere with 95% humidity.

4. Selection of extraction method

Three different extraction methods, *i.e.*, maceration, sonication, and heat-reflux were used to prepare AL extracts as follows:

4.1 Maceration method: Powdered plant material (10 g) was macerated in a stopper flask containing 300 ml of 95% ethanol at room temperature (25-30ºC) for 7 days with continuous stirring.

4.2 Sonication method: Powdered plant material (10 g) was put in a stopper flask containing 100 ml of 95% ethanol at room temperature (25-30ºC) and sonicated for 30 minutes.

4.3 Heat-reflux method: Powdered plant material (10 g) was put in a stopper flask containing 100 ml of 95% ethanol and heated on water bath (95 ºC) for 50 minutes.

The extracted solvent was removed and filtered through Whatman no.1 filter paper (GE Healthcare, Maidstone, UK). The solvent was pooled, evaporated under reduced pressure by rotary evaporation, and put on a water bath until dried. The dried extract was weighed and stored at 4ºC until use.

5. Optimization of the maceration method

Powdered plant material (200 g) was macerated in a stopper flask containing 1,000 ml of 95% ethanol at room temperature with agitation under four conditions as follows:

A: Maceration for 24 hours, once
B: Maceration for 24 hours, twice
C: Maceration for 24 hours for three times
D: Maceration for 72 hours, once

The extracted solvent was removed and filtered through Whatman no.1 filter paper (GE Healthcare, Maidstone, UK). The solvent was pooled, evaporated under reduced pressure by rotary evaporation, and finally dried by Freeze dryer. The dried extract was weighed and stored at 4ºC until use.

6. Cytotoxicity assay

CL-6 and OUMS-36T-1F cells (10,000 cells) were added into each well of a 96 well plate and treated with macerated extract of AL, as well as the active compounds β-eudesmol, atractylodin, and 5-FU (positive control drug) at concentrations ranging from 250 to 1.95 µg/ml and cell viability was assessed by MTT assay. IC_{50} (concentration that inhibits cell growth by

50%) was estimated using CalcuSyn software (Biosoft, Cambridge, UK). Selectivity index (SI) was calculated from the ratio of the IC_{50} of the extract/test compound in CL-6 and OUMS-36T-1F cell lines.

Results

1. Selection of extraction method

Brown and sticky extract products were obtained following the three extraction methods. The extraction efficiencies (% yields) of different methods in descending order were heat reflux (12.10%), followed by sonication (11.90%), and maceration (11.75%). Cytotoxic activities of the extracts prepared by the three methods including the active compounds against CL-6 and OUMS-36T-1F are shown in Table 1. All of the three extraction methods provided the extracts with comparable cytotoxic activities against CL-6 with IC_{50} values ranging from 26.15±0.47 to 33.61±4.70 µg/ml. The potency of activities of the AL extracts was about 3.3 - 4.2 fold of the positive control drug 5-FU. The maceration method was selected for further evaluation of the optimal extraction condition as it is relatively simple, cost-effective, and applicable to large scale production.

Table 1. IC_{50} (mean $\pm$ SD) and selectivity index (SI) of 5-FU and the extracts of *A. lancea* (Thunb.) DC. rhizome prepared by maceration, sonication, and heat-reflux (n = 3).

Plant/Drug	Extraction method	IC_{50}		SI
		CL-6	OUMS-36T-1F	
A. lancea (Thunb.) DC.	Maceration	33.02±0.18 µg/ml	77.79±3.53 µg/ml	2.33 2.35
	Sonication	26.15±0.47 µg/ml	63.50±3.17 µg/ml	2.42
	Heat-reflux	33.61±4.70 µg/ml	70.14±1.71 µg/ml	2.12 2.08
5-Flurouracil		107.72±1.69 µM	135.12±11.06 µM	4.87 1.25

2. Optimization of the maceration condition

The most efficient maceration condition which provided the highest extraction yield (10.74%) was the extraction duration of 24 hours for three times. The maceration which provided the extract with most potent cytotoxic activity (IC_{50} 27.49 $\pm$ 0.98 µg/ml) was the extraction duration of 24 hours, once **(Table 2).** Considering the compromised performance of the extraction efficiency (9.95%) and cytotoxic activity (IC_{50} 33.15 $\pm$ 2.50 µg/ml), the maceration condition of 24 hours extraction twice was selected as the most optimal condition for AL extraction. This extraction condition was therefore used to compare the cytotoxic activities of the macerated extract of AL and its two active compounds β-eudesmol, atractylodin, and 5-FU **(Table 3)**. β-Eudesmol was the most potent compound against CL-6

with mean IC_{50} of 29.60±1.00 µg/ml and relatively high SI (3.1). The potency of cytotoxic activities against CL-6 of the extract and the active compounds were about 2.4-3.8 times of 5-FU.

Table 2. Extraction efficiency (% yields), appearance and cytotoxic activities against CL-6 cells of the products following different maceration conditions used to prepare *A. lancea* (Thunb.) DC. extracts (n = 3).

A.lancea	%Yield	Appearance	IC_{50} (*µg/ml*)
A: Maceration for 24 hours, once	5.42	Brown and sticky	27.49 ± 0.98
B: Maceration for 24 hours, twice	9.95	Brown and sticky	33.15 ± 2.50
C: Maceration for 24 hours, three times	10.74	Brown and sticky	45.75 ± 1.82
B: Maceration for 72 hours, once	7.76	Brown and sticky	43.13 ± 0.67

Table 3. The IC_{50} values (mean $\pm$ SD) and SI for CL-6 and OUMS-36T-1F cell lines of the extract of *A.lancea* (Thunb.) DC. prepared by 24 hours maceration twice, β-eudesmol, atractylodin, and 5-flurouracil (n = 3).

	IC_{50}		SI
	CL-6	**OUMS-36T-1F**	
Macerated extract for 24 hours (twice)	33.15±2.50 µg/ml	113.98±3.39 µg/ml	3.28 3.44
β-Eudesmol	29.60±1.00 µg/ml	86.52±7.38 µg/ml	3.10 2.92
Atractylodin	45.69±3.40 µg/ml	95.27±17.86 µg/ml	2.11 2.08
5-Flurouracil (5-FU)	107.72±1.69 µM	135.12±11.06 µM	1.23 1.25

Discussion and Conclusion

All of the three extraction methods provided AL extracts with acceptable extraction yields (11.75-12.10%) and cytotoxic activities ($IC_{50} < 50$ µg/ml) against CL-6 cell line. Among the three methods, the heat reflux method provided the extract with highest yield, followed by maceration, and sonication. Due to its relative simplicity, cost effectiveness, and applicability to large scale production, the maceration method was selected for further evaluation for the optimal condition (extraction duration and number of repeated procedures. Results showed that maceration for 24 hours twice was the most suitable condition with regard to the extraction yield and cytotoxic activity against CL-6.) Based on the IC_{50} values, the cytotoxic activity of the crude extract is considered as potent as its purified active compounds. The selectivity of both the crude extract and purified compounds on cytotoxicity against CL-6 cells was relatively high compared with the standard drug 5-FU.

In conclusion, results signify the importance of optimization of the extraction method and condition for AL before further investigation of its biological activities. These optimized

methods will be applied for large scale production of the crude extract of AL for preparation of oral pharmaceutical formulation for future preclinical studies.

Acknowledgements

References

1. Sripa B, Pairojkul C. Cholangiocarcinoma: lessons from Thailand. Current Opinion in Gastroenterology. 2008;24(3):349-56.
2. Sripa B, Kaewkes S, Sithithaworn P, Mairiang E, Laha T, Smout M, et al. Liver fluke induces cholangiocarcinoma. PLoS Medicine. 2007;4(7):1148-55.
3. Thamavit W, Pairojkul C, Tiwawech D, Shirai T, Ito N. Strong promoting effect of *Opisthorchis viverrini* infection on dimethylnitrosamine-initiated hamster liver. Cancer Letters. 1994;78(1-3):121-5.
4. Malhi H, Gores GJ. Review article: the modern diagnosis and therapy of cholangiocarcinoma. Alimentary Pharmacology & Therapeutics. 2006;23(9):1287-96.
5. Kamangar F, Dores GM, Anderson WF. Patterns of cancer incidence, mortality, and prevalence across five continents: defining priorities to reduce cancer disparities in different geographic regions of the world. Journal of Clinical Oncology : official journal of the American Society of Clinical Oncology. 2006;24(14):2137-50.
6. Nakai Y, Kido T, Hashimoto K, Kase Y, Sakakibara I, Higuchi M, et al. Effect of the rhizomes of *Atractylodes lancea* and its constituents on the delay of gastric emptying. Journal of Ethnopharmacology. 2003;84(1):51-5.
7. Mahavorasirikul W, Viyanant V, Chaijaroenkul W, Itharat A, Na-Bangchang K. Cytotoxic activity of Thai medicinal plants against human cholangiocarcinoma, laryngeal and hepatocarcinoma cells in vitro. BMC Complementary and Alternative Medicine. 2010;10:55.

RESEARCH ARTICLE

Broad prediction of HLA-B*58:01 for allopurinol-induced Severe cutaneous adverse drug reactions in Thai population

Parnrat Kuntawong[1], Thawinee Jantararoungtong[1,2], Apichaya Puangpetch[1,2], Napatruporn Koomdee[1,2], Patompong Satapornpong[1], Patcharin Supapsophon[3], Jettanong Klaewsongkram[4,6], Ticha Rerkpattanapipat[5,6] , Chonlaphat Sukasem[1,2,6]

[1]Division of Pharmacogenomics and Personalized Medicine, Department of Pathology, Faculty of Medicine Ramathibodi Hospital, Mahidol University, Bangkok, Thailand
[2]Laboratory for Pharmacogenomics, Somdech Phra Debaratana Medical Center (SDMC), Ramathibodi Hospital, Bangkok, Thailand
[3]Department of Pharmacy, Somdech Phra Debaratana Medical Center (SDMC), Ramathibodi Hospital, Bangkok, Thailand
[4]Division of Allergy and Clinical Immunology, Department of Medicine, Faculty of Medicine, Allergy and Clinical Immunology Research Group, Chulalongkorn University, Bangkok, Thailand
[5]Division of Allergy Immunology and Rheumatology, Department of Medicine, Faculty of Medicine, Ramathibodi Hospital, Mahidol University, Bangkok, Thailand.
[6]The Thai Severe Cutaneous Adverse Drug Reaction (THAI-SCAR) research group.

*Corresponding Author: Chonlaphat Sukasem, Laboratory for Pharmacogenetics and Personalized Medicine, Department of Pathology, Faculty of Medicine, Ramathibodi Hospital, Mahidol University, Rama 6 Road, Bangkok 10400, Thailand
Tel (66)-2-201-1368, Fax: (66)-2-201-1324
E-mail: chonlaphat.suk@mahidol.ac.th

Abstract

Allopurinol is one of the common causes of severe cutaneous adverse reactions (SCARs), including Stevens-Johnson syndrome (SJS), toxic epidermal necrosis (TEN), and drug rash with eosinophilia and systemic symptoms (DRESS) in Thailand. Despite the HLA-B*58:01 are strongly associated with allopurinol-induced SJS/TEN, the association with allopurinol-induced DRESS has not been investigated in Thai population. The aim of this study was to investigate the predisposition to different types of allopurinol- induced cutaneous adverse drug reactions (CADRs) including SJS and SJS/TEN (n=11), DRESS (n=6) conferred by HLA-B*58:01 in a Thai population. This case-control association study included 17 cases with allopurinol-induced SCARs in comparison with allopurinol-tolerant control patients (n=95) and population control group (n=1,095) in Thailand. The control group was comprised of patients who had received allopurinol for $\geqslant$ 6 months without any adverse cutaneous event. HLA-B allele was genotyped by using a two-stage sequence-specific oligonucleotide probe system (PCR-SSOP). Regardless of the type of SCARs, 100% (n=17) of Thai with SCARs due to allopurinol have been found to be at least heterozygous for HLA-B*58:01. The risk of allopurinol-induced SCARs was significantly higher in the patients with HLA-B*5801 allele with an odd ration of 925 (95%CI: 45.73-18709.02, $p < 0.01$). This study demonstrated HLA-B*58:01 as a broad predictor for allopurinol-induced SJS/TEN and DRESS. These results suggest that screening tests for HLA-B*58:01 allele in patients who will be treated with

allopurinol will be clinically helpful in preventing the risk of developing SJS/TEN and DRESS in Thai population.

Keywords: HLA-B*58:01, allopurinol, Thais, SCARs, drug hypersensitivity, SJS/TEN, DRESS

Introduction

Allopurinol is a commonly prescribed medication that has been used to inhibit xanthine oxidase in patients with gouty arthritis, hyperuricemia and in cancer patients undergoing chemotherapy[1,2]. Allopurinol is a major cause of severe cutaneous adverse reactions (SCARs) including Stevens-Johnson syndrome (SJS), toxic epidermal necrolysis (TEN), drug reaction with eosinophillia and systemic symptoms (DRESS) in Thailand[3,4]. Several studies have reported that severe reactions to allopurinol are strongly associated with HLA-B*58:01, which is carried by 8% to 15% of Han Chinese and Thais[3,5,6], but occurs relatively infrequently in Japanese (0.6%) and European (0.8%) populations[7,8,9].

A previous publication from Thailand showed that the HLA-B*58:01 allele is a strong marker for allopurinol-induced SCARs in the Thai population[3]. However, that study reported only an association between allopurinol-induced SJS/TEN and HLA-B*58:01. More recently, a high frequency of HLA-B*58:01 was reported in Portuguese patients with allopurinol-induced DRESS[9].

Although allopurinol-induced DRESS is much more common than SJS/TEN, particularly in Thailand, there are no data describing whether HLA-B*58:01 could be used as a genetic marker for DRESS induced by allopurinol. Therefore, this study aims to determine the association of allopurinol-induced SCAR, which includes DRESS and SJS/TEN with the HLA-B*58:01 allele.

Materials and Methods

Subjects and characteristics

In this study, we carried out research as a retrospective and prospective case-controlled study. From 2011 to 2014, patients with allopurinol-induced SCAR admitted to the allergy clinic of Faculty of Medicine Ramathibodi Hospital, Mahidol University were enrolled. Seven teen patients with allopurinol-induced cutaneous adverse drug reactions (CADRs) were categorized into DRESS (6 cases) and SJS/TEN (11 cases). Patients who had been taking allopurinol for more than 6 months without evidence of cutaneous adverse effects were recruited as allopurinol-tolerant controls (n=95). In addition, healthy individuals who had not taken allopurinol and had no history of drug induced cutaneous adverse reactions were included in this study. Data for this healthy control group was obtained from 1,095 subjects undergoing HLA-B genotyping through the Laboratory for Pharmacogenomics, Somdech Phra Debaratana Medical Center (SDMC), Ramathibodi Hospital, Thailand. The study was performed and

approved by the Ramathibodi Hospital ethical review board, and informed consent was obtained from all of the participants.

Diagnosis of cutaneous adverse drug reactions (CADRs)

All CADR patients were assessed by a dermatologist and allergist who reviewed photographs, pathological slides, clinical morphology and medical records. The diagnosis of drug-induced DRESS, SJS, and TEN was made according to the RegiSCAR criteria[10]. In brief, DRESS was diagnosed in patients presenting with fever, maculopapular rash with internal organ involvement, and hematologic abnormalities. SJS was diagnosed in patients with skin rash and mucosal erosion covering 3% to 10% of body surface area (BSA) whereas SJS/TEN overlap was diagnosed in patients with epidermal necrosis whose blistering skin lesions affected between 10-30 % of BSA.

Genomic DNA extraction

Blood samples were collected into EDTA tubes. DNA was isolated using the MagNA Pure automated extraction system (Roche Diagnostics, USA) based on magnetic-bead technology. The quality of genomic DNA was assessed using a Nano Drop ND-1000 to measure quantity and purity of genomic DNA. All DNA was aliquotted and stored at -20∘C before analysis.

HLA-B typing

HLA-B genotyping was carried out using LuminexTM Multiplex Technology (Luminex®IS 100, USA) based on polymerase chain reaction-sequence specific oligonucleotide probe (PCR-SSOP) principles. Briefly, PCR products were hybridized against a panel of oligonucleotide probes coated on polystyrene microspheres that have sequences complementary to stretches of polymorphic sequence within the target HLA-B alleles. The amplicon-probe complex was visualized using a colorimetric reaction and fluorescence detection technology. Data analysis for the HLA-B assays was performed with HLA fusionTM2.0 software.

Statistical analysis

The association between HLA-B*58:01 and allopurinol-induced SCAR was evaluated by comparing the group of individuals with SCAR with the allopurinol-tolerant groups and the general population. Data was counted by presence or absence of HLA-B*58:01 allele. Chi-square test and Fisher's exact test were used to analyze the association between allopurinol-induced CADRs and HLA-B*58:01. Statistical analysis was performed using SPSS version 16.0 (SPSS Inc., Chicago, IL, USA). The strength of association was estimated by calculating the odds ratio (OR) with a 95% confidence interval (CI).

Results

Duration of allopurinol exposure to symptom onset, starting dose, indication of drug use, and the results of HLA-B genotyping are summarized in *Table 1*. In the allopurinol-

induced SCARs group, the subgroups of patients with SJS, SJS/TEN overlap and DRESS comprised 8 (47.06%), 3 (17.65%) and 6 (35.29%) patients, respectively. Among 17 patients with allopurinol-induced SCARs, all of them (100.00%; 6 DRESS, 11 SJS/TEN) had HLA-B*58:01. We observed a significant increase in HLA-B*58:01 allele frequency when comparing allopurinol-induced SCARs and -tolerant groups (100.00% vs. 3.2%, p<0.01: OR 925.00, 95%CI=45.73-18709.02). In addition, the risk of allopurinol-induced SCAR was significantly higher when comparing with the healthy population (100.00% vs. 10.10%, p<0.01; OR 309.04, 95% CI: 18.46-5174.25). In this study, there was a difference in the frequency of HLA-B*13:01 allele between the allopurinol-induced SCARs vs. allopurinol-tolerant and the untreated individuals (17.6% vs. 10.5% and 12.5%), but no significant association was found (*Table 2*).

In particular, HLA-B*58:01 was present in all 11 (100%) patients with allopurinol–induced SJS/TEN. As shown in *Table 3*, the HLA-B 58:01 allele occurred at significantly increased frequencies among the allopurinol–SJS/TEN patients compared to the allopurinol-tolerant group (100.00% vs. 3.2%, p<0.01; OR=607.86, 95%CI: 29.49-12530.13). When comparing the frequency of the HLA-B*58:01 allele between the allopurinol-induced DRESS and the allopurinol-tolerant patients, the OR of HLA-B*58:01 was highly significant (OR=343.57, 95% CI: 15.98-7387.26, p<0.01), as shown in *Table 4*.

Discussion

The case–controlled analysis included 17 cases of allopurinol-induced CADRs, which included DRESS (6 cases) and SJS/TEN (11 cases). The association study in Thai patients examined only a limited phenotype of allopurinol-induced SJS/TEN[3]. Previous studies have proposed association of immune mechanisms in the development of several forms of allopurinol-induced SCARs (SJS, TEN, and DRESS). Hung et al. has shown that the HLA-B*58:01 allele is a strong genetic factor in the incidence of SCAR for Han Chinese taking allopurinol[5]. Although, Tassaneeyakul et al. were the first to identify an association between HLA-B*58:01 and allopurinol-induced SJS/TEN[3], no published data have yet confirmed such a strong correlation of HLA-B*58:01 and allopurinol-induced DRESS in Thai patients. This finding reveals that the risk of developing SCARs among those allopurinol users with HLA-B*58:01 is significantly increased by 108.33 times (95% CI; 11.96-980.83) compared to allopurinol-tolerant controls. In this study, we confirmed the association between HLA-B* 58:01 and allopurinol-induced SCARs, including SJS/TEN and DRESS (OR 925).

Novelty, we also identified an association between HLA-B*58:01 and allopurinol-induced DRESS in Thai population (OR=925.00). The association is 100% in that the HLA-B*58:01 was present in all 6 patients with allopurinol-induced DRESS, similar to the study in Han Chinese and Japanese populations[5,8]. Based on the strong association of the presence of HLA-B*58:01 and DRESS and SJS/TEN, it is presumed that the attributable risk of SCARs due to the existence of this allele is larger - as high as 8% in Thailand, indicating that HLA-B*58:01 is associated with the pathogenesis of allopurinol-induced SCARs regardless of the

phenotype or severity. This is in contrast to carbamazepine-induced SCARs, with which HLA-B*15:02 only shows association with specific phenotype (SJS/TEN)[11-13].

In summary, a strong association between allopurinol-induced SCARs and the HLA-B*58:01 allele was confirmed. Incidence of the HLA-B*58:01 allele is strongly associated with individuals who are at risk for allopurinol-induced DRESS, SJS and SJS/ TEN in the Thai population. Our results suggest that the screening tests for the HLA-B*58:01 allele in patients who will be treated with allopurinol would be clinically helpful in reducing the risk of developing SCARs. Regarding to our findings, the pharmacogenetic interpretation could be generalized to SCARs, including DRESS, SJS and SJS/TEN. Physicians and national policy makers should consider genetic screening for the HLA-B*58:01 alleles prior to initiation of allopurinol therapy in Thai patients.

Conflicts of Interest Statement

The authors have no relevant affiliations or financial involvement with any organization or entity with a financial interest in or financial conflict with the subject matter or materials discussed in the manuscript.

Acknowledgements

Table 1 Summary of characteristics and genotyping data of allopurinol induced SCAR patients

No.	Age/Sex	Phenotype	Duration of exposure (day)	Dosage of allopurinol (mg/day)	Indication	HLA-B*5801	HLA-B genotyping
1	56/M	DRESS	34	200	Hyperuricemia	positive	4402/5801
2	72/F	SJS	26	300	gouty arthritis	positive	5701/5801
3	78/F	SJS	11	100	Hyperuricemia	positive	3501/5801
4	68/F	SJS	14	300	gouty arthritis	positive	4601/5801
5	38/F	SJS	10	200	gouty arthritis	positive	1301/5801
6	68/M	SJS	17	300	gouty arthritis	positive	1301/5801
7	49/M	SJS	19	300	gouty arthritis	positive	4001/5801
8	66/M	SJS/TEN	28	300	gouty arthritis	positive	4403/5801
9	74/F	SJS/TEN	10	100	gouty arthritis	positive	1502/5801
10	28/M	DRESS	18	200	Hyperuricemia	positive	3915/5801
11	37/F	DRESS	10	200	Hyperuricemia	positive	0801/5801
12	81/F	DRESS	12	300	Hyperuricemia	positive	1301/5801
13	76/F	SJS	7	300	gouty arthritis	positive	5801/5801
14	76/M	SJS	14	300	Hyperuricemia	positive	4001/5801
15	72/M	DRESS	30	100	gouty arthritis	positive	5201/5801
16	76/F	SJS/TEN	10	100	gouty arthritis	positive	1513/5801
17	61/M	DRESS	42	200	gouty arthritis	positive	5101/5801

Table 2 The association of individual HLA-B allele with allopurinol induced SCAR

HLA-B allele	Allopurinol induced SCAR (n=17)	Allopurinol tolerant (n=95)	General population (n=1095)	SCAR cases versus Allopurinol tolerant control		SCAR cases versus general population	
				OR (95% CI)	P value	OR (95% CI)	P value
5801	17 (100.0)	3 (3.2)	111 (10.1)	925.00 (45.73-18709.02)	<0.01	309.04 (18.46-5174.25)	<0.01
1301	3 (17.6)	10 (10.5)	137 (12.5)	1.82 (0.44-7.45)	0.404	1.50 (0.43-5.28)	0.529
1502	1 (5.9)	17 (17.9)	161 (14.7)	0.29 (0.04-2.31)	0.241	0.36 (0.05-2.75)	0.327
4001	2 (11.8)	27 (28.4)	162 (14.8)	0.34 (0.07-1.57)	0.165	0.77 (0.17-3.39)	0.727
4601	1 (5.9)	20 (21.1)	227 (20.7)	0.23 (0.03-1.88)	0.171	0.24 (0.03-1.81)	0.166
5101	1 (5.9)	12 (12.6)	65 (5.9)	0.43 (0.05-3.56)	0.436	1.02 (0.13-7.83)	0.983

Table 3 The association of individual HLA-B allele with allopurinol induced SJS/TEN

HLA-B allele	Allopurinol induced SJS/TEN (n=11)	Allopurinol tolerant (n=95)	General population (n=1095)	SJS/TEN cases versus Allopurinol tolerant control		SJS/TEN cases versus general population	
				OR (95% CI)	P value	OR (95% CI)	P value
5801	11 (100.0)	3 (3.2)	111 (10.1)	607.86(29.49-12530.13)	<0.01	203.08 (11.89-3469.77)	<0.01
1301	2 (18.2)	10 (10.5)	137 (12.5)	1.89 (0.36-10.00)	0.454	1.55 (0.33-7.27)	0.575
1502	1 (9.1)	17 (17.9)	161 (14.7)	0.46 (0.06-3.83)	0.471	0.58 (0.07-4.56)	0.605
4001	2 (18.2)	27 (28.4)	162 (14.8)	0.56 (0.11-2.76)	0.476	1.28 (0.27-5.98)	0.754
4601	1 (9.1)	20 (21.1)	227 (20.7)	0.38 (0.05-3.11)	0.363	0.38 (0.05-3.00)	0.361
5101	0 (0.0)	12 (12.6)	65 (5.9)	0.29 (0.01-5.24)	0.402	0.68 (0.04-11.74)	0.793

Table 4 The association of individual HLA-B alleles with allopurinol induced DRESS

HLA-B allele	Allopurinol induced DRESS (n=6)	Allopurinol tolerant (n=95)	General population (n=1095)	DRESS versus Allopurinol tolerant control		DRESS versus general population	
				OR (95% CI)	P value	OR (95% CI)	P value
5801	6 (100.0)	3 (3.2)	111 (10.1)	343.57(15.98-7387.26)	<0.01	114.78 (6.42-2051.26)	<0.01
1301	1 (16.7)	10 (10.5)	137 (12.5)	1.70 (0.18-16.05)	0.643	1.40 (0.16-12.06)	0.760
1502	0 (0.0)	17 (17.9)	161 (14.7)	0.35 (0.02-6.42)	0.476	0.45 (0.03-7.94)	0.582
4001	0 (0.0)	27 (28.4)	162 (14.8)	0.19 (0.01-3.52)	0.266	0.44 (0.02-7.88)	0.579
4601	0 (9.1)	20 (21.1)	227 (20.7)	0.28 (0.02-5.24)	0.397	0.29 (0.02-5.23)	0.404
5101	1 (16.7)	12 (12.6)	65 (5.9)	1.38 (0.15-12.87)	0.776	3.17 (0.36-27.53)	0.296

References

1. Min HK, Lee B, Kwok SK, Ju JH, Kim WU, Park YM, et al. Allopurinol hypersensitivity syndrome in patients with hematological malignancies: characteristics and clinical outcomes. The Korean journal of internal medicine. 2015;30(4):521-30.
2. Lam MP, Yeung CK, Cheung BM. Pharmacogenetics of allopurinol--making an old drug safer. Journal of clinical pharmacology. 2013;53(7):675-9.
3. Tassaneeyakul W, Jantararoungtong T, Chen P, Lin PY, Tiamkao S, Khunarkornsiri U, et al. Strong association between HLA-B*5801 and allopurinol-induced Stevens-Johnson syndrome and toxic epidermal necrolysis in a Thai population. Pharmacogenetics and genomics. 2009;19(9):704-9.
4. Saokaew S, Tassaneeyakul W, Maenthaisong R, Chaiyakunapruk N. Cost-effectiveness analysis of HLA-B*5801 testing in preventing allopurinol-induced SJS/TEN in Thai population. PloS one. 2014;9(4):e94294.
5. Hung SI, Chung WH, Liou LB, Chu CC, Lin M, Huang HP, et al. HLA-B*5801 allele as a genetic marker for severe cutaneous adverse reactions caused by allopurinol. Proceedings of the National Academy of Sciences of the United States of America. 2005;102(11):4134-9.
6. Puangpetch A, Koomdee N, Chamnanphol M, Jantararoungtong T, Santon S, Prommas S, et al. HLA-B allele and haplotype diversity among Thai patients identified by PCR-SSOP: evidence for high risk of drug-induced hypersensitivity. Frontiers in genetics. 2014;5:478.
7. Lonjou C, Borot N, Sekula P, Ledger N, Thomas L, Halevy S, et al. A European study of HLA-B in Stevens-Johnson syndrome and toxic epidermal necrolysis related to five high-risk drugs. Pharmacogenetics and genomics. 2008;18(2):99-107.
8. Kaniwa N, Saito Y, Aihara M, Matsunaga K, Tohkin M, Kurose K, et al. HLA-B locus in Japanese patients with anti-epileptics and allopurinol-related Stevens-Johnson syndrome and toxic epidermal necrolysis. Pharmacogenomics. 2008;9(11):1617-22.
9. Goncalo M, Coutinho I, Teixeira V, Gameiro AR, Brites MM, Nunes R, et al. HLA-B*58:01 is a risk factor for allopurinol-induced DRESS and Stevens-Johnson syndrome/toxic epidermal necrolysis in a Portuguese population. The British journal of dermatology. 2013;169(3):660-5.
10. Choudhary S, McLeod M, Torchia D, Romanelli P. Drug Reaction with Eosinophilia and Systemic Symptoms (DRESS) Syndrome. The Journal of clinical and aesthetic dermatology. 2013;6(6):31-7.
11. Lee MT, Mahasirimongkol S, Zhang Y, Suwankesawong W, Chaikledkaew U, Pavlidis C, et al. Clinical application of pharmacogenomics: the example of HLA-based drug-induced toxicity. Public health genomics. 2014;17(5-6):248-55.
12. Phillips EJ, Chung WH, Mockenhaupt M, Roujeau JC, Mallal SA. Drug hypersensitivity: pharmacogenetics and clinical syndromes. The Journal of allergy and clinical immunology. 2011;127(3 Suppl):S60-6.
13. Suresh Kumar PN, Thomas B, Kumar K, Kumar S. Stevens-Johnson syndrome-toxic epidermal necrolysis (SJS-TEN) overlap associated with carbamazepine use. Indian journal of psychiatry. 2005;47(2):121-3.

RESEARCH ARTICLE

Prevalence and antimicrobial susceptibility of enteric bacterial infection in Lao PDR, 2012

Phanthaneeya Teepruksa[1,2], Phengta Vongpachanh[2], Noikaseumsy Sithivong[2], Keseara Na-Bangchang[1], Wanna Chaijaroenkul[1*]

[1]*Chulabhorn International College of Medicine, Thammasat Univesity (Rangsit Campus), Pathumthani 12121, Thailand*
[2]*National Center for Laboratory and Epidemiology, Km 3 Thaduae Rd., Sisattanack District, Vientiane Capital, LAO PDR*
*corresponding author

Abstract

Diarrhea is an important health problem which is the second leading cause of deaths among children in developing countries. The antimicrobial resistance surveillance in Lao PDR was established in 2012. The aim of this study was to identify bacterial pathogens, the virulence of pathogenic *E. coli,* and the antimicrobial susceptibility profile of enteric pathogen from diarrhea patients in Lao PDR. Stool and rectal swab samples were collected from diarrheal patients during January to December 2012. The cultivation, biochemical method, multiplex PCR and antimicrobial susceptibility were performed. Results showed that 284 out of 708 specimens were infected with *Aeromonas* spp (1.7%), *Plesiomonas shigelloides* (1.7%), *Salmonella* spp (4.9%), *Shigella* spp (1.4%), *Vibrio* spp. (0.4%), rotavirus (0.4%), pathogenic *Escherichia coli* (17.8%), and mixed infection (11.5%). The prevalence of samples positive for *Aeromonas* spp., *Plesiomonas shigelloides*, and *Vibrio* spp. were significantly higher in patients aged > 5 years. The prevalence of samples with mixed infection was however significantly higher in children aged ≤5 years (*p* =0.020). Most samples infected with *Aeromonas* spp and *Plesiomonas shigelloides* were susceptible (resistance prevalence ≤ 35%) to amoxicillin-clavulanate, chloramphenicol, ciprofloxacin, ceftriaxone, gentamicin, trimethoprim-sulfamethoxazole, and tetracycline. Samples infected with *Vibrio* spp. were sensitive to amoxicillin-clavulanate, chloramphenicol, ciprofloxacin, ceftriaxone, gentamicin, and tetracycline. Those infected with *Salmonella* spp. was resistant to ampicillin and tetracycline (resistance prevalence = 80% and 67%, respectively). Most samples infected with *Shigella* spp. were resistant to ampicillin (69%), chloramphenicol (64%), trimethoprim-sulfamethoxazole (93%), and tetracycline (82%).

Keywords: Enteric bacteria, Antimicrobial, Lao PDR

Introduction

Diarrheal disease is an important health problem which is the second leading cause of deaths annually, especially children under five in developing countries (1, 2). Diarrhea is caused by several microorganisms such as viruses, parasites, and bacteria. The pathogenic bacteria associated with diarrhea include *Shigella, Salmonella, Vibrio,* and pathogenic *Escherichia coli*. *E. coli* is the most commonly found pathogen of acute diarrhea in developing countries. Although this microorganism is the normal flora of the human intestine, several strains of *E. coli* are pathogenic to humans (3). The virulent strains of *E. coli* that cause diarrheal diseases are enterotoxigenic *E. coli* (ETEC), enteroinvasive *E. coli* (EIEC), enterohemorrhagic *E. coli* (EHEC), enteropathogenic *E. coli* (EPEC), and enteroaggregative *E. coli* (EAEC) (3).

The antimicrobial resistance (AMR) is a worldwide public health concern. A number of AMR cases have been reported in the Asia pacific region (4, 5), but with limited reports from Lao PDR. AMR surveillance is recommended by the World Health Organization (WHO) as an approach to control microbial infections. To cope with the AMR issue in Lao PDR, the surveillance program of the causative microorganisms of diarrhea has been launched in 2012 by the National Center for Laboratory and Epidemiology. The information of surveillance program is essential for planning and implementing disease control in Lao PDR. The aim of this study was to identify bacterial pathogens that cause diarrhea, the virulence of pathogenic *E. coli*, and the antimicrobial susceptibility profiles of enteric pathogens from diarrhea patients in Lao PDR during 2012.

Materials and Methods

1. tudy areas and samples collection

A cross sectional study was conducted in Vientiane capital as indicator-based surveillance (IBS) in eight hospitals/health centers: Mother and Child hospital (MC), Sisattanak district hospital (SIS), Sikottabong district hospital (SKB), Hatsaifong district hospital (HAT), Banhom health center (SH), Mahosot hospital (MHS), Settathilath hospital (SET), and Mittapab hospital (MTB). Clinical samples were from all the diarrheal patients attending the Emergency clinic, Internal department, Infectious ward and Pediatric ward of these hospitals. The event-based surveillance (EBS) of the disease outbreak was conducted during January to December 2012 throughout the country. The samples were collected randomly from five diarrheal case clusters. Diarrhea was defined as the passage of three or more liquid stools during a 24-hour period. Fresh stool, stool swab in Cary blair transport medium, or rectal swab in Cary blair transport medium were collected. A total of 708 stool/ rectal swab samples were collected and transported to the microbiology laboratory of The National Center for Laboratory and Epidemiology (NCLE) for cultivation of the causative agents.

2. Isolation and identification of enteric pathogen

Each clinical sample was suspended in 0.5 ml 0.85% normal saline solution to obtain working sample. Then working sample was initially inoculated with MacConkey agar, Salmonella-Shigella (SS-) agar, and Xylose lysine deoxycholate (XLD) agar, at 35°C for 18 to 48 hours for observing colonies of *Salmonella, Shigella, Vibrio, Aeromonas* and *Plesiomonas*, respectively (**Figure 1**). To identify the colonies of *Vibrio* spp., the working sample was further inoculated in alkaline peptone water (APW) and incubated at 35°C for 4-6 hours, and then transferred to thiosulfate citrate bile salts sucrose (TCBS) agar and incubated at 35°C for 18-48 hours. To identify the colonies of *Salmonella*, all working samples were inoculated overnight in Selenite broth at 35°C and transferred to SS-agar and XLD agar incubated at 35°C for an additional 18-48 hours and Modification Semisolid Rappaport-Vassiliadis (MSRV) medium incubate at 42°C for overnight. To identify *Campylobacter* spp, inoculated working sample in Preston broth with 5%lysed horse blood to enrich the organism for overnight at 35°C then transfer onto cellulose acetate membrane on Charcoal ceforazone deoxycholate agar (CCDA) or Blood agar, incubate plate at 42°C microaerophilic condition for 48-72 hours. Observing the suspected organisms on culture media, identified by colony morphology, gram-stain, and traditional biochemical tests. Confirmation using commercial reagent- API identification kit (Biomerieux, France) was required for gram-negative glucose fermentation-oxidase positive. If biochemical test show *Shigella*- or *Salmonella*-likes, serological confirmation were further tested.
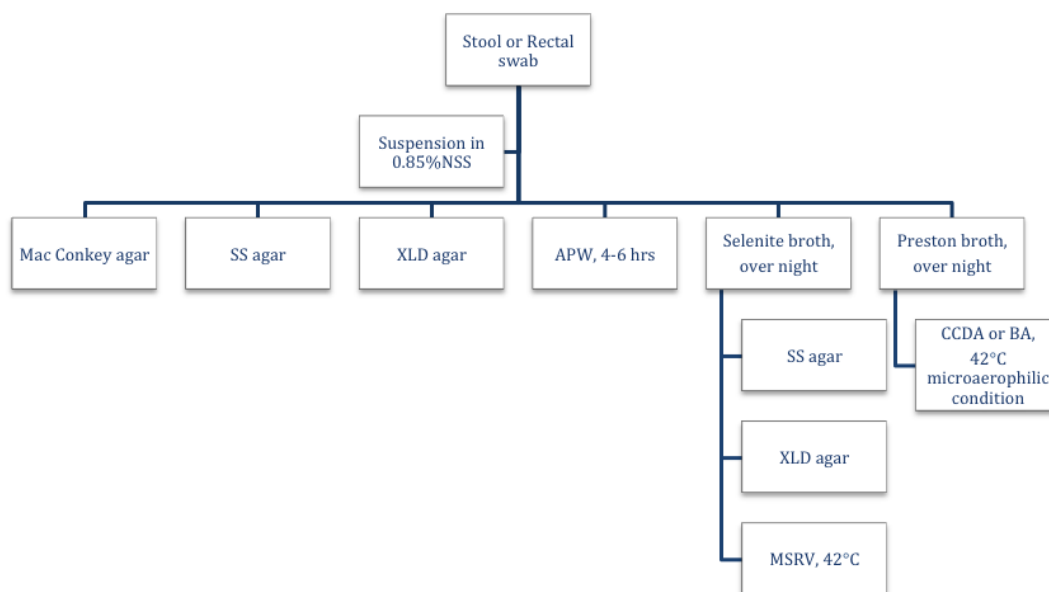
Figure 1 Diagram of bacterial culture process from stool/rectal swab

3. Identification of the virulence of pathogenic E. coli

Polymerase chain reaction (PCR) was used for identification of the virulence of *E. coli*. A loop-full of *E. coli*-like colonies from inoculated MC agar were swept and suspended into the extraction buffer (Tris-EDTA buffer) and DNA was extracted by boiling method. The

following target genes were used to differentiate pathogenic *E. coli*: *eae* and *bfp* (EPEC), *eae*, *stx1* and *stx2* (EHEC), *st* and *lt* (ETEC), and *ipaH* (EIEC). All primers sequences (Table 1) and PCR conditions were developed and/or modified by the Department of Bacteriology I, The National Institute of Infectious Diseases (NIID) Japan. The multiplex PCR conditions were as follows: 96°C for 2 min, 30 cycles of 96°C for 20 sec, 55°C for 20 sec, 72°C for 1 min, and 72°C for 1 min.

Table 1 Primer sequences for identification of pathogenic *E. coli*.

Target gene	Primer name	Sequence 5'-3'
eae	eaeA-newF	AACGGCTATTTCCGCATGAG
	eae-newR	CACATAAGCMGGCAAAATAGCCTG
bfp	bfpB-F	GACACCTCATTGCTGAAGTCG
	bfpB-newR	GCCCAGAACACCTCCGTTAT
stx1	mMK1-1	GAATTTACCTTAGACTTCTCGAC
	mMK1-2	TGTCACATATAAATTATTTCGTTCA
stx2	mMK2-1	GAGTTTACGATAGACCTTTCGAC
	mMK2-2	GGCCACATATAAATTATTTTGCTC
st	ST1a-s	GCAATTTTTATTTCTGTATTATCTT
	St1a-as	GGATTACAACAAAGTTCACAG
	ST1b-s	TTTATTTTTCTTTCTGTATTGTCTT
	St1b-as	GGATTACAACACAATTCACAG
lt	lt-Fv	CTATTACAGAACTATGTTCGGAATATC
	lt-Rv	GGGGGTTTTATTATTCCATACAC
ipaH	ipaH-F,	GTTCCTTGACCGCCTTTCCGATACCGTC
	ipaH-Rv	GCCGGTCAGCCACCCTCTGAGRGTAC

4. Antimicrobial susceptibility testing

Antimicrobial susceptibility test was performed on Mueller-Hinton agar (Becton Dickinson, USA) using disc diffusion technique. The antimicrobials under investigation included: ampicillin (10 µg), amoxicillin-clavulanate (20/10 µg), tetracycline (30 µg), gentamycin (10 µg), chloramphenicol (30 µg), ciprofloxacin (5 µg), trimethoprim-sulfamethoxazole (1.25/23.75 µg), and ceftriaxone (30 µg) (Oxoid, UK). The colonies 18- to 24-hours from non-selective media were selected and the working bacteria suspension was prepared in 0.85% sterile normal saline solution (0.85% NSS). Turbidity of the broth culture was equilibrated to match 0.5 McFarland standard. The surface of Mueller-Hinton agar plate was evenly inoculated with the culture using a sterile cotton swab. The antibiotic discs were applied to the surface of the inoculated agar. After 18–24 hours of incubation, the diameters of

growth inhibition around the discs were measured and interpreted as sensitive, intermediate, or resistant (6). The reference strain *E. coli* ATCC 25922 was used for quality control.

5. Data analysis

Statistical analysis was performed using SPSS version 12. Qualitative data are presented as number and percentage values. Comparison of the frequencies of microorganisms among all age groups was performed using Pearson's chi-square or Fisher exact test. Statistical significance was set at $\alpha = 0.05$.

Results

1. Identification of enteric pathogens

Of the 708 stool and rectal swab specimens collected in 2012, 554 were from acute watery diarrhea (AWD) surveillance program in Vientiane capital, 132 from diarrhea and/or food poisoning outbreak investigation, and 22 from public and private health facilities. Four hundred and sixty-seven samples were collected from patients aged less than 5 years. Two-hundred and eighty four samples were infected with *Aeromonas* spp. (1.7%), *Plesiomonas shigelloides* (1.7%), *Salmonella* spp. (4.9%), *Shigella* spp. (1.4%), *Vibrio* spp. (0.4%), pathogenic *E. coli* (17.9%), and mixed infection (11.6%) (**Table 2**). The prevalence of samples infected with *Aeromonas* spp., *Plesiomonas shigelloides*, *Shigella* spp. and *Vibrio* spp. were significantly higher in patients aged > 5 years ($p = 0.007$, < 0.0001, 0.042 and 0.009, respectively). In contrast, the prevalence of mixed infection with at least one enteric pathogen was significantly lower in children aged ≤ 5 years ($p = 0.013$) (**Table 3**).

Table 2 Identification of pathogenic microorganisms in the clinical samples. Data are presented as number (n) and percentage (%) values.

Bacterial identification	Number (n)	Percentage (%)
Aeromonas spp.	12	1.7
Plesiomonas shigelloides	12	1.7
Salmonella spp.	35	4.9
Shigella spp.	10	1.4
Vibrio spp.	3	0.4
Escherichia coli (*E. coli*)	127	17.9
- Enterohemorrhagic *E. coli* (EHEC)	20	2.8
- Enteroinvasive *E. coli* (EIEC)	26	3.7
- Enteropathogenic *E. coli* (EPEC)	58	8.2
- Enterotoxigenic *E. coli* - heat labile toxin (ETEC.LT)	9	1.3
- Enterotoxigenic *E. coli* - heat stable toxin (ETEC.ST)	14	2.0
Mixed infection with > 1 spp.	82	11.6
Negative	427	60.3
Total	708	100.0

2. *Antimicrobial susceptibility*

Antimicrobial susceptibility testing for the five microorganisms was successfully performed in 116 samples. Most samples infected with *Aeromonas* spp. and *Plesiomonas shigelloides* were susceptible to amoxicillin-clavulanate, chloramphenicol, ciprofloxacin, ceftriaxone, gentamicin, trimethoprim-sulfamethoxazole, and tetracycline; resistant isolates were found at the prevalence of 0-35%. Those infected with *Vibrio* spp. was sensitive to amoxicillin-clavulanate, chloramphenicol, ciprofloxacin, ceftriaxone, gentamicin, and tetracycline. Samples infected with *Salmonella* spp. were resistant to ampicillin and tetracycline (resistant rate = 80% and 67%, respectively). Most of the samples infected with *Shigella* spp. were resistant to ampicillin (69%), chloramphenicol (64%), trimethoprim-sulfamethoxazole (93%), and tetracycline (82%) (**Figure 2**).

Table 3 The enteric pathogens identified in clinical samples classified according to age groups. Data are presented as numbers (n).

Bacterial identification	Number of samples (n)		*p*-value
	≤ 5 years	> 5 years	
Aeromonas spp.	4	8	0.007*
Plesiomonas shigelloides	1	11	< 0.0001*
Salmonella spp.	26	9	0.596
Shigella spp.	4	6	0.042*
Vibrio spp.	0	3	0.009*
Escherichia coli (*E. coli*)	85	42	0.507
- Enterohemorrhagic *E. coli* (EHEC)	10	10	0.058
- Enteroinvasive *E. coli* (EIEC)	16	10	0.361
- Enteropathogenic *E. coli* (EPEC)	41	17	0.917
- Enterotoxigenic *E. coli* - heat labile toxin (ETEC.LT)	8	1	0.220
- Enterotoxigenic *E. coli* - heat stable toxin (ETEC.ST)	10	4	0.910
Mixed infection with > 1 spp.	46	36	0.013*
Total	166	115	

Discussion

The prevalence of death from diarrhea in children under 5 years reported In Lao PDR in 2004 was 16.9% (7). The outbreaks of diarrhea were reported in 1993 and 1994, and during the period 2000-2002. In 2007, the outbreak of diarrhea was investigated and more than 50% of *V. cholerae* was found to be the cause of diarrhea (8). Nevertheless, antimicrobial susceptibility of the pathogenic microorganisms was not investigated during these outbreaks. The susceptibility testing for *E. coli* was not accomplished due to technical problem at the step of bacterial purification.

Specimen were classified into 2 groups as age less than or equal five years old and greater than five years old as children ≤ 5 are age of pre-school which have lower immunity

and had several report of infectious diseases. Results of the present study show that only 40% of patients infected with bacterial pathogens and the major cause of diarrhea was *E. coli* (17.9%) with comparable prevalence in both age groups (≤ 5 and **>** 5 years). Some samples with negative bacterial infection were found to be infected with protozoas, helminthes, or viruses.

The previous study in Vientiane, Lao PDR during 1996-1997, showed the major cause of diarrhea were *E. coli* (35.8%) and *Shigella* spp. (16.8%) infections (9). The highest number of *E. coli* infection was also found in the present study but the *Shigella* spp. infection was only found 1.4%. The prevalence of enteropathogenic *E. coli* was similar to that reported previously, except the enterotoxigenic *E. coli* - heat stable toxin (ETEC.ST) (2.0 % *vs*. 17.2%) (9). It was noted however that the present study was conducted 15 years back and the prevalence and patterns of infected micro-organisms may be changed.

A trend of antimicrobial resistance in *Salmonella* spp. and *Shigella* spp. was observed in the study samples. Samples infected with *Shigella* spp. were resistant (multidrug resistant) to ampicillin, chloramphenicol, trimethoprim-sulfamethoxazole, and tetracycline. High level of resistance in samples infected with *Shigella* spp. has been observed in several countries (10-13). In this study, resistance to ciprofloxacin was not found and resistance to ceftriaxone and nalidixic acid was found at the prevalence of 20% and 35%, respectively. Continuous monitoring of antimicrobial resistance in Lao PDR and control use of antimicrobial drugs is required because there are still no policy or measurement to controlled the antibacterial use including imported of food animal and seafood from neighboring country.

Conclusion

The enteric pathogen is an important cause of diarrhea worldwide including Lao PDR. Our results show that most (40%) diarrhea in Lao PDR is caused by the bacterial pathogens *E. coli*, *Aeromonas* spp., *Plesiomonas shigelloides*, *Salmonella* spp., *Shigella* spp., and *Vibrio* spp. Those infected with *Shigella* spp. were multidrug resistant to several antimicrobial drugs. Continuous monitoring of antimicrobial resistance in Lao PDR and control use of antimicrobial drugs is required.

Acknowledgements
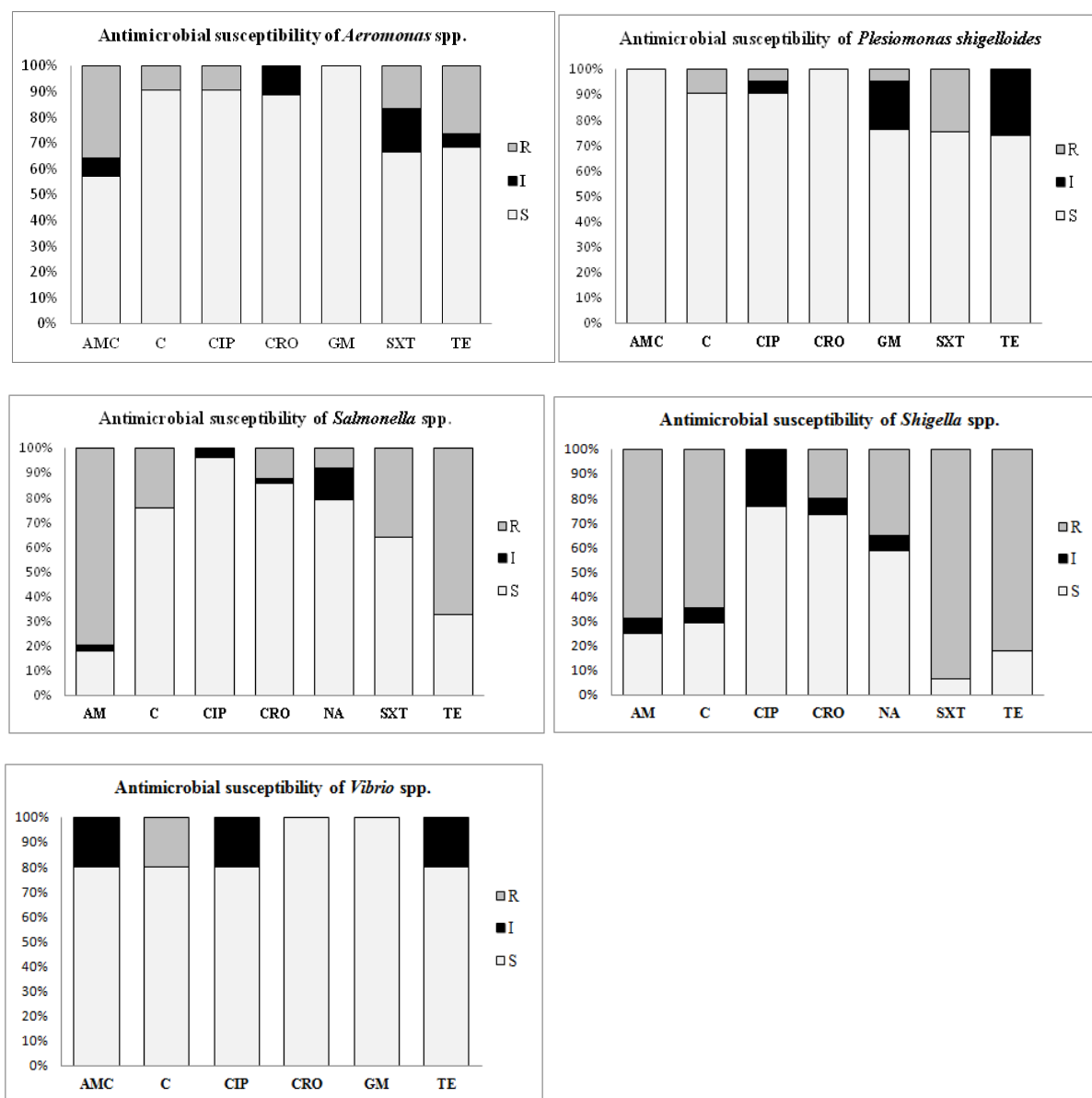
Figure 2 Antimicrobial susceptibility of the clinical samples infected with *Aeromonas* spp., *Plesiomonas shigelloides*, *Salmonella* spp., *Shigella* spp., and *Vibrio* spp.

AMC: Amoxicillin-clavulanate, AM: Ampicillin, C: Chloramphenicol,
CIP: Ciprofloxacin, CRO: Ceftriaxone, NA: Nalidixic acid, GM: Gentamicin,
SXT: Trimethoprim-sulfamethoxazole, TE: Tetracycline
R: Resistant, I: Intermediate, S: Susceptible

References

1. Boschi-Pinto C, Velebit L, Shibuya K. Estimating child mortality due to diarrhoea in developing countries. Bull World Health Organ. 2008;86(9):710-7.
2. Podewils LJ, Mintz ED, Nataro JP, Parashar UD. Acute, infectious diarrhea among children in developing countries. Semin Pediatr Infect Dis. 2004;15(3):155-68.
3. Nataro JP, Kaper JB. Diarrheagenic Escherichia coli. Clin Microbiol Rev. 1998;11(1):142-201.
4. Kang CI, Song JH. Antimicrobial resistance in Asia: current epidemiology and clinical implications. Infect Chemother. 2013;45(1):22-31.
5. Lestari ES, Severin JA, Verbrugh HA. Antimicrobial resistance among pathogenic bacteria in Southeast Asia. Southeast Asian J Trop Med Public Health. 2012;43(2):385-422.
6. CLSI. Performance Standards for Antimicrobial Susceptibility Testing. CLSI document 2015;35.
7. Infant mortality under 5 by cause, Diarrhoea (%) - for all countries [Internet]. factfish. 2010-2015. Available from: http://www.factfish.com/statistic/infant%20mortality%20under%205%20by%20cause%2C%20diarrhoea.
8. Lenglet A, Khamphaphongphane B, Thebvongsa P, Vongprachanh P, Sithivong N, Chantavisouk C, et al. A cholera epidemic in Sekong Province, Lao People's Democratic Republic, December 2007-January 2008. Jpn J Infect Dis. 2010;63(3):204-7.
9. Yamashiro T, Nakasone N, Higa N, Iwanaga M, Insisiengmay S, Phounane T, et al. Etiological study of diarrheal patients in Vientiane, Lao People's Democratic Republic. J Clin Microbiol. 1998;36(8):2195-9.
10. Gebrekidan A, Dejene TA, Kahsay G, Wasihun AG. Prevalence and antimicrobial susceptibility patterns of Shigella among acute diarrheal outpatients in Mekelle hospital, Northern Ethiopia. BMC Res Notes. 2015;8:611.
11. Kim JS, Kim JJ, Kim SJ, Jeon SE, Seo KY, Choi JK, et al. Outbreak of Ciprofloxacin-Resistant Shigella sonnei Associated with Travel to Vietnam, Republic of Korea. Emerg Infect Dis. 2015;21(7):1247-50.
12. Cui X, Wang J, Yang C, Liang B, Ma Q, Yi S, et al. Prevalence and antimicrobial resistance of Shigella flexneri serotype 2 variant in China. Front Microbiol. 2015;6:435.
13. Malakooti MA, Alaii J, Shanks GD, Phillips-Howard PA. Epidemic dysentery in western Kenya. Trans R Soc Trop Med Hyg. 1997;91(5):541-3.

RESEARCH ARTICLE

An updated systematic review of hyperpigmentation treatment

Napatchar Techataratip[1], Jitlada Meephansan[1], Phubodin Vongtaranavuth[2], Pichit Suvanprakorn[2]

[1]*Division of Dermatology, Chulabhorn International College of Medicine, Thammasat University, Pathum Thani, 12120, Thailand*
[2]*Pan Rajdhevee Suphannahong Foundation, Bangkok, 10330, Thailand.*

Address correspondence and reprint request to: Jitlada Meephansan, Chulabhorn international college of medicine, Thammasat University, Pathum Thani, Thailand. E-mail address: kae_mdcu@yahoo.com.

Abstract

Hyperpigmentation, including postinflammatory hyperpigmentation, melasma, and lentigines, is a common problem in cosmetic dermatology. Its treatment remains challenging because the results of topical treatment, chemical peeling, or even laser treatment are unpredictable, and relapse is frequent. Topical treatments mostly include depigmenting agents such as hydroquinone, azelaic acid, and retinoids. The most effective topical treatment is hydroquinone; however, it causes many adverse effects, such as irritation and permanent ochronosis. Using other modalities rather than hydroquinone may help to avoid these adverse effects. Therefore, we gathered data from articles published on hyperpigmentation treatments and conducted a systematic review. We found that various treatment methods including topical and laser treatment are as effective as the gold standard, with fewer adverse effects.

Keywords: Hyperpigmentation, botanical extracts, treatment of hyperpigmentation, depigmenting agents.

Introduction

A common complaint at Asian dermatology clinics is hyperpigmentation, including melasma and postinflammatory hyperpigmentation. In the past, hydroquinone or triple combination cream (TCC) (hydroquinone + retinoic acid + corticosteroid) was the gold standard treatment for hyperpigmented lesions. Currently, many depigmenting agents have been launched to replace hydroquinone because of its adverse effects. Although some depigmenting agents are not as effective as hydroquinone, they do not cause irritation, erythema, or ochronosis. It is required to find a new treatment modality that is better than hydroquinone and/or has fewer adverse effects.

Methods

This article reviews the brief pathogenesis of melanogenesis, and focuses on the treatment of hyperpigmentation. This review was based on a literature search of the PubMed database, using the terms "hyperpigmentation," "melanogenesis," "melanin," "depigmenting agents," and "skin lightening." Other sources of data included dermatological textbooks.

We searched the PubMed database by using the medical subject headings (MeSH) term, "Melasma". Our search yielded 8,404 results. Only clinical trials and full text articles were included, and 203 publications were identified. Furthermore, we limited our study to studies that occurred between January 2011 and December 2015 (five years). Seventy-five publications appeared during our search. The reviewers screened the abstracts of these publications.

Sixty-nine publications were removed from this study because they were not concerning melasma, did not evaluate the outcomes using the Melasma Area and Severity Index (MASI) score, and the standard treatment (hydroquinone or TCC) was not used in the control groups. Finally, six publications were eligible for our systematic review.

The outcome of interest for this study was the MASI score used to measure the improvement in melasma lesions after treatment. The results reflect the other treatment modalities for hyperpigmentation. We needed to collect data on melasma studies alone because the standard evaluation of melasma is similar.

Melanogenesis

Melanogenesis is a complex process of producing melanin pigment. It occurs in melanosomes, which are specialized intracellular vesicles present in melanocytes.[1, 2] Melanosomes are transferred to keratinocytes through the dendrites of melanocytes, where they protect the nuclei of keratinocytes from ultraviolet (UV) radiation.[1] Melanocytes may be stimulated by direct exogenous factors such as UV radiation or by indirect factors such as cytokines and growth factors of keratinocytes, fibroblasts, or other cells.[3] Keratinocytes produce paracrine and/or autocrine signals known as keratinocyte-derived factors, such as alpha-melanocyte stimulating hormone (α-MSH), adrenocorticotropic hormone (ACTH), basic fibroblast growth factor (bFGF), steel factor. These growth factors influence the proliferation and differentiation of melanocytes.[4]

Melanosomes contain a number of melanin-producing enzymes such as tyrosinase, tyrosinase-related protein 1 (TRP-1), tyrosinase-related protein 2 (TRP-2), and dopachrome tautomerase (Dct).[5, 6] Tyrosinase is one of the most important enzymes in melanogenesis.[2, 7] It controls two rate-limiting steps in melanogenesis.[8,9] Many depigmenting agents target tyrosinase, aiming to inhibit melanin production. Tyrosinase is a copper-dependent enzyme.[10] It converts tyrosine (substrate) to L-3,4-dihydroxyphenylalanine (L-DOPA) and then oxidizes L-DOPA to dopaquinone.[8, 11] Microphthalmia-associated transcriptional factor (MITF) is a key regulator of tyrosinase, TRP-1 and TRP-2 gene transcription in melanocytes.[5,12] MITF plays a

crucial role in binding to tyrosinase promoter and in turning on the melanin production process.[13] It regulates melanogenic enzymes and proliferation and differentiation of melanocytes, and is induced by Cyclic-AMP (cAMP).[14] c-AMP is a secondary messenger that regulates protein kinase A (PKA).[15] It affects cAMP-dependent PKA as well as cAMP-responsive element binding protein (CREB).[6,14]

Table 1: The mechanisms and efficacy of natural products for the management of hyperpigmentation

Natural products	Mechanisms	Efficacy
Arbutin	Competitive tyrosinase inhibitor Inhibits melanosome maturation	Topical deoxyarbutin application for 12 weeks resulted in a significant reduction in overall skin lightness in human clinical trial [16] Suppressed pigmentation by 43.5% in a clinical study in humans [17]
Aloesin	Dose-dependent competitive tyrosinase inhibitor	Suppressed pigmentation by 34% in a clinical study [17]
Ellagic acid	Tyrosinase inhibition via copper chelation	Suppressed pigmentation more than kojic acid or arbutin at the same dose in B16/F0 mouse melanoma cells [18]
Emblica extract	Antioxidant Inhibits melanogenesis	In facial dyschromia, products containing kojic acid, *Emblica* extract, and glycolic acid showed similar effectiveness to 4% HQ [19]
Flavonoids	Antioxidant Inhibits melanocyte proliferation Tyrosinase inhibitor	*Garcinia gardneriana* and kojic acid inhibited melanogenesis by 35.2% and 87%, respectively [20]
Hesperitin	Suppresses ultraviolet-induced oxidative damage Competitive and reversible tyrosinase inhibitor	Hesperetin bound more tightly to tyrosinase than kojic acid [21]
Niacinamide	Antioxidant Anti-inflammatory Inhibits melanosome transfer	In an *in vitro* study, inhibited melanosome transfer by 35%–68% [22]
Licorice	Antioxidant Anti-inflammatory Tyrosinase inhibitor	In a clinical trial, topical liquiritin was therapeutically effective in melasma, with complete disappearance in 18 (90%) out of 20 subjects at week four [23]
Mulberry	Antioxidant Tyrosinase inhibitor	Concentration of mulberroside F required to suppress mammalian tyrosinase activity by 50% was higher than kojic acid [24]

Many studies have investigated novel depigmenting agents, but the results have not been compared in a systematic review. (Table 1) Finally, we collected only publications on melasma (as described in the methods), as these studies have similarly evaluated methods (MASI score) (Figure 1, Table 2).

Table 2: Results of the studies

Study	Case	N (E/C)	Control	N (E/C)	MASI before treatment		MASI after treatment		Treatment duration
					Case	Control	Case	Control	
Farshi[25]	20% Azelaic acid	15/14	4% Hydroquinone	15/15	7.6 ± 3.5	7.2 ± 3.2	3.8 ± 2.8	6.2 ± 3.6	2 months
Kroon[26]	Nonablative 1550-nm fractional laser Therapy	10/10	Triple combination Cream	10/10	8.5 ± 3.6	9.8 ± 6.5	6.6 ± 3.8	6.9 ± 5.9	8 weeks
Passeron[27]	Pulse dye laser + TCC	18/17	Triple combination cream	18/17	6.20 ± 3.02	6.76 ± 3.25	2.79 ± 2.70	4.25 ± 2.76	4 months
Yousefi[28]	10% Zinc sulfate	40/38	4% Hydroquinone	42/42	6.3 ± 2.1	6.4 ± 1.6	5.1 ± 2	3.9 ± 1.4	2 months
Mendoza[29]	3% Rumex occidentalis cream	15/15	4% Hydroquinone	15/15	Diff = 0.6 SD = 0.86	Diff = 0.55 SD = 0.62			8 weeks
Ghorbel[30]	Copper Bromide laser + TCC	20/17	Triple combination cream	20/17	7.66 ± 5.11	7.29 ± 4.11	7.81 ± 4.58	6.58 ± 3.30	6 months
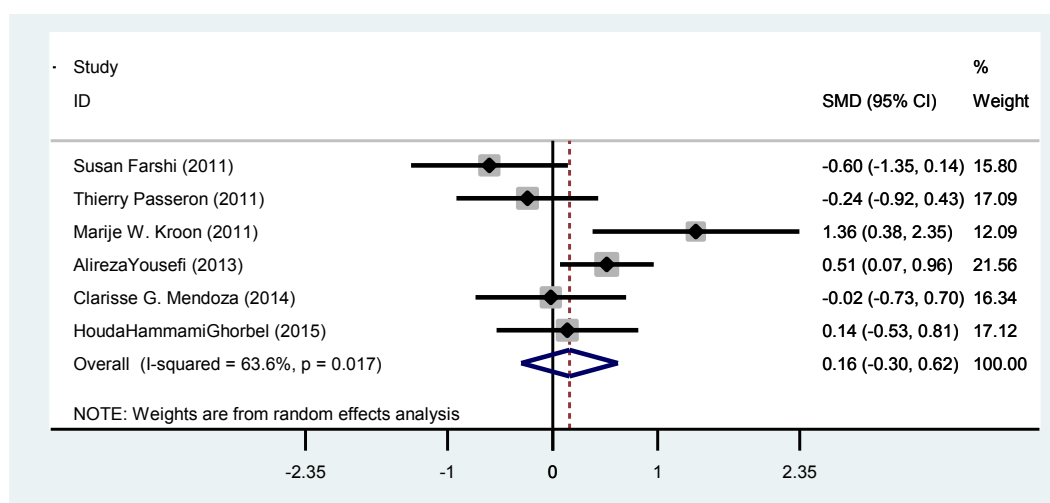
Figure 1: Forest plot of the difference in MASI score between baseline and after melasma treatment. Standardized mean difference (SMD),

Heterogeneity chi-squared = 13.73 (d.f. = 5) p = 0.017,

I-squared (variation in SMD attributable to heterogeneity) = 63.6%,

Estimate of between-study variance Tau-squared = 0.2032,

Test of SMD = 0: z = 0.69 p = 0.493

Table 3: Characteristics of Patients in Included Trials

Study	Year	Age Mean ± SD (Range) Years	Type of melasma			Fitzpatrick skin type	Wash out period
			Epidermal	Dermal	Mixed		
Farshi[25]	2011	34.6 ± 6.6	Inclusion criteria = epidermal melasma	-	-	Not mentioned	2 months
Kroon[26]	2011	Case = 35.3 Control = 42	Case = 6/10 pts. Control = 7/10 pts.	Case = 3/10 pts. Control = 1/10 pts.	Case = 1/10 pts. Control = 2/10 pts.	Type II = 5/20 pts. Type III = 8/20 pts. Type IV = 5/20 pts. Type V = 2/20 pts.	4 weeks
Passeron[27]	2011	41 (33-56)	Not mentioned			Type II = 4/18 pts. Type III = 8/18 pts. Type IV = 6/18 pts.	Not mentioned
Yousefi[28]	2013	Case = 33.1 ± 9.1 Control = 35.2 ± 8.1	Case = 60% Control = 64.2%	-	Case = 40% Control = 35.7%	Not mentioned	3 months
Mendoza[29]	2014	29.04 ± 7.8 (18-50)	Case = 86.7% Control = 73.3%	-	Case = 13.3% Control = 26.7%	Filipino patients Not mentioned skin type.	2 months
Ghorbel[30]	2015	38.4 ± 6.2 (30-53)	Not mentioned			Type II = 3/20 pts. Type III = 10/20 pts. Type IV = 7/20 pts.	Not mentioned

Results

We identified 75 publications in the PubMed database. Sixty-nine publications were excluded because of methodology, leaving six trials that were eligible for review and inclusion in the analysis.

Trial results are described in Table 2. All six trials compared MASI score in patients with melasma between standard treatment (hydroquinone or TCC), as a control group, and other treatment modalities such as topical therapies or laser.

The mean age of the patients in these trials ranged between 29.04 and 56 years. The patients had all types of melasma (epidermal, dermal, or mixed melasma). Patients with Fitzpatrick skin type II to V were enrolled in these studies. The patients had discontinued the use of any depigmenting agents between 4 weeks and 3 months before they were enrolled in the studies, but two of six publications did not mention the wash out period.

The forest plot in Figure 1 showed that the case and control group were different overall, with an SMD of 0.16. (95% confidence interval = -0.30 to 0.62) It demonstrated that the control group was better than the case group.

All six clinical trials included melasma treatment studies (Table 2). There was evidence of heterogeneity among these trials (I^2 = 63.6%, chi-squared = 13.73, p = 0.017). The heterogeneity may be due to the study design. The variety of patients, type of melasma, wash out period, duration of the study, and skin types of patients could all be the cause of heterogeneity. (Table 3)

Discussion

In this updated systematic review, we have summarized the current clinical outcomes of melasma treatment for the treatment of hyperpigmentation.

It might be evident that topical therapies or laser treatment for hyperpigmentation are as effective as the gold standard treatment, hydroquinone or TCC (hydroquinone 4% + tretinoin 0.05% + triamcinolone acetonide 0.1% cream). Although this result was not statistically significant, it could be applied to clinical use. Using other treatment modalities can prevent the adverse effects of hydroquinone, including irritation, erythema, or ochronosis.

Conclusion

The outcomes of melasma treatment were better in both case and control groups in our meta-analysis. However, we did not find that the case group was significantly better than the control group (p > 0.05). In this study, the duration of treatment, topical regimens, or even characteristics of patients were different, so further study should be done by randomized block design to get a precise result. Further studies must use similar treatment modalities in similar populations, with the same treatment duration.

In our study, we only chose publications in which hyperpigmentation treatment was compared with the gold standard treatment (hydroquinone or TCC). As a result, all treatment modalities in the case group can be applied in practice to prevent the adverse effects of standard treatment.

Reference:

1. Chandra M, Levitt J, Pensabene CA. Hydroquinone therapy for post-inflammatory hyperpigmentation secondary to acne: not just prescribable by dermatologists. *Acta Derm Venereol* 2012; **92**: 232-5.
2. Kolbe L, Mann T, Gerwat W, et al. 4-n-butylresorcinol, a highly effective tyrosinase inhibitor for the topical treatment of hyperpigmentation. *J Eur Acad Dermatol Venereol* 2013; **27**: 19-23
3. Jimbow K, Minamitsuji Y. Topical therapies for melasma and disorders of hyperpigmentation. *Dermatologic Ther* 2001; **14**: 35-45.
4. Costin GE, Hearing VJ. Human skin pigmentation: melanocytes modulate skin color in response to stress. *FASEB J* 2007; **21**: 976-94.
5. Lee SJ, Lee WJ, Chang SE, Lee G-Y. Antimelanogenic effect of ginsenoside Rg3 through extracellular signal-regulated kinase-mediated inhibition of microphthalmia- associated transcription factor. *J Ginseng Res* 2015; **39**: 238-42.
6. Chao HC, Najjaa H, Villareal MO, et al. Arthrophytum scoparium inhibits melanogenesis through the down-regulation of tyrosinase and melanogenic gene expressions in B16 melanoma cells. *Exp Dermatol* 2013; **22**: 131–6.
7. Lou SN, Yu MW, Ho CT. Tyrosinase inhibitory components of immature calamondin peel. *Food Chem* 2012; **135**: 1091-6.

8. Kang KH, Lee B, Son S, et al. (Z)-2-(Benzo[d]thiazol-2-ylamino)-5-(substituted benzylidene)thiazol- 4(5H)-one derivatives as novel tyrosinase inhibitors. *Biol Pharm Bull* 2015; **38**: 1227-33.

9. Nguyen BCQ, Tawata S. Mimosine dipeptide enantiomsers: improved inhibitors against melanogenesis and cyclooxygenase. *Molecules* 2015; **20**: 14334-47.

10. Dej-adisai S, Meechai I, Puripattanavong J, Kummee S. Antityrosinase and antimicrobial activities from Thai medicinal plants. *Arch Pharm Res* 2014; **37**: 473–83.

11. Jorge ATS, Arroteia KF, Santos IA, et al. Schinus terebinthifolius Raddi extract and linoleic acid from Passiflora edulis synergistically decrease melanin synthesis in B16 cells and reconstituted epidermis. *Int J Cosmet Sci* 2012; **34**: 435–40.

12. Baek SH, Lee SH. Proton pump inhibitors decrease melanogenesis in melanocytes. *Biomed Rep* 2015; **3**: 726-30.

13. Lee J, Jung K, Kim YS, Park D. Diosgenin inhibits melanogenesis through the activation of phosphatidylinositol-3-kinase pathway (PI3K) signaling. *Life Sci* 2007; **81**: 249-54.

14. Hwang E, Lee TH, Lee WJ, et al. A novel synthetic Piper amide derivative NED-180 inhibits hyperpigmentation by activating the PI3K and ERK pathways and by regulating Ca2+ influx via TRPM1 channels. *Pigment Cell Melanoma Res* 2016; **29**: 81-91.

15. Roh E, Yun CY, Yun JY, et al. cAMP-binding site of PKA as a molecular target of bisabolangelone against melanocyte-specific hyperpigmented disorder. *J Invest Dermatol* 2013; **133**: 1072-9.

16. RE B, M V, MA d. DeoxyArbutin: a novel reversible tyrosinase inhibitor with effective in vivo skin lightening potency. *Exp Dermatol* 2005; **14**: 601-8.

17. Choi S, Park YI, Lee SK, Kim JE, Chung MH. Aloesin inhibits hyperpigmentation induced by UV radiation. *Clin Exp Dermatol* 2002; **27**: 513-5.

18. Shimogaki H, Tanaka Y, Tamai H, Masda M. In vitro and in vivo evaluation of ellagic acid onmelanogenesis inhibition. *Int J Cosmet Sci* 2000; **22**: 291-303.

19. Draelos ZD, Yatskayer M, Bhushan P, Pillai S, Oresajo C. Evaluation of a kojic acid, emblica extract, and glycolic acid formulation compared with hydroquinone 4% for skin lightening. *Cutis* 2010; **86**: 153-8.

20. Campos PcM, Horinouchi CnDdS, Prudente AdS, Cechinel-Filho V, Cabrini DdA, Otuki MF. Effect of a Garcinia gardneriana (Planchon and Triana) Zappi hydroalcoholic extract on melanogenesis in B16F10 melanoma cells. *J Ethnopharmacol* 2013; **148**: 199-204.

21. Sia YX, Wanga ZJ, Parkb D, et al. Effect of hesperetin on tyrosinase: Inhibition kinetics integrated computational simulation study. *Int J Biol Macromol* 2012; **50**: 257–62.

22. Hakozaki T, Minwalla L, Zhuang J, et al. The effect of niacinamide on reducing cutaneous pigmentationand suppression of melanosome transfer. *Brit J Dermatol* 2002; **147**: 20-31.

23. Amer M, Metwalli M. Topical liquiritin improves melasma. *Int J Dermatol* 2000; **39**: 299-301.

24. Lee SH, Choi SY, Kim H, et al. Mulberroside F isolated from the leaves of Morus alba inhibits melaninbiosynthesis. *Biol Pharm Bull* 2002; **25**: 1045-8.

25. Farshi S. Comparative study of therapeutic effects of 20% azelaic acid and hydroquinone 4% cream in the treatment of melasma. *J Cosmet Dermatol* 2011; **10**: 282-7.

26. Kroon MW, Wind BS, Beek JF, Veen JPW, Nieuweboer-Krobotova L, Bos JD, et al. Nonablative 1550-nm fractional laser therapy versus triple topical therapy for the treatment of melasma: a randomized controlled pilot study. *J Am Acad Dermatol* 2011; **64**: 516-23.

27. Passeron T, Fontas E, Kang HY, Bahadoran P, Lacour J-P, Ortonne J-P. Melasma treatment with pulsed-dye laser and triple combination cream: a prospective, randomized, single-blind, split-face study. *Arch Dermatol* 2011; **147**: 1106-8.
28. Yousefi A, Khoozani ZK, Forooshani SZ, Omrani N, Moinni AM, Eskandari Y. Is topical zinc effective in the treatment of melasma? a double-blind randomized comparative study. *Deramatol Surg* 2014; **40**: 33-7.
29. Mendoza CG, Singzon IA, Handog EB. A randomized, double-blind, placebo-controlled clinical trial on the efficacy and safety of 3% Rumex occidentalis cream versus 4% hydroquinone cream in the treatment of melasma among Filipinos. *Int J Dermatol* 2014; **53**: 1412-6.
30. Ghorbel HH, Boukari F, Fontas E, Montaudie H, Bahadoran P, Lacour J-P, et al. Copper bromide laser vs triple-combination cream for the treatment of melasma: a randomized clinical trial. *JAMA Dermatol* 2015; **151**: 791-2**.**

RESEARCH ARTICLE

Systematic review: an updated review of botulinum toxin for the treatment of hyperhidrosis

Chanisa Chamnanvad[1], Panlop Chakkavittumrong[1], Mukarin Surapanpitak[2], Panida Laoratthapong[2]

[1]*Division of Dermatology, Department of Medicine, Chulabhorn International College of Medicine, Thammasat University, Pathum Thani 12120, Thailand*
[2]*Pan Rajdhevee Suphannahong Foundation, Bangkok 10330, Thailand*

Address correspondence and reprint request to: Chanisa Chamnanvad, email: pukbungchanisa@gmail.com.

Abstract

Botulinum toxin has recently emerged as a promising alternative for hyperhidrosis treatment. We conducted a systematic review to investigate the feasibility of botulinum toxin injections for the treatment of primary focal hyperhidrosis. Seven databases were searched for all literature published the previous ten years. Five studies were found that met our inclusion and exclusion criteria. Statistical analysis revealed that the standardized mean differences of the dermatology life quality index scores declined by an average of 1.65 units after treatment began ($p < 0.05$). Our results suggest that botulinum toxin (BoNT) is effective for primary focal hyperhidrosis, and may improve patients' dermatological quality of life.

Keywords: botulinum toxin, botulinum toxin type-A, hyperhidrosis, dermatology quality of life

Introduction

Primary hyperhidrosis is an idiopathic disorder that causes excessive sweating, typically in the axillae, palms, soles, and face. Several therapeutic strategies, including topical aluminum salts, tap-water iontophoresis, and oral anticholinergics, have yielded satisfactory results. However, their effects are usually temporary and often result in adverse effects and complications. Botulinum toxin (BoNT) has recently emerged as a promising alternative for hyperhidrosis treatment. It is a potent neurotoxin derived from the bacterium Clostridium botulinum. While there are seven distinct serotypes of BoNT (A, B, C1, D, E, F, and G), only BoNT types A and B are commercially available. Botulinum toxins block cholinergic stimulus of eccrine sweat glands by inhibiting the presynaptic release of acetylcholine while also binding to acetylcholine receptors at the postsynaptic membrane. Because focal HH likely results from neurogenic hyperactivity as opposed to structural abnormalities in the eccrine glands, BoNT may be the ideal treatment for focal HH[4]. We aimed to perform a systematic review of recent literature to explore the effectiveness of BoNT against hyperhidrosis with regards to improvement in dermatological quality of life.

Materials and Methods

Literature review

We used PubMed, Medline, EBSCO, Ovid, Embase, PROQUEST and Cochrane databases to search literature from 2005 to 2016. The search encompassed literature ahead of print and non-English articles. The following terms were used in various combinations: HH OR botulinum toxin OR botulinum toxin for HH OR HH treatment OR sweating OR therapy OR treatment OR axillary OR palmar OR plantar OR facial OR botulinum neurotoxin OR oral OR topical and surgical.

Study selection

We included data from several types of cohort studies that quantitatively assessed botulinum toxin for HH treatment except in the following cases: BoNT was noted as an exclusion criterion; the study subjects were not humans; the study was not published in a full text journal; the condition was not primary HH; gravimetric assessment was not performed; studies that did not contain DLQI scores. We also expanded medical subject headings (MeSH) search terms to include "botulinum toxins for therapeutic use."

Statistical analysis

For continuous outcomes, the mean differences between Dermatology Life Quality Index (DLQI) scores before and after treatment were summarized using standardized mean differences (SMDs). The presence of heterogeneity between the studies was assessed using the Cochran Q (heterogeneity chi-squared) test and I^2 test. The random effects model was applied for all pooling. A p-value < 0.05 was considered statistically significant except when the heterogeneity test was used, in which case $p < 0.10$ was considered significant. All data were analyzed with STATA version 13.0 (StataCorp LP, College Station, TX).

Results

Although results from several studies varied, our statistical analysis revealed that BoNT is effective and can significantly reduce sweating and increase patients' DLQI scores (Table 1). In fact, when we summarized the mean DLQI scores before and after treatment (Table 2) as SMDs, a significant difference before and after treatment with BoNT types A and B emerged ($p < 0.05$), with the SMDs of the DLQI scores declining by an average of 1.65 units from baseline (95% CI: 1.42–1.87). However, the heterogeneity chi-squared test result was 536.13 ($p < 0.001$), and I^2 (variation in SMD attributable to heterogeneity) = 99.3%, indicating that the 5 studies significantly differed (Figure 1).

To illustrate, figure 2 compares the SMDs of the DLQI change from baseline with the study durations. Kouris et al.[7] recorded the highest SMD of 17, but their study duration was 12 weeks. On the other hand, Rosell et al.[9] had a SMD of 10.3 with study duration of 3 weeks. The duration of the remaining studies was also 4 weeks. Therefore, we conclude that the amount of time required for BoNT to improve quality of life varies depending on the HH site.

Table 1. These studies found that the botulinum toxin for HH treatment significantly increases quality of life.

Author	N	Agent	Type of HH	Result
Karlqvist 2013 (6)	38	Botulinum toxin B	Craniofacial HH	DLQI scores significantly improved at 2,4 weeks
Kouris 2014 (7)	119	Botulinum toxin A (OnaA)	Axillary HH Palmar HH Plantar HH	DLQI scores significantly lower than the baseline values ($p < 0.0001$)
Marcella 2011 (8)	30	Botulinum toxin A	Axillary HH	DLQI scores significantly improved ($p < 0.001$)
Rosell 2013 (9)	84	Botulinum toxin A and B	Axillary HH Palmar HH	DLQI scores significantly improved: palmar HH 100%, axillary HH 95% ($p < 0.05$)
Weber 2005 (10)	70	Botulinum toxin A	Axillary HH Palmar HH Plantar HH	DLQI scores worsened with mean ± SD skin index score of 24.3 ± 5.7 at baseline

DLQI: Dermatology Life Quality Index

Table 2. Dermatology Life Quality Index scores before and after botulinum toxin treatment as SMDs.

Study	Name	Years	N	Before		After		SMD	Duration (weeks)
				Mean	SD.	Mean	SD.		
1	Karlqvist	2013	38	13	1	5	1	8	4
2	Kouris	2014	119	20	1	3	1	17	12
3	Marcella	2011	30	45.3	19.6	38.5	22.4	0.32	4
4	Rosell	2013	84	12	5.5	1.7	2.6	2.39	3
5	Weber	2004	70	24.3	5.7	17.6	15.5	0.57	4
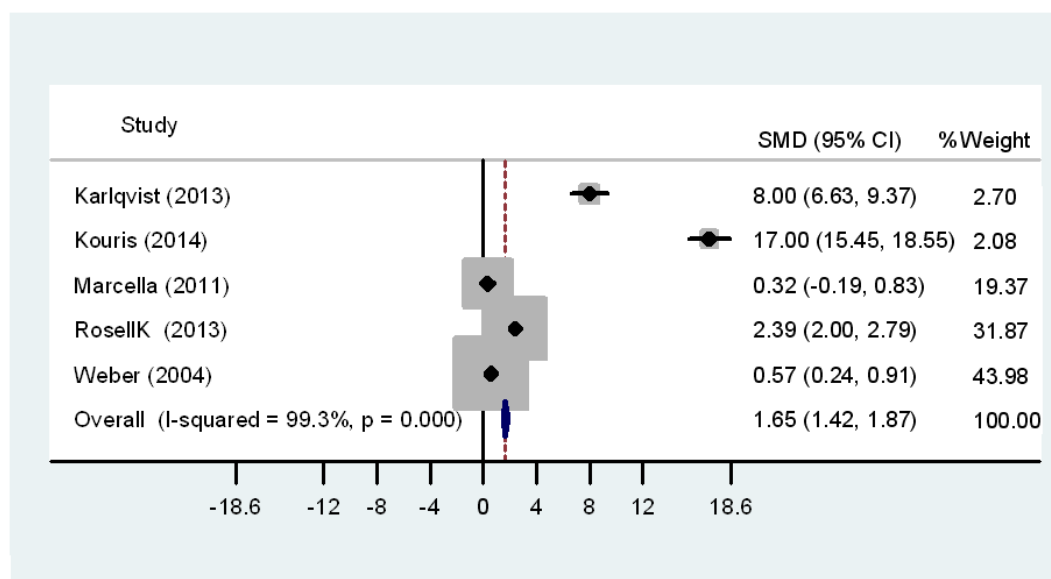
Figure 1: Pooling of the standardized mean differences between before and after botulinum toxin treatment. SMD: standardized mean difference. Heterogeneity chi-squared = 536.13 (d.f. = 4), $p < 0.001$. I^2 = 99.3%. Test of SMD = 0, z = 14.40, $p < 0.001$.
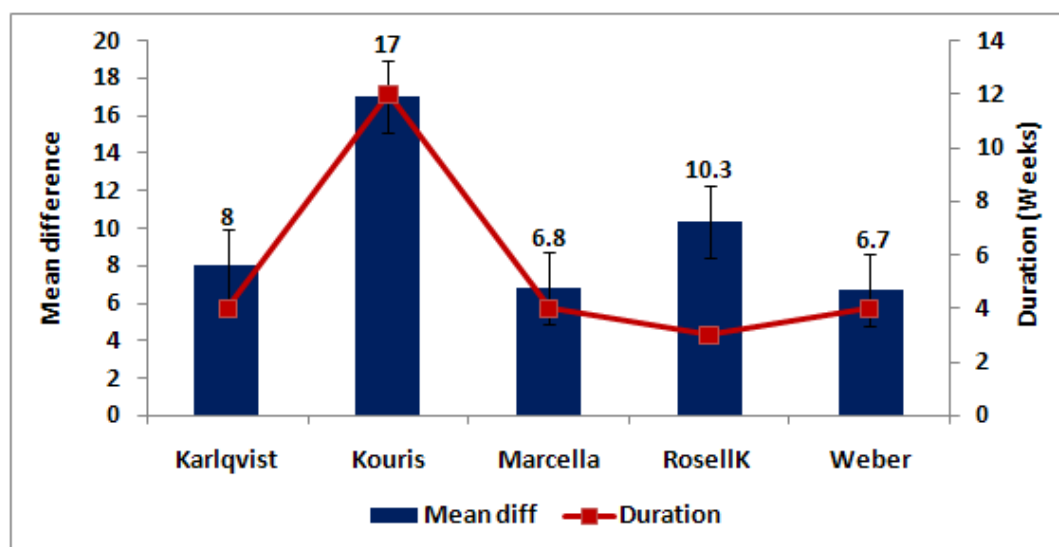
Figure 2: Decrease in Dermatology Life Quality Index (DLQI) scores from baseline and study duration.

Discussion

Axillary hyperhidrosis

Over the past 10 years, more than 20 studies have been conducted on the use of botulinum toxin for axillary HH therapy has been studied more than ten years, and that over twenty researches discussed about it. From these studies, it was found that the duration of action for the axillae HH ranged from 4 to 10 months. Studies comparing botulinum toxin type A

(BoNT-A) products— between OonabotulinumtoxinA (OnaA) and AabobotulinumtoxinA (AboA) —reported showed that OnaA has a faster onset of action, as (1 week for OnaA requires only one week, whileand 2 weeks for AboA) takes two weeks. [18]. Repeated However, repeated botulinum toxin type A (BoNT-A) injections results in a similar durations of effectiveness (4–10 months) between the two products of treatment, and neither product causes therapeutic the resistance towards botulinum toxin did not emerge during repeated treatment. In general, patients are claimed that they are satisfied with the results of botulinum toxin type BoNT-A injections, with more than 98% willing to recommend the therapy to persons with similar axillary HH indications[11-13]. Studies have found that the quality of life (as measured by DLQI scores) improves significantly after botulinum toxin injection for axillary HH treatments at 3 weeks. [9]

There are no standardized BoNT-A dilutions for axillary HH treatment[25], but studies have shown that BoNT-A mixed in either saline or lidocaine is equally effective[32]. The suggested technique for axillary injection is to always perform a Minor iodine-starch test before botulinum toxin injection[13]. In addition, the injection should be placed subcutaneously, as it is less painful than intradermal

Figure 3. Botulinum toxin injection pattern for axillary hyperhidrosis

Researchers have suggested using 50–100 units of OnaA divided by 10–20 intradermal injections per axilla[12]. Patients with severe axillary HH may require injections every 6 months to control sweating[30,31]. Adverse effects such as pain following an injection are usually minor, and precooling has been shown effective in relieving that pain.

Palmar hyperhidrosis

Numerous studies have demonstrated the beneficial effects of BoNT-A in the treatment of palmar HH. Most of these studies calculated the efficacy at around 80–90%, but the duration of action (approximately 6 months, as measured by the anhidrosis) is shorter than for axillary HH. Response rates to BoNT-A also vary more compared with that of axillary HH[16]. In previous study, patients with palmar HH who were treated with botulinum toxin type A

(Xeomin) and B (NeuroBloc) injections reported a 100% satisfaction rate and showed significant DLQI improvement at 3 weeks after treatment (P < 0.05)[9].

The optimal dose for BoNT-A is unknown, as it depends on the surface size of the palm. It is often reported to be between 100 and 240 units per hand for OnaA, and 120 units to 500 units per hand for AboA. Some studies have suggested using a defined dose per injection: 2–3 units spaced every 1–2 cm, approximately 40–50 injections in total (Figure 4). However, this may slightly vary, depending on the palm size. Adverse effects include transient weakness of the intrinsic hand muscles[2], which usually presents 1–3 days after an injection resolves within 10–14 days. Another adverse effect of palmar injection is intense pain owing to the sensitivity of the palms. This may require regional nerve block anesthesia prior to injections. Ice cube anesthesia to precool the site for about 5–10 sec has proven significantly effective, whereas topical anesthesia with cream will not sufficiently decrease discomfort.

Figure 4. Botulinum toxin injection pattern on the palm and digits for palmar hyperhidrosis

Plantar hyperhidrosis

There are few reports regarding the use of BoNT for the treatment of plantar HH. The thick stratum corneum on the soles of the feet make intradermal injections difficult[2], not to mention that dense innervation makes injections painful. Nevertheless, nonrandomized controlled trials have reported that BoNT-A injections are equally effective for plantar and palmar HH at similar dosages, and patients may experience approximately 6 months of symptom relief and improvement in dermatological quality of life[14].

Craniofacial hyperhidrosis

Botulinum toxin type A has been used successfully for forehead HH, with an effectiveness rate reaching approximately 75% and a duration of action of at least 5 months[18]. Botulinum toxin injections are usually applied in a band close to or along the hairline. Reported adverse effects included mild weakness of the frontalis muscle lasting approximately 3 months that sometimes result in a mild brow ptosis[17, 18]. Dermatology Life Quality Index scores significantly improve at 2–4 weeks.[6]

Although BoNT has been used to treat nearly all types of focal HH, the Food and Drug administration (FDA) has only approved it for the treatment for axillary HH. The use of BoNT-A for palmoplantar and craniofacial HH is considered unapproved[18, 19]. Still, high efficacy and safety rates have been reported for BoNT-A in the management of nearly all types of focal HH. Our statistical analysis revealed that botulinum toxin for primary HH significantly improved patients' dermatological quality of life (as indicated by DLQI scores). However, our forest plot suggests that the 5 included studies significantly differed from each other, and $I^2 = 99.3\%$, indicating heterogeneity. This heterogeneity might have resulted from the varying composition of HH sites investigated by each of the studies (e.g., axillary, palmar, plantar, and craniofacial). The types of BoNT, dose of BoNT, and dilution method could also have been a factor.

Conclusion

Botulinum toxin is an effective treatment option for primary HH and can considerably improve the dermatological quality of life, while it is safe, easy to use with minimal side effects. Botulinum toxin might be a useful alternative to current treatment modalities for primary HH.

Acknowledgements

The authors are very thankful to Thammasat University and its staff members for providing the facilities and encouragement to carry out this work.

References

1. Saadia D, Voustianiouk A, Wang AK, Kaufmann H. Botulinum toxin type A in primary palmar hyperhidrosis. Neurology. 2001;57:2095-9.
2. Hornberger J, Grimes K, Naumann M, Glaser DA, Lowe, NJ. Recognition, diagnosis, and treatment of primary focal hyperhidrosis. J Am Acad Dermatol. 2004;51(2):274-86.
3. Naumann M, Jankovic J. Safety of botulinum toxin type A: a systematic review and metaanalysis. Curr Med Res Opin. 2004;20(7):981-90.
4. Grunfeld A, Murray CA, Solish N. Botulinum toxin for hyperhydrosis: a review. Am J Clin Detmatol. 2009;10(2):87-102.
5. Khalid SG. Quantification of hyperhydrosis using electronic sudometer. Royal Institute of Technology KTH STH. 2013. oai: DiVA.org:kth-132250.
6. Karlqvist M, Rosell K, Rystedt A, Hymnelius K, Swartling C. Botulinum toxin B in the treatment of craniofacial hyperhidrosis. J Eur Acad Dermatol Venereol. 2014;28(10):1313-7.
7. Kouris A, Armyra K, Christodoulou C, Karimali P, Karypidis D, Kontochristopoulos G. Quality of lif in patients with focal hyperhidrosis before and after treatment with botulinum toxin A. ISRN Dermatol. 2014. doi: 10.1155/2014/308650.
8. Marcella S, Goodman G, Cumming S, Foley P, Morgan V. Thirty-five units of botulinum toxin type A for treatment of axillary hyperhidrosis in female patients. Australas J Dermatol. 2011;52(2):123-6.
9. Rosell K, Hymnelius K, Swartling C. Botulinum toxin type A and B improve quality of life in patients with axillary and palmar hyperhidrosis. Acta Derm Venereol. 2013;93(3):335-9.

10. Glogau RG. Botulinum A neurotoxin for axillary hyperhidrosis: no sweat Botox. Dermatol Surg. 1998;24(8):817-9.
11. Naumann M, Hamm H, Lowe NJ. Effect of botulinum toxin type A on quality of life measures in patients with excessive axillary sweating: a randomized controlled trial. Br J Dermatol. 2002;147(6):1218-26.
12. Naumann M, Lowe NJ. Botulinum toxin type A in treatment of bilateral primary axillary hyperhidrosis: randomised, parallel group, double blind, placebo controlled trial. BMJ. 2001;323(7313):596-9.
13. Heckmann M, Ceballos-Baumann AO, Plewig G. Botulinum toxin A for axillary hyperbidrosis (excessive sweating). N Engl J Med. 2001;344(7):488-93.
14. Naumann M, Hofmann U, Bergmann I, Hamm H Toyka KV, Reiners K. Focal hyperhydrosis: effective treatment with intracutancous botulinum toxin. Arch Dermatol. 1998;134(3):301-4.
15. Naver H, Swartling C, Aquilonius SM. Palmar and axillary hyperhidrosis treated with botulinum toxin: one-year clinical follow-up. Eur J Neurol. 2000;7(1):55-62.
16. Glogau RG. Hyperhidrosis and botulinum toxin A: patient selection and techniques. Clin Dermatol. 2004;22(1):45-52.
17. Vadoud-Seyedi J. Treatment of plantar hyperbidrosis with botulinum toxin type A. Int J Dermatol. 2004;43(12):969-71.
18. Tan SR, Solish N. Long-term efficacy and quality of life in the treatment of focal hyperhidrosis with botulinum toxin A. Dermatol Surg. 2002;28(6):495-9.
19. Pena MA, Alam M, Yoo S. Complications with the use of botulinum toxin type A for cosmetic applications and hyperhidrosis. Semin Cutan Med Surg. 2007;26(1):29-33.
20. Emmerson J. Botulinum toxin for spasmodie torticollis in a patient with myasthenia gravis. Mov Dissord. 1994;9(3):367.
21. Erbgutb F, Claus D, Engelhardt A. Systemic effect of local botulinum toxin injections unmasks subclinical Lambert-Eaton myasthenic syndrome. J Neurol Neurosurg Psychiatry. 1993;56(11):1235-6.
22. Fasano A, Bentivoglio AR, Lalongo T, Soleti F, Evoli A. Treatment with botulinum toxin in a patient with myasthenica gravis and cervical dystonia. Neurology. 2005;64(12):2155-6.
23. Klein AW. Contraindications and eomplications with the use of botulinum toxin. Clin Dermatol. 2004;22:66-75.
24. Thomas I, Brown J, Vafaie J, Schwartz RA. Palmoplantar hyperbidrosis: a therapeutic challenge. Am Fam Physician. 2004;69(5):1117-20.
25. Lecouflet M, Leux C, Fenot M, et al. Duration of efficacy increases with the repetition of botulinum toxin A injections in primary axillary hyperhidrosis: a study in 83 patients. J Am Acad Dermatol. 2013; 69(6):960-4.
26. Lakraj AA, Moghimi N, Jabbari B. Hyperhidrosis: anatomy, pathophysiology and treatment with emphasis on the role of botulinum toxins. Toxins. 2013;5(4):821-40.
27. Rosell K, Hymnelius K, Swartling C. Botulinum toxin type A and B improve quality of life in patients with axillary and palmar hyperhidrosis. Acta Derm Venereol. 2013;93:335-9.
28. Frasson E, Brigo F, Acler M, et al. Botulinum toxin type A vs type B for axillary hyperhidrosis in a case series of patients observed for 6 months. Arch Dermatol. 2011;147(1):122.3.
29. Skiveren J, Larsen HN, Kjaerby E, et al. The influence of needle size on pain perception in patients treated with botulinum toxin A injections for axillary hyperhidrosis. Acta Derm Venereol. 2011;91(1):72-4.

30. Trindade de Almeida AR, Secco LC, Carruthers A. Handling botulinum toxins: an updated literature re- view. Dermatol Surg. 2011;37(11):1553-65.
31. Bovell DL, MacDonald A, Meyer BA, et al. The secretory clear cell of the eccrine sweat gland as the probable source of excess sweat gland as the probable source of excess sweat production in hyperhidrosis. Exp Dermatol. 2011;20(12):1017-20.
32. Vergilis-Kalner IJ. Same-patient prospective comparison of Botox versus Dysport for treatment of primary axillary hyperhidrosis and review of literature. J Drugs Dermatol. 2011;10(9):1013-15.
33. Scamoni S, Valdatta L, Frigo C, et al. Treatment of primary axillary hyperhidrosis with botulinum toxin type A: our experience in 50 patients from 2007 to 2010. ISRN Dermatol. 2012;2012. doi: 10.5402/2012/70271

Sponsors

Review

Role of Matrix Metalloproteinases in Photoaging and Photocarcinogenesis

Pavida Pittayapruek [1,†], Jitlada Meephansan [1,†], Ornicha Prapapan [1], Mayumi Komine [2,*] and Mamitaro Ohtsuki [2]

[1] Division of Dermatology, Chulabhorn International College of Medicine, Thammasat University, Pathum Thani 12000, Thailand; p_ha_r@hotmail.com (P.P.); kae_mdcu@yahoo.com (J.M.); chad_naja@hotmail.com (O.P.)
[2] Department of Dermatology, Jichi Medical University, Tochigi 329-0498, Japan; mamitaro@jichi.ac.jp
* Correspondence: mkomine12@jichi.ac.jp; Tel.: +81-285-58-7360
† These authors contributed equally to this work.

Abstract: Matrix metalloproteinases (MMPs) are zinc-containing endopeptidases with an extensive range of substrate specificities. Collectively, these enzymes are able to degrade various components of extracellular matrix (ECM) proteins. Based on their structure and substrate specificity, they can be categorized into five main subgroups, namely (1) collagenases (MMP-1, MMP-8 and MMP-13); (2) gelatinases (MMP-2 and MMP-9); (3) stromelysins (MMP-3, MMP-10 and MMP-11); (4) matrilysins (MMP-7 and MMP-26); and (5) membrane-type (MT) MMPs (MMP-14, MMP-15, and MMP-16). The alterations made to the ECM by MMPs might contribute in skin wrinkling, a characteristic of premature skin aging. In photocarcinogenesis, degradation of ECM is the initial step towards tumor cell invasion, to invade both the basement membrane and the surrounding stroma that mainly comprises fibrillar collagens. Additionally, MMPs are involved in angiogenesis, which promotes cancer cell growth and migration. In this review, we focus on the present knowledge about premature skin aging and skin cancers such as basal cell carcinoma (BCC), squamous cell carcinoma (SCC), and melanoma, with our main focus on members of the MMP family and their functions.

Keywords: matrix metalloproteinase (MMP); photoaging; photocarcinogenesis; basal cell carcinoma; squamous cell carcinoma; malignant melanoma

1. Introduction

Skin is the primary means through which an organism interacts with its environment. Accordingly, it is regularly exposed to a direct oxidative environment, including ultraviolet (UV) radiation. Acute exposure to UV radiation causes sunburn, connective tissue deterioration, DNA injury, and immune suppression. Chronic or long-term exposure to UV radiation disrupts the normal skin structure leading to a host of skin issues including premature skin aging (photoaging) and skin cancer (photocarcinogenesis) [1,2].

UV radiation increases the expression of matrix metalloproteinases (MMPs) in human skin. MMPs are responsible for degrading the extracellular matrix (ECM) proteins such as collagen, fibronectin, elastin, and proteoglycans, contributing to photoaging [3,4]. MMPs play a crucial role in photocarcinogenesis by regulating/affecting various processes related to tumor progression including tumor institution, growth, angiogenesis, and metastasis [5].

This review focuses on human MMPs in relation to photoaging and photocarcinogenesis. The first half of the paper briefly summarizes the role of MMPs in relation to photoaging and the second half focuses on the involvement of MMPs in the pathophysiology of skin cancers such as melanoma, basal cell carcinoma (BCC), and squamous cell carcinoma (SCC).

2. MMPs

MMPs are zinc-containing endopeptidases with a broad range of substrate specificities. They mediate the degradation of the different components of the ECM [3,4]. They are secreted by keratinocytes and dermal fibroblasts in response to multiple stimuli such as oxidative stress, UV radiation, and cytokines [6,7]. To date, at least 28 different types of MMPs have been identified that play important roles in various pathophysiological processes including photoaging, wound healing, skeletal growth and remodeling, arthritis, inflammation, angiogenesis, and cancer [3,8,9].

MMPs can be categorized into five main subgroups based on their substrate specificity and structural organization. These are listed below in Table 1:

Table 1. Classification of human metalloproteinases (MMPs) and their function in relation to photoaging and photocarcinogenesis.

MMP Subgroup	MMP Number	Alternate Name	Role in Photoaging	Role in Photocarcinogenesis
Collagenases	MMP-1	- Interstitial collagenase -Type I Collagenase	- Collagen type I and III degradation	- Tumor growth in BCC and SCC - Facilitate tumor invasion in melanoma
	MMP-8	- Neutrophil collagenase	- Limited role	- Limited role in BCC and SCC - Increased risk of malignant melanoma
	MMP-13	- Collagenase-3	- Limited role	- Tumor invasion and angiogenesis in BCC and SCC - Involved in invasive VGP of melanoma
Gelatinases	MMP-2	- Gelatinase-A - 72 kDa type IV collagenase	- Collagen type IV degradation	- Growth initiation and tumor invasion in BCC and SCC - Hematogenous metastasis in melanoma
	MMP-9	- Gelatinase-B - 92-kDa type IV collagenase	- Degrade collagen type IV	- Growth initiation and tumor invasion in BCC and SCC - Related to the RGP of melanoma and tumor angiogenesis
Stromelysins	MMP-3	- Stromelysin-1 - Proteoglycanase - Transin-1	- Collagen type I degradation - Activate MMP-1, -7, and -9	- Tumor progression and metastasis in SCC - Activate pro-MMPs in melanoma
	MMP-10	- Stromelysin-2 - Transin-2	- Activate pro-MMPs	- Tumor initiation in SCC
	MMP-11	- Stromelysin-3	-	-
Matrilysins	MMP-7	- Matrilysin-1 - Pump-1	- Elastin degradation	- Tumor invasion
	MMP-26	- Matrilysin-2 - Endometase	-	-Limited role in BCC -Activate MMP-9 and promote tumor growth in SCC
Membrane-type	MMP-14	- MT1-MMP	-	- Tumor invasion - Activate MMP-2 - Tumor angiogenesis in melanoma
	MMP-15	- MT2-MMP	-	- Tumor invasion in melanoma
	MMP-16	- MT3-MMP	-	- Tumor invasion in melanoma
	MMP-17	- MT4-MMP	-	-
	MMP-24	- MT5-MMP	-	-
	MMP-25	- MT6-MMP	-	-
Other types	MMP-12	- Metalloelastase	- Elastin degradaion	- Tumor invasion, lymph node metastasis in melanoma
	MMP-19	- RASI-1	-	-
	MMP-20	- Enamelysin	-	-
	MMP-21	-	-	-
	MMP-22	-	-	-
	MMP-23	-	-	-
	MMP-28	- Epilysin	-	-

1. Collagenases (MMP-1, MMP-8, and MMP-13) recognize the substrate through a hemopexin-like domain and are able to degrade fibrillar collagen [10].

2. Gelatinases (MMP-2 and MMP-9) are able to digest a number of ECM components such as collagen type I and IV.

3. Stromelysins (MMP-3, MMP-10, and MMP-11) have a domain arrangement similar to that of collagenases; however, they do not cleave fibrillar collagen type I.

4. Matrilysins (MMP-7 and MMP-26) lack a hemopexin-like domain and degrade collagen type IV but not type I.

5. MT-MMPs (MMP-14, MMP-15, and MMP-16) have an additional C-terminal transmembrane domain with a short cytoplasmic tail. Both MMP-14 and MMP-16 degrade fibrillar collagen type I.

In addition to the five aforementioned subgroups of MMPs, there are few MMPs that are not grouped into any of these categories, such as metalloelastase (MMP-12), RASI-1 (MMP-19), enamelysin (MMP-20), and epilysin (MMP-28) [9].

3. Photoaging

Aging changes in the skin can be categorized in two groups: (1) intrinsic, or chronologic aging, an inherent degenerative process due to declining physiological functions and capacities; and (2) extrinsic, or photoaging, a distinctive deteriorating process caused by environmental factors. UV radiation is the major environmental factor that causes photoaging [11,12]. The action spectrum for UV-induced skin damage is divided into UV-A (320–400 nm) and UV-B (290–320 nm). UV-A rays account for up to 95% of the UV radiation reaching the Earth's surface and is only slightly affected by ozone levels. The amount of UV-B reaching the earth's surface is lesser than that of UV-A; however, its intensity is high enough to cause photoaging and skin cancer [13,14]. Nonetheless, both UV-A and UV-B irradiation can induce oxidative stress in human skin, leading to temporal and persistent genetic impairment, up-regulation of activator protein (AP)-1 activity, and increased MMP expression (Table 2) [15,16].

Table 2. Role of UV-A and UV-B in photoaging induced by MMPs.

MMPs	UV-A	UV-B
Collagenases		
MMP-1	+	++
MMP-8	NA	NA
MMP-13	+	+
Gelatinases		
MMP-2	+	+
MMP-9	+	+
Stromelysins		
MMP-3	+	++
MMP-10	+	++
Matrilysins		
MMP-7	+	+
MMP-26	NA	NA
MT-MMPs		
MMP-14	NA	NA
MMP-15,16	NA	NA
Other types		
MMP-12	++	+

Abbreviations: ++, highly upregulated; + upregulated; NA, no reported.

Photoaging involves prominent cutaneous transformation that is clinically characterized by fine and coarse wrinkles, blotchy dyspigmentation, telangiectasia, sallowness, increased fragility, and rough skin texture [3]. Additionally, histological and ultrastructural studies have revealed epidermal hyperplasia, damaged and disorganized collagen fibrils, and substantial accumulation of abnormal elastic material in dermal connective tissue [16,17].

Photoaging is caused by an imbalance in equilibrium between the accumulation and degradation of ECM components that provide structural and functional support to the skin tissue. Cumulative exposure to the sun results in continuous degradation of ECM proteins such as collagen and elastin,

and a decreased rate of renewal/synthesis of collagen. Collagen is the primary insoluble fibrous protein in the ECM and in connective tissue. Type I collagen is the most abundant subtype of collagen found within connective tissue of the skin, followed by small amounts of type III collagen. Fibroblasts, located within the dermis, mainly synthesize collagen, which imparts strength and elasticity to the skin [12,14,17].

Degradation of collagen is normally regulated by MMPs and by the activity of their natural inhibitors, tissue inhibitor of metalloproteinases (TIMPs). Increased MMP activity is an important factor influencing the development of age-related changes in skin [18] (Figure 1 and Table 1).

In the skin, epidermal keratinocytes and dermal fibroblasts mainly secrete MMP-1(interstitial collagenase or collagenase 1), a collagenase that degrades fibrillar collagens type I and III into specific fragments at a single site within the central triple helix. Other MMPs such as gelatinases, further hydrolyze these fragments, ultimately impairing the function of the collagen-rich dermis [1,4,8,19].
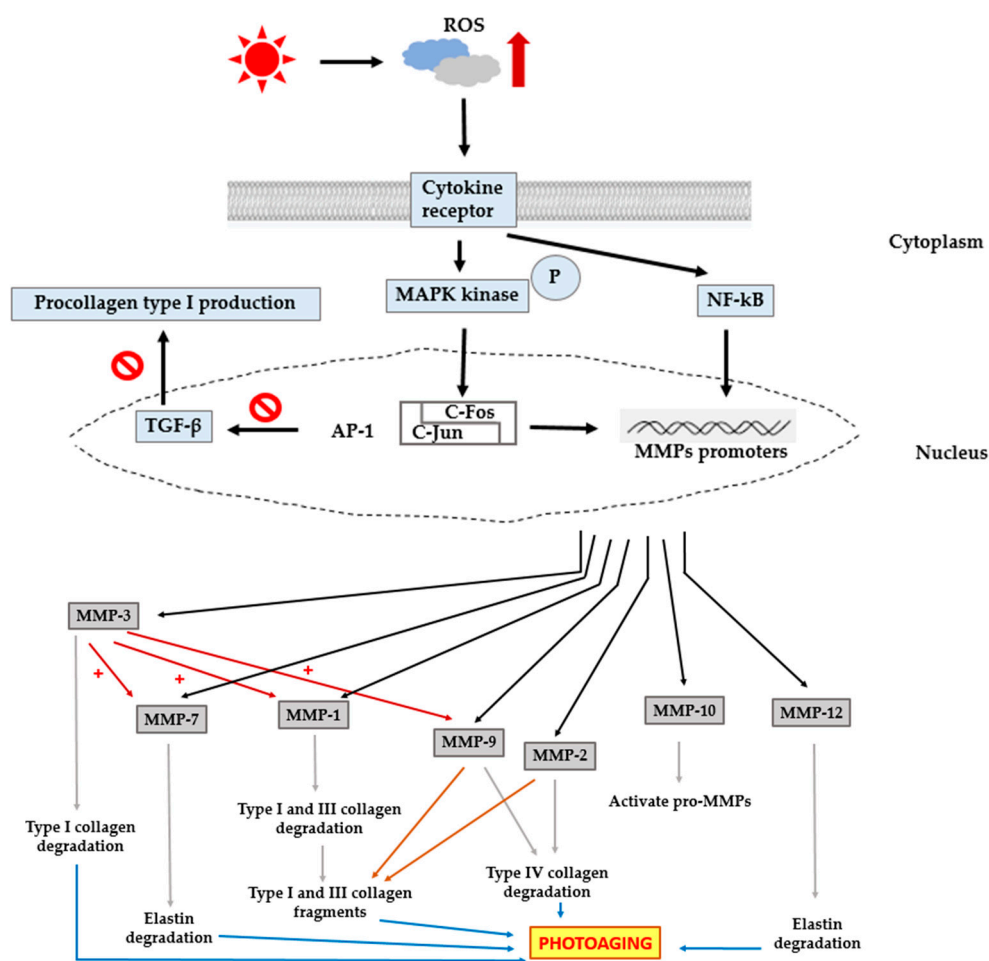
Figure 1. Schematic diagram showing the role of MMPs in photoaging. UV-induced excess intracellular reactive oxygen species (ROS) activates mitogen-activated protein kinases (MAPKs) and nuclear factor-kappa B (NF-κB), culminating in the transcriptional regulation of MMPs, and results in the degradation of collagen and elastin, subsequently leading to photoaging. In addition to collagen and elastin degradation, AP-1 inhibits transforming growth factor beta (TGF-β) signaling, causing a reduction in procollagen synthesis.

UV irradiation induces increased synthesis and expression of MMP-1 by dermal fibroblasts, which is stimulated by the generation of excess reactive oxygen species (ROS), and plays a critical role in photoaging. UV irradiation induces excess intracellular ROS such as singlet oxygen ($^1O_2$), superoxide

anion (O$_2$$^-$), hydrogen peroxide (H$_2O_2$), and hydroxyl radicals (OH$^.$) [17]. ROS, a secondary messenger, activates the mitogen-activated protein kinase (MAPK) family. MAPKs are a family of proline-directed Ser/Thr kinases comprising extracellular signal-regulated kinases (ERKs), p38, and c-Jun NH2-terminal kinase (JNK). ERK is important to stimulate the expression of c-Fos, whereas p38 and JNK activation are crucial for the expression of c-Jun. c-Jun in combination with c-Fos forms the transcription factor AP-1, which plays an essential role in the transcriptional regulation of MMP-1, MMP-3, and MMP-9 resulting in the degradation of collagen [4,17,20]. Additionally, AP-1 inhibits transforming growth factor-β (TGF-β) signaling, a major regulator for the production of procollagen type I in human skin. Impairment of the TGF-β pathway leads to decreased synthesis of procollagen [21–23]. Besides AP-1, nuclear factor-kappa B (NF-κB) is another important transcription factor that is activated in response to UV irradiation. NF-κB is a universal transcription factor that regulates the gene expression of growth factors, chemokines, cytokines, and cell adhesion molecules, in healthy as well as numerous diseased states. Generation of ROS induces NF-κB-mediated transcriptional activation and regulation of MMP gene expression. Thus, this factor is important to mediate the responses of UV irradiation. NF-κB activity is reported to be responsible for the up-regulation of MMPs such as MMP-1 and MMP-3 in dermal fibroblasts [2,20,24]. Thus, both AP-1 and NF-κB are involved in the process of photoaging.

UV-induced AP-1 activation enhances the expression of MMP-1, MMP-3, and MMP-9. MMP-3, known as stromelysin-1, differs from collagenases because of its inability to digest collagen type I. However, it does degrade a large number of ECM proteins, such as type IV, V, IX, and X collagens, gelatin, fibrillin-1, fibronectin, laminin, and proteoglycans. The primary function of MMP-3 is the activation of pro-MMPs such as collagenases, gelatinase B, and matrilysins during ECM turnover. In particular, the production of fully active MMP-1 MMP-3 is essential to partially activate pro-MMP-1 [9,25,26]. MMP-10, known as stromelysin-2, cleaves various ECM proteins and is involved in the activation of pro-MMPs. However, the catalytic function of collagen type IV and type V is quite weak compared to the MMP-3 activity [9,27].

MMP-9, known as gelatinase B or 92-kDa type IV collagenase, is a member of the gelatinase subgroup of MMPs, whose expression is largely dependent on the activation of AP-1. MMP-9 is produced by human keratinocytes and can digest collagen type IV, an important component of the basement membrane in skin. The epidermal basement membrane is responsible for the epidermal-dermal adhesion, which is crucial for epidermal integrity. It is also important in controlling epidermal differentiation [8,9,28,29]. Like MMP-9, MMP-2 (known as gelatinase A or 72-kDa type IV collagenase) is able to cleave collagen type IV [30]. Additionally, both these gelatinases can degrade other substrates such as collagen type V, VII, and X, fibronectin, and elastin. They are essential in degrading fibrillar collagen fragments after their initial degradation by collagenases [12,25,31].

Collagenases refer to a class of MMPs with the ability to degrade native collagen without unwinding the triple helical assembly of the substrate. Interstitial collagenase (MMP-1), neutrophil collagenase (MMP-8), and collagenase 3 (MMP-13) belong to this group [9]. They have similar configuration and enzymatic functions, despite small differences in substrate specificity. As mentioned above, MMP-1 plays an important role in the photoaging process. Recent studies suggest a limited role for MMP-8 in UV-mediated collagen damage in the skin. Although this enzyme was found to be induced by UV light, it is up-regulation was minimal [32]. MMP-13 shows higher cleavage specificity for collagen type II, a major collagen present in the cartilage, compared to collagen type I and III. MMP-13 is five times less potent than MMP-1 in cleaving collagen types I and III; however, it is 5–10 times more potent in cleaving collagen type II [9]. Hence, during photoaging, MMP-8 and MMP-13 probably contribute very little to the overall structural damage to collagen.

In addition to the degradation of collagens in skin, changes in the level of elastin have also been well documented in the process leading to photoaging. Elastin is a major component that contributes to the function of recoil and resilience, although it constitutes only 2%–4% of the total protein content of the skin. Reduced levels of elastin are associated with various diseases such as atherosclerosis and arthritis. Degradation of elastin results in an aged appearance of the skin [33–35]. MMP-12, known as

macrophage metalloelastase, is the most effective MMP against elastin. Macrophages and fibroblasts secrete MMP-12 in response to acute UV radiation. MMP-12 plays a crucial role in the development of solar elastosis as indicated by the association between the expression of MMP-12 and the amount of elastotic material in the upper dermis of photodamaged skin [30,33,35]. The process of solar elastosis refers to the collection of dystrophic elastotic material in the dermis [15,33]. In addition to elastin, MMP-12 can cleave many other substrates belonging to the ECM, such as collagen type IV fragments, fibronectin, fibrillin- 1, laminin, entactin, vitronectin, heparin, and chondroitin sulfates. MMP-12 is also responsible for the activation of other pro-MMPs, such as pro-MMP-1, MMP-2, MMP-3, and MMP-9 [9,34]. In addition to MMP-12, MMP-7 (called matrilysin) can efficiently degrade elastin. Upon UV irradiation, MMP-7 can cleave not only elastin but also many other substrates of the ECM, such as collagen type IV, entactin, fibronectin, laminin, and cartilage proteoglycan aggregates [9,30].

Neutral endopeptidase (NEP) or neprilysin, a 94-kDa membrane-bound type of metalloprotease, is identical to fibroblasts-derived elastase. It exhibits similarities in terms of its membrane-bound metalloproteinase nature and inhibitory profiles [36,37]. The enhanced NEP activity in dermal fibroblasts plays an important role in the UV-B-induced cascade of biological processes that lead to skin wrinkling and/or sagging. This occurs because of the deterioration of the three-dimensional structure of elastic fibers and the subsequent loss of skin elasticity [36,38]. The expression of NEP is associated with keratinocyte-derived cytokines including interleukin-1 alpha (IL-1α) and granulocyte macrophage colony stimulatory factor (GM-CSF). Repetitive exposure to UV-B radiation activates keratinocytes to secrete IL-1α, which then stimulates the secretion of GM-CSF in an autocrine manner. Additionally, UVB can directly stimulate keratinocytes to produce GM-CSF. Both, IL-1α and GM-CSF enter the dermis and stimulate fibroblasts to up-regulate NEP. NEP then destroys the three-dimensional architecture of the elastic fibers thereby impairing skin elasticity, resulting in wrinkle formation in the skin [36,38].

MMPs play a significant role in wrinkle formation, a characteristic of photoaging. Evolution of novel MMP inhibitors is promising as targets to combat photoaging. In recent years, there has been considerable interest in the use of botanical supplements for the prevention of solar UV radiation-induced skin photodamage (Table 3). *Galla chinensis*, a natural traditional Chinese medicine, is known to significantly suppresses UV-B-induced ROS and MMP-1 expression in normal human dermal fibroblasts [21]. Extracts of *Neonauclea reticulata*, a member of Rubiaceae, a flavonoid-enriched flowering plant, significantly decreases the expression of MMP-1, MMP-3, and MMP-9 by suppressing ERK, p38, and JNK phosphorylation. *Ixora parviflora* and *Coffea arabica*, polyphenol-enriched members of Rubiaceae family, exhibit anti-photoaging activity by inhibiting the expression of MMP-1, MMP-3, and MMP-9, and MAPK activity [12,17,39].

Table 3. Protective agents against photoaging.

Mechanisms	Protective Agents
MMP inhibitors	*Galla chinensis* *Neonauclea reticulate* *Coffea Arabica* *Ixora parviflora*
Free radical scavengers	*Coffea Arabica* *Terminalia catappa* *Emblica officinalis* Epigallocatechin-3-gallate (EGCG) *Gynura procumbens* *Caesalpinia sappan* L.

Another strategy to diminish the damaging effects of UV radiation on skin is the use of antioxidants or free radical scavengers (Table 3). Polyphenols, with a higher number of OH groups act as ROS scavengers and protect against cellular damage. Natural products with high polyphenol

contents such as *Emblica officinalis*, *Coffea arabica*, *Terminalia catappa*, and epigallocatechin-3-gallate (EGCG) render effective protection against photoaging [14,17,31]. In addition to phenolic compounds, coriander leaf extract, *Gynura procumbens*, and *Caesalpinia sappan* L. also exhibit strong protective effects against UV-induced oxidative stress [4,22,24].

## 4. Photocarcinogenesis

4.1. BCC

Overexposure of human skin to solar UV radiation is a major environmental risk factor for melanoma and nonmelanoma skin cancers [40]. Nonmelanoma skin cancers include BCC and SCC, which are responsible for approximately 80% and 20% of all nonmelanoma skin cancer cases, respectively [41–43].

In humans, skin neoplasms commonly arise in the epidermis or hair follicles where proliferating basaloid tumor cells are present. To date, most of the studies on BCC are based on Caucasian populations, as this type of cancer is less common in Asians and Black African races. It has been shown that the incidence of BCC in Asian individuals range from 16 to 20 per 100,000, and is increasing since the 1960s. In contrast, the incidence of BCC in Caucasians has been approximated to be higher than 200 and 400 per 100,000 in females and males, respectively [44,45].

BCC mostly occurs in parts of the body that are frequently exposed to the sun, such as the head and neck regions. In particular, BCC often develops on the face with the nose and the lip being the most commonly affected areas [42,46]. Though BCC is characterized by slow progression and low metastatic potential, it has a propensity to be locally destructive. If untreated, BCC may invade subcutaneous fat, muscles, and even bones [42,47,48]. The invasion of tumor cells is a complex, multistage process, which starts with proteases such as MMP degrading the basement membrane and the ECM surrounding the original tumor (Figures 2 and 3), altering cell-to-cell adhesion properties, reorganizing the ECM surroundings, suppressing anoikis, and rearranging the cytoskeleton to facilitate cell motility. These processes are governed by complex interactions between various biomarkers, especially MMPs, cell–cell adhesion molecules (such as β-catenin), and chemokine receptor-ligand complexes (SDF- 1/CXCR4) [42,47,49].
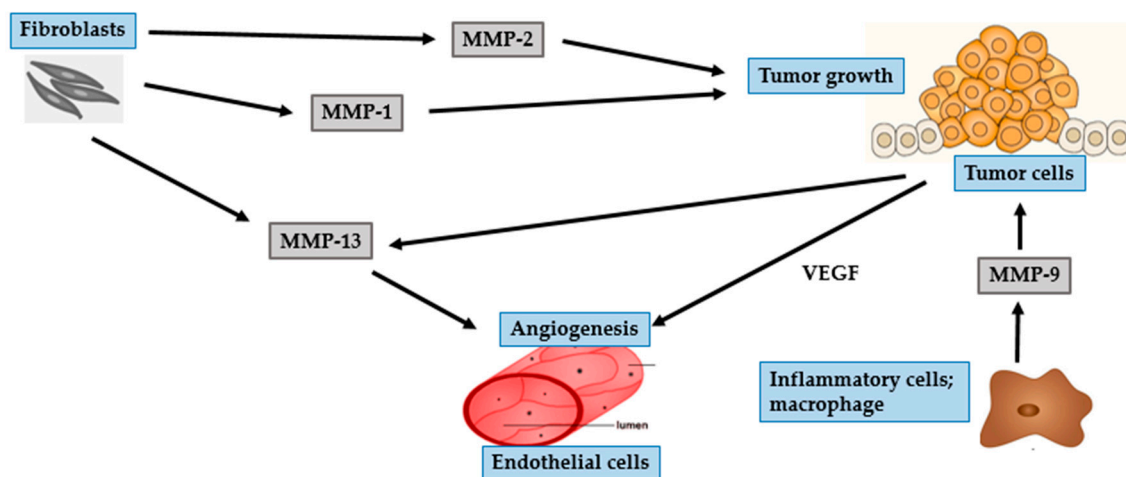
Figure 2. Role of MMPs in BCC and tumor growth. MMP-1 and MMP-2 secreted by fibroblasts facilitate tumor growth. MMP-13 secreted by fibroblasts and tumor cells promote tumor angiogenesis. MMP-9 secreted by inflammatory cells activates BCC cells to secrete VEGF, which in turn promotes angiogenesis.
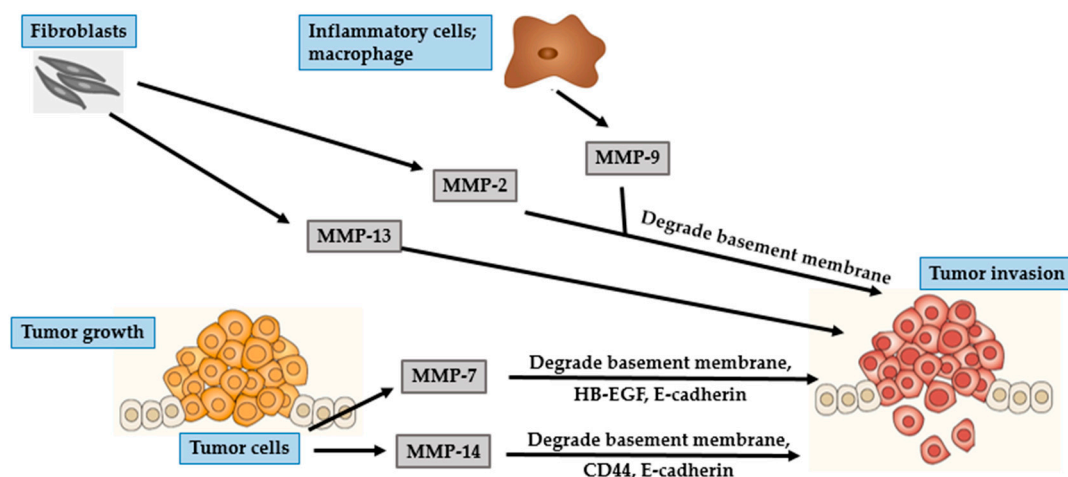
Figure 3. Role of MMPs in BCC tumor invasion. MMP-2 and MMP-13 secreted by fibroblasts facilitate tumor invasion. Inflammatory cells-derived MMP-9 degrades the basement membrane and promotes tumor invasion. BCC cells secrete MMP-7 and MMP-14. MMP-7 degrades the basement membrane, HB-EGF and E-cadherin, whereas, MMP-14 degrades the basement membrane, CD-44 and E-cadherin. Together, they play an important role in tumor invasion.

Two essential steps in tumor development are degradation of the basement membrane and invasion of the surroundings tissue by tumor cells [43,46,47,50]. Gelatinases are known to be associated with cancer invasion because of their ability to degrade crucial components of the basement membrane, especially collagen type IV [43,50]. MMP-2 is mostly secreted by fibroblast-like stromal cells surrounding BCC tumors, and rarely by keratinocytes and BCC tumor cells. Interaction of stromal fibroblasts and BCC tumor cells affects fibroblasts-derived MMP-2, suggesting a significant effect of this interaction in the development of cancer [5,51]. MMP-2 plays an important role in creating a suitable microenvironment for the proliferation of cancer cells and contributes to epithelial–mesenchymal transition (EMT). This transition depends upon the eliminating of adhesion molecules, such as cadherins and integrins, and a marked reorganization of the cytoskeleton, both of which facilitate the separation of malignant cells from the primary tissue. All of these processes are associated with the activity of MMP-2 [9].

MMP-9, is a gelatinase with proteolytic activity against the basement membrane components, including collagen type IV [5,41]. MMP-9 is mostly secreted by inflammatory cells such as macrophages, rather than by tumor cells [46,52]. Macrophages located within the tumor environment are called tumor-associated macrophages (TAMs). TAMs are a type of M2 macrophage that supports tumor growth. In addition to secreting proteases, TAMs can activate COX-2 in BCC cells. Overexpression of COX-2 induces secretion of angiogenic factors such as vascular endothelial growth factor (VEGF), and basic fibroblast growth factor (bFGF) [53].

Inflammatory cells surrounding BCC are typically positive for MMP-13, MMP-1, and MMP-9, indicating an essential role of inflammation in modulating tumor progression [42]. MMP-13 is involved in the degradation of ECM and its expression is associated with malignant transformation in skin carcinogenesis [42,46,47]. The expression of MMP-13 is not confined to tumor cells alone, as its expression is up-regulated in stromal cells surrounding epithelial tumors including fibroblasts, inflammatory cells, and endothelial cells. Endothelial cells-derived MMP-13 is associated with endothelial cell proliferation and vascular differentiation [42]. Of the other collagenases, MMP-1 is the primary collagenolytic enzyme in BCC. The expression of MMP-1 is significantly enhanced by fibroblasts at the invasive front of BCC, suggesting its role in the initial steps of tumor proliferation, which is mediated by cleaving the ECM proteins and active forms of growth factors that subsequently stimulate cancer cells [46,51].

UV irradiation increases tyrosine phosphorylation of β-catenin. The epidermal growth factor receptor (EGFR) activation signaling pathway facilitates nuclear translocation of phosphorylated β-catenin. In the nucleus, β-catenin regulates the Wnt/T-cell transcription factor (TCF) signaling, thereby stimulating gene transcription of MMPs, including MT1-MMP and matrilysin [42,48]. MT-MMPs are different from other soluble MMPs because of the presence of an additional C-terminal transmembrane domain and a short cytoplasmic tail. MT1-MMP or MMP-14, a classical type of MT-MMP, acts as a membrane activator of other soluble MMPs, such as MMP-2 [43,48]. Expression of MT1-MMP is involved in the degradation of ECM barrier, which then promotes tumor invasion because of its localization at the invasive front of tumor invading cells. In addition to its ability to degrade multiple components of the ECM, MT1-MMP can degrade cell adhesion molecules and signaling receptors such as CD44 and E-cadherin [48]. E-cadherin, a calcium-dependent cell adhesion protein, plays a primary role in intercellular adhesion in all the layers of the epidermis except the outermost layer [54]. CD44, a cell-surface glycoprotein, is a member of the hyaluronate receptor of cell adhesion molecules [55]. Loss of either CD44 or E-cadherin leads to impairment of epidermal cell adhesion, thereby promoting invasion of malignant tumor cells into the neighboring tissues [52].

MMP-7 or matrilysin is a widespread metalloproteinase that can degrade numerous ECM and cell surface proteins including E-cadherin and heparin-binding epidermal-like growth factor (HB-EGF) precursor. CD44 mediates the recruitment of active MMP-7 and HB-EGF precursor to form a complex on the surface of tumor cells. In this complex, MMP-7 processes HB-EGF precursor and the resultant HB-EGF activates and stimulates its receptor, ErbB4, resulting in the destruction of the basement membrane, which is an essential step towards tumor progression [52]. MMP-26, also known as matrilysin-2 or endometase, is the smallest known MMP to date. Its expression is barely detected in BCC epithelium or stromal cells and is therefore not considered significant in the development of BCC nor in the process of angiogenesis [46,56].

4.2. SCC

The second most common type of nonmelanoma skin cancer is SCC, accounting to approximately 20% of all skin malignancies [57–59]. It is characterized by malignant proliferation of epidermal keratinocytes. Causes for the development of SCC are multifactorial, including both host and environmental factors. The common host risk factors include genetic predisposition, immunosuppression, human skin type, and human papilloma virus infection. The common environmental risk factors include UV exposure, ionizing radiation, exposure to certain chemicals such as arsenic, and smoking. UV radiation is considered the predominant risk factor for SCC [57–59]. Unlike BCC, SCC exhibits an increased risk of metastasis, though the rate of metastasis is much lower than that of melanoma [58,60].

Metastasis of cancer cells is a complex multistep process involving altered cell-to-cell adhesion, degradation of the ECM and basement membrane, detachment of tumor cells from the original site, intravasation into lymphatic or blood vessels, and establishment of new tumor at distant sites [60–62]. The barrier that mainly restricts development of cancer by preventing tumor invasion and metastasis is composed of the ECM and basement membrane. Thus, it is well established that the degradation of ECM and basement membrane, which requires a wide range of proteolytic enzymes, enhance the ability of tumor cells to invade and metastasize. MMPs play an important role in this process and as they have been implicated in the degradation of ECM and basement membrane [60,63] (Figures 4 and 5).

MMP-2 and MMP-9, members belonging to the gelatinase subgroup, play an essential role in SCC invasion and metastasis. This ability is mainly attributed to the cleavage of collagen type IV, the major component of the basement membrane. Additionally, gelatinases function to regulate the activity of numerous growth factors and cytokines. This affects immune response and angiogenesis, leading to the proliferation and maintenance of primary and metastatic tumors [63–65]. The greater invasive property of SCC, compared to that of BCC, might be due to the enhanced expression and activity of gelatinases [5,43]. Gelatinolytic activity is initiated at the onset of invasive growth, mainly in the tumor stroma. Fibroblasts are potent producers of MMP-2 [64]. In contrast, neutrophils, mast

cells and macrophages are the predominant source of MMP-9 [5,65]. Fibroblast-derived MMP-2 is expressed to a greater degree during the earlier stages of squamous carcinogenesis, resulting in the initiation of tumor growth. Inflammatory cell-derived MMP-9 promotes tumor invasion and angiogenesis by mediating the release of TGF-β and VEGF [64,66,67]. The expression of VEGF is also governed by hypoxia-inducible factor-1α (HIF-1α). During tumor progression, the proliferating tumor cells increase oxygen consumption, thereby worsening hypoxia. In order to adapt to the hypoxic condition, tumor cells up-regulate the expression of HIF-1α, which further aids tumor development and angiogenesis [68,69].
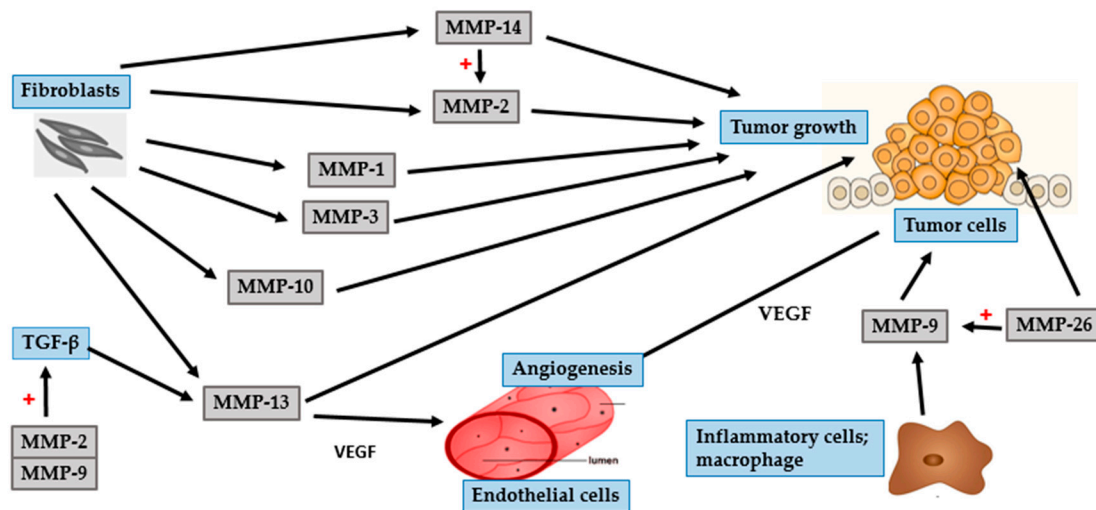
Figure 4. Role of MMPs in SCC and tumor growth. Fibroblasts secrete MMP-1, MMP-2 (also activated by MMP-14), MMP-3, MMP-10, MMP-13 (also enhanced by TGF-β that is activated by MMP-2 and MMP-9), and MMP-14 to promote tumor growth. In addition to tumor initiation, MMP-13 is involved in the maintenance of angiogenesis through the release of VEGF. Inflammatory cells-derived MMP-9 induces SCC cells to release VEGF to support tumor angiogenesis. MMP-26 can activate MMP-9 and promote tumor growth.
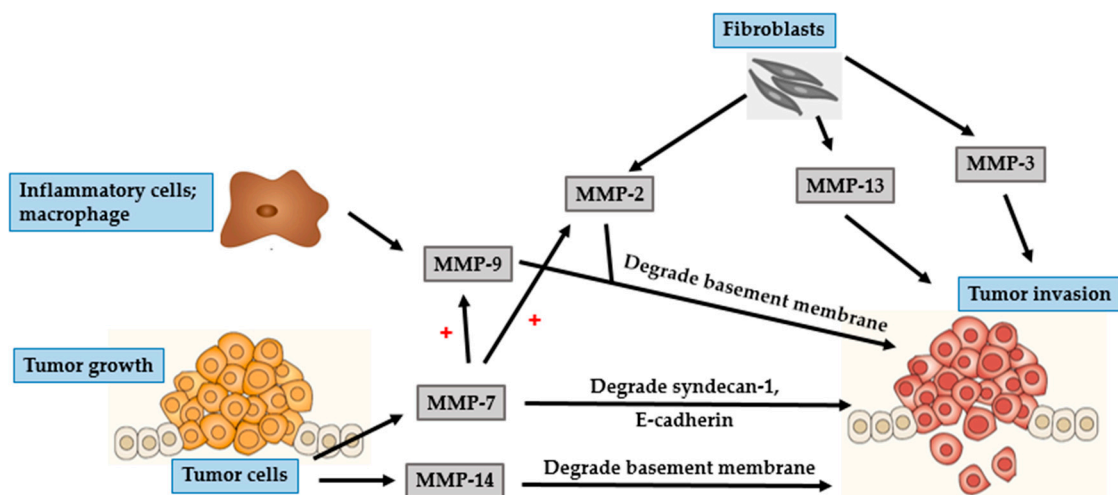
Figure 5. Role of MMPs in SCC tumor invasion. Fibroblasts secrete MMP-2, MMP-3, and MMP-13 to promote tumor invasion. Inflammatory cells secrete MMP-9 that degrades the basement membrane, leading to tumor invasion. SCC cells secrete MMP-7, which degrades syndecan-1, E-cadherin and induces the expression of MMP-2 and MMP-9. Additionally, SCC cells secrete MMP-14, which degrades the basement membrane. The expression of both MMP-7 and MMP-14 are important for tumor invasion.

Similar to MMP-2, the collagenases MMP-1 and MMP-13 are expressed in stromal cells, particularly in tumor-associated fibroblasts [61,70]. Both MMP-1 and MMP-13 are able to cleave native fibrillar collagen, an important step in tumor invasion and metastasis [67,71]. Expression of MMP-1 is reported to be associated with the initial steps of tumor growth in cutaneous SCC [72]. The involvement of cytokines in the initiation and development of tumor is an interesting fact in tumor biology. Interleukin (IL)-6, a potent pleiotropic cytokine, produced by various cell types such as activated keratinocytes, B- and T lymphocytes, macrophages, and endothelial cells, has a variety of biological functions. IL-6 is a key factor driving tumor progression [72]. The expression level of IL-6 is related to the expression of MMP-1. This indicates a role for MMP-1 in the regulation of cytokine and protease network, particularly related to SCC tumor progression [59]. Thus, overexpression of MMP-1 correlates positively with tumor aggressiveness and a poor clinical outcome.

MMP-13 has great substrate specificity and is a powerful tool for tumor invasion [73]. It is mainly produced by stromal cells that lie in close vicinity to tumor cells, which supports the crucial role of stroma in tumor progression. Furthermore, MMP-13 is involved in the maintenance of angiogenesis through the release of VEGF from the tumor ECM [67,71]. The level of MMP-13 is up-regulated by a multifunctional growth factor called TGF-β, which exerts various effects on ECM deposition, tumor cell proliferation and progression [73]. Interestingly, TGF-β is activated by gelatinolytic enzymes (MMP-2 and MMP-9) [61]. Taken together, tumor cell invasion and metastasis is mediated by the interaction between various MMPs and growth factors.

Several other MMPs are reported to be involved in the pathophysiology of SCC. Among them, MT1-MMP or MMP-14 acts as the most powerful pericellular proteolysis mediator. Tumor cells are controlled by processes that help them to pass through the ECM and to migrate and invade in the form of a single cell and as a collective tumor in a greatly arranged manner [61]. MT1-MMP, a member of the MT-MMP subgroup, plays an important role in the degradation of various ECM proteins and in activating pro-MMP-2. Both stromal fibroblasts and tumor cells in SCC, particularly at the invasive front of the tumor, secrete MMP-14. This finding suggests that the expression of MMP-14 in fibroblasts and tumor cells are related to tissue remodeling and invasive tumor growth, respectively [57,64]. The aggressive behavior of SCCs is illustrated by the fact that MMP-14 is expressed at the surface of tumor cells.

Although MMP-7 is the smallest member of the MMP family, it is able to digest a wide range of ECM proteins and cleave several cell surface proteins including-cadherin and syndecan-1 [50,54]. E-cadherin/syndecan-1 complex is a potent suppressor of invasion, and loss of E-cadherin or syndecan-1 on the cell surface leads to epithelial cell transformation [54]. In addition to enhancing tumor invasion and metastasis directly, MMP-7 exerts indirect effects through the activation of MMP-2 and MMP-9 [50]. Unlike several other MMPs that are involved in varied stages of tumor invasion, MMP-26 plays an essential role in the initial stages of skin cancer. MMP-9, the most important MMP in SCC tumor growth, is stimulated by MMP-26 [65].

MMP-10 or stromelysin-2, similar to other metalloproteases, facilitates the recruitment of infiltrating cells by remodeling the ECM. Moreover, MMP-10 up-regulates several other MMPs such as MMP-1, MMP-7, MMP-9, and MMP-13 that are essential for tumor progression. The function of this protease is restricted to the initial process of tumor initiation, indicating that it might not be important in invasion or metastasis [74]. MMP-10 is highly expressed in SCC stromal cells and is up-regulated by tumor-associated cytokines including TGF-β and TNF-α. Another stromelysin, MMP-3 is induced in the tumor stroma in the early stages of tumorigenesis. It can degrade a variety of matrix and non-matrix molecules such as growth factors, HB-EGF, and E-cadherin. Fibroblasts-derived MMP-3 is a necessary mediator of tumor vascularization and tumor progression, and thus plays an important role in mechanisms that modulate tumor metastasis [70,75].

Since MMPs appear to play a crucial role in the pathogenesis of SCC, many researchers have tried to develop specific inhibitors for each MMP as targeted therapeutics for the treatment of cancer. Vitamin D3 analogue, calcipotriol, down-regulates the expression of MMP-9 and MMP-13 in normal

human epidermal keratinocytes and human squamous-cell-carcinoma cell line [76]. Hence, suppressive effects of calcipotriol on the expression of MMP-9 and MMP-13 could be considered as a strategy for cancer treatment.

An natural compound,α-mangostin, a xanthone compound isolated from the pericarp of mangosteen, suppresses the activity of gelatinases, thus inhibiting the processes involved in metastasis [60].

4.3. Malignant Melanoma

Cutaneous melanoma, a type of cancer arising from pigment-producing cells called melanocytes, is known for its rapid progression, metastasis, and high morbidity and mortality in patients [77,78]. It accounts for 3%–5% of all cutaneous cancers, 75% of all skin cancer mortality, and has a 5-year survival rate lower than 15% for metastatic cases [77–79]. Development of melanoma is divided into two phases, radial growth phase (RGP) and vertical growth phase (VGP) or metastatic phase [79,80]. In the early stages of melanoma, RGP exists solely within the epidermis, with only a small number of non-dividing cells present within the superficial dermis. VGP melanomas may develop directly from RGP melanomas and are characterized by the invasion of dermal and subcutaneous tissues with the ability to disperse to regional lymph nodes and distant organs [80,81].

Like nonmelanoma skin cancers, the activity of MMPs can promote invasion of melanoma cells by altering the basement membrane and ECM proteins [77] (Figures 6 and 7). The gelatinases, MMP-2 and MMP-9, primarily cleave collagen type IV and are believed to play a crucial role in the progression of melanoma cells [78]. Fibroblasts secrete pro-MMP-2 which is activated by MMP-14 [82]. Overexpression of MMP-2 is correlated with architectural impairment, atypia progression, and hematogenous metastasis [83,84]. MMP-9 is strongly expressed in inflammatory cells such as macrophages, neutrophils, and mast cells. Its expression is related to the RGP rather than the VGP of melanomas, and is probably associated with early stages of tumor invasion [83,84].
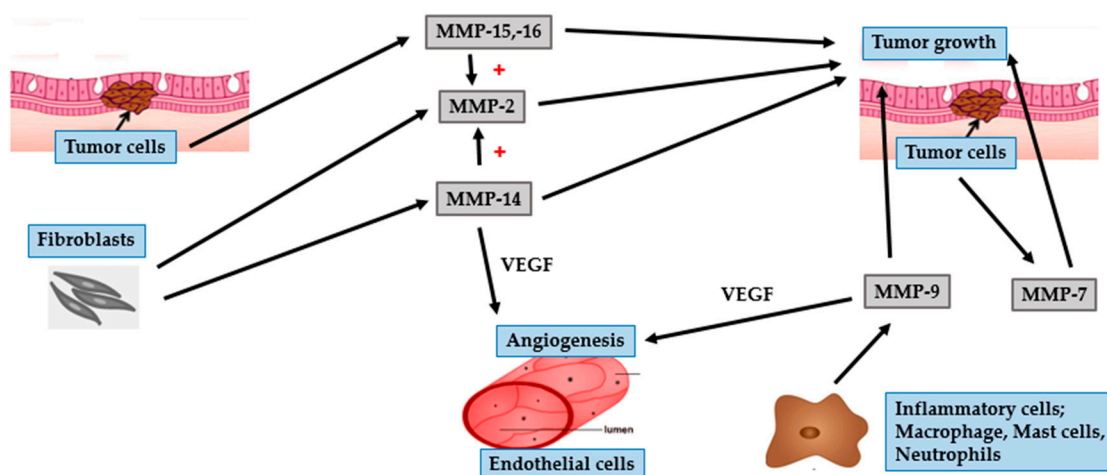
Figure 6. Role of MMPs in malignant melanoma and tumor growth. Melanoma cells secrete MMP-15 and MMP-16 to promote tumor growth. Fibroblasts secrete MMP-2 (also activated by MMP-14, MMP-15, and MMP-16) and MMP-14 to induce tumor growth. In addition to growth initiation, MMP-14 promotes tumor angiogenesis by enhancing the expression of VEGF. Inflammatory cells-derived MMP-9 is involved in tumor development and tumor angiogenesis. MMP-7 produced by melanoma cells can enhance tumor growth.

Angiogenesis is the initial process involved in the transition from a pre-neoplastic to a neoplastic stage [85]. Hypoxia is a strong stimulus for tumor angiogenesis. Tumor cells become hypoxic as they become distant from nearby vessels and respond to hypoxia-related angiogenic factors. HIF-1α,

a master regulator of cellular hypoxic response, is a transcription factor essential for the transcriptional activation of VEGF, resulting in tumor angiogenesis [86,87]. In addition to angiogenesis, under hypoxic conditions, HIF-1α plays an important role in the metastatic progression of melanoma by enhancing the expression of MMP such as MMP-2, MMP-9, and MMP-14 [87,88].
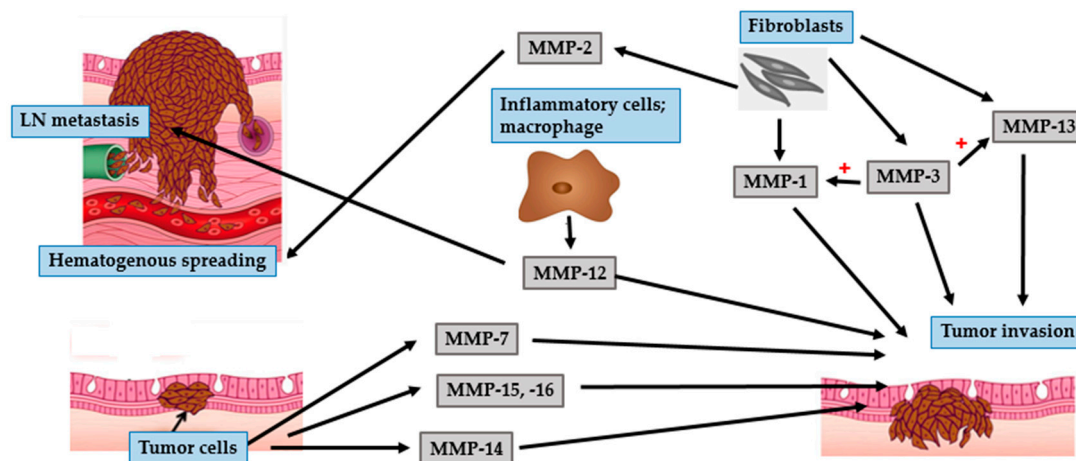
Figure 7. Role of MMPs in malignant melanoma tumor metastasis. Fibroblasts secrete MMP-1, MMP-3 (also activate MMP-1 and MMP-13) and MMP-13 to facilitate tumor invasion. Melanoma cells secrete MMP-7, MMP-14, MMP-15, and MMP-16 and facilitates tumor invasion. Inflammatory cells secrete MMP-12 to promote tumor invasion and are involved in lymph node (LN) metastasis. Fibroblasts-derived MMP-2 correlates with hematogenous spreading.

An adequate supply of oxygen and nutrients for tumor development, and a route for tumor cell migration and invasion, are highly correlated with tumor angiogenesis. Many angiogenic factors are secreted by tumor cells, including VEGF, bFGF, and platelet-derived growth factor (PDGF). The most essential pro-angiogenic factor is VEGF and its level is related to tumor vascularization [89,90]. Expression of MMP-9 plays an important role in tumor angiogenesis as it enhances the availability of VEGF in malignant tumors. VEGF can up-regulate MMP-2 expression in melanoma cells [89,90]. Taken together, interaction between gelatinases and VEGF promote tumor progression by regulating tumor angiogenesis and metastasis.

MT1-MMP plays a primary role in angiogenesis by promoting the expression of VEGF, mediating endothelial cell migration and vascular formation processes [91,92]. Furthermore, MT1-MMP cleaves a wide range of ECM components, promote tumor development and invasion, and activate pro-MMP-2 on the surface of melanoma cells [84,85]. Thus, MT1-MMP is crucial for tumor invasion and for activating pro-tumorigenic MMPs. Of the other MT-MMPs, the expression of MT2-MMP (MMP-15) and MT3-MMP (MMP-16) is increased in primary and metastatic melanoma cells [92]. Like MT1-MMP, MT3-MMP is also an efficient cell surface activator of pro-MMP2 [93].

Collagenases, MMP-1, MMP-8, and MMP-13, are the dominant extracellular proteinases with the ability to cleave native fibrillar collagen types I, II, III, and V. As they can degrade dermal collagen, they are particularly relevant in melanoma [81]. MMP-1, secreted by melanoma and activated stromal cells, contributes to the progression of melanoma in two ways. Firstly, it promotes invasion and metastasis of melanoma by breaking down interstitial collagens. Secondly, it promotes tumor invasion and vascularization via protease activator receptor-1 (PAR-1)-induced gene expression [81,94]. In addition to melanoma, PAR-1, an oncogene, is highly expressed in many types of cancer. The expression of PAR-1 correlates with the depth of melanoma invasion [81]. Hence, the process of tumor cell invasion requires a combination of PAR-1 activity and MMP-1 expression, both of which are responsible for the collagenolytic function.

MMP-13 is reported to be involved in the invasive VGP of melanomas. Its expression in stromal cells immediately adjacent to the tumor is higher upon tumor cell invasion [82,92]. An increased risk of malignant melanoma is correlated with the expression of MMP-8 [92].

MMP-3 can activate pro-MMPs, such as pro-MMP-1 and pro-MMP-13. It is expressed in metastatic melanoma and is correlated with shorter disease-free survival [92,95]. MMP-7 or matrilysin is expressed and produced by primary cutaneous and metastatic melanomas [92,96]. Matrilysin is secreted as a pro-enzyme and is activated extracellularly. Its expression in melanomas enhances tumor cell growth and metastasis, thereby reducing the survival rate [96]. Levels of MMP-12 correlates with melanoma cell invasion, lymph node metastasis, and tumor metastasis. It is a potential predictive marker for the prognosis of patients with melanoma [97].

The knowledge of events that are associated with the initiation and progression of melanoma could be used critically for the development of novel therapeutic agents aimed at increasing the effectiveness of cancer therapy and improving the survival rate of cancer patients.

5. Conclusions

Cutaneous exposure to UV irradiation causes the up-regulation of several different MMPs that virtually impair the various components of the ECM. These alterations in the ECM are known to cause skin wrinkling, a major characteristic of premature skin aging. Regulation of MMPs is one of the strategies to prevent photodamage to the skin as their activities contribute to wrinkle formation. Use of free radical scavengers or antioxidants is considered on a therapeutic basis to diminish the damaging effects of UV radiation and to prevent UV-initiated photoaging because of their ability to inhibit the expression and activity of MMPs.

MMPs play an important role in tumor development, growth, angiogenesis, and metastasis. Each of these proteinases has specific roles in determining the invasive capacity of the tumor. Hence, the function of distinct MMPs and their regulation should be considered the principal targets for development of antineoplastic drugs or chemotherapeutic agents.

Author Contributions: Pavida Pittayapruek and Jitlada Meephansan prepared the data and wrote the paper; Jitlada Meephansan was the advisor and Ornicha Prapapan was the co-advisor; Mayumi Komine and Mamitaro Ohtsuki supervised the writing.

Conflicts of Interest: The authors declare no conflict of interest.

Abbreviations

$^1O_2$	Singlet oxygen
AP-1	Activator protein 1
BCC	Basal cell carcinoma
bFGF	Basic fibroblast growth factor
COX-2	Cyclooxygenase 2
CXCR4	C-X-C chemokine receptor type 4
ECM	Extracellular matrix
EGCG	Epigallocatechin gallate
EGFR	Epidermal growth factor receptor
EMT	Epithelial-mesenchymal transition
ERK	Extracellular signal-regulated kinase
GM-CSF	Granulocyte macrophage colony stimulatory factor
H_2O_2	Hydrogen peroxide
HB-EGF	Heparin-binding epidermal-like growth factor
HIF-1α	Hypoxia-inducible factor-1α
IL-1α	Interleukin 1 alpha
IL-6	Interleukin 6
JNK	c-Jun NH2-terminal kinase
kDa	Kilodalton
LN	Lymph node
MAPK	Mitogen-activated protein kinase

MMPs	Matrix metalloproteases
MT-MMP	Membrane-type matrix metalloprotease
NEP	Neutral endopeptidase
NF-κB	Nuclear factor-kappa B
O_2-	Superoxide anion
OH groups	Hydroxyl group
OH.	Hydroxyl radical
PAR-1	Protease activator receptor 1
PDGF	Platelet-derived growth factor
RGP	Radial growth phase
ROS	Reactive oxygen species
SCC	Squamous cell carcinoma
SDF-1	Stromal cell-derived factor 1
TAMs	Tumor-associated macrophages
TCF	T-cell transcription factor
TGF-β	Transforming growth factor-beta
TIMP	Tissue inhibitors of matrix metalloprotease
TNF-α	Tumor necrosis factor alpha
UV	Ultraviolet
VEGF	Vascular endothelial growth factor
VGP	Vertical growth phase

References

1. Steinbrenner, H.; Ramos, M.C.; Stuhlmann, D.; Sies, H.; Brenneisen, P. UVA-mediated downregulation of MMP-2 and MMP-9 in human epidermal keratinocytes. *Biochem. Biophys. Res. Commun.* **2003**, *308*, 486–491. [CrossRef]

2. Vicentini, F.T.M.C.; He, T.; Shao, Y.; Fonseca, M.J.V.; Verri, W.A., Jr.; Fisher, G.J.; Xu, Y. Quercetin inhibits UV irradiation-induced inflammatory cytokine production in primary human keratinocytes by suppressing NF-κB pathway. *J. Dermatol. Sci.* **2011**, *61*, 162–168. [CrossRef] [PubMed]

3. Quan, T.; Qin, Z.; Xia, W.; Shao, Y.; Voorhees, J.J.; Fisher, G.J. Matrix-degrading metalloproteinases in photoaging. *J. Investig. Dermatol. Symp. Proc.* **2009**, *14*, 20–24. [CrossRef] [PubMed]

4. Kim, J.; Lee, C.W.; Kim, E.K.; Lee, S.J.; Park, N.H.; Kim, H.S.; Kim, H.K.; Char, K.; Jang, Y.P.; Kim, J.W. Inhibition effect of Gynura procumbens extract on UVB-induced matrix-metalloproteinase expression in human dermal fibroblasts. *J. Ethnopharmacol.* **2011**, *137*, 427–433. [CrossRef] [PubMed]

5. O'Grady, A.; Dunne, C.; O'Kelly, P.; Murphy, G.M.; Leader, M.; Kay, E. Differential expression of matrix metalloproteinase (MMP)-2, MMP-9 and tissue inhibitor of metalloproteinase (TIMP)-1 and TIMP-2 in non-melanoma skin cancer: Implications for tumour progression. *Histopathology* **2007**, *51*, 793–804.

6. Ham, S.A.; Yoo, T.; Hwang, J.S.; Kang, E.S.; Paek, K.S.; Park, C.; Kim, J.H.; Do, J.T.; Seo, H.G. Peroxisome proliferator-activated receptor d modulates MMP-2 secretion and elastin expression in human dermal fibroblasts exposed to ultraviolet B radiation. *J. Dermatol. Sci.* **2014**, *76*, 44–50. [CrossRef] [PubMed]

7. Hwang, Y.P.; Choi, J.H.; Kim, H.G.; Choi, J.M.; Hwang, S.K.; Chung, Y.C.; Jeong, H.G. Cultivated ginseng suppresses ultraviolet B–induced collagenase activation via mitogen-activated protein kinases and nuclear factor κB/activator protein-1–dependent signaling in human dermal fibroblasts. *Nutr. Res.* **2012**, *32*, 428–438. [CrossRef] [PubMed]

8. Jung, S.K.; Lee, K.W.; Kim, H.Y.; Oha, M.H.; Byun, S.; Lim, S.H.; Heo, Y.S.; Kang, N.J.; Bode, A.M.; Dong, Z.; *et al.* Myricetin suppresses UVB-induced wrinkle formation and MMP-9 expression by inhibiting Raf. *Biochem. Pharmacol.* **2010**, *79*, 1455–1461. [CrossRef] [PubMed]

9. Sbardella, D.; Fasciglione, G.F.; Gioia, M.; Ciaccio, C.; Tundo, G.R.; Marini, S.; Coletta, M. Human matrix metalloproteinases: An ubiquitarian class of enzymes involved in several pathological processes. *Mol. Asp. Med.* **2012**, *33*, 119–208. [CrossRef] [PubMed]

10. Bae, J.Y.; Choi, J.S.; Choi, Y.J.; Shin, S.Y.; Kang, S.W.; Han, S.J.; Kang, Y.H. Epigallocatechin gallate hampers collagen destruction and collagenase activation in ultraviolet-B-irradiated human dermal fibroblasts: Involvement of mitogen-activated protein kinase. *Food Chem. Toxicol.* **2008**, *46*, 1298–1307. [CrossRef] [PubMed]

11. Hwang, B.M.; Noh, E.M.; Kim, J.S.; Kim, J.M.; Hwang, J.K.; Kim, H.K.; Kang, J.S.; Kim, D.S.; Chae, H.J.; You, Y.O.; *et al.* Decursin inhibits UVB-induced MMP expression in human dermal fibroblasts via regulation of nuclear factor-κB. *Int. J. Mol. Med.* **2013**, *31*, 477–483. [PubMed]

12. Wen, K.C.; Fan, P.C.; Tsai, S.Y.; Shih, I.C.; Chiang, H.M. Ixora parviflora protects against UVB-induced photoaging by inhibiting the expression of MMPs, MAP kinases, and COX-2 and by promoting type I procollagen synthesis. *Evid. Based Complement. Altern. Med.* **2011**, *2012*, 1–11. [CrossRef] [PubMed]

13. Hwang, Y.P.; Kim, H.G.; Choi, J.H.; Han, E.H.; Kwon, K.I.; Lee, Y.C.; Choi, J.M.; Chung, Y.C.; Jeong, T.C.; Jeong, H.G. Saponins from the roots of Platycodon grandiflorum suppress ultraviolet A-induced matrix metalloproteinase-1 expression via MAPKs and NF-κB/AP-1-dependent signaling in HaCaT cells. *Food Chem. Toxicol.* **2011**, *49*, 3374–3382. [CrossRef] [PubMed]

14. Chiang, H.M.; Chen, H.C.; Lin, T.J.; Shih, I.C.; Wen, K.C. Michelia alba extract attenuates UVB-induced expression of matrix metalloproteinases via MAP kinase pathway in human dermal fibroblasts. *Food Chem. Toxicol.* **2012**, *50*, 4260–4269. [CrossRef] [PubMed]

15. Tewari, A.; Grys, K.; Kollet, J.; Sarkany, R.; Young, A.R. Upregulation of MMP12 and its activity by UVA1 in human skin: potential implications for photoaging. *J. Investig. Dermatol.* **2014**, *134*, 2598–2609. [CrossRef] [PubMed]

16. Parkinson, L.G.; Toro, A.; Zhao, H.; Brown, K.; Tebbutt, S.J.; Granville, D.J. Granzyme B mediates both direct and indirect cleavage of extracellular matrix in skin after chronic low-dose ultraviolet light irradiation. *Aging Cell* **2015**, *14*, 67–77. [CrossRef] [PubMed]

17. Chiang, H.M.; Chen, H.C.; Chiu, H.H.; Chen, C.W.; Wang, S.M.; Wen, K.C. Neonauclea reticulata (Havil.) merr stimulates skin regeneration after UVB exposure via ROS scavenging and modulation of the MAPK/MMPs/collagen pathway. *Evid. Based Complement. Altern. Med.* **2013**, *2013*, 1–9. [CrossRef] [PubMed]

18. Ham, S.A.; Kang, E.S.; Lee, H.; Hwang, J.S.; Yoo, T.; Paek, K.S.; Park, C.; Kim, J.H.; Lim, D.S.; Seo, H.G. PPAR-delta inhibits UVB-induced secretion of MMP-1 through MKP-7-mediated suppression of JNK signaling. *J. Investig. Dermatol.* **2013**, *133*, 2593–2600. [CrossRef] [PubMed]

19. Wang, Y.; Chen, H.; Wang, W.; Wang, R.; Liu, Z.L.; Zhu, W.; Lian, S. N-terminal 5-mer peptide analog P165 of amyloid precursor protein inhibits UVA-induced MMP-1 expression by suppressing the MAPK pathway in human dermal fibroblasts. *Eur. J. Pharmacol.* **2014**, *734*, 1–8. [CrossRef] [PubMed]

20. Park, J.E.; Pyun, H.B.; Woo, S.W.; Jeong, J.H.; Hwang, J.K. The protective effect of Kaempferia parviflora extract on UVB-induced skin photoaging in hairless mice. *Photodermatol. Photoimmunol. Photomed.* **2014**, *30*, 237–245. [CrossRef] [PubMed]

21. Sun, Z.W.; Hwang, E.; Lee, H.J.; Lee, T.Y.; Song, H.G.; Park, S.Y.; Shin, H.S.; Lee, D.G.; Yi, T.H. Effects of Galla chinensis extracts on UVB-irradiated MMP-1 production in hairless mice. *J. Nat. Med.* **2015**, *69*, 22–34. [CrossRef] [PubMed]

22. Hwang, E.; Lee, D.G.; Park, S.H.; Oh, M.S.; Kim, S.Y. Coriander leaf extract exerts antioxidant activity and protects against UVB-induced photoaging of skin by regulation of procollagen type I and MMP-1 expression. *J. Med. Food* **2014**, *17*, 985–995. [CrossRef] [PubMed]

23. Chen, B.; Li, R.; Yan, N.; Chen, G.; Qian, W.; Jiang, H.L.; Ji, C.; Bi, Z.G. Astragaloside IV controls collagen reduction in photoaging skin by improving transforming growth factor-β/Smad signaling suppression and inhibiting matrix metalloproteinase-1. *Mol. Med. Rep.* **2015**, *11*, 3344–3348. [PubMed]

24. Lee, Y.R.; Noh, E.M.; Han, J.H.; Kim, J.M.; Hwang, J.K.; Hwang, B.M.; Chung, E.Y.; Kim, B.S.; Lee, S.H.; Lee, S.J.; *et al.* Brazilin inhibits UVB-induced MMP-1/3 expressions and secretions by suppressing the NF-κB pathway in human dermal fibroblasts. *Eur. J. Pharmacol.* **2012**, *674*, 80–86. [CrossRef] [PubMed]

25. Yao, C.; Lee, D.H.; Oh, J.H.; Kim, M.K.; Kim, K.H.; Park, C.H.; Chung, J.H. Poly(I:C) induces expressions of MMP-1, -2, and -3 through various signaling pathways including IRF3 in human skin fibroblasts. *J. Dermatol. Sci.* **2015**, *80*, 54–60. [CrossRef] [PubMed]

26. Son, W.C.; Yun, J.W.; Kim, B.H. Adipose-derived mesenchymal stem cells reduce MMP-1 expression in UV-irradiated human dermal fibroblasts: Therapeutic potential in skin wrinkling. *Biosci. Biotechnol. Biochem.* **2015**, *79*, 919–925. [CrossRef] [PubMed]

27. Wertz, K.; Seifert, N.; Hunziker, P.B.; Riss, G.; Wyss, A.; Lankin, C.; Goralczyk, R. Beta-carotene inhibits UVA-induced matrix metalloprotease 1 and 10 expression in keratinocytes by a singlet oxygen-dependent mechanism. *Free Radic. Biol. Med.* **2004**, *37*, 654–670. [CrossRef] [PubMed]

28. Onoue, S.; Kobayashi, T.; Takemoto, Y.; Sasaki, I.; Shinkai, H. Induction of matrix metalloproteinase-9 secretion from human keratinocytes in culture by ultraviolet-B irradiation. *J. Dermatol. Sci.* **2003**, *33*, 105–111. [CrossRef] [PubMed]

29. Kim, H.S.; Song, J.H.; Youn, U.J.; Hyun, J.W.; Jeong, W.S.; Lee, M.Y.; Choi, H.J.; Lee, H.K.; Chae, S. Inhibition of UVB-induced wrinkle formation and MMP-9 expression by mangiferin isolated from Anemarrhena asphodeloides. *Eur. J. Pharmacol.* **2012**, *689*, 38–44. [CrossRef] [PubMed]

30. Fortino, V.; Maioli, E.; Torricelli, C.; Davis, P.; Valacchi, G. Cutaneous MMPs are differently modulated by environmental stressors in old and young mice. *Toxicol. Lett.* **2007**, *173*, 73–79. [CrossRef] [PubMed]

31. Vayalil, P.K.; Mittal, A.; Hara, Y.; Elmets, C.A.; Katiyar, S.K. Green tea polyphenols prevent ultraviolet light-induced oxidative damage and matrix metalloproteinases expression in mouse skin. *J. Investig. Dermatol.* **2004**, *122*, 1480–1487. [CrossRef] [PubMed]

32. Brennan, M.; Bhatti, H.; Nerusu, K.C.; Bhagavathula, N.; Kang, S.; Fisher, G.J.; Varani, J.; Voorhees, J.J. Matrix metalloproteinase-1 is the major collagenolytic enzyme responsible for collagen damage in UV-irradiated human skin. *Photochem. Photobiol.* **2003**, *78*, 43–48. [CrossRef]

33. Chen, Z.; Seo, J.Y.; Kim, Y.K.; Lee, S.R.; Kim, K.H.; Cho, K.H.; Eun, H.C.; Chung, J.H. Heat modulation of tropoelastin, fibrillin-1, and matrix metalloproteinase-12 in human skin *in vivo*. *J. Investig. Dermatol.* **2005**, *124*, 70–78. [CrossRef] [PubMed]

34. Taddese, S.; Weiss, A.S.; Neubert, R.H.; Schmelzer, C.E. Mapping of macrophage elastase cleavage sites in insoluble human skin elastin. *Matrix Biol.* **2008**, *27*, 420–428.

35. Taddese, S.; Weiss, A.S.; Jahreis, G.; Neubert, R.H.; Schmelzer, C.E. *In vitro* degradation of human tropoelastin by MMP-12 and the generation of matrikines from domain 24. *Matrix Biol.* **2009**, *28*, 84–91. [PubMed]

36. Imokawa, G.; Nakajima, H.; Ishida, K. Biological mechanisms underlying the ultraviolet light-induced formation of skin wrinkling and sagging II: over-expression of Neprilysin/Neutral endopeptidase via epithelial-mesenchymal interaction plays an essential role in wrinkling and sagging. *Int. J. Mol. Sci.* **2015**, *16*, 1–25. [CrossRef] [PubMed]

37. Morisaki, N.; Moriwaki, S.; Sugiyama-Nakagiri, Y.; Haketa, K.; Takema, Y.; Imokawa, G. Neprilysin is identical to skin fibroblast elastase. *J. Biol. Chem.* **2010**, *285*, 39819–39827. [CrossRef] [PubMed]

38. Nakajima, H.; Ezaki, Y.; Nagai, T.; Yoshioka, R.; Imokawa, G. Epithelial–mesenchymal interaction during UVB-induced up-regulation of neutral endopeptidase. *Biochem. J.* **2012**, *443*, 297–305. [CrossRef] [PubMed]

39. Chiang, H.M.; Lin, T.J.; Chiu, C.Y.; Chang, C.W.; Hsu, K.C.; Fan, P.C.; Wen, K.C. Coffea arabica extract and its constituents prevent photoaging by suppressing MMPs expression and MAP kinase pathway. *Food Chem. Toxicol.* **2011**, *49*, 309–318. [CrossRef] [PubMed]

40. Mantena, S.K.; Roy, A.M.; Katiyar, S.K. Epigallocatechin-3-Gallate inhibits photocarcinogenesis through inhibition of angiogenic factors and activation of CD8 + T cells in tumors. *Photochem. Photobiol.* **2005**, *81*, 1174–1179. [CrossRef] [PubMed]

41. Poswar, F.O.; Fraga, C.A.; Farias, L.C.; Feltenberger, J.D.; Cruz, V.P.; Santos, S.H.; Silveira, C.M.; de Paula, A.M.B.; Guimarães, A.L.S. Immunohistochemical analysis of TIMP-3 and MMP-9 in actinic keratosis, squamous cell carcinoma of the skin, and basal cell carcinoma. *Pathol. Res. Pract.* **2013**, *209*, 705–709. [CrossRef] [PubMed]

42. Ciurea, M.E.; Cernea, D.; Georgescu, C.C.; Cotoi, O.S.; Patrascu, V.; Parvanescu, H.; Popa, D.; Pârvănescu, V.; Ciurea, R.N.; Mercut, R. Expression of CXCR4, MMP-13 and β-catenin in different histological subtypes of facial basal cell carcinoma. *Rom. J. Morphol. Embryol.* **2013**, *54*, 949–951.

43. De Oliveira Poswar, F.; de Carvalho Fraga, C.A.; Gomes, E.S.B.; Farias, L.C.; Souza, L.W.F.; Santos, S.H.S.; Gomez, R.S.; de-Paula, A.M.B.; Guimarães, A.L.S. Protein expression of MMP-2 and MT1-MMP in actinic keratosis, squamous cell carcinoma of the skin, and basal cell carcinoma. *Int. J. Surg. Pathol.* **2015**, *23*, 20–25. [CrossRef] [PubMed]

44. Tan, E.S.; Ee, M.; Shen, L.; Chua, H.; Chan, Y.H.; Tan, S.H. Basal cell carcinoma in Singapore: A prospective study on epidemiology and clinicopathological characteristics with a secondary comparative analysis between Singaporean Chinese and Caucasian patients. *Australas. J. Dermatol.* **2015**, *56*, 175–179. [CrossRef] [PubMed]

45. Moore, M.G.; Bennett, R.G. Basal cell carcinoma in Asians: A retrospective analysis of ten patients. *J. Skin Cancer* **2012**, 1–5. [CrossRef] [PubMed]

46. Boyd, S.; Tolvanen, K.; Virolainen, S.; Kuivanen, T.; Kyllönen, L.; Saarialho-Kere, U. Differential expression of stromal MMP-1, MMP-9 and TIMP-1 in basal cell carcinomas of immunosuppressed patients and controls. *Virchows. Arch.* **2008**, *452*, 83–90. [CrossRef] [PubMed]

47. Chu, C.Y.; Cha, S.T.; Chang, C.C.; Hsiao, C.H.; Tan, C.T.; Lu, Y.C.; Jee, S.H.; Kuo, M.L. Involvement of matrix metalloproteinase-13 in stromal-cell-derived factor 1a-directed invasion of human basal cell carcinoma cells. *Oncogene* **2007**, *26*, 2491–2501. [CrossRef] [PubMed]

48. Oh, S.T.; Kim, H.S.; Yoo, N.J.; Lee, W.S.; Cho, B.K.; Reichrath, J. Increased immunoreactivity of membrane type-1 matrix metalloproteinase (MT1-MMP) and b-catenin in high-risk basal cell carcinoma. *Br. Assoc. Dermatol.* **2011**, *165*, 1197–1204. [CrossRef] [PubMed]

49. Nan, H.; Niu, T.; Hunter, D.J.; Han, J. Missense polymorphisms in matrix metalloproteinase genes and skin cancer risk. *Cancer Epidemiol. Biomark. Prev.* **2008**, *17*, 3551–3557. [CrossRef] [PubMed]

50. Chuang, H.C.; Su, C.Y.; Huang, H.Y.; Huang, C.C.; Chien, C.Y.; Du, Y.Y.; Chuang, J.H. Active matrix metalloproteinase-7 is associated with invasion in buccal squamous cell carcinoma. *Mod. Pathol.* **2008**, *21*, 1444–1450. [CrossRef] [PubMed]

51. Chen, G.S.; Lu, M.P.; Wu, M.T. Differential expression of matrix metalloproteinase-2 by fibroblasts in co-cultures with keratinocytes, basal cell carcinoma and melanoma. *J. Dermatol.* **2006**, *33*, 609–615. [CrossRef] [PubMed]

52. Hartmann-Petersen, S.; Tammi, R.H.; Tammi, M.I.; Kosma, V.M. Depletion of cell surface CD44 in nonmelanoma skin tumours is associated with increased expression of matrix metalloproteinase 7. *Br. J. Dermatol.* **2009**, *160*, 1251–1257. [CrossRef] [PubMed]

53. Tjiu, J.W.; Chen, J.S.; Shun, C.T.; Lin, S.J.; Liao, Y.H.; Chu, C.Y.; Tsai, T.F.; Chiu, H.C.; Dai, Y.S.; Inoue, H.; *et al.* Tumor-associated macrophage-induced invasion and angiogenesis of human basal cell carcinoma cells by cyclooxygenase-2 induction. *J. Investig. Dermatol.* **2009**, *129*, 1016–1025. [CrossRef] [PubMed]

54. Kivisaari, A.K.; Kallajoki, M.; Mirtti, T.; McGrath, J.A.; Bauer, J.W.; Weber, F.; Königová, R.; Sawamura, D.; Sato-Matsumura, K.C.; Shimizu, H.; *et al.* Transformation-specific matrix metalloproteinases (MMP)-7 and MMP-13 are expressed by tumour cells in epidermolysis bullosa-associated squamous cell carcinomas. *Br. J. Dermatol.* **2008**, *158*, 778–785. [CrossRef] [PubMed]

55. Goodison, S.; Urquidi, V.; Tarin, D. CD44 cell adhesion molecules. *J. Clin. Pathol. Mol. Pathol.* **1999**, *52*, 189–196. [CrossRef]

56. Ahokas, K.; Skoog, T.; Suomela, S.; Jeskanen, L.; Impola, U.; Isaka, K.; Saarialho-Kere, U. Matrilysin-2 (matrix metalloproteinase-26) is upregulated in keratinocytes during wound repair and early skin carcinogenesis. *J. Investig. Dermatol.* **2005**, *124*, 849–856. [CrossRef] [PubMed]

57. Roh, M.R.; Zheng, Z.; Kim, H.S.; Kwon, J.E.; Jeung, H.C.; Rha, S.Y.; Chung, K.Y. Differential expression patterns of MMPs and their role in the invasion of epithelial premalignant tumors and invasive cutaneous squamous cell carcinoma. *Exp. Mol. Pathol.* **2012**, *92*, 236–242. [CrossRef] [PubMed]

58. Briso, E.M.; Guinea-Viniegra, J.; Bakiri, L.; Rogon, Z.; Petzelbauer, P.; Eils, R.; Wolf, R.; Rincón, M.; Angel, P.; Wagner, E.F. Inflammation-mediated skin tumorigenesis induced by epidermal c-Fos. *Genes Dev.* **2013**, *27*, 1959–1973. [CrossRef] [PubMed]

59. Prasad, N.B.; Fischer, A.C.; Chuang, A.Y.; Wright, J.M.; Yang, T.; Tsai, H.L.; Westra, W.H.; Liegeois, N.J.; Hess, A.D.; Tufaro, A.P. Differential expression of degradome components in cutaneous squamous cell carcinomas. *Mod. Pathol.* **2014**, *27*, 945–957. [CrossRef] [PubMed]

60. Wang, J.J.; Sanderson, B.J.; Zhang, W. Significant anti-invasive activities of α-mangostin from the mangosteen pericarp on two human skin cancer cell lines. *Anticancer Res.* **2012**, *32*, 3805–3816. [PubMed]

61. Kessenbrock, K.; Wang, C.Y.; Werb, Z. Matrix metalloproteinases in stem cell regulation and cancer. *Matrix Biol.* **2015**, *44*, 184–190. [CrossRef] [PubMed]

62. Junttila, M.; Ala-aho, R.; Jokilehto, T.; Peltonen, J.; Kallajoki, M.; Grenman, R.; Jaakkola, P.; Westermarck, J.; Kähäri, V.M. p38a and p38d mitogen-activated protein kinase isoforms regulate invasion and growth of head and neck squamous carcinoma cells. *Oncogene* **2007**, *26*, 5267–5279. [CrossRef] [PubMed]

63. Xia, Y.H.; Li, M.; Fu, D.D.; Xu, S.L.; Li, Z.G.; Liu, D.; Tian, Z.W. Effects of PTTG down-regulation on proliferation and metastasis of the SCL-1 cutaneous squamous cell carcinoma cell line. *Asian Pac. J. Cancer Prev.* **2013**, *14*, 6245–6248. [CrossRef] [PubMed]

64. Hernández-Pérez, M.; El-hajahmad, M.; Massaro, J.; Mahalingam, M. Expression of gelatinases (MMP-2, MMP-9) and gelatinase activator (MMP-14) in actinic keratosis and in *in situ* and invasive squamous cell carcinoma. *Am. J. Dermatopathol.* **2012**, *7*, 723–728. [CrossRef] [PubMed]

65. Kuivanen, T.; Jeskanen, L.; Kyllonen, L.; Isaka, K.; Saarialho-Kere, U. Matrix metalloproteinase-26 is present more frequently in squamous cell carcinomas of immunosuppressed compared with immunocompetent patients. *J. Cutan. Pathol.* **2009**, *36*, 929–936. [CrossRef] [PubMed]

66. Ahmed Haji Omar, A.; Haglund, C.; Virolainen, S.; Häyry, V.; Atula, T.; Kontio, R.; Salo, T.; Sorsa, T.; Hagström, J. MMP-7, MMP-8, and MMP-9 in oral and cutaneous squamous cell carcinomas. *Oral Surg. Oral Med. Oral Pathol. Oral Radiol.* **2015**, *119*, 459–467. [CrossRef] [PubMed]

67. Lederle, W.; Hartenstein, B.; Meides, A.; Kunzelmann, H.; Werb, Z.; Angel, P.; Mueller, M.M. MMP13 as a stromal mediator in controlling persistent angiogenesis in skin carcinoma. *Carcinogenesis* **2010**, *31*, 1175–1184. [CrossRef] [PubMed]

68. Shen, L.; Lio, L.; Yang, Z.; Jiang, N. Identification of genes and signaling pathways associated with squamous cell carcinoma by bioinformatics analysis. *Oncol. Lett.* **2016**, *11*, 1382–1390. [CrossRef] [PubMed]

69. An, X.; Xu, G.; Yang, L.; Wang, Y.; Li, Y.; Mchepange, U.O.; Shen, G.; Tu, Y.; Tao, J. Expression of hypoxia-inducible factor-1alpha, vascular endothelial growth factor and prolyl hydroxylase domain protein 2 in cutaneous squamous cell carcinoma and precursor lesions and their relationship with histological stages and clinical features. *J. Dermatol.* **2014**, *41*, 76–83. [CrossRef] [PubMed]

70. Vosseler, S.; Lederle, W.; Airola, K.; Obermueller, E.; Fusenig, N.E.; Mueller, M.M. Distinct progression-associated expression of tumor and stromal MMPs in HaCaT skin SCCs correlates with onset of invasion. *Int. J. Cancer* **2009**, *125*, 2296–2306. [CrossRef] [PubMed]

71. Meides, A.; Gutschalk, C.M.; Devel, L.; Beau, F.; Czarny, B.; Hensler, S.; Neugebauer, J.; Dive, V.; Angel, P.; Mueller, M.M. Effects of selective MMP-13 inhibition in squamous cell carcinoma depend on estrogen. *Int. J. Cancer* **2014**, *135*, 2749–2759. [CrossRef] [PubMed]

72. Lederle, W.; Depner, S.; Schnur, S.; Obermueller, E.; Catone, N.; Just, A.; Fusenig, N.E.; Mueller, M.M. IL-6 promotes malignant growth of skin SCCs by regulating a network of autocrine and paracrine cytokines. *Int. J. Cancer* **2011**, *128*, 2803–2814. [CrossRef] [PubMed]

73. Leivonen, S.K.; Ala-aho, R.; Koli, K.; Grénman, R.; Peltonen, J.; Kahari, V.M. Activation of Smad signaling enhances collagenase-3 (MMP-13) expression and invasion of head and neck squamous carcinoma cells. *Oncogene* **2006**, *25*, 2588–2600. [CrossRef] [PubMed]

74. Boyd, S.; Virolainen, S.; Parssinen, J.; Skoog, T.; Van Hogerlinden, M.; Latonen, L.; Kyllönen, L.; Toftgard, R.; Saarialho-Kere, U. MMP-10 (Stromelysin-2) and MMP-21 in human and murine squamous cell cancer. *Exp. Dermatol.* **2009**, *18*, 1044–1052. [CrossRef] [PubMed]

75. McCawley, L.J.; Wright, J.; LaFleur, B.J.; Crawford, H.C.; Matrisian, L.M. Keratinocyte expression of MMP3 enhances differentiation and prevents tumor establishment. *Am. J. Pathol.* **2008**, *173*, 1528–1539. [CrossRef] [PubMed]

76. Meephansan, J.; Komine, M.; Tsuda, H.; Ohtsuki, M. Suppressive effect of calcipotriol on the induction of matrix metalloproteinase (MMP)-9 and MMP-13 in a human squamous cell carcinoma cell line. *Clin. Exp. Dermatol.* **2012**, *37*, 889–896. [CrossRef] [PubMed]

77. Leight, J.L.; Tokuda, E.Y.; Jones, C.E.; Lin, A.J.; Anseth, K.S. Multifunctional bioscaffolds for 3D culture of melanoma cells reveal increased MMP activity and migration with BRAF kinase inhibition. *Proc. Natl. Acad. Sci. USA* **2015**, *112*, 5366–5371. [CrossRef] [PubMed]

78. Rotte, A.; Martinka, M.; Li, G. MMP2 expression is a prognostic marker for primary melanoma patients. *Cell Oncol.* **2012**, *35*, 207–216. [CrossRef] [PubMed]

79. Chen, Y.; Chen, Y.; Huang, L.; Yu, J. Evaluation of heparanase and matrix metalloproteinase-9 in patients with cutaneous malignant melanoma. *J. Dermatol.* **2012**, *39*, 339–343. [CrossRef] [PubMed]

80. Ye, S.; Dhillon, S.; Turner, S.J.; Bateman, A.C.; Theaker, J.M.; Pickering, R.M.; Day, I.; Howell, W.M. Invasiveness of cutaneous malignant melanoma is influenced by matrix metalloproteinase-1 gene polymorphism. *Cancer Res.* **2001**, *61*, 1296–1298. [PubMed]

81. Blackburn, J.S.; Liu, I.; Coon, C.I.; Brinckerhoff, C.E. A matrix metalloproteinase-1/Protease activated receptor-1 signaling axis promotes melanoma invasion and metastasis. *Oncogene* **2009**, *28*, 4237–4248. [CrossRef] [PubMed]

82. Kondratiev, S.; Gnepp, D.R.; Yakirevich, E.; Sabo, E.; Annino, D.J.; Rebeiz, E.; Laver, N.V. Expression and prognostic role of MMP2, MMP9, MMP13, and MMP14 matrix metalloproteinases in sinonasal and oral malignant melanomas. *Hum. Pathol.* **2008**, *39*, 337–343. [CrossRef] [PubMed]

83. Väisänen, A.H.; Kallioinen, M.; Turpeenniemi-Hujanen, T. Comparison of the prognostic value of matrix metalloproteinases 2 and 9 in cutaneous melanoma. *Hum. Pathol.* **2008**, *39*, 377–385. [CrossRef] [PubMed]

84. Hofmann, U.B.; Houben, R.; Bröcker, E.B.; Becker, J.C. Role of matrix metalloproteinases in melanoma cell invasion. *Biochimie* **2005**, *87*, 307–314. [CrossRef] [PubMed]

85. Foda, H.D.; Zucker, S. Matrix metalloproteinases in cancer invasion, metastasis and angiogenesis. *Drug Discov. Today* **2001**, *6*, 478–482. [CrossRef]

86. Hwang, H.W.; Baxter, L.L.; Loftus, S.K.; Cronin, J.C.; Trivedi, N.S.; Borate, B.; Pavan, W.J. Distinct microRNA expression signatures are associated with melanoma subtypes and are regulated by HIF1A. *Pigment. Cell Melanoma Res.* **2014**, *27*, 777–787. [CrossRef] [PubMed]

87. Sun, B.; Zhang, D.; Zhang, S.; Zhang, W.; Guo, H.; Zhao, X. Hypoxia influences vasculogenic mimicry channel formation and tumor invasion-related protein expression in melanoma. *Cancer Lett.* **2007**, *249*, 188–197. [CrossRef] [PubMed]

88. Hanna, S.C.; Krishnan, B.; Bailey, S.T.; Moschos, S.J.; Kuan, P.F.; Shimamura, T.; Osborne, L.D.; Siegel, M.B.; Duncan, L.M.; O'Brien III, E.T.; *et al.* HIF1α and HIF2α independently activate SRC to promote melanoma metastasis. *J. Clin. Investig.* **2013**, *123*, 2078–2093. [CrossRef] [PubMed]

89. Kim, A.; Im, M.; Yim, N.H.; Ma, J.Y. Reduction of metastatic and angiogenic potency of malignant cancer by Eupatorium fortunei via suppression of MMP-9 activity and VEGF production. *Sci. Rep.* **2014**, *4*, 1–10. [CrossRef] [PubMed]

90. Tas, F.; Duranyildiz, D.; Oguz, H.; Camlica, H.; Yasasever, V.; Topuz, E. Circulating levels of vascular endothelial growth factor (VEGF), matrix metalloproteinase-3 (MMP-3), and BCL-2 in malignant melanoma. *Med. Oncol.* **2008**, *25*, 431–436. [CrossRef] [PubMed]

91. Shaverdashvili, K.; Zhang, K.; Osman, I.; Honda, K.; Jobava, R.; Bedogni, B. MT1-MMP dependent repression of the tumor suppressor SPRY4 contributes to MT1-MMP driven melanoma cell motility. *Oncotarget* **2015**, *6*, 33512–33522. [PubMed]

92. Moro, N.; Mauch, C.; Zigrino, P. Metalloproteinases in melanoma. *Eur. J. Cell Biol.* **2014**, *93*, 23–29. [CrossRef] [PubMed]

93. Tatti, O.; Arjama, M.; Ranki, A.; Weiss, S.J.; Keski-Oja, J.; Lehti, K. Membrane-type-3 matrix metalloproteinase (MT3-MMP) functions as a matrix composition-dependent effector of melanoma cell invasion. *PLoS ONE* **2011**, *6*, 1–13. [CrossRef] [PubMed]

94. Whipple, C.A.; Brinckerhoff, C.E. BRAFV600E melanoma cells secrete factors that activate stromal fibroblasts and enhance tumourigenicity. *Br. J. Cancer* **2014**, *111*, 1625–1633. [CrossRef] [PubMed]

95. Vlaykova, T.; Kurzawski, M.; Tacheva, T.; Dimov, D.; Gulubova, M.; Yovchev, Y.; Chakarov, S.; Drozdzik, M. Investigation of the role of MMP3 -1171insA polymorphism in cutaneous malignant melanoma a preliminary study. *Biotechnol. Biotechnol. Equip.* **2014**, *28*, 904–910. [CrossRef] [PubMed]

96. Kawasaki, K.; Kawakami, T.; Watabe, H.; Itoh, F.; Mizoguchi, M.; Soma, Y. Expression of matrilysin (matrix metalloproteinase-7) in primary cutaneous and metastatic melanoma. *Br. J. Dermatol.* **2007**, *156*, 613–619. [CrossRef] [PubMed]

97. Zhang, Z.; Zhu, S.; Yang, Y.; Ma, X.; Guo, S. Matrix metalloproteinase-12 expression is increased in cutaneous melanoma and associated with tumor aggressiveness. *Tumor Biol.* **2015**, *36*, 8593–8600. [CrossRef] [PubMed]

第31回

The 31st Annual Meeting of
the Japanese Society for Psoriasis Research

日本乾癬学会学術大会

プログラム・抄録集

会期　2016年9月2日金・3日土
会場　ホテル東日本宇都宮
会長　大槻 マミ太郎 ［自治医科大学皮膚科学講座］

The 31st

Ψ

The 31st Annual Meeting of the Japanese Society for Psoriasis Research
JSPR 2016 in UTSUNOMIYA

乾癬、その深淵へ